INTERNATIONAL DOCTORAL
SCHOOL OF THE USC

Iago
González Prada

PhD Thesis

# Electrospun mats for drug repositioning: antimicrobial and antitumor applications

Santiago de Compostela, 2024

**Doctoral Programme in Drug Research and Development**

USC
UNIVERSIDADE
DE SANTIAGO
DE COMPOSTELA

ESCOLA DE DOUTORAMENTO
INTERNACIONAL DA USC

TESIS DOCTORAL

# ELECTROSPUN MATS FOR DRUG REPOSITIONING: ANTIMICROBIAL AND ANTITUMOR APPLICATIONS

Iago González Prada

Directores: Carmen Álvarez Lorenzo y Ángel Concheiro Nine

Tutor: Ángel Concheiro Nine

PROGRAMA DE DOCTORADO EN INVESTIGACIÓN Y DESARROLLO DE MEDICAMENTOS

SANTIAGO DE COMPOSTELA

USC
UNIVERSIDADE
DE SANTIAGO
DE COMPOSTELA

# AGRADECIMIENTOS

Primeiro de todo, quero expresar o meu agradecemento os meus directores de tese *Ángel Concheiro e Carmen Álvarez Lorenzo*, por abrirme as portas do seu laboratorio para poder realizar esta fermosa Tese, que finalmente vai ser concluída, e por ser uns bos referentes cos que tiven o privilexio de dar os meus primeiros pasos no mundo da ciencia e sobre todo no eido da Farmacia e da Tecnoloxía farmacéutica; aprendendo un sinfín de coñecementos e actitudes que de seguro serán imprescindíbeis en futuras etapas. Nunca esquecerei a primeira reunión que tivemos para planificar o que ía ser o traballo desta longa viaxe, na que finalmente optouse por non seguir no mundo das micelas e comezar cunha nova e apaixonante técnica que para mín era totalmente descoñecida nese momento, chamada electrofiado. A partir dese momento e eu sen terme percatado, toda a miña vida ía xirar o redor deste monotema, sendo as miñas palabras máis usadas "electrospinning", "electrospun", "fibers" e "mats". Todo isto, supuxo un enorme reto de moito traballo, superación, amargura e ledicia ata conseguir as tan esperadas fibras e, como unha forte, duradeira e resistente malla de electrofiado, tamén fun facendo grandes amizades e relacións de traballo con outras persoas que tiven o pracer de coñecer nesta etapa da miña vida; o que quero agradecer con estas verbas que perdurarán para sempre.

E como todo bó comezo, nunca esquecerei a primeira persoa que coñecín neste laboratorio e do que orgullosísimo podo chamar aínda agora despois dun lustro "O meu amigo Valenciano", que lonxe de afastarnos por mor de que só estaba facendo unha estadía de tres meses e que a súa volta a Valencia sempre tivo data de volta; o tempo e a distancia non foron suficientes para afastarnos dese sitio no que comezamos chamado sólidos pulverulentos. Moltes gràcies per tot, amic *Caravaca*.

Despois deses tres incríbeis meses tocaba cambio de sitio, no cal estaría o meu escritorio durante os próximos catro anos de doutoramento. O lugar chamábase o "zulo" e alí estábame esperando a miña futura compañeira e amiga tuga *Ana Filipa*, coa que compartín moitas experiencias tanto boas como non tan boas; a *Claudia Sanhueza* coa

USC UNIVERSIDADE DE SANTIAGO DE COMPOSTELA

que fixen as miñas primeiras fibras no meu querido equipo de electrofiado e por último estaba *Xela* a que quero agradecer os seus consellos como veterana e que en poucos meses presentou a súa tese dando paso o que sería o meu compañeiro e amigo máis internacional, pertencente a ONU debido as súas múltiples nacionalidades *Axel* e non Alex. A pesar de todo o choque cultural e de moitos xiros de guión na nosa amizade, sei que sempre poderei contar cun cuarto e cun abarco en calquera parte do mundo. À la prochaine fois, mon ami *Axel*.

Co pasar do tempo, vas pasando de principiante a veterano e como todos sabemos as primeiras veces nunca se esquecen. Por este motivo quero agradecer a todos os meus veteranos por toda a incalculable axuda prestada aínda sabendo de que nunca ía ser devolta. Moitas grazas aos meus veteranos de pecera *Xian* e *María* "*farmatips*" e a os meus veteranos de ciclodextrinas *Clara* e *Victor* "*Viti*". Tamén quero agradecer o "laboratorio de Fran", en especial a Victoria, Iria, Carlos, Xurxo e Rubén por dar toda a súa axuda desinteresadamente o longo deste doutoramento a pesar de non pertencer o seu grupo. Claramente, un día decátaste que agora eres tí o veterano e ademais de ensinar tamén podes aprender, por iso quero agradecer ás expertas de impresión 3D *Lucía* e *Paola*, a meu primeiro TFM *Fernando* e a miña TFG *Nati* por todos eses bos momentos.

Como toda boa Tese, as colaboracións son imprescindibles para aprender novas aptitudes e habilidades. Por este motivo quero dedicar estas verbas a miña primeira colaboración a cal converxeu na miña primeira estadía no laboratorio do profesor *Manuel Simões no Porto*. Nestes tres meses, fun incribelmente recibido pola que sería a miña postdoc *Anabela Borges*, a cal introduciume no mundo da microbioloxía e ensinoume todo o necesario para desenvolver unha parte importante desta Tese a pesar do pouco tempo que dispoñía. Todo este traballo e coñecemento trasladouse ó CIBUS, agradecendo á profesora *Beatriz Magariños* a apertura desta nova posibilidade e a estimable axuda de *Beatriz Santos*. Despois destas frutíferas colaboracións, chegaría a terceira e a última deste doutoramento da man do profesor *Emmanuel Garcion* e o seu equipo *Marine Dion* e *Arthur Barcelos*, e que a pesar da distancia entre Santiago e Angers fixéronme sentilo moi cerca. Por todo isto, síntome un gran afortunado de ter compartido longas xornadas de traballo con persoas dun talento incalculable. Muito obrigado!, Merci beaucoup!.

Quero destacar a última incorporación dentro destra etapa doutoral e da miña vida, a cal supuxo un xiro de 360 grados e que cambiou totalmente a miña perspectiva das

cousas. Converténdose en compañeira, amiga e confidente dentro desde laboratorio e que sen ela esta Tese non sería o que é. Muito obrigado *Dianinha*, por todo o que fas todos os días por mín, por darme as forzas e os ánimos necesarios para enfrontar todos os problemas finais desta Tese, por incrementar o nivel ata cotas inimaxinábeis, por ensinarme o lado bo e amable da vida e, sobre todo, por ensinarme que aínda que o mundo vírense contra nós e que este estea cheo de obstáculos tan grande como a Torre da Serra da Estrela, todos poderanse superar con traballo, sacrificio, constancia e decoro. Estou seguro que sempre poderei contar contigo aínda que os nosos camiños podan separase, sen dubidar que sempre estaremos preto un do outro malia a distancia e quen sabe se voltearemos outra vez a traballar e a compartir o noso tempo xuntos outra vez. Creo que fáltanme verbas que aínda non existen para expresar todo o que sinto por ti.

Por último quero expresar que antes do doutorado e do doutoramento está a persoa, por iso quero agradecer a todas a persoas que apareceron o longo da miña vida e que de certa forma van aportando e modificando a túa personalidade de forma sixilosa.

No meu caso quero agradecer a todas as persoas que coñecín durante a carreira de Farmacia e que foron e serán os meus "amigos de farmacia", *Santi* e *Adrí* , os que ademais foron compañeiros de piso; as miñas amigas *Silvia*, *Lorena* e *Uxía* por toda a axuda prestada e a o meu amigo e dottore *Felipe* o cal tamén decidiu seguir o camiño da ciencia e que sempre estarei esperando por el en Vigo. Nesta fermosa etapa, puiden coñecer o meu irmán de outra mai, o cal recorrín todo o camiño académico enteiro e sendo un dos maiores apoios nesta etapa. Moitas grazas *Javi*.

Tamén quero agradecer os meus amigos de toda a vida, "os meus amigos do Barco", cos que compartín desde os tres anos infinidade de historias e aínda que algúns xa se foron e outros foron formando parte do grupo, todos aportaron nalgún momento da miña vida unha inmensa ledicia. Moitas grazas *a  Carlos, Patri, Sergio, Javi, Pablo* e *Dani* por todos este anos.

E como non podería ser doutra forma quero agradecer a toda a miña familia, en especial ao meu irmán *David* e aos meus pais *Fermi* e *Seve*, por ser o piar principal na miña vida, por darme sempre todo e máis e polo apoio inesgotable. Definitivamente esta Tese vai dedicada a vos, porque sería imposible de ter comezado e menos terminado sen toda a axuda prestada tanto económica como anímicamente e só espero que estedes

USC UNIVERSIDADE DE SANTIAGO DE COMPOSTELA

orgullosos do voso fillo, que espera darvos moitas alegrías futuras para compensar todo ese cariño e esforzo recibido. Podo terminar dicindo, que teño os mellores pais do mundo.

USC
UNIVERSIDADE
DE SANTIAGO
DE COMPOSTELA

# INDEX

**RESUMO** ..... **XIII**

**LIST OF ABBREVIATIONS** ..... **XXI**

**I. INTRODUCTION** ..... **25**

1.1. ELECTROSPINNING AS A FORMULATION TOOL: AN OVERVIEW ..... 27

*1.1.1 Electrospinning components and procedure* ..... *29*

*1.1.2. Role of instrument parameters on electrospinning* ..... *36*

*1.1.3 Role of solution characteristics* ..... *40*

*1.1.4 Types of electrospinning* ..... *45*

*1.1.5 Types of matrices* ..... *51*

*1.1.6 Modifications post-manufacture* ..... *54*

1.2. BIOMEDICAL APPLICATIONS OF ELECTROSPUN MATS ..... 55

*1.2.1 Drug delivery* ..... *55*

*1.2.2. Bacterial infections: A global threat* ..... *59*

*1.2.3 Cancer diagnosis and therapy* ..... *83*

1.3. REFERENCES ..... 97

**II.AIM** ..... **125**

**III. ANTIMICROBIAL CYCLODEXTRIN-ASSISTED ELECTROSPUN FIBERS LOADED WITH CARVACROL, CITRONELLOL AND CINNAMIC ACID FOR WOUND HEALING** ..... **131**

ABSTRACT ..... 134

KEYWORDS ..... 134

GRAPHICAL ABSTRACT ..... 135

3.1. INTRODUCTION ..... 136

3.2. MATERIALS AND METHODS ..... 139

*3.2.1 Materials* ..... *139*

*3.2.2 Preparation of electrospinning solutions* ..... *140*

*3.2.3 Electrospinning process* ..... *140*

*3.2.4 Biofilm prevention studies of the electrospun mats* ..... *142*

*3.2.5 Fibers characterization* ..... *144*

*3.2.6 EOC release tests* ..... *145*

USC UNIVERSIDADE DE SANTIAGO DE COMPOSTELA

*3.2.7 Antioxidant activity* ..... *148*
*3.2.8 Hemolysis test* ..... *149*
*3.2.9 In ovo tissue integration and angiogenesis evaluation* ..... *149*
*3.2.10 Statistical Analysis* ..... *150*
3.3. RESULTS AND DISCUSSION ..... 150
*3.3.1 Fibers preparation* ..... *151*
*3.3.2 Antibiofilm activity* ..... *156*
*3.3.4 Structural characterization and release pattern of the antibiofilm fibers* ..... *181*
*3.3.5 Surface polarity* ..... *193*
*3.3.6. Mechanical properties of electrospun mats* ..... *199*
*3.3.7 Antioxidant activity* ..... *200*
*3.3.8 Hemolysis test* ..... *201*
*3.3.9 In ovo tissue integration and angiogenesis evaluation* ..... *203*
3.4. CONCLUSIONS ..... 205
3.5. REFERENCES ..... 207

**IV. DISULFIRAM-LOADED ELECTROSPUN FIBERS WITH ANTIMICROBIAL AND ANTITUMORAL PROPERTIES FORGLIOBLASTOMA TREATMENT..217**

ABSTRACT ..... 220
KEYWORDS ..... 220
GRAPHICAL ABSTRACT ..... 221
4.1 INTRODUCTION ..... 222
4.2 MATERIALS AND METHODS ..... 226
*4.2.1 Materials* ..... *226*
*4.2.2 Preparation of polymeric solution and electrospinning* ..... *227*
*4.2.3 Fibers characterization* ..... *230*
*4.2.4 In vitro release study* ..... *230*
*4.2.5 Blood compatibility* ..... *233*
*4.2.6 Antimicrobial activity* ..... *234*
*4.2.7 In Vitro test* ..... *235*
*4.2.8 Evaluation of the toxicity of fibers In Vivo* ..... *237*
*4.2.9 Statistical Analysis* ..... *238*
4.3 RESULTS AND DISCUSSION ..... 239

USC UNIVERSIDADE DE SANTIAGO DE COMPOSTELA

*4.3.1 Fibers preparation and morphological and mechanical analysis* ..... *239*
*4.3.2 Mechanical, spectroscopical and hydrophobic properties of the fibers* ..... *245*
*4.3.3 Disulfiram release profile* ..... *248*
*4.3.4 Hemolysis* ..... *252*
*4.3.5 Antimicrobial activity* ..... *252*
*4.3.6 Anticancer activity on glioblastoma cells* ..... *254*
*4.3.7 In vivo medium-term biocompatibility of SF-fibers: locoregional histological analysis* ..... *259*
4.4. CONCLUSIONS ..... 262
4.5. REFERENCES ..... 264

**V. GENERAL DISCUSSION ..... 273**

REFERENCES ..... 287

**VI. CONCLUSIONS ..... 293**

**VII. GENERAL BIBLIOGRAPHY ..... 297**

**VII. ANNEXES ..... 357**

ANNEX A ..... 359
*A.1. CONFLICT OF INTEREST* ..... *359*
*A.2. LIST OF PUBLICATIONS* ..... *359*
*A.3. Figures Authorship* ..... *360*
ANNEX B ..... 361
*B.1. PERMISSION FOR THE IN VIVO STUDY* ..... 361
*B.2. ARRIVE CHECKLIST* ..... 362

USC UNIVERSIDADE DE SANTIAGO DE COMPOSTELA

USC
UNIVERSIDADE
DE SANTIAGO
DE COMPOSTELA

# RESUMO

USC
UNIVERSIDADE
DE SANTIAGO
DE COMPOSTELA

USC
UNIVERSIDADE
DE SANTIAGO
DE COMPOSTELA

# RESUMO

A sociedade actual ten experimentado cambios demográficos e tecnolóxicos moi notables nas últimas décadas. A pesar do aumento na esperanza de vida, a prevalenza de enfermidades dexenerativas coma cancro, diabetes e Alzheimer, e as infecciosas lonxe de decrecer estase a incrementar. Cada ano, organizacións de todo o mundo publican listas das dez principais causas de morte, sendo a maioría lideradas polos diferentes tipos de cancros (8.2 millóns) e progresivamente van aparecendo as resistencias antimicrobianas con 700.000 falecementos no 2016. As enfermidades infecciosas amosan unha clara tendencia ascendente, con 1.9 millóns de mortes no 2019 e espérase 10 millóns para o 2050, converténdose na principal causa de falecemento a nivel mundial. O continuo aumento de mortes vaticinan un escenario escuro debido a múltiples mecanismos de resistencia, perdida da eficacia de antibióticos, maior desinterese da industria e dos gobernos na procura de novos enfoques, mal uso dos antibióticos debido á automedicación e a incorrectas prescricións médicas, pouca hixiene ou ineficiente depuración de auga e residuos, cambio climático ou malas practicas agrícolas. Todo isto crea un escenario similar á era preantibiótica.

Diferentes tipos de patóxenos, tales como bacterias, virus, fungos ou parásitos son os responsables desta dramática situación debido ós seus múltiples mecanismos de defensa fronte a diversos axentes activos como antibióticos, antiparasitarios ou antifúnxicos. Dentro deste grupo destacan as infeccións producidas por bacterias, sendo as mais comúns, as de maior diversidade, podendo localizarse en calquera parte do corpo e acontecendo en todo tipo de ambientes e lugares. Este grupo de microorganismos contribúe maioritariamente ó escenario das resistencias antimicrobianas debido aos seus múltiplos mecanismos de resistencia, preferentemente: degradación ou modificación da estrutura dos antibióticos; cambios nas dianas terapéuticas dos antibióticos como a protección; e diminución da cantidade de antibiótico dentro da bacteria pola actividade das bombas de efluxo ou porinas presentes na membrana bacteriana. Todos estes mecanismos de resistencia débense a cambios xenómicos nas bacterias debido a razóns intrínsecas, adaptativas ou adquiridas. Ademais dos mecanismos de resistencia, hai que ter en conta que as bacterias son seres vivos que viven en sociedade onde os individuos encontran un ambiente axeitado para crecer, alimentarse, comunicarse, protexerse e

USC UNIVERSIDADE

dividirse. Estas comunidades chamadas biofilmes están altamente protexidas por unha envoltura ou matriz polimérica que representa o 90% do biofilme mentres que o 10% restantes son as propias bacterias pertencentes a un só tipo ou a varios tipos de cepas que viven en sintonía e de forma altamente organizada. Estas comunidades non son estáticas; todo comeza pola adhesión de unha ou varias bacterias a un estrato ou material, crecerán en número, madurarán e por último conseguirán espallarse a outros lugares onde o ciclo repetirase infinitamente.

Todas as características están presentes en maior ou menor medida nos dous grandes grupos de bacterias Gram positivas ao que pertencen as familias como *Streptococcus* e *Staphylococcus* e Gram negativas ao que pertencen as familias como *Enterobacteriaceae*, *Vibrionaceae* ou *Pseudomonaceae*; diferenciados porque estes últimos presentan unha densa membrana lipopolisacárida. Moitas bacterias conviven co ser humano dun xeito harmonioso, en simbiose formando parte da microbiota natural da pel ou intestino, por exemplo, facilitando certos procesos ou evitando a invasión de outros potencial patóxenos. Non obstante, ao longo da súa vida unha persoa experimentará certas circunstancias que romperán esta boa relación, desenvorcando na aparición de diversas infeccións de diferente calibre, que sen unha intervención axeitada poden causar a morte do individuo. Unha destas circunstancias é a aparición de feridas na pel, rompendo a barreira natural do organismo e propiciando a invasión e máis tarde colonización de bacterias como *Staphylococcus aureus* e *Staphylococcus epidermidis, Pseudomonas aeruginosa* ou *Escherichia coli*.

Acotío, unha pequena ferida non supón maiores problemas na poboación sa, sendo que normalmente non é preciso ningún tipo de intervención xa que o corpo ten os seus propios mecanismos para remediar de forma axeitada este tipo de eventualidades. A reparación e restauración da ferida consta de catro etapas perfectamente sincronizadas, as cales son hemostase, inflamación, proliferación e remodelación. As primeiras 24 horas son críticas para a estabilización e comezo da rexeneración do tecido podendo alargarse aos tres meses ata a total recuperación do tecido. Non obstante algún destes catro procesos pode fallar debido a varios factores como ausencia de resposta inmune, falta de actividade plaquetaria e doutras células como os fibroblastos ou queratinocitos, ou a invasión e colonización de bacterias. Todos estes factores determinan a cronificación das feridas, aparecendo ulceras diabéticas (aproximadamente o 15% dos doentes diabéticos desenvólvena e desta porcentaxe entre o 14-24% sufrirán amputación), úlceras venosas

USC DE SANTIAGO DE COMPOSTELA

localizadas na perna (prevalencia ente 1-1.5% da poboación) ou úlceras por presión en doentes con mobilidade reducida (prevalencia do 1 ao 5%).

A cronificación das feridas débese principalmente a factores sistémicos ou locais. Os sistémicos están relacionados co alcance do dano (tamaño, profundidade, ou localización da ferida), a idade da persoa, enfermidades crónicas (obesidade, cancro, diabetes ou hipertensión), interacción de fármacos (corticosteroides, inmunosopresores ou diuréticos), malnutrición ou certos hábitos (tabaco ou alcol). Os factores locais que abranden enfermidades vasculares tanto arteriais como venosas, neuropatías, cirurxías, inflamacións crónicas, tecido necrosado, radiación o condicións exteriores desfavorábeis como pouca osixenación, mal balance hídrico, temperatura ou acidez, senescencia de fibroblastos, tratamentos ou practicas incorrectas como mal uso de antibióticos ou fallo no debridamento da infección.

O descubrimento dos antibióticos na segunda metade do século XX supuxo un auténtico pulo na abordaxe das feridas e a resolución das infeccións. Sen embargo, na actualidade estase a vivir un auténtico chanzo atrás debido a aparición das resistencias antimicrobianas, que limitan a utilidade do arsenal terapéutico dispoñible e supoñen un aumento da taxa de mortalidade por infección de feridas crónicas. Todo isto motiva que se estea a procurar novos enfoques para o tratamento das infeccións, como a estimulación inmune con vacinas e anticorpos, e a procura de lisinas ou fagos mais eficaces que permitan controlar infeccións minimizando as resistencias antimicrobianas. Un destes novos enfoques é o uso de aceites esenciais. Os aceites esenciais son compostos de orixe natural, formados por unha variedade de terpenos, terpenoides ou fenilpropanoides e outras moléculas como alcois, ácidos, hidrocarburos alifáticos lactonas ou esteres entre outros, os cales ofrecen varias vantaxes como actividade de amplo espectro contra algúns microorganismos pertencentes o grupo ESKAPE, mecanismos de accións multi-diana, reducindo a presión selectiva e combatendo a resistencia antimicrobiana e por último ofrecendo un rendemento versátil e polivalente, por exemplo actividade antiinflamatoria, antioxidante e anxioxénica. Esas características fan dos aceites esenciais unha prometedora alternativa ao uso dos antibióticos para tratar todo tipo de feridas. Dentro dos múltiples aceites esenciais identificados, destacan o carvacrol, un monoterpenoide fenólico presente na planta do ourego, o citronellol un alcol monoterpénico presente na planta da citronela, e o ácido cinámico que é un ácido carboxílico fenólico presente na árbore da canela. Estes tres aceites esenciais presentan boas propiedades antimicrobianas

USC
DE SANTIAGO
DE COMPOSTELA

(baixa concentración mínima inhibitoria e concentración mínima bactericida), gran capacidade antioxidante debido a presencia de grupos hidroxilo na súa estrutura, anxioxénicas ou antiinflamatorios por medio da inhibición das especies ROS, radicais libres ou inhibición de varias enzimas ou citokinas como COX-2 ou a liooxigenasa. Ademais, estes tres aceites esenciais posúen diferentes mecanismos de acción antimicrobianos, tales como desestabilización e degradación de varios compoñentes presentes na membrana bacteriana (ácidos graxos, proteínas, polisacáridos e fosfolípidos) desencadeando pérdida de ións e organoides da bacteria, unión coa bomba de protóns provocando pérdida da actividade da membrana, incrementan a permeabilidade provocando a pérdida de compoñentes, inhiben a síntese de ATP e inactivan unha serie de enzimas. Ademais de todos estes mecanismos, os aceites esenciais interferen nas comunicacións das bacterias presentes no biofilme. As bacterias comunícanse mediante pequenas moléculas sinalizadoras denominadas en inglés "quorum sensing" ou "autoinducers" que regulan diversos procesos de adaptación e formación do biofilme, polo que interromper esta comunicación supón o dano do biofilm. Os aceites esenciais teñen a capacidade de alterar esta comunicación mediante a inhibición, secuestro ou o trasporte das devanditas moléculas.

A pesar de que o escenario das resistencias antimicrobianas é cada vez mais preocupante e xera unha maior conciencia dentro da sociedade, a prevalencia que actualmente ten o conxunto de enfermidades designadas como "cancro" é moito maior. O que explica que, a maioría de recursos, esforzos e investimentos nos países desenvolvidos se centren no achado de posíbeis tratamentos e solucións e que cada ano se reporten novos datos do aumento da esperanza de vida dos doentes de cancro e incluso a total curación de cancros que fai un par de décadas parecían intratábeis. Malia isto, algúns cancros todavía teñen moi mal prognóstico. Este é o caso do glioblastoma, un tumor cerebral moi agresivo no que a ausencia dun diagnóstico temperán xunto cun arsenal terapéutico pouco eficiente determinan que a taxa de supervivencia sexa menor de dous anos despois da diagnose. Este tumor maligno representa o 49% de todos os tumores primarios de cerebro entre adultos de entre 45 e 74 anos de idade, cunha incidencia de 4.6 por 100.000 habitantes. O tratamento farmacolóxico basease na administración sistémica da temozolamida ou na administración local de carmustina (GLIADEL®). Estas dúas terapias son moi limitadas conseguindo supervivencia media de 15 meses, xunto cun ratio de supervivencia de máximo 5 anos no 4.7% dos doentes.

Neste século tan só aprobáronse dous tratamentos novos baseados no anticorpo monoclonal bevacizumab (2009) e un novo produto antimitótico, coñecido co nome comercial NovoTTF-100A System™ (2015), que xera campos eléctricos alternos de baixa intensidade e frecuencia intermedia a través de conxuntos de transdutores non invasivos adheridos o coiro cabeludo do paciente.

Dado que o descubrimento de novos fármacos innovadores é moi complexo e ten uns elevados custos en tempo e diñeiro, estase a desenvolver unha estratexia alternativa que consiste no reposicionamento de fármacos aprobados para outros usos mediante a identificación de novos mecanismos de acción. No caso do glioblastoma, está recibindo atención o fármaco disulfiram, aprobado pola FDA para o tratamento do alcolismo, como posible alternativa terapéutica o ter demonstrado actividade antitumoral e antimicrobiana. O reposicionamento de fármacos ofrece vantaxes como o coñecemento do perfil toxicolóxico e redución dos costes de desenvolvemento e do tempo requirido para a investigación e o rexistro. O principal mecanismo de acción do disulfiram é a inhibición da enzima aldehido dehidroxenasa que participa en procesos metabólicos do alcol, pero tamén é usado polas células cancerígenas. Mecanismos de acción complementarios como a quelación de organometais presentes en elevadas concentracións en todas as células cancerígenas para diversas funcións, a restricción da anxioxénexe, a limitación que produce na metástase do tumor ou a regulación inmunosupresiva fan do disulfiram un fármaco prometedor contra o glioblastoma.

Tanto as infeccións como o cancro precisan de novos enfoques para aumentar a eficiencia terapéutica, evitar mortes prematuras e mellorar a calidade de vida dos doentes. O obxectivo desta Tese Doutoral foi o deseño, preparación e caracterización de fibras obtidas por electrofiado útiles para dúas aplicacións: como apósitos para tratar feridas crónicas, e como sistemas implantables na resección do tumor para erradicar glioblastoma. Para a primeira aplicación, as fibras incorporan varios aceites esenciais para acadar a actividade antimicrobiana evitando contribuír a aparición de resistencias antimicrobianas. Mentres que para a segunda aplicación, avaliarase o potencial terapéutico do fármaco de reposicionamento disulfiram en canto a propiedades antimicrobianas e antitumorais.

Tanto os aceites esenciais coma o disulfiram supoñen un reto para a súa formulación como medicamentos xa que presentan propiedades fisicoquímicas inadecuadas, como

USC UNIVERSIDADE

baixa solubilidade en medios acuosos, alta volatilidade, e pouca estabilidade a factores externos (quecemento, exposición continuada a luz, oxidación). Para preparar as formulacións optouse pola técnica do electrofiado, que permite a obtención de fibras de tamaño micro- ou nanométrico cunha superficie específica elevada, porosidade e maleabilidade versátiles e adaptables as características dos tecidos cos que teñen que entrar en contacto, de fácil escalabilidade industrial e baixo custo. Para levar a cabo o traballo, seleccionáronse o polímero sintético policaprolactona e polímero de orixe natural fibroína procedente do verme da seda *Bombyx mori.* Estes polímeros destacan polas súas excelentes propiedades como alta biocompatibilidade, escasa resposta inmune ou inflamatoria, alta estabilidade mecánica, e modulable biodegradabilidade. A técnica de electrospinning xurdiu a principios do século XX e nos últimos anos tense desenvolvido moito coa aparición de novos deseños de procesado que fan do electrofiado unha técnica moi valiosa en múltiples campos incluido o biomédico. Esta Tese de Doutoramento céntrase na preparación, caracterización e avaliación de apósitos xerados pola técnica de electrofiado para o tratamento de feridas crónicas infectadas, xa que a maior parte das infección comezan tras cortes, queimaduras e enfermidades subxacentes (envellecemento, diabetes ou problemas de mobilidade), e de mallas implantables na zona de resección trala cirurxía de glioblastoma, cargados cos axentes terapéuticos nomeados anteriormente.

Na primeira etapa da Tese centrouse en apósitos preparados a partir do polímero biocompatíbel sintético policaprolactona para obter unha estrutura adecuada que poida incorporar varios tipos de ciclodextrinas (por exemplo, αCD, βCD e HPβCD) con diferentes tamaños moleculares e propiedades fisicoquímicas para mellorar as propiedades mecánicas das fibras, formando deste xeito poli(pseudorrotaxanos) entre a policaprolactona e as ciclodextrinas. Ademais, explorouse a formación do complexo de inclusión entre ciclodextrina e os aceites esenciais cavacrol, citronellol e ácido cinámico para mellorar as súas propiedades fisicoquímicas, tales como a baixa estabilidade, pobre disolución en auga e a alta taxa de volatilidade. Estes aceites esenciais incorporáronse de diferentes formas na matriz polimérica da policaprolactona, ou ben sos, en combinación dos tres aceites esenciais ou formando os diferentes complexos de inclusión coas ciclodextrinas. Desta maneira intentouse aproveitar ó máximo as múltiples propiedades que ofrecen estes compostos naturais, tales como a antimicrobiana, antioxidante e anxioxénica. Neste parte da Tese púxose de manifesto a gran capacidade de

USC UNIVERSIDADE DE SANTIAGO

encapsulamento das ciclodextrinas, formado as αCD complexos de inclusión coa larga cadea polimérica de policaprolactona dotando ó sistema de mellores propiedades mecánicas ata chegar a unha concentración máxima. Non en tanto, comprobouse que as HPβCD son mellores encapsulando os aceites esenciais. Deste xeito, os aceites esenciais encapsulados na matriz polimeríca da policaprolactona mostraron perfís de cesión controlados e sostidos mentres que os aceites que previamente foron encapsulados polas HPβCD liberaron grandes cantidades de aceite esencial ó medio acuoso e obtendo un perfil de liberación moito mais rápido. Estes resultados tiveron un impacto notorio na actividade antimicrobiana frente *S. aureus* e *P. aeruginosa*, dous dos principais microorganismos responsables da maioría das infeccións de feridas e pertencentes ao grupo denominado ESKAPEE, na actividade antioxidante e na actividade anxioxénica. Todos os apósitos preparados mostraron boa hemocompatibilidade e unha gran capacidade de integración e biocompatibilidade nos estudos *in ovo*. Debe destacarse que a avaliación microbiolóxica e antibiofilm desta investigación foi posible grazas a colaboración multidisciplinar que se estableceu entre o grupo I+D Farma da Universidade de Santiago de Compostela co equipo do Profesor Manuel Simões e a doutora Anabela Borges na Facultade de Engenharia da Universidade do Porto (FEUP) e co grupo da Profesora Beatriz Magariños no centro de investigacións biolóxicas da USC (CIBUS). O doutorando levou a cabo unha estancia no FEUP financiada polo programa Iacobus.

A segunda parte desta tese tivo coma obxectivo o desenvolvemento de mallas de electrofiado implantables no cerebro utilizando o polímero natural fibroína obtida a partir do verme da seda *Bombyx mori*, para aproveitar algunhas das súas características e vantaxes como as superiores capacidades mecánicas, biocompatibilidade, e actividade antiinflamatoria, rexenerativa, restauradora e neuroprotectora . Estas propiedades poden contribuír a reparación do dano tisular despois dunha cirurxía de resección da cavidade, imprescindible para a recuperación do paciente. O principal obxectivo era a incorporación do fármaco de reposicionamento, disulfiram aprobado pola FDA en 1951 para o tratamento do alcolismo, xa que este fármaco inhibe a aldehído deshidroxenase. Esta inhibición é útil contra as células cancerosas e varios microorganismos, proporcionando o apósito actividade antitumoral e antimicrobiana. Nesta parte da Tese demostrouse a posibilidade de preparar fibras a partir de fibroína liofilizada e a alta capacidade destas para encapsular grandes cantidades de disulfiram, dando lugar a unha liberación sostida e controlada do fármaco. Todo isto, sen perder as excelentes propiedades mecánicas que

USC UNIVERSIDADE DE SANTIAGO

demostrou a fibroína en lámina beta tralo proceso de liofilización. Non obstante, para mellorar a actividade antimicrobiana e antitumoral, optouse pola incorporación da ciclodextrina HPβCD e do ion Cu(II) presente no $CuCl_2$. A incorporación de HPβCD permitiu obter o complexo de inclusión co disulfiram mellorando a solubilidade en auga e a inestabilidade deste fármaco. Ademais, como aconteceu cos aceites esenciais, a HPβCD permitiu liberar cantidades máis altas de disulfiram no medio acuoso nas primeiras horas. Isto permitiu obter excelente actividade antitumoral e antimicrobiana fronte *S. aureus* e *P. aeruginosa*. Aínda que estas fibras mostraron unha boa hemocompatibilidade, e coa premisa de obter biocompatibilidade coas células do cerebro, obtouse por reducir a cantidade de disulfiram das fibras pero mantendo a capacidade antimicrobiana e antitumoral. Deste xeito, incorporánronse pequenas cantidades de $CuCl_2$ para mellorar proceso de electrofiado e aproveitar as propiedades de formación de quelatos do disulfiram para xerar o complexo $Cu(DDC)_2$. Deste modo observouse unha diminución do tamaño da fibra, incrementouse a actividade antitumoral fronte as células de glioblastoma, obtendo actividade antimicrobiana fronte *S. aureus* e mellorando a biocompatibilidade cos astrocitos. Esta segunda parte da Tese de Doutoramento abordouse tamén dende unha perspectiva multidisciplinar coa colaboración do Profesor Emmanuel Garcion e o seu grupo dentro do Institut National de la Santé et de la Recherche Médicale (INSERM-CRCI2NA) na Universidade de Angers (Francia), co que o grupo I+D Farma mantén unha estreita colaboración desde a participación conxunta no proxecto europeo EURONANOMED3 "Gliosilk". O grupo do Prof. Garción está especializado en neurociencia, en particular no desenvolvemento de modelos de glioblastoma en animais, identificación dos mecanismos fundamentais subxacentes ao desenvolvemento do glioblastoma e de tratamentos loco-rexionais relevantes. É importante destacar que nun primeiro ensaio *in vivo* en modelo de resección cerebral as fibras de electrofiado preparadas amosaron unha boa biocompatibilidade na primeira semana post-implantación. Tomando como base estes resultados *in vitro* e *in vivo*, está previsto abordar nun futuro próximo a avaliación da eficacia das fibras de disulfiram nun modelo animal de glioblastoma.

En conxunto, os resultados desta Tese de Doutoramento amosan as posibilidades da formulación de aceites esenciais e de fármacos reposicionados en mallas de electrofiado, para unha abordaxe novidosa do tratamento das feridas crónicas e de tumores que prantexan necesidades terapéuticas que non están suficientemente cubertas.

USC UNIVERSIDADE DE SANTIAGO

# LIST OF ABBREVIATIONS

| | |
|---|---|
| **ABC** | ATP Binding Cassette |
| **AC** | Alternating Current |
| **AcOH** | Acetic Acid |
| **AHL** | Acyl-Homoserine Lactone |
| **AI** | Autoinducer |
| **AIP** | Autoinducing Peptide |
| **ALDH** | Enzyme Aldehyde Dehydrogenase |
| **AMR** | Antimicrobial Resistance |
| **BBB** | Blood-Brain Barrier |
| **BCE** | Before Common Era |
| **$CHCl_3$** | Chloroform |
| **CIP** | Cisplatin |
| **CNS** | Central Nervous System |
| **CSF** | Cerebrospinal Fluid |
| **Cu** | Copper |
| **DC** | Direct Current |
| **DCM** | Dichloromethane |
| **DMF** | Dimethylformamide |
| **DMSO** | Dimethyl Sulfoxide |
| **DNA** | Deoxyribonucleic Acid |
| **DSF** | Disulfiram |
| **DTR** | Difficult-To-Treat Resistance |
| **ECM** | Extracellular Matrix |
| **EGF** | Epidermal Growth Factor |
| **EMA** | European Medicines Agency |
| **EOC** | Essential Oil Component |
| **ETOH** | Ethanol |
| **FDA** | Food And Drug Administration |
| **FGF** | Fibroblast Growth Factor |
| **GBM** | Glioblastoma Multiforme |
| **GDP** | Gross Domestic Product |

USC UNIVERSIDADE DE SANTIAGO DE COMPOSTELA

| | |
|---|---|
| **GMP** | Good Manufacturing Practice |
| **HIV** | Human Immunodeficiency Virus |
| **HTAB** | Hexadecyl Trimethyl Ammonium Bromide |
| **IRN** | Irinotecan |
| **ISF** | Interstitial Fluid |
| **LiCl** | Lithium Chloride |
| **LPS** | Lipopolysaccharides |
| **MATE** | Multidrug And Toxic Compound Extrusion |
| **MeOH** | Methanol |
| **MFS** | Major Facilitator Superfamily |
| **MMP** | Matrix Metalloproteinase |
| **NaCl** | Sodium Chloride |
| **NAP-2** | Neutrophil Activating Peptide-2 |
| **NK** | Natural Killer |
| **NO** | Nitric Oxide |
| **OCDE** | Economic Co-Operation and Development |
| **OM** | Outer Membrane |
| **PAM** | Polyacrylamide |
| **PCL** | Polycaprolactone |
| **PDGF** | Platelet-Derived Growth Factor |
| **PDR** | Pan-Drug Resistant |
| **PEG** | Polyethylene Glycol |
| **PEI** | Polyethyleneimine |
| **PEO** | Polyethylene Oxide |
| **PF-4** | Platelet Factor 4 |
| **PGA** | Poly(Glutamic Acid) |
| **PLA** | Poly(Lactic Acid) |
| **PLGA** | Poly(Lactic-Co-Glycolic Acid) |
| **PP** | Polypropylene |
| **PS** | Polystyrene |
| **PTX** | Paclitaxel |
| **PU** | Polyurethane |
| **PVA** | Polyvinyl Alcohol |

USC UNIVERSIDADE DE SANTIAGO DE COMPOSTELA

| | |
|---|---|
| **PVP** | Polyvinyl Pyrrolidone |
| **QS** | Quorum Sensing |
| **RNA** | Ribonucleic Acid |
| **RND** | Resistance Nodulation Division |
| **ROS** | Reactive Oxygen Species |
| **SCFA** | Short-Chain Fatty Acid |
| **SDF-1** | Platelet Derived Stromal Cell Derived Factor-1 |
| **SDS** | Sodium Dodecylsulphate |
| **SMR** | Small Multidrug Resistance |
| **TGF- β** | Transforming Growth Factor-B |
| **THF** | Tetrahydrofuran |
| **TMZ** | Temozolomide |
| **TTField** | Tumor Treating Field |
| **USA** | United States of America |
| **VEGF** | Vascular Endothelial Growth Factor |
| **WHO** | World Health Organization |
| **XDR** | Extensively Drug Resistant |

USC
UNIVERSIDADE DE SANTIAGO DE COMPOSTELA

USC
UNIVERSIDADE
DE SANTIAGO
DE COMPOSTELA

# I. INTRODUCTION

USC
UNIVERSIDADE
DE SANTIAGO
DE COMPOSTELA

USC
UNIVERSIDADE
DE SANTIAGO
DE COMPOSTELA

# I. INTRODUCTION

## 1.1. ELECTROSPINNING AS A FORMULATION TOOL: AN OVERVIEW

The electrospinning technique is a fascinating, simple, and versatile method for preparing microscale to nanoscale fibers with tunable surface morphology, high surface area to volume ratios, and modifiable compositions [1]. This approach has received increasing attention as a promising research tool in numerous fields, namely medical and healthcare, filtration, protective clothing, optical and chemical sensors, electronics, nanocatalysis, biotechnology, pharmaceutical, and environmental engineering [2].

Typically, the electrospinning technique involves the preparation of polymer solution based on both natural or synthetic polymers, selection of proper solvents, and the use of optimal solution parameters (*e.g.,* molecular weight of the polymer, polymer concentration, viscosity and solution conductivity) [1]. The obtained electrospun fiber mats can present different sizes and often feature a high encapsulation efficiency, high surface-to-volume ratio ideal for the co-delivery of a wide range of active agents, tunable porosity, malleability, easy handling and reliability, reproducibility, cost-effectiveness, and scalability [2–4]. All these properties make electrospinning to be considered a preferable and highly effective procedure in tissue engineering, wound healing, and local cancer treatment [5] As illustrated in **Figure 1.1.**, a conventional electrospinning system is usually composed of four main parts: (i) a spinneret, which is typically a syringe attached to a needle; (ii) a syringe pump for the controlled release of the polymer solution; (iii) a metallic collector to receive the electrospun fiber mat; (iv) a power supply to create an electric field between the spinneret and the collector [2]. In this technique, the polymer to be electrospun is either dissolved in a proper solvent or melted and transferred to the spinneret using the syringe. Then, an electrical field between the spinneret and the collector creates a cone-shaped deformation of the liquid droplet, known as Taylor cone, and a jet stream. This jet stream further elongates, and its large surface area allows the rapid solvent evaporation rapidly or rapid cooling of the melted polymer, which results in the formation of continuous solid fiber mats. Finally, these fiber mats are deposited on

USC DE SANTIAGO DE COMPOSTELA

the ground collector. It should be highlighted that the described fundamental configuration of the electrospinning equipment has remained unchanged since the beginning of its development in 1897 by Rayleigh, two centuries ago [2]. Later, the electrospraying technique was created by Zeleny in 1924. In the following ten years, Formhals started to publish several patents about a new experimental setup for polymeric filaments using electrostatic forces. [6,7]. In 1969, Taylor described the development of a conical shape of a jet as a result of a hydrostatic balance between electrostatic forces and the surface tension [8]. Although the term electrospinning derived from "electrostatic spinning" did not become popular until the mid-1990s, it has been gaining importance in the subsequent decade due to interest in nanotechnology applications [9]. Nowadays, electrospinning has become a research widespread in both academia and industry, giving rise to numerous scientific articles and patents every year [10]. For instance, in the last decade, a total of 29.767 scientific articles and 9.375 patents were published about new emerging approaches to solve a plethora of important problems worldwide [9,10].

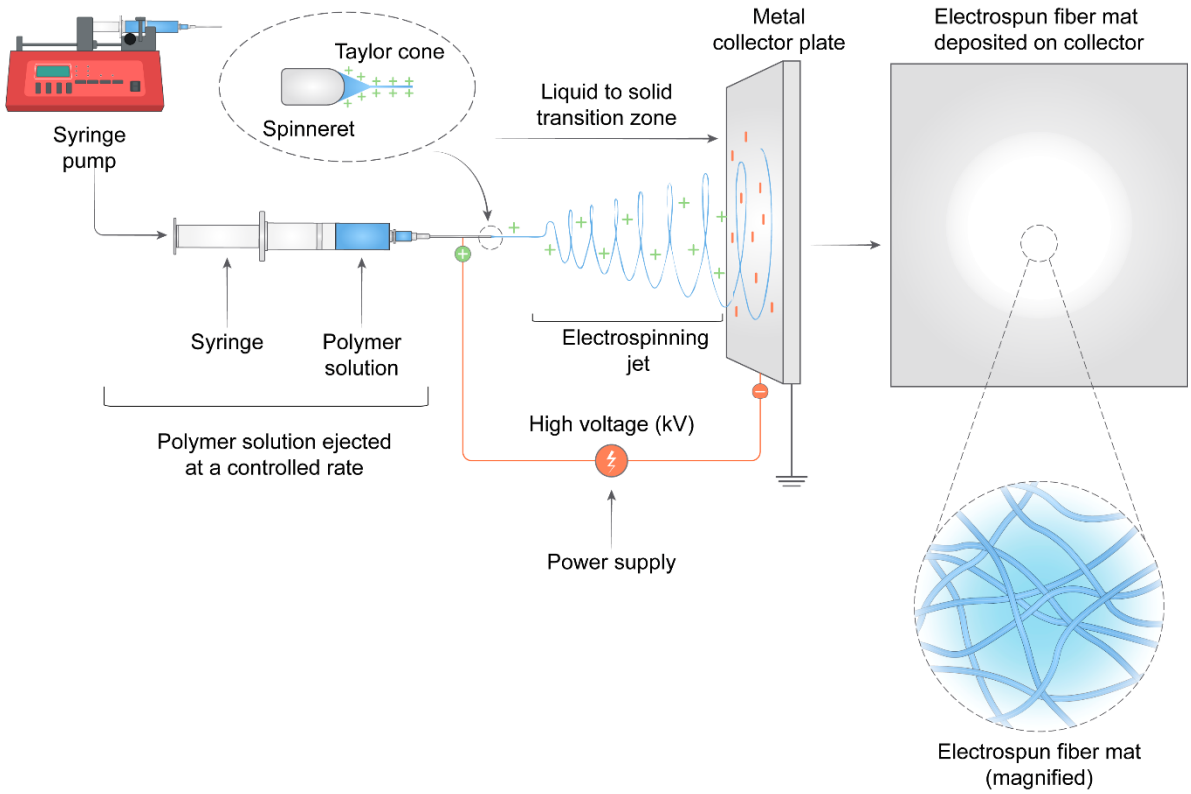



**Figure 1.1. Example of a conventional setup of electrospinning for preparing fiber mats. The key elements of electrospinning consist of a syringe pump, a spinneret, a high voltage power supply, and a conductive collector. The Figure was made by the author of the Thesis.**

USC UNIVERSIDADE DE SANTIAGO DE COMPOSTELA

### 1.1.1 Electrospinning components and procedure

#### 1.1.1.1 Voltage supply

Typically, the electrospinning process starts with the formation of a cone-shaped solution, also identified as a Taylor cone **(Figure 1.1.)**, at the end of the spinneret when the charged polymer solution is released at high voltage (>10 kV) [11]. Therefore, a high voltage power supply is essential to provide sufficient voltage to overcome the repulsion forces that occur at the end of the spinneret. Without this device it would be impossible to form the Taylor cone and, consequently, the intertwining of the polymer chains and evaporation of the solvent [12]. The distance between the spinneret and collector determines the initiation voltage for electrospinning, which is often approximately 6 kV [13]. For example, a closer distance results in a lower initiation voltage. Then, the voltage of the power supply can be increased steadily up to a magnitude of 50 kV and 0.5 A of electricity [12].

#### 1.1.1.2 Syringe pump

The syringe pump has two important functions: (i) holding the syringe that contains the spinnable polymer solution and (ii) driving the liquid sample through the spinneret towards the collector at the suitable flow rate for the preparation of the fiber mats. Depending on the desired type of fibers, the electrospinning system can incorporate one or more syringe pumps, which can simultaneously hold two or more syringes. For instance, the preparation of uniaxial only requires a syringe pump, while two pumps are necessary for preparing coaxial fibers [12]. It should be noted that different types of needles may be integrated in the same syringe, since the diameters of the needles influences the size of the fibers that are produced (*i.e.*, large needle diameters give rise to fibers with large diameters). This strategy can be particularly useful in the preparation of coaxial, tri-axial, multi-needle, magnetic field-assisted electrospun fibers [12]. All types of fibers will be described in the **Section 1.4**.

#### 1.1.1.3 Spinneret

Over the years, the voltage supply and the syringe pump did not suffer relevant changes as they are devices that are not directly in contact with the polymeric solution and the formation of electrospun fiber mats [14]. Researchers have focused more efforts on the parts that are in contact with the polymeric solution and can notably determine

fiber formation, namely the spinneret and the collector. Typically, the spinneret is the structure where a drop of polymeric solution became a Taylor cone for jet formation due to the voltage applied and gravity forces. Besides, spinnerets can be divided in three main types: spinnerets with needles, spinnerets for nozzle-type electrospinning and spinnerets for free surface electrospinning. Both types include stationary or rotating spinnerets [15].

1.1.1.3.1 Needle electrospinning

Spinnerets can incorporate one or more needles with different configurations. The simplest appearance of electrospinning arises from the single needle electrospinning method, which is often applied to improve the solubility, drug loading, and stability of dosage forms. A single needle consists of a single hollow blunt metal needle suitable for preparing monolithic, blend, and emulsion matrices. This type of fibers represents approximately 80% of publications due to the simplicity, easy implementation, and first source for checking the newest electrospinnable solutions and solvents [15]. The single needle is included in several electrospinning types such as uniaxial, melt, 3D electrospinnable, and portable electrospinning (explained in detail in **Section 2.1.4.**) However, the low production rate implies the implentation of some modifications in the single needle configuration, namelly electroblowing with auxiliary air flow inside to generate multiple jets and increase the yield. Nevertheless, searching for an increase in production rate more complex needle types are being developed [15].

Multiple needles consist of complex electrospinning systems that use more than one needle in different configurations or spatial disposition have been adopted to increase the production of fibers [15]. There exist multiple noodle configurations, such as linear array (*e.g.*, nine needles in a linear fashion), square or rectangle disposition *(e.g.,* 3x3 matrix square), hexagon organization (*e.g.*, six-needle setup surrounding one center needle or hexagon with an equilateral triangle), concentric arrangement, among other configurations. The optimization and development of new and continuous arrangements are a response to the multiple challenges for implementing multi-needle systems due to their associated problems in terms of repulsion between jets with same charge that causes instability of the process, clogging, and lack of uniformity in fiber distribution [15]. Thereby, the needle distribution plays an important role in the optimal space fiber formation, avoiding undesirable repulsion between jets.

USC UNIVERSIDADE DE SANTIAGO DE COMPOSTELA

*1.1.1.3.2 Nozzle-type electrospinning*

Nozzle-type technologies, in contrast to the previously discussed numerous needles, have been developed for the industrial bulk production of electrospun fibers **(Figure 1.2.)**. This approach aims to avoid jet repulsion and includes different types of configurations, including cylindrical porous tube, flat spinnerets, centrifugal, implementation of auxiliary electrodes, and needle accessories. In this system, the electrospinning setup contains needles, holes, or channels where each nozzle produces a Taylor cone (or bubble in some cases), after the feed polymer solution to be ejected straight from nozzles or enclosed capillaries [15]. For instance, cylindrical porous tubes produce multiple jets with broader fiber distribution. In turn, flat spinnerets have several perforations with optimal distribution to prevent repulsion and clogging. The incorporation of auxiliary electrodes (*e.g.*, ring, cylindrical, or plate) can intensify the electric field by applying similar polarity needles to improve the morphology of the fibers (*i.e.*, thin and uniform fibers) and increase the production rate. Besides, different accessories of needles like holes or channels with microfluidic systems for the solution feeding or substituting needles by holes to produce more uniform and finer fibers than using needles [15–18].

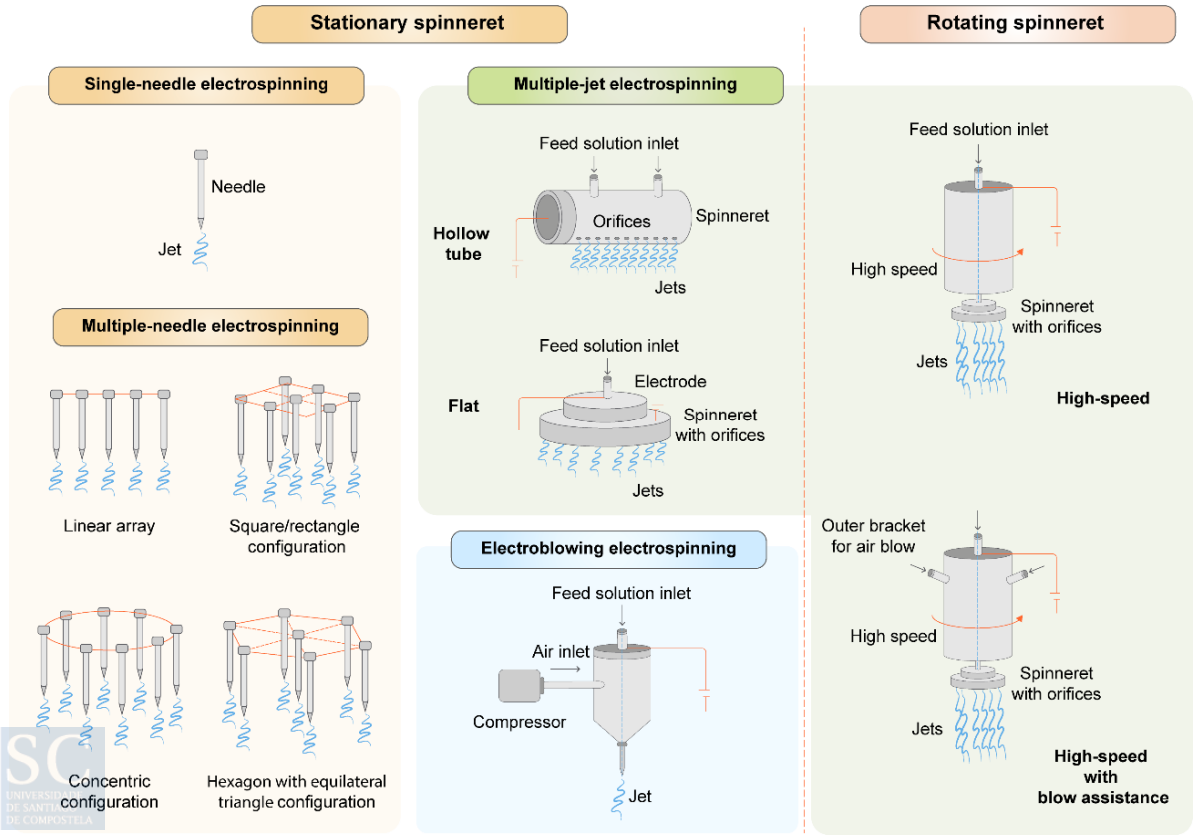


**Figure 1.2. Schematic illustration of different types of spinnerets containing needles and spinnerets for nozzle-type electrospinning. Stationary spinnerets: linear array, square/rectangle configuration, concentric arrangement, hexagon with equilateral triangle outline, hollow tube, flat and electroblowing. Rotating spinnerets: nozzle-based high-speed and high-speed with blow assistance. The Figure was made by the author of the Thesis.**

*1.1.1.3.3 Free surface electrospinning*

Free needle, also known as free surface or tipless electrospinning replaces the needles with a surface connected to high voltage for triggering multiple Taylor cones and jets formation at several localizations and to obtain great fiber formation rate [19]. This approach provides several advantages including major fiber throughput, and it is useful for unelectrospinnable solutions that generate unstable Taylor cone and jets [20]. However, this tipless approach demands that the surface is connected to high voltages to overcome the surface tension of the great area occupied by the polymeric solution [15]. Moreover, the implementation of free surface electrospinning in the pharmaceutical industry following the requirements of the Good Manufacturing Practices (GMPs) is challenging, due to the possible variations in polymeric solution (e.g., conductivity, viscosity) owing to the prolonged air exposition of the solution associated with high evaporation rates of the solvents. Free surface electrospinning involves using stationary or rotating spinnerets **(Figure 1.3.)**. The first group has a static spinneret aided by gravitational force for feed the system. Bowl, wire, conical wire, stepped pyramid, slit, slot, cleft and plate edges are examples of stationary spinnerets. Bowl spinneret generates multiple jets at the edge in the presence of high voltage from a polymeric solution that fills the bowl and redistributes spontaneously for equal curve space [21]. Wire spinnerets allow the production of core-shell fibers using an emulsion solution through two wires forming multiple jets. The various positions that wires may adopt have a strong influence on the process, being vertically twisted positions more stable than straight wire designs [22]. Conical wire coil avoids the use of two wires obtaining superior quality fibers. Stepped pyramid spinneret produces thinner fibers using a similar concept as bowl spinneret but increasing the production rate due to the presence of more edge area [23]. Slit-fixtures spinnerets are usually used for preparing core-shell fibers with uniform distribution and easy monitoring process [24]. Different convexly curved slots were designed using a variety of shapes namely, straight line, triangles and rectangles that leverage the convex curvature of the systems and enhance the uniform intensity of voltage distribution to prepare consistent fibers with great production rates [25]. Linear cleft

USC DE SANTIAGO DE COMPOSTELA

spinnerets were inspired on surface waves dynamic theory to prepare fibers using the crest structures for multiple jet formation when voltage is applied. Finally, plate edges use numerous piled up plates trying to mimic a waterfall structure, which the control flow rate changing the angle of the plate to produce good quality fibers and avoid undesirable clogging [26]. Furthermore, corona, rotatory wire, spiral coil, beaded-chain, rotary disk, cylinder, ball, bubble, centrifugal electrospinning and magnetic fluid were categorized as rotating electrospinning. These approaches commonly use a polymeric solution bath with immersed spinnerets with different movements and shape types to form multiple jets when voltage is applied for the preparation of fibers. Corona spinneret is formed by sharp-edge circular electrodes, requiring low amounts of solution [27]. Rotatory wire is totally immersed in a solution bath with an into and out movement forming droplets and erupting jets [28]. The rotating spiral coils prepare finer fibers when a high-intensity voltage is applied throughout coils [29]. Plane beaded chain has two horizontal sections, the bottom section is immersed in the solution bath whilst the top section forms the fibers when a strong intensity field is applied [30]. Rotating disk consists of the formation of multiple jets in the surface disk aided by a rotation that prevents the coagulation of the solution. This last approach generates more uniform fibers than the cylinder spinneret since need more applied voltage [31]. Ball spinneret formed multiple jets in the upper half of the ball when an electric field is applied, reporting low production of fibers in comparison with the two last approaches [32]. Bubble spinneret are inspired by bubble electrospinning; the bubbles are produced by air injection and when reach the surface of the solvent bath, split into multiple jets for the voltage applied [33]. Applying a magnetic field into a solution top assisted by supplemented ferromagnetic fluid bottom allows for reducing the voltage applied for obtaining thinner fibers [34].

USC
UNIVERSIDADE DE SANTIAGO DE COMPOSTELA

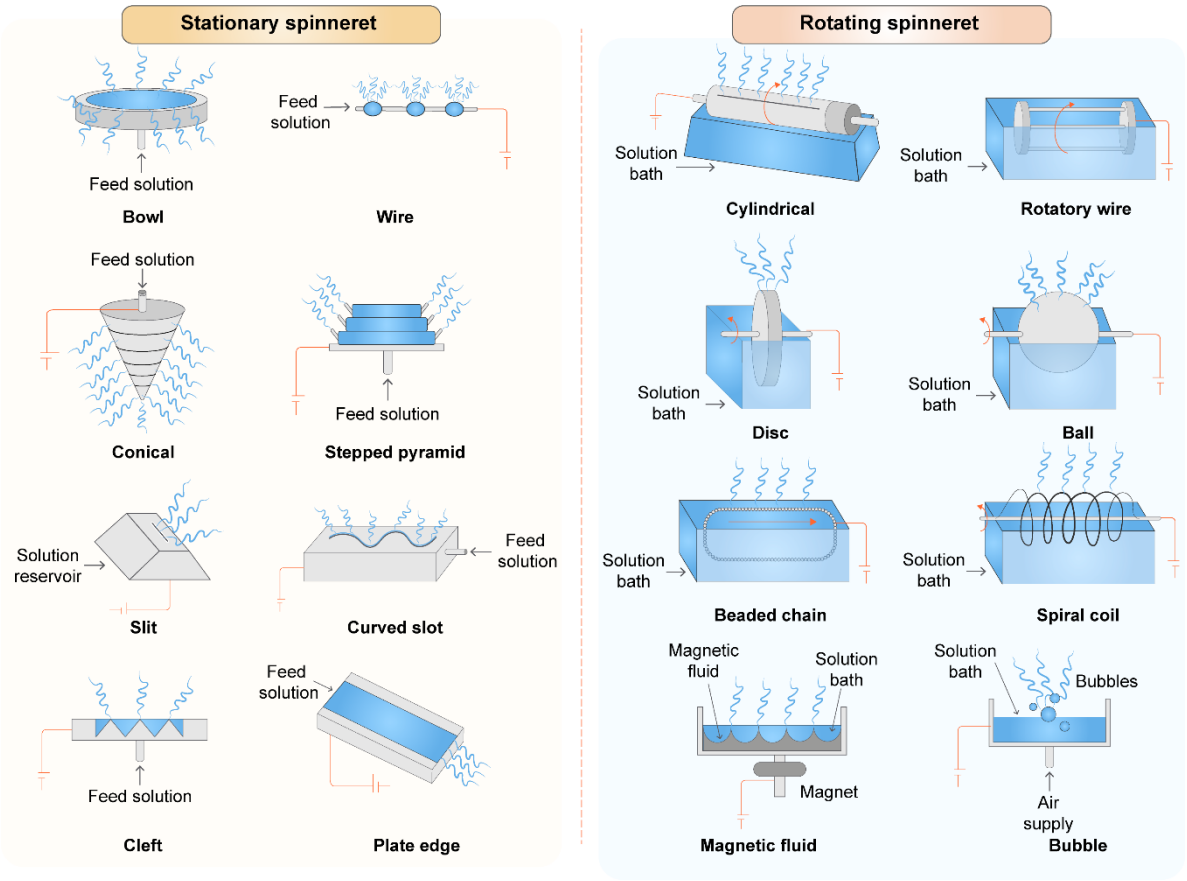



**Figure 1.3. Different types of spinnerets for free surface electrospinning. Stationary spinnerets (left-side): bowl, wire, conical wire, stepped pyramid, slot, cleft, and plate edge. Rotating spinnerets (right-side): cylindrical, rotatory wire, disk, ball, beaded-chain, spiral coil, magnetic fluid, and bubble. The Figure was made by the author of the Thesis.**

#### 1.1.1.4 Collector

The collector is the place where the fibers formed after the solvent evaporates are deposited and collected **(Figure 1.1.)**. Depending on the configuration of the electrospinning equipment, the deposition of the fibers is affected by different mechanisms. If the equipment is in a vertical position, the fibers ejected from the needle will be attracted by the action of gravity and by the attraction of charges since negative voltage is applied to the collector, while positive voltage is applied to the needle. On the other hand, if the electrospinning equipment is in a horizontal position, the fibers will only be attracted by the different charges existing between the needle and the collector [5]. Different types of collectors have been developed to control the morphology, the orientation and the distribution of the fibers. Currently, there are two different collector groups, stationary and rotating collectors **(Figure 1.4.)**. Flat plate, parallel plate, blade,

ring, liquid bath, and electrode array collectors belong to stationary ones, while pins drum, wires drums, disc, knife edge, and rotating bath belong to the rotating group [11,35].

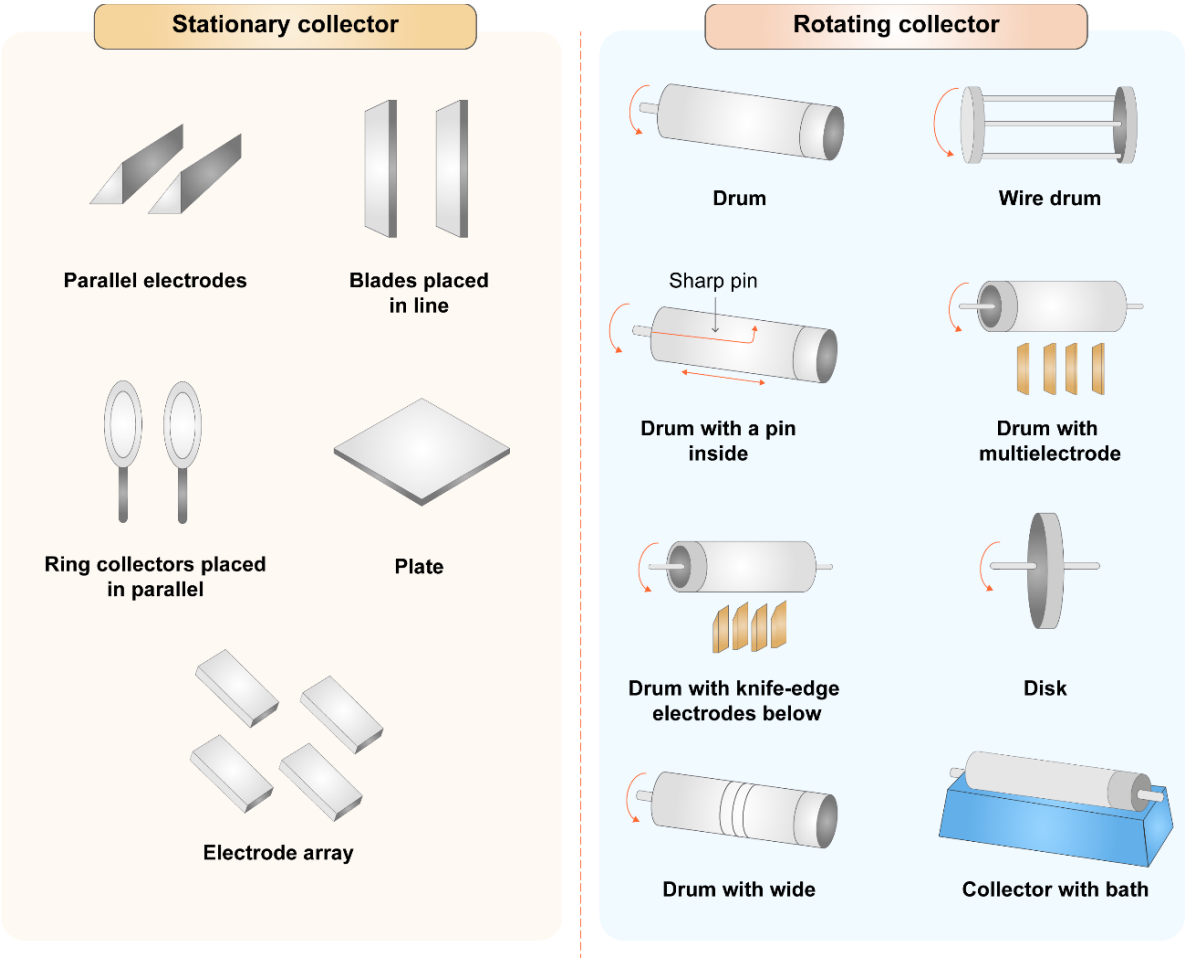



**Figure 1.4. Different types of collectors that are often used in electrospinning: static collectors (left-side) or rotatory collectors (right-side). The Figure was made by the author of the Thesis.**

Flat plate is the most widely used collector type to prepare randomly distributed electrospun mats, being the reference collector [35]. Parallel plates allow aligned fibers using a stationary collector [36]. Parallel rings create twisted fiber yarns [37]. Electrode arrays offer a precise control of fiber orientation. A liquid bath collector enables 3D electrospinning structures [11]. Pins drums are useful to obtain fine and aligned fibers. Knife edge electrodes offer an aligned coarse fiber. Wire drums provide the control of alignment area. Disc collector facilitates the alignment of the fiber through speed synchronization for enhanced integrity fiber. Rotating bath incorporates a rotating drum for twisted the solidified fiber with the aim of forming a polymeric electrospun yarn [38].

USC UNIVERSIDADE DE SANTIAGO DE COMPOSTELA

### 1.1.2. Role of instrument parameters on electrospinning

The electrospinning process is governed by certain parameters that can be customized including, applied voltage, flow rate, distance between tip-to-collector, solution properties (*i.e.*, viscosity, surface tension, concentration, molecular weight of polymer, conductivity, homogeneity, and solvents), environments parameters (*i.e.*, temperature, humidity, and pressure) [1].

#### 1.1.2.1 Applied voltage

Technically, electrospinning is a process that uses a strong electrical field to draw a polymer solution or melt into fine filaments by overcoming the surface tension of the polymer solution. The fiber formation could be divided in four steps: charging and deformation; jet formation; jet thinning; and solidification and collection [11]. Thus, the process starts with a droplet liquid or melt polymer at the needle being distorted into a cone shape, known as Taylor cone, under a high electrification [39]. The high voltage application creates an imbalance between bulk and surface of the drop [8]. This charge imbalance generates electrostatic forces sufficiently high to overcome the surface tension of the drop, acquiring the Taylor cone shape **(Figure 1.5.)**. The process is mathematically described by the Coulomb´s law, being F the force between objects ($q_1$,$q_2$) at the distance (r), and *k* the Coulomb´s constant $9\times 10^9$ $Nm^2$ $C^{-2}$ **Equation 1.1.** [11]:

$$F=\frac{(k\times q_1\times q_2)}{r^2} \qquad (1.1.)$$

The effect of the electric current on a drop to become in a shaped cone was also mathematically described by Taylor through the following **Equation 1.2.**, in which V is the potential, R the radial, $P_{1/2}(\cos\theta)$ the Legendre function in order ½ [40]:

$$V=V_0+AR^{1/2}P_{1/2}(\cos\theta) \qquad (1.2.)$$

Once the drop started the elongation, the electrostatic forces should increase until reaching the critical electrospun voltage ($V_c$), where the charged polymer is ejected from the cone. The **Equation 1.3.** is based on the Taylor equations to explain this phenomenon, considering the viscosity and surface tension [41]:

USC UNIVERSIDADE DE SANTIAGO DE COMPOSTELA

$$V_c^2 = 4\frac{H^2}{h^2}\left(\ln\left(\frac{2h}{R}\right) - 1.5\right)(1.3\pi R\gamma)(0.09) \quad (1.3.)$$

$V_c$ is the critical voltage, H represents the distance between spinneret to collector in centimeters, h denotes liquid column length in centimeters, $R$ is the spinneret inner radius in centimetres, $\gamma$ is the surface tension of the solution in dyne per centimeter, and 0.09 is the constant that give a voltage estimate. The critical electrospun voltage is different for different polymer solutions.

The application of strong electrostatic forces causes a great electrostatic repulsion by the induction of charges on the surface, producing a shear stress that provokes the jet formation [11]. This process was described by Rayleigh instability **Equation 1.4.**:

$$\lambda = \frac{k \times Q^2}{\varepsilon \times d^4} \quad (1.4.)$$

being $\lambda$ the instability wavelength, $k$ is the droplet charge, $\varepsilon$ is the surrounding medium permittivity, and $d$ is droplet diameter [11]. Then, the jet is ejected due to the intertwining of the polymer chains, creating a whipping and elongating movement [12].

The electrical current generated along the electrospun distance depends on the charge carriers that are obtained by ionizing the air from the needle to the collector, passing through the polymer jet solution. Furthermore, the electrical current in the jet is affected by some parameters such as solvent, relative humidity, applied voltage, conductivity of the solution, the diameter of the needle (gap) and some geometric properties. The electrical current in the polymeric jet was determined by Charles using the following **Equation 1.5.** [42] :

$$I_{total} = EQ^{0.5}K^{0.5} \quad (1.5.)$$

I is electrical current flow through the jet, E is filed strength, Q is flow rate and K is the conductivity solution. Through the process, the jet travels through the air experimenting charge dissipation and evaporation, provoking jet thinning and solidification into fibers until it reaches the collector where finishes solidifying and collected. Taylor predicted and described the size and the shape of the jet while is ejected from the spinneret [10] as follow **Equation 1.6.**:

USC UNIVERSIDADE DE SANTIAGO DE COMPOSTELA

$$Q=\frac{2\pi\times\varepsilon\times d\times V}{\ln\left(\frac{r_2}{r_1}\right)} \qquad (1.6.)$$

where $\varepsilon$ is the surrounding medium permittivity, $d$ is droplet diameter, $V$ is the applied voltage, $r_2$ is the jet radius and $r_1$ is the cone radius. Commonly, the applied voltage ranges between 1 and 30 kV to surpass the surface tension of the polymeric solution [39]. The voltage has influence in the diameter of the fibers as a general rule when the voltage is increased the diameter of the fibers is decreased due to the stretching of the polymer solution until reaching the critical voltage. Too high or two low voltages cause the formation of noticeable beads lengthwise the fibers [42,43].

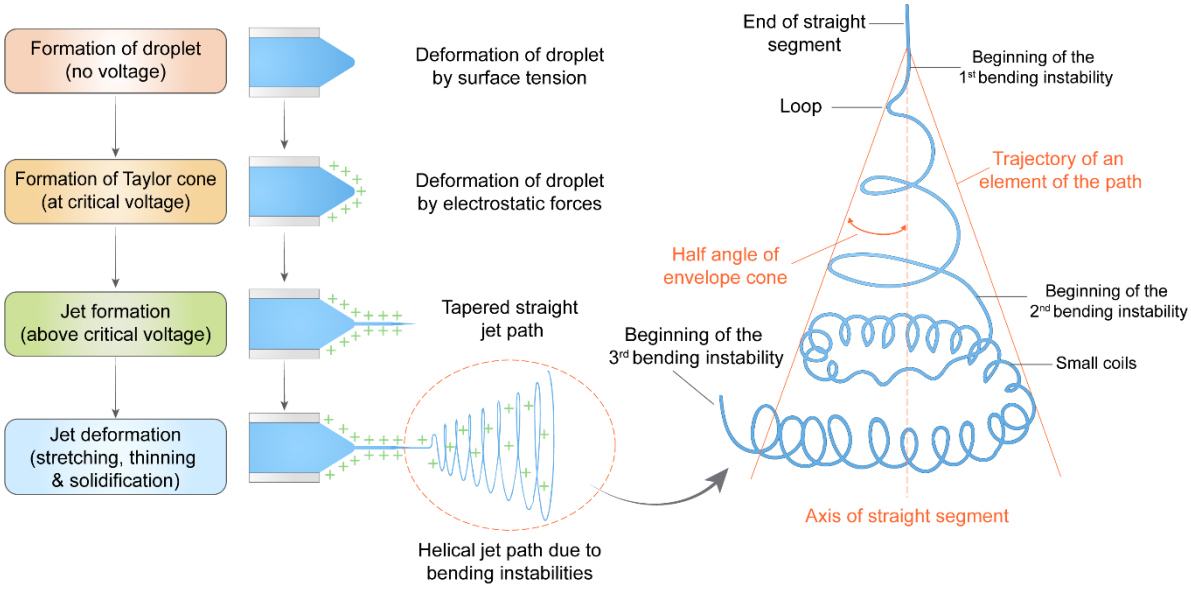



**Figure 1.5. Phases of jet formation during electrospinning procedure. Formation of the Taylor cone (left-side): (i) pendant drop; (ii) hemispherical shape droplet; (iii) conical shape droplet. Formation of the electrospinning jet (right-side): (i) formation of a droplet in the absence of voltage; (ii) formation of Taylor cone at critical voltage; (iii) formation of jet above critical voltage; and (iv) jet deformation (stretching, thinning, and solidification of jet). The Figure was made by the author of the Thesis.**

### 1.1.2.2 Distance between spinneret and collector

The distance between the spinneret and the collector ($H$) determines the diameter and morphology of the fibers because the distance is related with the time of flow and the evaporation. Moreover, $H$ determines the electric field strength ($E = V/H$), and changing the distance modifies $E$ and the distribution of electric flux lines that affects the fiber formation [44]. If the distance is increased, the time that the jet has for evaporating the

USC UNIVERSIDADE DE SANTIAGO

solvent and for elongating the polymeric chains is increased, leading to a decrease in the diameter size. Moreover, the jet always experimented with thins until reach at the collector due to the increase of surface charge density, resulting in the obtention of thinner fibers. Conversely, if the distance is decreased, the time for evaporation of the solvent is reduced and less elongation of the polymer chains occurs, causing the apparition of fused fibers on the collector and beads lengthwise the fibers [12]. Furthermore, as the distance is reduced, the time that the jet remains in contact with the air decreases increasingly since the electric field accelerate it because of the intensity of the electric field is inversely proportional to the distance [42]. The selection between direct current (DC) and alternating current (AC) is essential owing to impact in the formation fiber since DC use a commonly voltage range between (10-20 kV) ensuring jet stability and continuous fiber formation whilst AC uses a range of voltage between (1-20 kV) with polarity changes that provoke bead formation and jet disruption. However, this disadvantage of AC could be used for obtaining a customizable morphology [44].

#### 1.1.2.3 Solution flow rate

The morphology, structure, and diameter of the fibers depends on the rate flow applied. Setting the correct flow is essential to get smooth, homogeneous, and continuous fibers without beads. If the rate flow increases, the diameter and the pore size increase because of a reduction in the time of the jet flight and uncomplete evaporation of the solvent [42]. Moreover, the viscosity and the solvent used are closely related to the flow rate. Polymeric dispersions with low viscosity require faster flow rate due to the fast evaporation rate of the solvent into the needle, avoiding obstruction. This effect is more relevant when volatile organic solvents are used such as acetic acid (AcOH), ethanol (ETOH), dimethyl sulfoxide (DMSO), methanol (MeOH), chloroform ($CHCl_3$), dichloromethane (DCM), tetrahydrofuran (THF), or dimethylformamide (DMF) [43]. A minimal flow rate is needed to prepare nanofibers and achieve a stable jet cone, avoiding the apparition of beads and great variability of distribution size. The commonly flow rate is in the range of $0.05 – 5$ mL $h^{-1}$, and applied feed rates upper than 10 mL $h^{-1}$ should be avoided to prevent periodically splashes and bead fiber formation [11]. Overall, the flow rate applied will depend on a variety of solution parameters, including the polymers selected and their molecular weights, the concentration of the several other components, the solvents selected and their evaporation rate, and the total viscosity of the polymeric solution.

USC DE COMPOSTELA

### 1.1.3 Role of solution characteristics

#### 1.1.3.1 Types of polymers

A properly selection of a wide range of materials, including polymers, ceramics, bioglasses, and organometallics is a crucial aspect for the development and preparation of electrospun mats, considering the applicability and functionality of the electrospun mats. These materials should be biocompatible, nontoxic, mechanically stable, and non-immunogenic for biomedical applications [45].

Polymers are the most widely and commonly used components of electrospun fibers. Natural polymers have unique and beneficial properties such as biocompatibility, chemical versatility, ability to interact with host tissue to induce cell adhesion, proliferation, differentiation, and angiogenesis, different biodegradability rates through several cellular metabolisms, low immune and inflammatory response, environment friendly, and unlimited resource. However, preparation of electrospun fibers with natural polymers can become a tough task because this type of polymers present complex structures and inter-lot variability for optimal fiber obtention, short working window (*e.g.,* thermolabile, mostly organic solvents rejection), sensitiveness to environmental conditions (*i.e.*, temperature, relative humidity, or light), and uncontrollable degradation.

Natural polymers can be classified in different families due to source of origin as polysaccharides (*e.g.*, dextran, alginate, chitosan and hyaluronic acid), cellulose derivatives (*e.g.,* methylcellulose, carboxymethyl cellulose, hydroxypropylmethylcellulose, ethylcellulose, or hydroxyethylcellulose) and proteins (*e.g.,* collagen, gelatine, silk fibroin, elastin, chitosan, casein, or fibrinogen) [2,46,47].

Synthetic polymers have a long carbon chain in their structure mainly produced from petrol derivatives using several chemical processes and are endowed with a wide range of characteristics or properties. They can be classified in non-biodegradable and biodegradable ones, depending on the time needed for enzymatic, hydrolytic, environmental or microbial activity. They are more cost-effective in most cases, especially if compare with natural polymers, and can be produced in large quantities [48,47]. Many hydrophobic, hydrophilic, and amphiphilic polymers have been tested for electrospinning, highlighting polyvinyl alcohol (PVA), polyvinyl pyrrolidone (PVP), Polyethylene oxide (PEO), poly(glutamic acid) (PGA), poly(lactic-co-glycolic acid)

USC UNIVERSIDADE DE SANTIAGO DE COMPOSTELA

PLGA, polyacrylamide (PAM), polyethyleneimine (PEI), polycaprolactone (PCL), poly(lactic acid) (PLA), polyurethane (PU), polystyrene (PS), polypropylene (PP), polyethylene glycol (PEG), and several poloxamer varieties [2].

#### 1.1.3.2 Solution Properties

##### *1.1.3.2.1 Concentration*

Preparation of continuous, homogeneous, and smooth fibers demands a minimum solution concentration. A polymeric solution can be in different stage or phases, regarding the polymer concentration. Some researchers describe a minimum or critical polymer concentration required for obtaining electrospun fibers due to the formation of enough chain entanglements interactions. A low concentration (*i.e.*, dilute regimen far below the minimum concentration) results in droplets containing free (individualized) polymer chains that lead to electrospray process. If the concentration is increased and the polymer chains start to overlap among them, then a semi-dilute regime is achieved in which the entanglement is not sufficient and thus both beads and fibers are obtained. The obtention of undesirable beads will be until the entanglement concentration ($C_e$) is surpassed. In general, optimal fibers require polymer concentrations 2-2.5 fold higher than $C_e$ [47]. However, if the concentration is too high, the typical cylindrical shape of the fibers starts changing to a flat shape, denominated as ribbon structure that presents an increased diameter [49]. Beyond this concentration the electrospinning process is prohibited owing to the inability to maintain the correct flow [50]. Thus, there exist a positive correlation between fiber diameter and polymer concentration [51].

##### *1.1.3.2.2 Molecular weight*

The molecular weight of a polymer plays an important role in the solution properties owing to the significant impact in the viscosity, conductivity, surface tension, and dielectric strength, which are involved in morphology, rheological, and electrical properties [49]. Molecular weight has a power relationship with the number of entanglements of polymer chains in a solution. As mentioned above, the chain entanglements are critical for ensuring a minimum level of viscosity to avoid break the jet during electrospinning process and to reduce the surface tension effects [52]. Thereby, in electrospinning technique high molecular weight polymers are preferred due to their lower entanglement concentration, which reduces the probability that the jet breakes,

USC UNIVERSIDADE DE SANTIAGO

enhances the mechanical strength of the fibers and decreases the likelihood of bead formation lengthwise the fibers [53]. However, many publications also demonstrated the interest of low molecular weight polymers to prepare electrospun fibers, whereby enough intermolecular interactions (*e.g.,* van der Waals forces, hydrophobic interactions, and hydrogen bonding) can alleviate the weaker interchain connectivity through physical entanglements [54].

*1.1.3.2.3 Viscosity*

The viscosity depends on many factors such as molecular weight and molar concentration of the polymer, the solvent, impurities in the solution, temperature and pressure [12]. Moreover, these factors are not independent of each other but are related. Thereby, the viscosity of a polymeric dispersion increases with an increase of the molecular weight or molar concentration and depends on temperature. The intrinsic viscosity directly depends on the molecular weight as indicated by Mark-Houwink Sakurada [42] in the following **Equation 1.7.**:

$$[\eta]=KM^{a} \qquad (1.7.)$$

In this equation $[\eta]$ is the intrinsic viscosity, M is the molecular weight, and K and $a$ are Mark-Houwink parameters or calculated empirically constants parameters that depend on the polymer-solvent interactions. Indeed, the value of $a$ predicts the best solvent for different type of polymers, being a 0.5 value for theta solvents (polymer coils act like ideal chains), 0.5-0.8 value for solvents suitable for flexible polymers, and > 0.8 values for solvents suitable for semiflexible polymers [42].

The electrospinning process is strongly dependent on the viscosity of the polymeric dispersion. High interaction among polymeric chains is needed for obtaining a continuous jet. If the viscosity of the polymeric dispersion is below a minimum, electrospray occurs. As the polymer concentration increases some fragment forms of fibers appear, and continuous fibers with beads are formed until the optimal viscosity is reached. Likewise, if the optimal viscosity is overcome ribbon fibers star to appear and the possibilities to obstruct the needle increases due to solvent evaporation [55]. Thus, the optimal viscosity should be in the range of 1-20 Pa·s since larger viscosities cause flow instability by high cohesiveness forces. If the viscosity is lower than 1 Pa·s droplets

USC UNIVERSIDADE DE SANTIAGO DE COMPOSTELA

could be formed [1]. Ultimately, this is the main parameter that affect the morphology and the diameter of the fibers [56].

*1.1.3.2.4 Surface tension*

The surface tension is linked with the solvent that was used for preparing the solution, becoming the main opposite force against the fiber formation. Thereby, this parameter solution plays an important role since it is necessary apply voltage for overcoming the electrostatic repellent force on the polymeric solution [49]. Consequently, solvents with high surface tension unable the electrospun process since an unstable Taylor cone is obtained and instability of jets occurs, provoking generation of sprayed droplets and increases the probabilities to bead appear [57]. Thus, solvents with low surface tension values are preferred as they do not require high voltage rates, generating fibers in a gentle process. However, sometimes high surface tension solvents have to be used to dissolve the polymer and cannot be replaced by other most friendly solvent. In that case, a variety of strategies have been developed, including the use of auxiliary substances such as ionic salts or surfactants that can reduce the surface tension of the polymeric solution (*e.g.,* sodium chloride (NaCl), Lithium Chloride (LiCl), Triton-X, sodium dodecylsulphate (SDS), and hexadecyl trimethyl ammonium bromide (HTAB)) [58,59].

*1.1.3.2.5 Conductivity/ surface charge density*

The conductivity of a polymeric solution is given by the type of the polymer, the solvent used and the enable of ionizable salts, providing charge ions that have great influence in jet formation [2]. Polymers are conductive except for dielectric materials; natural polymers are usually more conductive than synthetic polymers [60]. Moreover, each solvent has its own conductivity. Conductivity could modify the morphology and the diameter of the fibers. A polymeric dispersion with high conductivity requires less voltage to obtain a stable Taylor cone and thus less diameter fibers could be obtained [61]. Meanwhile, low conductivity provokes insufficient jet elongation, resulting in bead fibers. Likewise, the conductivity of the polymeric dispersion can be enhanced using salts such as NaCl, $KH_2PO_4$, nickel acetate and cobalt acetate [62]. However, the salts added have a limit, since could change the viscosity of polymeric dispersion, leading to alterations in fiber preparation. Moreover, extremely conductive solutions result in unstable processes under the applied electric field (bending instability) [62].

USC DE COMPOSTELA

#### 1.1.3.3 Environmental conditions

Commonly, the environmental parameters that affect the process and preparation of electrospun fiber mats are temperature, humidity, and pressure [64].

##### *1.1.3.3.1 Temperature*

The most environmental parameter that change the condition of the experiments is the temperature, since it can affect greatly the viscosity of the polymer dispersion and the evaporation rate of the solvent [63]. Depending on the polymer, an increase in temperature could either increase or decrease the viscosity. Indeed, electrospinning is not only affected by the viscosity but also by the evaporation rate of the solvent, which also impacts on the morphology and the diameter of the fibers. Commonly, an increase of the temperature implies a decrease in fiber diameter due to faster solvent evaporation and reduction of the probability of fibers fusion [64].

##### *1.1.3.3.2 Humidity*

Humidity affects the volatility of the solvent. High relative humidity reduces the volatility of the solvent. In parallel, if hydrophilic polymers are being used, they can absorb water that will be incorporated into the fibers. In the case of hydrophobic polymers, the humidity can create pores lengthwise the fibers due to the changes in the evaporation of organic solvents [65].These pores could alter the mechanical properties, wettability and surface area of the fibers [11]. Thereby, the humidity should not surpass the 40% wt.% to not affect the electrospun process and the fibers formation since high humidity rates triggers undesirable increases in the size, distribution and number of surface pores [60].

##### *1.1.3.3.3 Pressure*

The atmospheric pressure is directly related with the boiling point of liquids. A decrease of pressure implies a decrease of boiling point and increase of the volatility of the solvent. Therefore, if the volatility of the solvent changes, the fiber formation will be altered. [65].

USC UNIVERSIDADE DE SANTIAGO DE COMPOSTELA

### 1.1.4 Types of electrospinning

Over the years, electrospinning approaches and new setups arise for overcoming limitations and challenges that the applications of electrospun fibers in different fields were emerging. The present section describes the most common electrospinning types and the most recent setups for preparing different types of fiber mats **(Figure 1.6.)**.

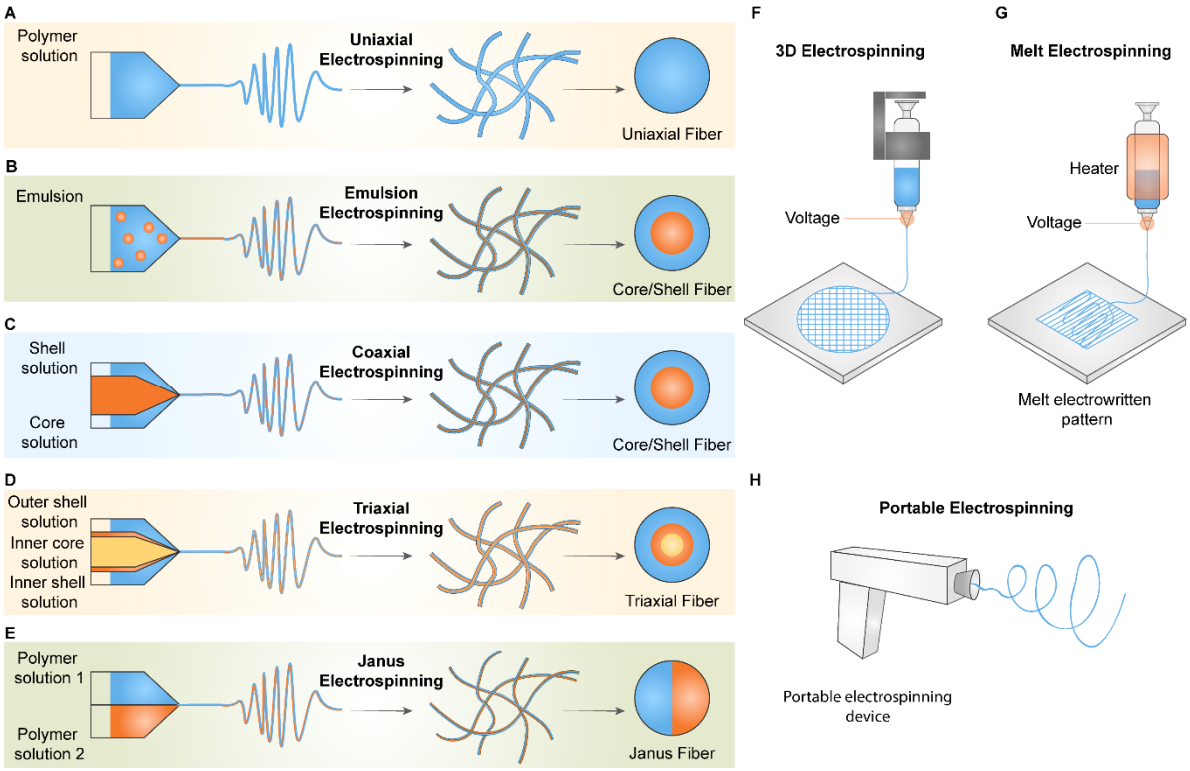



**Figure 1.6. Process diagram for preparing different types of fiber mats through electrospinning technology (i.e., uniaxial, core/shell, triaxial or janus fibers). These optimized electrospinning approaches can then be incorporated with other new or traditional technologies (3D printing or melt spinning) to produce tailor-made functional formulations for different biomedical applications. The Figure was made by the author of the Thesis.**

#### 1.1.4.1 Uniaxial electrospinning

It is was first and the oldest electrospinning approach introduced by Cooley and Morton in 1902 [14]. Although more than a hundred years have passed, currently uniaxial electrospinning is the most commonly and widely used electrospun technique worldwide due to their simplicity, versatility, easy operability and handling [1]. This technique is the reference model to explain the electrospun setup since all electrospun modifications include it. Thereby, uniaxial electrospinning is composed of one syringe pump, high-

voltage power supply connected to a single blunt metallic needle, and collector. Eventually, electrospun equipment is incorporated into video equipment for monitoring the Taylor cone shape [2].

Different approaches have been developed to surpass a variety of limitations of this technique, namely using different solution types (*e.g.* blend or emulsion solution), sequential electrospinning, co-electrospinning or electrospinning-co-electrospraying. Emulsion and blend solution are explained in **Section 1.5.2.** Sequential electrospinning involves the electrospinning of a first solution for producing a mat in the collector, then the syringe is changed with the second solution for deposition of new fibers on top of the former ones. When two opposite spinnerets arranged in a different special place (*i.e.*, vertically, antiparallel and horizontally) are fed at the same time and the same collector is used to prepare a single mat, the approach is designed as co-electrospinning. If in this technique one of the electrospun solutions is replaced by an electrospray solution (less polymeric concentrate), electrospinning-co-electrospraying can be obtained. Thereby, these different uniaxial approaches offer new electrospun mats such as layer-by-layer or mixed mats, improving the physicochemical properties, biocompatibility or obtaining different release profile of widely different drugs [66]. Uniaxial electrospinning offers several advantages namely, simple and less complex setup (suitable for laboratory use) but highly reproducible results. It is the first technique for use to check the spinnability of new material and its optimization. However, the simplicity of this technique implies a variety of disadvantages including the limited production capacity (0.01-0.03 $gh^{-1}$ of solid dry fibers), and that the mats have small-diameter pores that hinder the inner penetration by large particles or mammalian cells. [14].

#### 1.1.4.2 Coaxial electrospinning

Coaxial electrospinning appeared in 2003 [67]. In this approach the spinneret consists of two concentrically aligned needles with an inner needle fitted within the outer needle. Each needle is fed by two different syringe pumps with different composition solutions and connected at one high-voltage power supply in the coaxial orifice, when both polymeric solution travel, the outer (shell) solution entraps the inner (core) solution [14,68]. This process produces fibers with core-shell structure and enhanced properties; namely, diverse and incompatible polymers can be combined in the same fiber, unstable active compounds (*e.g.,* enzymes or growth factors) can be incorporated, protection from

USC UNIVERSIDADE DE SANTIAGO

external environment agents(*e.g.,* light, oxygen and other free radicals, temperature and humidity) can be improved, hollow fibers can be generated by removing the core material using thermal or chemical processes post-electrospinning, and the mechanical properties and release of simultaneous drugs can be finely tuned [10,14,68,69]. Nevertheless, core-shell fiber formation is a complex process owing to disbalances in the rheological, chemical, and physical properties of both solutions and the complexity for maintaining a stable Taylor cone. The optimal shell solution should be more viscosity and conductive than the core solution to overcome the interfacial tension of the two solutions and minimize structural discontinuities induced by core elongation. Thus, solvents with low vapor pressure but not too rapid evaporation are preferable [70]. Moreover, adjusting the parameters process is hard due to the different flow rates for each solution; the flow rate has to be higher in shell than in the core. The shell flow rate must has a good balance since a low rate disrupts the fiber and a high rate provokes fragmented sheath fibers [14]. Besides, certain compatibility between polymers is needed to avoid phase separation. Finally, this technique is more expensive, and the cleaning is more difficult when clogging appears. Overall, it demands more time in comparison with uniaxial electrospinning.

#### 1.1.4.3 Triaxial and multi-axial electrospinning

Triaxial electrospinning relies on a concept similar to coaxial electrospinning, adding an extra needle for obtaining three concentrically aligned needles; the inner, the intermediate and the outer needle. Therefore, three syringe pumps, one high-voltage power supply and single collector are needed. This concept was developed in 2009 triggering the implementation of more extra needles at the concentric system resulting in multi-axial electrospinning (more than three needles) [71]. Thereby, triaxial electrospinning has comparable advantages and disadvantages to coaxial electrospinning. Thus, this technique is useful for unable electrospinnable materials or sensitive active compounds, to enhance mechanical properties of deficient materials, to prepare more complex and multitask electrospun mat using the same process and saving money and time, to provide an extra protection or loading greater amounts of active compounds in the same matrix fiber, to obtein more complex or multi drug release profiles (*e.g.,* combining zero order, first order, Higuchi or Korsmeyer-Peppas kinetics profiles), or to combine different release mechanisms (*e.g.,* combinations of Fick diffusion with erosion, swelling or stimuli responsiveness) [72,73]. Nonetheless, triaxial electrospinning displays

USC DE COMPOSTELA

difficulties for its implementation owing to amplification of the coaxial problems related to the need of synchronization of the three different flow rates to obtain stable Taylor cone and avoid the undesirable elongation or separation, the need of using compatible polymers with similarly physicochemical properties, and of design a quality spinneret, respecting intraneedle spacing and inner diameter for an optimal distribution of each matrix [14,74].

#### 1.1.4.4 Janus electrospinning

Herein, two phases with their interfaces are closely attached, similar to coaxial electrospinning, but sharing both matrix the same external environment due to spatial position in left-right structure [75]. Usually, Janus fibers are composed by two uniaxial fibers with monolithic matrix, however, some authors report more than two fibers or fusion of different techniques, for instance, electrospraying. Thus, different strategies were explored to develop different Janus fiber type, namely side-by-side, conjugate electrospinning and electrospinning combined with electrospraying [75]. Some critical aspects are compatibility of solution (*i.e.*, prevent discontinuation owing to a blocked spinneret) and the furcation due to Taylor cone, straight jet and bending region. This technique offers some unique advantages, including particular morphology (*i.e.*, helical structure), good tensile properties, combination of contrasting properties in each face of the Janus, and thus novel medical applications could be envisioned [75].

Side-by-side electrospinning is the most traditional Janus electrospinning, using an uniaxial electrospinning concept by stratified solutions that are pumped at the same time through a single needle. Side-by-side technique is composed of typical electrospinning setup, namely pumps, high voltage supply, collector, and modified needles as Janus spinneret that includes two parallel metal capillaries [76]. To obtain optimal side-by side fibers, low voltage should be applied to increase adhesive forces of solution and prevent the solution furcates since high voltage increases electrostatic repulsion between the solutions for surpassing the adhesive forces [77]. Another critical variable is the angle set between needles, which modifies the width and the interface area. As a general rule, when the angle between needles decreases, the width increases, and the interface area decreases [78]. Additionally, the flow rate could change the morphology, inner structure, and interface area [79]. For Janus fibers, interface area modification is an unique aspect of this technique. Also, the optimal flow rate for each polymeric solution is difficult to set

USC UNIVERSIDADE DE SANTIAGO

since using the same flow rate for both solutions could cause a different width of each region, affecting the overall diameter and properties of the fibers [79].

Some strategies to improve the Janus process include the use of a parallel spinneret with supererogatory metal sheet that provides an extra force preventing the fluid separation or the extension of the contact of both solutions before the tip of the needle [80]. Another approach based on Janus fibers is conjugate electrospinning, using polymeric solutions with opposite charges that by electrostatic attraction will form conjugate fibers [81]. Probably, conjugate electrospinning is one of the tough electrospun methods for obtaining Janus fibers owing to the difficulty of combining both jets. Moreover, in this case, a rotative collector is indispensable to avoid the furcation [82].

#### 1.1.4.5 Melt electrospinning

Melt electrospinning is still less used than solution electrospinning or its variations. Nevertheless, melt electrospinning continues to be a fascinating technique since it does not require the preparation of a polymer dispersion as solvents are not needed and the fibers produced by this method can be superior in optical, mechanical, electrical properties and less energy consumption [83]. Avoiding the use of solvents makes this technique more cost effective and environment friendly, especially when class 2 or 3 organic solvents are used, being harmful and very expensive [84]. However, this great advantage is also the greatest limitation, since it is necessary to melt the polymers at high temperatures in a range of 45 °C - 330 °C, which prevents the incorporation of most active biomolecules and thermolabile drugs into the fiber [83].

#### 1.1.4.6 3D electrospinning

Electrospinning is commonly known to produce 2D structures. However, the bidimensional structures have some restrictions in comparation with three-dimensional layout, for instance in deeper wounds where complex and great 3D porous tissue scaffolds are required to enhance cell and factors infiltration (*e.g.*, fibroblast and keratinocytes) for wound healing applications [85]. For many years, several research have focused on multi-layering, template-assisted systems and postprocessing techniques, including freeze-drying, gas foaming or folding to create a 3D structure from the conventional 2D mats [86]. Nowadays, only two electrospun technologies have been developed with the capacity of prepare 3D electrospun mats by instantaneous one-step, being wet and cold-

USC UNIVERSIDADE DE SANTIAGO

plate electrospinning and 3D fibrous self-assembly via electrospinning [14]. Wet and cold-plate electrospinning was developed in two different spatial and time lapses, being wet electrospinning developed in 2009 to fabricate 3D spongiform fibers [87] and later, cold-plate electrospinning approach appeared in 2015 to produce 3D fibrous electrospun mats with large pores using silk fibroin as main structural material [88]. Wet electrospinning is inspired by conventional electrospinning changing the collector for a bath filled with a low surface tension organic solvent (*e.g.,* tertiary-butyl alcohol), attracting and solidifying the formed fibers for produce 3D structures with low bulk density, high porosity, and relative short size [14]. Cold-plate electrospinning is characterized by forming ice crystals on the collector that can be cooled up to -90ºC. The ice crystals formed improve the conductivity and the fiber position in layer-by-layer structure [14]. With the apparition and development of the first 3D printers to prepare three-dimensional layout, some researchers explored the possibility for combine electrospinning and 3D printing for leveraging all the advantages offered by these two fascinating technologies. In 2018 the first 3D fibrous self-assembly via electrospinning using a extrusion 3D printing was achieved by changing the printhead for a typical electrospun needle switched to a high-voltage power supply [89]. These 3D electrospinning approaches are assisted by Computer Aided Design (CAD) software and the deposition fiber are controlled similarly a 3D printing by x-y-z motion control for prepare the 3D electrospun mats. These electrospun mats are influenced by great evaporation of solvents, polarization, and electrostatic induction, using extra electrodes on the collector and including a conductive additive (*e.g.,* $H_3PO_4$) at the ink or electrospun solution [14]. These techniques have significant advantages including, no handling required due to guide by CAD software, direct 3D electrospun mats obtention without subsequent post-manufactured process, avoid of wasting materials, or obtention of microporous electrospun mats for cell migrations. However, these techniques need more development since the structures processing by 3D electrospinning are usually soft and fluffy, for 3D assembly is necessary materials with great conductivity and the precision decreases with the height; cold plate electrospinning requires water-solvent process and post fabrication, and the morphology of the electrospun mat is uncontrollable; wet electrospinning requires coagulation solvents and lack of voltage in the deep of the bath. Currently these techniques are unable for upscaling [14].

USC UNIVERSIDADE DE SANTIAGO DE COMPOSTELA

#### 1.1.4.7 Portable electrospinning

Handheld and lightweight electrospinning rely on using a conventional electrospinning to prepare fiber on-site and was initially proposed in 2013 to treat diverse skin wounds [90]. The first prototype was semi-portable since it was switched a cord to power the high-voltage power supply, minimizing the accessibility and portability outside a building. The second model fixed this main limitation by integrating a relative tiny and lightweight battery as power supply, being the first truly portable electrospun system [91]. Then, new applications and models had arisen until the commercialization of Spincare® by an Israeli company [14]. The portable electrospinning is suitable for producing a painless wound dressing directly in the injury site and can offer a variety of advantages in wound management such as enhanced homeostasis, wound protection against several microbial colonization, promoted tissue regeneration, immediately alleviation of pain, or application of unstable substances that suffer degradation by prolonged storage periods. It is claimed to be useful in emergency situations (*e.g.,* medical, fire, military, and rescue services), and economically and environmental friendly [14,92]. However, this is a new technology have some challenges for its application in healthcare systems in terms of regulations, patient compliance, safety, fibers stability (lack of opposite potential charge), low voltages (maximum 10 kV), polymers, additives and solvents (avoiding most organic solvents of class II and III), and difficulties for ensuring reproducibility and quality [14].

### 1.1.5 Types of matrices

#### 1.1.5.1 Monolithic or monophasic matrix

The most common method for incorporation of drugs in electrospun mats consists in dissolving or dispersing the active component in the same solvent as the polymer. During the electrospinning process, the active component is encapsulated into the polymeric matrix of the fibers. This method has some advantages such as easy production and high loading efficiency [93]. However, an effective encapsulation requires that the drug and the polymer have certain chemically compatibility or at least are miscible. Thus, hydrophilic active compounds are usually combined with hydrophilic polymers, and vice versa, hydrophobic active compounds are added to hydrophobic polymers solutions. If the active compounds are partial soluble in the mixture, burst release is quite likely to occur due to the low interaction with polymeric chains [94].

UCC UNIVERSIDADE

#### 1.1.5.2 Biphasic matrix

##### *1.1.5.2.1 Blended matrix*

Blended matrices offer the chance to make use of the advantages offered by different types of polymers or alleviate some disadvantage of the main polymer. The mixture of different types of biomaterials from different origins (*e.g.,* polymers, cyclodextrins, metals, ceramics, glass) confers new biological activities or advantages to the electrospun mat and mitigates or eliminates the possible disadvantages of using a single polymer [95]. Blending can improve the mechanical properties and wetting and biodegradation requirements, reduce the toxicity, and allow the use of bioactive compounds with low compatibility with one of the polymers. Both random distribution and ordered distribution of the components in the blend fibers have been reported. Random distribution involves mixing two or more compatible polymers and solvents at the same vial and requires basic setup (*e.g.,* one syringe, one pump and one needle). Thereby, the procedure is simple, fast and cost-effective but demands good compatibility between polymers and good miscibility between solvents to obtain optimal dispersion before and during electrospinning [95]. Despite of this disadvantage, some authors report on the use of a variety of polymers and solvents, including mixtures of synthetic polymers with natural polymers, cyclodextrins with polymers, metals with polymers, ceramics with polymers, glass with polymers, etc. Moreover, mixing of drugs with different properties and different hydrophilicities is possible to perform [96]. To overcome incompatibility problems, different techniques suffer modifications to produce ordered distribution of the components in the matrix, resulting in core-shell-, Janus-, and emulsion matrices. These types of matrices allow combining incompatible polymers or bioactive compounds and obtaining release kinetics to fit to specific therapeutic demands [95].

##### *1.1.5.2.2 Emulsion matrix*

This type of fibers is prepared using two immiscible solvents with different hydrophobicity polymers and commonly adding surfactants at the solution before of mixing, applying a great energy for emulsion droplets formation [97]. When a voltage is applied, emulsion droplets become stretched into an elliptical shape whilst the continuous phase solvent is evaporated, increasing the viscosity and observing droplet enrichment in the axial region for obtaining the core matrix of the fiber and pushing the other polymer towards the surface to form the shell matrix [98]. Most emulsion matrices are prepared

from O/W emulsions using an uniaxial electrospinning setup and resulting in a core-shell matrix formation. This matrix type can provide sustained release profiles during weak or months, even surpassing the fibers prepared with coaxial electrospinning [99].

*1.1.5.2.3 Core-shell matrix*

A core-shell matrix consists in two different regions: the inner layer called core, and the outer layer called shell. Commonly, the hydrophilic layer or the layer with less adequate mechanical properties is positioned in the inner section (core), while the hydrophobic layer or that providing adequate mechanical properties is in the outer section (shell). This is only a general rule and combination of the same hydrophilic or hydrophobic components in both layers with different properties (*e.g.,* different biocompatibilities, different type of drug release such as diffusion or erosion or different properties) has been reported [100].

Two large families of core-shell matrices can be distinguished attending to the application or proposal; namely, reservoir core-shell matrix and multi-matrix core-shell [95]. Reservoir core-shell matrices are usually used for hydrophilic active compounds that require controlled release; loading the drug into the inner in a hydrophilic matrix and coating with a hydrophobic matrix barrier for obtaining sustained release [101]. If the application of the electrospun mat requires the release of more than one active compound, preparation of a multi-matrix core shell matrix may be required. As a general rule, hydrophilic active compounds are placed in the core and hydrophobic compounds are in the shell, but it is possible prepare multi- matrix core shell with hydrophilic material in the shell and hydrophobic materials in the core [102]. Such a variety of combinations has been explored to facilitate the attachment of cells or other biologic compounds increasing the biocompatibility and reducing the side effects (*e.g.,* natural polymer as gelatine in the shell and synthetic polymer as PCL for the sustained release). Moreover, matrices with both layers of the same hydrophilic compounds or hydrophobic compounds can be obtained, leading to two different release patterns, which may even combine sustained release (for prolonged effects) with burst release (for fast start of therapeutic action) [103]. For instance, when a cut occurs, fast effect is necessary to stop bleeding, reduce cute pain and eradicate external agents, namely bacterial, virus and parasites that could colonize the affected area, while prolonged effect is required for damage repair of the wound or chronic pain. Furthermore, other disease that could require this type of

USC UNIVERSIDADE DE SANTIAGO

electrospun mats are heart stroke (fast effect to treat cute pain or vasodilator and prolonged effect to repair the damage zone due to cardiac cells death and chronic pain) or cancer disease (fast effect to kill cancer cells that were impossible to remove after resection surgery and prolonged effect to apply adjuvant chemotherapy).

#### 1.1.5.3 Combination of different matrix types

Bilayer or Janus systems and sandwich systems consist in a mixture of different components, including polymers, ceramics, metals and glasses. They offer some advantages such as multiple release profiles, improved biocompatibility, combination of incompatible materials, and processability under different techniques (*i.e.*, electrospinning with 3D printing, superfluid technology with electrospinning) [95].

Bilayer systems are the combination of two different materials being randomly or orderly oriented. If the system clearly differentiates two layers, this type or system follows ordered orientation. On the other hand, if it is impossible to differentiate or separate the components, these systems are considered randomly oriented [104]. This random distribution has some advantages in terms of simplicity and fastness but requires two needles and two pumps or extruders working at same time and thus could be an equipment limitation. Another limitation refers to the percentage of each component in the final mat. To get a 50% of each layer, the same flow rates are necessary and sometimes this is impossible to achieve owing to the different rheological and characteristics of both polymeric dispersions. To overcomes these limitations, side by side or Janus matrix could be an interesting approach as it requires one needle and pump, but there is the risk of layers separation owing to incompatibility of the components (*i.e.*, charge repulsion, different rheological properties and weak bounding between materials). These disadvantages could be overcome using additives that work as a glue (*e.g.*, surfactants, cross-linkers that are activated with temperature changes or UV radiation), preparation of an intermediate layer with adhesive properties (*e.g.,* PVP, PVA) or applying other techniques such as sintering (*e.g.,* supercritical fluids, laser) in absence of modification of composition, or morphology of both layers [105,106].

### 1.1.6 Modifications post-manufacture

USC UNIVERSIDADE DE SANTIAGO

Electrospinning and its approaches have some limitations that make it difficult the incorporation of different types of active compounds such as thermolabile drugs, light

sensitive drugs, proteins derivates (enzymes, fractions of ribonucleic acid (RNA) and deoxyribonucleic acid (DNA)), different type of cells (immune cells, regenerative cells) and brittle polymers (collagen, hyaluronic acid). Thus, post-electrospinning modifications are sometimes required to adapt the obtained fibers to specific applications.

Every material can be susceptible to some types of modification at a molecular or macroscopic level [93]. Usually, the fibers show remarkable absorption properties through physical or chemical interactions with a variety of substances without the need for any additional post-processing. However, for a specifical grafting or to increase the amount of active compound loaded, post-processing may be needed. One of the most used method is the grafting of ligands such as amine groups at polymers structure (*e.g.,* adding 1-6-diaminohexane to PCL, using PEG diamine or polydopamine) to obtain a covalent conjugation [107–111]. Grafting of carboxylic groups has been explored to incorporate several metal ions (*e.g.,* Ag, Cu or Au) and immobilization of polypeptides allows attracting several active compounds [112]. Post-spinning surface immobilization has a variety of advantages, nevertheless this approach is limited by the number of chemical reactions and the stability of the fibers during the post-processing [107].

## 1.2. Biomedical applications of electrospun mats

### 1.2.1 Drug delivery

Electrospun mats can be designed to finely tune the bioactive release profile for assuring a desire effect therapeutic effect depending on the characteristics of the disease/damage and patient needs. Using different preparation protocols, type of polymers or additives ca variety of kinetics can be obtained. Some considerations have to be taken into account for the rational design of the electrospun mat such as application site, type of drug administration intended (systemic or local), timing, amount of drug required for therapeutic target, and toxicity [95]. Before implanting or placing the electrospun mat it is necessary to know the characteristics and localization of the damage or the therapeutic action of the drug. For instance, its necessary know the type of tissue to which the electrospun material will enter into contact with soft mucosa, fatty tissue or hard (bond or muscle), the depth and shape of the wound, the environment of the organ (pH, enzyme) and accessibility (contact with blood, immune system, other types of fluids such as cerebrospinal, interstitial or exudates). Furthermore, depending on type and route of administration the drug release kinetics may be different. Thus, appropriate

USC UNIVERSIDADE DE SANTIAGO DE COMPOSTELA

combination of polymer solution (solvents, polymers), process parameters (depending on the technique) and environmental conditions (temperature, humidity and pressure) [95] has to be considered for a suitable release profile. Burst drug release, sustained drug release, biphasic drug release and stimulus-activated drug release are illustrated in **Figure 1.7** and tackled below [95].

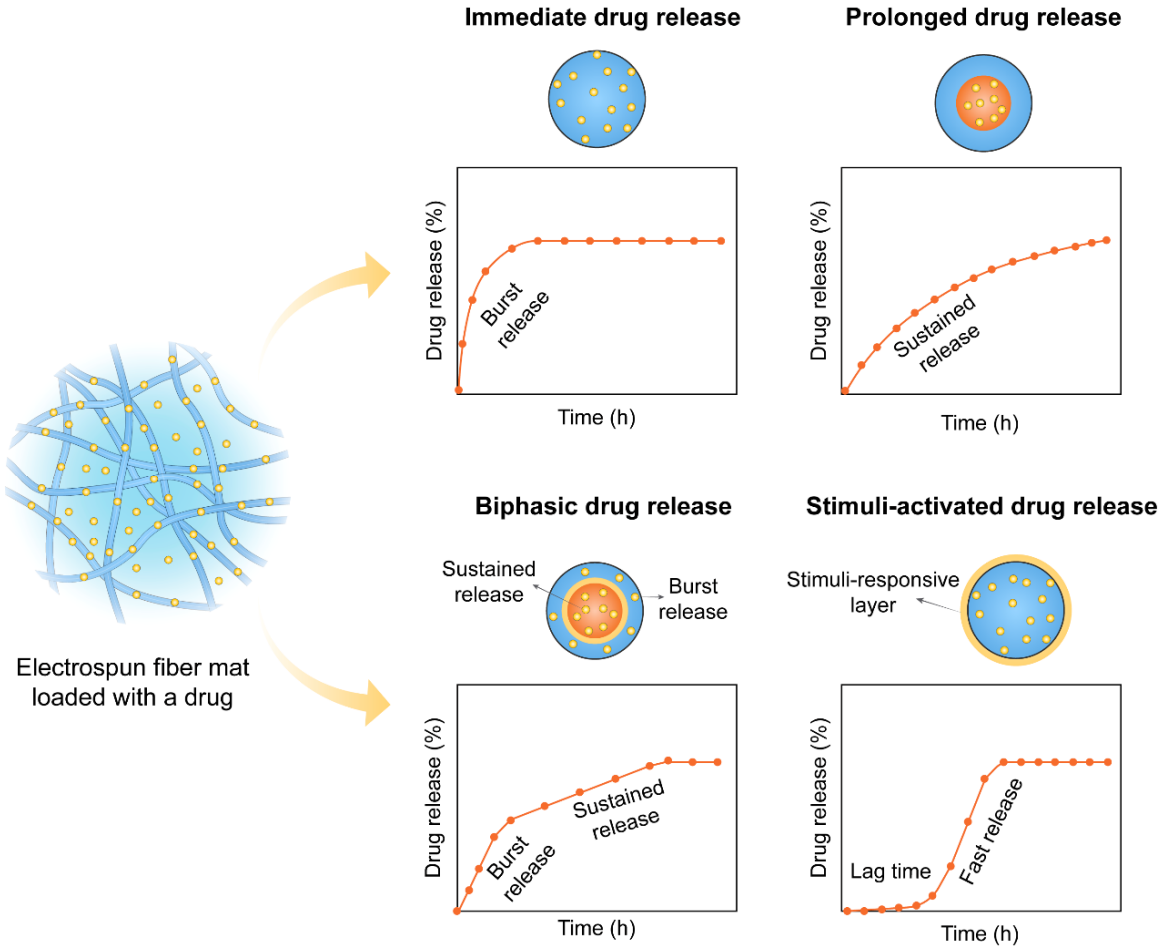



**Figure 1.7. Classification of nanofibers based on their drug-release profiles. The Figure was made by the author of the Thesis.**

1.2.1.1 Burst release profile

Electrospun mats that release the most amount of the active compound in the release medium in the first hours are classified as burst or fast release systems. This type of release profile consists of an immediate diffusion of all drug owing to a high permeability, wettability, solubility or erosion of the polymer by the release medium. Thus, the electrospun mat needs to have some properties such as high porosity, high surface-to-volume ratio, incorporate highly degradable or swellable polymers with weak affinity for the drug, and load the drug as amorphous dispersion [95]. Fibers with burst release profile

USC DE SANTIAGO DE COMPOSTELA

are being considered as an alternative to freeze-dried powders to obtain fast dissolution for extemporaneous preparation of injectables and as fast release oral/buccal formulations [113]. Compared to classical solid oral dosage forms (tablets and capsules), burst release fibers may allow reaching therapeutic effects in less minutes due to significantly faster and higher plasma drug concentration-time curve (AUC) [114].

#### 1.2.1.2 Controlled release profile

Electrospun mats able to regulate the release profile for prolonged time periods allow multiple drug administration for non-invasive (*i.e.*, oral, transdermal) or invasive (subcutaneous, intravenous) routes. Controlled release profile offers some advantages that improve the quality of patient treatment, for instance, reduce administration frequency leading to an improved patient compliance, avoid failed on the therapeutic response because of reduction of human/patient failures (*i.e.*, forget or repetition of the administration), fewer visits to the hospital or avoid the intervention of qualified professionals (*i.e.*, administration of drugs that need constant supervision, or special or difficult administration rotes, such as intravitreal administration). Even, it is possible to avoid secondary disease due to side effects of the treatment, for instance inflammation, traumas, or infections [101]. Also, implantation of drug-loaded fibers into the resection cavity after surgery allows very localized treatment of the disease where it is needed, increasing therapeutic efficacy and reducing the number of interventions to the patient. Several strategies are being investigated to endow electrospun mats with sustained release capabilities, such as blends of different compatible polymer in a single matrix, the use of hydrophobic polymers with slow erosion via enzymatic or chemical degradation, the incorporation of drugs in crystalline form (more stable and with slower dissolution rate), the design of complex matrices (*e.g.,* core-shell, Janus) [95,115–117]. Usually, controlled release profiles are fitted to first orden and Higuchi mathematical models [118].

#### 1.2.1.3 Biphasic drug release

There are matrix electrospun mats that combine burst and controlled release. This release type is useful for obtaining a fast effect for an initial control of the disease at first hours, following sustained release to prolong the drug effects to restore the damage or control the effects of the disease for weeks or months. Biphasic drug release is common in polymeric matrix or materials that load the majority of active compounds on the surface

USC DE COMPOSTELA

(*e.g.,* ceramic, metal or glass). Some approaches, including core-shell, and Janus (side by side) are designed to obtain this type of release [95].

#### 1.2.1.4 Stimulus-activated drug release

Electrospun mats can be prepared combining different biomaterials (*e.g.,* polymers, metals, ceramics) that react to some stimulus or changes in the environment such as pH [119], temperature [120], light [121], or electrical field [122]. These types of systems are characterized by displaying a lag time where the electrospun mat does not release the active compound until activation [95].

##### *1.2.1.4.1 Thermo-responsive drug release*

Compounds that suffer physicochemical modifications with temperature changes are candidates to endow the electrospun mats with thermo-responsiveness. An increase or decrease in the temperature can cause a change in the hydrophobicity of the polymer; *e.g.,* poly(N-isopropylacrylamide) (PNIPAAm) undergoes a transition from hydrophilic to hydrophobic when the temperature rises above 32ºC [120]. Under health conditions our body regulates the temperature in a range of 36-37ºC to maintain and produce the optimal biological reactions that are essential for life. Sometimes and in a short period of time, this range of value could be affected with an increase or decrease of the temperature due to external factors such as bacterial or viral infections. Small increments in temperature facilitate several body defenses to improve their activity, while weakens the external factors, decreasing their activity and possible damage. In recent years, several electrospun mats try to mimic this event, increasing the temperature to kill bacteria or virus and also cancer cells by applying external stimulus that modify or excite several compounds into the electrospun mat (*e.g.,* organometallic compounds or polymers) [123]. Depending on the external stimulus, therapies such as photothermal- (laser and other light types are the source) or magnetic- (excitation by waves at different) treatments can be implemented [121].

##### *1.2.1.4.2 pH-responsive drug release*

In our body there exist different areas with different values of pH. These pH values changes depend on the administration via, being the oral administration showing the most abrupt changes, including neutral-basic pH (7.4) in the mouth-pharyngeal tract, follow to super acidic environment of stomach with pH (2) and finishing with basic pH (7-8) in gut

USC DE COMPOSTELA

and colon [124]. Interestingly, the standardized pH body is 7.4 (*e.g.,* in blood and other media) whereas different organs present different local pH such as eyes, brain, or vagina. Moreover, different diseases modify the pH, namely bacterial wound infections, burns, inflammatory processes and cancer leading. These changes are taken into account for the design of electrospun mats that only release the drug when the disease starts to develop [95].

*1.2.1.4.3 Electro-responsive drug release*

Different materials (polymers, ceramics, glasses) are sensitive to electric fields that can be used to trigger drug release. This type of release method is commonly used for transdermal delivery systems and allows for precise control of the amount released, reversible and absence of pain, and high drug penetration on deep tissues [125].

### 1.2.2. Bacterial infections: A global threat

Until the 20$^{th}$ century, the humanity only benefited from the immune system response, naturally-occurring compounds (*e.g.,* herbal medicines have been therapeutically used for more than 5000 years), and metal salts (*e.g.,* gold, silver, arsenic, mercury) as available resources to combat infectious diseases [126]. The discovery of penicillin by Alexander Fleming in 1928 changed the course of medicine in treating bacterial infections with antibiotics [127]. This important milestone led to the Golden Era, where the main classes of broad-spectrum antibiotics were discovered in a fairly short period of time (*e.g.,* tetracycline, chloramphenicol, and streptomycin) [128]. Nevertheless, this was a short-lived groundbreaking phase, since the knowledge on mechanisms of action of antibiotics began to accumulate, the evolution of antibiotic-resistant bacteria occurred, and the emergence of antimicrobial resistance (AMR) became a reality and a global crisis [129,130]. This is a problem that has not only been confined to bacteria, but also to all pathogens that have the potential to render the currently available antimicrobial drugs ineffective.

Nowadays, infectious diseases remain an ominous public health concern, contributing substantially to global mortality trends and imposing a significant burden on healthcare systems worldwide. This concerning scenario has been prompted by several factors, including pathogen outbreaks, pandemics, slow and inaccurate detection of infections,

USC UNIVERSIDADE DE SANTIAGO DE COMPOSTELA

misuse or overuse of antimicrobial drugs, limited pipeline of new antimicrobial drugs, and expanding AMR.

#### 1.2.2.1 The Antimicrobial resistance crisis

Until 2014, drug resistant infections were responsible for at least 700,000 deaths per year worldwide [131]. In a short period of time this number increased, with 1.7 million of deaths directly caused by AMR in 2019 [132]. This alarming scenario encouraged World Health Organization (WHO) included AMR among top 10 public health threats facing humanity [133,134], since the increase in incidence of drug-resistant infections may pose a global health crisis with the number of deaths (*ca.,* 10 million deaths) exceeding those due to cancer by 2050 [135,136].

Antimicrobial drugs consist of therapeutic agents that are active against a range of infections caused by different microorganisms, namely bacteria (antibiotics), viruses (antivirals), fungi (antifungals), and parasites (antiparasitic agents). When microorganisms no longer respond to antimicrobial drugs, these therapies become ineffective, the infection persists, and the so-called AMR arises. Consequently, AMR limits the current therapeutic options, intensifies the risk of clinical complications, increases hospital admissions, requires more costly therapies, and ultimately raises mortality rates.

Over the years, several definitions have emerged to categorize AMR: (i) multidrug resistant (MDR), to describe microorganisms resistant to at least one agent in three or more different antimicrobial categories; (ii) extensively drug resistant (XDR), microorganisms resistant to all antimicrobial agents except one or two categories; and (iii) pan-drug resistant (PDR), microorganisms resistant to all agents in all antimicrobial categories. In addition, the term difficult-to-treat resistance (DTR) has been used to define Gram-negative bacteria that are resistant to first-line antibiotics. This type of infections are characterized by a high mortality and the only available treatments are less effective or highly toxic (also known as “Reserve” antibiotics) [137].

#### 1.2.2.2 Understanding the mechanisms and drivers of antimicrobial resistance

AMR is a major global health challenge caused by a plethora of important driving factors, namely mechanisms of bacterial resistance, loss of efficacy of antibiotics, poor antibiotics pipeline, overuse and misuse of antibiotics, inappropriate prescription or self-

USC DE SANTIAGO DE COMPOSTELA

medication, poor hygiene practice and lack of safe water or sanitation, climate change, agriculture practices, among others [138,139]. There are several molecular mechanisms of bacterial resistance to antibiotics, namely (i) enzymatic degradation of the antibiotics, (ii) enzymatic modification of antibiotic targets, (iii) protection, modification or bypass of antibiotic targets, and (iv) decreased influx or active efflux of antibiotics mediated by membrane efflux pumps, which individually or collectively reduce cellular concentrations of antibiotics required to inhibit the bacterial growth and ultimately kill them **(Figure 1.8.)** [140].

Bacteria can be intrinsically resistant to antibiotics but can also acquire or adapt their resistance to these therapeutic agents by chromosomal mutations and/or horizontal gene transfer. Therefore, all the aforementioned mechanisms of bacterial resistance can be categorized in three main groups: intrinsic resistance, acquired resistance and adaptative resistance [141]. Intrinsic resistance is an innate ability present in all species, independently of antibiotic exposure since a particular species could have an unavailability or absence of target for different antibiotics [142]. Acquired resistance is a gene or chromosomal mutation addition by horizontal information transferences between bacteria such as plasmids, integrins, transposons, and genomic islands [143]. Bacteria have three main methods to acquire gene resistance, namely transduction (resistant gene acquisition from the environment), bacterial conjugation (resistant gene transformation between resistant bacterial strains) and transduction (resistant gene from bacteriophage) [144]. Adaptative resistances are gene expression alterations due to environmental changes or exposition to non-lethal selective pressure (*e.g.,* temperature, growth state, pH, nutrient conditions, and infra inhibitory levels of antibiotic concentration) and there are passed down through several generations [145,146].

USC
UNIVERSIDADE DE SANTIAGO DE COMPOSTELA

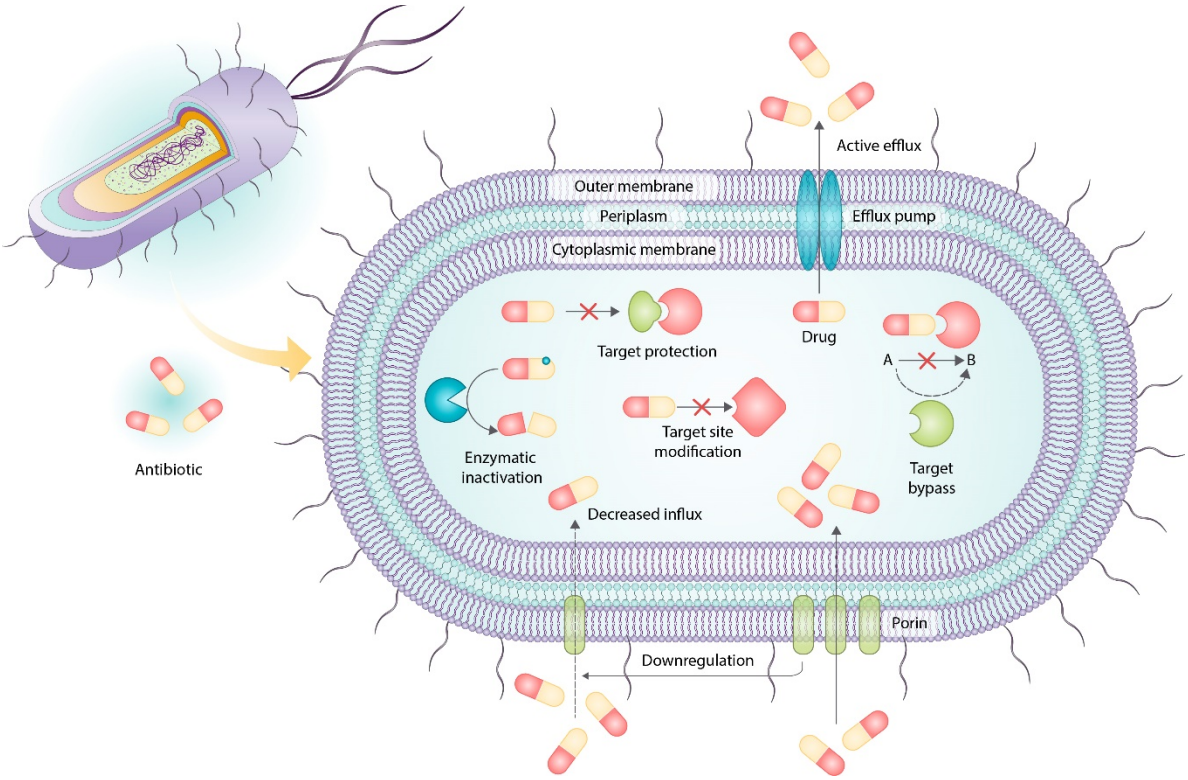



**Figure 1.8. Overview of the molecular mechanisms involved in antibiotic resistance emergence.**

**The figure was made by the autor of the Thesis.**

Bacteria has the capability to limit intracellular drug accumulation by two different mechanisms, developing porins mutations and efflux pumps. Porins are proteins channels present in Gram-negative bacteria membrane allowing the entry of several molecules, including antibiotics. A reduction of this protein channels expression results in less antibiotic incorporation into the bacteria contributing to AMR [141]. Efflux pumps maintain the correct and optimal internal bacterial environment removing toxic substances and other antimicrobial components and the overexpression plays an important role in AMR due to the removal of antimicrobial agents from the cytoplasm and easy horizontal information transfer of efflux pump encoded by plasmid or bacterial chromosome [141,147]. There exist 5 major efflux pumps families in bacteria: ATP binding cassettes (ABC), small multidrug resistance (SMR), major facilitator superfamily (MFS), multidrug and toxic compound extrusion (MATE), and resistance nodulation division (RND) [147]. In this group MFS encoded by Gram-positive and Gram-negative bacteria are the most common efflux pumps, and RND are exclusively encoded by Gram-negative bacteria. These two types are the main contributors to resistance against different antibiotics families (*e.g.,* penicillins, macrolides, fluoroquinolones, tetracyclines and others) [148].

USC DE COMPOSTELA

The ability of bacteria to transform and change the structure of antibiotics and their own susceptibility plays an important role in antibiotic resistance. Enzymes are involved in large bacterial process, namely disorganization of the cytoplasmic membrane, metabolites, protein synthesis, nucleic acids and bacteria cell wall biosynthesis [149]. It is well known the activity of penicillin-binding proteins synthesizing the main component of bacterial wall peptidoglycan, being the target of β-lactam antibiotics. Different mutations in this type of enzymes develop resistances to these antibiotics [150]. Tetrameric enzymes like Topoisomerase IV and DNA gyrase catalyze spatial DNA configuration in transcription, replication and cell division, being target of quinolones. If these enzymes suffer mutations or their production is decreased quinolones loss their activity [151]. The modification of the structure of antibiotics are provided by three enzymatic categories: oxidoreductases, hydrolases and transferases using two commonly pathways for this proposal, adding a chemical group and degrading the drug. β-Lactamases belong to drug-hydrolyzing enzymes, enabling a several range of antibiotics with β-lactam ring in their structure (*e.g.,* imipenem, amoxicillin, ceftazidime, and penicillin) [152]. Furthermore, the bacteria could modify the antibiotics target, for instance, using methylation. Aminoglycosides bind to ribosomal ARN and this agent loss its activity when several bacterial enzymes methylated the ribosomal ARN for avoid the bind [152].

Bacteria live in communities, commonly described as biofilm. These authentic communities consist in a single or mixture of several microbial species living together surrounded by a polymeric matrix, in which microbial population is embedded [153]. This polymeric matrix envelope represents the 90% of the biofilm, being only 10% of bacteria population [154]. Moreover, in Gram-negative bacteria this polymeric matrix envelope is formed from lipopolysaccharides (LPS) [141]. Biofilms are not static communities, but participate in a cyclical process with four identified steps: adhesion, growth, maturation, and detachment [155]. Biofilms make bacteria 1000-fold less susceptibility at antibiotics compared to single (planktonic) bacteria due to the protective effect of the polymer matrix, which prevents the antibiotic penetration and facilitates efficient horizontal genetic information transfer by plasmid or other mobile genetic compound [156,157]. In biofilms exit a group of bacteria described as “ESKAPE” that easily and rapidly suffer the aforementioned resistance mechanisms, and which are a health concern. This group is formed by *Enterococcus faecium, Staphylococcus aureus,*

USC UNIVERSIDADE DE SANTIAGO

*Klebsiella pneumoniae, Acinetobacter baumannii, Pseudomonas aeruginosa* and *Enterobacter spp* including their resistant subspecies. They are called as "superbugs" [139,158].

The extensive use of antibiotics created a selective pressure since antibiotics are commonly used to treat hospital-acquired infections, sepsis, diarrhea, sexually transmitted infections, and urinary tract infections [128]. The last century supposes major sociodemographic and environmental changes that disrupted the equilibrium between humans and bacteria. The population growth supposed a massive exodus to the cities, increasing the population density in healthcare centers, allowing the rapidly dissemination of resistant bacteria into the community [159]. The misuse of antibiotics in health care systems is related to unnecessary prescriptions due to incorrect assessment and diagnosis methods or outdated medical guidelines [160,161]. Furthermore, the increase in population every year facilitated the introduction of intensive agriculture, provoking the antibiotic overuse in this field [128]. The control of weeds and pests in plants and livestock increased the use of antibiotics and pesticides to promote rapid growth, better yield and prevent infections. These practices increase the risk of the apparition of resistant genes in animals, and zoonotic diseases could be transferred to humans by directly food exposure [127]. Moreover, the globalization has allowed an increase in number and speed of the journeys with reduction in travelling expenses, trade and commercial transportations, and easy population migration, enabling fast dissemination of bacterial resistance [159]. The industrialization era improves the life of people but triggered huge environmental changes such as deforestation, melting ice, increase greenhouse gases, loss of flora and fauna, and increase sea levels and global temperatures, leading to the emergence of new infections and resistances. In addition, poor governance promotes a lack of health resources (*i.e.*, inadequate infrastructure, insufficient trained personnel, and lack of medical protocols or diagnostic tools) and sanitation practices that contaminate water systems and spread antibiotics and their resistance in wastewater. These factors combined lead to inappropriate use of antibiotics and indirectly and directly affect antibiotic consumption. [128,162,163].

#### 1.2.2.3 Consequences of antimicrobial resistance in a global health context

USC UNIVERSIDADE DE SANTIAGO

One of the immediate benefits that antibiotics have provided was higher survival rates of preterm babies, children affected by infectious diseases, patients with cancer,

immunosuppressive therapy or autoimmune disease (*e.g.,* transplant therapies, human immunodeficiency viruses (HIV) patients), chronic diseases (*e.g.,* renal insufficient, diabetes), and people that requires large surgeries [159]. Thus, antibiotics are behind the increase in life expectancy, and conversely, AMR can notably compromise the achievements conquered in the last century. Currently, 70% of pathogenic bacteria have developed resistance against commercially available antibiotics [164]. AMR prolongs the time of sickness, increasing the hospital stays, requiring more costly therapies and raises fatality rates [139]. When first-line antimicrobial therapy fails, second- and third-line therapies have to be implemented using more toxic compounds, and higher doses for more prolonged treatment time, which increases the costs [165]. AMR is already increasing the risks associated to organ transplants, surgery and chemotherapy [128].

AMR is not only associated with deaths and healthcare problems, but also with economic efforts [131]. AMR has an important impact in global economic with directly and indirectly consequences. In Europe, bacterial resistance involves an expenditure of €900 million and extra hospital cost were estimated in €595 million, making a total expenditure of €1,5 billion annually by 2050 [166]. Different economists predicted that United States of America (USA) will loss $20 billion (0.11% of Gross Domestic Product (GDP)) and China will losses $42 billion (0.37% of GDP) in terms of global production, resulting in a global economic burden of $100 trillion (>5% GDP) by 2050 [167,168]. Thereby, several organizations estimate that 24 million of people will be pushed into extremely poverty in 2030 due to the bacterial resistance [168]. Currently, the cost for patient in USA associated to drug-resistant infections are approximately $18,588-$29,069 per patient, and the organization for Economic Co-operation and Development (OCDE) published an additional cost of $10,000-$40,000 per patient infected with antibiotic resistant bacteria [148]. Indirect consequences are related to lower productivity due to premature deaths and loss of work hours during the extended hospitalizations [163].

The loss of therapeutic arsenal is one of the major problems that explain the increasing death rates and possible dramatic future associated to infections. The lack of new antibiotics is in part due to the low interest and investment by different governments and private sectors in new antibiotics while the available ones were still effective. During the past decades the pharmaceutical companies were focused on development of treatments with higher commercial returns whilst antibiotics research suffered continuous divestments [131]. Moreover, the big families of antibiotics and their modification

USC DE SANTIAGO DE COMPOSTELA

reached a limit, and the innovation was more difficult. Thereby, the perfect storm appears, increasing the resistances and decreasing the therapeutical arsenal [139]. In 2021, WHO published a list for priority infections with 32 antibiotics in clinical development and only 6 were innovative [133]. The increase in clinical trial cost, the difficulty for discovering new antimicrobial agents using traditional methods, and the uncertainty in new regulatory approval requirements and economic returns could be behind the currently poor arsenal of antibiotics [128]. New niches for finding antimicrobial molecules and application of artificial intelligence tools may help reversing the situation [169–173].

#### 1.2.2.4 Wound healing process: Normal vs chronic wounds

##### *1.2.2.4.1 Normal cutaneous wound healing*

Approaches, methods, and management of wound healing process appeared in the first medical manuscripts with date back to 2200 Before Common Era (BCE) and consisted in "three healing gestures": wound washing, plasters preparation and wound covering. Sumerian, Egyptian, or Chinese old civilizations extensively reported different materials for covering or treat wounds (*e.g.,* wine, milk, honey, leaves, resin trees and boiling water) [174]. However, humans had to wait until 19th century with the introduction of antiseptic technique that it was a real revolution in acute and chronic wound healing management. More recently, modern wound healing is part of tissue engineering concept and steps [175].

Wounds healing is a response of an organism to a physical or chemical disruption of a tissue to re-establish homeostasis and stabilize the normal physiology [176]. This complex process involves four overlapping and coordinated phases: homeostasis, inflammation, proliferation and remodeling [177]. Homeostasis phase occurs immediately after a damage and is mediated by hydrogen peroxide gradient starting cell recruitment, including platelet and fibrin that triggers the coagulation cascade and vasoconstriction process for blood clot formation [178]. When endothelial cells suffer damage, collagen exposition stimulates the activation, adhesion, and aggregation of platelets. In this process several chemotactic growth factors are released, namely epidermal growth factor (EGF), platelet-derived growth factor (PDGF) and transforming growth factor-β (TGF-β); platelet-specific proteins (*e.g.*, platelet factor 4 (PF-4)); fibrinogen, thrombin; anti- and pro- angiogenic factors (*i.e.*, endostatin and vascular endothelial growth factor (VEGF)) and variety cytokines (platelet derived stromal cell

USC DE COMPOSTELA

derived factor-1 (SDF-1 α) and neutrophil activating peptide-2 (NAP-2)) [179]. Thereby, these factors activate and attract several cells such as neutrophils, macrophages, endothelial cells, fibroblast, and smooth muscle. Moreover, fibroin arises from platelet-derived fibrinogen and acts as matrix for incoming fibroblast and macrophages [180,177].

The inflammatory phase starts a few hours after injury, when neutrophils adhere endothelium using collagenase and elastase to facilitate the migration at extracellular space. These neutrophils release several compounds such as matrix metalloproteinases (MMPs), Reactive Oxygen Species (ROS), antimicrobial peptides and several growth factors to develop several functions, namely degrade matrix proteins, phagocytose of bacteria, and attraction of new neutrophils and macrophages [181,182]. Monocytes arrive within 24h and suffer transformation in macrophages M1 (pro-inflammatory) [177]. These macrophages are the most important inflammatory cells, and they degrade wound debris, stimulate granulation tissue formation and angiogenesis, and release growth factors (*i.e.*, nitric oxide (NO), reROS, fibroblast growth factor, interleukin-1, 6 and 8, PDGF, TGF- β, and tumor necrosis factor -α) until 3 to 5 days in acute wounds [183]. For a later stage, macrophages M2 arise from macrophages M1 or monocytes, releasing fibroblast growth factor (FGF), TGF-β1, VEGF, PDGF, insulin growth factor (IGF-1), and IL-10 in order to induce cell migration, proliferation and matrix formation. Finally, lymphocytes are the last inflammatory cells in the process of wound niche attachment [184].

Proliferation phase involved fibroplasia, granulation, epithelization, and angiogenesis at first 24 hours of damage [177]. The main goal is to develop the granulation tissue to restore vascular network, covering the wound surface [185]. TGF- β stimulates keratinocytes, while vascular endothelial growth factors are upregulated by low oxygen tension increasing angiogenesis and stimulating the recruitment of capillary endothelial cells for re-epithelization [183,186]. Other cells that play an important role in this phase are fibroblasts, producing structural proteins (*i.e.*, elastin, collagen, extracellular matrix proteins, and MMPs). MMPs degrade the initial fibrin to facilitate fibroblast access. Collagen type II is secreted between 5- and 7-days post injury, and it is stimulated by TGF-β [187]. Mesenchymal stem cells have immunosuppressive effects by increasing the secretion of indoleamine 2,3-dioxigenase downregulating TNFα and IL-1 and other proinflammatory cells such as T cells, Natural Killer (Nk) cells and B cells.

USC DE SANTIAGO DE COMPOSTELA

Mesenchymal stem cells produce and remodel new extracellular matrix (ECM), differentiate several cell types and increase angiogenesis [188,189].

Finally, the last step is the remodeling that could occur during weeks where the collagen type III changes into a stronger network collagen type I by the reorganization produced by MMPs. This collagen is weaker (20% of tensile strength) after three months in comparison to collagen deposited one year later (80% of tensile strength) [177,180].

*1.2.2.4.2 Chronic wounds (Insufficient healing)*

Chronic wound appears as a result of skin microenvironment disruption and tissue repair mechanism failure due to several factors including bacterial invasion and colonization, absence of immune response, or lack of platelet and fibroblast activity. If the anatomic and functional integrity are not restored after 1 month, it is considered as chronic wound [190]. Chronic wound could appear in different forms such us venous leg ulcers (prevalence of 1-1.5%), diabetic ulcers (approximately 15% of diabetic patients develop diabetic ulcers annually and a range of 14-24% diabetic foot ulcers patients suffer amputation), pressure ulcers (prevalence of 1-5% in hospitalize patients) [177,191].

The correct wound healing depends on multiple systemic or local factors. Systemic factors, namely the severity of the damage (*i.e.*, size, depth, and localization of wound), patient age, chronic diseases (*e.g.*, obesity, cancer, diabetes, hypertension, and endocrine disorders), use of some drugs (*e.g.,* corticosteroids, immunosuppressants, and diuretics), malnutrition, and habits (*e.g.,* tabaco and alcohol consumption) predispose the patient to suffer chronic wounds. Local factors are also relevant: vascular disease (arterial or venous), neuropathy, surgical intervention, chronic inflammation, necrotic tissue, radiation, unfavorable environment (*e.g.,* poor oxygenation and balance between dry or wet, temperature, pH), fibroblast absence, inappropriate treatments (*e.g.,* misuse of antibiotics, debridement fail), fibroblast senescence, critical or impaired levels of cytokines and growth factors, bacterial infection and colonization **(Figure 1.9.)** [192].

Wound healing usually fails in the inflammatory or the proliferative phases. In proliferation phase the failure is associated to the absence of mitogenic capacity of fibroblasts [193]. Moreover, growth factors could be downregulated or overexpressed such as TGF-β type II, improperly functioning, or MMPs are overactive [177]. The environment of a chronic wound consists mainly in keratinocytes and fibroblasts embedded in a ECM composed by collagen, elastin, fibrin, fibronectin, laminin,

glycosaminoglycans, and proteoglycans that provide an optimal space for survival, proliferation and function of different cell for a correct wound repair [194]. Unfortunately, this optimal environment serves for bacteria to grow and develop infections. Bacteria embedded in the ECM readily form a biofilm that protects them against host immune [195].

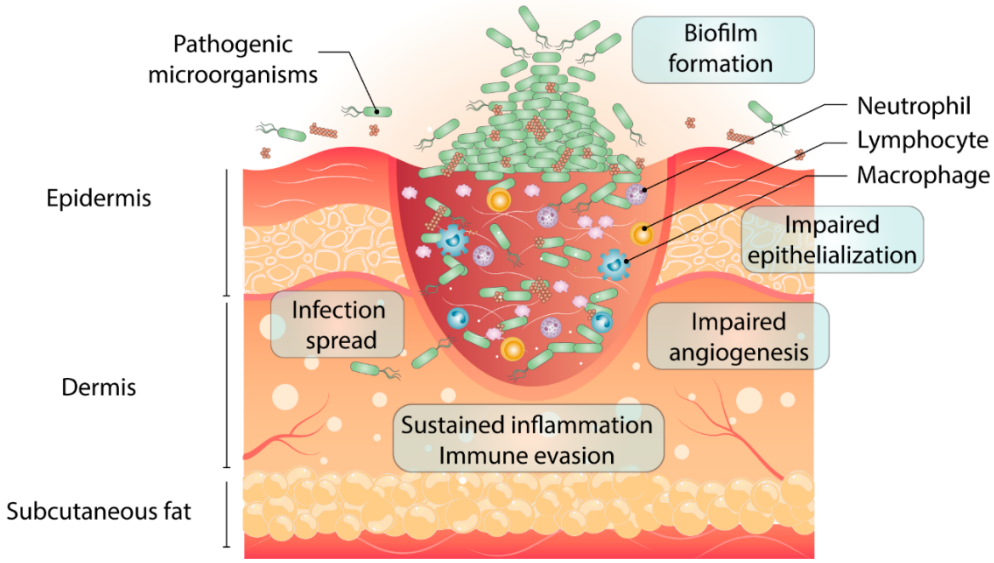



**Figure 1.9. Development of a chronic wound, which often leads to systemic infections or complications. Several factors that contribute to wound chronicity, including hyperproliferative epidermal keratinocytes that fail to migrate, sustained inflammation, immune dysregulation, abnormal protease production, impaired angiogenesis, and fibroblast senescence. The Figure was made by the author of the Thesis.**

Biofilm interacts with immune cells, inflammatory factors, host cellular and matrix elements, mechanical cues, and signaling components [195]. Biofilms are typical in chronic wounds with 60% of prevalence in biopsy specimens, while in acute wounds they represent only a 6% [191]. Moreover, biofilm structure provide some advantages such as self-repair in case of damage, increase metabolic efficiency, and wider substrates accessibility [196]. Overall, bacteria in biofilm have greater immune, chemical, mechanical, and antimicrobial resistance [197]. Moreover, bacteria secrets several microbial components such as toxins, virulence factors (exotoxins and proteases), short-chain fatty acids (SCFAs), and quorum sensing signals, that degrade proteins and affect several host elements between immune and inflammatory cells, namely neutrophils, leukocytes, macrophages, keratinocytes and fibroblast functions that interfere in chemotaxis and release of growth factors (*e.g.,* vascular endothelial growth factors,

USC UNIVERSIDADE

epidermal growth factor or platelet-derived growth factor), cytokines (IL-6,TNFα or CXCL8/IL8 chemokine), MMPs, and cause inflammation or damage [191,198–201]. Neutrophils are the first infiltrate cells in wound site, phagocyting a range of microbes and releasing proteolytic enzymes (*i.e.*, elastase, cathepsin G, and MMPs), plethora of cytokines and antimicrobial peptides [182]. The MMPs overproduction accelerates the ECM components digest and decreases the TIMPS (inhibitors of MMPs), prolongs the inflammatory state and causes the production of abnormal ECM forms (chronic granulation tissue) [202]. Then, monocytes differentiate in macrophages for phagocytosis and release of grow factors (interleukins and TNFα). Finally, keratinocytes induce the production of cytokines, immune cells recruit and antimicrobial peptides [203].

Chemical factors, like oxygen and pH, also play an important role in wound healing. Oxygen is necessary for several biochemical and cellular processes, namely production of reactive oxygen species, inflammatory signaling cascades, ECM remodeling and antimicrobial killing [204]. An optimal balance of oxygen is essential for correct healing since low concentrations or hypoxia impair angiogenesis and allow facultative microbes growth. Differently, high levels of oxygen provoke an excess in ROS species (*i.e.*, hydroxyl radicals, hydrogen peroxide, and superoxide anions) from an oxidative burst release from macrophages and neutrophils, which trigger proteolytic enzymes activation, endothelial injure, and re-epithelialization fail. This cascade leads to a perpetual cycle of damage and chronic inflammation [205,206]. When a skin injury occurs, the pH changes. Comparable to oxygen, pH is involved in several processes, including fibroblast and keratinocyte migration, MMPs activity, angiogenesis and microbial proliferation. Low pH is preferable for a good wound healing process as prevents from undesirable antimicrobial growth and colonization, whilst alkaline pH is involved in non-healing process owing to inadequate oxygenation and feasibility of bacterial colonization and biofilm formation [198,207]. At first stage of wound healing the pH increase as neutral pH facilitates the Gram-positive bacteria colonization, such as coagulase-negative Staphylococci [208].

Mechanical tension, stretching, compression, osmotic forces, and shear stress are biophysical factors that also mediate in wound healing process, changing the biofilms and host and immune cells behavior [209]. Thereby, these forces could exacerbate the progression of the infection by breakup, dispersal, and seeding of new biofilm [210]. Other biomechanical forces, such as vacuum and cyclical stretching, enhance the wound

USC DE SANTIAGO DE COMPOSTELA

healing by increasing proliferation, migration, and signaling of fibroblast and keratinocytes [211].

Infected wounds can be colonized by two or more bacterial species (aerobic and anaerobic), mostly S.*aureus, P. aeruginosa* and the other bacteria belonging to ESKAPE group. These two bacteria together with β-haemolytic streptococci are the primary cause of chronic wound infection [212]. Indeed, a *S.aureus* and *P. aeruginosa* co-infection is the condition with great inflammatory responses, upper antimicrobial resistances and high rate of chronic non-healing states. These bacteria adopt a peculiar wound spatial arrangement, with *S. aureus* located at the surface whilst *P. aeruginosa* is located deeper, producing virulence factors to destroy neutrophils and provoking persistent inflammatory state due to a constant cycle of neutrophil recruitment [195,213].

One of the major problems in chronic wounds is the colonization by bacteria and the subsequent development of biofilm, being an important cause of delayed wound healing and healthcare burden such as hospitalization, amputation, and death. Approximately 40 million of patients worldwide suffer chronic wounds, showing similar numbers in terms of epidemiology and rivaling with the mortality of cancer patients [214]. Only in USA, 2% of population (5.7 million of people) suffer chronic wounds and nearly 60% of these wounds are infected by bacterial biofilm [215]. Chronic wound healing supposed approximately $18 billion worldwide in 2016 according to "Global Wound Care Market" [216].

#### 1.2.2.5 Approaches for controlling antimicrobial resistance

Chronic wound-related infections constitute a worldwide health serious problem, since conventional antimicrobial agents are becoming ineffective. Besides, these therapies are highly associated with systemic toxicity and emergence of AMR due to prolonged and repeated treatments [217]. Antimicrobial agents are often administered by systemic routes and their oral administration encompasses degradation and low absorption in the gastrointestinal tract [218]. Also, systemic off-target distribution of antimicrobial agents is related to poor targeting of wound biofilms. In this context, topical drug delivery systems can afford several benefits, including higher concentrations at the target site, lower systematic toxicity, potential synergism between different therapeutic agents, minimized incidence of AMR, the possibility of using antimicrobial agents not available for systemic therapy, and the increased adherence to therapy due to their non-

USC DE SANTIAGO DE COMPOSTELA

invasive nature [219]. Nevertheless, challenges persist due to low cutaneous permeation, local hypersensitivity, microbiome alteration, and requirement to repeated applications. Thereby, electrospun fiber mats may boost conventional topical treatments efficacy, which typically involve long-lasting treatments. Electrospun fiber mats can protect antimicrobial agents from degradation by wound protease, improve skin retention, modify kinetics release, and bioavailability, facilitating wound healing and effective tissue regeneration, contributing for cost reduction and a patient-friendly wound management [220].

*1.2.2.5.1 Essential oils: A promising therapeutic alternative*

The antibiotic pipeline remains insufficient for current and anticipated future global needs. Therefore, alternative antimicrobial therapies capable of accelerating wound healing with improved efficacy and safety are urgently needed. New approaches under development by academia and industry, include antibodies, immune stimulation, vaccines, lysins, wildtype and engineered phages, and probiotics already in clinical trials [221].

Plant-derived formulations are an attractive solution to promote would healing and simultaneously circumvent AMR due to their multi-target effects. Particularly, essential oil components (EOCs) are promising wound healing agents due to their anti-inflammatory, angiogenic, antioxidant, antibacterial and antifungal properties. It was identified at least Essential oils are commonly presented as a volatile and colored liquid, displaying lower density than water and hydrophobicity nature [222]. Essential oils are composed by mixtures of terpenes, terpenoids, phenylpropanoids, and several other molecules, including alcohols, acids, aliphatic hydrocarbons, aldehydes, lactones or acylic esters that confer the most relevant biological properties, namely, antibacterial, anticancer, antifungal, antidiabetic, antiviral, antimutagenic, and anti-inflammatory properties [223]. Thus, EOCs are use in different fields such as health, cosmetic, agriculture and food industry [223].

Terpenes are hydrocarbons resulting from the combination of several isoprene units (C5H8) synthetized by mevalonic acid pathway and acetyl Coa within the cytoplasm of vegetal cells. There exists a variety of terpenes, the most commonly are monoterpenes (C10), sesquiterpenes (C15), and diterpenes (C20) and triterpenes (C30) [222]. Limonene, p-Cymene, terpinene sabinene and pinene belong to this family. However,

USC DE SANTIAGO DE COMPOSTELA

mostly of terpenes show none or slight antimicrobial activity, especially against Gram-negative bacteria [224].

Terpenoids are one of the most important active compounds of EOCs with similar terpenes structure, adding oxygen molecules and methyl groups in specific positions. Thymol, menthol, linalool, carvacrol, geraniol and citronellol are the most used terpenoids. Indeed, the presence of hydroxyl groups and delocalized electrons confer the antimicrobial activity [222]. For instance, p-cymene and carvacrol have similarly structure but carvacrol has a hydroxyl group, which modifies the hydrophobicity and increases the antimicrobial properties [222,225]. Carvacrol is a phenolic monoterpenoid from oregano with several antimicrobial ways of action; namely, it disintegrates the membrane and the proteins in Gram-negative bacteria, increases the fluidity and permeability of membranes owing to the change in fatty acid, and inhibits the microbial protein synthesis or fledgling, leading to the death of bacteria [226,227].

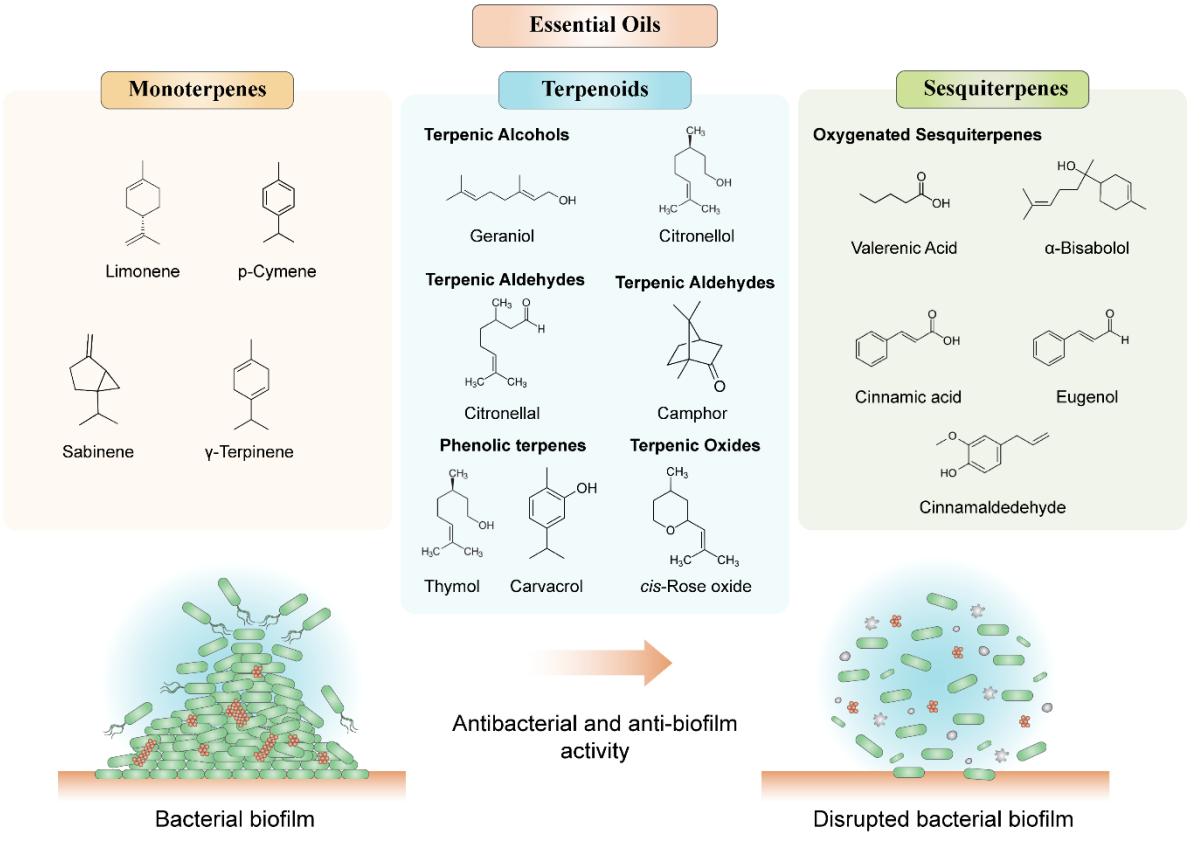



**Figure 1.10. Chemical structure of essential oils with antimicrobial activity and ability to target and disassemble bacterial biofilms. The Figure was made by the author of the Thesis.**

USC UNIVERSIDADE DE SANTIAGO

Phenylpropenes contain a 6-carbon aromatic phenol group and three-carbon propene tail from cinnamic acid. The antimicrobial activity of this group depends on the

free hydroxyl group and the type and number of aromatic substitutions [228]. Several phenylpropenes are currently available, including eugenol, isoeugenol, cinnamaldehyde, vanillin, and carvone, which display good antimicrobial properties against Gram-positive and Gram-negative bacteria [229]. To explain the mechanism of phenylpropenes, cinnamaldehyde is a good representative of this group. This molecule inhibits enzymes essential for cytokine interactions at low concentration, acts as an ATPase inhibitor, and alter the lipid profile of bacterial wall membrane [230].

*1.2.2.5.2 Possible mechanisms of action of essential oils*

Bacteria develop less resistance or tolerances to EOCs than antibiotics because EOCs display several simultaneous mechanisms of action, including bacterial membrane destabilization and degradation by interaction with a variety of components (*e.g.,* fatty acids, proteins, polysaccharides, and phospholipids) triggering a loss of ions and cellular contents, interference in proton pump activity with loss of membrane activity; denaturation of cytoplasmatic proteins; increasing permeability leading to leakage of bacteria components; decreasing the proton motive force and ATP synthesis; and inactivation of a diverse range of enzymes. Thereby, the bacteria could not maintain the integrity and normal function [222, 226, 231, 232].

One of the main antimicrobial activities of EOCs is the destabilization of membrane structure in both bacterial types. Gram-positive and Gram-negative bacteria have different cell walls, being the first type of bacteria constituted in a 90-95% of peptidoglycan and other molecules (*e.g.,* teichoic acid and different proteins) whilst the last type of bacteria is more complex, composed by peptidoglycan (2-3 nm thinner than Gram-positive bacteria) representing the 20% of dry weight of bacteria and it is enveloped by an outer membrane (OM), linked using a covalently bound by Braun lipoprotein [222]. OM is composed of a double phospholipids layer and linked to an LPS inner membrane. Thus, Gram-positive wall bacteria are more permeable to hydrophobic molecules such as phenolic compounds, which can then arrive to the cytoplasm or bacterial wall inner and depending on their concentration cause a change in enzymes activity (at low concentrations) or denaturalize the proteins (at high concentrations). Gram-negative bacteria wall allows diffusion of small hydrophilic solutes through porins at OM membrane that act as truly hydrophilic transmembrane channels. They avoid the pass of hydrophobic molecules, including antibiotics, toxic compounds or EOCs [233,

USC UNIVERSIDADE DE SANTIAGO

234]. Thereby, Gram-negative bacteria are more resistant to several active compounds than Gram-positive bacteria [235].

EOCs use different routes or mechanisms for destabilization of the bacterial membrane [236]. Thymol and carvacrol increase the amount of saturated C16 and C18 fatty acids and decrease the amount of unsaturated C18, leading to a change in the fluidity of the membrane. Moreover, EOCs affect the enzymes responsible for the optimal maintaining and synthesis of fatty acids (*e.g.,* multicomponent membrane desaturase enzyme) increasing the cis isomers, reducing the chain length and decreasing the abundance of unsaturated fatty acids [226]. Proteins are involved in bacteria division or in bacteria wall membrane such as Fts Z (prokaryotic homolog of tubulin). Several EOCs including cinnamaldehyde or thymol bind the aforementioned protein, hindering bacterial division [237]. Furthermore, EOCs down-regulate or up-regulate other proteins, triggering bacteria stress owing to accumulation of mis-folded OM proteins [238]. ATP is essential for the normal bacteria functions, and it is produced in wall membrane and cytosol by glycolysis, existing an optimal balance between extracellular and intracellular ATP. It has been demonstrated that EOCs alter the ATP balance, provoking the wall bacterial membrane disruption [239].

Biofilms develop a complex communication via small organic signaling molecules that regulate adaptation and formation of biofilm and injury response, being important in the five biofilm stages [240]. Both type of bacteria, Gram-positive and negative bacteria use quorum sensing (QS) or *autoinducers* (AIs) that regulate a gene expression when binds to a corresponding receptor. AIs diffuse through bacterial membrane to activate intracellular receptors, altering directly gene expression or transmembrane receptors. Both mechanisms produce signal transduction and the consequent downstream modifications in gene expressions [190]. Each type of bacteria produces their own QS with different morphology, characteristics and properties. Gram-positive bacteria release small peptides as signaling molecules, termed *Autoinducing Peptide Pheromones* (AIPs), while Gram-negative bacteria release Acyl-homoserine Lactones (AHLs) produced by LuxI, an autoinducer synthase and binding with a transcriptional activator protein LuxR, promoting the transcription of downstream genes itself or others closets bacterial cells [241,242]. Moreover, there exist universal QS molecules, termed *autoinducer 2* (AIs) produced approximately by 50 species of Gram-positive and Gram-negative bacteria [243]. QS is involved in the biofilm formation in

USC DE SANTIAGO DE COMPOSTELA

different bacterial species: *S. aureus, P. aeruginosa* and *Vibrio cholera* [244]. QS regulate numerous activities, namely virulence factor production, exoproducts and bioluminescence. EOCs can alter bacterial communication through a variety of mechanisms such as QS synthesis inhibition, sequestration, transport or secretion, or developing an antagonist action to several QS [245].

Several health problems or metabolic processes (*i.e.*, damage regeneration, arteriosclerosis, diabetes, ageing, asthma, Parkinson and Alzheimer disease) provoke the apparition of oxidative stress owing to the ROS and free radicals generation, leading to cellular damage [246]. Flavonoids, terpenoids and phenolic compounds exhibit strong antioxidant effects [247]. For example, the EOCs with major antioxidant activity and free radical-scavenging are clove, cinnamon, basil, nutmeg, carvacrol, and thymol [247],[248]. Likewise, EOCs displayed anti-inflammatory activity owing to the neutralization of ROS and free radicals, prevention of leukotriene synthesis, repression of pro-inflammatory genes, and inhibition of several factors and mechanism such as COX-2 enzyme, lipoxygenase, pro-inflammatory cytokines, TNFα and IL-1 [248].

Overall, EOCs have a variety of advantages for healthcare applications. However, these active agents are unstable, volatile and fragile compounds, and display easy degradation by several external factors, namely, heating, light, and oxidation [249]. Thus, an optimal encapsulation is essential for reach all the potential offered by these natural compounds, increasing the stabilization and obtaining a controlled release for a prolonged antimicrobial action [250]. **Table 1.1.** displays main studies related to the use of electrospinning technique to encapsulate essential oils as antimicrobial or wound healing agent in different polymeric fibers and prepared with different electrospun techniques, thatwere published between 2019- 2024 (Web of Science database) **(Figure 1.11.)**.

USC
UNIVERSIDADE DE SANTIAGO DE COMPOSTELA

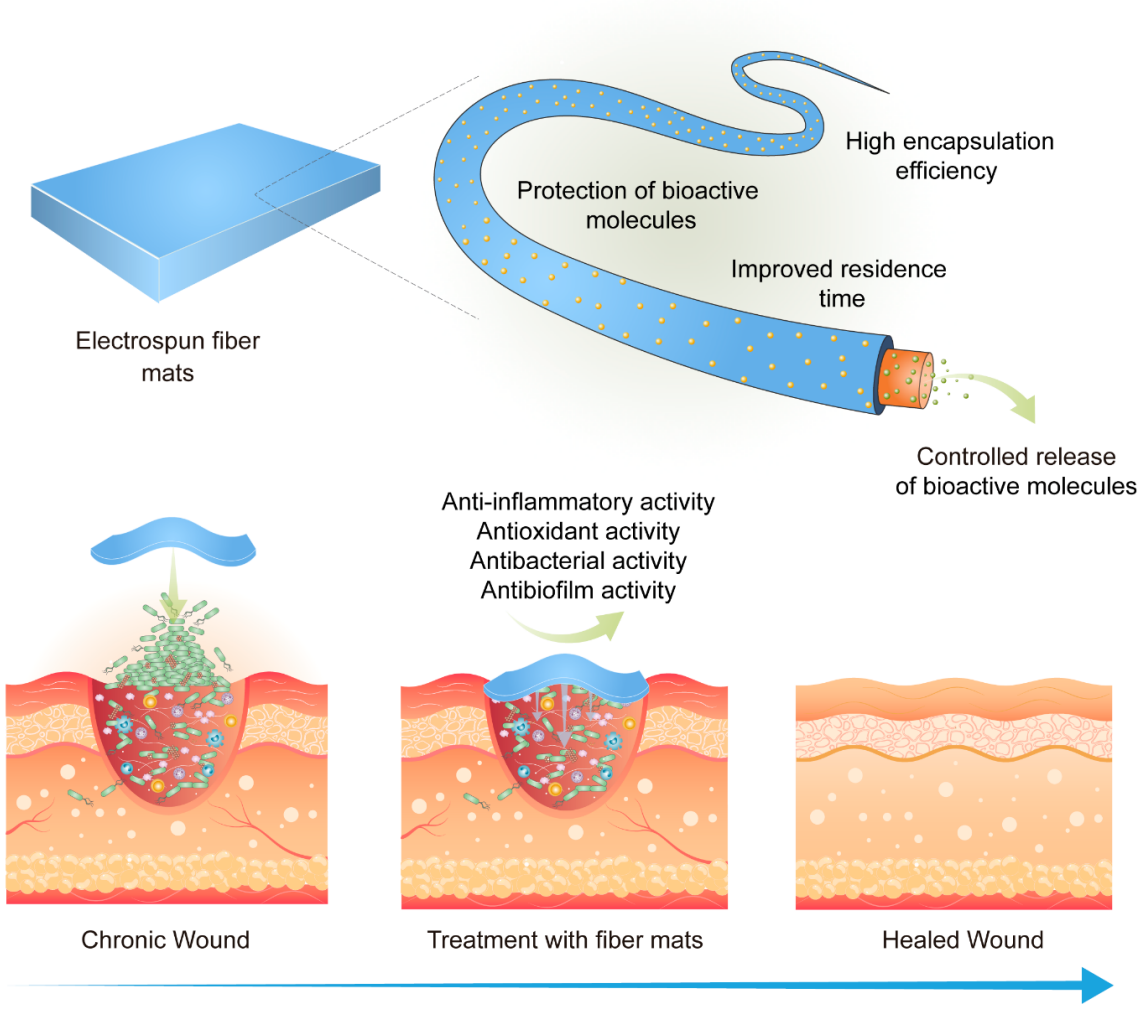



**Figure 1.11. Schematic representation of the different properties that electrospun fiber mats loaded with EOCs could display in wound healing. The Figure was made by the author of the Thesis.**

USC UNIVERSIDADE DE SANTIAGO DE COMPOSTELA

**Table 1.1. Electrospun fibers loaded with different essential oils for wound healing (published between 2019 and 2024 according to Web of Science database).**

| Plant extract / Essential oils | Materials | Electrospinning type | *In vitro* studies | *In vivo* model | Treatment duration | Ref. |
|---|---|---|---|---|---|---|
| *Zataria multiflora* (*lamiaceae*) | PVA<br>Chitosan<br>Gelatin | Uniaxial | Fibroblast cells (cytotoxicity)<br>*S. aureus*, *P. aeruginosa* and *C. albicans* (MIC, MBC, and reduction colonies) | N.A | N.A | [251] |
| Clove EOC<br>*Eugenia caryophyllata* | PCL<br>Gelatin | Uniaxial | Fibroblast cells (cytotoxicity and Scratch test)<br>*S. aureus* and *E. coli* (bacterial viability) | N.A | N.A | [252] |
| Lavander oil<br>*(Lavandula angustifolia)*<br><br>Silver nitrate ($AgNO_3$)<br>NP | PU | Uniaxial | Fibroblast cells (cytotoxicity, cellular attachment)<br>*S. aureus* and *E. coli* (disk diffusion assay) | N.A | N.A | [253] |
| Peppermint EOCs<br>*Mentha piperita*<br>(lamiaceae) | PCL | Uniaxial | Fibroblast cells (cytotoxicity)<br>*S. aureus* and *E. coli* (bacterial viability) | N.A | N.A | [254] |
| Clove EOC<br>*Eugenia caryophyllata* | Zein<br>PEO | Uniaxial (portable electrospinning) | Fibroblast cells (cytotoxicity)<br>*S. aureus* and *E. coli (*disk diffusion assay) | Kunming mice | 11 days | [255] |
| Thyme EOC | Zein<br>PEO | Uniaxial (portable electrospinning) | *S. aureus* and *E. coli* (disk diffusion assay) | Kunming mice | 11 days | [256] |

| | | | | | | |
|---|---|---|---|---|---|---|
| Palmarosa oil (*Cymbopo-gon martinii*)<br>Phytoncide oil (*Chamaecyparis obtusa)* | PVA<br>Tween 80 | Emulsion (O/W) | *S. aureus* and *C. albicans* (disk diffusion assay) | N.A | N.A | [220] |
| Cinnamon EOC | PCL<br>Gelatin | Uniaxial | Fibroblast cells (cytotoxicity)<br>Microbial penetration assay (absorbance profile) | Wistar rats | 14days | [257] |
| Cinnamon EOC (*Clevenger apparatus*) | PU | Uniaxial | Fibroblast cells (cytotoxicity)<br>*S. aureus* and *P. aeruginosa* (RT-PCR) | N.A | N.A | [258] |
| *Zingiber cassumunar* Roxb | PLA<br>PEO | Uniaxial | Fibroblast cells and keratinocytes (cytotoxicity)<br>*S. aureus* and *E. coli* (disk diffusion assay) | N.A | N.A | [259] |
| Black pepper (Piper nigrum)<br>Limonene | PLA<br>Chitosan | Uniaxial<br>Post-treatment fibers (coated with chitosan) | Fibroblast cells (cytotoxicity)<br>*S. aureus, S. epidermidis, P. aeruginosa and E. coli* (CFUs) | N.A | N.A | [260] |
| *Nigella sativa* | PU | Uniaxial | Human umbilical vein endothelial cell line (cytotoxicity)<br>*S. aureus* and *E. coli* (CFUs/mL) | Sprague Dawley rats | 21 days | [261] |
| Ajwain (*Trachyspermum Mami*) | Core:<br>PVA<br>Gelatin<br>Shell:<br>Aloe vera<br>Arabinose | Coaxial | Fibroblast cells (cytotoxicity)<br>*S. aureus, P. aeruginosa, E. coli, E. faecalis, C. dubliniensis* and *C. albicans* (MIC, MBC, and % of reduction colonies) | Sprague-Dawley male rats | 14 days | [262] |

| | | | | | | |
|---|---|---|---|---|---|---|
| | PVP | | | | | |
| *Thymus vulgaris, Salvia officinalis folium*, and *Hyperici herba* | PVA | Uniaxial | *S. aureus* and *E. coli* (disk diffusion assay) | N.A | N.A | [263] |
| Lavander oil<br>Silver nanoparticle | PCL<br>Cellulose acetate | Janus | *S. aureus* and *E. coli* (disk diffusion assay) | N.A | N.A | [264] |
| Cinnamon EOC<br><br>Nanoceria<br>(precursor cerium nitrate) | 1. syringe<br>PU<br>2. syringe<br>PVA<br>Gelatin | Uniaxial<br>(Dual spinneret) | Adipose-derived mesenchymal stem cells (cytotoxicity)<br>*S. aureus* and *E. coli*<br>(log CFUs/mL and % of bacterial viability) | N.A | N.A | [265] |
| *Pistacia atlantica* | PVA<br>Sodium alginate | Uniaxial | Radical scavenging assay<br>(DPPH scavening) | N.A | N.A | [266] |
| Rosemary EOC<br>*(Rosmarinus officinalis)*<br><br>Silver nitrate<br>($AgNO_3$)<br>NP | PU<br>Cellulose acetate | Uniaxial | Human embryonic kidney cells<br>(cytotoxicity and cell attachment)<br>*S. aureus* and *E. coli* (disk diffusion assay and absorbance profile) | N.A | N.A | [267] |
| *Calophyllum inophyllum* (EOC) | PCL | Uniaxial | Fibroblast cells and macrophages (cytotoxicity and antioxidant activity)<br>*S. aureus* and *E. colin* (bacterial viability) | N.A | N.A | [268] |

| | | | | | | |
|---|---|---|---|---|---|---|
| Tea tree oil<br>*(Melaleuca alternifolia)* | PVP<br>Polyamide-6 | Uniaxial | Fibroblast cells (cytotoxicity and cell attachment)<br>*S. aureus* and *E. coli* (disk diffusion assay) | N.A | N.A | [269] |
| Thymus EOC<br>*(Thymus daenensis)*<br>Licorice extract<br>*(Glycyrrhiza glabra)* | Core:<br>PVA<br>Gelatin<br>Thymus<br>Shell:<br>PVA<br>Gelatin<br>Licorice | Coaxial | Fibroblast cells (cytotoxicity, attachment, and scratch test)<br>*S. aureus* and *K. pneumoniae* (disk diffusion assay) | N.A | N.A | [270] |
| Watermelon, Jackfruit, and papaya EOCs | PCL<br>Gelatin | Uniaxial | Fibroblast cells (cytotoxicity)<br>*MRSA* and *P.aeruginosa* (disk diffusion assay) | N.A | N.A | [271] |
| *Plectranthusamboinicus* | PCL | Uniaxial | Keratinocytes (HaCaT) (cytotoxicity)<br>No bacterial strain specified (disk diffusion assay) | N.A | N.A | [272] |
| Chamomile EOC<br>(*Matricaria chamomilla*) | PCL<br>N-(3-sulfopropyl) chitosan | Uniaxial | Fibroblast cells (HFF-2) (cytotoxicity)<br>*S. aureus* and *E. coli* (disk diffusion assay) | N.A | N.A | [273] |
| *Lavandula angustifolia* extract<br>Mupirocin | First layer:<br>Polyacrylonitrile<br>Second layer:<br>Gum (0.7%) | Uniaxial<br>Hydrogel (sprayed) | Fibroblast cells (HDF) (cytotoxicity)<br>*S. aureus* and *E. coli* (disk diffusion assay) | N.A | N.A | [274] |

| | | | | | | |
|---|---|---|---|---|---|---|
| *Eucalyptus* oil (*Eucalyptus camaldulensis*) | Chitosan Cellulose acetate | Uniaxial | Human normal melanocyte cell line (HFB4, cytotoxicity and scratch test) *S. aureus*, *P. aeruginosa*, *P. vulgaris*, *E. coli*, *K. pneumonia*, *A. baumannii*, and *C. albicans* (MIC, MBC, Live/Dead, $Log_{10}$ CFU/mL, and disk diffusion assay) | Albino rats (Rattus norvegicus Albinus) | 7 days | [275] |
| *p*-cymene | PVA Gellan gum | Uniaxial | Fibroblast cells (NIH3T3, (cytotoxicity) *C. albicans*, and *C. glabrata* (% of reduction and inhibition of colonies, morphology wall bacteria by FESEM) | Male Wistar rats | 24 days | [276] |
| Clove EOC Retinyl palmitate | Cellulose acetate | Uniaxial | Fibroblast cells (L929, cytotoxicity) *S. aureus* and *E. coli* (inhibition of colonies) | N.A | N.A | [277] |
| *Pistacia atlántica* Gum-resin | PCL | Uniaxial | Human umbilical vein endothelial cells (HUVEC, cytotoxicity) *S. aureus* and *E. coli* (disk diffusion assay) | N.A | N.A | [278] |
| Helichrysum italicum EOC | PVA PVP | Uniaxial | Human skin cells (SSCs) and BJ fibroblasts (cell viability under UV stress, and *β*-Galactosidase Stain) | N.A | N.A | [279] |

### 1.2.3 Cancer diagnosis and therapy

Cancer is a complex and multifactorial disease that constitutes a significant challenge to global health. Despite significant advances in surgical, radiotherapeutic, and immunological therapeutic approaches to improve cancer treatment outcomes, chemotherapy remains the key therapeutic option. However, this important therapeutic option is characterized by a narrow therapeutic index, low bioavailability, lack of specificity, and requires multiple dosing at high concentrations. Therefore, the clinical efficacy of chemotherapeutic agents is often limited by the emergency of MDR resistance and severe systemic toxicity. In this context, flexible and highly porous electrospun fiber mats can be promising local delivery systems for different chemotherapeutic agents due to their high encapsulation efficiency and surface-to-volume ratio. In contrast to conventional clinical dosage protocols, this strategy specifically targets the tumor site, improving the bioavailability of the chemotherapeutic agents and reducing their side effects through the modification of the drug release profiles. Moreover, this local delivery strategy is useful to enhance the stability of chemotherapeutic agents, protecting them from degradation within the body. Besides, these structures can be obtained from either one single polymer or combined polymers with different properties (*e.g.,* both natural and synthetic polymers on the same electrospun mat) [280–283].

#### 1.2.3.1 Glioblastoma: An unmet medical need

Glioblastoma multiforme (GBM) remains one of the most common and extremely lethal neurological malignancies, accounting for around 49% of all primary brain tumors worldwide among human adults (age from 45 to 75 years old) [284]. Due to the highly aggressive nature of GBM, the WHO classified it as a grade IV cancer with an average annual age-adjusted incidence rate of 4.6 per 100,000 population [285]. Emerging from glial cells or their precursors, GBM is distinguished by a poor prognosis due to its location, fast progression, and invasiveness throughout the Central Nervous System (CNS) [286]. The current standard of care for treating newly diagnosed GBM includes surgical resection followed by radiation and chemotherapy with the alkylating agent Temozolomide (TMZ), providing less than 15 months of median overall survival after disease diagnosis and a 5-year survival rate of only 4.7% [287]. TMZ is considered the gold standard therapy due to its ability to penetrate the blood–brain barrier (BBB). Its antitumoral efficacy on its ability to deliver a methyl group to purine bases of DNA (*i.e.,*

USC UNIVERSIDADE DE SANTIAGO DE COMPOSTELA

N7-guanine, N3-guanine, O6-guanine, and N3-adenine), which can induce cell cycle arrest at the G2/M phase and, ultimately, lead to apoptosis. However, TMZ is ineffective against *ca.,* 50% of primary or recurrent GBMs and its clinical application finds the limitations of its short half-life, absence of treatment specificity related with significant side effects, poor drug accumulation in tumor location, and frequent development of resistances [288].

Apart from TMZ (*i.e.,* Temodar® capsules), few new therapies have been approved by the US Food and Drug Administration (FDA) and the European Medicines Agency (EMA) for GBM since 1976, namely the nitrosourea compounds lomustine (*i.e.*, CeeNU® capsules only by FDA in 1976) and carmustine (*i.e.,* GLIADEL® wafer implants by FDA in 1996 and EMA in 2000), the monoclonal antibody bevacizumab (*i.e.,* Avastin® intravenous solution by FDA in 2009 and EMA in 2014), and an anti-mitotic agent that generates Tumor Treating Fields (TTFields) (*i.e.*, Optune™, formerly known as the NovoTTF-100A System™ in 2015) [289]. TTFields, inhibitors of rapid cell division, may also be applied in combination with chemotherapy. Alternatively, different chemotherapeutic agents (*i.e.*, nimustine, egorafenib, sunitinib, doxorubicin, paclitaxel (PTX), irinotecan (IRN), and cisplatin (CIP)), alongside combination therapies are in preclinical and clinical studies [288]. Nevertheless, all these therapeutic strategies for GBM have not significantly advanced in the last years and have failed to prolong the long-term prospects for patients with GBM mainly due to the inevitable cancer relapse and resistance to treatment.

Such poor outcomes mainly result from a marked therapy resistance resulting from several distinctive features of GBM, including genetic and phenotypic heterogeneity, abundance of different deregulated signaling pathways, different DNA repair pathways, invasive nature, unique features of the immunosuppressive TME, intrinsic resistance to treatment of GBM stem cells, microenvironmental cellular communication, and the presence of the BBB [290,291]. Particularly, GBM stem cells recruit several healthy cells in their vicinity (*i.e.*, monocytes, macrophages, microglia, oligodendrocytes, mast and T cells, neurons, astrocytes, endothelial cells) to change their phenotype for supporting tumor growth, promoting angiogenesis, and suppressing adaptative antitumor immune responses. A multidimensional communication is required for this recruitment enrolled by GBM stem cells, namely secretion of soluble factors (*i.e.*, chemokines and cytokines), direct cell–cell contact, extracellular vesicles (*i.e.*, exosomes

USC DE SANTIAGO DE COMPOSTELA

and microvesicles) and connecting nanotubes and/or microtubes [292]. GBM stem cells invasion deep into the brain also precludes the effective treatment of GBM only with surgical resection. Besides, GBM stem cells are often highly refractory to conventional chemotherapy, which promotes tumor recurrence and emergence of multiple drug resistance. Other important unique features of the TME that challenge the treatment of GBM include the BBB, the existence of myelinated and interconnected axon projections, and particularly soft hyaluronic acid-rich extracellular matrix. Although BBB loses integrity during tumor progression, continues to hinder the passage of systemically administered chemotherapeutic agents and remains intact in the actively invading tumor regions [293]. In the perivascular area, haptotactic signals from the vascular basement membrane and enrichment of vascular-derived chemotactic signals promote tumor cell invasion and treatment resistance [294]. Interconnected axon projections also release haptotactic signals and represent a major obstacle to surgical resection [287]. Together, all these multi-faceted roles of the components in the complex TME of GBM play a pivotal role in tumor progression, invasion, and resistance to treatment. Collectively, all aforementioned constrains dictate the urgent need for developing new therapeutic strategies with improved efficacy and safety.

#### 1.2.3.2 Drug repurposing for glioblastoma reatment: An underutilized resource

Research and development of novel therapeutic approaches is an extremely complex, expensive, and time-consuming process characterized by high failure rates. In recent years, one promising strategy that has become very popular is drug repurposing (also described as drug repositioning, reprofiling or re‑tasking). This emerging strategy consists of identifying new indications for clinically approved drugs, leveraging completed pharmaceutical development process to maximize the therapeutic utility of the already developed products. Generally, a drug repurposing strategy includes three main steps before pursuing with the drug candidate further through the development pipeline: **(i)** identification of a candidate molecule for a new therapeutic indication (hypothesis generation) *via* data-driven strategies or experimental approaches; **(ii)** mechanistic assessment of the drug effect in preclinical models; and **(iii)** evaluation of efficacy in phase II clinical trials, considering that reliable data on safety, tolerability, pharmacokinetics were already obtained from phase I studies performed for the original indication [295] .

In the context of cancer research, drug repurposing can be considerably advantageous, since repurposed drugs present already well-established safety profiles, they are usually more affordable, and can significantly expedite the drug development process with timelines decreased by up to 3–5 years [219]. For instance, repurposing of therapeutic agents for GBM treatment can introduce promising alternative therapeutic alternatives in a short period of time with low associated costs, improved treatment compliance, and minor risks neurologic deficits and severe side effects (*i.e.,* suppression of bone marrow, hepatotoxicity, nephrotoxicity, necrosis, neurotoxicity, hematologic toxicity, and skin toxicity [296]. Currently, a plethora of drugs on the market have shown promising therapeutical effects based preclinical data using GBM models, being considered possible candidates for repurposing in GBM treatment [297,298] . Only a fraction of these drugs has already entered in clinical trials, demonstrating favorable outcomes alone or combined with TMZ **(Table 1.2.)**. Typically drugs with therapeutic value for GBM treatment should be able to penetrate the BBB and present good site accumulation characteristics. Therefore, the overwhelming majority of candidates for drug repurposing are originally indicated for CNS due to their proven capacity to cross the BBB in therapeutic concentrations. For instance, disulfiram (DSF, Antabuse®) is a good illustration of a drug repositioning opportunity that might offer an effective treatment for GBM therapy [299]. The FDA has approved DSF for several years to treat chronic alcoholism by inhibiting the enzyme aldehyde dehydrogenase (ALDH) [300]. In the last years, an increasing amount of independent preclinical data have support DSF as an anticancer agent [301]. DSF presents a copper-dependent antitumoral with the disulfiram−copper complex playing a pivotal role in reversing MDR, restraining angiogenesis, limiting tumor metastasis, and regulating immunosuppressive TMEs [300;302,303]. Consequently, several clinical trials have been performed to corroborate the preclinical antitumoral effect of DSF combined with copper (Cu) by enhancing TMZ antitumoral effect in patients who have newly diagnosed or recurrent GBM (clinicaltrials.gov, NCT02770378, NCT03034135, NCT02715609, NCT01777919, NCT01907165, NCT02678975, and NCT03363659). Another candidate for drug repurposing in GBM is the antidiabetic metformin, a highly potent, selective, and reversible inhibitor of sodium-glucose co-transporter 2 (SGLT2). Both *in vitro* and *in vivo* studies have demonstrated that metformin may play an important role in regulating several signaling pathways involved in cellular proliferation, autophagy, apoptosis, angiogenesis, invasion, and MDR reversal [304,305]. These favorable outcomes

USC DE COMPOSTELA

motivated the performance of clinical trials with metformin in combination with DSF (clinicaltrials.gov, NCT03151772), since both drugs may be part of a novel paradigm in GBM treatment.

#### 1.2.3.3 Local drug delivery for a local effect

The treatment of patients with advanced-stage GBM typically involves a multimodality approach (including surgery, chemotherapy, radiotherapy, and/or targeted therapy), which is often ultimately ineffective. Drug delivery strategies for GBM treatment can be implemented either systemically or locally using different administration routes: parenteral administration, invasive local administration (*i.e.,* implanted and injected modalities by intrathecal and intraparenchymal delivery), and alternative administration routes (*i.e.,* intranasal or nose-to-brain and peripheral delivery) [306]. However, several drugs systemically administered present limited bioavailability in the CNS, mainly imposed by the tight junctions between endothelial cells of the BBB. Among the drugs that can potentially surpass the BBB, systemic toxicity becomes a concern due to the require multiple dosing at high concentrations to achieve therapeutic levels in the brain-tumor site. Moreover, short drug half-life and early clearance of the interstitial fluid (ISF) and cerebrospinal fluid (CSF) prevent drugs from remaining at therapeutic concentrations in the brain-tumor. Consequently, GBM almost always recurs within 2 cm of the tumor resection margin (more than 90% of clinical cases), within the radiotherapy field [287,307]

Local therapeutic strategies provide a unique opportunity to surpass the BBB and deliver high therapeutic doses of drugs directly to the tumor area, aiming to reduce dosing frequency, mitigate systemic toxicity, and ultimately improve patient compliance [308]. An example of a locally administered drug delivery system intended to have a local effect in GBM treatment is the Gliadel® wafer technology. Approved by the FDA in 1996, Gliadel® wafer is the only post-surgical local chemotherapy indicated for the treatment of patients with newly-diagnosed high-grade glioma in combination with surgery and radiation, and recurrent glioblastoma as an adjunct to surgery. Gliadel® wafers consist of white round wafers (*ca.,* 1.45 cm in diameter and 1 mm thickness) containing the chemotherapeutic drug carmustine (BCNU, 7.7 mg) and the biodegradable polyanhydride copolymer Polifeprosan 20 that controls the release of the drug. Following tumor resection, Gliadel wafers (up to 8 wafers) can be placed in the region of interest to cover

USC UNIVERSIDADE DE SANTIAGO

as much of the resection cavity as possible. Oxidized regenerated cellulose (Surgicel®) may also be placed over the wafers to secure them against the cavity surface. Upon exposure to the aqueous environment of the resection cavity, the anhydride bonds in the copolymer are hydrolyzed, releasing BCNU into the surrounding brain tissue for nearly 7 days (90%) [309,310] . Gliadel® wafers have been shown to increase the mean overall survival in patients with recently diagnosed GBM by 2 months This limited survival benefit emphasizes how challenging it to find effective drug delivery systems to the brain, even when the BBB has been circumvented. Besides, Gliadel® wafers have been associated with numerous clinical complications, including edema, seizures, abnormal wound healing, and surgical site infections. Furthermore, short half-life of BCNU (*ca.,* 20 min) and its limited tissue penetration (1–5 mm) persisted as significant obstacles. Several preclinical sutidies have been performed with a wide range of polymeric drug delivery systems (*e.g.,* polymeric implants [311–313] microparticles [314], microcapsules [315], microchips [316], and nanoparticles [317,318]) loaded with different chemotherapeutic drugs (e.g. TMZ [319]–[321], PTX [312,322,323], Doxorubicin [324,325], 5-Fluorouracil [326], and Camptothecin [327]). However, the majority of the developed systems have critically failed to maintain a sustained drug release for more than 2–3 weeks. Therefore, novel local and controlled delivery systems of drugs directly in brain-tumor for prolonged periods are urgently needed to improve the prognosis of recurrent GBM.

Electrospun mats constitute promising long-acting local drug-delivery systems (also described as depot systems) for GBM treatment due to their capacity to achieve a local, slow, constant, and sustained release of chemotherapeutic drugs at brain-tumor site over a prolonged period of time, ranging from a few hours to months **(Figure 1.12)** [328]. Consequently, these formulations can decrease the systemic toxicity of chemotherapy, while enhancing its therapeutic efficacy against GBM and inhibiting post-surgery tumor recurrence [328]. Adopting the electrospinning technique, versatile ultra-fine fiber mats can be created with scalability and reproducibility by spinning multiple polymer-drug compositions into a single biodegradable mat [3,4].

USC UNIVERSIDADE DE SANTIAGO DE COMPOSTELA

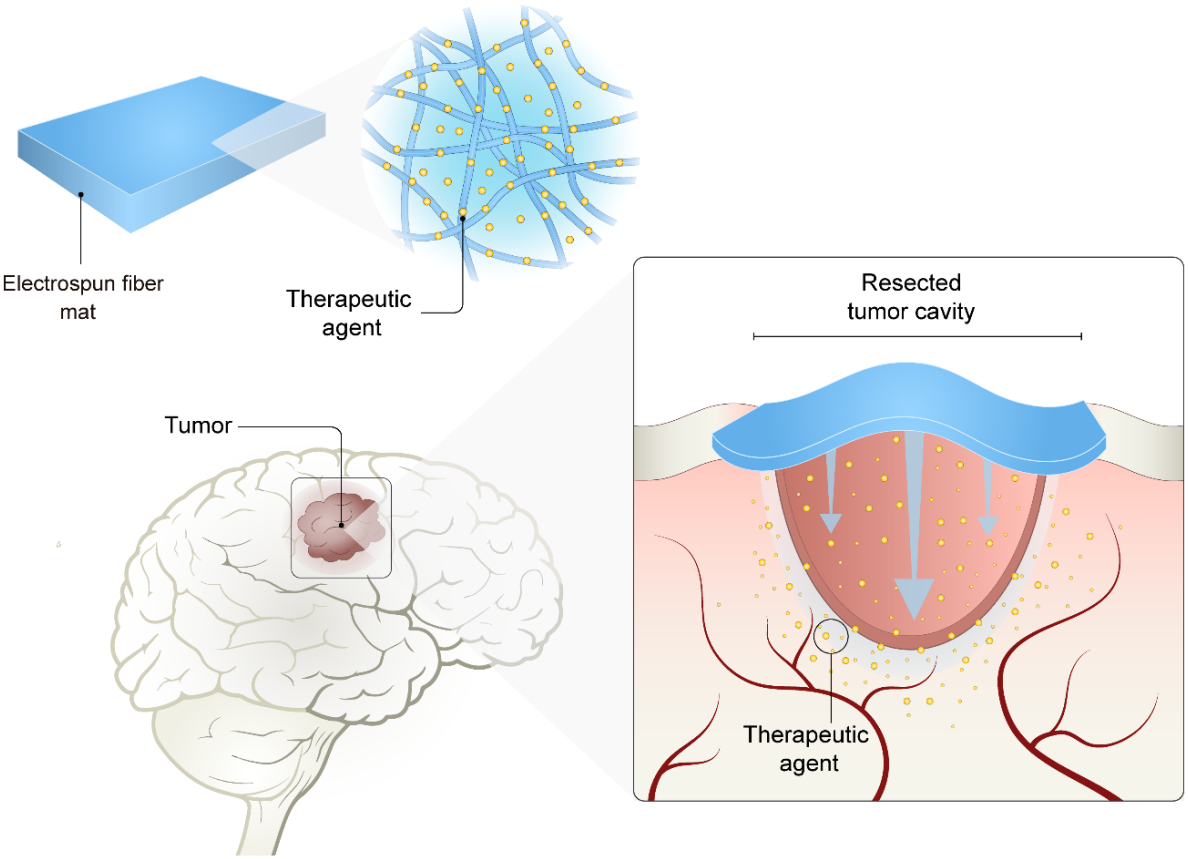



**Figure 1.12. Following tumor resection, electrospun fiber mats can be placed in the region of interest to cover as much of the resection cavity as possible. The Figure was made by the author of the Thesis.**

Several natural or synthetic polymers have been successfully electrospun into ultrafine fiber mats, with diameters in the range of nanometers to micrometers, for GBM treatment. Among all the synthetic polymers, the FDA-approved bulk-eroding polyesters such as PLGA, PLA, PCL, and PVA are the options that have been most widely explored to prepare electrospun fiber mats for prolonged and localized treatment of GBM with different chemotherapeutic drugs (*e.g.,* paclitaxel (PTX), TMZ, and BCNU) [312,308,329]. **Table 1.2.** presents an overview of relevant examples of electrospun fiber mats tested *in vivo* for GBM treatment. For all cases suitable solvents were chosen to dissolve the selected polymer, since solvent properties (*i.e.,* conductivity and volatility) considerably affect the stability of the electrospinning process and the morphology of the resulting mats.

PLGA remains a popular choice do prepare electrospun fiber mats owing to its excellent biocompatibility, biodegradability, and mechanical strength. In long-acting pharmaceutical formulations like electrospun mats, the biodegradability of PLGA should

USC DE SANTIAGO DE COMPOSTELA

be balanced with the prolonged and sustained duration of release desired for the therapeutic agent [63]. PLGA is a polymer composed of lactic acid and glycolic acid monomers and the proportion of these two monomers in the polymer composition can be tuned to simultaneously obtained the desired degradation rate of the polymer and the suitable release rate of the therapeutic agent. For instance, PLGA (50:50) is a copolymer of 50% poly lactic acid (PLA) and 50 % poly glycolic acid (PGA) and displays the fastest degradation rate, being completely degraded in about 2 months [330]. However, increasing the molar ratio of PLA in the PLGA polymer will make it more hydrophobic. Consequently, the capacity of the PLGA polymer to absorb water molecules will be reduced and its degradation will be much slower. Besides, the molecular weight or inherent viscosity of the PLGA polymer is also an important to consider, since the higher molecular weight provides a slower drug release [330]. This is perfectly exemplified in one study work where PTX-loaded electrospun fiber mats were prepared from two different PLGA co-polymers, PLGA 50:50 and PLGA 85:15 [312] . Different flow rates and DMF contents were also used to yield fibers with different mean diameters, since low polymer flow rates produces fin fibers from the jet and high DMF content increases the conductivity of the polymer solution providing more fluidity. Thus, PLGA 50:50 was electrospun at a high flow rate combined with a high DMF content to yielded microfibers of mean diameter around 3.5 ± 0.32 μm, whereas PLGA 85:15 was electrospun with a low flow rate and high DMF content to yield submicrofibers of mean diameter around 930 ± 35 nm. *In vitro* drug release studies showed that both formulations provided a PTX sustained release over 80 days, in which the submicro-fibers showed a higher release rate than microfibers due to the higher surface area:volume ratio and higher degradation rate of the PLGA polymer by hydrolysis [312]. It is should be highlighted that PTX loaded-fibers locally applied showed superior inhibition on the tumor growth compared to PTX systemically administered in subcutaneous C6-bearing BALB/c nude mice models, demonstrating significant advantages in providing a local and sustained release of PTX from fiber mats [312]. In a similar study, PTX-loaded PLGA (50:50) continuous nanofibers (*ca.,* 100 nm mean diameter) were prepared using electrospinning. In this case, nano-structuring of the fibers resulted from the use of TATPB to increase the conductivity of the solution combined with a thin jet resulting from a low polymer concentration, low flow rate, and high voltage difference. *In vivo* studies showed that PLGA nanofibers exhibited a PTX sustained release and enhanced penetration of PTX in the mouse brain up to 5 mm from the implant site even after 42 days post-implantation, while the slow-

USC DE COMPOSTELA

release rate of PTX from PLGA microfibers impaired the PTX penetration in the brain. Besides, the PTX-loaded PLGA nanofibers demonstrated a significant tumor inhibition (*ca.,* 30-fold) following 41 days of treatment in intracranial U87 MG-luc2 GBM mouse models as compared to placebo controls [322]. PLGA nanofibers have been also explored as an alternative to overcome some the major drawbacks of Gliadel® wafers, namely fast release of a considerable amount of BCNU within first 5–7 days and its rigidness. Particularly, biodegradable electrospun nanofiber mats (375-1200 nm) based on PLGA 50:50 were able to provide a sustained of BCNU for more than 6 weeks in the cerebral cavity of orthotopic C6-bearing Wistar rats. In contrast to BCNU-loaded wafers, the prepared thin (*ca.,* 0.12 mm) and flexible nanofibers demonstrated improved adaptability to geometry of the brain tissue and better capacity to cover the tumor resection cavity, ensuring a better penetration of BCNU without inducing inflammatory reactions neither interfering with the normal function of the brain [309]. Electrospun fiber mats composed of PLGA have been study as a strategy to overcome the emergence of MD by combining multiple chemotherapeutic agents or other anticancer bioactive molecules in one single local drug delivery system. Ideally, chemotherapy with a combination of two or more drugs would provide a synergistic effect between the drugs, suppress the emergence of MDR via several pathways, and ultimately enhance the overall therapeutic efficacy. For instance, three chemotherapeutic drugs (*i.e.,* BCNU, irinotecan, and cisplatin) were co-loaded in PLGA (50:50) nanofibers and an antiangiogenic agent in PLGA (75:25) nanofibers. *In vitro* studies showed a fast release of all chemotherapeutic agents from the nanofibers, whereas antiangiogenic agent presented a sustained release profile over 2 weeks. Nevertheless, all therapeutic agents locally applied remained at high in the brain tissues for more than 8 weeks compared with the ones systemically. Moreover, nanofiber mats containing the four therapeutic agents showed an effective tumor growth inhibition with prolonged survival in C6 GBM-bearing rats in contrast to nanofibers without the antiangiogenic agent [331]. In a similar study, PTX-loaded PLGA (50:50) continuous nanofibers (*ca.,* 100 nm mean diameter) were prepared using electrospinning. In this case, nano-structuring of the fibers resulted from the use of TATPB to increase the conductivity of the solution combined with a thin jet resulting from a low polymer concentration, low flow rate, and high voltage difference. *In vivo* studies showed that PLGA nanofibers exhibited a PTX sustained release and enhanced penetration of PTX in the mouse brain up to 5 mm from the implant site even after 42 days post-implantation, while the slow-release rate of PTX from PLGA microfibers impaired the PTX penetration in the brain.

USC DE SANTIAGO DE COMPOSTELA

Besides, the PTX-loaded PLGA nanofibers demonstrated a significant tumor inhibition (*ca.,* 30-fold) following 41 days of treatment in intracranial U87 MG-luc2 GBM mouse models as compared to placebo controls [322]. PLGA nanofibers have been also explored as an alternative to overcome some the major drawbacks of Gliadel® wafers, namely fast release of a considerable amount of BCNU within first 5–7 days and its rigidness. Particularly, biodegradable electrospun nanofiber mats (375-1200 nm) based on PLGA 50:50 were able to provide a sustained of BCNU for more than 6 weeks in the cerebral cavity of orthotopic C6-bearing Wistar rats. In contrast to BCNU-loaded wafers, the prepared thin (*ca.,* 0.12 mm) and flexible nanofibers demonstrated improved adaptability to geometry of the brain tissue and better capacity to cover the tumor resection cavity, ensuring a better transport of BCNU without inducing inflammatory reactions neither interfering with the normal function of the brain.

USC
UNIVERSIDADE DE SANTIAGO DE COMPOSTELA

**Table 1.2. Applications of electrospun mats for the therapy of glioblastoma: *in vivo* evidence.**

| Therapeutic agent | Polymer/ Precursor | Solvent | Applied voltage (kV) | Spinning type | Mean diameter (nm) | Release studies | *In vivo* model | Treatment duration | Outcomes | Ref. |
|---|---|---|---|---|---|---|---|---|---|---|
| PTX | PLGA (50:50) | DCM/DMF 70/30 % (v/v) | 12–20 | Uniaxial (single nozzle) | 930 | PTX release (30%) for 80 days (pH~7.4) | Subcutaneous C6-bearing BALB/c nude mice | 32 days | Effective tumor growth inhibition (~78%) over placebo control group | [312] |
| PTX | PLGA (50:50) | TATPB DCM | 18–20 | Uniaxial (single nozzle) | 102 | Initial burst release of PTX followed by a sustained release up to 60 days | U87 MG xenograft in BALB/c nude mice | 42 days | Deep penetration (5 mm) of PTX released from fibers in mouse brain observed even 42 days post implantation | [322] |
| TMZ | PLGA (50:50) PLA (150 kD) PCL (100 kD) | Acetone Chloroform | 15–18 | Uniaxial (single nozzle) | 400-600<br>800-1000 | Sustained release of TMZ up to 30 days | Orthotopic C6-bearing Wistar rats | 74 days | Significant (~30 fold) tumor inhibition over placebo control group<br>1-month releasing fibers provided prolonged survival (>4 months), whereas 7-day releasing-fibers provided a median survival of only 2 months | [308] |
| BCNU | PLGA (50:50) | HFIP | 17 | Uniaxial (single nozzle) | 375-2000 | Initial burst BCNU release up to 2 days, then controlled release up to 11 days, followed | Orthotopic C6-bearing Wistar rats | 6 weeks | Biodegradable nanofibers released high concentrations of BCNU during 6 weeks in the cerebral cavity of rats | [329] |

| | | | | | | | | | |
|---|---|---|---|---|---|---|---|---|---|
| BCNU<br>IRN<br>CIP<br>CA4P | PLGA<br>(75:25) | HFIP | 17 | Uniaxial<br>(single nozzle) | 375-2000 | by a second peak release up 15 days<br>Burst release of several chemotherapeutic agents (BCNU, IRN, and CP) followed by the release of the antiangiogenic agent (CA4P) after 2 weeks | Orthotopic C6-bearing Wistar rats | 20 weeks | Effective tumor growth inhibition with prolonged survival (86 days) over control group (23 days) | [331] |
| PTX<br>MMP-2<br>mRNA | PLGA<br>50:50<br>PEG<br>(MW~4600) | DCM<br>TATPB<br>Span 80 | 12–20 | Emulsion electrospinning | 850 | Sustained gene/drug dual delivery for 42 days | U87 MG xenograft in BALB/c nude mice | 34 days | Synergistic therapeutic efficacy imposed significant tumor regression over single drug delivery fibers and free drug | [332] |
| TRAIL | PLA<br>(MW~70000) | Chloroform/DMF<br>3:1 % (v/v) | 15 | Uniaxial<br>(single nozzle) | 450 | N.A. | U87 MG xenograft in BALB/c nude mice | 35 days | Suppression of post-surgical GBM recurrence with prolonged survival | [333] |
| DOX | PLA<br>(Mn 3800 kDa)<br>Gelatine<br>Type A | N.A. | N.A. | Uniaxial<br>(single nozzle) | 799 | Initial burst release of DOX (~20%) followed by a sustained release up to 30 days | U87 MG xenograft in BALB/c nude mice | 20 days | Significant tumor volume reduction without no oblivious side effects | [334] |
| iNek1<br>TMZ | PVA | $dH_2O$<br>DMSO | 9 | Uniaxial<br>(single nozzle) | 2900 | Sustained release of TMZ and iNek1 for 8 days | Wistar rats | 60 days | High concentrations of TMZ within the brain | [335] |

| | | | | | | | | | | |
|---|---|---|---|---|---|---|---|---|---|---|
| SDF-1α | PEO (MW~2000) | $dH_2O$ Chitosan/1 M Acetic Acid | 30 | Uniaxial (single nozzle) | 251 | Sustained release of SDF-1α for 5 weeks | Fischer rats | 7 days | Effective tumor growth inhibition without oblivious side effects<br>Absence of adverse effects on implanted rats with slow biodegradability | [336] |

USC UNIVERSIDADE DE SANTIAGO DE COMPOSTELA

Stimuli-responsive PEGylated-PLGA electrospun nanofibrous mats co-loaded with the antitumoral natural flavonoid silibinin and iron oxide nanoparticles have also demonstrated the capacity to provide a remotely control and activation of drug release for at least 60 hours, without an initial burst effect [337]. Additionally, this type of nanofibers containing both therapeutic agents and metallic nanoparticles can be applied as theranostic nanoplatforms, since simultaneously allow diagnostic and therapeutic functions. Accordingly, theranostic nanofibers can be useful in detecting target tumors and monitoring the response to treatment [308,337],. Despite all the progress mentioned above, achieving a sustained drug release from electrospun nanofiber mats within brain-tumor site for a long period of time remains a challenge due to the abrupt biodegradation properties of the polymers in physiological conditions [308]. Therefore, the combination different proportions of bulk-eroding polyesters with different biodegradation rates (fast release for PLGA or slow for PLA/PCL) in one single electrospun mat can effectively enable a controlled drug release for 1-2 moths in a challenging TME like GBM [322].

USC
UNIVERSIDADE DE SANTIAGO DE COMPOSTELA

## 1.3. References


[1] X. Hu, S. Liu, G. Zhou, Y. Huang, Z. Xie, and X. Jing, "Electrospinning of polymeric nanofibers for drug delivery applications," *J. Control. Release*, vol. 185, no. 1, pp. 12–21, 2014, doi: 10.1016/j.jconrel.2014.04.018.

[2] N. Bhardwaj and S. C. Kundu, "Electrospinning: A fascinating fiber fabrication technique," *Biotechnol. Adv.*, vol. 28, no. 3, pp. 325–347, 2010, doi: 10.1016/j.biotechadv.2010.01.004.

[3] S. Chakraborty, I. C. Liao, A. Adler, and K. W. Leong, "Electrohydrodynamics: A facile technique to fabricate drug delivery systems," *Adv. Drug Deliv. Rev.*, vol. 61, no. 12, pp. 1043–1054, 2009, doi: 10.1016/j.addr.2009.07.013.

[4] N. Aminu *et al.*, "Journal of Drug Delivery Science and Technology Applications of nanofibers drug delivery system in cancer therapy," *J. Drug Deliv. Sci. Technol.*, vol. 90, no. October, p. 105128, 2023, doi: 10.1016/j.jddst.2023.105128.

[5] S. Thenmozhi, N. Dharmaraj, K. Kadirvelu, and H. Y. Kim, "Electrospun nanofibers: New generation materials for advanced applications," *Mater. Sci. Eng. B*, vol. 217, pp. 36–48, 2017, doi: 10.1016/j.mseb.2017.01.001.

[6] J. Zeleny, "The electrical discharge from liquid points, and a hydrostatic method of measuring the electric intensity at their surfaces," *Phys. Rev.*, vol. 3, no. 2, pp. 69–91, 1914, doi: 10.1103/PhysRev.3.69.

[7] A. Formhals, "PROCESS AND APPARATUS FOR PREPARING ARTIFICIAL THREADS," *United States paatent Off.*, vol. 1,095,504, 1934, doi: 10.1016/0042-6822(72)90565-x.

[8] G. Taylor and P. R. S. L. A, "Electrically driven jets," *Proc. R. Soc. London. A. Math. Phys. Sci.*, vol. 313, no. 1515, pp. 453–475, 1969, doi: 10.1098/rspa.1969.0205.

[9] Z. M. Huang, Y. Z. Zhang, M. Kotaki, and S. Ramakrishna, "A review on polymer nanofibers by electrospinning and their applications in nanocomposites," *Compos. Sci. Technol.*, vol. 63, no. 15, pp. 2223–2253, 2003, doi: 10.1016/S0266-3538(03)00178-7.

[10] D. Han and A. J. Steckl, "Coaxial Electrospinning Formation of Complex Polymer Fibers and their Applications," *Chempluschem*, vol. 84, no. 10, pp. 1453–1497, 2019, doi: 10.1002/cplu.201900281.

[11] D. Ji *et al.*, "Electrospinning of nanofibres," *Nat. Rev. Methods Prim.*, vol. 4, no. 1, 2024, doi: 10.1038/s43586-023-00278-z.

[12] P. R. Patel and R. V. N. Gundloori, "A review on electrospun nanofibers for multiple biomedical applications," *Polym. Adv. Technol.*, vol. 34, no. 1, pp. 44–63, 2023, doi: 10.1002/pat.5896.

[13] A. Ghaderpour, Z. Hoseinkhani, R. Yarani, S. Mohammadiani, F. Amiri, and K. Mansouri, "Altering the characterization of nanofibers by changing the electrospinning parameters and their application in tissue engineering, drug delivery, and gene delivery systems," *Polym. Adv. Technol.*, vol. 32, no. 5, pp. 1924–1950, 2021, doi: 10.1002/pat.5242.


USC UNIVERSIDADE DE SANTIAGO DE COMPOSTELA

[14] A. Keirouz, Z. Wang, V. S. Reddy, and Z. K. Nagy, "The History of Electrospinning : Past , Present , and Future Developments," vol. 2201723, pp. 1–34, 2023, doi: 10.1002/admt.202201723.

[15] S. Mei *et al.*, "Journal of Drug Delivery Science and Technology Electrospinning and its potential in fabricating pharmaceutical dosage form," vol. 76, no. May, 2022.

[16] G. H. Kim, Y. S. Cho, and W. D. Kim, "Stability analysis for multi-jets electrospinning process modified with a cylindrical electrode," *Eur. Polym. J.*, vol. 42, no. 9, pp. 2031–2038, 2006, doi: 10.1016/j.eurpolymj.2006.01.026.

[17] Y. Zheng, S. Xie, and Y. Zeng, "Electric field distribution and jet motion in electrospinning process: From needle to hole," *J. Mater. Sci.*, vol. 48, no. 19, pp. 6647–6655, 2013, doi: 10.1007/s10853-013-7465-8.

[18] Y. Zheng, R. H. Gong, and Y. Zeng, "Multijet motion and deviation in electrospinning," *RSC Adv.*, vol. 5, no. 60, pp. 48533–48540, 2015, doi: 10.1039/c5ra06049d.

[19] C. J. Angammana and S. H. Jayaram, "Fundamentals of electrospinning and processing technologies," *Part. Sci. Technol.*, vol. 34, no. 1, pp. 72–82, 2016, doi: 10.1080/02726351.2015.1043678.

[20] N. M. Thoppey, J. R. Bochinski, L. I. Clarke, and R. E. Gorga, "Unconfined fluid electrospun into high quality nanofibers from a plate edge," *Polymer (Guildf).*, vol. 51, no. 21, pp. 4928–4936, 2010, doi: 10.1016/j.polymer.2010.07.046.

[21] N. M. Thoppey, J. R. Bochinski, L. I. Clarke, and R. E. Gorga, "Edge electrospinning for high throughput production of quality nanofibers," *Nanotechnology*, vol. 22, no. 34, 2011, doi: 10.1088/0957-4484/22/34/345301.

[22] J. Holopainen, T. Penttinen, E. Santala, and M. Ritala, "Needleless electrospinning with twisted wire spinneret," *Nanotechnology*, vol. 26, no. 2, p. 25301, 2015, doi: 10.1088/0957-4484/26/2/025301.

[23] G. Jiang, S. Zhang, and X. Qin, "High throughput of quality nanofibers via one stepped pyramid-shaped spinneret," *Mater. Lett.*, vol. 106, pp. 56–58, 2013, doi: 10.1016/j.matlet.2013.04.084.

[24] X. Yan *et al.*, "Slit-surface electrospinning: A novel process developed for high-throughput fabrication of core-sheath fibers," *PLoS One*, vol. 10, no. 5, pp. 1–11, 2015, doi: 10.1371/journal.pone.0125407.

[25] G. Yan, H. Niu, H. Shao, X. Zhao, H. Zhou, and T. Lin, "Curved convex slot: an effective needleless electrospinning spinneret," *J. Mater. Sci.*, vol. 52, no. 19, pp. 11749–11758, 2017, doi: 10.1007/s10853-017-1315-z.

[26] D. Lukas, A. Sarkar, and P. Pokorny, "Self-organization of jets in electrospinning from free liquid surface: A generalized approach," *J. Appl. Phys.*, vol. 103, no. 8, 2008, doi: 10.1063/1.2907967.

[27] K. Molnar and Z. K. Nagy, "Corona-electrospinning: Needleless method for high-throughput continuous nanofiber production," *Eur. Polym. J.*, vol. 74, pp. 279–286, 2016, doi: 10.1016/j.eurpolymj.2015.11.028.

USC UNIVERSIDADE DE SANTIAGO DE COMPOSTELA

[28] I. Bhattacharyya, M. C. Molaro, R. D. Braatz, and G. C. Rutledge, "Free surface electrospinning of aqueous polymer solutions from a wire electrode," *Chem. Eng. J.*, vol. 289, pp. 203–211, 2016, doi: 10.1016/j.cej.2015.12.067.

[29] X. Wang, H. Niu, X. Wang, and T. Lin, "Needleless electrospinning of uniform nanofibers using spiral coil spinnerets," *J. Nanomater.*, vol. 2012, 2012, doi: 10.1155/2012/785920.

[30] S. L. Liu, Y. Y. Huang, H. D. Zhang, B. Sun, J. C. Zhang, and Y. Z. Long, "Needleless electrospinning for large scale production of ultrathin polymer fibres," *Mater. Res. Innov.*, vol. 18, pp. S4833–S4837, 2014, doi: 10.1179/1432891714Z.000000000802.

[31] C. Huang, H. Niu, J. Wu, Q. Ke, X. Mo, and T. Lin, "Needleless electrospinning of polystyrene fibers with an oriented surface line texture," *J. Nanomater.*, vol. 2012, 2012, doi: 10.1155/2012/473872.

[32] T. Miloh, B. Spivak, and A. L. Yarin, "Needleless electrospinning: Electrically driven instability and multiple jetting from the free surface of a spherical liquid layer," *J. Appl. Phys.*, vol. 106, no. 11, 2009, doi: 10.1063/1.3264884.

[33] H. Niu, X. Wang, and T. Lin, "Needleless electrospinning: Influences of fibre generator geometry," *J. Text. Inst.*, vol. 103, no. 7, pp. 787–794, 2012, doi: 10.1080/00405000.2011.608498.

[34] A. L. Yarin and E. Zussman, "Upward needleless electrospinning of multiple nanofibers," *Polymer (Guildf).*, vol. 45, no. 9, pp. 2977–2980, 2004, doi: 10.1016/j.polymer.2004.02.066.

[35] Y. Li *et al.*, "Developments of Advanced Electrospinning Techniques : A Critical Review," vol. 2100410, pp. 1–29, 2021, doi: 10.1002/admt.202100410.

[36] D. Li, Y. Wang, and Y. Xia, "Electrospinning of polymeric and ceramic nanofibers as uniaxially aligned arrays," *Nano Lett.*, vol. 3, no. 8, pp. 1167–1171, 2003, doi: 10.1021/nl0344256.

[37] P. D. Dalton, D. Klee, and M. Möller, "Electrospinning with dual collection rings," *Polymer (Guildf).*, vol. 46, no. 3, pp. 611–614, 2005, doi: 10.1016/j.polymer.2004.11.075.

[38] J. Wu *et al.*, "Electrospun nanoyarn scaffold and its application in tissue engineering," *Mater. Lett.*, vol. 89, pp. 146–149, 2012, doi: 10.1016/j.matlet.2012.08.141.

[39] C. G. Taylor and E. L. Pendleton, "Characterization of an Epoxy-Anhydride Ablative System Using Computer Treatment of Analytical Results," *J. Macromol. Sci. Part A - Chem.*, vol. 3, no. 3, pp. 453–470, 1969, doi: 10.1080/10601326908053822.

[40] G. Taylor and P. R. S. L. A, "Disintegration of water drops in an electric field," *Proc. R. Soc. London. Ser. A. Math. Phys. Sci.*, vol. 280, no. 1382, pp. 383–397, 1964, doi: 10.1098/rspa.1964.0151.

[41] M. Jr and W. Ep, "Electrohydrodynamics of a current-carrying semi-insulating jet," vol. 47, pp. 127–143, 1971.

USC UNIVERSIDADE DE SANTIAGO DE COMPOSTELA

[42] S. Kailasa, M. S. B. Reddy, M. R. Maurya, B. G. Rani, K. V. Rao, and K. K. Sadasivuni, "Electrospun Nanofibers: Materials, Synthesis Parameters, and Their Role in Sensing Applications," *Macromol. Mater. Eng.*, vol. 306, no. 11, pp. 1–36, 2021, doi: 10.1002/mame.202100410.

[43] C. Zhang and X. Yuan, "EUROPEAN POLYMER Study on morphology of electrospun poly ( vinyl alcohol ) mats," vol. 41, pp. 423–432, 2005, doi: 10.1016/j.eurpolymj.2004.10.027.

[44] N. Joy, R. Anuraj, A. Viravalli, H. N. Dixit, and S. Samavedi, "Coupling between voltage and tip-to-collector distance in polymer electrospinning: Insights from analysis of regimes, transitions and cone/jet features," *Chem. Eng. Sci.*, vol. 230, p. 116200, 2021, doi: 10.1016/j.ces.2020.116200.

[45] A. Asti and L. Gioglio, "Natural and synthetic biodegradable polymers: Different scaffolds for cell expansion and tissue formation," *Int. J. Artif. Organs*, vol. 37, no. 3, pp. 187–205, 2014, doi: 10.5301/ijao.5000307.

[46] H. Seddiqi *et al.*, *Cellulose and its derivatives: towards biomedical applications*, vol. 28, no. 4. Springer Netherlands, 2021. doi: 10.1007/s10570-020-03674-w.

[47] H. Rodríguez-Tobías, G. Morales, and D. Grande, "Comprehensive review on electrospinning techniques as versatile approaches toward antimicrobial biopolymeric composite fibers," *Mater. Sci. Eng. C*, vol. 101, no. March, pp. 306–322, 2019, doi: 10.1016/j.msec.2019.03.099.

[48] V. Siracusa, "Microbial Degradation of Synthetic Biopolymers Waste," *Polymers (Basel).*, vol. 11, no. 6, 2019, doi: 10.3390/polym11061066.

[49] A. K. Haghi and M. Akbari, "Trends in electrospinning of natural nanofibers," *Phys. Status Solidi Appl. Mater. Sci.*, vol. 204, no. 6, pp. 1830–1834, 2007, doi: 10.1002/pssa.200675301.

[50] S. Sukigara, M. Gandhi, J. Ayutsede, M. Micklus, and F. Ko, "Regeneration of Bombyx mori silk by electrospinning - Part 1: Processing parameters and geometric properties," *Polymer (Guildf).*, vol. 44, no. 19, pp. 5721–5727, 2003, doi: 10.1016/S0032-3861(03)00532-9.

[51] C. S. Ki, D. H. Baek, K. D. Gang, K. H. Lee, I. C. Um, and Y. H. Park, "Characterization of gelatin nanofiber prepared from gelatin-formic acid solution," *Polymer (Guildf).*, vol. 46, no. 14, pp. 5094–5102, 2005, doi: 10.1016/j.polymer.2005.04.040.

[52] P. Gupta, C. Elkins, T. E. Long, and G. L. Wilkes, "Electrospinning of linear homopolymers of poly(methyl methacrylate): Exploring relationships between fiber formation, viscosity, molecular weight and concentration in a good solvent," *Polymer (Guildf).*, vol. 46, no. 13, pp. 4799–4810, 2005, doi: 10.1016/j.polymer.2005.04.021.

[53] S. S. Ojha, M. Afshari, R. Kotek, R. E. Gorga, and N. Carolina, "Morphology of Electrospun Nylon-6 Nanofibers as a Function of Molecular Weight and Processing Parameters," 2007, doi: 10.1002/app.

[54] M. G. McKee, J. M. Layman, M. P. Cashion, and T. E. Long, "Phospholipid nonwoven electrospun membranes," *Science (80-. ).*, vol. 311, no. 5759, pp. 353–

USC UNIVERSIDADE DE SANTIAGO COMPOSTELA

355, 2006, doi: 10.1126/science.1119790.

[55] V. Pillay *et al.*, "A Review of the Effect of Processing Variables on the Fabrication of Electrospun Nanofibers for Drug Delivery Applications," *J. Nanomater.*, vol. 2013, p. 22, 2013, doi: http://dx.doi.org/10.1155/2013/789289.

[56] S. Tan, R. Inai, M. Kotaki, and S. Ramakrishna, "Systematic parameter study for ultra-fine fiber fabrication via electrospinning process," vol. 46, pp. 6128–6134, 2005, doi: 10.1016/j.polymer.2005.05.068.

[57] M. M. Hohman, M. Shin, G. Rutledge, and M. P. Brenner, "Electrospinning and electrically forced jets. II. Applications," *Phys. Fluids*, vol. 13, no. 8, pp. 2221–2236, 2001, doi: 10.1063/1.1384013.

[58] E. Polyetherimide, A. Abutaleb, D. Lolla, A. Aljuhani, and H. U. Shin, "Effects of Surfactants on the Morphology and," pp. 1–14, doi: 10.3390/fib5030033.

[59] D. P. Bhattarai, L. E. Aguilar, C. H. Park, and C. S. Kim, "A Review on Properties of Natural and Synthetic Based Electrospun Fibrous Materials for Bone Tissue Engineering," 2018, doi: 10.3390/membranes8030062.

[60] B. C. Xinhua Zonga, Kwangsok Kima, Dufei Fangb, Shaofeng Rana, Benjamin S. Hsiaoa,*, "Structure and process relationship of electrospun bioabsorbable nanofiber membranes," vol. 43, pp. 4403–4412, 202AD.

[61] I. Hayati, A. Bailey, and T. . Tadros, "Investigations into the mechanism of electrohydrodynamic spraying of liquids," *J. Colloid Interface Sci.*, vol. 117, no. 1, pp. 222–230, 1987, doi: 10.1016/0021-9797(87)90186-x.

[62] N. A. M. Barakat, M. A. Kanjwal, F. A. Sheikh, and H. Yong, "Spider-net within the N6 , PVA and PU electrospun nanofiber mats using salt addition : Novel strategy in the electrospinning process," *Polymer (Guildf).*, vol. 50, no. 18, pp. 4389–4396, 2009, doi: 10.1016/j.polymer.2009.07.005.

[63] A. Ghaderpour and F. Amiri, "Altering the characterization of nanofibers by changing the electrospinning parameters and their application in tissue engineering , drug delivery , and gene delivery systems," no. January, 2021, doi: 10.1002/pat.5242.

[64] Y. Su *et al.*, "Temperature effect on electrospinning of nanobelts: The case of hafnium oxide," *Nanotechnology*, vol. 22, no. 28, 2011, doi: 10.1088/0957-4484/22/28/285609.

[65] J. Pelipenko, J. Kristl, B. Jankovi, and P. Kocbek, "The impact of relative humidity during electrospinning on the morphology and mechanical properties of nanofibers," vol. 456, pp. 125–134, 2013, doi: 10.1016/j.ijpharm.2013.07.078.

[66] Y. Montoya, J. Cardenas, J. Bustamante, and R. Valencia, "Effect of sequential electrospinning and co-electrospinning on morphological and fluid mechanical wall properties of polycaprolactone and bovine gelatin scaffolds , for potential use in small diameter vascular grafts," *Biomater. Res.*, vol. 25, no. 38, pp. 1–17, 2021, doi: https://doi.org/10.1186/s40824-021-00240-8.

[67] B. Z. Sun, E. Zussman, A. L. Yarin, J. H. Wendorff, and A. Greiner, "Compound Core ± Shell Polymer Nanofibers," no. 22, pp. 1929–1932, 2003, doi: 10.1002/adma.200305136.

USC UNIVERSIDADE DE SANTIAGO DE COMPOSTELA

[68] W. Huang, T. Hibino, S. Suye, and S. Fujita, "Electrospun collagen core/poly-l-lactic acid shell nanofibers for prolonged release of hydrophilic drug," pp. 5703–5711, 2021, doi: 10.1039/d0ra08353d.

[69] Y. Xia, "Electrospinning of nanofibers with core-sheath , hollow , or porous structures Jesse T . McCann , Dan Li and Younan Xia *," *J. Mater. Chem.*, vol. 15, no. 7, pp. 727–734, 2005, doi: https://doi.org/10.1039/B415094E.

[70] A. Khalf and S. V Madihally, "European Journal of Pharmaceutics and Biopharmaceutics Recent advances in multiaxial electrospinning for drug delivery," *Eur. J. Pharm. Biopharm.*, vol. 112, pp. 1–17, 2017, doi: 10.1016/j.ejpb.2016.11.010.

[71] V. Kalra, J. H. Lee, J. H. Park, M. Marquez, and Y. L. Joo, "Confined Assembly of Asymmetric Block-Copolymer Nanofibers via Multiaxial Jet Electrospinning," pp. 2323–2332, 2009, doi: 10.1002/smll.200900157.

[72] D. Yu, X. Li, X. Wang, J. Yang, S. W. A. Bligh, and G. R. Williams, "Nano fi bers Fabricated Using Triaxial Electrospinning as Zero Order Drug Delivery Systems," 2015, doi: 10.1021/acsami.5b06007.

[73] X. Li, Y. He, J. Hou, G. Yang, and S. Zhou, "A Time-Programmed Release of Dual Drugs from an Implantable Trilayer Structured Fiber Device for Synergistic Treatment of Breast Cancer," vol. 1902262, pp. 1–14, 2020, doi: 10.1002/smll.201902262.

[74] W. K. Son, J. H. Youk, and W. H. Park, "Preparation of Ultrafine Oxidized Cellulose Mats via Electrospinning," vol. 5, no. 1, pp. 197–201, 2004, doi: https://doi.org/10.1021/bm034312g.

[75] M. Wang, D. Yu, S. Wan, and A. Bligh, "Progress in preparing electrospun Janus fibers and their applications," *Appl. Mater. Today*, vol. 31, no. October 2022, p. 101766, 2023, doi: 10.1016/j.apmt.2023.101766.

[76] P. Gupta and G. L. Wilkes, "Some investigations on the fiber formation by utilizing a side-by-side bicomponent electrospinning approach," vol. 44, pp. 6353–6359, 2003, doi: 10.1016/S0032-3861(03)00616-5.

[77] Y. Su, M. B. Taskin, M. Dong, X. Han, F. Besenbacher, and M. Chen, "A biocompatible artificial tendril with a spontaneous 3D Janus multi-helix-perversion configuration," *Mater. Chem. Front.*, vol. 4, no. 7, pp. 2149–2156, 2020, doi: 10.1039/d0qm00125b.

[78] G. Chen, Y. Xu, D. Yu, D. Zhang, N. P. Chatterton, and K. N. White, "Structure-tunable Janus fibers fabricated using spinnerets with varying port angles †," *Chem. Commun.*, vol. 51, pp. 4623–4626, 2015, doi: 10.1039/C5CC00378D.

[79] G. Jin, S. Lee, S. Kim, M. Kim, and J. Jang, "Bicomponent electrospinning to fabricate three-dimensional hydrogel-hybrid nanofibrous scaffolds with spatial fiber tortuosity," pp. 793–804, 2014, doi: 10.1007/s10544-014-9883-z.

[80] Y. Li *et al.*, "Developments of Advanced Electrospinning Techniques: A Critical Review," *Adv. Mater. Technol.*, vol. 6, no. 11, pp. 1–29, 2021, doi: 10.1002/admt.202100410.

USC UNIVERSIDADE DE SANTIAGO DE COMPOSTELA

[81] Y. Chen *et al.*, "Preparation of Charged Mosaic Membrane of Sodium Polystyrene Sulfonate and Poly ( 4-vinyl pyridine ) by Conjugate Electrospinning," vol. 40716, pp. 1–9, 2014, doi: 10.1002/app.40716.

[82] J. He, K. Qi, Y. Zhou, and S. Cui, "Multiple Conjugate Electrospinning Method for the Preparation of Continuous Polyacrylonitrile Nanofiber Yarn," vol. 40137, pp. 2–7, 2014, doi: 10.1002/app.40137.

[83] R. S. Bhattarai, R. D. Bachu, S. H. S. Boddu, and S. Bhaduri, "Biomedical Applications of Electrospun Nanofibers : Drug and Nanoparticle Delivery," 2018, doi: 10.3390/pharmaceutics11010005.

[84] R. Nayak, R. Padhye, and L. Arnold, *Melt-electrospinning of nanofibers*. Elsevier Ltd., 2017. doi: 10.1016/B978-0-08-100907-9.00002-7.

[85] W. Feng *et al.*, "Coaxial electrospun membranes with thermal energy storage and shape memory functions for simultaneous thermal / moisture management in personal cooling textiles," *Eur. Polym. J.*, vol. 145, no. November 2020, p. 110245, 2021, doi: 10.1016/j.eurpolymj.2020.110245.

[86] H. Zhong, J. Huang, J. Wu, and J. Du, "Electrospinning nanofibers to 1D , 2D , and 3D scaffolds and their biomedical applications," *Nano Res.*, vol. 15, no. 2, pp. 787–804, 2022, doi: https://doi.org/10.1007/s12274-021-3593-7.

[87] Y. Yokoyama, S. Hattori, C. Yoshikawa, Y. Yasuda, and H. Koyama, "Novel wet electrospinning system for fabrication of spongiform nano fi ber 3-dimensional fabric," *Mater. Lett.*, vol. 63, no. 9–10, pp. 754–756, 2009, doi: 10.1016/j.matlet.2008.12.042.

[88] R. Nanomedicine *et al.*, "3D electrospun silk fibroin nanofibers for fabrication of artificial skin," *Nanomedicine Nanotechnology, Biol. Med.*, vol. 11, no. 3, pp. 681–691, 2015, doi: 10.1016/j.nano.2014.11.007.

[89] M. Vong, E. Speirs, C. Klomkliang, I. Akinwumi, W. Nuansing, and N. Radacsi, "RSC Advances," pp. 15501–15512, 2018, doi: 10.1039/c7ra13278f.

[90] P. Sofokleous, E. Stride, W. Bonfield, and M. Edirisinghe, "Design, construction and performance of a portable handheld electrohydrodynamic multi-needle spray gun for biomedical applications," *Mater. Sci. Eng. C*, vol. 33, no. 1, pp. 213–223, 2013, doi: 10.1016/j.msec.2012.08.033.

[91] S. C. Xu *et al.*, "A battery-operated portable handheld electrospinning apparatus," *Nanoscale*, vol. 7, no. 29, pp. 12351–12355, 2015, doi: 10.1039/c5nr02922h.

[92] R. A. Revia, B. A. Wagner, and M. Zhang, "A portable electrospinner for nanofiber synthesis and its application for cosmetic treatment of alopecia," *Nanomaterials*, vol. 9, no. 9, 2019, doi: 10.3390/nano9091317.

[93] M. M. Abdul Hameed, S. A. P. Mohamed Khan, B. M. Thamer, N. Rajkumar, H. El-Hamshary, and M. El-Newehy, "Electrospun nanofibers for drug delivery applications: Methods and mechanism," *Polym. Adv. Technol.*, vol. 34, no. 1, pp. 6–23, 2023, doi: 10.1002/pat.5884.

USC UNIVERSIDADE DE SANTIAGO DE COMPOSTELA

[94] Y. Liu, X. Chen, Y. Liu, Y. Gao, and P. Liu, "Electrospun Coaxial Fibers to Optimize the Release of Poorly Water-Soluble Drug," *Polymers (Basel).*, vol. 14, no. 469, pp. 1–13, 2022, doi: https://doi.org/ 10.3390/polym14030469.

[95] S. Kajdič, O. Planinšek, M. Gašperlin, and P. Kocbek, "Electrospun nanofibers for customized drug-delivery systems," *J. Drug Deliv. Sci. Technol.*, vol. 51, no. March, pp. 672–681, 2019, doi: 10.1016/j.jddst.2019.03.038.

[96] P. P. P.Preetha, A.Srinivasa Rao, "Biphasic drug delivery in controlled release formulations – A review," *Int. J. Pharm. Technol.*, vol. 6, no. 10, pp. 3046–3060, 2015.

[97] N. Nikmaram *et al.*, "Emulsion-based systems for fabrication of electrospun nanofibers: Food, pharmaceutical and biomedical applications," *RSC Adv.*, vol. 7, no. 46, pp. 28951–28964, 2017, doi: 10.1039/c7ra00179g.

[98] P. McClellan and W. J. Landis, "Recent Applications of Coaxial and Emulsion Electrospinning Methods in the Field of Tissue Engineering," *Biores. Open Access*, vol. 5, no. 1, pp. 212–227, 2016, doi: 10.1089/biores.2016.0022.

[99] X. Luo, C. Xie, H. Wang, C. Liu, S. Yan, and X. Li, "Antitumor activities of emulsion electrospun fibers with core loading of hydroxycamptothecin via intratumoral implantation," *Int. J. Pharm.*, vol. 425, no. 1–2, pp. 19–28, 2012, doi: 10.1016/j.ijpharm.2012.01.012.

[100] S. P. Miguel *et al.*, "Electrospun polymeric nanofibres as wound dressings: A review," *Colloids Surfaces B Biointerfaces*, vol. 169, pp. 60–71, 2018, doi: 10.1016/j.colsurfb.2018.05.011.

[101] A. Szentivanyi, T. Chakradeo, H. Zernetsch, and B. Glasmacher, "Electrospun cellular microenvironments : Understanding controlled release and scaffold structure," *Adv. Drug Deliv. Rev.*, vol. 63, no. 4–5, pp. 209–220, 2011, doi: 10.1016/j.addr.2010.12.002.

[102] W. Song, Z. Ma, C. Wang, H. Li, and Y. He, "Pro-chondrogenic and immunomodulatory melatonin-loaded electrospun membranes for tendon-to-bone healing," *J. Mater. Chem. B*, vol. 7, no. 42, pp. 6564–6575, 2019, doi: 10.1039/c9tb01516g.

[103] G. Kuang, Z. Zhang, S. Liu, and D. Zhou, "Biomaterials Science Biphasic drug release from electrospun polyblend nano fi bers for optimized local cancer treatment †," 2017, doi: 10.1039/c7bm01018d.

[104] A. Laha, C. S. Sharma, and S. Majumdar, "Sustained drug release from multi-layered sequentially crosslinked electrospun gelatin nano fi ber mesh," *Mater. Sci. Eng. C*, vol. 76, pp. 782–786, 2017, doi: 10.1016/j.msec.2017.03.110.

[105] C. A. García-González, A. Concheiro, and C. Alvarez-Lorenzo, "Processing of Materials for Regenerative Medicine Using Supercritical Fluid Technology," *Bioconjug. Chem.*, vol. 26, no. 7, pp. 1159–1171, 2015, doi: 10.1021/bc5005922.

[106] K. Li *et al.*, "Three-dimensional magnetic fibrous scaffold with icariin expanded by supercritical CO2 for bone tissue engineering under static magnetic field," *Compos. Part B Eng.*, vol. 226, no. July, p. 109304, 2021, doi: 10.1016/j.compositesb.2021.109304.

[107] J. Wang and M. Windbergs, "Functional electrospun fibers for the treatment of human skin wounds," *Eur. J. Pharm. Biopharm.*, vol. 119, pp. 283–299, 2017, doi: 10.1016/j.ejpb.2017.07.001.

USC DE SANTIAGO DE COMPOSTELA

[108] R. S. Tiğli, N. M. Kazaroğlu, B. Maviş, and M. Gumusderelioglu, "Cellular behavior on epidermal growth factor (EGF)-immobilized PCL/gelatin nanofibrous scaffolds," *J. Biomater. Sci. Polym. Ed.*, vol. 22, no. 1–3, pp. 207–223, 2011, doi: 10.1163/092050609X12591500475424.

[109] H. Daemi, M. Mashayekhi, and M. Pezeshki Modaress, "Facile fabrication of sulfated alginate electrospun nanofibers," *Carbohydr. Polym.*, vol. 198, no. May, pp. 481–485, 2018, doi: 10.1016/j.carbpol.2018.06.105.

[110] J. S. Choi, K. W. Leong, and H. S. Yoo, "In vivo wound healing of diabetic ulcers using electrospun nanofibers immobilized with human epidermal growth factor (EGF)," *Biomaterials*, vol. 29, no. 5, pp. 587–596, 2008, doi: 10.1016/j.biomaterials.2007.10.012.

[111] X. Sun *et al.*, "BFGF-grafted electrospun fibrous scaffolds via poly(dopamine) for skin wound healing," *J. Mater. Chem. B*, vol. 2, no. 23, pp. 3636–3645, 2014, doi: 10.1039/c3tb21814g.

[112] Z. Yang, H. Peng, W. Wang, and T. Liu, "Crystallization behavior of poly(ε-caprolactone)/layered double hydroxide nanocomposites," *J. Appl. Polym. Sci.*, vol. 116, no. 5, pp. 2658–2667, 2010, doi: 10.1002/app.

[113] S. Nam, S. Y. Lee, and H. Cho, "Journal of Colloid and Interface Science Phloretin-loaded fast dissolving nanofibers for the locoregional therapy of oral squamous cell carcinoma," *J. Colloid Interface Sci.*, vol. 508, pp. 112–120, 2017, doi: 10.1016/j.jcis.2017.08.030.

[114] K. Anjireddy and S. Karpagam, "International Journal of Biological Macromolecules Chitosan nanofilm and electrospun nanofiber for quick drug release in the treatment of Alzheimer ' s disease : In vitro and in vivo evaluation," *Int. J. Biol. Macromol.*, vol. 105, pp. 131–142, 2017, doi: 10.1016/j.ijbiomac.2017.07.021.

[115] W. Cui, X. Li, X. Zhu, G. Yu, S. Zhou, and J. Weng, "Investigation of Drug Release and Matrix Degradation of Electrospun Poly ( DL -lactide ) Fibers with Paracetanol Inoculation," *Biomacromolecules*, vol. 7, pp. 1623–1629, 2006, doi: 10.1021/bm060057z.

[116] J. Zeng *et al.*, "Biodegradable electrospun fibers for drug delivery," vol. 92, pp. 227–231, 2003, doi: 10.1016/S0168-3659(03)00372-9.

[117] Y. You, B. Min, S. J. Lee, T. S. Lee, and W. H. Park, "In Vitro Degradation Behavior of Electrospun Polyglycolide , Polylactide , and Poly ( lactide- co - glycolide )," pp. 2–9, 2004, doi: 10.1002/app.21116.

[118] X. Zhu *et al.*, "Anti-Neoplastic Cytotoxicity of SN-38-Loaded PCL / Gelatin Electrospun Composite Nanofiber Scaffolds against Human," *J. Pharm. Sci.*, vol. 104, no. 12, pp. 4345–4354, 2015, doi: 10.1002/jps.24684.

[119] Q. Sang, G. R. Williams, H. Wu, K. Liu, H. Li, and L. Zhu, "Materials Science & Engineering C Electrospun gelatin / sodium bicarbonate and poly ( lactide- co - ε - caprolactone )/ sodium bicarbonate nano fi bers as drug delivery systems," *Mater. Sci. Eng. C*, vol. 81, no. July, pp. 359–365, 2017, doi: 10.1016/j.msec.2017.08.007.

[120] J. Hu, H. Li, G. R. Williams, H. Yang, L. Tao, and L. Zhu, "Electrospun Poly ( N-

USC UNIVERSIDADE DE SANTIAGO DE COMPOSTELA

isopropylacrylamide )/ Ethyl Cellulose Nano fi bers as Thermoresponsive Drug Delivery Systems," vol. 105, pp. 1104–1112, 2016, doi: 10.1016/S0022-3549(15)00191-4.

[121] Y. Li *et al.*, "Light responsive hybrid nanofibres for on-demand therapeutic drug and cell delivery," 2016, doi: 10.1002/term.

[122] J. Yun, J. S. Im, Y. Lee, and H. Kim, "Electro-responsive transdermal drug delivery behavior of PVA / PAA / MWCNT nanofibers," *Eur. Polym. J.*, vol. 47, no. 10, pp. 1893–1902, 2011, doi: 10.1016/j.eurpolymj.2011.07.024.

[123] Y. Kim, M. Ebara, and T. Aoyagi, "FULL PAPER A Smart Hyperthermia Nanofi ber with Switchable Drug Release for Inducing Cancer Apoptosis," pp. 1–9, 2013, doi: 10.1002/adfm.201300746.

[124] X. Wang, D. Yu, X. Li, S. W. A. Bligh, and G. R. Williams, "Electrospun medicated shellac nano fi bers for colon-targeted drug delivery," *Int. J. Pharm.*, vol. 490, no. 1–2, pp. 384–390, 2015, doi: 10.1016/j.ijpharm.2015.05.077.

[125] Y. Sakai *et al.*, "Corticostriatal functional connectivity in non-medicated patients with," vol. 26, pp. 463–469, 2011, doi: 10.1016/j.eurpsy.2010.09.005.

[126] M. Ekor, "The growing use of herbal medicines : issues relating to adverse reactions and challenges in monitoring safety," vol. 4, no. January, pp. 1–10, 2014, doi: 10.3389/fphar.2013.00177.

[127] C. L. Ventola, "The Antibiotic Resistance Crisis Part 1 : Causes and Threats," *Pharm. Ther.*, vol. 40, no. 4, pp. 277–283, 2015.

[128] D. Chinemerem Nwobodo *et al.*, "Antibiotic resistance: The challenges and some emerging strategies for tackling a global menace," *J. Clin. Lab. Anal.*, vol. 36, no. 9, pp. 1–10, 2022, doi: 10.1002/jcla.24655.

[129] C. H. Rammelkamp and T. Maxon, "Experimental Biology and Medicine," 1942, doi: 10.3181/00379727-51-13986.

[130] M. Gajdács, "The Continuing Threat of Methicillin-Resistant Staphylococcus aureus," *Antibiotics*, vol. 8, p. 52, 2019, doi: 10.3390/antibiotics8020052.

[131] J. O'Neill, "Tackling Drug-Resistance Infections Globally: Final Report and Recommendations. The review on Antimicrobial Resistance Chaired by Jim O'Neill.[Online …," no. May, pp. 1–84, 2016, [Online]. Available: https://amr-review.org/sites/default/files/160518_Final paper_with cover.pdf

[132] The Lancet, "Antimicrobial resistance: time to repurpose the Global Fund," *Lancet*, vol. 399, no. 10322, p. 335, 2022, doi: 10.1016/S0140-6736(22)00091-5.

[133] M. Hosseini *et al.*, "Prediction of tsunami of resistance to some antibiotics is not fetched which used during COVID- - 19 pandemic," no. January, pp. 1–10, 2023, doi: 10.1002/jcla.24959.

[134] EClinicalMedicine, "Antimicrobial resistance: a top ten global public health threat," *eClinicalMedicine*, vol. 41, p. 101221, 2021, doi: 10.1016/j.eclinm.2021.101221.

USC UNIVERSIDADE DE SANTIAGO DE COMPOSTELA

[135] C. J. Murray *et al.*, "Global burden of bacterial antimicrobial resistance in 2019: a

systematic analysis," *Lancet*, vol. 399, no. 10325, pp. 629–655, 2022, doi: 10.1016/S0140-6736(21)02724-0.

[136] A. Cassini *et al.*, "Attributable deaths and disability-adjusted life-years caused by infections with antibiotic-resistant bacteria in the EU and the European Economic Area in 2015: a population-level modelling analysis," *Lancet Infect. Dis.*, vol. 19, no. 1, pp. 56–66, 2019, doi: 10.1016/S1473-3099(18)30605-4.

[137] S. Basak, P. Singh, and M. Rajurkar, "Multidrug Resistant and Extensively Drug Resistant Bacteria: A Study," *J. Pathog.*, vol. 2016, pp. 1–5, 2016, doi: 10.1155/2016/4065603.

[138] H. Endale, M. Mathewos, and D. Abdeta, "Potential Causes of Spread of Antimicrobial Resistance and Preventive Measures in One Health Perspective-A Review," *Infect. Drug Resist.*, vol. 16, no. December, pp. 7515–7545, 2023, doi: 10.2147/IDR.S428837.

[139] S. K. Ahmed *et al.*, "Antimicrobial resistance: Impacts, challenges, and future prospects," *J. Med. Surgery, Public Heal.*, vol. 2, no. March, p. 100081, 2024, doi: 10.1016/j.glmedi.2024.100081.

[140] H. Mohanty, S. Pachpute, and R. P. Yadav, "Mechanism of drug resistance in bacteria: efflux pump modulation for designing of new antibiotic enhancers," *Folia Microbiol. (Praha).*, vol. 66, no. 5, pp. 727–739, 2021, doi: 10.1007/s12223-021-00910-z.

[141] A. Asghar *et al.*, "An insights into emerging trends to control the threats of antimicrobial resistance (AMR): an address to public health risks," *Arch. Microbiol.*, vol. 206, no. 2, 2024, doi: 10.1007/s00203-023-03800-9.

[142] J. L. Martinez, "Drug resistance General principles of antibiotic resistance in bacteria," *Drug Discov. Today Technol.*, vol. 11, pp. 33–39, 2014, doi: 10.1016/j.ddtec.2014.02.001.

[143] E. Van Duijkeren, A. Schink, M. C. Roberts, Y. Wang, and S. Schwarz, "Mechanisms of Bacterial Resistance to Antimicrobial Agents," *Microbiol. Spectr.*, vol. 6, no. 2, 2017, doi: 10.1128 /microbiolspec.ARBA-0019-2017.

[144] J. M. A. Blair, M. A. Webber, A. J. Baylay, D. O. Ogbolu, and L. J. V Piddock, "Molecular mechanisms of antibiotic resistance," *Nat. Publ. Gr.*, vol. 13, no. 1, pp. 42–51, 2014, doi: 10.1038/nrmicro3380.

[145] G. Zhou, Q. Shi, X. Huang, and X. Xie, "The Three Bacterial Lines of Defense against Antimicrobial Agents," pp. 21711–21733, 2015, doi: 10.3390/ijms160921711.

[146] A. Tello, B. Austin, and T. C. Telfer, "Selective pressure of antibiotic pollution on bacteria of importance to public health," *Environ. Health Perspect.*, vol. 120, no. 8, pp. 1100–1106, 2012, doi: 10.1289/ehp.1104650.

[147] H. N. Xian-Zhi Li, "Efflux-Mediated Drug Resistance in Bacteria: an Update," *Drugs*, vol. 69, no. 12, pp. 1555–1623, 2010, doi: 10.2165/11317030-000000000-00000.Efflux-Mediated.

[148] T. Li *et al.*, "Bacterial resistance to antibacterial agents: Mechanisms, control strategies, and implications for global health," *Sci. Total Environ.*, vol. 860, no.

November 2022, p. 160461, 2023, doi: 10.1016/j.scitotenv.2022.160461.

[149] M. A. Kohanski, D. J. Dwyer, and J. J. Collins, "How antibiotics kill bacteria: From targets to networks," *Nat. Rev. Microbiol.*, vol. 8, no. 6, pp. 423–435, 2010, doi: 10.1038/nrmicro2333.

[150] V. Kumar, S. L. Viviani, J. Ismail, S. Agarwal, A. Bonomo, and F. V. D. A. Id, "Structural analysis of the boronic acid β - lactamase inhibitor vaborbactam binding to Pseudomonas aeruginosa penicillin-binding protein 3," pp. 1–16, 2021, doi: 10.1371/journal.pone.0258359.

[151] L. S. Redgrave, S. B. Sutton, M. A. Webber, and L. J. V Piddock, "Fluoroquinolone resistance : mechanisms , impact on bacteria , and role in evolutionary success," *Trends Microbiol.*, vol. 22, no. 8, pp. 438–445, 2014, doi: 10.1016/j.tim.2014.04.007.

[152] R. R. N. A. Methyltransferases, "A m i n o g l y c o s i d e Re s i s t a n c e The Emergence of Acquired 16S," *Infect. Dis. Clin. NA*, vol. 30, no. 2, pp. 523–537, 2016, doi: 10.1016/j.idc.2016.02.011.

[153] M. H. Muhammad, A. L. Idris, X. Fan, Y. Guo, Y. Yu, and X. Jin, "Beyond Risk : Bacterial Biofilms and Their Regulating Approaches," vol. 11, no. May, pp. 1–20, 2020, doi: 10.3389/fmicb.2020.00928.

[154] H. Flemming and J. Wingender, "Relevance of microbial extracellular polymeric substances ( EPSs ) – Part I : Structural and ecological aspects," *Water Sci. Technol.*, vol. 43, no. 6, pp. 1–8, 2001, doi: https://doi.org/10.2166/wst.2001.0326.

[155] G. Laverty, S. P. Gorman, and B. F. Gilmore, "Biomolecular Mechanisms of Pseudomonas aeruginosa and Escherichia coli Biofilm Formation," pp. 596–632, 2014, doi: 10.3390/pathogens3030596.

[156] A. J. Weisberg and J. H. Chang, "Mobile Genetic Element Flexibility as an Underlying Principle to Bacterial Evolution," *Annu. Rev. Microbiol.*, vol. 77, pp. 603–624, 2023, doi: 10.1146/annurev-micro-032521-022006.

[157] P. Gilbert, T. Maira-litran, and J. M, "The Physiology and Collective Recalcitrance of Microbial Biofilm Communities," *Adv. Microb. Physiol.*, vol. 46, pp. 203–256, 2002, doi: https://doi.org/10.1016/S0065-2911(02)46005-5.

[158] W. R. Miller and C. A. Arias, "ESKAPE pathogens: antimicrobial resistance, epidemiology, clinical impact and therapeutics," *Nat. Rev. Microbiol.*, vol. 22, no. 10, pp. 598–616, 2024, doi: 10.1038/s41579-024-01054-w.

[159] M. Vouga and G. Greub, "Emerging bacterial pathogens: The past and beyond," *Clin. Microbiol. Infect.*, vol. 22, no. 1, pp. 12–21, 2016, doi: 10.1016/j.cmi.2015.10.010.

[160] G.-H. Tan, Q.-W. Low, H.-C. Lim, H.-K. Seah, and H.-K. Chan, "Inappropriate Antibiotic Utilization: Outpatient Prescription Review of a Regional Secondary Hospital in Kedah, Malaysia," *J. Pharm. Pract. Community Med.*, vol. 3, no. 4, pp. 215–219, 2017, doi: 10.5530/jppcm.2017.4.62.

[161] P. Dadgostar, "Antimicrobial resistance: implications and costs," *Infect. Drug Resist.*, vol. 12, pp. 3903–3910, 2019, doi: 10.2147/IDR.S234610.

USC COMPOSTELA

[162] I. Boszczowski, B. S. Kliemann, A. S. Levin, M. Luı, and J. J. Lewis, “Socioeconomic Determinants of Antibiotic Consumption in the State of S ã o Paulo , Brazil : The Effect of Restricting Over-The-Counter,” no. Did, pp. 1–14, 2016, doi: 10.5061/dryad.mt685.

[163] T. Pulingam *et al.*, “Antimicrobial resistance: Prevalence, economic burden, mechanisms of resistance and strategies to overcome,” *Eur. J. Pharm. Sci.*, vol. 170, p. 106103, 2022, doi: 10.1016/j.ejps.2021.106103.

[164] T. Mahtab *et al.*, “Journal of Infection and Public Health Antibiotic resistance in microbes : History , mechanisms , therapeutic strategies and future prospects,” vol. 14, pp. 1750–1766, 2021, doi: 10.1016/j.jiph.2021.10.020.

[165] R. Smith and J. Coast, “The true cost of antimicrobial resistance,” *BMJ*, vol. 346, no. 7899, pp. 1–5, 2013, doi: 10.1136/bmj.f1493.

[166] E. Kobeissi, M. Menassa, K. Moussally, E. Repetto, I. Soboh, and M. Hajjar, “The socioeconomic burden of antibiotic resistance in conflict-affected settings and refugee hosting countries : a systematic scoping review,” *Confl. Health*, vol. 15, no. 21, pp. 1–9, 2021, doi: https://doi.org/10.1186/s13031-021-00357-6.

[167] W. Wang *et al.*, “Antibiotic resistance : a rundown of a global crisis,” *Infect. Drug Resist.*, vol. 11, pp. 1645–1658, 2018, doi: http://dx.doi.org/10.2147/IDR.S173867.

[168] X. Zhen, C. S. Lundborg, X. Sun, X. Hu, and H. Dong, “Economic burden of antibiotic resistance in ESKAPE organisms : a systematic review,” *Antimicrob. Resist. Infect. Control*, vol. 7, no. 8, p. 137, 2019, doi: https://doi.org/10.1186/s13756-019-0590-7.

[169] F. Wan, M. D. T. Torres, J. Peng, and C. de la Fuente-Nunez, “Deep-learning-enabled antibiotic discovery through molecular de-extinction,” *Nat. Biomed. Eng.*, vol. 8, no. 7, pp. 854–871, 2024, doi: 10.1038/s41551-024-01201-x.

[170] F. Wong, C. de la Fuente-Nunez, and J. J. Collins, “Leveraging artificial intelligence in the fight against infectious diseases,” *Science (80-. ).*, vol. 381, no. 6654, pp. 164–170, 2023, doi: 10.1126/science.adh1114.

[171] Y. Wang, K. J. Stebe, C. de la Fuente-Nunez, and R. Radhakrishnan, “Computational Design of Peptides for Biomaterials Applications,” *ACS Appl. Bio Mater.*, vol. 7, no. 2, pp. 617–625, 2024, doi: 10.1021/acsabm.2c01023.

[172] M. D. T. Torres *et al.*, “Mining human microbiomes reveals an untapped source of peptide antibiotics,” *Cell*, vol. 187, no. 19, pp. 5453-5467.e15, 2024, doi: 10.1016/j.cell.2024.07.027.

[173] C. de la Fuente-Nunez, “Toward Autonomous Antibiotic Discovery,” *mSystems*, vol. 4, no. 3, pp. 10–14, 2019, doi: 10.1128/msystems.00151-19.

[174] R. D. Forrest, “Early history of wound treatment,” *J. R. Soc. Med.*, vol. 75, no. 3, pp. 198–205, 1982, doi: 10.1177/014107688207500310.

[175] J. B. Shah, “The history of wound care,” *J. Am. Col. Certif. Wound Spec.*, vol. 3, no. 3, pp. 65–66, 2011, doi: 10.1016/j.jcws.2012.04.002.

[176] A. Scalise *et al.*, “Microenvironment and microbiology of skin wounds: The role

USC UNIVERSIDADE DE SANTIAGO DE COMPOSTELA

of bacterial biofilms and related factors," *Semin. Vasc. Surg.*, vol. 28, no. 3–4, pp. 151–159, 2015, doi: 10.1053/j.semvascsurg.2016.01.003.

[177] L. M. Morton and T. J. Phillips, "Wound healing and treating wounds Differential diagnosis and evaluation of chronic wounds," *J. Am. Acad. Dermatol.*, vol. 74, no. 4, pp. 589–605, 2016, doi: 10.1016/j.jaad.2015.08.068.

[178] B. K. Sun, Z. Siprashvili, and P. A. Khavari, "Advances in skin grafting and treatment of cutaneous wounds," *Science (80-. ).*, vol. 346, no. 6212, pp. 941–945, 2014, doi: 10.1126/science.1253836.

[179] M. Rodrigues, N. Kosaric, C. A. Bonham, and G. C. Gurtner, "Wound healing: A cellular perspective," *Physiol. Rev.*, vol. 99, no. 1, pp. 665–706, 2019, doi: 10.1152/physrev.00067.2017.

[180] J. R. S. Andrei Z. Budzynski, "Fibrinogen and fibrin: Biochemistry and pathophysiology," *Crit. Rev. Oncol. Hematol.*, vol. 6, no. 2, p. Pages 97-146, 1986, doi: https://doi.org/10.1016/S1040-8428(86)80019-1.

[181] J. C. McDaniel, S. Roy, and T. A. Wilgus, "Neutrophil activity in chronic venous leg ulcers - A target for therapy?," *Wound Repair Regen.*, vol. 21, no. 3, pp. 339–351, 2013, doi: 10.1111/wrr.12036.

[182] T. A. Wilgus, S. Roy, and J. C. McDaniel, "Neutrophils and Wound Repair: Positive Actions and Negative Reactions," *Adv. Wound Care*, vol. 2, no. 7, pp. 379–388, 2013, doi: 10.1089/wound.2012.0383.

[183] M. F. Shah, D. C. Mancuso, L. He, and S. Kozak, "Evaluation of the Medicaid Buy-In Program in Washington State: Outcomes for Workers With Disabilities Who Purchase Medicaid Coverage," *J. Disabil. Policy Stud.*, vol. 22, no. 4, pp. 220–229, 2012, doi: 10.1177/1044207311427162.

[184] P. Krzyszczyk, R. Schloss, A. Palmer, and F. Berthiaume, "The role of macrophages in acute and chronic wound healing and interventions to promote pro-wound healing phenotypes," *Front. Physiol.*, vol. 9, no. MAY, pp. 1–22, 2018, doi: 10.3389/fphys.2018.00419.

[185] I. Aukhil, "Biology of wound healing," *Periodontol. 2000*, vol. 22, no. 1, pp. 44–50, 2000, doi: 10.1034/j.1600-0757.2000.2220104.x.

[186] C. L. Grosskreutz *et al.*, "Vascular endothelial growth factor-induced migration of vascular smooth muscle cells in vitro," *Microvasc. Res.*, vol. 58, no. 2, pp. 128–136, 1999, doi: 10.1006/mvre.1999.2171.

[187] Brainbridge P, "Wound Healing and The Role of Fibroblast," *J. Wound Care*, vol. 22, no. 8, pp. 407–412, 2013, doi: https://doi.org/10.12968/jowc.2013.22.8.407.

[188] A. W. S. Yeung, A. C. Terentis, N. J. C. King, and S. R. Thomas, "Role of indoleamine 2,3-dioxygenase in health and disease," *Clin. Sci.*, vol. 129, no. 7, pp. 601–672, 2015, doi: 10.1042/CS20140392.

[189] S. ichiro Motegi and O. Ishikawa, "Mesenchymal stem cells: The roles and functions in cutaneous wound healing and tumor growth," *J. Dermatol. Sci.*, vol. 86, no. 2, pp. 83–89, 2017, doi: 10.1016/j.jdermsci.2016.11.005.

[190] A. Clinton and T. Carter, "Chronic wound biofilms: Pathogenesis and potential

USC UNIVERSIDADE DE SANTIAGO DE COMPOSTELA

therapies," *Lab Med.*, vol. 46, no. 4, pp. 277–284, 2015, doi: 10.1309/LMBNSWKUI4JPN7SO.

[191] G. A. James *et al.*, "Biofilms in chronic wounds," *Wound Repair Regen.*, vol. 16, no. 1, pp. 37–44, 2008, doi: 10.1111/j.1524-475X.2007.00321.x.

[192] B. A. Mast and G. S. Schultz, "Interactions of cytokines, growth factors, and proteases in acute and chronic wounds," *Wound Repair Regen.*, vol. 4, no. 4, pp. 411–420, 1996, doi: 10.1046/j.1524-475X.1996.40404.x.

[193] N. J. Trengove, H. Bielefeldt-Ohmann, and M. C. Stacey, "Mitogenic activity and cytokine levels in non-healing and healing chronic leg ulcers," *Wound Repair Regen.*, vol. 8, no. 1, pp. 13–25, 2000, doi: 10.1046/j.1524-475X.2000.00013.x.

[194] L. E. Tracy, R. A. Minasian, and E. J. Caterson, "Extracellular Matrix and Dermal Fibroblast Function in the Healing Wound," *Adv. Wound Care*, vol. 5, no. 3, pp. 119–136, 2016, doi: 10.1089/wound.2014.0561.

[195] S. Kadam, S. Nadkarni, J. Lele, S. Sakhalkar, P. Mokashi, and K. S. Kaushik, "Bioengineered Platforms for Chronic Wound Infection Studies: How Can We Make Them More Human-Relevant?," *Front. Bioeng. Biotechnol.*, vol. 7, no. December, 2019, doi: 10.3389/fbioe.2019.00418.

[196] P. Taylor, S. L. Percival, and J. T. Walker, "Potable water and biofilms: A review of the public health implications," *Biofouling*, vol. 14, no. 2, pp. 99–115, 1999, doi: https://doi.org/10.1080/08927019909378402.

[197] T. K. Fisher, R. Wolcott, D. M. Wolk, M. Bharara, H. R. Kimbriel, and D. G. Armstrong, "Diabetic foot infections: A need for innovative assessments," *Int. J. Low. Extrem. Wounds*, vol. 9, no. 1, pp. 31–36, 2010, doi: 10.1177/1534734610363459.

[198] K. Rumbaugh, C. Watters, and T. Yuan, "Beneficial and deleterious bacterial–host interactions in chronic wound pathophysiology," *Chronic Wound Care Manag. Res.*, p. 53, 2015, doi: 10.2147/cwcmr.s60317.

[199] M. Zhou, A. Yu, G. Wu, C. Xia, X. Hu, and B. Qi, "Role of different negative pressure values in the process of infected wounds treated by vacuum-assisted closure: An experimental study," *Int. Wound J.*, vol. 10, no. 5, pp. 508–515, 2013, doi: 10.1111/j.1742-481X.2012.01008.x.

[200] A. Tankersley, M. B. Frank, M. Bebak, and R. Brennan, "Early effects of Staphylococcus aureus biofilm secreted products on inflammatory responses of human epithelial keratinocytes," *J. Inflamm. (United Kingdom)*, vol. 11, no. 1, pp. 1–11, 2014, doi: 10.1186/1476-9255-11-17.

[201] R. Prabhakara, J. M. Harro, J. G. Leid, M. Harris, and M. E. Shirtliff, "Murine immune response to a chronic Staphylococcus aureus biofilm infection," *Infect. Immun.*, vol. 79, no. 4, pp. 1789–1796, 2011, doi: 10.1128/IAI.01386-10.

[202] E. R. Zielins *et al.*, "Wound healing: An update," *Regen. Med.*, vol. 9, no. 6, pp. 817–830, 2014, doi: 10.2217/rme.14.54.

[203] C. Albanesi, S. Madonna, P. Gisondi, and G. Girolomoni, "The interplay between keratinocytes and immune cells in the pathogenesis of psoriasis," *Front. Immunol.*, vol. 9, no. JUL, pp. 1–7, 2018, doi: 10.3389/fimmu.2018.01549.

USC DE SANTIAGO DE COMPOSTELA

[204] C. W. Hall and T. F. Mah, "Molecular mechanisms of biofilm-based antibiotic resistance and tolerance in pathogenic bacteria," *FEMS Microbiol. Rev.*, vol. 41, no. 3, pp. 276–301, 2017, doi: 10.1093/femsre/fux010.

[205] D. M. Castilla, Z.-J. Liu, and O. C. Velazquez, "Oxygen: Implications for Wound Healing," *Adv. Wound Care*, vol. 1, no. 6, pp. 225–230, 2012, doi: 10.1089/wound.2011.0319.

[206] C. Dunnill *et al.*, "Reactive oxygen species (ROS) and wound healing: the functional role of ROS and emerging ROS-modulating technologies for augmentation of the healing process," *Int. Wound J.*, vol. 14, no. 1, pp. 89–96, 2017, doi: 10.1111/iwj.12557.

[207] S. L. Percival, S. McCarty, J. A. Hunt, and E. J. Woods, "The effects of pH on wound healing, biofilms, and antimicrobial efficacy," *Wound Repair Regen.*, vol. 22, no. 2, pp. 174–186, 2014, doi: 10.1111/wrr.12125.

[208] G. Daeschlein, "Antimicrobial and antiseptic strategies in wound management," *Int. Wound J.*, vol. 10, no. S1, pp. 9–14, 2013, doi: 10.1111/iwj.12175.

[209] L. A. Barnes *et al.*, "Mechanical Forces in Cutaneous Wound Healing: Emerging Therapies to Minimize Scar Formation," *Adv. Wound Care*, vol. 7, no. 2, pp. 47–56, 2018, doi: 10.1089/wound.2016.0709.

[210] P. Thomen, J. Robert, A. Monmeyran, A. F. Bitbol, C. Douarche, and N. Henry, "Bacterial biofilm under flow: First a physical struggle to stay, then a matter of breathing," *PLoS One*, vol. 12, no. 4, pp. 1–24, 2017, doi: 10.1371/journal.pone.0175197.

[211] R. Agha, R. Ogawa, G. Pietramaggiori, and D. P. Orgill, "A review of the role of mechanical forces in cutaneous wound healing," *J. Surg. Res.*, vol. 171, no. 2, pp. 700–708, 2011, doi: 10.1016/j.jss.2011.07.007.

[212] P. G. Bowler, B. I. Duerden, and D. G. Armstrong, "Wound microbiology and associated approaches to wound management," *Clin. Microbiol. Rev.*, vol. 14, no. 2, pp. 244–269, 2001, doi: 10.1128/CMR.14.2.244-269.2001.

[213] M. Fazli *et al.*, "Nonrandom distribution of Pseudomonas aeruginosa and Staphylococcus aureus in chronic wounds," *J. Clin. Microbiol.*, vol. 47, no. 12, pp. 4084–4089, 2009, doi: 10.1128/JCM.01395-09.

[214] K. Las Heras, M. Igartua, E. Santos-Vizcaino, and R. M. Hernandez, "Chronic wounds: Current status, available strategies and emerging therapeutic solutions," *J. Control. Release*, vol. 328, no. September, pp. 532–550, 2020, doi: 10.1016/j.jconrel.2020.09.039.

[215] S. Guo and L. A. DiPietro, "Critical review in oral biology & medicine: Factors affecting wound healing," *J. Dent. Res.*, vol. 89, no. 3, pp. 219–229, 2010, doi: 10.1177/0022034509359125.

[216] C. D. Weller, V. Team, and G. Sussman, "First-Line Interactive Wound Dressing Update: A Comprehensive Review of the Evidence," *Front. Pharmacol.*, vol. 11, no. February 2020, pp. 1–13, 2020, doi: 10.3389/fphar.2020.00155.

USC UNIVERSIDADE DE SANTIAGO DE COMPOSTELA

[217] T. Mustoe, "Understanding chronic wounds: A unifying hypothesis on their

pathogenesis and implications for therapy," *Am. J. Surg.*, vol. 187, no. 5 SUPPL. 1, pp. S65–S70, 2004, doi: 10.1016/S0002-9610(03)00306-4.

[218] V. Dubey, D. Mishra, A. Asthana, and N. K. Jain, "Transdermal delivery of a pineal hormone: Melatonin via elastic liposomes," *Biomaterials*, vol. 27, no. 18, pp. 3491–3496, 2006, doi: 10.1016/j.biomaterials.2006.01.060.

[219] Y. Xia, M. Sun, H. Huang, and W. L. Jin, "Drug repurposing for cancer therapy," *Signal Transduct. Target. Ther.*, vol. 9, no. 1, 2024, doi: 10.1038/s41392-024-01808-1.

[220] K. Lee and S. Lee, "Electrospun Nanofibrous Membranes with Essential Oils for Wound Dressing Applications," *Fibers Polym.*, vol. 21, no. 5, pp. 999–1012, 2020, doi: 10.1007/s12221-020-9300-6.

[221] L. Czaplewski *et al.*, "Alternatives to antibiotics-a pipeline portfolio review," *Lancet Infect. Dis.*, vol. 16, no. 2, pp. 239–251, 2016, doi: 10.1016/S1473-3099(15)00466-1.

[222] F. Nazzaro, F. Fratianni, L. De Martino, R. Coppola, and V. De Feo, "Effect of essential oils on pathogenic bacteria," *Pharmaceuticals*, vol. 6, no. 12, pp. 1451–1474, 2013, doi: 10.3390/ph6121451.

[223] J. S. Raut and S. M. Karuppayil, "A status review on the medicinal properties of essential oils," *Ind. Crops Prod.*, vol. 62, pp. 250–264, 2014, doi: https://doi.org/10.1016/j.indcrop.2014.05.055.

[224] C. F. Bagamboula, M. Uyttendaele, and J. Debevere, "Inhibitory effect of thyme and basil essential oils, carvacrol, thymol, estragol, linalool and p-cymene towards Shigella sonnei and S. flexneri," *Food Microbiol.*, vol. 21, no. 1, pp. 33–42, 2004, doi: 10.1016/S0740-0020(03)00046-7.

[225] A. Ben Arfa, S. Combes, L. Preziosi-Belloy, N. Gontard, and P. Chalier, "Antimicrobial activity of carvacrol related to its chemical structure," *Lett. Appl. Microbiol.*, vol. 43, no. 2, pp. 149–154, 2006, doi: 10.1111/j.1472-765X.2006.01938.x.

[226] R. Di Pasqua, G. Betts, N. Hoskins, M. Edwards, D. Ercolini, and G. Mauriello, "Membrane toxicity of antimicrobial compounds from essential oils," *J. Agric. Food Chem.*, vol. 55, no. 12, pp. 4863–4870, 2007, doi: 10.1021/jf0636465.

[227] C. V. Gabel and H. C. Berg, "The speed of the flagellar rotary motor of Escherichia coli varies linearly with protonmotive force," *Proc. Natl. Acad. Sci. U. S. A.*, vol. 100, no. 15, pp. 8748–8751, 2003, doi: 10.1073/pnas.1533395100.

[228] A. Pauli and K. H. Kubeczka, "Antimicrobial properties of volatile phenylpropanes," *Nat. Prod. Commun.*, vol. 5, no. 9, pp. 1387–1394, 2010, doi: 10.1177/1934578x1000500910.

[229] M. Hyldgaard, T. Mygind, and R. L. Meyer, "Essential oils in food preservation: Mode of action, synergies, and interactions with food matrix components," *Front. Microbiol.*, vol. 3, no. JAN, pp. 1–24, 2012, doi: 10.3389/fmicb.2012.00012.

USC DE SANTIAGO DE COMPOSTELA

[230] I. M. Helander *et al.*, "Characterization of the Action of Selected Essential Oil Components on Gram-Negative Bacteria," *J. Agric. Food Chem.*, vol. 46, no. 9, pp. 3590–3595, 1998, doi: 10.1021/jf980154m.

[231] N. Y. Saad, C. D. Muller, and A. Lobstein, "Major bioactivities and mechanism of action of essential oils and their components," *Flavour Fragr. J.*, vol. 28, no. 5, pp. 269–279, 2013, doi: 10.1002/ffj.3165.

[232] S. Burt, "Essential oils: Their antibacterial properties and potential applications in foods - A review," *Int. J. Food Microbiol.*, vol. 94, no. 3, pp. 223–253, 2004, doi: 10.1016/j.ijfoodmicro.2004.03.022.

[233] B. K. Tiwari, V. P. Valdramidis, C. P. O'Donnell, K. Muthukumarappan, P. Bourke, and P. J. Cullen, "Application of natural antimicrobials for food preservation," *J. Agric. Food Chem.*, vol. 57, no. 14, pp. 5987–6000, 2009, doi: 10.1021/jf900668n.

[234] H. Nikaido, "Prevention of Drug Access to Bacterial Targets: Permeability Barriers and Active Efflux," *Science (80-. ).*, vol. 264, no. 5157, pp. 382–388, 1994, doi: 10.1126/science.8153625.

[235] D. Trombetta *et al.*, "Mechanisms of antibacterial action of three monoterpenes," *Antimicrob. Agents Chemother.*, vol. 49, no. 6, pp. 2474–2478, 2005, doi: 10.1128/AAC.49.6.2474-2478.2005.

[236] S. A. Burt and R. D. Reinders, "Antibacterial activity of selected plant essential oils against Escherichia coil O157:H7," *Lett. Appl. Microbiol.*, vol. 36, no. 3, pp. 162–167, 2003, doi: 10.1046/j.1472-765X.2003.01285.x.

[237] P. Domadia, S. Swarup, A. Bhunia, J. Sivaraman, and D. Dasgupta, "Inhibition of bacterial cell division protein FtsZ by cinnamaldehyde," *Biochem. Pharmacol.*, vol. 74, no. 6, pp. 831–840, 2007, doi: 10.1016/j.bcp.2007.06.029.

[238] R. Di Pasqua, G. Mauriello, G. Mamone, and D. Ercolini, "Expression of DnaK, HtpG, GroEL and Tf chaperones and the corresponding encoding genes during growth of Salmonella Thompson in presence of thymol alone or in combination with salt and cold stress," *Food Res. Int.*, vol. 52, no. 1, pp. 153–159, 2013, doi: 10.1016/j.foodres.2013.02.050.

[239] M. Oussalah, S. Caillet, L. Saucier, and M. Lacroix, "Antimicrobial effects of selected plant essential oils on the growth of a Pseudomonas putida strain isolated from meat," *Meat Sci.*, vol. 73, no. 2, pp. 236–244, 2006, doi: 10.1016/j.meatsci.2005.11.019.

[240] Y. H. Li and X. Tian, "Quorum sensing and bacterial social interactions in biofilms," *Sensors*, vol. 12, no. 3, pp. 2519–2538, 2012, doi: 10.3390/s120302519.

[241] P. Williams, "Quorum sensing, communication and cross-kingdom signalling in the bacterial world," *Microbiology*, vol. 153, no. 12, pp. 3923–3938, 2007, doi: 10.1099/mic.0.2007/012856-0.

[242] B. L. Bassler, "How bacteria talk to each other: Regulation of gene expression by quorum sensing," *Curr. Opin. Microbiol.*, vol. 2, no. 6, pp. 582–587, 1999, doi: 10.1016/S1369-5274(99)00025-9.

[243] M. E. Taga, J. L. Semmelhack, and B. L. Bassler, "The LuxS-dependent autoinducer Al-2 controls the expression of an ABC transporter that functions in Al-2 uptake in Salmonella typhimurium," *Mol. Microbiol.*, vol. 42, no. 3, pp. 777–793, 2001, doi: 10.1046/j.1365-2958.2001.02669.x.

USC UNIVERSIDADE DE SANTIAGO DE COMPOSTELA

[244] B. K. Hammer and B. L. Bassler, "Quorum sensing controls biofilm formation in Vibrio cholerae," *Mol. Microbiol.*, vol. 50, no. 1, pp. 101–104, 2003, doi: 10.1046/j.1365-2958.2003.03688.x.

[245] F. Nazzaro, F. Fratianni, and R. Coppola, "Quorum sensing and phytochemicals," *Int. J. Mol. Sci.*, vol. 14, no. 6, pp. 12607–12619, 2013, doi: 10.3390/ijms140612607.

[246] J. M. McCord, "The evolution of free radicals and oxidative stress," *Am. J. Med.*, vol. 108, no. 8, pp. 652–659, 2000, doi: 10.1016/S0002-9343(00)00412-5.

[247] A. Tomaino *et al.*, "Influence of heating on antioxidant activity and the chemical composition of some spice essential oils," *Food Chem.*, vol. 89, no. 4, pp. 549–554, 2005, doi: 10.1016/j.foodchem.2004.03.011.

[248] M. G. Miguel, "Antioxidant and anti-inflammatory activities of essential oils: A short review," *Molecules*, vol. 15, no. 12, pp. 9252–9287, 2010, doi: 10.3390/molecules15129252.

[249] A. El Asbahani *et al.*, "Essential oils: From extraction to encapsulation," *Int. J. Pharm.*, vol. 483, no. 1–2, pp. 220–243, 2015, doi: 10.1016/j.ijpharm.2014.12.069.

[250] Z. Drulis-Kawa and A. Dorotkiewicz-Jach, "Liposomes as delivery systems for antibiotics," *Int. J. Pharm.*, vol. 387, no. 1–2, pp. 187–198, 2010, doi: 10.1016/j.ijpharm.2009.11.033.

[251] N. T. Ardekani, M. Khorram, K. Zomorodian, S. Yazdanpanah, H. Veisi, and H. Veisi, "Evaluation of electrospun poly (vinyl alcohol)-based nanofiber mats incorporated with Zataria multiflora essential oil as potential wound dressing," *Int. J. Biol. Macromol.*, vol. 125, pp. 743–750, 2019, doi: 10.1016/j.ijbiomac.2018.12.085.

[252] I. Unalan *et al.*, "Evaluation of Electrospun Poly(E-Caprolactone)/Gelatin Nanofiber Mats Containing Clove Essential Oil for Antibacterial Wound Dressing," *Pharmaceutics*, vol. 11, no. 11, p. 570, 2019, doi: https://doi.org/10.3390/pharmaceutics11110570.

[253] H. S. Sofi, T. Akram, A. H. Tamboli, A. Majeed, N. Shabir, and F. A. Sheikh, "Novel lavender oil and silver nanoparticles simultaneously loaded onto polyurethane nanofibers for wound-healing applications," *Int. J. Pharm.*, vol. 569, no. April, 2019, doi: 10.1016/j.ijpharm.2019.118590.

[254] I. Unalan, B. Slavik, A. Buettner, W. H. Goldmann, G. Frank, and A. R. Boccaccini, "Physical and Antibacterial Properties of Peppermint Essential Oil Loaded Poly (ε-caprolactone) (PCL) Electrospun Fiber Mats for Wound Healing," *Front. Bioeng. Biotechnol.*, vol. 7, no. November, pp. 1–11, 2019, doi: 10.3389/fbioe.2019.00346.

[255] M. Qin *et al.*, "In Situ Electrospinning Wound Healing Films Composed of Zein and Clove Essential Oil," *Macromol. Mater. Eng.*, vol. 305, no. 3, pp. 1–6, 2020, doi: 10.1002/mame.201900790.

[256] J. X. Liu *et al.*, "In Situ Electrospun Zein/Thyme Essential Oil-Based Membranes as an Effective Antibacterial Wound Dressing," *ACS Appl. Bio Mater.*, vol. 3, no. 1, pp. 302–307, 2020, doi: 10.1021/acsabm.9b00823.

USC UNIVERSIDADE DE SANTIAGO DE COMPOSTELA

[257] M. Salehi *et al.*, "Porous electrospun poly(ε-caprolactone)/gelatin nanofibrous mat containing cinnamon for wound healing application: in vitro and in vivo study," *Biomed. Eng. Lett.*, vol. 10, no. 1, pp. 149–161, 2020, doi: 10.1007/s13534-019-00138-4.

[258] H. Hosseinpor, A. Khaledi, and D. Esmaeili, "The properties of nanofiber scaffolds of polyurethane-Cinnamomum zeylanicum against pathogens of Pseudomonas aeruginosa and Staphylococcus aureus," *Polym. Bull.*, vol. 78, no. 1, pp. 223–245, 2021, doi: 10.1007/s00289-019-03095-1.

[259] P. Sinsup *et al.*, "Zingiber cassumunar roxb. Essential oil-loaded electrospun poly(lactic acid)/poly(ethylene oxide) fiber blend membrane for antibacterial wound dressing application," *Membranes (Basel).*, vol. 11, no. 9, 2021, doi: 10.3390/membranes11090648.

[260] G. Milanesi, B. Vigani, S. Rossi, G. Sandri, and E. Mele, "Chitosan-coated poly(Lactic acid) nanofibres loaded with essential oils for wound healing," *Polymers (Basel).*, vol. 13, no. 16, pp. 1–16, 2021, doi: 10.3390/polym13162582.

[261] C. Aras, E. Tümay Özer, G. Göktalay, G. Saat, and E. Karaca, "Evaluation of Nigella sativa oil loaded electrospun polyurethane nanofibrous mat as wound dressing," *J. Biomater. Sci. Polym. Ed.*, vol. 32, no. 13, pp. 1718–1735, 2021, doi: 10.1080/09205063.2021.1937463.

[262] M. Reza, M. Khorram, S. Barzegar, F. Asadian, and K. Zomorodian, "Antimicrobial core – shell electrospun nanofibers containing Ajwain essential oil for accelerating infected wound healing," *Int. J. Pharm.*, vol. 603, no. February, p. 120698, 2021, doi: 10.1016/j.ijpharm.2021.120698.

[263] D. Serbezeanu *et al.*, "Electrospun polyvinyl alcohol loaded with phytotherapeutic agents for wound healing applications," *Nanomaterials*, vol. 11, no. 12, pp. 1–13, 2021, doi: 10.3390/nano11123336.

[264] M. Wang, D. G. Yu, G. R. Williams, and S. W. A. Bligh, "Co-Loading of Inorganic Nanoparticles and Natural Oil in the Electrospun Janus Nanofibers for a Synergetic Antibacterial Effect," *Pharmaceutics*, vol. 14, no. 6, 2022, doi: 10.3390/pharmaceutics14061208.

[265] A. S. Mohamed Ahmed Mohamady Hussein, Oguzhan Gunduz and M. M. Ibrahim Mohamed El-Sherbiny, "Dual Spinneret Electrospun Polyurethane/PVA-Gelatin Nanofibrous Scaffolds Containing Cinnamon Essential Oil and Nanoceria for Chronic Diabetic Wound Healing: Preparation, Physicochemical Characterization and In-Vitro Evaluation," *Molecules*, vol. 27, p. 2146, 2022, doi: https://doi.org/10.3390/molecules27072146.

[266] M. Najafiasl, S. Osfouri, R. Azin, and S. Zaeri, "Modeling of drug release and simultaneous enhancement of tensile strength and antioxidant activity of the electrospun nanofibres using naturally extracted oil from Pistacia atlantica," *Polym. Test.*, vol. 107, p. 107492, 2022, doi: 10.1016/j.polymertesting.2022.107492.

[267] A. H. Rather *et al.*, "Polyurethane and cellulose acetate micro-nanofibers containing rosemary essential oil, and decorated with silver nanoparticles for wound healing application," *Int. J. Biol. Macromol.*, vol. 226, no. September 2022,

USC UNIVERSIDADE DE SANTIAGO DE COMPOSTELA

pp. 690–705, 2023, doi: 10.1016/j.ijbiomac.2022.12.048.

[268] C. R. ustundag and M. B. Piskin, "Investigation of electrospun poly (ε-caprolactone) fiber mats loaded with Calophyllum inophyllum essential oil for wound dressing applications: Morphology, drug release and in vitro evaluation," *Mater. Technol.*, vol. 38, no. 1, 2023, doi: 10.1080/10667857.2023.2223018.

[269] S. Khataei, M. H.Al-Musawi, K. Asadi, S. Ramezani, M. Abbasian, and M. Ghorbani, "Effect of molecular weight and content of polyvinylpyrrolidone on cell proliferation, loading capacity and properties of electrospun green tea essential oil-incorporated polyamide-6/polyvinylpyrrolidone nanofibers," *J. Drug Deliv. Sci. Technol.*, vol. 82, no. September 2022, p. 104310, 2023, doi: 10.1016/j.jddst.2023.104310.

[270] V. Reisi-Vanani *et al.*, "Engineering of a core-shell polyvinyl alcohol/gelatin fibrous scaffold for dual delivery of Thymus daenensis essential oil and Glycyrrhiza glabra L. extract as an antibacterial and functional wound dressing," *J. Drug Deliv. Sci. Technol.*, vol. 81, no. February, p. 104282, 2023, doi: 10.1016/j.jddst.2023.104282.

[271] V. Sadaiyandi, R. Ramalingam, K. D. Arunachalam, and J. T. D, "Essential Oils Infused Poly-ε-Caprolactone/Gelatin Electrospun Nanofibrous Mats: Biocompatibility and Antibacterial Study," *Appl. Biochem. Biotechnol.*, vol. 196, no. 1, pp. 296–313, 2024, doi: 10.1007/s12010-023-04530-w.

[272] S. Rathinavel, M. Sugumar, E. Swaminathan, S. Kubendren, K. Samvasivan, and D. Sangeetha, "Development of electrospun Plectranthus amboinicus loaded PCL polymeric nanofibrous scaffold for skin wound healing application: in-vitro and in-silico analysis," *J. Polym. Res.*, vol. 30, no. 3, 2023, doi: 10.1007/s10965-023-03474-3.

[273] P. Nezhad-Mokhtari *et al.*, "Matricaria chamomilla essential oil-loaded hybrid electrospun nanofibers based on polycaprolactone/sulfonated chitosan/ZIF-8 nanoparticles for wound healing acceleration," *Int. J. Biol. Macromol.*, vol. 247, no. July, p. 125718, 2023, doi: 10.1016/j.ijbiomac.2023.125718.

[274] M. Heydari *et al.*, "A two-layer nanofiber-Tragacanth hydrogel composite containing Lavender extract and Mupirocin as a wound dressing," *Polym. Bull.*, vol. 81, no. 1, pp. 373–389, 2024, doi: 10.1007/s00289-022-04655-8.

[275] N. A. Elbhnsawi *et al.*, "Nano-Chitosan/Eucalyptus Oil/Cellulose Acetate Nanofibers: Manufacturing, Antibacterial and Wound Healing Activities," *Membranes (Basel).*, vol. 13, no. 6, 2023, doi: 10.3390/membranes13060604.

[276] P. Mishra, P. Gupta, R. Srivastava, A. K. Srivastava, K. M. Poluri, and R. Prasad, "Exploration of Antibiofilm and In Vivo Wound Healing Activity of p-Cymene-Loaded Gellan/PVA Nanofibers," *ACS Appl. Bio Mater.*, vol. 6, no. 5, pp. 1816–1831, 2023, doi: 10.1021/acsabm.3c00047.

[277] A. Akturk, "Enrichment of Cellulose Acetate Nanofibrous Scaffolds with Retinyl Palmitate and Clove Essential Oil for Wound Healing Applications," *ACS Omega*, vol. 8, no. 6, pp. 5553–5560, 2023, doi: 10.1021/acsomega.2c06881.

[278] Z. Fakhri, N. Karimi, F. Saba, and M. Ghorbanpour, "Synthesis composit electrospun based gum-resin/polycaprolactone fibers for biomedical application,"

USC UNIVERSIDADE DE SANTIAGO DE COMPOSTELA

*J. Drug Deliv. Sci. Technol.*, vol. 100, no. July, p. 106010, 2024, doi: 10.1016/j.jddst.2024.106010.

[279] D. Serra *et al.*, "Electrospun Nanofibers Encapsulated with Natural Products: A Novel Strategy to Counteract Skin Aging," *Int. J. Mol. Sci.*, vol. 25, no. 3, pp. 1–16, 2024, doi: 10.3390/ijms25031908.

[280] D. Hanahan and R. A. Weinberg, "The Hallmarks of Cancer," *Cell*, vol. 100, pp. 57–100, 2000, doi: 10.1016/S0092-8674(00)81683-9.

[281] D. Hanahan and R. A. Weinberg, "Hallmarks of cancer: The next generation," *Cell*, vol. 144, no. 5, pp. 646–674, 2011, doi: 10.1016/j.cell.2011.02.013.

[282] D. Hanahan, "Hallmarks of Cancer: New Dimensions," *Cancer Discov.*, vol. 12, no. 1, pp. 31–46, 2022, doi: 10.1158/2159-8290.CD-21-1059.

[283] D. Hanahan and M. Monje, "Cancer hallmarks intersect with neuroscience in the tumor microenvironment," *Cancer Cell*, vol. 41, no. 3, pp. 573–580, 2023, doi: 10.1016/j.ccell.2023.02.012.

[284] O. Visser *et al.*, "Survival of adults with primary malignant brain tumours in Europe ; Results of the EUROCARE-5 study," pp. 2231–2241, 2015, doi: 10.1016/j.ejca.2015.07.032.

[285] D. Abdelnabi *et al.*, "Local administration of irinotecan using an implantable drug delivery device stops high-grade glioma tumor recurrence in a glioblastoma tumor model," *Drug Deliv. Transl. Res.*, vol. 14, no. 11, pp. 3070–3088, 2024, doi: 10.1007/s13346-024-01524-x.

[286] D. N. Louis *et al.*, "The 2021 WHO classification of tumors of the central nervous system: A summary," *Neuro. Oncol.*, vol. 23, no. 8, pp. 1231–1251, 2021, doi: 10.1093/neuonc/noab106.

[287] K. J. Wolf, J. Chen, J. D. Coombes, M. K. Aghi, and S. Kumar, "Dissecting and rebuilding the glioblastoma microenvironment with engineered materials," *Nat. Rev. Mater.*, vol. 4, no. 10, pp. 651–668, 2019, doi: 10.1038/s41578-019-0135-y.

[288] P. Peruzzi *et al.*, "Intratumoral drug-releasing microdevices allow in situ high-throughput pharmaco phenotyping in patients with gliomas," *Sci. Transl. Med.*, vol. 15, no. 712, 2023, doi: 10.1126/SCITRANSLMED.ADI0069.

[289] D. Lenz, M. Ries, and P. Johann, "The drug development pipeline for glioblastoma—A cross sectional assessment of the FDA Orphan Drug Product designation database," *PLoS One*, vol. 16, no. 7 July, pp. 1–14, 2021, doi: 10.1371/journal.pone.0252924.

[290] T. S. van Solinge, L. Nieland, E. A. Chiocca, and M. L. D. Broekman, "Advances in local therapy for glioblastoma — taking the fight to the tumour," *Nat. Rev. Neurol.*, vol. 18, no. 4, pp. 221–236, 2022, doi: 10.1038/s41582-022-00621-0.

[291] K. Lin, S. E. Gueble, R. K. Sundaram, E. D. Huseman, R. S. Bindra, and S. B. Herzon, "Mechanism-based design of agents that selectively target drug-resistant glioma," *Science (80-. ).*, vol. 377, no. 6605, pp. 502–511, 2022, doi: 10.1126/science.abn7570.

USC UNIVERSIDADE DE SANTIAGO DE COMPOSTELA

[292] M. L. Broekman, S. L. N. Maas, E. R. Abels, T. R. Mempel, A. M. Krichevsky,

and X. O. Breakefield, "Multidimensional communication in the microenvirons of glioblastoma," *Nat. Rev. Neurol.*, vol. 14, no. 8, pp. 482–495, 2018, doi: 10.1038/s41582-018-0025-8.

[293] N. A. De Vries, J. H. Beijnen, W. Boogerd, and O. Van Tellingen, "Blood-brain barrier and chemotherapeutic treatment of brain tumors," *Expert Rev. Neurother.*, vol. 6, no. 8, pp. 1199–1209, 2006, doi: 10.1586/14737175.6.8.1199.

[294] C. Nimsky *et al.*, "Preoperative and intraoperative diffusion tensor imaging-based fiber tracking in glioma surgery," *Neurosurgery*, vol. 56, no. 1, pp. 130–137, 2005, doi: 10.1227/01.NEU.0000144842.18771.30.

[295] S. Pushpakom *et al.*, "Drug repurposing: progress, challenges and recommendations," *Nat. Rev. Drug Discov.*, vol. 18, no. 1, pp. 41–58, 2019, doi: 10.1038/nrd.2018.168.

[296] F. Ragucci *et al.*, "Insights into Healthcare Professionals ' Perceptions and Attitudes toward Nanotechnological Device Application : What Is the Current Situation in Glioblastoma Research ?," *Biomedicines*, vol. 11, p. 1854, 2023, doi: https://doi.org/10.3390/ biomedicines11071854 Academic.

[297] J. Basso, A. Miranda, J. Sousa, A. Pais, and C. Vitorino, "Repurposing drugs for glioblastoma: From bench to bedside," *Cancer Lett.*, vol. 428, pp. 173–183, 2018, doi: 10.1016/j.canlet.2018.04.039.

[298] S. Alomari *et al.*, "Drug repurposing for glioblastoma and current advances in drug delivery—A comprehensive review of the literature," *Biomolecules*, vol. 11, no. 12, 2021, doi: 10.3390/biom11121870.

[299] B. Cvek, "Nonprofit drugs as the salvation of the world's healthcare systems: the case of Antabuse (disulfiram)," *Drug Discov. Today*, vol. 17, no. 9–10, pp. 409–412, 2012, doi: 10.1016/j.drudis.2011.12.010.

[300] Z. Skrott *et al.*, "Alcohol-abuse drug disulfiram targets," *Nat. Publ. Gr.*, 2017, doi: 10.1038/nature25016.

[301] Y. Lu *et al.*, "Leveraging disulfiram to treat cancer: Mechanisms of action, delivery strategies, and treatment regimens," *Biomaterials*, vol. 281, no. September 2021, p. 121335, 2022, doi: 10.1016/j.biomaterials.2021.121335.

[302] M. Pan *et al.*, "Seesaw conformations of Npl4 in the human p97 complex and the inhibitory mechanism of a disulfiram derivative," *Nat. Commun.*, vol. 12, no. 1, 2021, doi: 10.1038/s41467-020-20359-x.

[303] Y. Terashima *et al.*, "Targeting FROUNT with disulfiram suppresses macrophage accumulation and its tumor-promoting properties," *Nat. Commun.*, vol. 11, no. 1, 2020, doi: 10.1038/s41467-020-14338-5.

[304] J. Sesen *et al.*, "Metformin inhibits growth of human glioblastoma cells and enhances therapeutic response," *PLoS One*, vol. 10, no. 4, pp. 1–24, 2015, doi: 10.1371/journal.pone.0123721.

[305] M. Gritti *et al.*, "Metformin repositioning as antitumoral agent: Selective antiproliferative effects in human glioblastoma stem cells, via inhibition of CLIC1-mediated ion current," *Oncotarget*, vol. 5, no. 22, pp. 11252–11268, 2014, doi: 10.18632/oncotarget.2617.

USC UNIVERSIDADE DE SANTIAGO DE COMPOSTELA

[306] E. Nance, S. H. Pun, R. Saigal, and D. L. Sellers, "Drug delivery to the central nervous system," *Nat. Rev. Mater.*, vol. 7, no. 4, pp. 314–331, 2022, doi: 10.1038/s41578-021-00394-w.

[307] M. Weller *et al.*, "Glioma," *Nat. Rev. Dis. Prim.*, vol. 10, no. 1, 2024, doi: 10.1038/s41572-024-00516-y.

[308] R. Ramachandran *et al.*, "Theranostic 3-Dimensional nano brain-implant for prolonged and localized treatment of recurrent glioma," *Sci. Rep.*, vol. 7, no. October 2016, pp. 1–16, 2017, doi: 10.1038/srep43271.

[309] Y. Y. Tseng, J. Y. Liao, W. A. Chen, Y. C. Kao, and S. J. Liu, "Sustainable release of carmustine from biodegradable poly[(d,l)-lactide-co- glycolide] nanofibrous membranes in the cerebral cavity: In vitro and in vivo studies," *Expert Opin. Drug Deliv.*, vol. 10, no. 7, pp. 879–888, 2013, doi: 10.1517/17425247.2013.758102.

[310] A. B. Fleming and W. M. Saltzman, "Pharmacokinetics of the carmustine implant," *Clin. Pharmacokinet.*, vol. 41, no. 6, pp. 403–419, 2002, doi: 10.2165/00003088-200241060-00002.

[311] F. Ahmed, R. I. Pakunlu, A. Brannan, F. Bates, T. Minko, and D. E. Discher, "Biodegradable polymersomes loaded with both paclitaxel and doxorubicin permeate and shrink tumors, inducing apoptosis in proportion to accumulated drug," *J. Control. Release*, vol. 116, no. 2 SPEC. ISS., pp. 150–158, 2006, doi: 10.1016/j.jconrel.2006.07.012.

[312] S. H. Ranganath and C. H. Wang, "Biodegradable microfiber implants delivering paclitaxel for post-surgical chemotherapy against malignant glioma," *Biomaterials*, vol. 29, no. 20, pp. 2996–3003, 2008, doi: 10.1016/j.biomaterials.2008.04.002.

[313] P. Kumar Naraharisetti, B. Yung Sheng Ong, J. Wei Xie, T. Kam Yiu Lee, C. H. Wang, and N. V. Sahinidis, "In vivo performance of implantable biodegradable preparations delivering Paclitaxel and Etanidazole for the treatment of glioma," *Biomaterials*, vol. 28, no. 5, pp. 886–894, 2007, doi: 10.1016/j.biomaterials.2006.09.044.

[314] D. Hernán Pérez de la Ossa *et al.*, "Local Delivery of Cannabinoid-Loaded Microparticles Inhibits Tumor Growth in a Murine Xenograft Model of Glioblastoma Multiforme," *PLoS One*, vol. 8, no. 1, pp. 2–9, 2013, doi: 10.1371/journal.pone.0054795.

[315] A. W. Scott *et al.*, "Intracranial microcapsule drug delivery device for the treatment of an experimental gliosarcoma model," *Biomaterials*, vol. 32, no. 10, pp. 2532–2539, 2011, doi: 10.1016/j.biomaterials.2010.12.020.

[316] G. Y. Kim *et al.*, "Resorbable polymer microchips releasing BCNU inhibit tumor growth in the rat 9L flank model," *J. Control. Release*, vol. 123, no. 2, pp. 172–178, 2007, doi: 10.1016/j.jconrel.2007.08.003.

[317] M. Y. Hua *et al.*, "The effectiveness of a magnetic nanoparticle-based delivery system for BCNU in the treatment of gliomas," *Biomaterials*, vol. 32, no. 2, pp. 516–527, 2011, doi: 10.1016/j.biomaterials.2010.09.065.

[318] R. Ramachandran *et al.*, "A polymer-protein core-shell nanomedicine for

USC UNIVERSIDADE DE SANTIAGO DE COMPOSTELA

inhibiting cancer migration followed by photo-triggered killing," *J. Biomed. Nanotechnol.*, vol. 10, no. 8, pp. 1401–1415, 2014, doi: 10.1166/jbn.2014.1847.

[319] V. R. Recinos *et al.*, "Combination of intracranial temozolomide with intracranial carmustine improves survival when compared with either treatment alone in a rodent glioma model," *Neurosurgery*, vol. 66, no. 3, pp. 530–537, 2010, doi: 10.1227/01.NEU.0000365263.14725.39.

[320] S. Brem *et al.*, "Local delivery of temozolomide by biodegradable polymers is superior to oral administration in a rodent glioma model," *Cancer Chemother. Pharmacol.*, vol. 60, no. 5, pp. 643–650, 2007, doi: 10.1007/s00280-006-0407-2.

[321] S. Anai *et al.*, "Antitumor effect of fibrin glue containing temozolomide against malignant glioma," *Cancer Sci.*, vol. 105, no. 5, pp. 583–591, 2014, doi: 10.1111/cas.12397.

[322] S. H. Ranganath *et al.*, "The use of submicron/nanoscale PLGA implants to deliver paclitaxel with enhanced pharmacokinetics and therapeutic efficacy in intracranial glioblastoma in mice," *Biomaterials*, vol. 31, no. 19, pp. 5199–5207, 2010, doi: 10.1016/j.biomaterials.2010.03.002.

[323] B. Y. S. Ong *et al.*, "Paclitaxel delivery from PLGA foams for controlled release in post-surgical chemotherapy against glioblastoma multiforme," *Biomaterials*, vol. 30, no. 18, pp. 3189–3196, 2009, doi: 10.1016/j.biomaterials.2009.02.030.

[324] M. S. Lesniak, U. Upadhyay, R. Goodwin, B. Tyler, and H. Brem, "Local delivery of doxorubicin for the treatment of malignant brain tumors in rats," *Anticancer Res.*, vol. 25, no. 6 B, pp. 3825–3831, 2005.

[325] Y. Manome *et al.*, "Local delivery of doxorubicin for malignant glioma by a biodegradable PLGA polymer sheet," *Anticancer Res.*, vol. 26, no. 5 A, pp. 3317–3326, 2006.

[326] P. Menei *et al.*, "Local and sustained delivery of 5-fluorouracil from biodegradable microspheres for the radiosensitization of glioblastoma: A pilot study," *Cancer*, vol. 86, no. 2, pp. 325–330, 1999, doi: 10.1002/(SICI)1097-0142(19990715)86:2<325::AID-CNCR17>3.0.CO;2-S.

[327] J. D. Weingart, R. C. Thompson, B. Tyler, O. M. Colvin, and H. Brem, "Local delivery of the topoisomerase I inhibitor camptothecin sodium prolongs survival in the rat intracranial 9L gliosarcoma model," *Int. J. Cancer*, vol. 62, no. 5, pp. 605–609, 1995, doi: 10.1002/ijc.2910620519.

[328] J. Zhao and W. Cui, "Functional Electrospun Fibers for Local Therapy of Cancer," *Adv. Fiber Mater.*, vol. 2, pp. 229–245, 2020, doi: https://doi.org/10.1007/s42765-020-00053-9.

[329] X. Xu *et al.*, "BCNU-loaded PEG – PLLA ultrafine fibers and their in vitro antitumor activity against Glioma C6 cells," vol. 114, pp. 307–316, 2006, doi: 10.1016/j.jconrel.2006.05.031.

[330] Z. Jiang *et al.*, *Nanofiber Scaffolds as Drug Delivery Systems Promoting Wound Healing*, vol. 15, no. 7. 2023. doi: 10.3390/pharmaceutics15071829.

[331] Y. Y. Tseng *et al.*, "Advanced interstitial chemotherapy combined with targeted treatment of malignant glioma in rats by using drug-loaded nanofibrous

membranes," *Oncotarget*, vol. 7, no. 37, pp. 59902–59916, 2016, doi: 10.18632/oncotarget.10989.

[332] C. Lei, Y. Cui, L. Zheng, P. K. Chow, and C. Wang, "Biomaterials Development of a gene / drug dual delivery system for brain tumor therapy : Potent inhibition via RNA interference and synergistic effects," *Biomaterials*, vol. 34, no. 30, pp. 7483–7494, 2013, doi: 10.1016/j.biomaterials.2013.06.010.

[333] J. R. Bagó *et al.*, "Biomaterials Electrospun nanofibrous scaffolds increase the efficacy of stem cell-mediated therapy of surgically resected glioblastoma," vol. 90, pp. 116–125, 2016, doi: 10.1016/j.biomaterials.2016.03.008.

[334] B. Liu *et al.*, "Electrospun poly ( L-lactic acid )/ gelatine membranes loaded with doxorubicin for effective suppression of glioblastoma cell growth in vitro and in vivo," no. July, pp. 1–12, 2021, doi: 10.1093/rb/rbab043.

[335] J. Gustavo *et al.*, "Nek1-inhibitor and temozolomide-loaded microfibers as a co-therapy strategy for glioblastoma treatment," vol. 617, no. November 2021, 2022, doi: 10.1016/j.ijpharm.2022.121584.

[336] M. Haji *et al.*, "Nanoparticle-containing electrospun nanofibrous scaffolds for sustained release of SDF-1 α," vol. 610, no. May, 2021, doi: 10.1016/j.ijpharm.2021.121205.

[337] S. Spadaro *et al.*, "PEG-PLGA electrospun nanofibrous membranes loaded with Au@Fe2O3 nanoparticles for drug delivery applications," *Front. Phys.*, vol. 13, no. 1, pp. 1–9, 2018, doi: 10.1007/s11467-017-0703-9.

[338] A. Contreras-García, E. Bucio, A. Concheiro, and C. Alvarez-Lorenzo, "Polypropylene grafted with NIPAAm and APMA for creating hemocompatible surfaces that load/elute nalidixic acid," *React. Funct. Polym.*, vol. 70, no. 10, pp. 836–842, 2010, doi: 10.1016/j.reactfunctpolym.2010.07.019.

[339] K. J. Figueroa-Lopez *et al.*, "Development of electrospun active films of poly(3-hydroxybutyrate-co-3-hydroxyvalerate) by the incorporation of cyclodextrin inclusion complexes containing oregano essential oil," *Food Hydrocoll.*, vol. 108, no. January, 2020, doi: 10.1016/j.foodhyd.2020.106013.

[340] J. E. Meneguello *et al.*, "Systematic review of disulfiram as an antibacterial agent: what is the evidence?," *Int. J. Antimicrob. Agents*, vol. 59, no. 5, p. 106578, 2022, doi: 10.1016/j.ijantimicag.2022.106578.

[341] M. Lemos *et al.*, "The effects of ferulic and salicylic acids on Bacillus cereus and Pseudomonas fluorescens single- and dual-species biofilms," *Int. Biodeterior. Biodegrad.*, vol. 86, pp. 42–51, 2014, doi: 10.1016/j.ibiod.2013.06.011.

[342] M. H. Cavanagh, R. E. Burrell, and P. L. Nadworny, "Evaluating antimicrobial efficacy of new commercially available silver dressings," *Int. Wound J.*, vol. 7, no. 5, pp. 394–405, 2010, doi: 10.1111/j.1742-481X.2010.00705.x.

[343] M. Weller *et al.*, "Glioma," *Nat. Rev. Dis. Prim.*, vol. 1, no. July, 2015, doi: 10.1038/nrdp.2015.17.

[344] C. Y. Foo *et al.*, "Medical Device Advances in the Treatment of Glioblastoma," pp. 1–33, 2022.

USC COMPOSTELA

[345] T. Iqbal *et al.*, "Frontiers in the treatment of glioblastoma : Past , present and emerging," *Adv. Drug Deliv. Rev.*, vol. 171, pp. 108–138, 2021, doi: 10.1016/j.addr.2021.01.012.

[346] B. J. Mason and C. J. Heyser, "A LCOHOL U SE D ISORDER : T HE R OLE OF M EDICATION IN R ECOVERY," vol. 41, no. 1, pp. 1–17, 2021.

[347] N. Ramadhani, M. Shabir, and C. McConville, "Preparation and characterisation of Kolliphor®P 188 and P 237 solid dispersion oral tablets containing the poorly water soluble drug disulfiram," *Int. J. Pharm.*, vol. 475, no. 1, pp. 514–522, 2014, doi: 10.1016/j.ijpharm.2014.09.013.

[348] F. Nazzaro, F. Fratianni, and L. De Martino, "Effect of Essential Oils on Pathogenic Bacteria," pp. 1451–1474, 2013, doi: 10.3390/ph6121451.

[349] S. Chouhan, K. Sharma, and S. Guleria, "Antimicrobial Activity of Some Essential Oils—Present Status and Future Perspectives," *Medicines*, vol. 4, no. 3, p. 58, 2017, doi: 10.3390/medicines4030058.

USC
UNIVERSIDADE DE SANTIAGO DE COMPOSTELA

USC
UNIVERSIDADE
DE SANTIAGO
DE COMPOSTELA

# II. AIM

USC
UNIVERSIDADE
DE SANTIAGO
DE COMPOSTELA

USC
UNIVERSIDADE
DE SANTIAGO
DE COMPOSTELA

# II.AIM

The aim of this Doctoral Thesis was to implement electrospinning protocols to formulate essential oil compounds (EOCs) and disulfiram as fiber mats with enhanced antimicrobial and antitumoral properties. According to this general aim, three specific aims were identified and developed as follows:

a) To prepare electrospun fiber mats that can host high amounts of EOCs and regulate their release to provide concentration levels well above the minimum inhibitory concentration (MIC) of two common human pathogens, *Staphylococcus aureus* and *Pseudomonas aeruginosa*. To carry out the work, three EOCs of quite different chemical structure, that is, carvacrol (phenolic monoterpenoid), citronellol (monoterpene alcohol) and cinnamic acid (phenolic carboxylic acid), were chosen to evaluate the feasibility of their incorporation into electrospun fibers. The non-specific mechanism of action converts these EOCs into broad-spectrum antimicrobial agents, effective against Gram-positive and Gram-negative pathogens. Moreover, they have been referred to have antioxidant and angiogenic capabilities, which may facilitate wound healing. Thus, EOCs are versatile and interesting compounds with polyvalent performances. Despite these advantages, there are also numerous constraints that compromise the handling and the effectiveness of EOCs. Generally, EOCs are volatile substances with strong organoleptic flavor, low water solubility and low stability. Therefore, the development of wound dressings or skin scaffolds loaded with EOCs is not straightforward and should consider efficient encapsulation ways that enhance stability and local solubility in order to increase penetration and effectiveness in the skin tissues. This work relies on the hypothesis that electrospun dressings of poly-ε-caprolactone (PCL) containing cyclodextrins (CDs) may act as scaffolds able to encapsulate EOCs and to deliver therapeutic concentrations to the wounds for effective prophylaxis or treatment of infections.

USC
UNIVERSIDADE DE SANTIAGO DE COMPOSTELA

Several mixtures of PCL with alpha-cyclodextrin (αCD) and hydroxypropyl-β-cyclodextrin (HPβCD) were first prepared, and adequate solvents for electrospinning of the mixtures were identified. In terms of safety, the chosen cyclodextrins show an excellent safety profile whether administered dermally or parenterally and are easily cleared from the body by renal filtration if they enter the bloodstream. Morphological, mechanical, thermal and surface properties of the fibers were investigated. Then, fibers loaded with selected EOCs were tested for their preventive action on *S. aureus* and *P. aeruginosa* biofilm set-up, as well as antioxidant and anti-inflammatory properties. Additional studies were also conducted with fibers prepared with binary and ternary combinations of EOCs in an attempt to enhance the antimicrobial efficiency while still preserving biocompatibility. Part of this work was carried out in collaboration with the group of Prof. Manuel Simoes and Dr. Anabela Borges in the Faculty of Engineering at University of Porto, in which the candidate acquired training in antimicrobial and antibiofilm studies during a research stay.

b) To prepare electrospun fiber mats that can host disulfiram and/or its complex with cupper ions and regulate their release to provide concentration levels well above the minimum inhibitory concentration (MIC) of *S. aureus* and *P. aeruginosa.* DSF is a biopharmaceutical classification system (BCS) class II drug (i.e., low solubility and high permeability). Therefore, to carry out the work, HPβCD was chosen as encapsulating agent able to form inclusion complexes with DSF and to facilitate drug incorporation in the electrospun mats and subsequent release in contact with the physiological fluids. Silk fibroin from *Bombyx mori* cocoons was selected as the main component of the mat due to its mechanical behavior, low immunogenicity, and non-carcinogenic and hemostatic properties. Pristine SF is composed of two polypeptide chains, a heavy chain (391.367 kDa) and light chain (25 kDa) and a glycoprotein of the P25 type. One of the most important advantages of use SF isolated from silkworm rather than other type of insects sources is its protein sequence and high content in hydrophobic amino acids (i.e. glycine, alanine, serine, and tyrosine) that contribute for its crystalline structure. Thereby, SF can experiment a conformational change from α -helix and random coil conformation (silk I, hydrophilic) to a ß-sheet conformation (silk II, hydrophobic) characterized by a robust mechanical strength and toughness. The DSF-loaded electrospun mats were produced by electrospinning and characterized using different spectral and analytical techniques including FTIR and SEM analyses, and mechanical tests. After the structural

USC UNIVERSIDADE DE SANTIAGO

characterization, the biocompatibility and microbial properties were investigated. Release of both pristine DSF and its complex with cupper ions was monitored using HPLC developed methods. Moreover, the antimicrobial properties against *S. aureus* and *P. aeruginosa* of electrospun mats evaluated following recognised and standardised protocols (*e.g.*; AATCC 100).

c) To prepare electrospun fiber mats that can host disulfiram and/or its complex with cupper ions and regulate their release to serve as antitumoral treatment against glioblastoma. The clinical application of DSF in GBM treatment is limited by its short plasma half-life (ca. 7 hours), physiological instability, lipophilicity (logP around 4.16), and poor water solubility (0.2 mg/mL). Systemic administration demands high doses of free DSF (ca. 500-1000 mg once daily) or in combination with temozolomide (ca. 500 mg once daily) to guarantee the desired therapeutic effect, but this causes marked hepatotoxicity, neurotoxicity, and low patient compliance. The aim of the last part of the Doctoral Thesis was to design and characterize cost-effective and safe electrospun mats composed of SF or SF combined with HPβCD for the controlled and sustained release of DSF to treat GBM locally post-surgery. The DSF-loaded electrospun mats were produced as explained in step b) by electrospinning and characterized regarding their anticancer activity in collaboration with the group of Dr. Emmanuel Garcion at the Institute National de la Santé et de la Recherche Médicale (National Institute of Health and Medical Research, INSERM) and the University of Angers.

USC
UNIVERSIDADE DE SANTIAGO DE COMPOSTELA

USC
UNIVERSIDADE
DE SANTIAGO
DE COMPOSTELA

# III. ANTIMICROBIAL CYCLODEXTRIN-ASSISTED ELECTROSPUN FIBERS LOADED WITH CARVACROL, CITRONELLOL AND CINNAMIC ACID FOR WOUND HEALING

USC
UNIVERSIDADE DE SANTIAGO DE COMPOSTELA

USC
UNIVERSIDADE
DE SANTIAGO
DE COMPOSTELA

# III. ANTIMICROBIAL CYCLODEXTRIN-ASSISTED ELECTROSPUN FIBERS LOADED WITH CARVACROL, CITRONELLOL AND CINNAMIC ACID FOR WOUND HEALING

Iago Gonzalez-Prada[1], Anabela Borges[2,3], Beatriz Santos-Torres[4], Beatriz Magariños[4], Manuel Simões[2,3], Angel Concheiro[1], and Carmen Alvarez-Lorenzo[1*]

[1]Departamento de Farmacología, Farmacia y Tecnología Farmacéutica, I+D Farma (GI-1645), Faculty of Pharmacy, Institute of Materials (iMATUS), and Health Research Institute of Santiago de Compostela (IDIS), Universidade de Santiago de Compostela, Spain

[2]LEPABE - Department of Chemical Engineering, Faculty of Engineering, University of Porto, Portugal

[3]ALiCE - Associate Laboratory in Chemical Engineering, Faculty of Engineering, University of Porto, Portugal

[4]Departamento de Microbiología y Parasitología, Facultad de Biología, CIBUS, Universidade de Santiago de Compostela, Spain.

This chapter has been already published in International Journal of Biological Macromolecules as Iago Gonzalez-Prada, Anabela Borges, Beatriz Santos-Torres, Beatriz Magariños, Manuel Simões, Angel Concheiro, Carmen Alvarez-Lorenzo, Antimicrobial cyclodextrin-assisted electrospun fibers loaded with carvacrol, citronellol and cinnamic acid for wound healing, 2024, 134154. DOI: https://doi.org/10.1016/j.ijbiomac.2024.134154. Online ISSN: 0141-8130.

USC UNIVERSIDADE DE SANTIAGO DE COMPOSTELA

**Abstract**

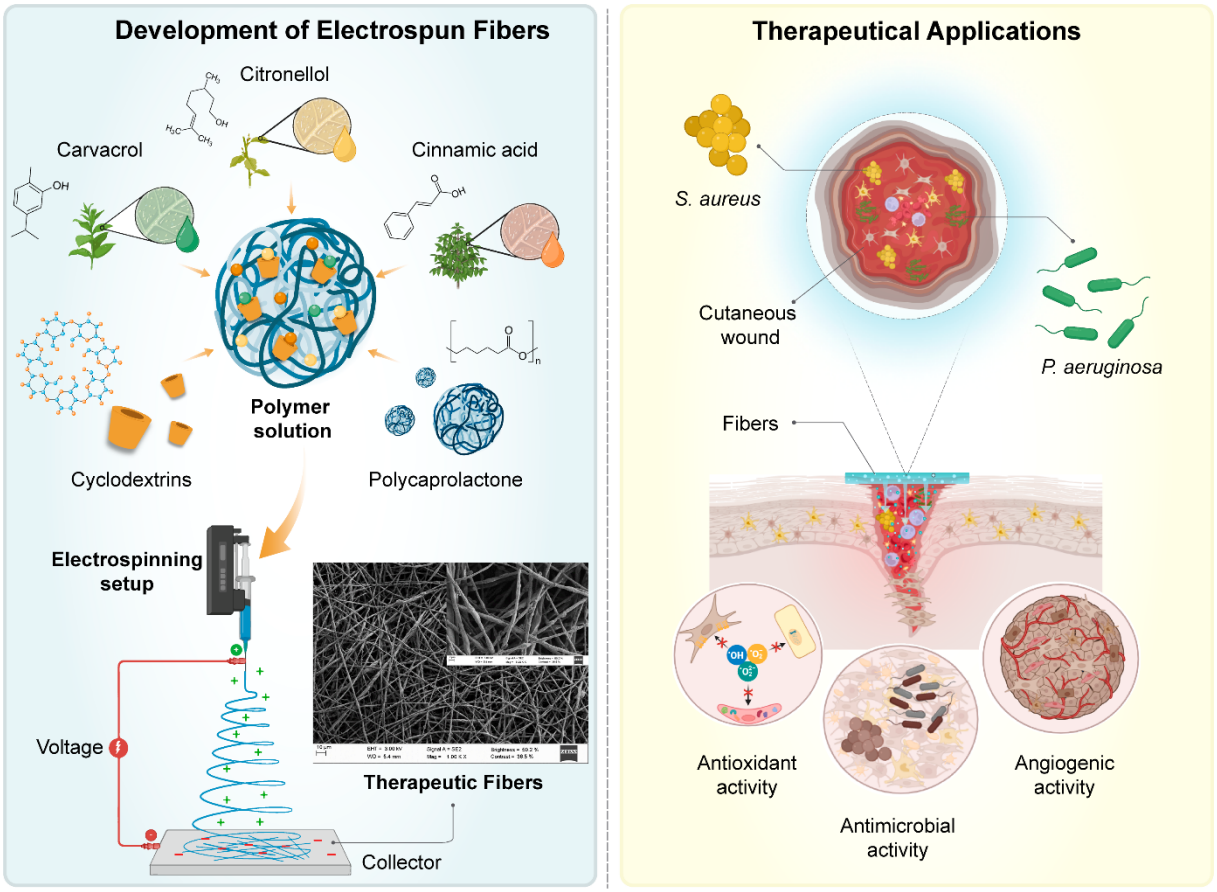
This work aimed to explore an alternative to the use of antibiotics for prevention and treatment of wounds infection caused by two of the most common bacterial pathogens *Staphylococcus aureus* and *Pseudomonas aeruginosa*. For this purpose, three promising essential oil components (EOCs), namely carvacrol, citronellol and cinnamic acid, were loaded into electrospun fibers of poly-ε-caprolactone (PCL) aided by alpha-cyclodextrin (αCD) and hydroxypropyl-β-cyclodextrin (HPβCD). Electrospun-fibers prepared with single, binary and ternary mixtures of the EOCs were screened for antimicrobial properties. The fibers were also characterized regarding their morphological, mechanical, thermal, surface polarity, antibiofilm and antioxidant properties. Differently to αCD that formed poly(pseudo)rotaxanes with PCL and weakly interacted with EOCs, HPβCD facilitated EOC encapsulation and the formation of continuous, smooth, homogeneous fibers (0.5-1 μm diameter) without beads. PCL/HPβCD fibers with high concentration of EOCs showed strong antibiofilm properties (> 3 log CFU reduction) and a high antioxidant activity (10-50 % DPPH scavenging effects). Relevant different performances were recorded for the three EOCs and their mixtures. All fibers showed good biocompatibility as verified using hemolysis tests and *in ovo* tissue integration and angiogenesis evaluation assays. Overall, HPβCD facilitated the complete release of EOCs from the fibers to the aqueous medium, being a promising, environment-friendly, and cost-effective strategy for the treatment of infected wounds.

**Keywords**

Electrospinning; cyclodextrin; essential oil components; antimicrobial; antioxidant; in ovo CAM test.

USC
UNIVERSIDADE DE SANTIAGO DE COMPOSTELA

## Graphical abstract



## 3.1. INTRODUCTION

Skin and soft tissue infections (SSTIs) are inflammatory microbial invasions of the epidermis, dermis and subcutaneous tissue with a lesion size area of at least 75 $cm^2$ [1,2]. They occur when skin defences and microbial invasion interact for different reasons, such as trauma and surgery [3]. SSTIs encompass a wide spectrum of clinical presentations, including cellulitis, impetigo, folliculitis, erysipelas, furuncles and carbuncles [4], with an estimated incidence about 24.6 per 1000 person-year in developed societies [5].

SSTIs range from mild, superficial forms that respond to local care (simple drainage) and oral antibacterial agents, to life-threatening, necrotizing processes, which involve the invasion of deeper tissues, penetrating subcutaneous layers (necrotizing cellulitis), fascia (necrotizing fasciitis) and the muscle (pyomyositis and myonecrosis). Underlying diseases may hinder the response to therapy, and complicated wounds require hospitalization, surgical intervention such as drainage and debridement, and parenteral antibacterial therapy. If the treatment is delayed, the mortality rate can be as high as 20–40% [3]. Complicated abscesses, infected burn wounds, infected diabetics ulcers, and deep space wound infections are particularly challenging [1,4]. This scenario has worsened due to the intensive and indiscriminate use of antibiotics, which has induced bacterial resistance against most conventional treatments available [6].

Antimicrobial resistance (AMR) is becoming one of the greatest threats to human health in the 21st century, returning to the level of the pre-antibiotic era [7,8]. It is estimated that by 2050, the AMR mortality rate will balloon to 10 million lives per year at a cost of one hundred trillion dollars. For these reasons, the World Health Organization placed the AMR in the top 10 urgent threats [7]. Most of these infections, including SSTIs, are caused by *Staphylococcus aureus* in Europe (39.9% of isolates) [9] and North America (44.6 % of isolates) [10]. *S. aureus* forms part of the common skin microbiome. Traditionally, infections caused by *Staphylococcus* species have responded well to penicillin derivatives, but decades of intensive use produced resistance to β-lactamase (in 1948) and latter to methicillin (MRSA in 1965) and vancomycin (VRSA) [12].

Chronic wounds can also be colonized by the Gram-negative *Escherichia coli* and *Pseudomonas aeruginosa*. *P. aeruginosa* is the second most isolated bacterial specie in North America (11.1% of isolates) and Europe (12.5% of isolates) [9] and the first Gram-negative pathogen in SSTIs. These pathogens belong to the group called ESKAPEE, an

USC UNIVERSIDADE DE SANTIAGO

acronym of bacteria which are the most dangerous drug-resistant microbes [7]. Therefore, there is an urgent need of developing new approaches to combat AMR [8]. Alternative agents to current antibiotics must meet certain characteristics, such as low toxicity, low risk of inducing resistance, and adequate economic viability [12]. A good alternative that meets these requirements are secondary metabolites synthesized by plants and other organisms necessary for reproduction and the defense mechanisms against other forms of life such as bacteria, fungi, viruses, vertebrates, etc. [8]. These secondary metabolites can be found in essential oils.

Secondary metabolites can be divided into three major categories, namely terpenes, phenolic compounds and nitrogen-containing compounds [8]. These secondary metabolites can be found in essential oils, which are mixtures of 20 to 100 low molecular weight plant secondary metabolites [7]. Essential oils represent a good alternative to the use of antibiotics, since they are not selective. Their hydrophobicity allows them to partition with the lipids present in the cell membrane or to attach the surface of the cell, penetrate the phospholipid bilayer of bacteria, making the membranes to be more permeable and disrupting many cellular activities, including energy production (membrane-coupled), membrane transport, and cell metabolism, causing cell death [12,13]. Overall, essential oils are less prone to be affected by the resistance mechanisms that bacteria commonly use, such as drug inactivation/alteration, modification of drug binding sites/targets, and changes in cell permeability resulting in reduced intracellular drug accumulation [11].

The non-specific mechanism of action turns essential oil components (EOCs) into broad-spectrum antimicrobial agents, effective against Gram-positive and Gram-negative pathogens [14]. Moreover, most EOCs have antioxidant, anti-parasitic, insecticidal, antiviral, antitumor, and anti-inflammatory capabilities [7,12,15]. Thus, EOCs are versatile and interesting compounds with polyvalent performances. Despite these advantages, there are also numerous constraints that compromise the handling and the effectiveness of EOCs. Generally, EOCs are volatile substances with strong organoleptic flavor, low water solubility and low stability [12]. Therefore, the development of wound dressings or skin scaffolds loaded with EOCs is not straightforward and should consider efficient encapsulation ways that enhance stability and local solubility in order to increase penetration and effectiveness in the skin tissues [16].

USC
DE SANTIAGO
DE COMPOSTELA

This work relies on the hypothesis that electrospun dressings of poly-ε-caprolactone (PCL) containing cyclodextrins (CDs) may act as scaffolds able to encapsulate EOCs and to deliver therapeutic concentrations to the wounds for effective prophylaxis or treatment of infections. Electrospinning is a versatile, economical method to prepare ultrafine fibers with tunable porosity and soft-tissue compatible mechanical properties [17-19]. It can be carried out at room temperature, which is useful for preventing the chemical degradation or volatilization of bioactive substances [16,20]. PCL is a linear aliphatic semi-crystalline polyester of recognized biocompatibility that degrades slowly without altering the surrounding pH [17,21]. Incorporation of CDs may overcome the hydrophobicity of the PCL networks and facilitate the hosting of EOCs by forming inclusion complexes [22-24]. Also, CDs may form poly(pseudo)rotaxanes with a variety of electrospinnable polymers to improve the mechanical properties of the mats, the wettability and the interaction with cells as well as cell proliferation and differentiation [25-27]. Inclusion complexes of EOCs formed during electrospinning can increase the apparent solubility (higher local concentration) and facilitate the diffusion of the EOCs through the soft tissue towards the bacteria [23]. The reports on electrospun fibers containing EOC inclusion complexes are still just a few and mainly intended for fast antimicrobial effect on food preservation [28-31].

To carry out the work, three EOCs were selected: carvacrol, citronellol and cinnamic acid. Carvacrol is a phenolic monoterpenoid, major component of oregano oil [32], that alters the composition of fatty acids in membrane cell, increasing fluidity and permeability [12], depletes the internal ATP pool of bacterial cells and inhibits the synthesis of flagellin, a microbial protein required for bacterial motility [13]. Carvacrol has been shown to be active against planktonic *S. aureus*, including methicillin-resistant *S. aureus* (MRSA), and *S. epidermidis* as well as Gram-negative bacteria [33]. It is classified as fast acting compound, an important quality for obtaining a good response in the first hours of infection [12]. Citronellol is a monoterpene alcohol found in the essential oil of plants of the genus *Cymbopogon*, which can modify the hydrophobicity and disrupt bacteria membrane integrity, leading to the leakage of $K^+$ ions [13,15,34]. Cinnamic acid is a phenolic carboxylic acid found in several plants such as *Cinnamomum cassia* and *Panax ginseng,* which exhibits antioxidant, antimicrobial, anticancer, neuroprotective, anti-inflammatory and antidiabetic properties [35]. It is active against both planktonic and sessile forms of *S. aureus*; the reduction of sessile bacteria being comparable to that of

USC UNIVERSIDADE DE SANTIAGO

peracetic acid and sodium hypochlorite and more efficient than that of hydrogen peroxide [36,37]. Cinnamic acid can cross the cell membrane by passive diffusion as undissociated acid (pKa ≈ 4.2), disturb or even disrupt the cell membrane structure, acidify the cytoplasm and cause denaturation of proteins as well as increasing bacterial permeability [36].

The aim of this work was to obtain a resistant but flexible electrospun scaffold that allows the patients mobility while not deteriorating, carrying a high content in EOCs to provide antibiofilm, angiogenic and antioxidant activity and be used as safer and cost-effective alternative to antibiotics. Several mixtures of PCL with alpha-cyclodextrin (αCD) and hydroxypropyl-β-cyclodextrin (HP-β-CD) were first prepared, and adequate solvents for electrospinning of the mixtures were identified. Morphological, mechanical, thermal and surface properties of the fibers were investigated. Then, fibers loaded with selected EOCs were tested for their preventive action on *S. aureus* and *P. aeruginosa* biofilm set-up, as well as antioxidant and anti-inflammatory properties. Additional studies were also conducted with fibers prepared with binary and ternary combinations of EOCs in an attempt to enhance the antimicrobial efficiency [38] while still preserving biocompatibility.

## 3.2. MATERIALS AND METHODS

### 3.2.1 Materials

Poly-ε-caprolactone (PCL) (80 kDa), 1- bromonaphthalene, carvacrol and 2,2-diphenyl-1-picrylhydrazyl (DPPH) were purchased from Sigma-Aldrich (Steinheim, Germany). Citronellol and cinnamic acid were from Acros (Waltham, MA, USA). Alpha-cyclodextrin (α-CD) Cavamax W6 was from Wacker Chemie (Munich, Germany) and hydroxypropyl-β-cyclodextrin (HPβCD) was purchased from Roquette (Lestrem, France). Tetrahydrofuran (THF), dimethylformamide (DMF) and Live/Dead™ *Bac*Light™ Bacterial Viability Kit were provided by Thermo Fisher Scientific (Waltham, MA, USA). Phosphate-buffered saline (PBS) pH ~7.4 medium was prepared as indicated in the European Pharmacopoeia 6$^{th}$ edition, mixing 8 g/L NaCl, 2.38 g/L $Na_2HPO_4$ and 0.19 g/L $KH_2PO_4$ in ultrapure water. Mueller-Hinton (MH) medium was from Oxoid (Hampshire, UK), Luria-Bertani (LB) from Liofilchem (Roseto degli Abruzzi, Italy), plate count agar (PCA) from Merck (Darmstadt, Germany) and formamide from Merck (Darmstadt, Germany). Acetonitrile and ethanol were provided

USC DE SANTIAGO DE COMPOSTELA

by VWR Chemicals (Leuven, Belgium). Paraformadehyde 3.7-4% was from Panreac (Castellar del Vallès, Barcelona, Spain). Ultrapure water (resistivity > 18.2 MΩ cm; Milli-Q®, Millipore Ibérica, Madrid, Spain) was obtained by reverse osmosis.

### 3.2.2 Preparation of electrospinning solutions

PCL (1.5 g) was dissolved in a mixture of 6 mL of THF and 4 mL of DMF at 45 ºC under stirring for 6 h to obtain a 15% PCL solution. Similarly, 18% and 22% PCL solutions were also prepared. When the solution reached room temperature, carvacrol, citronellol or cinnamic acid were added in various amounts to cover a wide range of concentrations 1%, 2%, 5%, 10% and 20% (w/v). The dispersions remained overnight under gentle agitation.

PCL/αCD fibers were prepared in two steps. PCL (1.5 or 1.8 g) was dissolved in 6 mL of THF and heated at 45 °C with stirring for 24 h. In separate, αCD (0.2, 0.5, 0.7 and 1 g) was dissolved in 4 mL of DMF under stirring for 24 h at room temperature. Then, α-CD/DMF solutions were added to the PCL/THF solutions with stirring. The mixture was magnetically stirred (200 rpm) at room temperature for 7 days. Once a homogeneous solution was obtained, the EOC was added at room temperature with gentle stirring overnight.

PCL/HPβCD fibers preparation followed the same steps as for PCL/αCD, except for the use of 1.5 g PCL and 0.7 g HPβCD instead of αCD.

### 3.2.3 Electrospinning process

A climate-controlled Yflow® Professional Electrospinning Machine (Yflow® S.D., Málaga, Spain) was used for fibers preparation. A series of experiments were carried out varying the electrospinning parameters to optimize the process. The applied voltages ranged between 10 and 15 kV, the collection distance was set at 25.0 cm, and the feeding rates were 1.0-2.0 mL/h for αCD and HPβCD. Composition and electrospinning conditions for each fiber are summarized in **Table 3.1.**.

**Table 3.1. Electrospinning parameters for the manufacture of electrospun fibers. The distance to the collector was 25 cm in all cases.**

| Composition (%) | EOC (%) | THF:DMF (vol:vol) | Temp (ºC) | RH (%) | Voltage (Kv) | | Flow rate (mL/h) |
|---|---|---|---|---|---|---|---|
| | | | | | Nozzle | Collector | |
| PCL 15% | Carvacrol 1% | 60:40 | 21.70 | 28.05 | +9.37 | -3.59 | 1 |

USC UNIVERSIDADE DE SANTIAGO DE COMPOSTELA

| | | | | | | | |
|---|---|---|---|---|---|---|---|
| PCL 15% | Carvacrol 2% | 60:40 | 23.90 | 35.98 | +9.16 | -3.39 | 1 |
| PCL 15% | Carvacrol 5% | 60:40 | 23.60 | 37.04 | +9.16 | -3.39 | 1 |
| PCL 15% | Citronellol 1% | 60:40 | 24.20 | 34.42 | +8.95 | -3.41 | 1 |
| PCL 15% | Citronellol 2% | 60:40 | 24.00 | 32.18 | +9.52 | -3.41 | 1 |
| PCL 15% | Citronellol 5% | 60:40 | 28.20 | 22.14 | +9.52 | -3.41 | 1 |
| PCL 15% | Cinnamic acid 1% | 60:40 | 22.35 | 35.26 | +9.52 | -3.41 | 1 |
| PCL 15% | Cinnamic acid 2% | 60:40 | 22.80 | 38.68 | +11.29 | -3.58 | 1 |
| PCL 15% | Cinnamic acid 5% | 60:40 | 22.90 | 41.80 | +10.20 | -3.57 | 1 |
| PCL 15% | Carvacrol 1%<br>Citronellol 1% | 60:40 | 24.10 | 36.81 | +11.28 | -3.57 | 1 |
| PCL 15% | Carvacrol 2%<br>Citronellol 2% | 60:40 | 23.10 | 52.63 | +10.82 | -3.57 | 1 |
| PCL 15% | Carvacrol 5%<br>Citronellol 5% | 60:40 | 22.30 | 51.62 | +11.09 | -3.57 | 1 |
| PCL 15% | Carvacrol 1%<br>Cinnamic acid 1% | 60:40 | 24.10 | 36.81 | +11.28 | -3.57 | 1 |
| PCL 15% | Carvacrol 2%<br>Cinnamic acid 2% | 60:40 | 23.10 | 41.58 | +12.18 | -3.57 | 1 |
| PCL 15% | Carvacrol 5%<br>Cinnamic acid 5% | 60:40 | 22.30 | 51.62 | +11.09 | -3.57 | 1 |
| PCL 15% | Citronellol 1%<br>Cinnamic acid 1% | 60:40 | 23.10 | 41.58 | +12.18 | -3.57 | 1 |
| PCL 15% | Citronellol 2%<br>Cinnamic acid 2% | 60:40 | 23.10 | 52.63 | +10.82 | -3.57 | 1 |
| PCL 15% | Citronellol 5%<br>Cinnamic acid 5% | 60:40 | 24.37 | 44.24 | +10.20 | -3.57 | 1 |
| PCL 15%<br>2% αCD | Carvacrol 5% | 60:40 | 23.80 | 41.26 | +9.37 | -3.57 | 1 |
| PCL 15%<br>αCD 2% | Citronellol 5% | 60:40 | 23.40 | 42.18 | +12.07 | -3.57 | 1 |
| PCL 15%<br>αCD 2% | Cinnamic acid 5% | 60:40 | 23.40 | 42.18 | +12.07 | -3.57 | 1 |
| PCL 15%<br>αCD 7% | Carvacrol 5% | 60:40 | 23.80 | 36.57 | +13.41 | -3.57 | 1 |
| PCL 15%<br>αCD 7% | Citronellol 5% | 60:40 | 24.37 | 44.24 | +10.20 | -3.57 | 1 |
| PCL 15%<br>αCD 7% | Cinnamic acid 5% | 60:40 | 23.80 | 36.57 | +13.41 | -3.57 | 1 |
| PCL 18% | Carvacrol 10% | 60:40 | 23.40 | 52.12 | +10.90 | -3.61 | 1 |
| PCL 20% | Carvacrol 20% | 60:40 | 24.10 | 52.20 | +15.10 | -3.65 | 1 |
| PCL 22% | Carvacrol 10% | 60:40 | 24.90 | 45.03 | +12.22 | -3.65 | 1 |
| PCL 15% | Citronellol 10% | 60:40 | 24.40 | 45.49 | +12.02 | -3.65 | 1 |
| PCL 18% | Citronellol 10% | 60:40 | 24.90 | 45.03 | +12.22 | -3.65 | 1 |
| PCL 18% | Citronellol 20% | 60:40 | 24.30 | 44.00 | +15.77 | -3.65 | 1 |
| PCL 20% | Citronellol 20% | 60:40 | 22.40 | 45.77 | +12.21 | -3.65 | 1 |
| PCL 15% | Cinnamic acid 20% | 60:40 | 24.15 | 44.90 | +11.89 | -3.65 | 1 |
| PCL 18% | Cinnamic acid 30% | 60:40 | 22.40 | 45.77 | +12.21 | -3.65 | 1 |
| PCL 20% | Carvacrol 10%<br>Citronellol 10% | 60:40 | 22.50 | 58.83 | +14.07 | -3.65 | 1 |

USC UNIVERSIDADE DE SANTIAGO DE COMPOSTELA

| | | | | | | | |
|---|---|---|---|---|---|---|---|
| PCL 20% | Carvacrol 20%<br>Citronellol 20% | 60:40 | 22.70 | 49.95 | +12.29 | -3.65 | 1 |
| PCL 18% | Carvacrol 10%<br>Cinnamic acid 10% | 60:40 | 22.10 | 45.77 | +12.21 | -3.65 | 1 |
| PCL 20% | Carvacrol 20%<br>Cinnamic acid 20% | 60:40 | 23.00 | 54.19 | +12.30 | -3.65 | 1 |
| PCL 18% | Citronellol 10%<br>Cinnamic acid 10% | 60:40 | 21.90 | 49.33 | +11.79 | -3.65 | 1 |
| PCL 20% | Citronellol 20%<br>Cinnamic acid 20% | 60:40 | 23.00 | 54.19 | +11.95 | -3.65 | 1 |
| PCL 18%<br>αCD 2% | Carvacrol 10% | 60:40 | 22.70 | 49.95 | +12.29 | -3.65 | 1 |
| PCL 18%<br>αCD 7% | Carvacrol 10% | 60:40 | 21.70 | 43.94 | +12.29 | -3.65 | 1 |
| PCL 18%<br>αCD 2% | Citronellol 10% | 60:40 | 23.50 | 50.18 | +15.13 | -3.65 | 1 |
| PCL 18%<br>αCD 7% | Citronellol 10% | 60:40 | 24.00 | 53.15 | +11.29 | -3.65 | 1 |
| PCL 18%<br>αCD 2% | Cinnamic acid 10% | 60:40 | 24.00 | 53.15 | +11.29 | -3.65 | 1 |
| PCL 18%<br>αCD 7% | Cinnamic acid 10% | 60:40 | 22.80 | 44.46 | +12.66 | -3.65 | 1 |
| PCL 15% | Cinnamic acid 10% | 60:40 | 23.10 | 50.85 | +12.61 | -3.65 | 1 |
| PCL 15%<br>HPβCD 7% | Cinnamic acid 10% | 50:50 | 20.40 | 34.77 | +9.72 | -3.46 | 2 |
| PCL 15%<br>HPβCD 7% | Carvacrol 5% | 50:50 | 26.10 | 33.56 | +7.44 | -4.26 | 2 |
| PCL 15%<br>HPβCD 7% | Carvacrol 10% | 50:50 | 24.20 | 26.26 | +7.56 | -4.26 | 2 |
| PCL 15%<br>HPβCD 7% | Citronellol 5% | 50:50 | 27.60 | 27.98 | +8.46 | -4.26 | 2 |
| PCL 15%<br>HPβCD 7% | Citronellol 10% | 50:50 | 27.30 | 36.40 | +9.37 | -2.87 | 2 |
| PCL 15%<br>HPβCD 7% | Cinnamic acid 10% | 50:50 | 27.50 | 30.27 | +10.88 | -2.87 | 2 |
| PCL 15%<br>HPβCD 7% | Carvacrol 10%<br>Citronellol 10% | 50:50 | 24.30 | 21.48 | +10.03 | -2.87 | 2 |
| PCL 15%<br>HPβCD 7% | Carvacrol 10%<br>Cinnamic acid 10% | 50:50 | 25.30 | 27.75 | +11.07 | -2.87 | 2 |
| PCL 15%<br>HPβCD 7% | Cinnamic acid 20% | 50:50 | 25.20 | 41.20 | +10.01 | -2.87 | 2 |
| PCL 15%<br>HPβCD 7% | Carvacrol 5%<br>Citronellol 5% | 50:50 | 28.60 | 23.12 | +10.78 | -2.87 | 2 |
| PCL 15%<br>HPβCD 7% | Carvacrol 5%<br>Citronellol 5%<br>Cinnamic acid 5% | 50:50 | 28.40 | 23.12 | +9.78 | -2.87 | 2 |
| PCL 15%<br>HPβCD 7% | Citronellol 10%<br>Cinnamic acid 10% | 50:50 | 27.10 | 25.45 | +10.33 | -4.07 | 2 |

### 3.2.4 Biofilm prevention studies of the electrospun mats

#### 3.2.4.1 Biofilm cells culturability

The activity of the electrospun nanofiber mats was assessed on preventing *S. aureus* (strains CECT 976 and ATCC 25923) and *P. aeruginosa* (CECT 110) biofilm set-up (24 h biofilms formed in the presence of electrospun nanofiber mats) following a modification

USC DE SANTIAGO

of the AATCC 100– Test Method for Antibacterial Finishes on Textile Materials. These strains are commonly used as model to validate the antimicrobial and antibiofilm activity of natural-based molecules [39,40]. Briefly, the nanofiber mats were cut into square pieces of 1.0 cm x 1.0 cm (≈10 mg) and sterilized under UV light for 30 min per side. The sterilized fibers were placed in a sterile 24 well polystyrene microtiter plate (Orange Scientific, Braine-l'Alleud, Belgium). Then, bacterial suspension (2 mL) of *S. aureus* in MH broth (0.04 optical density at 620 nm) or *P. aeruginosa* in LB broth (0.04 optical density at 620 nm) was prepared and added to each well and incubated for 24 h at 37 ºC under mild stirring (100 rpm). After that contact time, the fibers were removed and placed in 2 mL PBS (pH =7.4) in falcons and shaken using a vortex for about 1 min. Subsequently, 100 µL of the falcon solution was transferred to an Eppendorf with 900 µL of PBS and 10-fold serial dilutions were conducted. For each dilution factor, 20 µL were spread on PCA plates and incubated at 37 ºC for 24 h. After the incubation period the number of colony forming units (CFU) were counted and expressed as CFU/mL using **Equation 3.1.** [39].

$$\frac{\text{CFU}}{\text{mL}} = \frac{\text{N}}{\text{SV} \times \text{Dilution}} \qquad (3.1.)$$

where *N* is the number of CFU on the PCA plates and *SV* is the sample volume in mL.

Four replicate experiments were performed for each sample, testing two replicates in different weeks and the growth reduction was evaluated according to the Japanese Industrial Standard, as follows: no antimicrobial activity (< 0.5 log microbial growth reduction), slight antimicrobial activity (0.5 to 1 log microbial growth reduction), significant antimicrobial activity (1 to 3 log microbial growth reduction) and strong antimicrobial activity (> 3 log microbial growth reduction) [41].

#### 3.2.4.2 Biofilm cells membrane integrity

The selective staining exclusion method was used to evaluate the integrity of the biofilm cells membrane of *S. aureus* (strain CECT 976) following the method of Oliveira et al. [42]. For this assay, the Live/Dead BacLight™ kit (Invitrogen, USA) was used, which comprises two nucleic acid binding stains, SYTO 9™ and propidium iodide (PI). The green fluorescent SYTO 9 is capable to penetrate all cell membranes and stains the cells green, whereas fluorescent red PI is assumed to penetrate only cells with damaged

USC UNIVERSIDADE DE SANTIAGO DE COMPOSTELA

cytoplasmic membranes and stains the cells red. For this, after the biofilms grown during 24 h on PCL and PCL/αCD mats, the fibers were removed, transferred to falcons containing PBS and vortexed (as described in section 2.4). Then, 700 µL of each bacterial suspension was stained with 250 µL SYTO9™ and 50 µL PI, allowed to react in the dark for 7 min, and the resulting mixture filtred through a black polycarbonate membrane (Whatman International Ltd., Maidstone, UK). Then, the membranes were mounted on a microscope slide, and the samples visualized with a LEICA DMLB2 epifluorescence microscope (LEICA Microsystems Ltd., Weltzlar, Germany), and photos were taken for a subsequent analysis.

3.2.4.3 Biofilm cellular density

PCL/HPβCD fibers nanofiber mats were cut as square pieces of 1.0 $cm^2$, sterilized under UV light for 30 min per side, and placed in a sterile 24 well-plate. Then, bacterial suspension of either *S. aureus* (ATCC 25923) in MH medium or *P. aeruginosa* (CECT 110) in LB medium (2 mL) was added to each well and incubated for 24 h at 37 ºC under slight stirring (100 rpm). After that contact time, the fibers were removed and placed in 2 mL PBS, pH =7.4. Then 500 µL of SYTO 9/PBS (0.5% v/v) and 500 µL of PI/PBS (0.5% v/v) were added directly to the well with the fiber. The dyes were allowed to react for 15 min in the dark. Then, the fibers were removed from the wells with the help of tweezers, mounted on a slide and analyzed under a Leica STELLARIS 5 confocal microscope (Leica Microsystems, Germany). LAS X® version 3.7.4.23463 (2020 Leica microsystems CMS GmbH), image processing and archiving software were used to acquire the images. A total of 20 fields were counted and at least three independent membranes were used to calculate total cells per square centimeter of biofilm.

### 3.2.5 Fibers characterization

Electrospun mats were coated by sputtering iridium under argon (Sputter Coater (Ir) - QUORUM Q150T-S) and observed using a ZEISS FESEM ULTRA Plus (Carl Zeiss, Oberkochen, Germany). The average diameter of 150 measurements made in 4-6 different areas of each electrospun mat was recorded using the ImageJ analysis software.

Mechanical properties of each type of fibers were investigated using a TA.XT plus Texture Analyzer (Stable Micro Systems, Surrey, UK) equipped with a 30 Kgf (~294 N) load cell under a crosshead speed of 10 mm/min. The fibers were cut as square pieces of

USC UNIVERSIDADE DE SANTIAGO

2.0 cm x 2.0 cm. Ten specimens were tested and the Young's modulus was calculated as the slope of the linear (elastic) region of the stress-strain curve.

X-ray powder diffraction (XRPD) pattern of PCL, αCD and HPβCD and the different fibers without EOCs were recorded to verify the formation of inclusion complexes between PCL and CDs. A Philips powder diffractometer fitted with a PW1710 control unit, a PW1820/00 goniometer and an Enraf Nonius FR590 generator was used. Spectra were made by measuring the scintillation response to Cu Kα radiation in the 2-50° 2θ range, with a step size of 0.04° and counting time of 6 s per step.

Differential scanning calorimetry (DSC) scans of the raw materials and the fibers with and without EOCs were performed using a Q100 DSC (TA Instruments, New Castle, DE, USA). The specimens were accurately weighed in a 40 μL aluminum pan, covered with a tap, and then heated from 25 to 65°C, cooled to -20°C and then heated to 300°C at a scanning rate of 10°C/min in nitrogen atmosphere (50 mL/min).

Contact angles of water, formamide and 1-bromonaphthalene on the electrospun mats were measured using a OCA 15 Plus contact angle system (Dataphysics Instruments, Germany), fitted with a videocamera that allowed for image acquisition and data analysis, following a previously described protocol [43]. Fiber pieces (1 cm x 6 cm) were glued to a glass slide with double-sided tape. For each fiber sample, 6 to 10 measurements were made at room temperature (23 ± 2 ºC). Hydrophobicity was evaluated after contact angles measurement following the van Oss' approach [44-46]. The surface tension components of the solvents were obtained from literature [47].

### 3.2.6 EOC release tests

PCL and PCL/HPβCD fibers (1-30 mg) were immersed in vials containing PBS (pH 7.4) 10-25 mL (depending on the mass of the samples) and placed in a mini-shaker (VWR) at 37ºC and 100 rpm. At predetermined times, aliquots from the release medium were taken, replaced with same volume of fresh medium and filtered (Scharlau® Syringe Filter, 0.22 μm 13 mm PTFE hydrophilic). The concentration in EOC was quantified by HPLC (AS-4140 autosampler, PU-4180 pump, LC-NetII/ADC interface box, CO-4060 column oven, MD-4010 photodiode array detector, JASCO, Tokyo, Japan) fitted with a C18 column (Waters Symmetry C18, 5 μm, 4.6 × 250 mm) and operated with ChromNAV software v.2. The mobile phase was used in a gradient elution. Briefly, the

USC UNIVERSIDADE

mobile phase was initially set as water:acetonitrile in the ratio 70:30 (v/v) and then linearly changed to 20:80 (v/v) over 15 min. Eluent was pumped at flow rate of 1 mL/min and the sample injection volume was 30 µL. Carvacrol was quantified at a wavelength of 276 nm (retention time 10.56 min), citronellol at 210 nm (retention time 11.11 min) and cinnamic acid at 270 nm (retention time 2.01 min). The detection limit (LOD) and the quantification limit (LOQ) were determined for each EOC, as follows: carvacrol 0.381 ppm and 1.154 ppm, citronellol 1.177 ppm and 4.173 ppm, and cinnamic acid 1.848 ppm and 4.909 ppm, respectively. The experiments were carried out in triplicate. HPLC calibration curves of each EOC are shown in **Figures 3.1. to 3.3.**

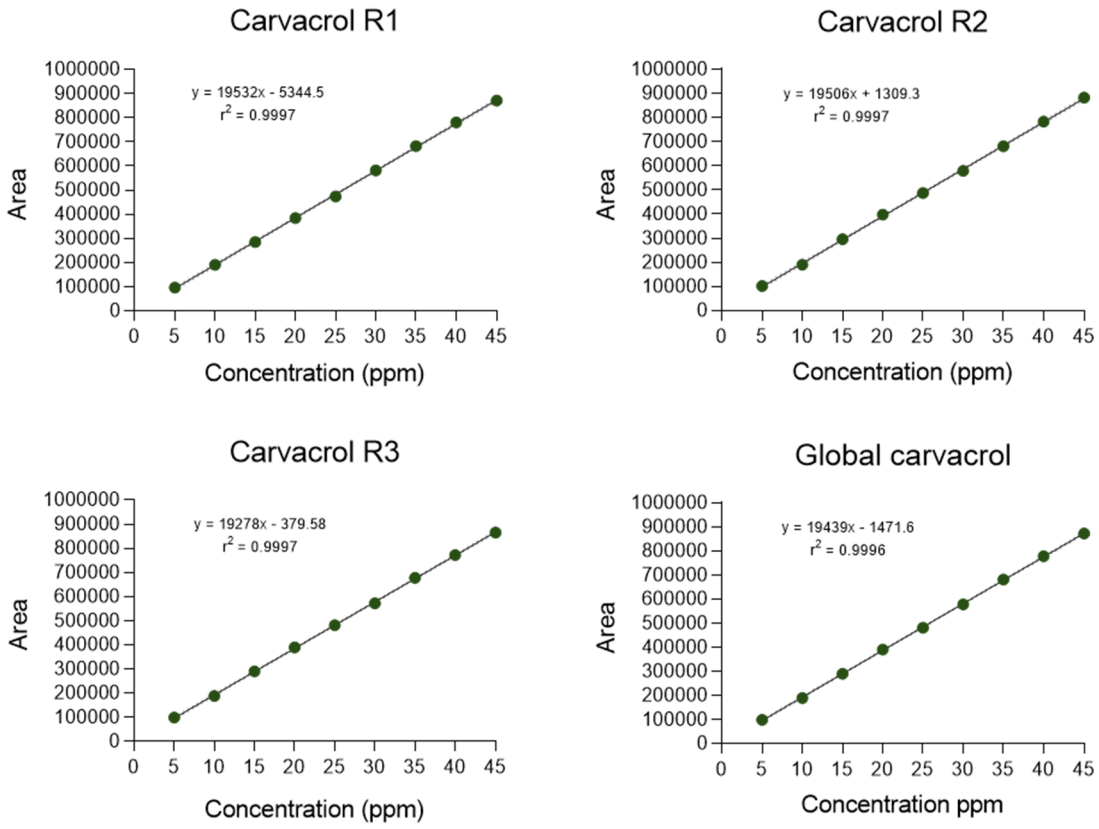



**Figure 3.1. Calibration curves of carvacrol determined by HPLC method.**

USC UNIVERSIDADE DE SANTIAGO DE COMPOSTELA

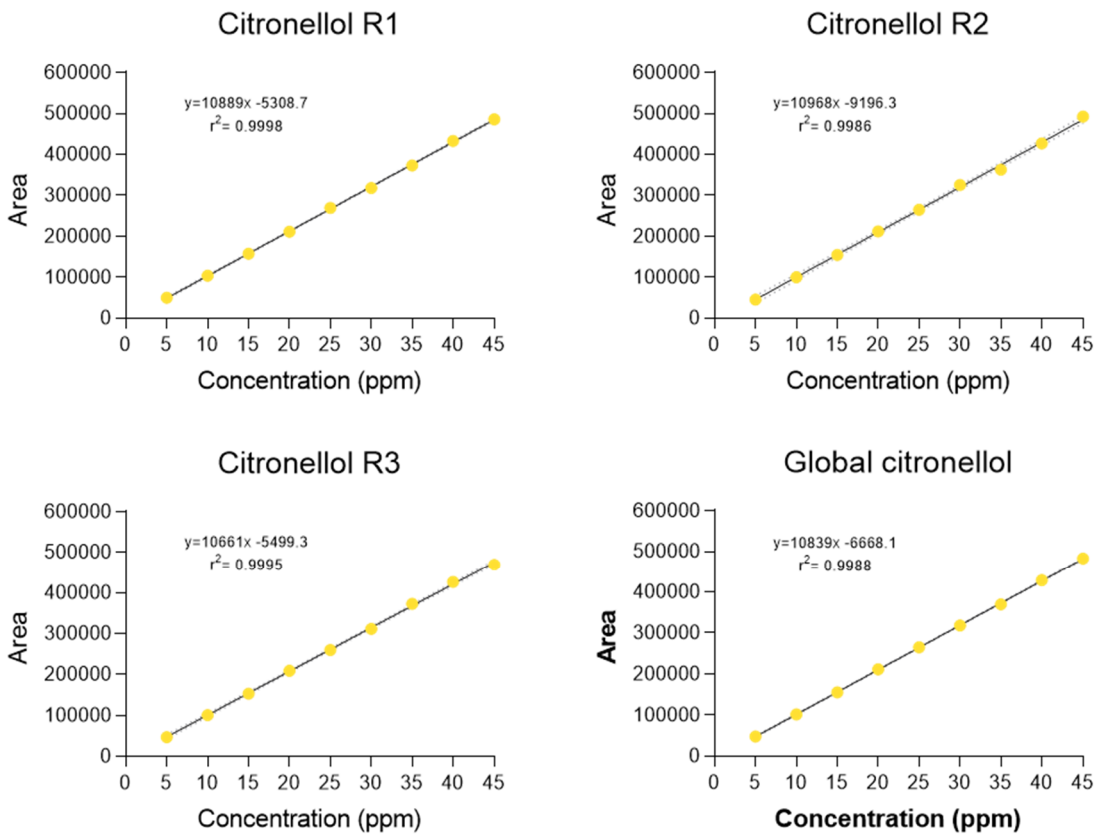



**Figure 3.2. Calibration curves of citronellol determined by HPLC method.**

USC
UNIVERSIDADE DE SANTIAGO DE COMPOSTELA

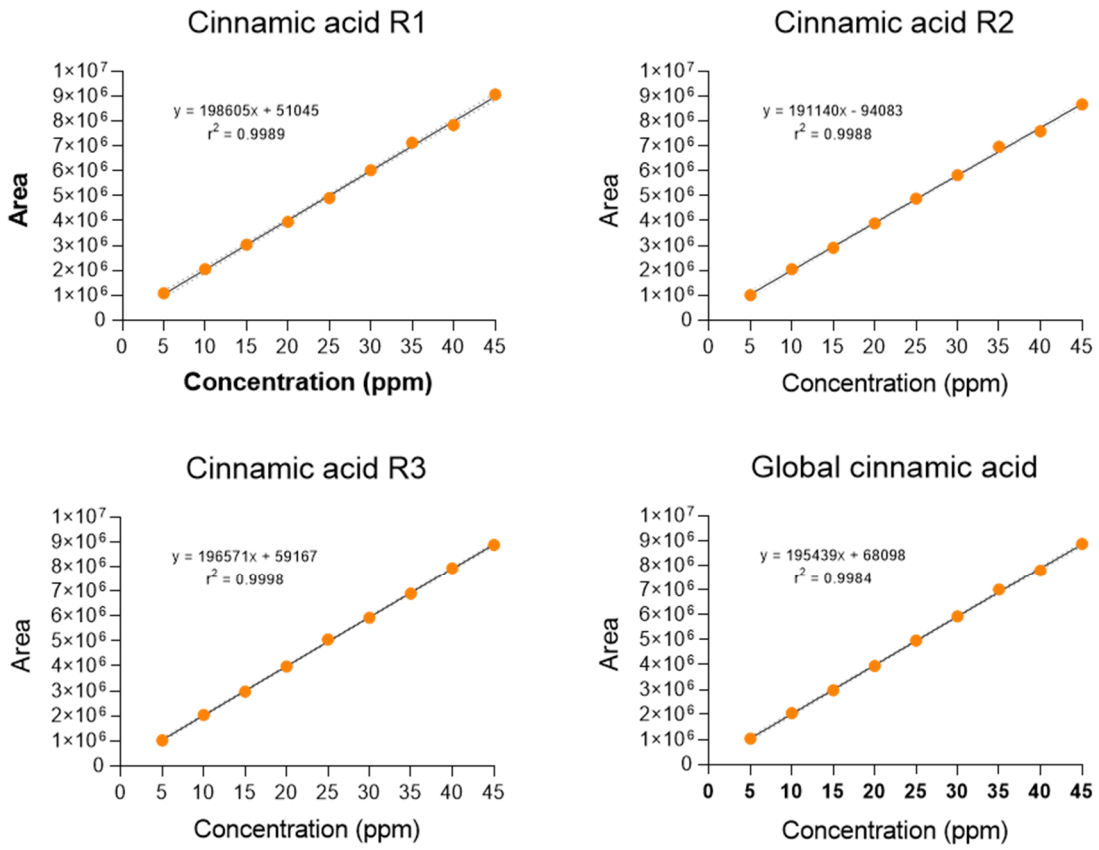



**Figure 3.3 Calibration curves of cinnamic acid determined by HPLC method.**

### 3.2.7 Antioxidant activity

The antioxidant activity was determined using the DPPH free radical method. A 24-hour release study was performed at 37 ºC and 100 rpm, immersing the fibers in 2 mL of PBS. Release medium samples (200 µL) were taken at stablished time points. DPPH solution (200 µL; 80 µg/mL) in ethanol:PBS 50:50 (v/v) was added to each aliquot of the fiber release medium, and the mixtures were kept protected from light and oxygen. After 2 h at 37°C and 100 rpm, the absorbance was recorded at 517 nm by UV spectrophotometry (Agilent 8453, Boeblingen, Germany).

Control experiments were carried out with fresh carvacrol, citronellol and cinnamic acid solutions obtained from a previously prepared high concentration stock solution. To this end, 1000 mg of EOC were diluted in 1 mL of DMSO. Then, 60 µL of each stock solution were taken and added to 1940 µL of ethanol:PBS 50:50 (v/v) to obtain a final concentration of 30 mg/mL. For preparing 11 serial dilutions, 1.4 mL were taken from this solution and mixed with 400 µL of ethanol:PBS 50:50 (v/v). Finally, for each dilution factor, 400 µL was taken and mixed with 400 µL of a previously prepared DPPH

USC DE COMPOSTELA

stock solution (4 mg/100 mL of ethanol:PBS 50:50 (v/v)). After mixing each diluted solution with DPPH solution, all prepared solutions were agitated at 100 rpm and 37°C for 2 h with protection from light. Then, the absorbance was recorded at 517 nm by UV spectrophotometry.

### 3.2.8 Hemolysis test

Square pieces of fibers (1x1 cm) were hydrated with PBS (pH 7.4) for 2 h and placed in Eppendorf tubes. A blood stock solution was prepared by diluting 6.25 mL of total volunteers' blood (Galician Transfusion Center, Spain) previously anticoagulated with EDTA in 250 mL of PBS (pH 7.4). Aliquots (1.5 mL) of the stock solution were added to each Eppendorf. After incubation for 1 h at 37 °C in a minishaker, the tubes were centrifuged at 10,000 g for 10 min [48][338]. The supernatant (150 µL) was taken and placed in 96 well plate.

The hemolytic activity was calculated as a function of the released hemoglobin, which was measured by recording the absorbance (Abs) of the supernatant using a UV–visible microplate reader (Testal, Germany) at 510 nm. Triton 1% solution was used as the positive control (PC) (100% lysis) and blood stock solution was used as the negative control (NC). The hemolysis percentage was calculated using **Equation 3.2.**:

$$\%\ \text{Hemolysis} = \frac{(\text{Abs}_{\text{sample}} - \text{Abs}_{\text{NC}})}{(\text{Abs}_{\text{PC}} - \text{Abs}_{\text{NC}})} \times 100 \qquad (3.2.)$$

### 3.2.9 *In ovo* tissue integration and angiogenesis evaluation

Fertilized hen eggs were supplied by Coren (San Cibrao das Viñas, Spain) and placed in an incubator at 37ºC and 60% relative humidity (Incubato IN-EI-528; Expondo, Zielona Góra, Poland). The position of the eggs was changed (180º) three times per day to mimic the movements by the hen. Lapsed 3 days, a small window (1x1 cm) was opened with a scalpel and scissors to verify that the eggs were fertilized and in optimal conditions to continue with the test. Moreover, this window provoked the retraction of the chicken chorioallantoic membrane (CAM) creating a greater empty space, facilitating the incorporation the scaffolds in the following days. The window was covered with a piece of parafilm to prevent contaminating agents from invading the internal part of the eggs, which were placed back in the incubator in an upright position until day 8. Then, the state of the egg was checked, and the fibers previously sterilized by UV and cut into 8 mm

USC UNIVERSIDADE DE SANTIAGO

circles (with the help of a punch) were incorporated. Two fibers of the same type were placed in each egg to reduce the number of eggs used. The experiment was done in quadruplicate for each fiber composition. The window was closed again.

On day 12, after 5 days of contact of the fibers with the CAM, tissue integration and angiogenesis were evaluated. First, the parafilm was removed and the size of the window was increased using scissors. Then, the CAM was fixed by adding a few drops of 3.7-4% paraformadehyde until the entire surface was covered. After 3 h, the membrane was well fixed and the perimeter of CAM in contact with the fibers was cut. The fiber-CAM system was washed three times with PBS and placed on a slide to obtain the corresponding images with the help of a stereo microscope with an integrated SZ-CTV camera (Olympus, Japan). Finally, the images were analyzed using the ImageJ program to determine the area occupied by the vessels in contact with the fibers. A score of integration (SI) was given to each scaffold, based on the neovascularization and attachment of the scaffold to the CAM. This score ranged from 0 (poor integration) to 3 (excellent integration) [49].

### 3.2.10 Statistical Analysis

Statistical analysis was performed using SPSS v.26.0 (IBM Co., Armonk, NY, USA). All results were expressed as mean ± standard deviation. Statistical analyses of the antimicrobial and antioxidant results (one-way ANOVA) were conducted, followed by the post hoc Tukey HSD multiple comparison test. Previously statistical analysis normality of all variables was evaluated using Kolmogorov-Smirnov test for groups ($n \geq 50$) and Shapiro–Wilk test for groups ($n \leq 50$). A confidence interval was used at least 95%, to define statistical significance (* $p < 0.05$, ** $p < 0.005$, *** $p < 0.001$ and **** $p < 0.0001$).

## 3.3. Results and discussion

EOCs may offer a variety of performances during wound healing, but this study was particularly focused on their capability to prevent/treat infections as an alternative to the use of conventional antibiotics. Thus, the first steps were devoted to find the best conditions to incorporate sufficiently higher amounts of EOCs in electrospun nanofibers by either increasing the concentration in PCL or adding cyclodextrins that can modulate the mechanical properties of the fibers (mainly αCD) and form inclusion complexes with the EOCs (mainly HPβCD). Then, the electrospun fibers were first challenged against

USC DE COMPOSTELA

biofilm formation, which is a major concern for chronic wound healing. Detailed structural and mechanical characterization and EOC release pattern of the fibers was carried out to find correlations with their biofilm prevention performance. Finally, biocompatibility of the most potent antibiofilm and antioxidant electrospun mats was preliminary screened in an *in ovo* model stablished as a suitable alternative to *in vivo* testing.

### 3.3.1 Fibers preparation

Preliminary studies were carried out with solutions prepared with PCL varieties of different molecular weight (50 kDa and 80 kDa) and covering a wide range of concentrations. The use of PCL with a molecular weight of 50 kDa generated irregular fibers of very diverse sizes (**Figure 3.4.**). To overcome this drawback, PCL with a molecular weight of 80 kDa was chosen. Different concentrations of PCL (8%, 12%, 15% and 18%) were tested in THF:DMF 60:40 v/v mixtures. Solutions of 8% PCL rendered nanofibers with beads throughout the entire fibers (**Figure 3.4.c**). Differently, 12% PCL solutions allowed obtaining continuous, smooth, homogeneous fibers without beads (**Figure 3.4.d**). Image analysis performed using Image J software showed diameters of 0.83 ± 0.25 µm according to normal distribution (**Figure 3.5.**).

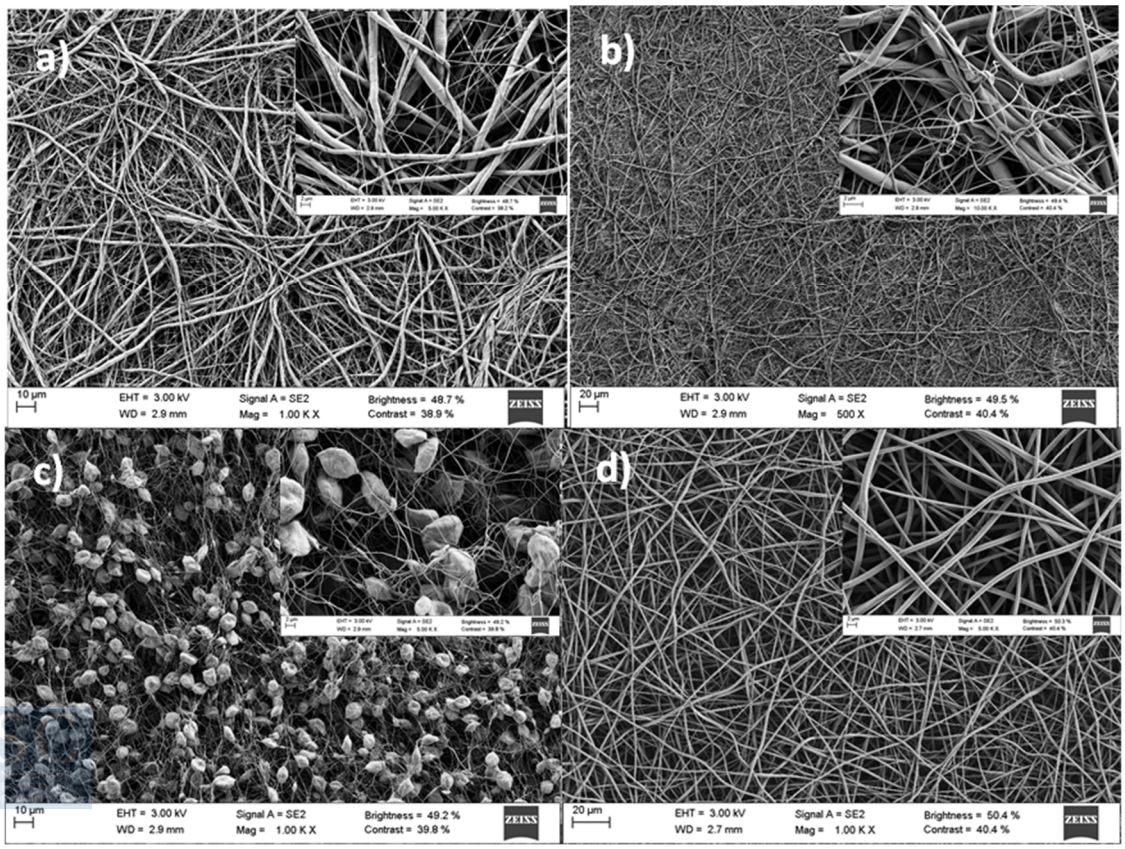


**Figure 3.4. Electrospun fibers of a) PCL (50 kDa) 25% (w/v) THF:DMF (60:40), b) PCL (50 kDa) 30% (w/v) THF:DMF (60:40), c) PCL (80 kDa) 8% (w/v) THF:DMF (60:40), and d) PCL (80 kDa) 12% (w/v) THF:DMF (60:40) solutions.**

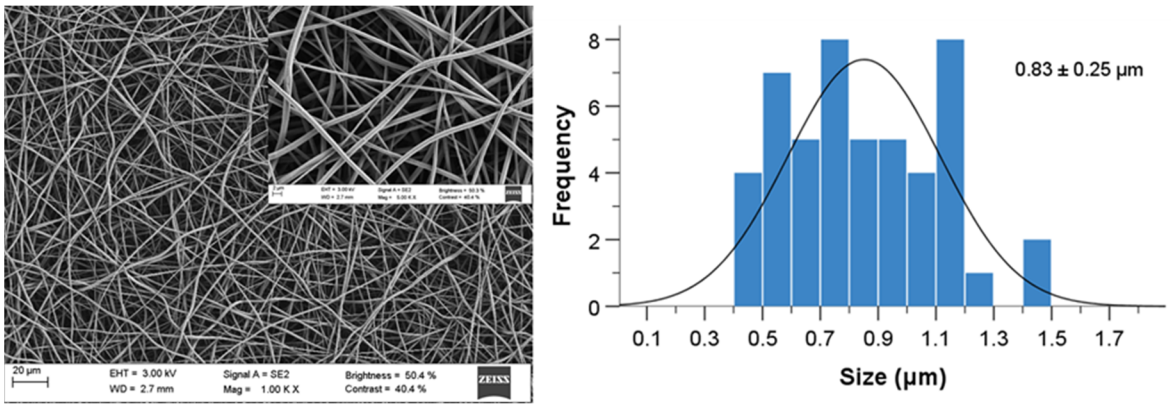



**Figure 3.5. Appearance and size analysis of PCL (80kDa) 12% (w/v) THF:DMF (60:40) fibers.**

PCL (80kDa) and αCD nanofiber mats were successfully electrospun from dispersions containing 15% of PCL and 2-7% of αCD (**Figure 3.6.**). At the time of mixing the two dispersions, the system was transparent, but the two dispersions were perfectly distinguishable (probably due to a difference in density), and after 24 h of stirring the dispersion was completely white suggesting an interaction between PCL and αCD [50]. PCL 15% αCD 2% nanofiber mats were composed of continuous, cylindrical fibers, of average diameters of 0.57 ± 0.14 µm (**Figure 3.7.A**). Increasing the amount of αCD in the polymer dispersion, some beads appeared along some fibers, but did not cause an increase in the fiber diameter. PCL 15% αCD 7% fibers had average diameter of 0.54 ±0.17 µm (n = 50), like PCL 15% αCD 2% fibers (**Figures 3.8 -3.12.**). PCL 18% αCD 2% fibers had average fiber diameters of 0.83 ± 0.25 µm (n = 50). PCL 18% αCD 7% fibers had diameters of 0.88 ± 0.40 µm (n = 50). Compared to PCL 15% fibers, an increase in PCL concentration to 18% caused an increase in fibers diameter, and the addition of αCD did not induce bead formation. Besides, the incorporation of HPβCD 7% (w/v) to PCL 15% (w/v) solution did not cause changes in size compared with the control PCL 15% fibers (**Figure 3.4.A**). The different effects of αCD and HPβCD on the fibers diameter can be attributed to differential interactions of PCL with these cyclodextrins. αCD can tread along PCL chain forming a poly(pseudo)rotaxane as also observed by other authors [22,25] causing the aggregation of PCL chains, as further investigated by X-ray diffraction (**Figure 3.7.B**). Meanwhile, the treading of HPβCD is less favourable due to the larger size of the cavity, and most HPβCD is expected to remain free lengthwise the fiber forming nanowebs.

USC
DE SANTIAGO
DE COMPOSTELA

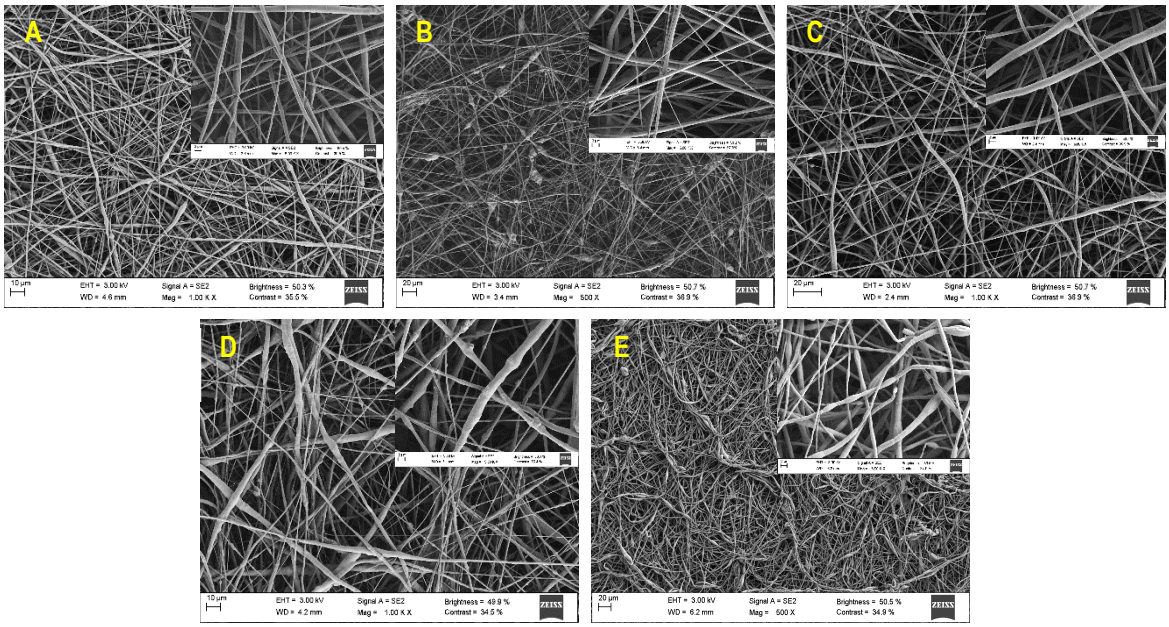



**Figure 3.6. FESEM images recorded at 500× (scale bar 20 µm) and 1000× (scale bar 10 µm), with inserts at 5,000× magnification (scale bar 2 µm) of electrospun mats: A) PCL (80kDa) 15% (w/v) αCD 2% (w/v) THF:DMF (60:40); B) PCL (80kDa) 15% (w/v) αCD 7% (w/v) THF:DMF (60:40); C) PCL (80kDa) 18% (w/v) αCD 2% (w/v) THF:DMF (60:40); D) PCL (80kDa) 18% (w/v) αCD 7% (w/v) THF:DMF (60:40); and E) PCL 15% HPβCD 7% (w/v) THF:DMF (50:50).**

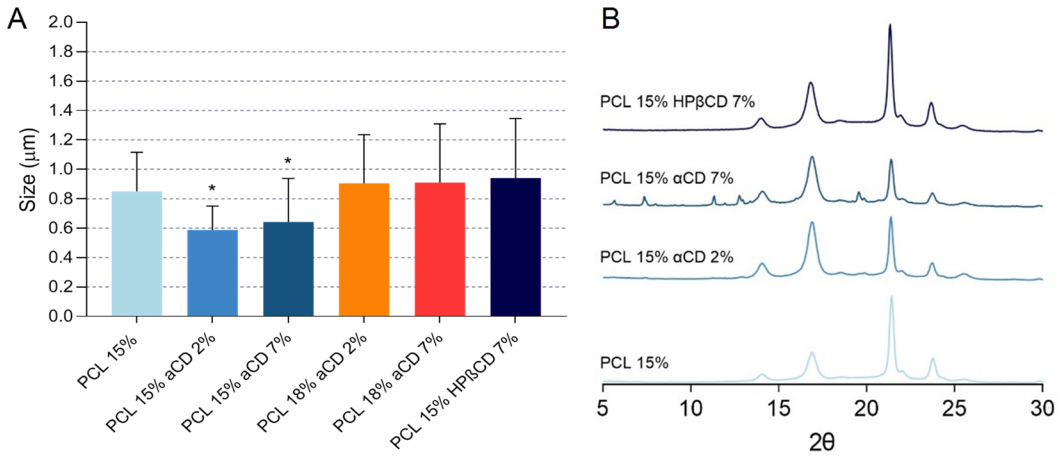



**Figure 3.7. (A) Diameters (n = 50) and (B) X-ray diffractograms of PCL fibres prepared with different contents in αCD and HPβCD.**

XRP diffractograms of PCL 15%, PCL 15% αCD 2%, PCL 15% αCD 7% and PCL 15% HPβCD 7% fibers are shown in **Figure 3.7.B** PCL is semi-crystalline (60% crystallinity with an orthorhombic crystal structure) and has strong characteristic peaks at 14, 16, 22 and 24 °2θ. The fibers maintained those peaks. Poly(pseudo)rotaxane formation with αCD was evidenced as a new peak at 20 º2θ due to its columnar packing, which was not observed for a physical mixture of PCL and αCD [22]. Clearly, this peak

USC UNIVERSIDADE DE SANTIAGO

was more intense in the fibers with the highest content in αCD, in good agreement with literature [50]. In addition, PCL 15% αCD 7% fibers showed peaks at 7 and 12 °2θ which may correspond to free αCD (native cage state) probably due to an excess of αCD not interacting with PCL. Differently, the fibers with HPβCD 7% did not show any additional peak, indicating that the interactions between both PCL and HPβCD, if any, are weak and do not increase the crystallinity of the fibers. This means that this cyclodextrin can remain free to form inclusion complexes with the EOCs. Lower contents in HPβCD were not tested aiming to have sufficiently cyclodextrins to accommodate the EOCs.

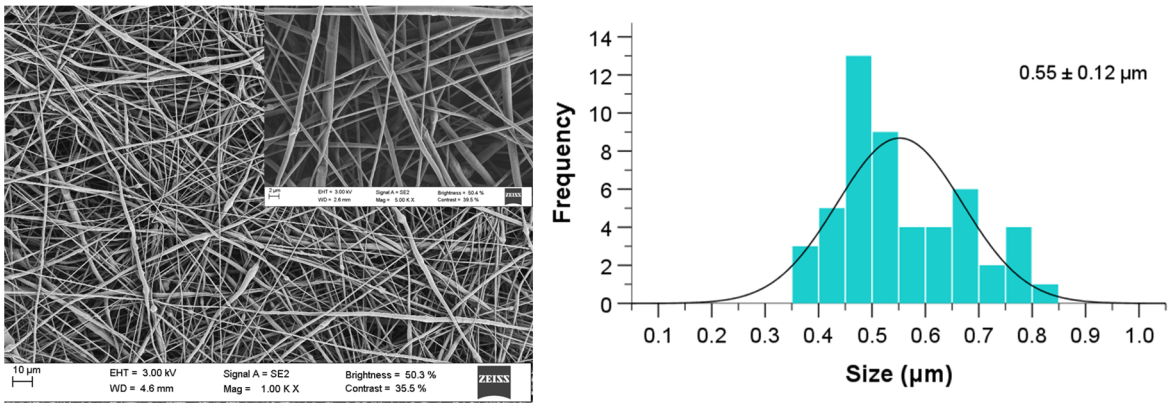



**Figure 3.8. Characterization of PCL (80 kDa) 15% (w/v) αCD 2% (w/v) THF:DMF (60:40) electrospun mat. A) FESEM images with 1000× and 5000× magnification with scale bar 10 µm and 2 µm, respectively. B) The fiber diameter distribution, n > 200.**

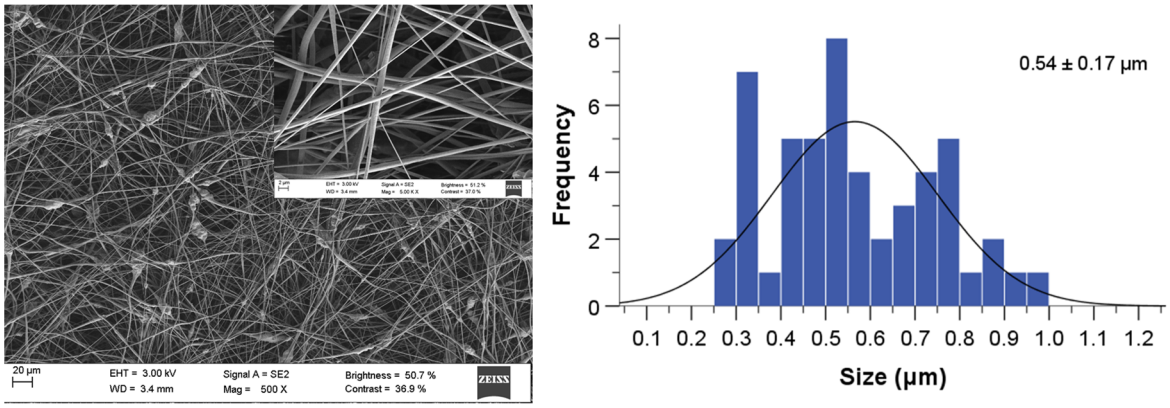



**Figure 3.9. Characterization of PCL (80 kDa) 15% (w/v) αCD 7% (w/v) THF:DMF (60:40) electrospun mat. A) FESEM images with 500× and 5000× magnification with scale bar 20 µm and 2 µm, respectively. B) The fiber diameter distribution, n > 200.**

USC
UNIVERSIDADE DE SANTIAGO DE COMPOSTELA

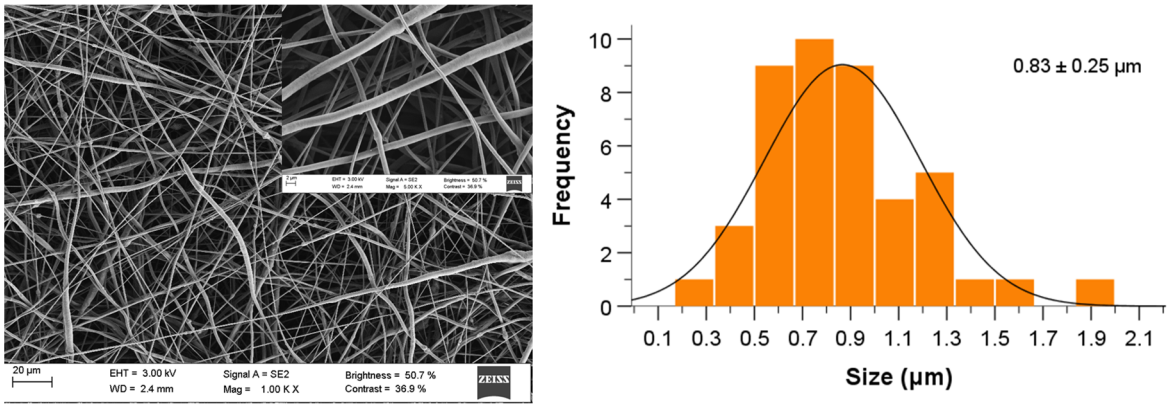



**Figure 3.10. Characterization of PCL (80 kDa) 18% (w/v) αCD 2% (w/v) THF:DMF (60:40) electrospun mat. A) FESEM images with 1000× and 5000× magnification with scale bar 20 µm and 2 µm, respectively. B) The fiber diameter distribution, n > 200.**

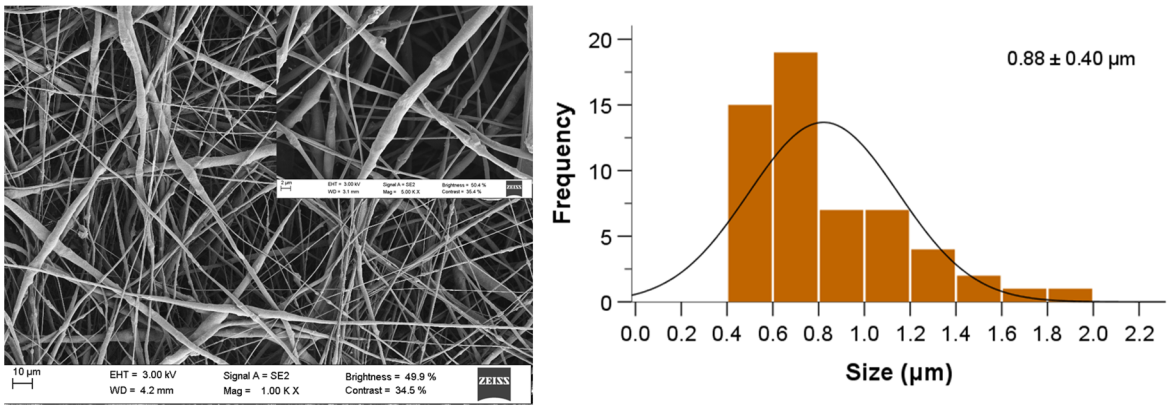



**Figure 3.11. Characterization of PCL (80 kDa) 18% (w/v) αCD 7% (w/v) THF:DMF (60:40) electrospun mat. A) FESEM images with 1000× and 5000× magnification with scale bar 10 µm and 2 µm, respectively. B) The fiber diameter distribution, n > 200.**

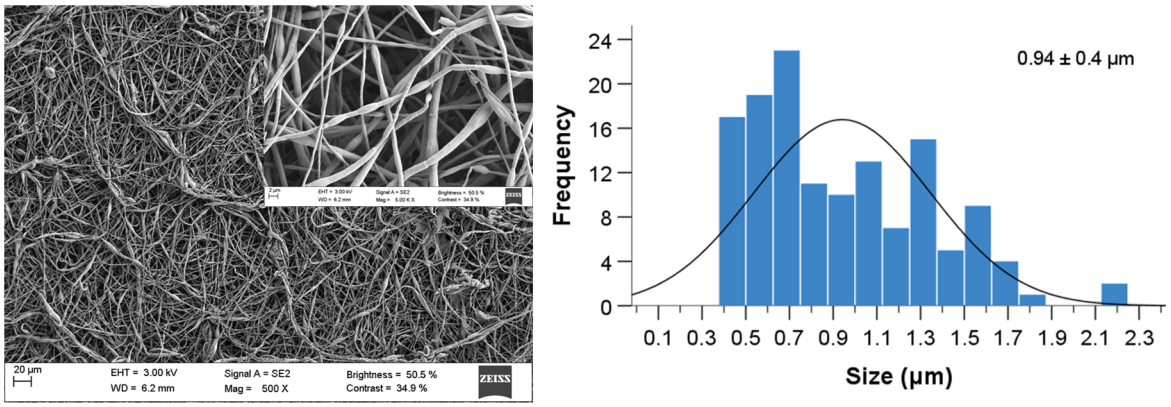



**Figure 3.12. Characterization of PCL 15% HPβCD 7% (w/v) THF:DMF (50:50) electrospun mat. A) FESEM images with 500× and 5000× magnification with scale bar 20 µm and 2 µm, respectively. B) The fiber diameter distribution, n > 200.**

USC UNIVERSIDADE DE SANTIAGO DE COMPOSTELA

### 3.3.2 Antibiofilm activity

Once the concentration of PCL and cyclodextrins and the electrospinning conditions were set, fibers were prepared with the EOCs and their antibiofilm activity (in terms of biofilm cells culturability) was screened before further assessment.

#### 3.3.2.1 *S. aureus* biofilm prevention

PCL 15% fibers with concentrations of 1%, 2% or 5% of carvacrol did not trigger antibiofilm effects against *S. aureus* **(Figure 3.13.)**. The next step was to increase the concentration of PCL to 18%, 20% and 22% (w/v) to encapsulate a greater amount of carvacrol (up to 20% (w/v)) but minor improvements in biofilm prevention properties (0.5-1 log CFU/mL reduction) were obtained, probably due to an inefficient release of carvacrol (the fibers were fused together). To overcome this problem, αCD was incorporated into the fibers in different amounts: 2% and 7% (w/v).

The fibers with αCD 2% did not show antibacterial activity (< 0.5 log CFU/mL reduction) while the fibers with αCD 7% showed a slight microbial activity (0.5-1 log CFU/mL reduction). No statistical differences were observed when carvacrol 5% was included in the fibers. Incorporation of carvacrol at higher proportions improved the antimicrobial activity; PCL 15% αCD 7% carvacrol 20% caused 1-3 log CFU/mL reduction ($p < 0.0001$, with respect to the control fibres and fibers without cyclodextrins). Nevertheless, fibers prepared with αCD 7% showed high variability in the antimicrobial performances **(Figure 3.13.)**. Thus, it was replaced by HPβCD at 7%. Fibers incorporating HPβCD 7% showed strong antimicrobial activity (>3 log CFU/mL reduction) and presented great improvements ($p < 0.0001$) with respect to the fibers prepared with 5% and 10% carvacrol. These results suggested that the fibers require a carvacrol concentration of 5% or higher and that an effective release of carvacrol from the fiber should be ensured, which could be provided by HPβCD as verified in subsequent sections.

USC UNIVERSIDADE DE SANTIAGO DE COMPOSTELA

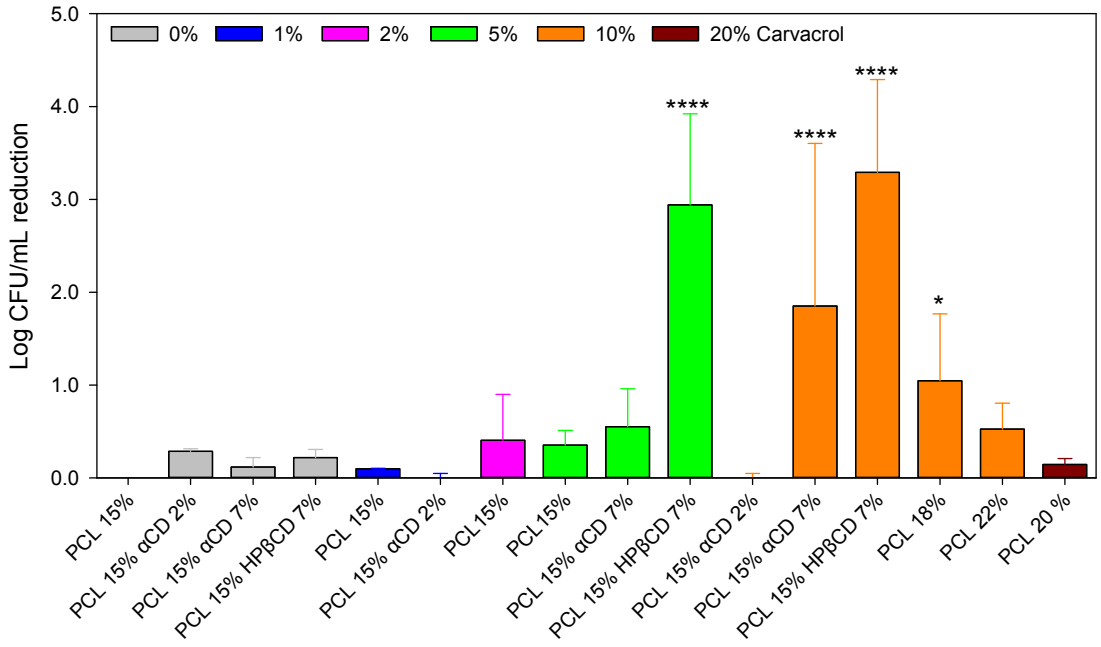



**Figure 3.13. Preventive action of PCL, PCL-αCD and PCL-HPβCD fibers loaded with carvacrol at different concentrations (from 1 to 20%, as indicated in the legend) against *S. aureus* biofilms, in terms of reduction of culturable cells (log (CFU/mL) reduction) after 24 h contact time. Mean ± standard deviation, n=4, * p < 0.05, ** p < 0.005, *** p < 0.001 and **** p < 0.0001.**

Similar results were observed for PCL 15% fibers containing 1%, 2%, or 5% (w/v) of citronellol, indicating the lack of antimicrobial properties due to either an inefficient release of the EOC (PCL forms a hydrophobic network) or an insufficient content of citronellol (**Figure 3.14.**). PCL 18% fibers that were prepared containing 10% citronellol did not display antimicrobial activity either. Differently, PCL 18% citronellol 20% showed a strong antimicrobial activity (>3 log CFU/mL reduction; $p < 0.0001$).

PCL 15% with αCD fibers were prepared in an attempt to improve the antimicrobial properties using less amount of citronellol to minimize possible toxic effects that citronellol 20% may have on human skin. PCL 15% αCD 2% citronellol 5% fibers showed significant activity (1-3 log CFU/mL reduction). A further increase in αCD concentration (7 %) did not improve the results, which may be related to the preferential binding of citronellol to PCL through hydrophobic interactions and the poor capability of αCD to solubilize citronellol by forming inclusion complexes [51]. αCD may also form poly(pseudo)rotaxanes with PCL increasing the hydrophobicity of the mat [22]. Differently, replacement of αCD by HPβCD (7%) allowed reaching significant antimicrobial activity (1-3 log CFU/mL reduction), and similar to that obtained for PCL 15% αCD 2% citronellol 5% mats.

USC
UNIVERSIDADE DE COMPOSTELA

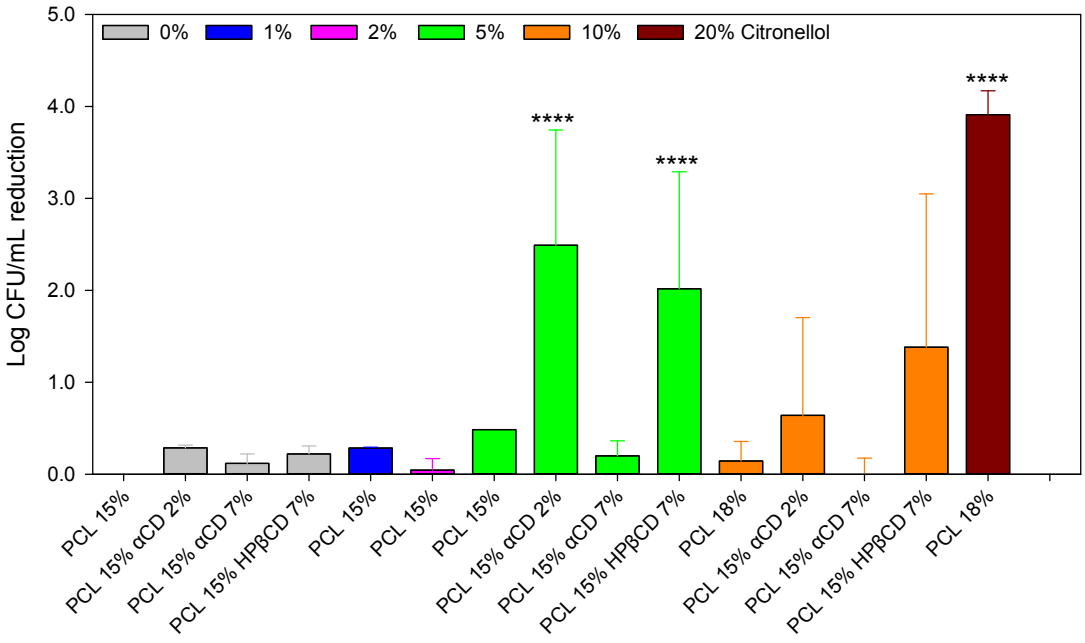



**Figure 3.14. Preventive action of PCL, PCL-αCD and PCL-HPβCD fibers loaded with citronellol at different concentrations (from 1 to 20%, as indicated in the legend) against *S. aureus* biofilms, in terms of reduction of culturable cells (log (CFU/mL) reduction) after 24 h contact time. Mean ± standard deviation, n=4, * p < 0.05, ** p < 0.005, *** p < 0.001 and **** p < 0.0001.**

Cinnamic acid performed differently from carvacrol and citronellol since PCL 15% fibers efficiently encapsulated cinnamic acid up to 20%. PCL 15% fibers prepared with 1, 2, 5 and 10% cinnamic acid did not show antibacterial activity, but those prepared with 20% cinnamic acid displayed significant log CFU/mL reduction (1-3 log CFU/mL reduction; $p < 0.0001$) with respect the other fibers (**Figure 3.15.**). Similar bacterial inhibition was recorded for PCL 18% cinnamic acid 30% fibers. The incorporation of αCD at the concentrations of 2% and 7% (w/v) did not improve the antibacterial properties. Differently, the incorporation of HPβCD at 7% strongly increased the antibacterial activity (>3 log CFU/mL reduction), reaching a total reduction of CFUs after 24 h contact.

USC UNIVERSIDADE DE SANTIAGO DE COMPOSTELA

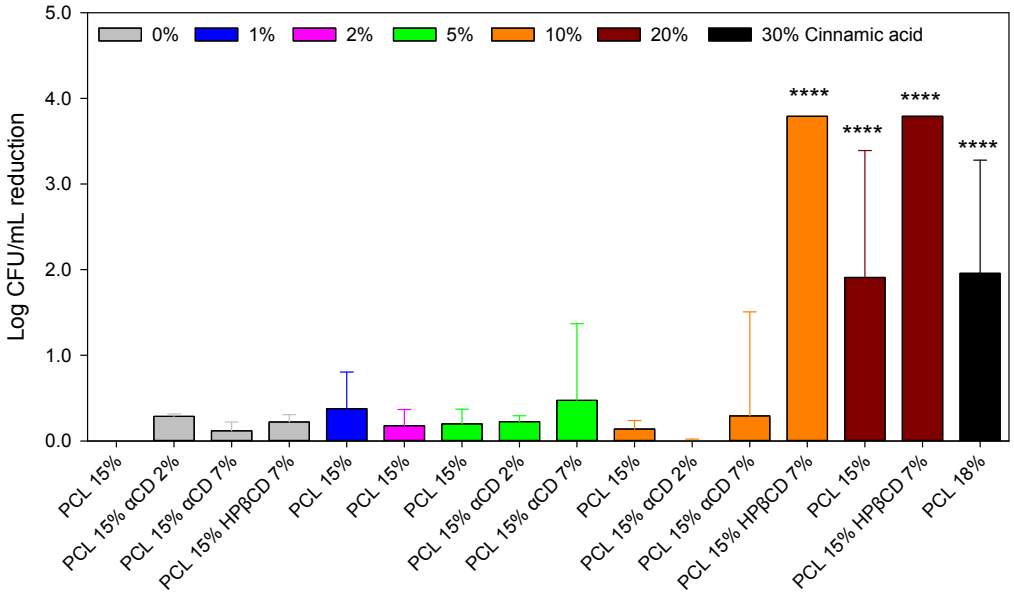



**Figure 3.15. Preventive action of PCL, PCL-αCD and PCL-HPβCD fibers loaded with cinnamic acid at different concentrations (from 1 to 30%, as indicated in the legend) against *S. aureus* biofilms, in terms of reduction of culturable cells (log (CFU/mL) reduction) after 24 h contact time. Mean ± standard deviation, n=4, * p < 0.05, ** p < 0.005, *** p < 0.001 and **** p < 0.0001.**

The next step was to explore the synergy that combinations of EOCs may provide to enhance the antimicrobial activity. The antimicrobial activity of fibers containing carvacrol-citronellol, carvacrol-cinnamic acid, and citronellol-cinnamic acid at 1%, 2%, 5%, 10% and 20% (w/v) was investigated at PCL concentration of 15%, 18% and 20% (w/v) (**Figure 3.16.**). Note that the percentage of EOC refers to each EOC in the mixture; namely carvacrol-citronellol 5% means that a 5% in each EOC was used to prepare the fibers. Fibers prepared with concentrations lower than 5% (w/v) of each EOC did not show antimicrobial activity, except for PCL 15% carvacrol-citronellol 5% which displayed significantly greater activity (1-3 log CFU/mL reduction; $p < 0.0001$) with respect to other fibers also prepared without HPβCD. Similarly, PCL 18% fibers prepared with citronellol-cinnamic acid mixture at 10-20% exhibited significant antimicrobial activity (1-3 log CFU/mL reduction).

USC UNIVERSIDADE DE SANTIAGO DE COMPOSTELA

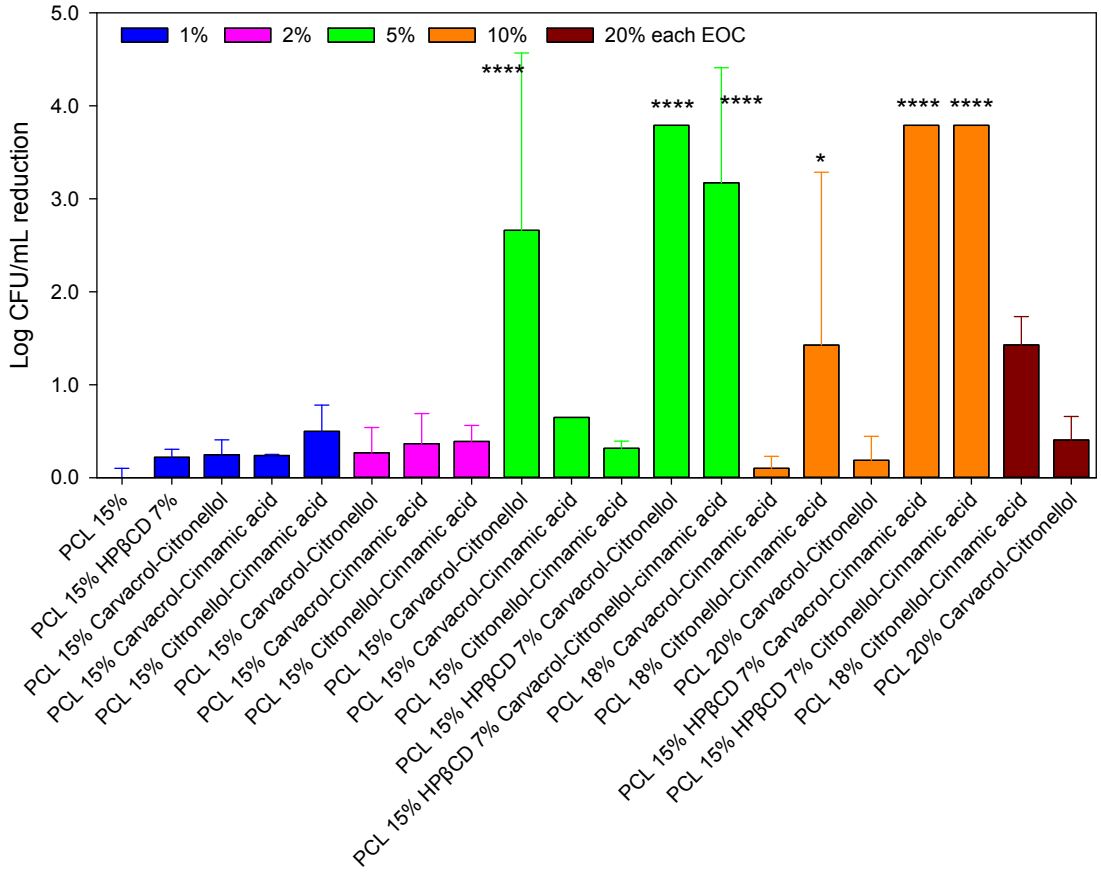



**Figure 3.16. Preventive action of PCL, PCL-αCD and PCL-HPβCD fibers loaded with binary (1:1) and ternary (1:1:1) mixtures of carvacrol, citronellol and cinnamic acid (from 1 to 20%, as indicated in the legend) against *S. aureus* biofilms, in terms of reduction of culturable cells (log (CFU/mL) reduction) after 24 h contact time. Mean ± standard deviation, n=4, * p < 0.05, ** p < 0.005, *** p < 0.001 and **** p < 0.0001.**

Since the results of the PCL 15-20% fibers with the different mixtures at low concentrations of EOCs did not exhibit relevant antimicrobial activity, HPβCD 7% was incorporated (**Figure 3.16.**). All PCL 15% HPβCD 7% fibers prepared with binary and ternary combinations of EOCs showed strong antimicrobial activity (> 3 log CFU/mL reduction; $p < 0.0001$ with respect to the other fibers). Indeed, the fibers containing binary combinations of EOCs completely inhibited bacterial growth.

Overall, the three EOCs tested exhibited strong antimicrobial properties when they were loaded into PCL 15% HPβCD 7% fibers, notably surpassing the antimicrobial activity of PCL 15-20% or PCL 15% αCD 2-7% fibers loaded with the same EOC concentrations. Only the PCL 18% fibers that incorporated citronellol 20% alone (not mixed with other EOC) were shown to be equally efficient. Thus, HPβCD improved the

USC
UNIVERSIDADE DE SANTIAGO DE COMPOSTELA

antimicrobial properties of the EOCs against *S. aureus* facilitating a log CFU/mL reduction greater than 3 or 4; namely these fibers could kill 99.9% bacteria. This improvement in the antimicrobial activity was mainly due to the high efficiency of the inclusion complex formation of EOCs with HPβCD [52], which resulted in fibers of adequate morphology (avoiding fiber fusion), with a high content in EOCs, and that increased the apparent solubility of the EOCs in the aqueous release medium (PBS), as further investigated in section 3.4. This finding is in good agreement with the decrease in MIC and MBC (up to 8 times) recorded for inclusion complexes of EOCs with different CDs against *S. aureus* and *P. aeruginosa* [53][339]. Subsequent release tests confirmed the facilitated release of EOCs from PCL 15% HPβCD 7% fibers, as tackled in section 3.4. The antimicrobial efficacy shown by the EOCs-loaded PCL 15% HPβCD 7% fibers against *S. aureus* were comparable with that of commercial formulations containing silver for treatment of wound infections such as Algicell™, PolyMem® Silver Non-Adhesive Pads, and PolyMem® Silver Shapes [54] that offer an efficacy ≤ 99.99% of bacterial reduction against *S. aureus*.

3.3.2.2 *P. aeruginosa* biofilm prevention

The therapeutic arsenal against Gram-negative bacteria, especially *P. aeruginosa,* is scarce and consists mainly of ceftazidime (cephalosporin) and ciprofloxacin (fluoroquinolone) [55]. Resistance against other antibiotics is a major concern. Thus, for *P. aeruginosa* CECT 110 biofilm prevention studies the most efficient fibers against *S. aureus* (CECT 976) were selected, i.e. those made with HPBCD 7% (**Figure 3.17.**).

The PCL 15% HPBCD 7% carvacrol 5% fibers caused a significant log CFU/mL reduction (1-3 log CFU/mL reduction; $p < 0.005$). An increase in carvacrol to 10% reduced further the CFUs (4 log CFU/mL reduction; $p < 0.0001$). Differently, citronellol-loaded fibers did not display relevant antimicrobial activity. Poor results were obtained also by the fibers loaded with cinnamic acid. Despite these fibers caused the greatest bacterial inhibition against *S. aureus*, the amount of cinnamic acid that they supplied was not enough to alter *P. aeruginosa* growth. According to literature, cinnamic acid MIC of *P. aeruginosa* is close to 12 mg/mL [56], suggesting that cinnamic acid is not a good candidate for use against this Gram-negative bacterium.

USC UNIVERSIDADE DE SANTIAGO DE COMPOSTELA

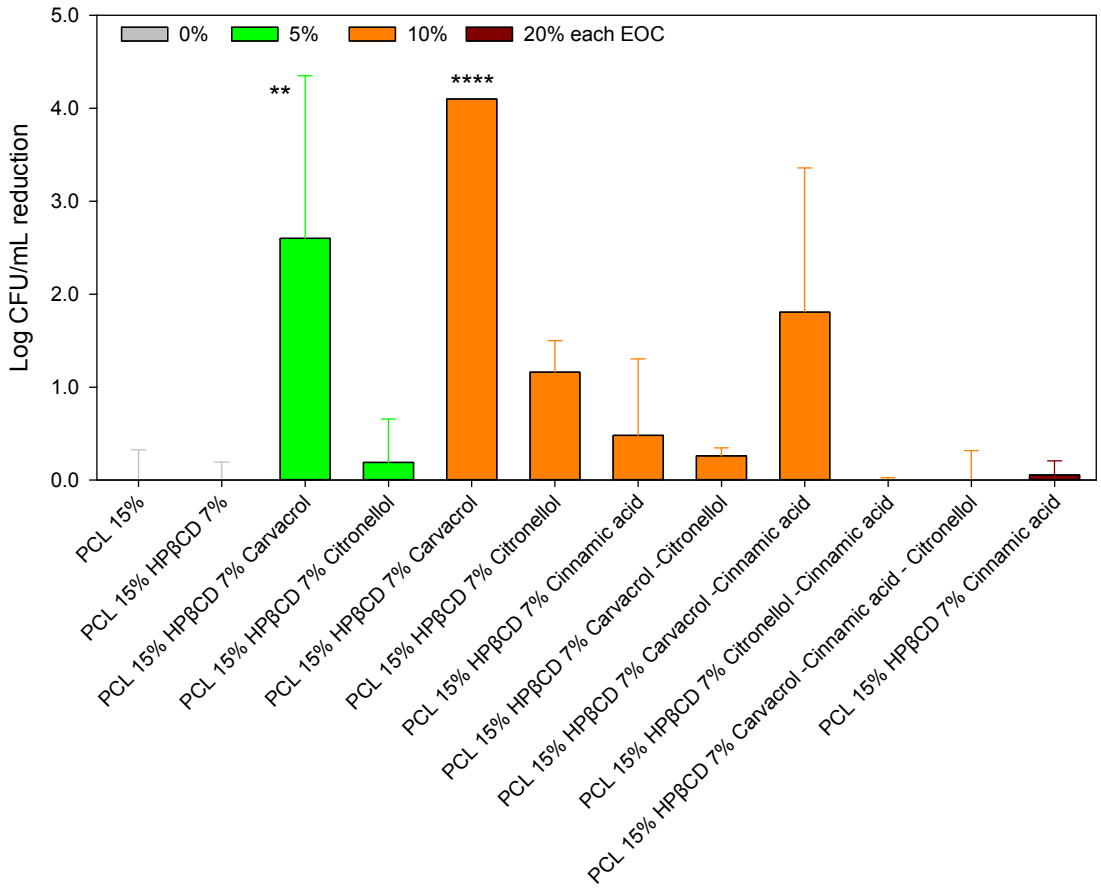



**Figure 3.17. Preventive action of PCL 15% HP-β-CD 7% fibers loaded with single, binary (1:1) and ternary (1:1:1) mixtures of carvacrol, citronellol and cinnamic acid (from 1 to 20%, as indicated in the legend) against *P. aeruginosa* biofilms, in terms of reduction of culturable cells (log (CFU/mL) reduction) after 24 h contact time. Mean ± standard deviation, n=4, * p < 0.05, ** p < 0.005, *** p < 0.001 and **** p < 0.0001.**

The fibers prepared with binary mixtures of EOCs at 10% (w/v) showed minor antimicrobial efficacy against *P. aeruginosa*, quite the opposite to what was observed when tested against *S. aureus*. Only the PCL 15% HPBCD 7% carvacrol-cinnamic acid 10% fibers caused 2 log CFU/mL reduction. Thus, compared to the non-active citronellol and cinnamic acid either alone or mixed together, the presence of carvacrol was required to endow the fibers with antimicrobial efficacy against *P. aeruginosa*. These results agree well with previous reports on the relevant antimicrobial activity of carvacrol against *P. aeruginosa* (MIC 1.18 mg/mL and MBC 2.25 mg/mL) and its capability to inhibit biofilm formation through disruption of the quorum sensing, thus decreasing bacteria pathogenicity [57].

USC UNIVERSIDADE DE SANTIAGO DE COMPOSTELA

3.3.3 Biofilm cellular density characterization

To gain a further insight into the *S. aureus* CECT 976 antibiofilm activity of the electrospun fibers, PCL/αCD electrospun mats, epifluorescence microscopy analysis was carried out for a qualitative assessment of the membrane integrity of biofilm cells. Meanwhile, the preventive action of PCL/HPβCD electrospun fibers on *S. aureus* ATCC 25923 and *P. aeruginosa* CECT 110 biofilm set-up was qualitative and quantitative assessed by confocal microscopy.

Regarding epifluorescence microscopy, the control groups showed a high population density of *S. aureus* CECT 976 (**Figure 3.18.A-C**), with most intact cell membranes (green color) that occupied the greatest area of the field. Meanwhile, few or no cells with membrane damaged (red-stained cells) were observed. Collectively, the electrospun mats loaded with EOC (**Figure 3.18.D-L**) displayed an increase in the population of cells with membrane damaged, highlighting PCL 15% carvacrol-citronellol 5%, PCL 18% citronellol 20%, PCL 15% cinnamic acid 20%, and PCL 18% cinnamic acid 20%. These results are consistent with CFU counting in the section above, showing an equal or more than significant log CFU/mL reduction (1-3 log CFU/mL reduction; $p < 0.05$). Nonetheless, bacterial cells with intact membranes were detected in all fibers despite the high amounts of EOC loaded. In parallel with former section, an improvement in the antibiofilm activity using lower concentrations of EOCs to minimize toxicity in human cells was searched by incorporating HPβCD to the fibers.

USC UNIVERSIDADE DE SANTIAGO DE COMPOSTELA

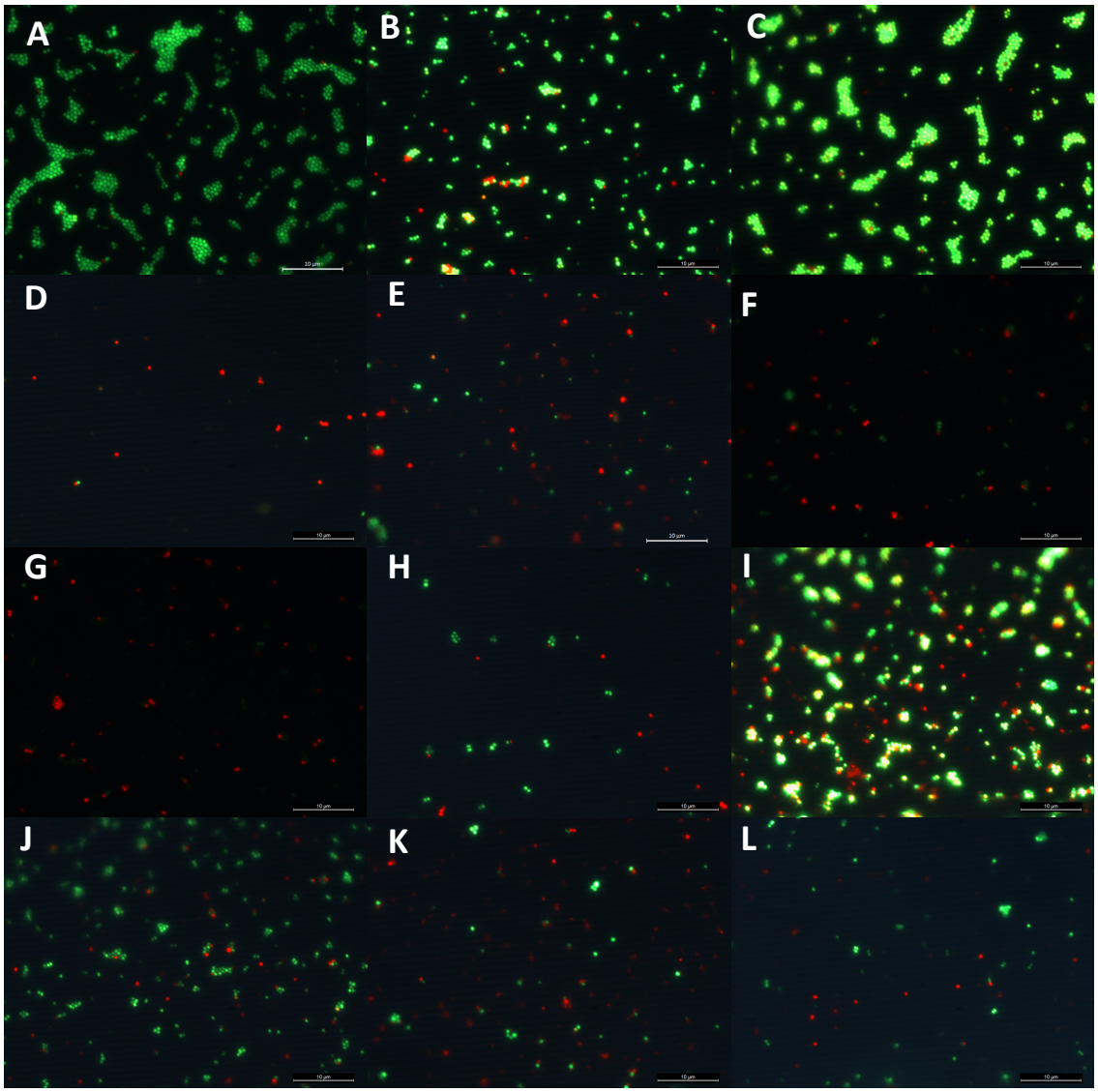



**Figure 3.18. Representative epifluorescence microscopy images of *S. aureus* CECT 976 sessile cells (stained by the Live/dead BacLight bacterial viability kit®) from biofilms grown during 24 h on A) PCL 15% (Control), B) PCL 15% αCD 2% (Control), C) PCL 15% αCD 7%, D) PCL 15% carvacrol-citronellol 5%, E) PCL 18% citronellol 20%, F) PCL 15% cinnamic acid 20%, G) PCL 18% cinnamic acid 30%, H) PCL 20% citronellol-cinnamic acid 20%, I) PCL 18% αCD 7% citronellol 5%, J) PCL 15% αCD7% carvacrol 5%, K) PCL 18% CD2% citronellol 10%, and L) PCL 18% αCD 7% citronellol 10%. Green cells are cell with intact membrane and red cells are cells with damaged membrane.**

In good agreement with section 3.4 results, the PCL/HPβCD fibers loaded with EOCs exhibited strong antimicrobial activity against sessile cells as revealed by confocal microscopy (**Figure 3.19-3.34**). For each type of fiber, three sets of images were taken: (A) the population of bacterial cells, both alive (intact) and dead, attending only to the emission of fluorescence; (B) the location of the bacterial cells within the fiber; and (D) a three-dimensional representation from which the area occupied by intact/dead bacteria cell layers was calculated (C). Regarding *S. aureus* ATCC 25923, the control PCL 15%

USC UNIVERSIDADE DE SANTIAGO DE COMPOSTELA

electrospun mat (**Figure 3.19.**) displayed a high and significant intact population attached to the fibers ($p < 0.0001$) compared to dead bacterial cells, as expected due to the lack of antimicrobial agent. Some bacterial death may be related to the fact that the staining was performed after 24 hours of incubation and, therefore, some cells may have entered the death phase. Interestingly, PCL 15% HPβCD 7% fibers without EOCs (**Figure 3.20.**) showed some bacterial cells attached to their surface with the same population of intact and dead bacteria, which could be due to a change in surface hydrophobicity, as investigated further in section 3.5.

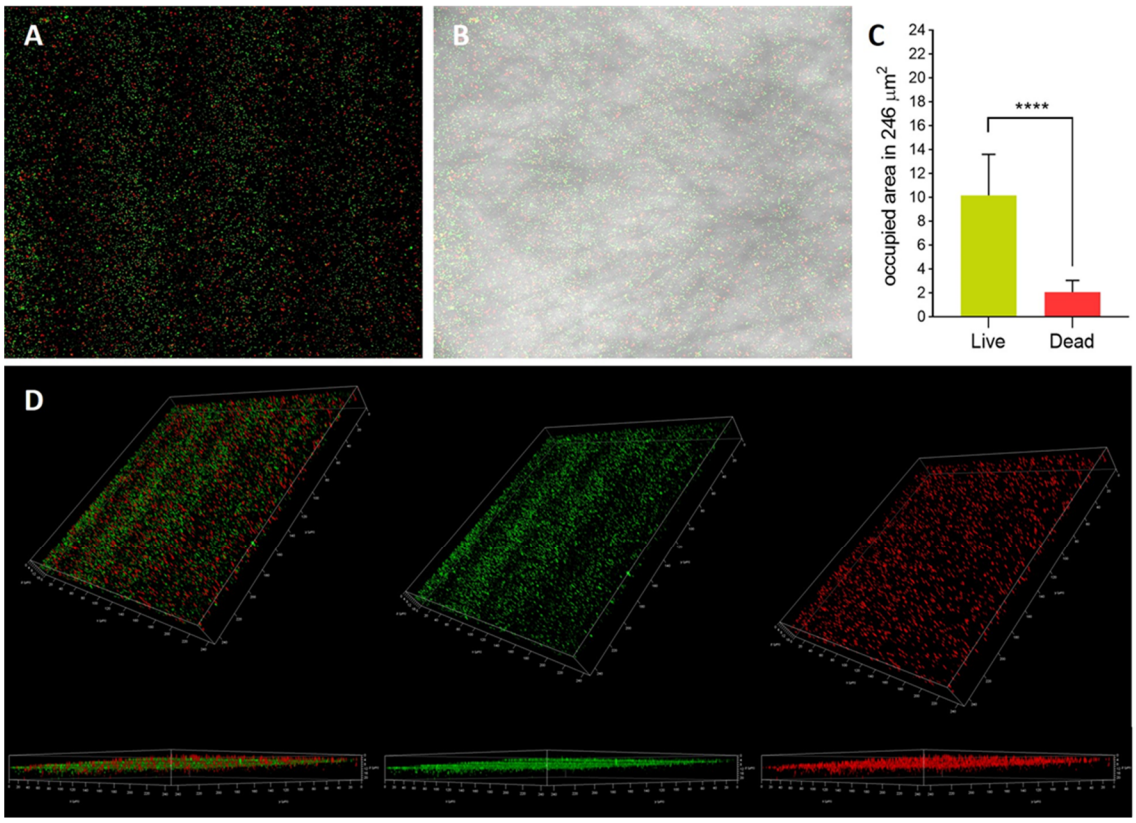



**Figure 3.19. Confocal microscopy images of *S. aureus* ATCC 25923 biofilms grown on PCL 15% fibers for 24 h under 100 rpm at 37 °C, stained by the Live/dead BacLight bacterial viability kit®. Alive bacterial cells with intact membrane present green fluorescence conferred by SYTO™ 9 dye, while dead bacterial cells present red fluorescence conferred by propidium iodide (PI) dye. (A) Top view of the electrospun mats using the green and red channels; (B) bacterial cells attached on the surface of lengthwise fibers from the electrospun mat; (C) occupied area in 246 µm² by intact and dead cells, mean ± standard deviation, n=5; and (D) 3D images of the electrospun mat (length, height, and depth) with the comparation of dead (right) and intact bacteria (center), and both types bacteria (left) on the same plane.**

USC UNIVERSIDADE DE SANTIAGO DE COMPOSTELA

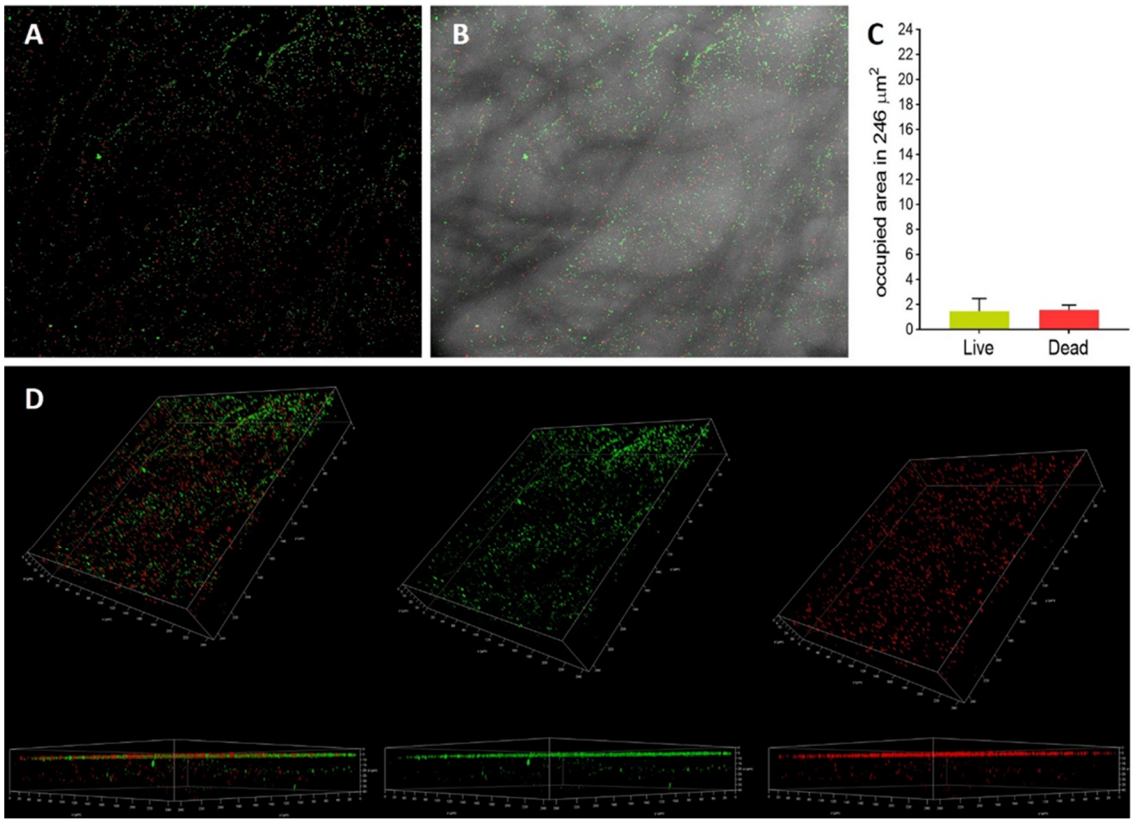



**Figure 3.20. Confocal microscopy images of *S. aureus* ATCC 25923 biofilms grown on PCL 15% HPβCD 7% fibers for 24 h under 100 rpm at 37°C, stained by the Live/dead BacLight bacterial viability kit®. Alive bacterial cells with intact membrane present a green fluorescence conferred by the SYTO™ 9 dye, while dead bacterial cells present a red fluorescence conferred by the propidium iodide (PI) dye. (A) Top view of the electrospun mats using the green and red channels; (B) bacterial cells attached on the surface of lengthwise fibers from the electrospun mat; (C) occupied area in 246 µm² by intact and dead cells expressed as mean ± standard deviation, n=5; (D) 3D images of the electrospun mat (length, height, and depth) with the comparation of dead (right) and intact bacteria (center), and both types of bacteria (left) on the same plane.**

USC
UNIVERSIDADE DE SANTIAGO DE COMPOSTELA

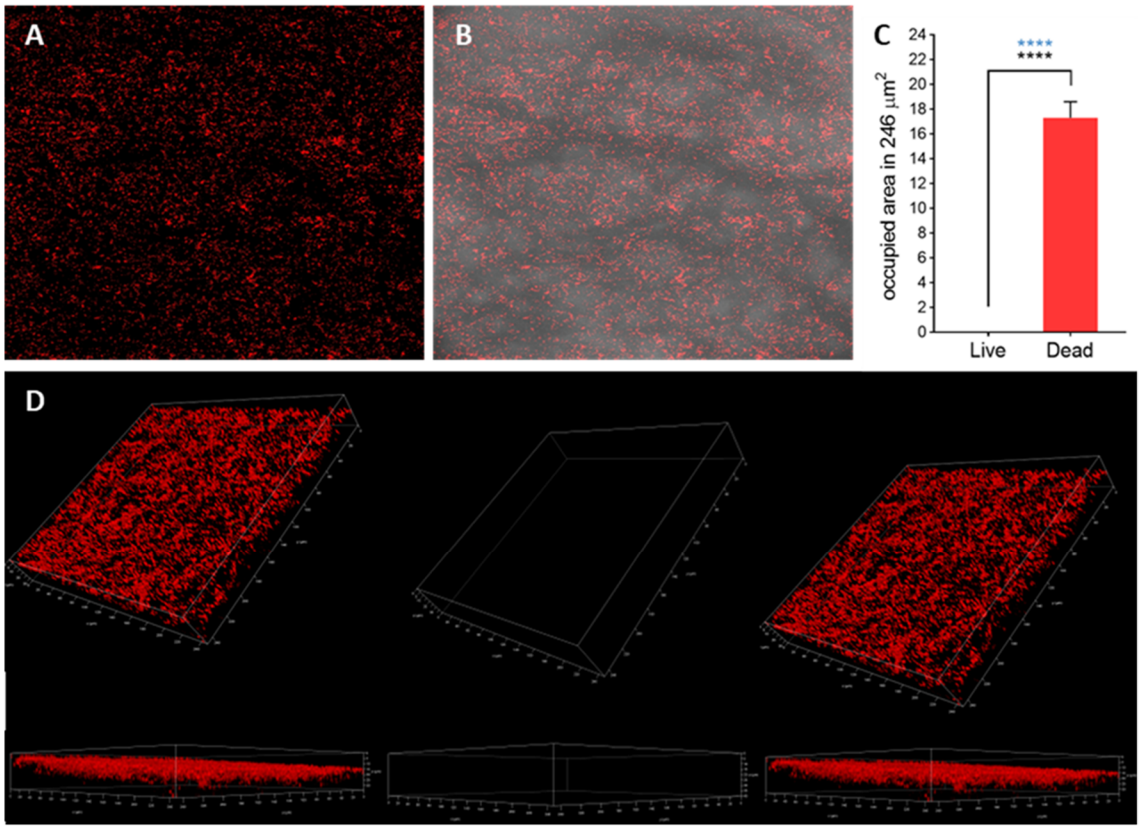



**Figure 3.21. Confocal microscopy images of *S. aureus* ATCC 25923 biofilms grown on PCL 15% HPβCD 7% carvacrol 5% fibers for 24 h under 100 rpm at 37°C, stained by the Live/dead BacLight bacterial viability kit®. Alive bacterial cells with intact membrane present a green fluorescence conferred by the SYTO™ 9 dye, while dead bacterial cells present a red fluorescence conferred by the by propidium iodade (PI) dye. (A) Top view of the electrospun mats using the green and red channels; (B) bacteria cells attached on the surface of lengthwise fibers from the electrospun mat; (C) occupied area in 246 µm² by intact and dead cells, expressed as mean ± standard deviation, n=5. Black asterisk (*) was used to compare intact-dead bacterial belonging to the same sample, and blue asterisk (*) was used to compare dead bacteria of each sample against PCL 15% fibers (control). Both types of asterisks indicate the following statistical significance: * p < 0.05, ** p < 0.005, *** p < 0.001 and **** p < 0.0001. (D) 3D images of the electrospun mat (length, height, and depth) with the comparation of dead (right) and intact bacteria (center), and both types of bacteria (left) on the same plane.**

USC
UNIVERSIDADE DE SANTIAGO DE COMPOSTELA

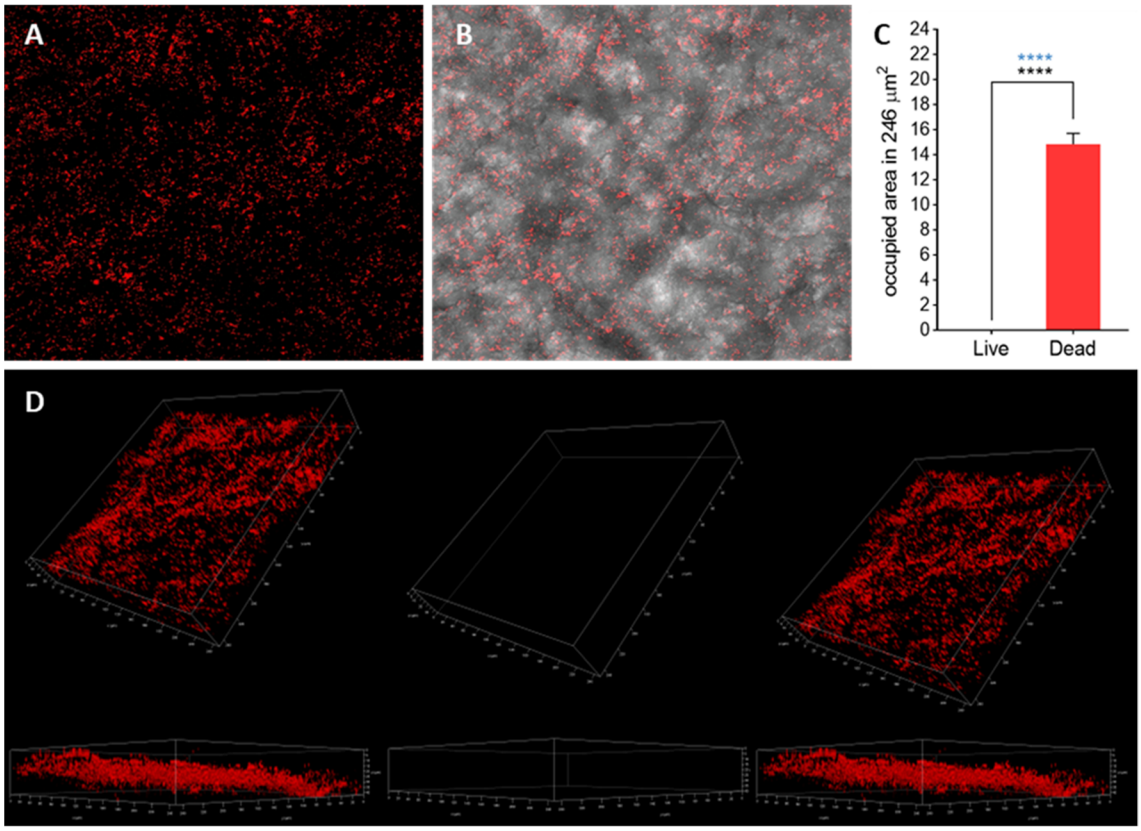



**Figure 3.22. Confocal microscopy images of *S. aureus* ATCC 25923 biofilms grown on PCL 15% HPβCD 7% carvacrol 10% fibers for 24 h under 100 rpm at 37°C, stained by the Live/dead BacLight bacterial viability kit®. Alive bacterial cells with intact membrane present a green fluorescence conferred by the SYTO™ 9 dye, while dead bacterial cells present a red fluorescence conferred by propidium iodide (PI) dye. (A) Top view of the electrospun mats using the green and red channels; (B) bacteria cells attached on the surface of lengthwise fibers from the electrospun mat; (C) occupied area in 246 μm² by intact and dead cells, expressed as mean ± standard deviation, n=5. Black asterisk (*) was used to compare intact-dead bacterial belonging to the same sample, and blue asterisk (*) was used to compare dead bacteria of each sample against PCL 15% fibers (control). Both types of asterisks indicate the following statistical significance: * p < 0.05, ** p < 0.005, *** p < 0.001 and **** p < 0.0001. (D) 3D images of the electrospun mat (length, height, and depth) with the comparation of dead (right) and intact bacteria (center), and both types of bacteria (left) on the same plane.**

USC UNIVERSIDADE DE SANTIAGO DE COMPOSTELA

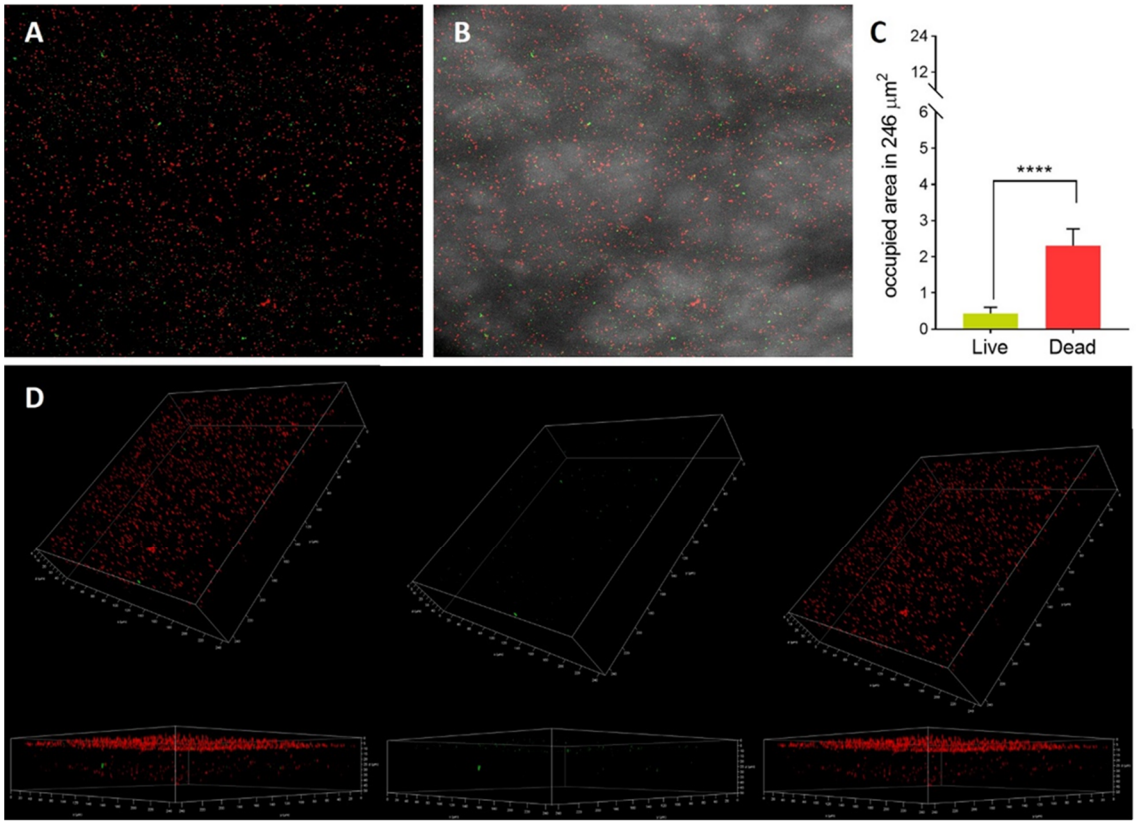



**Figure 3.23. Confocal microscopy images of *S. aureus* ATCC 25923 biofilms grown on PCL 15% HPβCD 7% citronellol 5% fibers for 24 h under 100 rpm at 37°C, stained by the Live/dead BacLight bacterial viability kit®. Alive bacterial cells with intact membrane present a green fluorescence conferred by the SYTO™ 9 dye, while dead bacterial cells present a red fluorescence conferred by propidium iodide (PI) dye. (A) Top view of the electrospun mats using the green and red channels; (B) bacteria cells attached on the surface of lengthwise fibers from the electrospun mat; (C) occupied area in 246 µm² by intact and dead cells, expressed as mean ± standard deviation, n=5. Black asterisk (*) was used to compare intact-dead bacterial belonging to the same sample, and blue asterisk (*) was used to compare dead bacteria of each sample against PCL 15% fibers (control). Both types of asterisks indicate the following statistical significance: * p < 0.05, ** p < 0.005, *** p < 0.001 and **** p < 0.0001. (D) 3D images of the electrospun mat (length, height, and depth) with the comparation of dead (right) and intact bacteria (center), and both types of bacteria (left) on the same plane.**

USC UNIVERSIDADE DE SANTIAGO DE COMPOSTELA

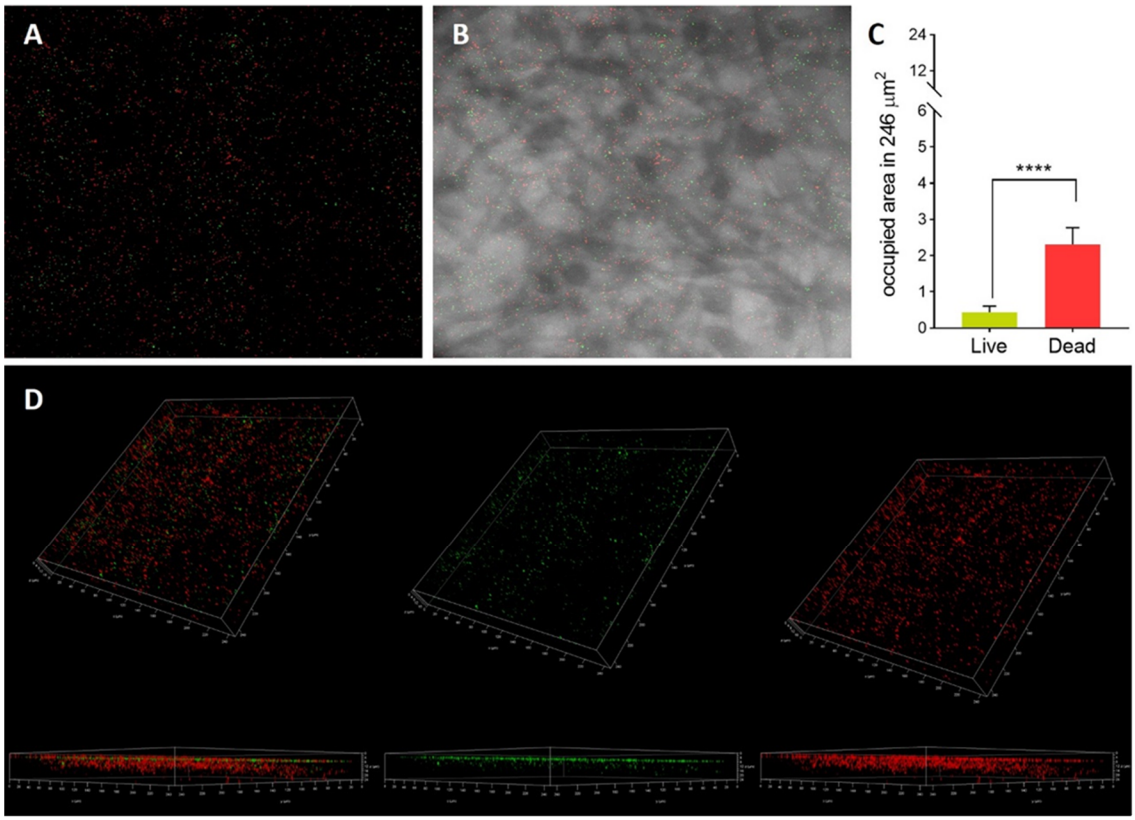



**Figure 3.24. Confocal microscopy images of *S. aureus* ATCC 25923 biofilms grown on PCL 15% HPβCD 7% citronellol 10% fibers for 24 h under 100 rpm at 37°C, stained by the Live/dead BacLight bacterial viability kit®. Alive bacterial cells with intact membrane present a green fluorescence conferred by the SYTO™ 9 dye, while dead bacterial cells present a red fluorescence conferred by propidium iodide (PI) dye. (A) Top view of the electrospun mats using the green and red channels; (B) bacteria cells attached on the surface of lengthwise fibers from the electrospun mat; (C) occupied area in 246 µm² by intact and dead cells, expressed as mean ± standard deviation, n=5. Black asterisk (*) was used to compare intact-dead bacterial belonging to the same sample, and blue asterisk (*) was used to compare dead bacteria of each sample against PCL 15% fibers (control). Both types of asterisks indicate the following statistical significance: * p < 0.05, ** p < 0.005, *** p < 0.001 and **** p < 0.0001. (D) 3D images of the electrospun mat (length, height, and depth) with the comparation of dead (right) and intact bacteria (center), and both types of bacteria (left) on the same plane.**

USC
UNIVERSIDADE DE SANTIAGO DE COMPOSTELA

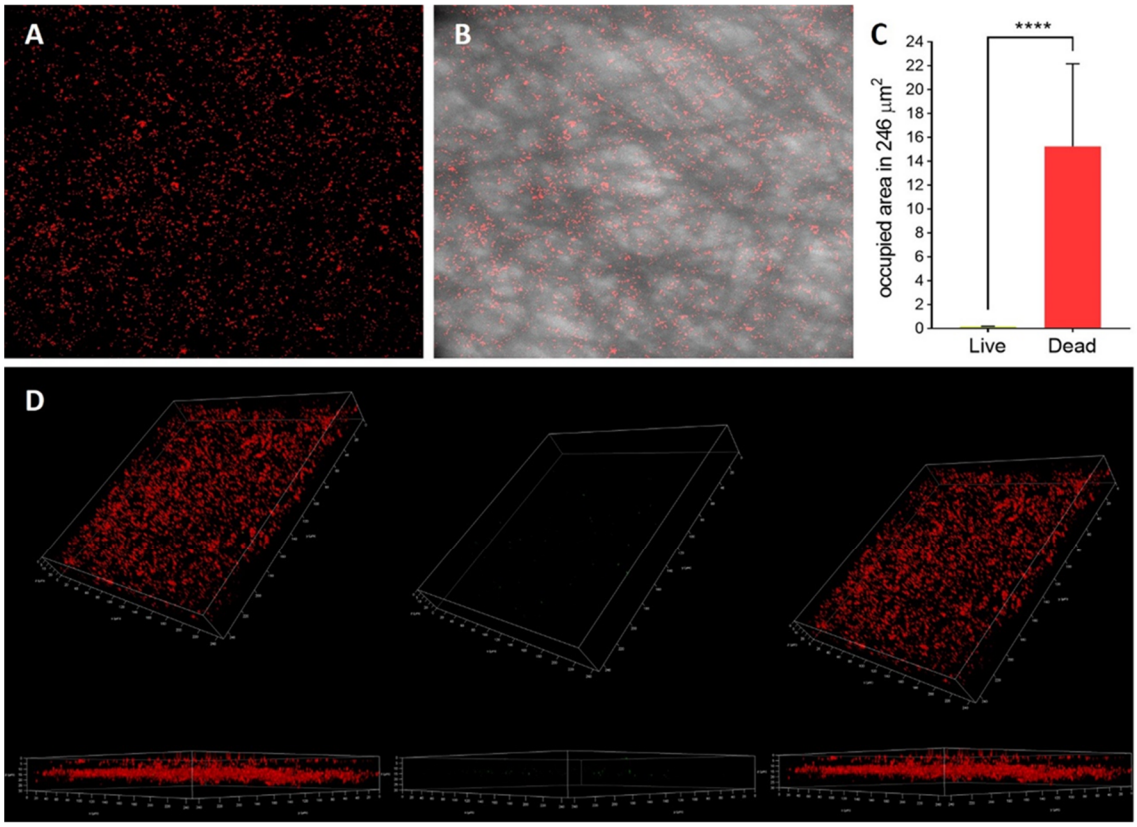



**Figure 3.25. Confocal microscopy images of *S. aureus* ATCC 25923 biofilms grown on PCL 15% HPβCD 7% cinnamic acid 10% fibers for 24 h under 100 rpm at 37°C, stained by the Live/dead BacLight bacterial viability kit®. Alive bacterial cells with intact membrane present a green fluorescence conferred by the SYTO™ 9 dye, while dead bacterial cells present a red fluorescence conferred by propidium iodide (PI) dye. (A) Top view of the electrospun mats using the green and red channels; (B) bacteria cells attached on the surface of lengthwise fibers from the electrospun mat; (C) occupied area in 246 μm² by intact and dead cells, expressed as mean ± standard deviation, n=5. Black asterisk (*) was used to compare intact-dead bacterial belonging to the same sample, and blue asterisk (*) was used to compare dead bacteria of each sample against PCL 15% fibers (control). Both types of asterisks indicate the following statistical significance: * p < 0.05, ** p < 0.005, *** p < 0.001 and **** p < 0.0001. (D) 3D images of the electrospun mat (length, height, and depth) with the comparation of dead (right) and intact bacteria (center), and both types of bacteria (left) on the same plane.**

USC UNIVERSIDADE DE SANTIAGO DE COMPOSTELA

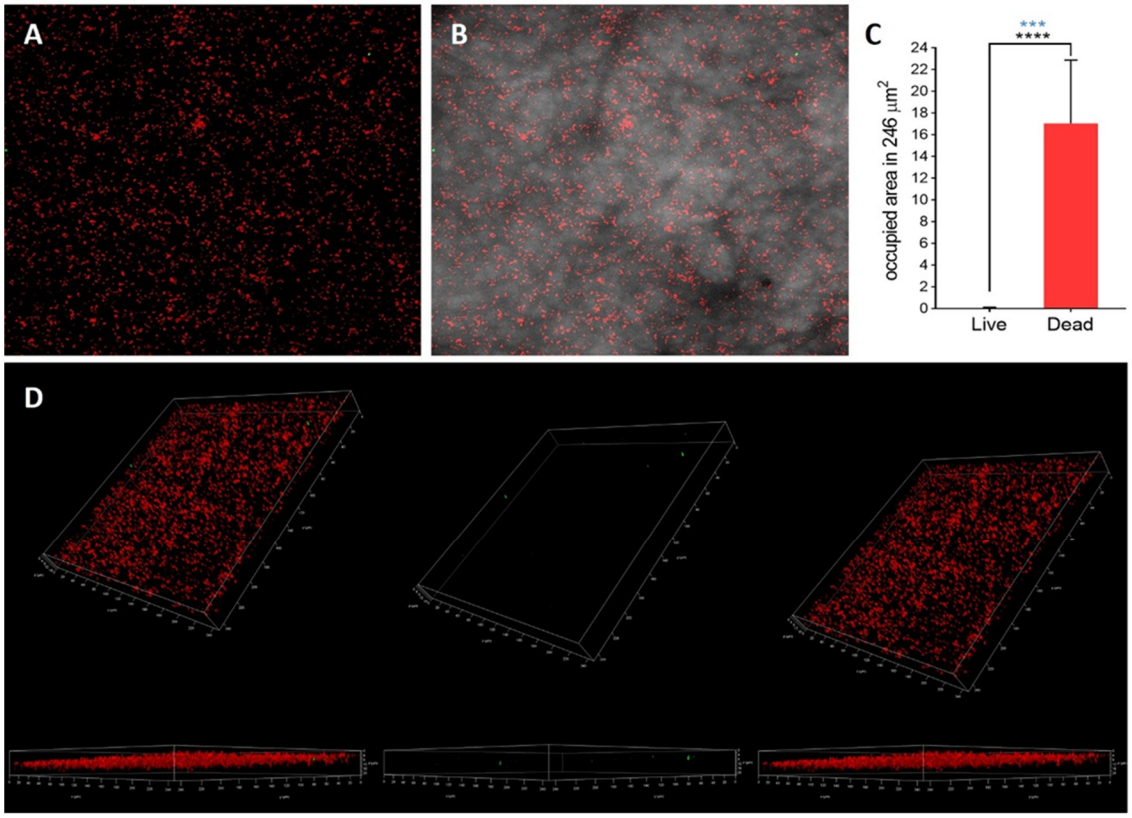



**Figure 3.26. Confocal microscopy images of *S. aureus* ATCC 25923 biofilms grown on PCL 15% HPβCD 7% cinnamic acid 20% fibers for 24 h under 100 rpm at 37°C, stained by the Live/dead BacLight bacterial viability kit®. Alive bacterial cells with intact membrane present a green fluorescence conferred by the SYTO™ 9 dye, while dead bacterial cells present a red fluorescence conferred by propidium iodide (PI) dye. (A) Top view of the electrospun mats using the green and red channels; (B) bacteria cells attached on the surface of lengthwise fibers from the electrospun mat; (C) occupied area in 246 µm$^2$ by intact and dead cells, expressed as mean ± standard deviation, n=5. Black asterisk (*) was used to compare intact-dead bacterial belonging to the same sample, and blue asterisk (*) was used to compare dead bacteria of each sample against PCL 15% fibers (control). Both types of asterisks indicate the following statistical significance: * p < 0.05, ** p < 0.005, *** p < 0.001 and **** p < 0.0001. (D) 3D images of the electrospun mat (length, height, and depth) with the comparation of dead (right) and intact bacteria (center), and both types of bacteria (left) on the same plane.**

USC
UNIVERSIDADE DE SANTIAGO DE COMPOSTELA

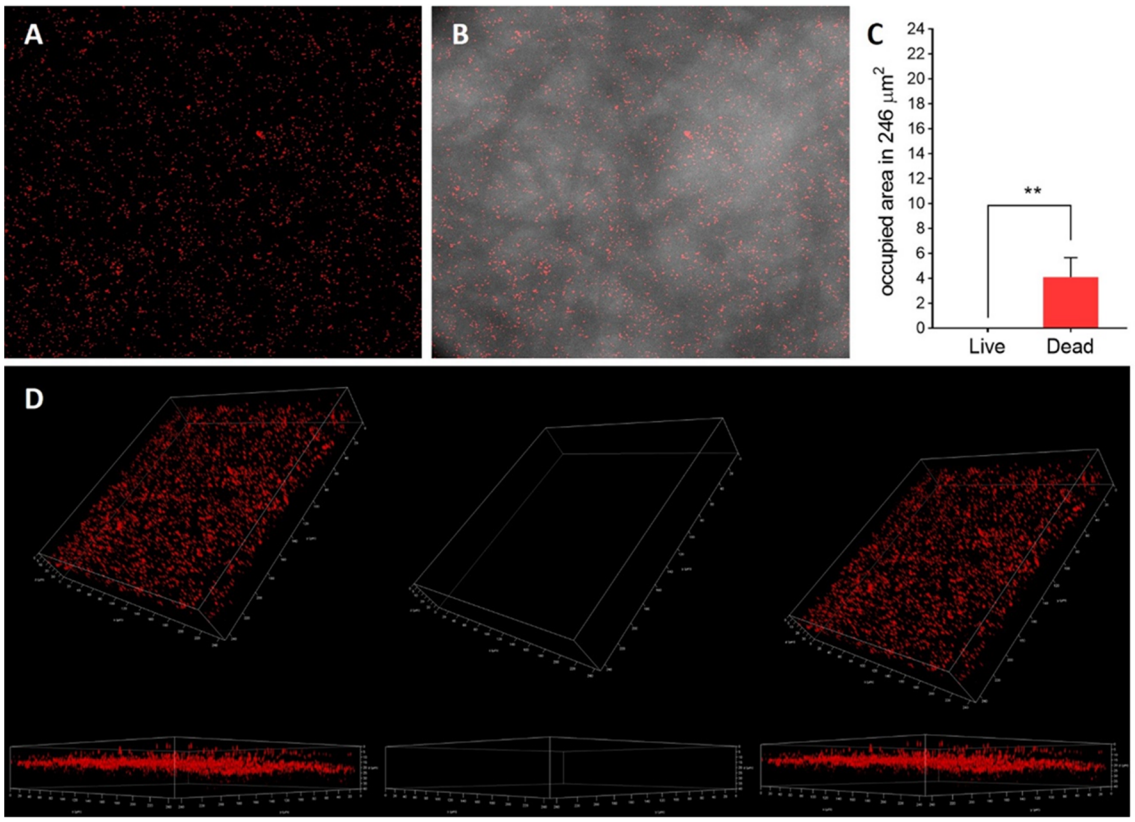



**Figure 3.27. Confocal microscopy images of *S. aureus* ATCC 25923 biofilms grown on PCL 15% HPβCD 7% carvacrol-citronellol 5% fibers for 24 h under 100 rpm at 37°C, stained by the Live/dead BacLight bacterial viability kit®. Alive bacterial cells with intact membrane present a green fluorescence conferred by the SYTO™ 9 dye, while dead bacterial cells present a red fluorescence conferred by propidium iodide (PI) dye. (A) Top view of the electrospun mats using the green and red channels; (B) bacteria cells attached on the surface of lengthwise fibers from the electrospun mat; (C) occupied area in 246 μm$^2$ by intact and dead cells, expressed as mean ± standard deviation, n=5. Black asterisk (*) was used to compare intact-dead bacterial belonging to the same sample, and blue asterisk (*) was used to compare dead bacteria of each sample against PCL 15% fibers (control). Both types of asterisks indicate the following statistical significance: * p < 0.05, ** p < 0.005, *** p < 0.001 and **** p < 0.0001. (D) 3D images of the electrospun mat (length, height, and depth) with the comparation of dead (right) and intact bacteria (center), and both types of bacteria (left) on the same plane.**

USC UNIVERSIDADE DE SANTIAGO DE COMPOSTELA

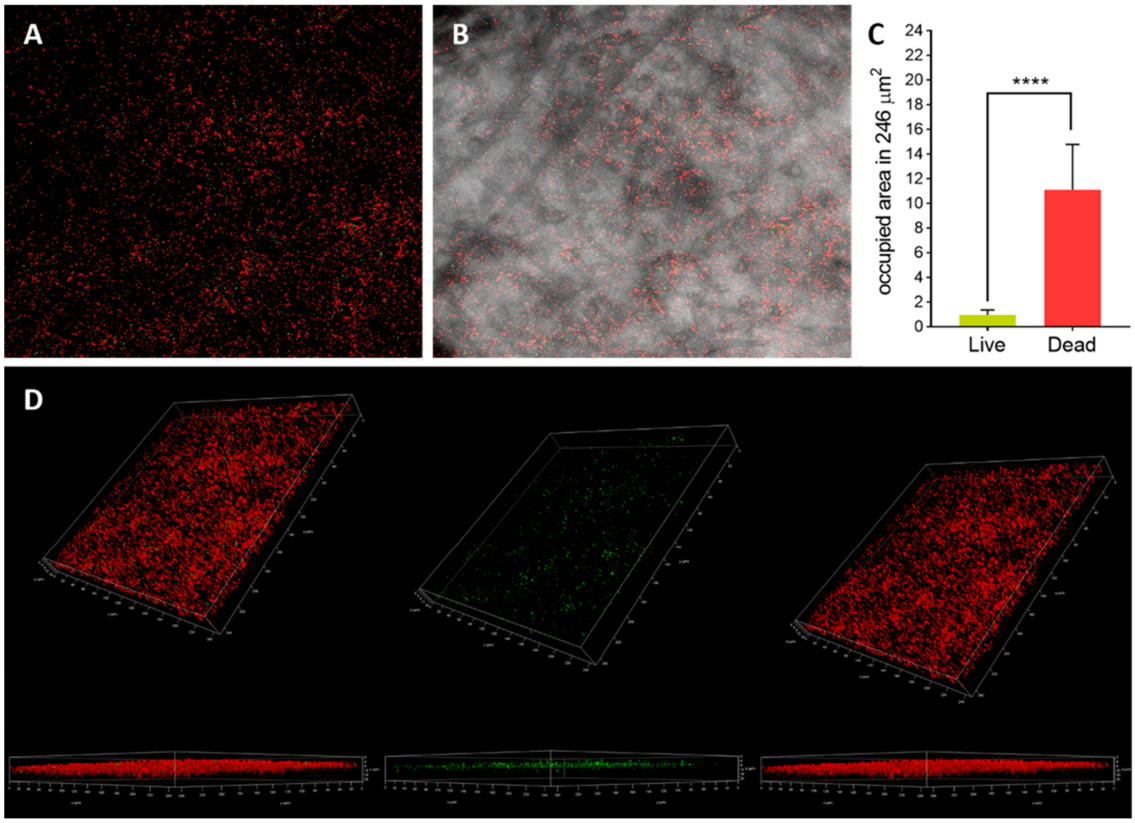



**Figure 3.28. Confocal microscopy images of *S. aureus* ATCC 25923 biofilms grown on PCL 15% HPβCD 7% citronellol-cinnamic acid 10% fibers for 24 h under 100 rpm at 37°C, stained by the Live/dead BacLight bacterial viability kit®. Alive bacterial cells with intact membrane present a green fluorescence conferred by the SYTO™ 9 dye, while dead bacterial cells present a red fluorescence conferred by propidium iodide (PI) dye. (A) Top view of the electrospun mats using the green and red channels; (B) bacteria cells attached on the surface of lengthwise fibers from the electrospun mat; (C) occupied area in 246 µm² by intact and dead cells, expressed as mean ± standard deviation, n=5. Black asterisk (*) was used to compare intact-dead bacterial belonging to the same sample, and blue asterisk (*) was used to compare dead bacteria of each sample against PCL 15% fibers (control). Both types of asterisks indicate the following statistical significance: * p < 0.05, ** p < 0.005, *** p < 0.001 and **** p < 0.0001. (D) 3D images of the electrospun mat (length, height, and depth) with the comparation of dead (right) and intact bacteria (center), and both types of bacteria (left) on the same plane.**

USC UNIVERSIDADE DE SANTIAGO DE COMPOSTELA

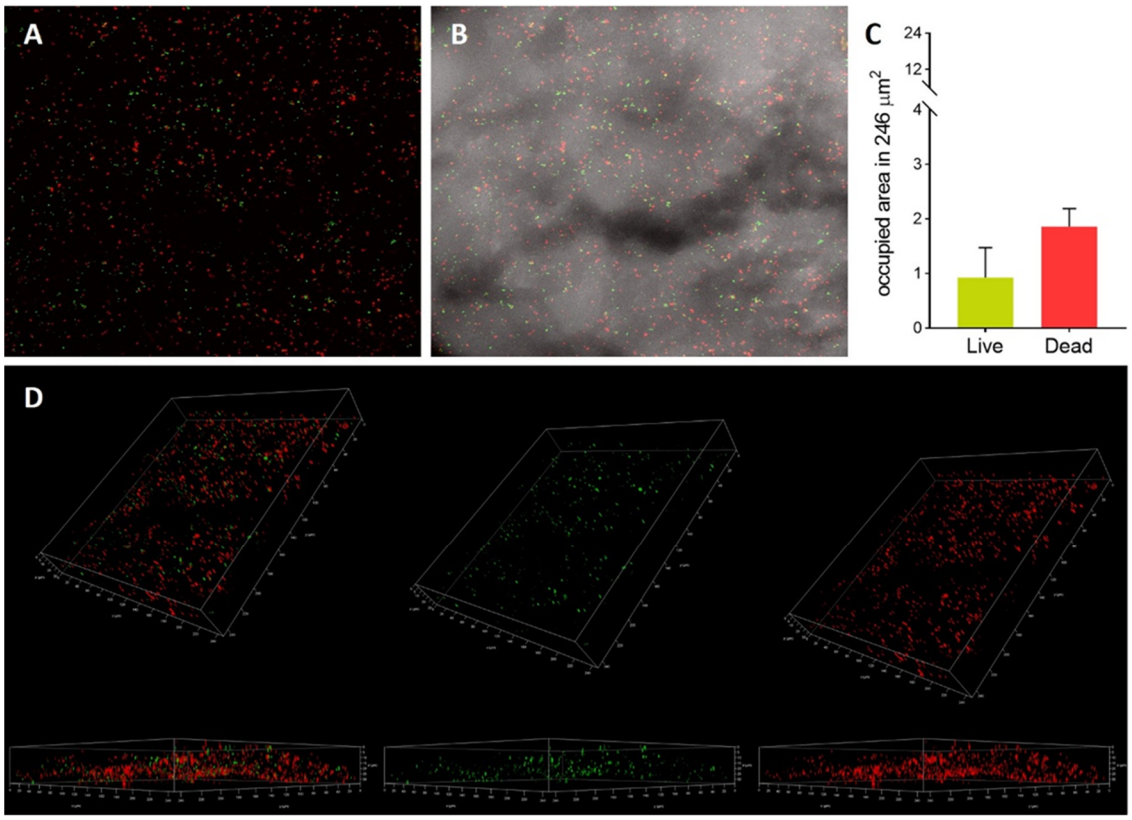



**Figure 3.29. Confocal microscopy images of *S. aureus* ATCC 25923 biofilms grown on PCL 15% HPβCD 7% carvacrol-citronellol-cinnamic acid 5% fibers for 24 h under 100 rpm at 37°C, stained by the Live/dead BacLight bacterial viability kit®. Alive bacterial cells with intact membrane present a green fluorescence conferred by the SYTO™ 9 dye, while dead bacterial cells present a red fluorescence conferred by propidium iodide (PI) dye. (A) Top view of the electrospun mats using the green and red channels; (B) bacteria cells attached on the surface of lengthwise fibers from the electrospun mat; (C) occupied area in 246 µm$^2$ by intact and dead cells, expressed as mean ± standard deviation, n=5. Black asterisk (*) was used to compare intact-dead bacterial belonging to the same sample, and blue asterisk (*) was used to compare dead bacterial of each sample against PCL 15% fibers (control). Both types of asterisks indicate the following statistical significance: * p < 0.05, ** p < 0.005, *** p < 0.001 and **** p < 0.0001. (D) 3D images of the electrospun mat (length, height, and depth) with the comparation of dead (right) and intact bacteria (center), and both types of bacteria (left) on the same plane.**

PCL 15% HPBCD 7% fibers prepared with carvacrol (**Figure 3.21 and 3.22**) and cinnamic acid (**Figure 3.25 and 3.26**) showed a large population of dead bacteria and no population of alive bacteria, obtaining significant differences ($p < 0.0001$) when compared with the controls without EOCs. These results agreed well with the logarithmic reduction > 3 that was obtained in the CFUs. In the case of citronellol-containing fibers (**Figure 3.23 and 3.24**) both intact and dead bacteria were observed, although with a predominance of dead bacteria ($p < 0.0001$), but the differences were not significant compared to the control.

USC DE SANTIAGO DE COMPOSTELA

The fibers prepared with a mixture of EOCs, PCL15% HPBCD 7% carvacrol-citronellol 5% (**Figure 3.27.**) and PCL15% HPBCD 7% citronellol-cinnamic acid 10% (**Figure 3.28.**) showed good antibiofilm activity, since most *S. aureus* cells were dead (stained red). Differently, the fibers with the mixture of the three EOCs (**Figure 3.2.9**) had less antimicrobial activity (log CFU/mL reduction 3) and showed an intact population, which can be explained by the relative decrease in the content in carvacrol and cinnamic acid, i.e. the two most efficient EOCs against *S. aureus*.

The antibiofilm properties against *P. aeruginosa* were investigated similarly (**Figure 3.30-3.34**). According to the results obtained in section 3.2.2, only the controls and carvacrol-loaded mats were tested. As expected, PCL 15% (w/v) control mats (**Figure 3.30.**) showed a large proportion of intact bacteria and some dead bacteria cells. Interestingly, PCL 15% HPβCD 7% control fibers (**Figure 3.31.**) displayed less bacteria attached, and the dead population occupied an area similar to that of intact population. This result, also observed when the fibers were exposed to *S. aureus*, suggests that HPβCD interferes with cell adhesion and biofilm development. The capability of HPβCD to alter quorum sensing mechanisms by trapping the communication signals has been previously demonstrated in solution and for gauzes grafted with cyclodextrins [58]. Similarly, the PCL 15% HPβCD 7% fibers can release some HPβCD units to the culture medium and most HPβCD remaining in the fibers can have their cavities available for hosting of quorum sensing signals, as no poly(pseudo)rotaxane formation is expected.

PCL 15% HPβCD 7% loaded with carvacrol at 5% - 10% (w/v) (**Figure 3.32 and 3.33**) evidenced that most area was occupied by dead bacteria. No intact bacteria were detected. Moreover, these electrospun mats displayed significant differences ($p < 0.05$) with respect to the control. The area occupied by dead bacteria was lower in the PCL 15% HPβCD 7% carvacrol-cinnamic acid 10% mats (**Figure 3.34.**), but still their capability to kill *P. aeruginosa* was remarkable. Quenching of the quorum sensing mechanism of communication among bacteria has been demonstrated as an efficient way of haltering *P. aeruginosa* biofilm formation [59], and both HPβCD and carvacrol in separate have demonstrated capability to inhibit quorum sensing through different mechanisms [57,60]. Such a capability explains the successful results recorded for electrospun mats that combine HPβCD and carvacrol.

USC UNIVERSIDADE DE SANTIAGO DE COMPOSTELA

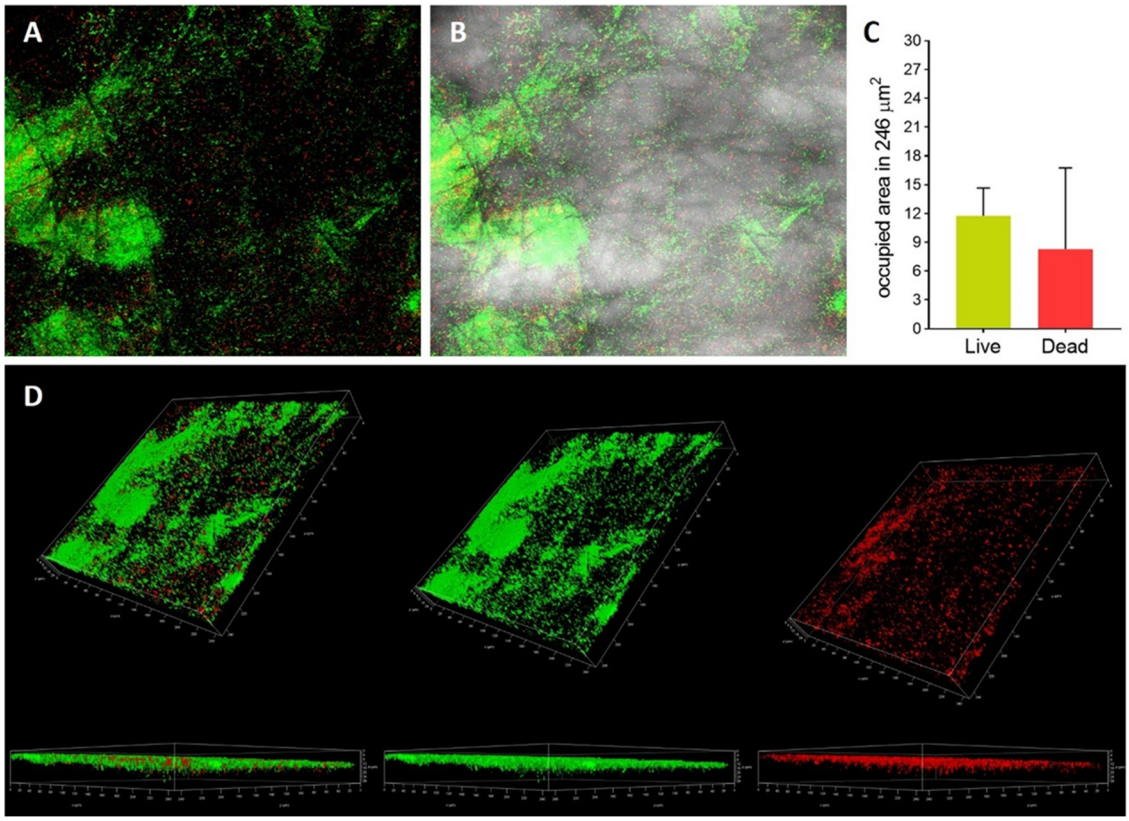



**Figure 3.30. Confocal microscopy images of *P. aeruginosa* CECT 110 biofilms grown on PCL 15% fibers for 24 h under 100 rpm at 37°C, stained by the Live/dead BacLight bacterial viability kit®. Alive bacterial cells with intact membrane present a green fluorescence conferred by the SYTO™ 9 dye, while dead bacterial cells present a red fluorescence conferred by propidium iodide (PI) dye. (A) Top view of the electrospun mats using the green and red channels; (B) bacteria cells attached on the surface of lengthwise fibers from the electrospun mat; (C) occupied area in 246 µm$^2$ by intact and dead cells, expressed as mean ± standard deviation, n=5. (D) 3D images of the electrospun mat (length, height, and depth) with the comparation of dead (right) and intact bacteria (center), and both types of bacteria (left) on the same plane.**

USC
UNIVERSIDADE DE SANTIAGO DE COMPOSTELA

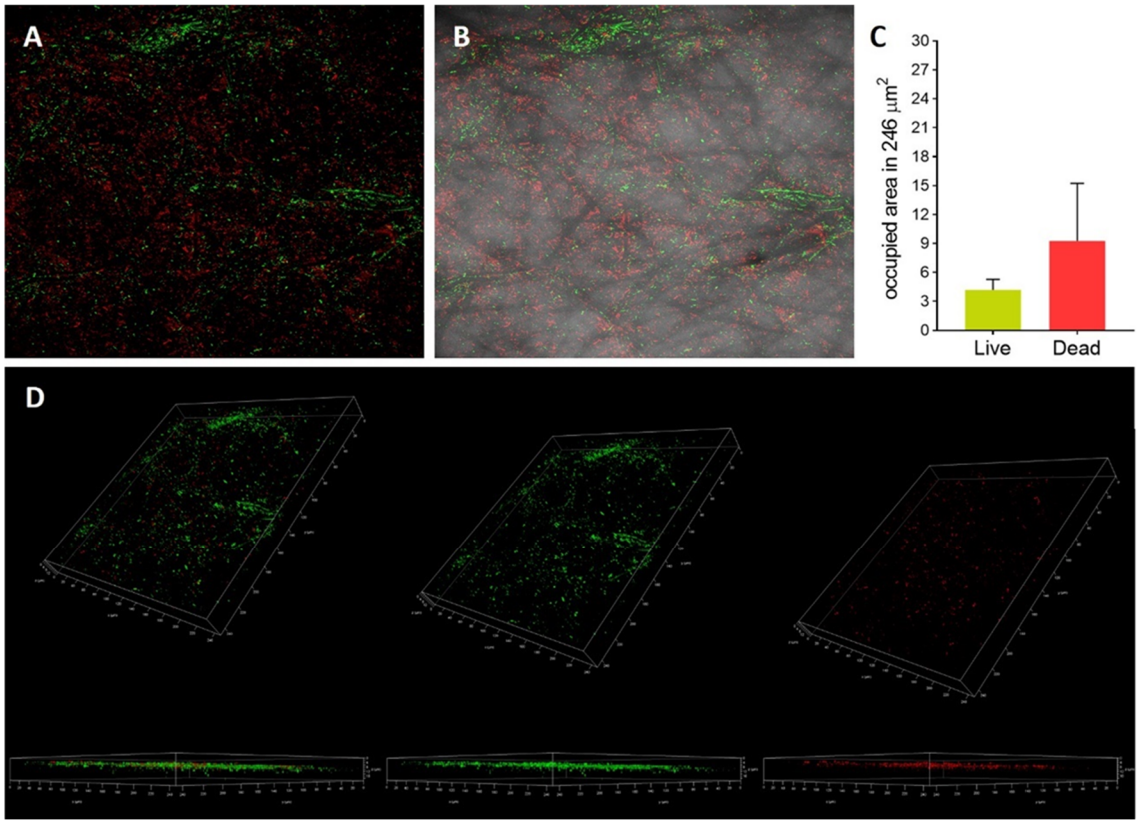



**Figure 3.31. Confocal microscopy images of *P. aeruginosa* CECT 110 biofilms grown on PCL 15% HPβCD 7% fibers for 24 h under 100 rpm at 37°C, stained by the Live/dead BacLight bacterial viability kit®. Alive bacterial cells with intact membrane present a green fluorescence conferred by the SYTO™ 9 dye, while dead bacterial cells present a red fluorescence conferred by propidium iodide (PI) dye. (A) Top view of the electrospun mats using the green and red channels; (B) bacteria cells attached on the surface of lengthwise fibers from the electrospun mat; (C) occupied area in 246 μm² by intact and dead cells, expressed as mean ± standard deviation, n=5. (D) 3D images of the electrospun mat (length, height, and depth) with the comparation of dead (right) and intact bacteria (center), and both types of bacteria (left) on the same plane.**

USC
UNIVERSIDADE DE SANTIAGO DE COMPOSTELA

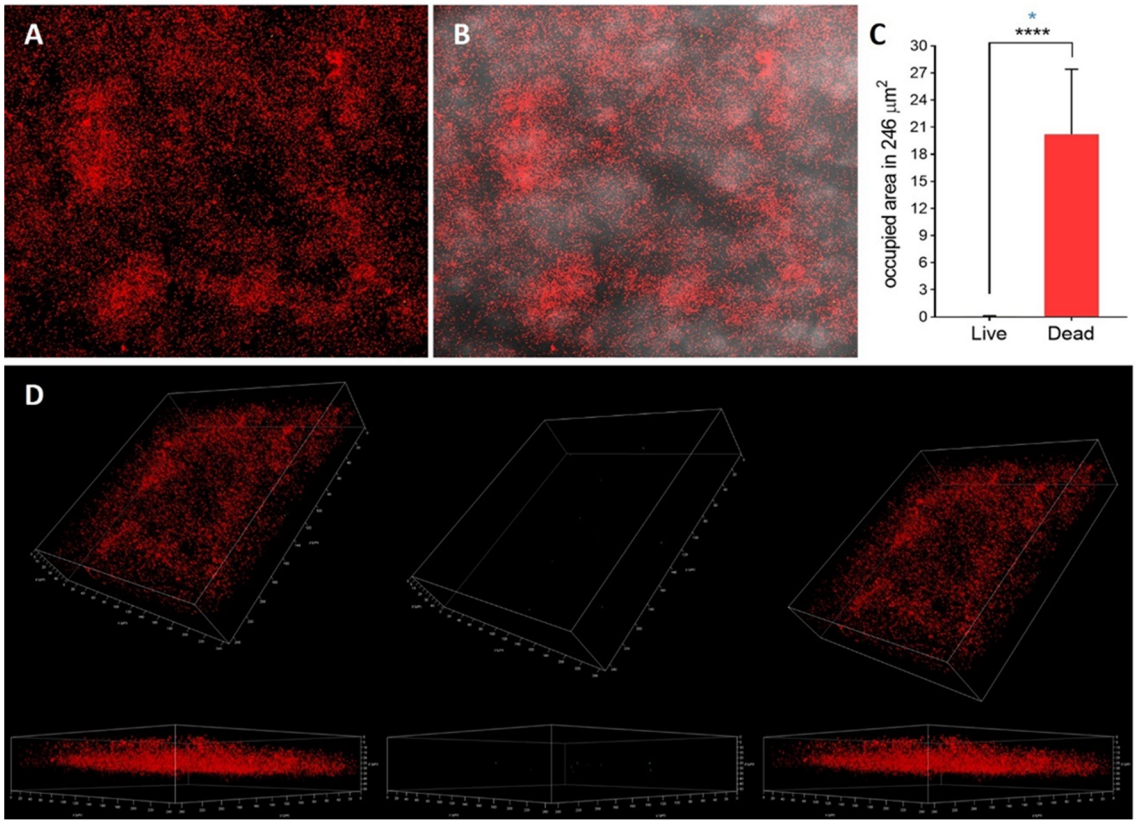



**Figure 3.32. Confocal microscopy images of *P. aeruginosa* CECT 110 biofilms grown on PCL 15% HPβCD 7% carvacrol 5% fibers for 24 h under 100 rpm at 37°C, stained by the Live/dead BacLight bacterial viability kit®. Alive bacterial cells with intact membrane present a green fluorescence conferred by the SYTO™ 9 dye, while dead bacterial cells present a red fluorescence conferred by propidium iodide (PI) dye. (A) Top view of the electrospun mats using the green and red channels; (B) bacteria cells attached on the surface of lengthwise fibers from the electrospun mat; (C) occupied area in 246 µm2 by intact and dead cells, expressed as mean ± standard deviation, n=5. Black asterisk (*) was used to compare intact-dead bacterial belonging to the same sample, and blue asterisk (*) was used to compare dead bacteria of each sample against PCL 15% fibers (control). Both types of asterisks indicate the following statistical significance: * p < 0.05, ** p < 0.005, *** p < 0.001 and **** p < 0.0001. (D) 3D images of the electrospun mat (length, height, and depth) with the comparation of dead (right) and intact bacteria (center), and both types of bacteria (left) on the same plane.**

USC
UNIVERSIDADE DE SANTIAGO DE COMPOSTELA

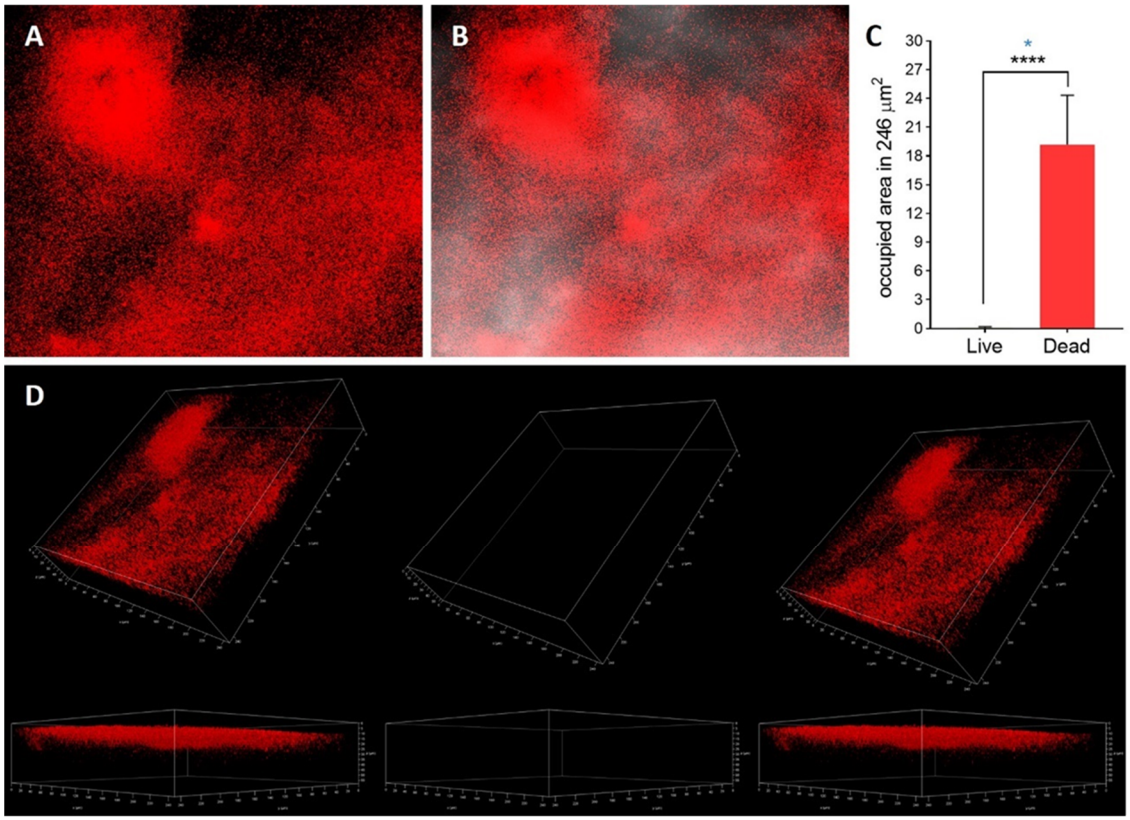



**Figure 3.33. Confocal microscopy images of *P. aeruginosa* CECT 110 biofilms grown on PCL 15% HPβCD 7% carvacrol 10% fibers for 24 h under 100 rpm at 37°C, stained by the Live/dead BacLight bacterial viability kit®. Alive bacterial cells with intact membrane present a green fluorescence conferred by the SYTO™ 9 dye, while dead bacterial cells present a red fluorescence conferred by propidium iodide (PI) dye. (A) Top view of the electrospun mats using the green and red channels; (B) bacteria cells attached on the surface of lengthwise fibers from the electrospun mat; (C) occupied area in 246 µm$^2$ by intact and dead cells, expressed as mean ± standard deviation, n=5. Black asterisk (*) was used to compare intact-dead bacterial belonging to the same sample, and blue asterisk (*) was used to compare dead bacteria of each sample against PCL 15% fibers (control). Both types of asterisks indicate the following statistical significance: * p < 0.05, ** p < 0.005, *** p < 0.001 and **** p < 0.0001. (D) 3D images of the electrospun mat (length, height, and depth) with the comparation of dead (right) and intact bacteria (center), and both types of bacteria (left) on the same plane**

USC UNIVERSIDADE DE SANTIAGO DE COMPOSTELA

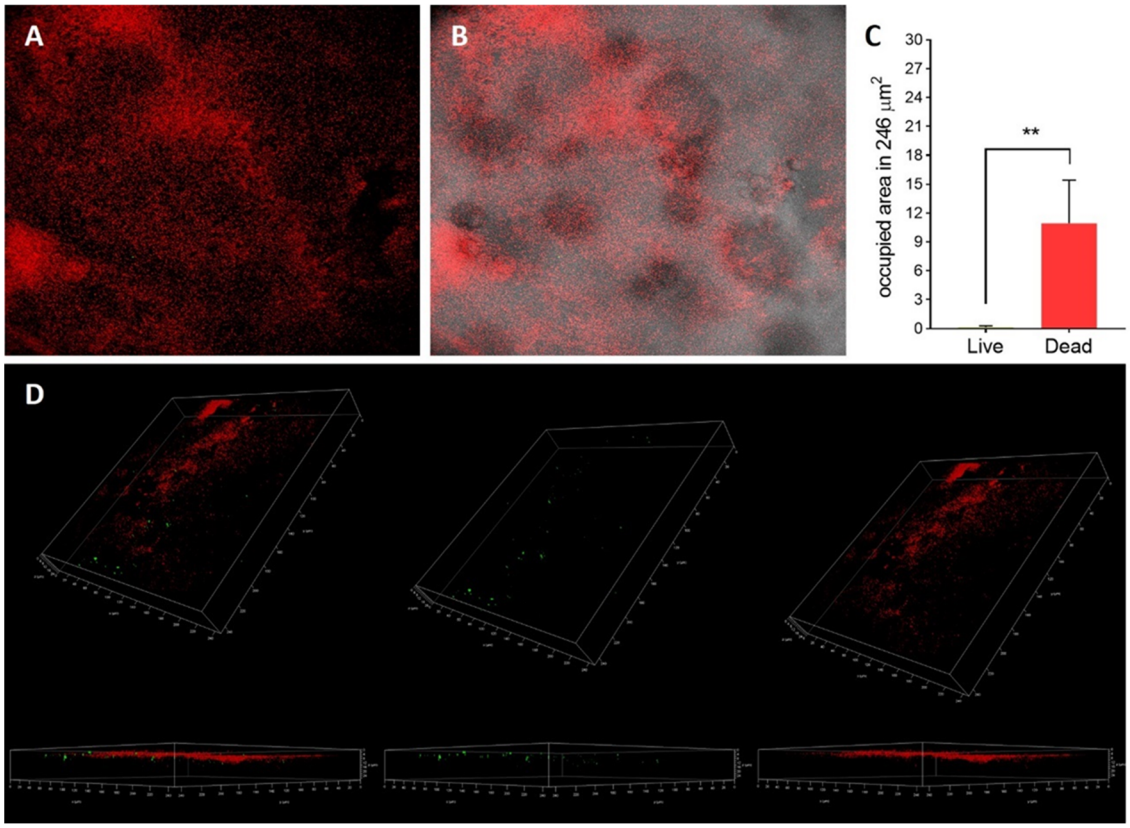



**Figure 3.34. Confocal microscopy images of *P. aeruginosa* CECT 110 biofilms grown on PCL 15% HPβCD 7% carvacrol-cinnamic acid 10% fibers for 24 h under 100 rpm at 37°C, stained by the Live/dead BacLight bacterial viability kit®. Alive bacterial cells with intact membrane present a green fluorescence conferred by the SYTO™ 9 dye, while dead bacterial cells present a red fluorescence conferred by propidium iodide (PI) dye. (A) Top view of the electrospun mats using the green and red channels; (B) bacteria cells attached on the surface of lengthwise fibers from the electrospun mat; (C) occupied area in 246 µm² by intact and dead cells, expressed as mean ± standard deviation, n=5. Black asterisk (*) was used to compare intact-dead bacterial belonging to the same sample, and blue asterisk (*) was used to compare dead bacteria of each sample against PCL 15% fibers (control). Both types of asterisks indicate the following statistical significance: * p < 0.05, ** p < 0.005, *** p < 0.001 and **** p < 0.0001. (D) 3D images of the electrospun mat (length, height, and depth) with the comparation of dead (right) and intact bacteria (center), and both types of bacteria (left) on the same plane.**

### 3.3.4 Structural characterization and release pattern of the antibiofilm fibers

Fibers exhibiting antibiofilm activity were investigated in more detail regarding morphology (FESEM images), crystallinity (DSC) and release profiles of the EOC/s in PBS (pH 7.4) at 37ºC. It should be noted that pristine carvacrol and citronellol are liquid at room temperature while cinnamic acid is formed by crystalline particles that melt at 135 ºC (**Figure 3.35.**).

USC UNIVERSIDADE DE SANTIAGO DE COMPOSTELA

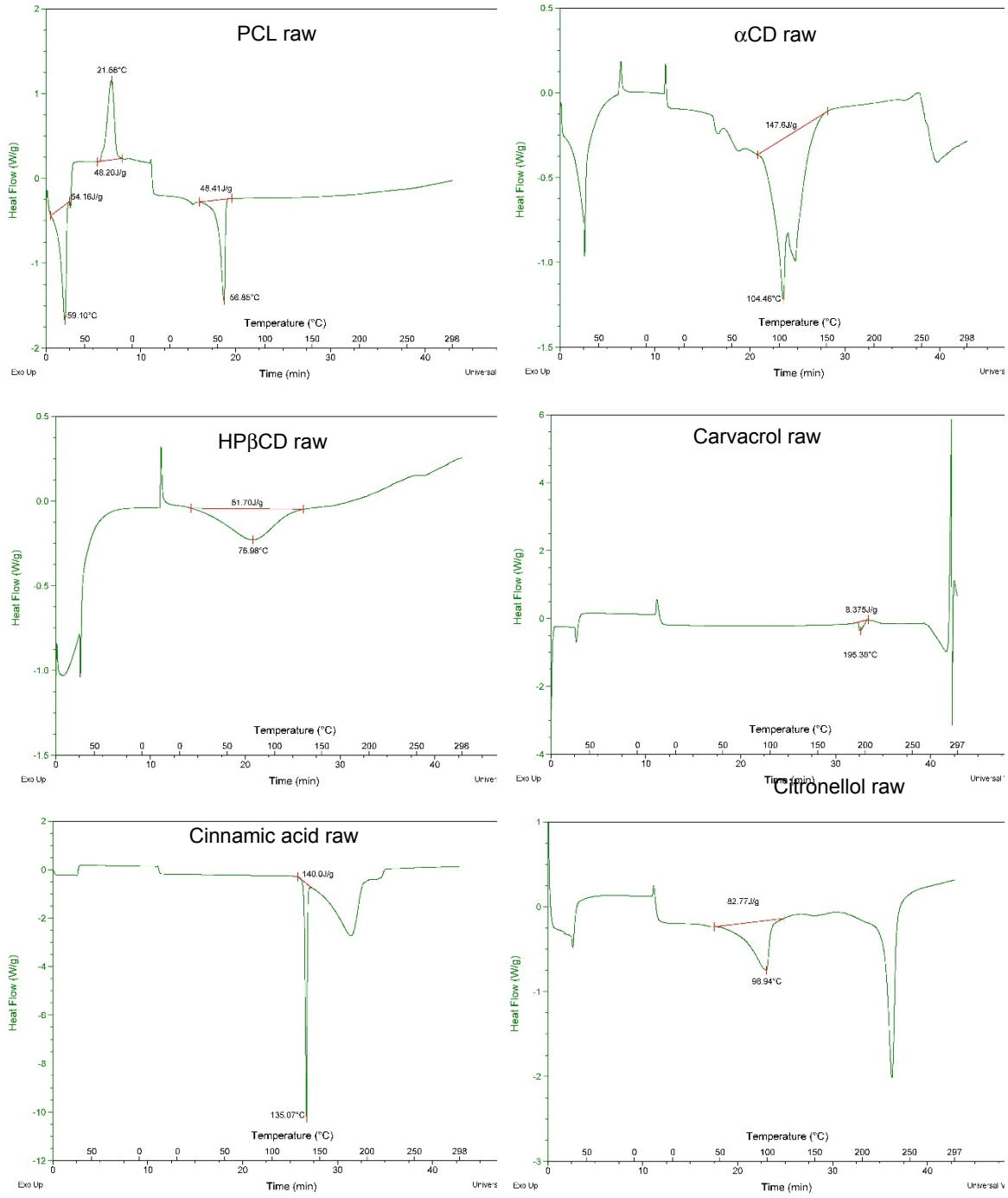



**Figure 3.35. DSC scans of the raw materials used to prepare the fibers. The samples were heated from 25 to 65°C, cooled to -20°C and then heated to 300°C at 10°C/min.**

Three fibers prepared with PCL solely were first characterized: PCL 18% citronellol 20%, PCL 15% cinnamic acid 20%, and PCL 18% cinnamic acid 30%. These fibers had in common that they were loaded with the maximum content in EOC that the fibers allowed. PCL 18% citronellol 20% fibers (1.66 ± 0.48 μm) maintained the cylindrical shape without beads despite the high amount of citronellol that was

USC UNIVERSIDADE DE SANTIAGO

incorporated (**Figure 3.37.A**). This electrospun mat showed sustained release of citronellol, with 170 mg released per gram of fiber at 24 h. Such a slow release may be related to the moderate solubility of citronellol in water (200 mg/L) and logP 3.2 (PubChem database) and to an efficient encapsulation inside the fibers. No relevant changes were recorded in the DSC scans of these fibers compared to raw PCL (**Figure 3.35.**) and PCL solely fibers (**Figure 3.36.**), showing similar melting temperature (57 ºC) and enthalpy (59.7 J/g).

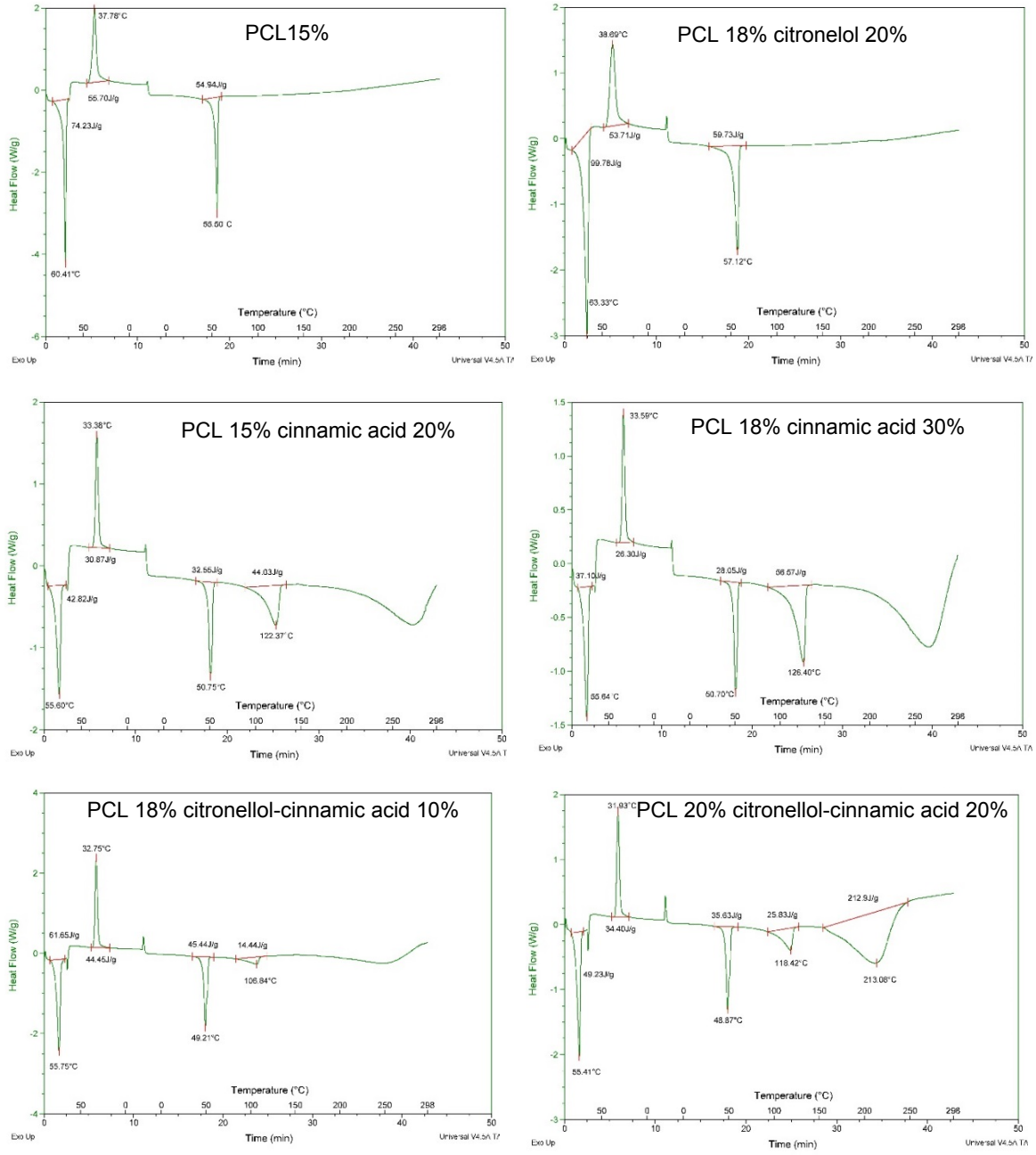



**Figure 3.36. DSC scans of fibers prepared with PCL and EOCs in the absence of cyclodextrins. The samples were heated from 25 to 65°C, cooled to -20°C and then heated to 300°C at 10°C/min.**

PCL fibers saturated with cinnamic acid, i.e. PCL 15% cinnamic acid 20% (1.73 ± 0.16 μm; **Figure 3.37.B**) and PCL 18% cinnamic acid 30% (0.61± 0.24 μm; **Figure 3.37.C**), had homogeneous, smooth and continuous shape, including cinnamic acid aggregates attached lengthwise the fiber. These two electrospun mats released rapidly a first fraction of the amount loaded (310 mg/g and 510 mg/g, respectively) in the first 2-3 hours. This burst release is related to cinnamic acid particles crystallized on the surface of the fibers, as confirmed by the DSC characteristic peaks of cinnamic acid melting (122-126 ºC) (**Figure 3.36**) although they appeared at slightly lower temperature than for the raw EOC (135 ºC). The melting enthalpy values revealed that 55% and 64% cinnamic acid remained as crystalline particles on the PCL 15% cinnamic acid 20% and PCL 18% cinnamic acid 30% fibers, respectively. The subsequent slower release step could correspond to cinnamic acid encapsulated inside the fibers. After 24 h in the release medium, PCL 15% cinnamic acid 20% released 650 mg/g, and PCL 18% cinnamic acid 30% released 530 mg/g, which corresponded to ca. 100% loaded.

USC UNIVERSIDADE DE SANTIAGO DE COMPOSTELA

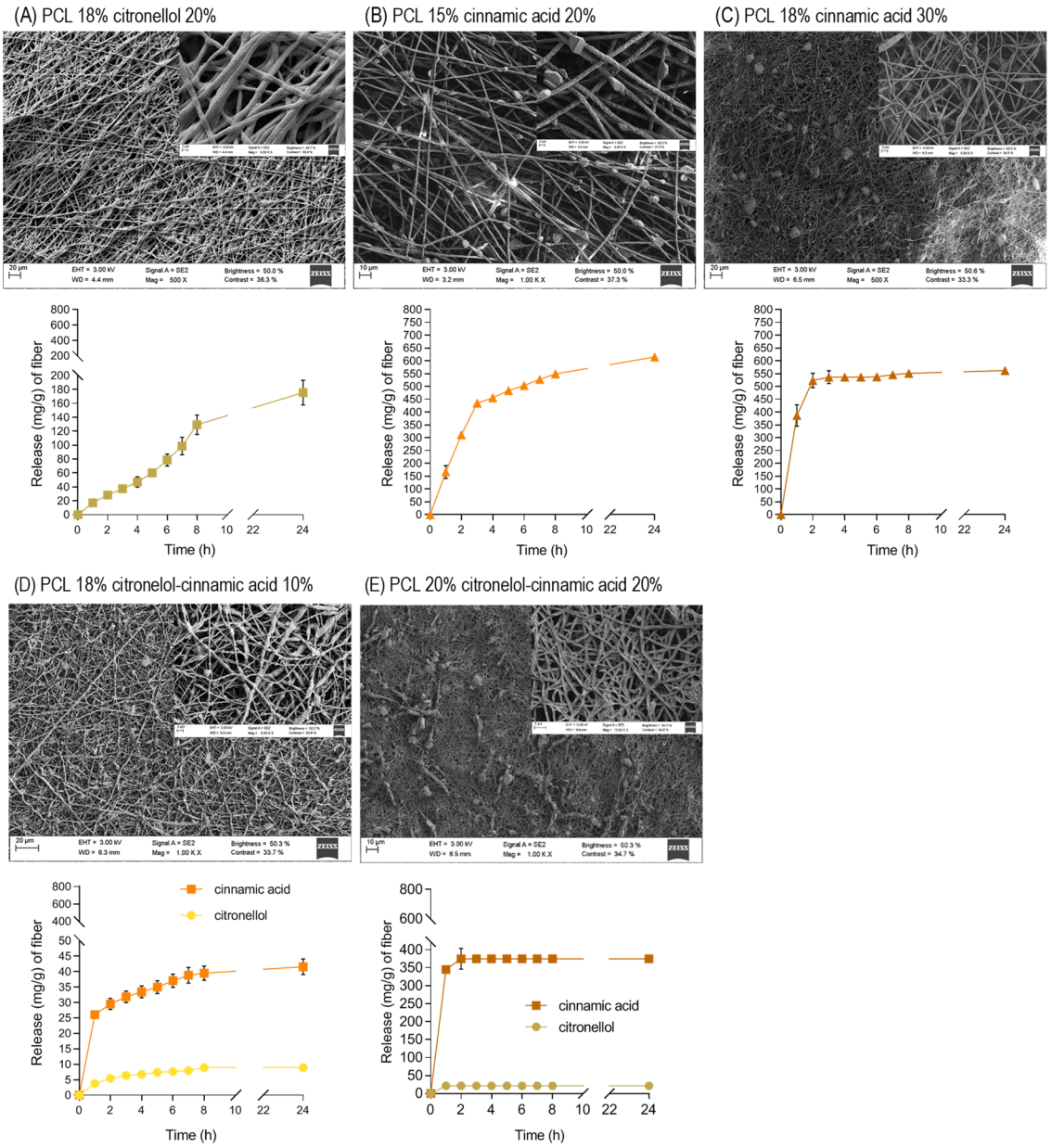



**Figure 3.37. FESEM images with 500× and 5000× magnification with scale bar 20 µm and 2 µm, respectively, and, below, the release profiles of EOCs in PBS (pH 7.4), under 100 rpm and 37°C for 24 hours (n = 3) recorded for (A) PCL 18% citronellol 20%, (B) PCL 15% cinnamic acid 20%, (C) PCL 18% cinnamic acid 30%, (D) PCL 18% citronelol-cinnamic acid 10%, and (E) PCL 20% citronelol-cinnamic acid 20% electrospun mats.**

PCL fibers prepared with mixtures of citronellol and cinnamic acid were also evaluated. The PCL 18% citronellol-cinnamic acid 10% fibers had cylindric shape but with some aggregates lengthwise of the fibers (fibers size 0.41 ± 0.14 µm; **Figure 3.37.D**) that resembled the cinnamic acid crystals. Interestingly, PCL 20% citronellol-cinnamic acid 20% mat was formed by more homogeneous fibers without beads, but they lost the cylindrical shape and adopted a ribbon-like structure due to the increase in the

EOCs:polymer ratio (fibers size 0.40 ± 0.04 μm; **Figure 3.37.E**). These dually loaded fibers also showed a very rapid release of cinnamic acid and slow release of citronellol, in good agreement with the results recorded for the fibers prepared with only one EOC. As explained above, fast dissolution of cinnamic acid correlated well with the presence of the crystals of this EOC on the mat surface. However, interestingly, the fibers co-loaded with citronellol and cinnamic acid evidenced lower melting temperature and enthalpy of cinnamic acid (**Figure 3.36.**) than those of raw cinnamic acid, which suggests that cinnamic acid can partially dissolve in citronellol and thus less crystals are formed. Concerning to citronellol release profile, both mats released similar amounts, 7-8 mg/g, despite PCL 20% citronellol-cinnamic acid 20% were prepared with double concentration of citronellol than PCL 18% citronellol-cinnamic acid 10% fibers. Citronellol (200 mg/L aq. solubility; log P 3.1) is more hydrophobic than cinnamic acid (500 mg/L aq. solubility; log P 2.2; PubChem database), being more compatible with PCL. Citronellol may establish hydrophobic interactions, dipole-dipole or van der Waals forces with PCL, more favourably than cinnamic acid, which may help citronellol to remain inside the PCL fiber matrix. Differently, migration to the surface of PCL matrices has already been described for polar active ingredients, similar to cinnamic acid, which facilitates drug release [61].

Regarding the fibers containing cyclodextrins, PCL 15% αCD 7% carvacrol 10% mats were formed by homogeneous, continuous fibers without bead (fibers diameter 1.04 ± 0.2 μm; **Figure 3.38.A**). Although the fibers were partially fused together, the mat was still porous and efficiently released carvacrol to the aqueous medium. The addition of αCD improved the loading of high amounts carvacrol and controlled the release for 24 h. PCL 15% αCD 2% citronellol 5% mat, which also exhibited antimicrobial properties, was made of continuous fibers (0.72 ± 0.42 μm; **Figure 3.38.B**). This mat showed a burst release in the first 4 h with 5 mg citronellol released per gram of fiber, which corresponded to a 22% of the initial content. These two mats showed the characteristic thermal events of PCL, but the fibers containing carvacrol had a second endothermic peak at 67.39 ºC (**Figure 3.39.**). This unexpected peak, which also appeared in PCL 15% HPβCD 7% carvacrol 10% mats, may suggest that carvacrol forms cocrystals with other components of the fibers. It has been reported that carvacrol itself crystallizes at -20 ºC and melts between 0 and 3.5ºC [62] and that readily forms cocrystals with a variety of molecules [63]. The crystallization of carvacrol was not seen in the DSC scans of the fibers, mainly because the crystallization process is quite slow and the sample requires

USC UNIVERSIDADE DE SANTIAGO

time to trigger crystal formation [62]. To the best of our knowledge, co-crystallization of carvacrol with a polymer has only been reported so far for polystyrene films processed in organic solvents like those used to prepare our fibers [64]. These authors found that such a co-crystallization decreased the desorption rate of carvacrol and provided prolonged antimicrobial effects.

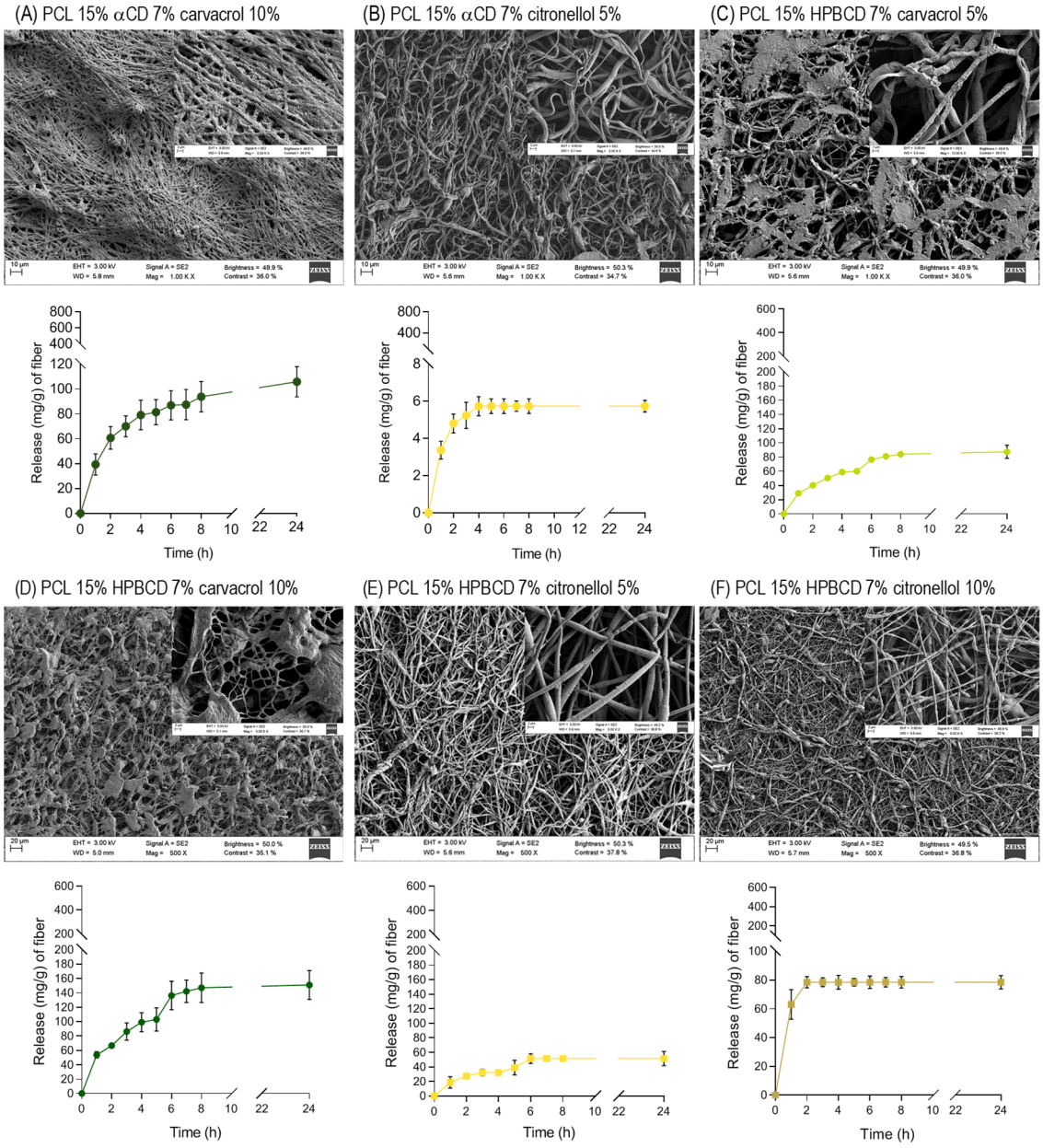
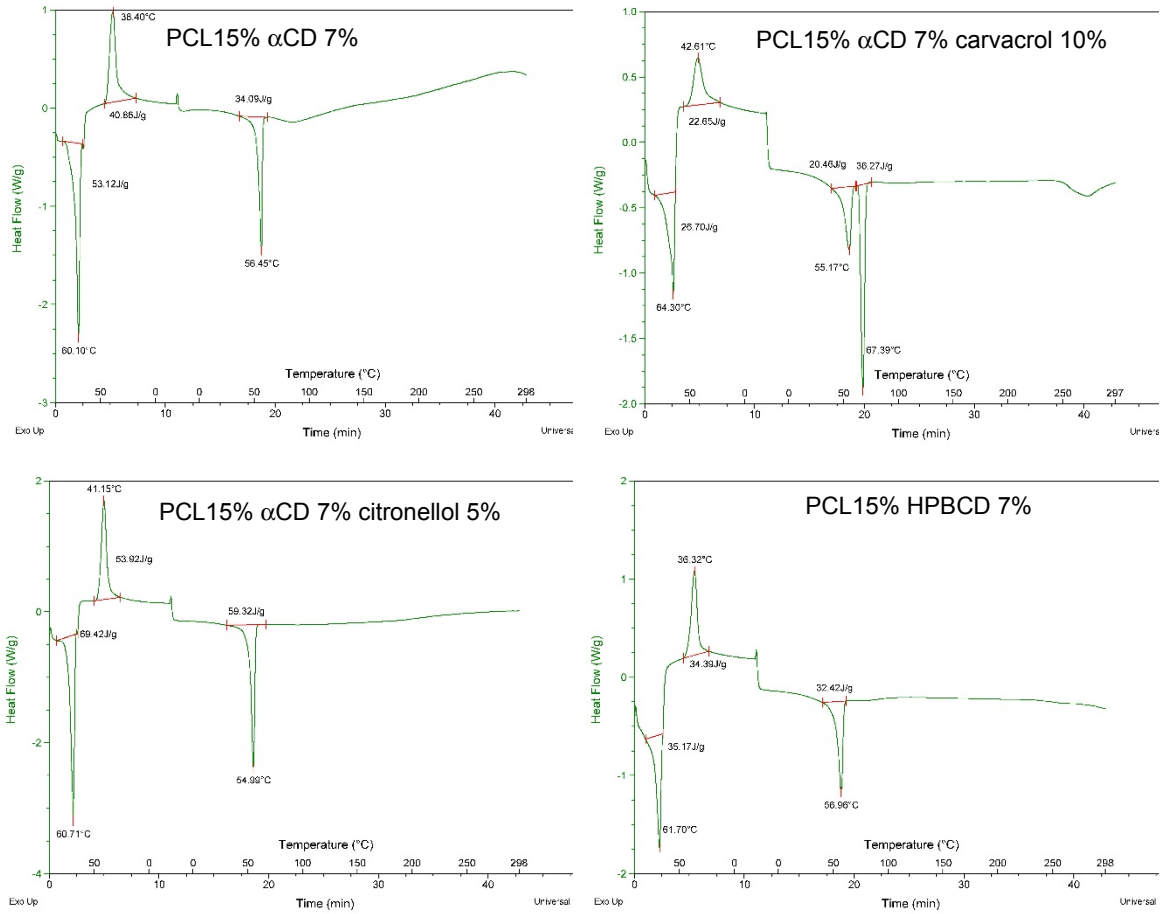



**Figure 3.38. FESEM images with 500× and 5000× magnification with scale bar 20 μm and 2 μm, respectively, and, below, the release profiles of EOCs in PBS (pH 7.4), under 100 rpm and 37°C for 24 hours (n = 3) recorded for (A) PCL 15% αCD 7% carvacrol 10%, (B) PCL 15% αCD 7% citronellol 5%, (C) PCL 15% HPβCD 7% carvacrol 5%, (D) PCL 15% HPβCD 7% carvacrol 10%, (E) PCL 15% HPβCD 7% citronellol 5%, and (F) PCL 15% HPβCD 7% citronellol 10% electrospun mats.**

Replacement of HPβCD by αCD did not prevent completely the fusion of fibers containing carvacrol. PCL 15% HPβCD 7% fibers prepared with carvacrol 5% (0.96 ± 0.55 μm; **Figure 3.38.C**) and carvacrol 10% (0.52 ± 0.27 μm; **Figure 3.38.D**) were continuous, but aggregation of fibers was observed. Both mats released carvacrol gradually during 8 h, and the amounts released at that time were 80 mg/g and 140 mg/g, respectively, which corresponded to 43.2% and 44.9% loaded. Only the mat with the highest content in carvacrol showed, in addition to the PCL melting peak, an additional endothermic event which might be related to co-crystallization (**Figure 3.39.**).




USC UNIVERSIDADE DE SANTIAGO DE COMPOSTELA

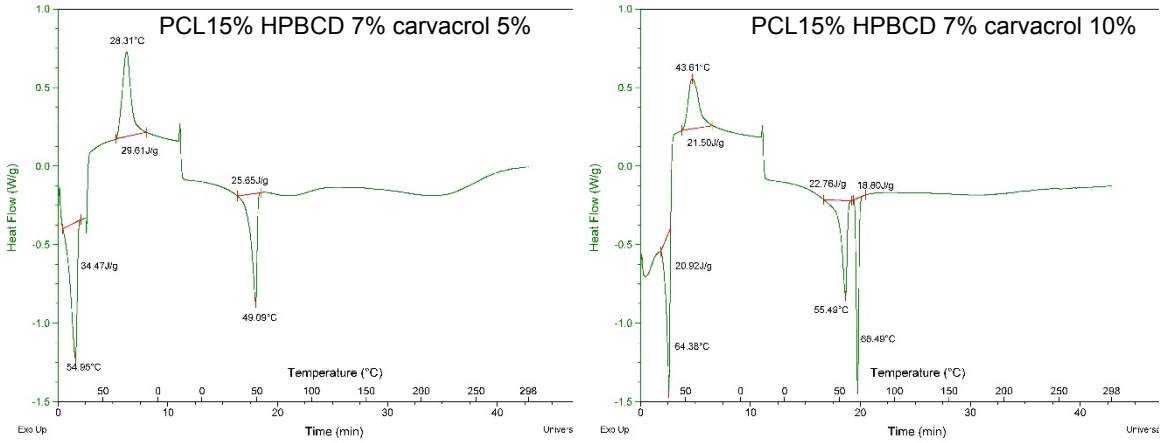
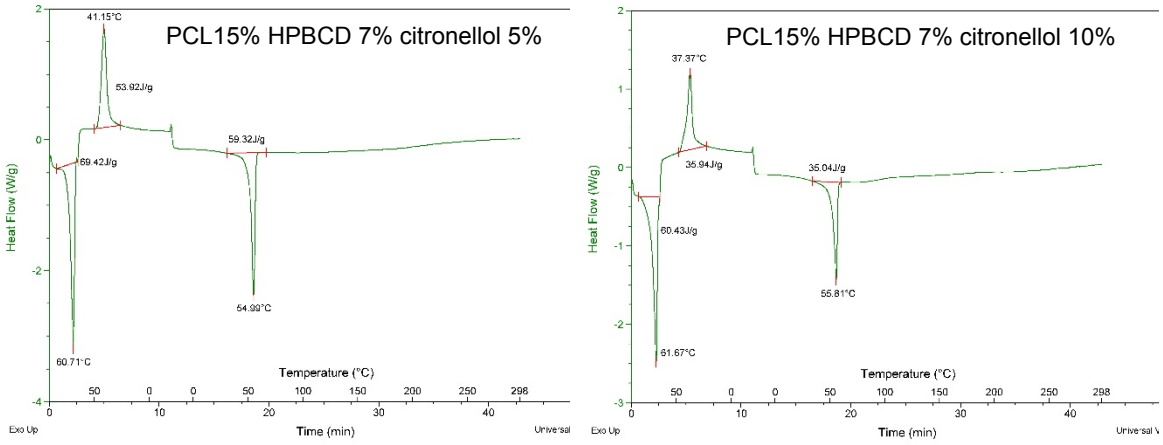



**Figure 3.39. DSC scans of fibers prepared with PCL, cyclodextrins and the indicated EOCs. The samples were heated from 25 to 65˚C, cooled to -20˚C and then heated to 300˚C at 10˚C/min.**

PCL 15% HPBCD 7% citronellol 5% fibers were continuous and without beads (0.52 ± 0.27 µm; **Figure 3.38.E**). Doubling the content in citronellol caused some beads to appear in the fibers (0.53± 0.20 µm; **Figure 3.38.F**) but fusion was not observed. The small diameter of citronellol-loaded fibers could be due to a decrease in the dielectric constant of the solutions caused by the EOC. These results agreed well with other fibers loaded with citronellol. These fibers released 40 mg/g and 80 mg/g, respectively, which corresponded to 21.6% and 25.6% loaded. The slower release rate of citronellol compared to carvacrol from fibers of the same composition can be related to lower solubility in aqueous medium of citronellol (200 mg/L) compared to carvacrol (1.2 g/L). Thus, these citronellol mats exhibited slightly lower antimicrobial activity against *S. aureus* and higher MBC (citronellol 1 mg/mL; carvacrol 0.8 mg/mL). These two mats only showed the characteristic thermal events of PCL (**Figure 3.40.**).




USC UNIVERSIDADE DE SANTIAGO DE COMPOSTELA

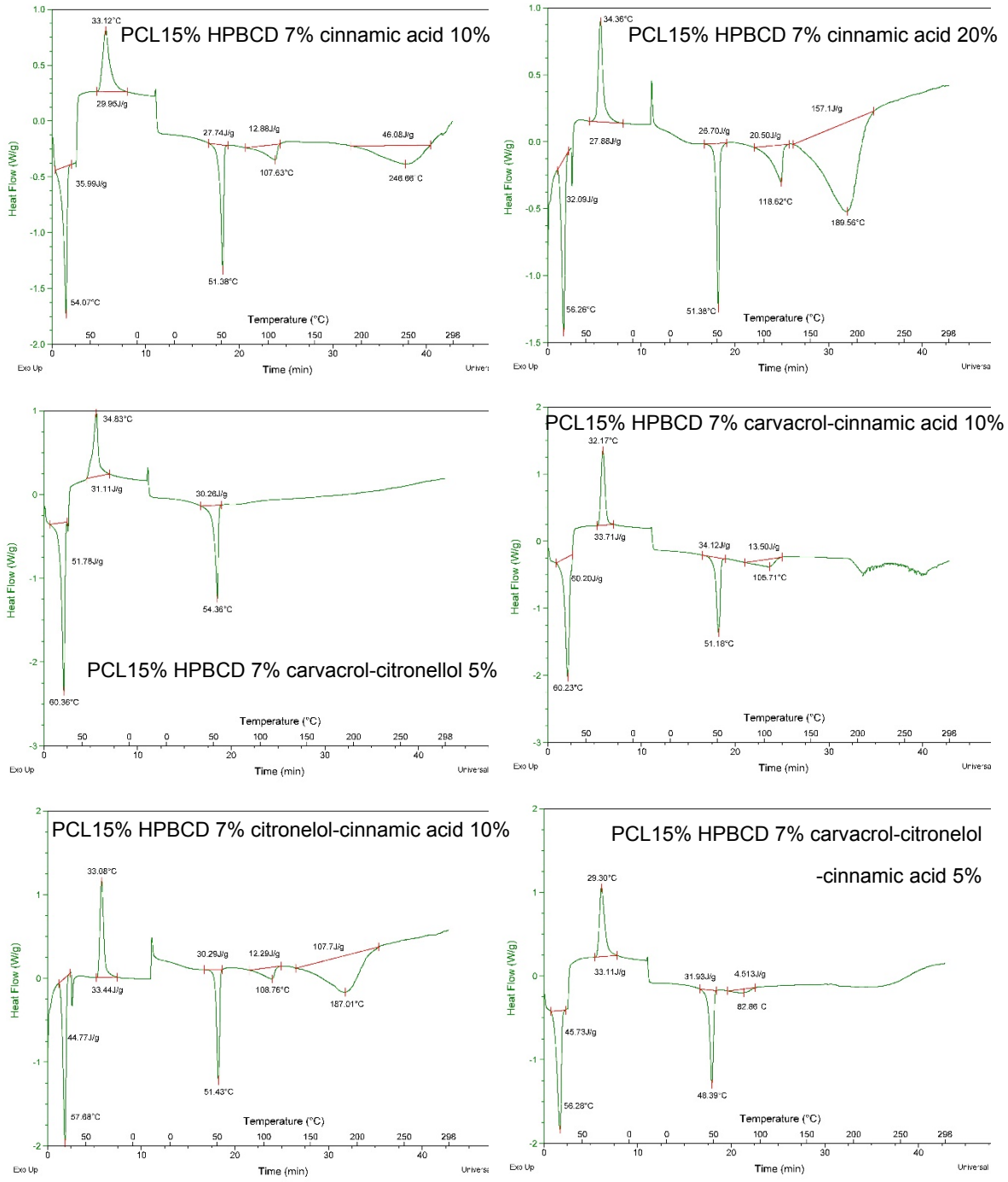



**Figure 3.40. DSC scans of fibers prepared with PCL, HPβCD, and the indicated EOCs. The samples were heated from 25 to 65°C, cooled to -20°C and then heated to 300°C at 10°C/min.**

In the case of cinnamic acid-loaded fibers, the addition of HPβCD favored the encapsulation of cinnamic acid into the PCL fibers and reduced to a minimum the formation of EOC crystals on the mats surface, as confirmed by the marked decrease in the melting enthalpy of the cinnamic acid (**Figure 3.40.**). These mats showed the characteristic melting peak of cinnamic acid at 107-118 ºC but the enthalpy values reflected that only 20-23% cinnamic acid remaining as free crystalline particles. PCL

USC UNIVERSIDADE DE SANTIAGO

15% HPBCD 7% fibers prepared with cinnamic acid 10% (1.13 ± 0.34 μm; **Figure 3.41.A**) or cinnamic acid 20% (1.22 ± 0.3 μm; **Figure 3.41.B**) displayed a huge burst release in first hour, releasing 300 mg/g and 500 mg/g, respectively, which corresponded to approx. 100% loaded. Therefore, the inclusion complex formation of cinnamic acid with HPβCD prevented cinnamic acid crystallization and notably accelerated the dissolution, which explains the higher antimicrobial activity of these fibers compared to those lacking HPβCD (PCL solely and PCL-αCD fibers).

Results obtained for electrospun mats loaded with binary and tertiary mixtures of EOCs are summarized in (**Figure 3.41.C-3.41.F)**. PCL 15% HPβCD 7% carvacrol-citronellol 5% displayed continuous fibers without beads but presented a variety of sizes (0.52 ± 0.27 μm) due to an irregular encapsulation by an excess of EOCs (**Figure 3.41.C**). HPβCD prevented the complete fusion of the fibers recorded for PCL 15% fibers with these two EOCs. Moreover, the mixture of two EOCs displayed important advantages with positive synergism; PCL 15% HPβCD 7% carvacrol-citronellol 5% released amounts of EOCs similar to those released by fibers containing carvacrol (**Figure 3.41.C**) and citronellol (**Figure 3.41.E**) in separate: 80 mg/g carvacrol and 50 mg/g citronellol at same time 24 h. These values corresponded to 51.3 and 32.1% loaded, respectively, which means that the fibers loaded with a binary mixture released the EOCs at the same rate or even faster than the single loaded fibers.

Similar results were obtained with the carvacrol and cinnamic acid mixture showing a positive synergism. PCL 15% HPβCD 7% carvacrol-cinnamic acid 10% mats displayed continuous fibers (0.74 ± 0.47 μm) and without beads but exhibit thickening lengthwise the fiber and some characteristic cinnamic aggregates, which can be due to a preferential interaction of carvacrol with HPβCD, triggering the migration of cinnamic acid towards the fibers surface. Nevertheless, the melting enthalpy of cinnamic acid peak was relatively small suggesting amorphization in these fibers (**Figure 3.40.**). These fibers released 50 mg/g of carvacrol, which was less than the amount released by single carvacrol 5% mat. Differently, cinnamic acid reached 100% release.

USC UNIVERSIDADE DE SANTIAGO DE COMPOSTELA

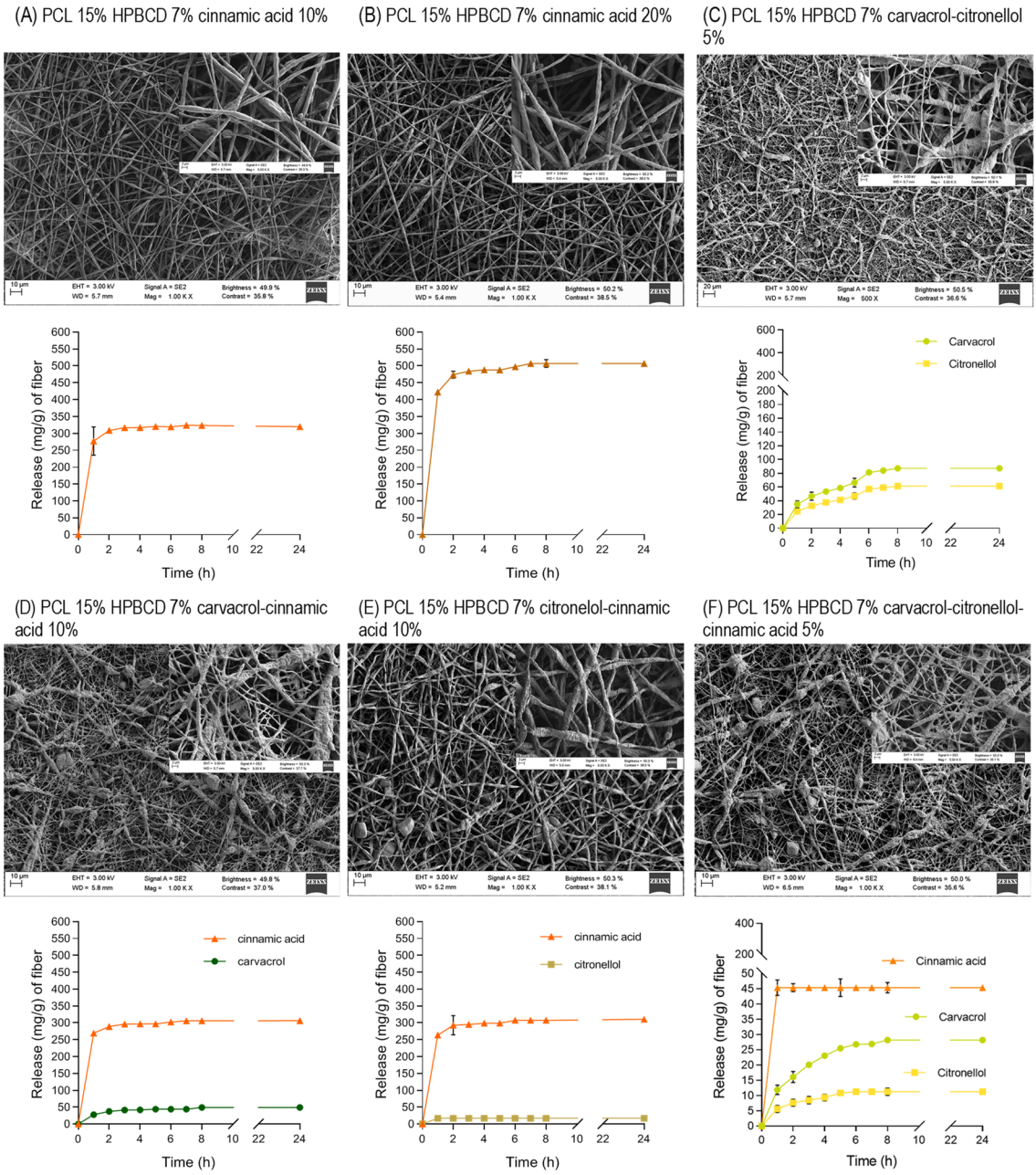



**Figure 3.41. FESEM images with 500× and 5000× magnification with scale bar 20 µm and 2 µm, respectively, and, below, the release profiles of EOCs in PBS (pH 7.4), under 100 rpm and 37°C for 24 hours (n = 3) recorded for (A) PCL 15% HPβCD 7% cinnamic acid 10%, (B) PCL 15% HPβCD 7% cinnamic acid 20%, (C) PCL 15% HPβCD 7% carvacrol-citronellol 5%, (D) PCL 15% HPβCD 7% carvacrol-cinnamic acid 10%, (E) PCL 15% HPβCD 7% citronellol-cinnamic acid 10%, and (F) PCL 15% HPβCD 7% carvacrol-citronellol-cinnamic acid 5% electrospun mats.**

USC UNIVERSIDADE DE SANTIAGO

Similarly, PCL 15% HPBCD 7% citronellol-cinnamic acid 10% were formed by continuous fibers (1.28 ± 0.6 µm; **Figure 3.41.E**) with some cinnamic acid crystals on

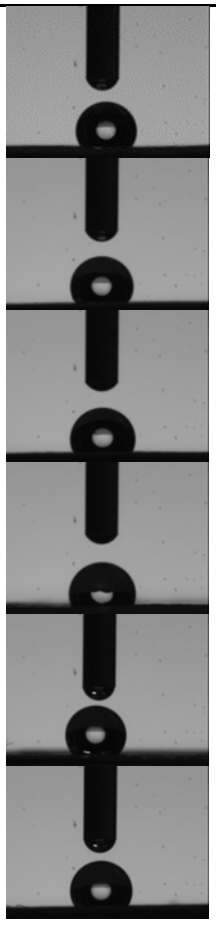
the surface and showed a fast and complete release of cinnamic acid. Instead, less amount of citronellol, 20 mg/g, was released.

Fibers prepared with a mixture of the three EOCs, PCL 15% HPBCD 7% carvacrol-citronellol-cinnamic acid 5% were continuous, homogeneous, without beads (0.56 ± 0.19 μm) but with thickening lengthwise due to an improper encapsulation of hydrophobic carvacrol and citronellol and some characteristic cinnamic acid aggregates. The fibers released the three EOCs at different rates as a function of their polarity, as clearly depicted in (**Figure 3.41.F**).

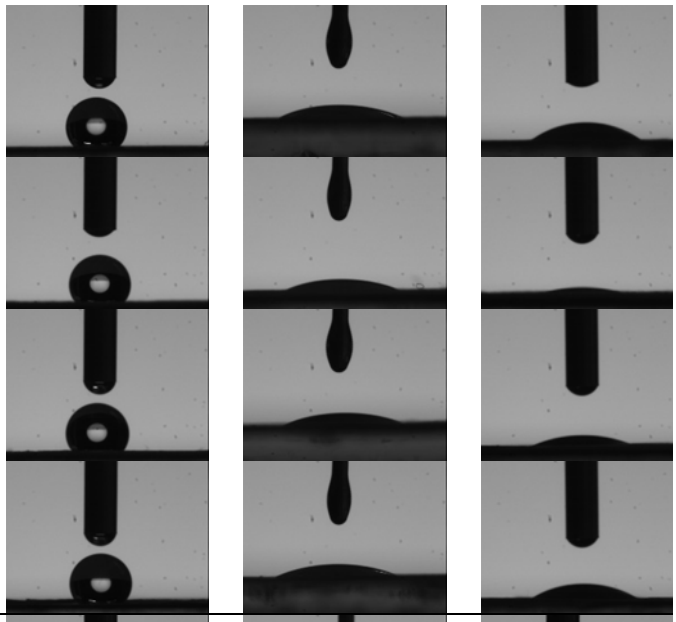
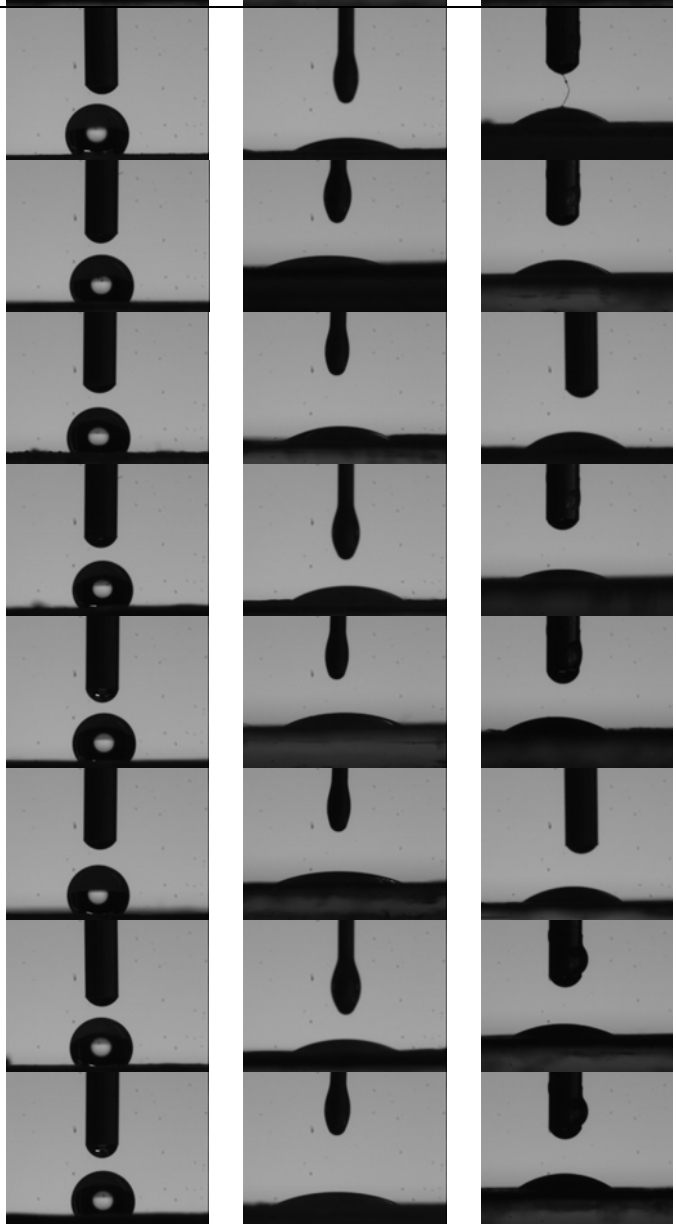
### 3.3.5 Surface polarity

The hydrophobic, polar, and apolar components of the surface tension of the mats prepared with and without EOCs are summarized in **Table 3.2** and **3.3.**

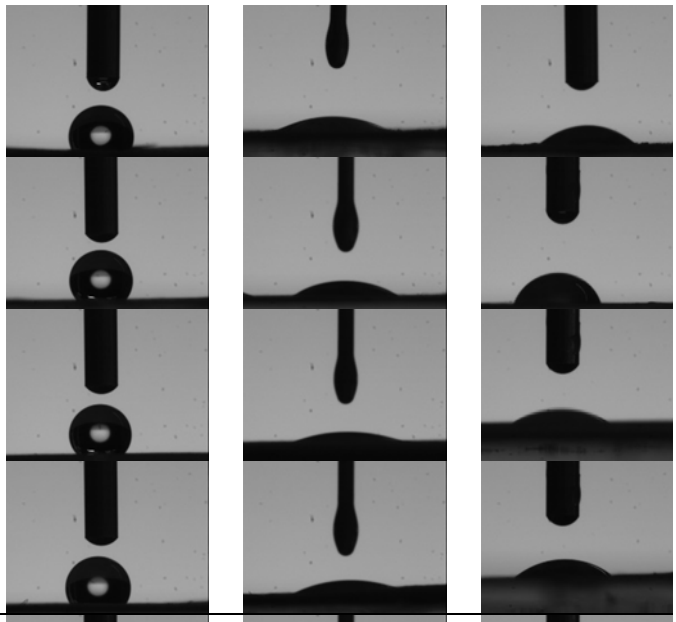
**Table 3.2. Contact angle of PCL, PCL αCD 2% and PCL αCD 7% fibers loaded carvacrol, citronellol and cinnamic acid using water, bromonaphthalene and formamide at 23 ± 2ºC.**

| Fiber | Surface tension parameters (mJ/m$^2$) | | | | $\Delta G^{TOT}$ (mJ/m$^2$) | Picture | | |
|---|---|---|---|---|---|---|---|---|
| | $\gamma^{LW}$ | $\gamma^{AB}$ | $\gamma^{+}$ | $\gamma^{-}$ | | Water | Bromonaphthalene | Formamide |
| PCL 15% (Control) | 40.68 | 0 | 2.67 | 0 | -74.82 |  | | |
| PCL 15% Carvacrol 1% | 40.97 | 0 | 14.94 | 0 | -29.92 | | | |
| PCL 15% Carvacrol 2% | 36.73 | 0 | 11.21 | 0 | -38.26 | | | |
| PCL 15% Carvacrol 5% | 39.34 | 0 | 6.44 | 0 | -55.88 | | | |
| PCL 15% Citronellol 1% | 38.79 | 0 | 17.50 | 0 | -22.35 | | | |
| PCL 15% Citronellol 2% | 35.67 | 0 | 11.50 | 0 | -36.88 | | | |

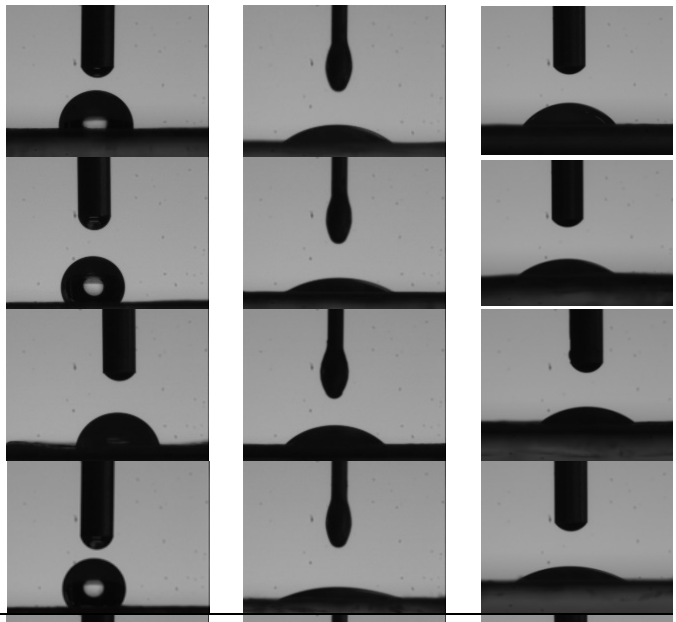
USC UNIVERSIDADE DE SANTIAGO DE COMPOSTELA

| | | | | | | |
|---|---|---|---|---|---|---|
| PCL 15% Citronellol 5% | 39.00 | 0 | 14.83 | 0 | -29.19 |  |
| PCL 15% Cinnamic 1% | 36.40 | 0 | 15.09 | 0 | -27.27 | |
| PCL 15% Cinnamic 2% | 40.95 | 0 | 14.85 | 0 | -30.14 | |
| PCL 15% Cinnamic 5% | 38.97 | 0 | 18.46 | 0 | -20.17 | |
| PCL 15% Carvacrol 1% Citronellol 1% | 39.37 | 0 | 17.84 | 0 | -21.84 |  |
| PCL 15% Carvacrol 2% Citronellol 2% | 37.16 | 0 | 16.33 | 0 | -24.46 | |
| PCL 15% Carvacrol 5% Cinnamic 5% | 38.04 | 0 | 13.15 | 0 | -33.25 | |
| PCL 15% Citronellol 1% Cinnamic 1% | 40.69 | 0 | 17.78 | 0 | -22.68 | |
| PCL 15% Citronellol 2% Ac Cinnamic 2% | 38.55 | 0 | 18.44 | 0 | -20.01 | |
| PCL 15% Citronellol 5% Cinnamic 5% | 36.53 | 0 | 4.032 | 0 | -65.22 | |
| PCL 15% Carvacrol 1% Citronellol 1% | 39.45 | 0 | 17.64 | 0 | -22.34 | |
| PCL 15% Carvacrol 2% Citronellol 2% | 36.21 | 0 | 13.79 | 0 | -30.62 | |

USC UNIVERSIDADE DE COMPOSTELA

| | | | | | | |
|---|---|---|---|---|---|---|
| PCL 15% Carvacrol 5% Citronellol 5% | 36.70 | 0 | 6.11 | 0 | -55.92 |  |
| PCL 15% αCD 2% | 36.53 | 0 | 4.03 | 0 | -65.22 | |
| PCL 15% αCD 2% Carvacrol 5% | 39.31 | 0 | 17.05 | 0 | -23.73 | |
| PCL 15% αCD 2% Citronellol 5% | 34.56 | 0 | 20.84 | 0 | -12.73 | |
| PCL 15% αCD 2% Cinnamic 5% | 41.39 | 0 | 14.02 | 0 | -32.60 | |
| PCL 15% αCD 7% | 37.62 | 0 | 0 | 0 | -106.29 | |
| PCL 15% αCD 7% Carvacrol 5% | 36.39 | 0 | 12.59 | 0 | -34.06 | |
| PCL 15% αCD 7% Citronellol 5% | 36.92 | 0 | 15.61 | 0 | -25.93 | |
| PCL 15% αCD 7% Cinnamic 5% | 41.87 | 0 | 14.95 | 0 | -30.36 | |
| PCL 22% Carvacrol 10% | 39.63 | 0 | 2.65 | 0 | -74.39 | |
| PCL 18% Carvacrol 10% | 32.99 | 0 | 9.97 | 0 | -40.51 | |
| PCL 20% Carvacrol 20% | 38.68 | 0 | 2.20 | 0 | -76.83 | |

USC UNIVERSIDADE DE SANTIAGO DE COMPOSTELA

| | | | | | | |
|---|---|---|---|---|---|---|
| PCL 15% Citronellol 20% | 38.41 | 0 | 1.23 | 0 | -84.23 |  |
| PCL 18% Citronellol 10% | 38.96 | 0 | 12.44 | 0 | -35.71 | |
| PCL 18% Citronellol 20% | 33.66 | 0 | 2.18 | 0 | -43.40 | |
| PCL 15% Cinnamic acid 10% | 40.47 | 0 | 12.39 | 0 | -36.63 | |
| PCL 15% Cinnamic acid 20% | 42.05 | 0 | 17.00 | 0 | -25.32 | |
| PCL 18% Cinnamic acid 30% | 41.82 | 0 | 17.94 | 0 | -22.91 | |
| PCL 20% Carvacrol 10% Citronellol 10% | 38.01 | 0 | 0 | 0 | -106.48 | |
| PCL 18% Citronellol 10% Cinnamic acid 10% | 40.1 | 0 | 12.40 | 0 | -36.42 | |
| PCL 20% Citronellol 20% Cinnamic acid 20% | 41.65 | 0 | 11.14 | 0 | -40.94 | |

The apolar and polar surface properties of the electrospun fibers were determined by Lifshitz-van der Waals component $\gamma^{LW}$ and the Lewis acid-base component $\gamma^{AB}$, respectively.The values of the nonpolar component $\gamma^{LW}$ were close to 40 mJ/m$^2$, which is a common value for organic polymers and biopolymers [44]. PCL electrospun mat had a value of 40.68 mJ/m$^2$. Indeed, the values of $\gamma^{LW}$ of the electrospun mats hardly changed with the incorporation of EOCs because the main component was PCL. The polar surface tension component, $\gamma^{AB}$, of the fibers had a value of 0 for PCL and PCL/αCD fibers. These

USC UNIVERSIDADE DE SANTIAGO

kinds of fibers displayed 0 proton acceptor or electron donor γ. The $\gamma^{AB}$ values were calculated applying **Equation 3.3.** [44]:

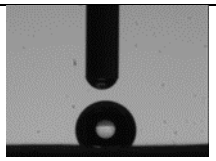
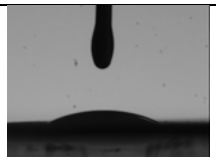
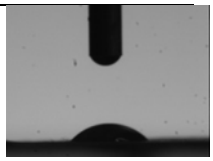
$$\gamma^{AB} = 2\sqrt{\gamma^{+}\gamma^{-}} \quad (3.3.)$$

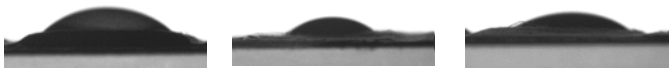
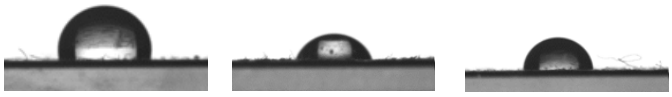
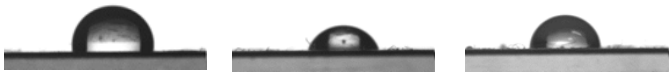
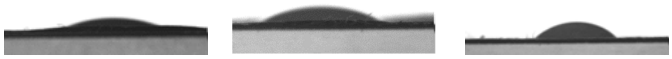
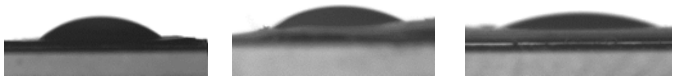
Where γ is the proton acceptor or electron donor component and $\gamma^{+}$ the electron acceptor component. The values of $\gamma^{+}$ increased slightly with the addition of EOCs to the fibers because they have electron-accepting functional groups. Cinnamic acid has a COOH acid group in its structure, while carvacrol and citronellol have OH groups. These later groups are strong electron donors and decreased the $\gamma^{+}$ values. The same phenomenon occurred for fibers with cyclodextrins which also had lower $\gamma^{+}$ values than fibers with only PCL mainly due to their OH groups. Meanwhile, some PCL/HPβCD fibers showed opposite behavior, $\gamma^{+} > \gamma$, being electron donor due to the structural differences between αCD and HPβCD.

PCL and PCL αCD fibers showed $\Delta G^{TOT} < 0$ mJ/m$^2$, indicating the hydrophobic character of these fibers, which could be increased due to poly(pseudo)rotaxane formation [65]. Differently, some PCL/HPβCD fibers displayed a $\Delta G^{TOT} > 0$ mJ/m$^2$ indicating hydrophilic character. This change of hydrophobicity could be relevant in terms of bacteria adhesion since the adhesion is hindered when $\Delta G^{TOT} > 0$ mJ/m$^2$, while $\Delta G^{TOT} < 0$ mJ/m$^2$ may favor the adhesion [66].

Overall, the fibers tested in this study had hydrophobic surface, as expected for PCL materials, except for some fibers prepared with HPβCD. The incorporation of EOCs attenuated the hydrophobicity, reducing the $\Delta G^{TOT}$. This reduction could be due to the presence of free EOC on the surface of the fibers. Also, the formation of EOC-cyclodextrin inclusion complexes in the vials before the electrospinning process can attenuate the poly(pseudo)rotaxane formation with PCL.

**Table 3.3. Contact angle of PCL HPβCD 7% fibers loaded carvacrol, citronellol and cinnamic acid using water, bromonaphthalene and formamide at 23 ± 2°C.**

| Fiber | Surface tension parameters (mJ/m$^2$) | | | | $\Delta G^{TOT}$ (mJ/m$^2$) | Picture | | |
|---|---|---|---|---|---|---|---|---|
| | $\gamma^{LW}$ | $\gamma^{AB}$ | $\gamma^{+}$ | $\gamma^{-}$ | | Water | Bromonaphthalene | Formamide |
| PCL 15% (Control) | 40.68 | 0 | 2.67 | 0 | -74.82 |  |  |  |

| | | | | | | |
|---|---|---|---|---|---|---|
| PCL 15% HPβCD 7% (Control) | 39.95 | 0 | 0 | 0 | -107.46 |  |
| PCL 15% HPβCD 7% Carvacrol 5% | 38.43 | 5.93 | 1.63 | 5.39 | -45.85 |  |
| PCL 15% HPβCD 7% Carvacrol 10% | 39.65 | 0 | 0 | 13.32 | -33.58 |  |
| PCL 15% HPβCD 7% Citronellol 5% | 37.93 | 7.57 | 0.33 | 43.61 | 23.38 |  |
| PCL 15% HPβCD 7% Citronellol 10% | 38.87 | 9.61 | 1.23 | 18.83 | -16.11 |  |
| PCL 15% HPβCD 7% Cinnamic acid 10% | 22.43 | 0.47 | 0.02 | 2.67 | -67.05 |  |
| PCL 15% HPβCD 7% Cinnamic acid 20% | 39.80 | 12.92 | 1.25 | 33.20 | 5.82 |  |
| PCL 15% HPβCD 7% Carvacrol-Citronellol 5% | 21.80 | 0.7 | 0.04 | 2.96 | -64.52 |  |
| PCL 15% HPβCD 7% Carvacrol-Cinnamic acid 10% | 40.53 | 0 | 0 | 63.58 | 53.31 |  |
| PCL 15% HPβCD 7% Citronellol-Cinnamic acid 10% | 41.77 | 8.20 | 0.40 | 41.70 | 18.43 |  |
| PCL 15% HPβCD 7% Carvacrol-Citronellol-Cinnamic acid 5% | 39.76 | 8.61 | 0.94 | 19.64 | -15.43 |  |

### 3.3.6. Mechanical properties of electrospun mats

The tensile properties of PCL, PCL/αCD and PCL/HPβCD mats with different concentration of EOC were characterized in terms of Young's modulus, tensile strength and elongation at break (**Table 3.4.**). Addition of EOC to PCL solely fibers caused a decrease in Young´s modulus and the fibers became brittle, suggesting that intercalation of EOC disrupted the intermolecular bonding among PCL chains. Relevantly, PCL 15% αCD 2% control mat had remarkably higher Young´s modulus and tensile strength, conforming the reinforcement of the fibers when poly(pseudo)rotaxanes are formed, in good agreement with previous results [22]. However, an excess in αCD (7%) restored the balance of intermolecular forces and the fibers performed similarly to PCL 15% mats. As expected, incorporation of EOCs, although weakly interacting with αCD compared to HPβCD [67], weakened the mechanical properties of the fibers as EOCs can attenuate poly(pseudo)rotaxane formation. In the case of PCL/HPβCD mats the results were similar to those recorded for PCL mats, with the exception of PCL 15% HPβCD7% carvacrol 10%, which were more rigid. Regarding the fibers prepared with the three AOE (**Table 3.4.**, last row), they were very brittle and broke easily when handled.

**Table 3.4. Mechanical properties of fibers prepared with different contents in EOCs.**

| Fiber type | Young's modulus (MPa) | Tensile strength (MPa) | Elongation at break (%) |
|---|---|---|---|
| **PCL 15%** | 367.36 | 80.72 | 97.43 |
| **PCL 15% αCD 2%** | 5291.7 | 1274.99 | 85.34 |
| **PCL 15% αCD 7%** | 167.79 | 55.93 | 92.05 |
| **PCL 20% citronellol 20%** | 32.20 | 4.65 | 97.56 |
| **PCL 18% cinnamic acid 20%** | 9.54 | 0.44 | 6.23 |
| **PCL 20% cinnamic acid 30%** | 2.62 | 1.64 | 72.98 |
| **PCL 18% citronellol-cinnamic acid 10%** | 4.27 | 0.19 | 0.2 |
| **PCL 20% citronellol-cinnamic acid 20%** | 3.74 | 0.12 | 4.89 |
| **PCL 15% αCD 2% carvacrol 10%** | 151.87 | 20.53 | 114.63 |
| **PCL 15% αCD 2% citronellol 5%** | 88.48 | 10.63 | 197.96 |
| **PCL 15% HPβCD7%** | 222.42 | 37.48 | 198.00 |

| | | | |
|---|---|---|---|
| **PCL 15% HPβCD7% carvacrol 5%** | 56.24 | 16.49 | 198.00 |
| **PCL 15% HPβCD7% carvacrol 10%** | 7850.8 | 354.72 | 45.67 |
| **PCL 15% HPβCD7% citronellol 5%** | 19.57 | 1.58 | 117.09 |
| **PCL 15% HPβCD7% citronellol 10%** | 0.7 | 0.26 | 42.51 |
| **PCL 15% HPβCD7% cinnamic acid 10%** | 16.62 | 3.56 | 22.97 |
| **PCL 15% HPβCD7% cinnamic acid 20%** | 83.99 | 3.78 | 5.60 |
| **PCL 15% HPβCD7% carvacrol-citronellol 5%** | 19.21 | 6.11 | 109.77 |
| **PCL 15% HPβCD7% carvacrol-cinnamic acid 10%** | 157.13 | 1.26 | 0.49 |
| **PCL 15% HPβCD7% citronellol-cinnamic acid 10%** | 5.98 | 0.06 | 4.74 |
| **PCL 15% HPβCD7% carvacrol-citronellol-cinnamic acid 5%** | 378.52 | 0.61 | 6.65 |

### 3.3.7 Antioxidant activity

In addition to antimicrobial properties, EOCs are commonly characterized by antioxidant activity, exerting synergic outcomes during wound healing [15,30]. First, the antioxidant properties of each free EOC was tested using concentrations in the 0.01 – 15.0 mg/mL in EtOH:PBS (50:50) medium. At the highest concentration, the DPPH scavenging capability ranked in the order cinnamic acid (50%) > carvacrol (30%) > citronellol (10%). Interestingly, carvacrol displayed 10% DPPH scavenging effect at 0.01 mg/mL (the lowest concentration tested), while cinnamic acid needed 0.94 mg/mL to achieved 10% DPPH scavenging effect.

In good agreement with the results obtained for free EOCs, fibers loaded with carvacrol surpassed 20% DPPH scavenging after 24 h contact, showing statistical differences ($p < 0.0001$) with respect to the PCL 15% HPβCD 7% (control) mats (**Table 3.5.**). The electrospun mat that displayed the highest scavenging effect (55.30 ± 4.50%) was PCL 15% HPβCD 7% carvacrol-cinnamic acid 10% owing to the high antioxidant activity of carvacrol and cinnamic acid, indicating a positive synergic effect since their antioxidant activity was twofold higher than that of fibers with same concentration of carvacrol. The second more efficient mats were those of PCL 15% HPβCD 7% carvacrol-citronellol-cinnamic acid 5% and PCL 15% HPβCD 7% carvacrol-citronellol 5%, which had 29.99 ± 2.21% and 27.62 ± 2.52% scavenging capability, respectively (**Table 3.5.**).

USC

Cinnamic acid electrospun mats displayed a notably DPPH scavenging only when the content in this EOC reached 20%, while citronellol-loaded fibers were the ones with the lowest antioxidant capability.

**Table 3.5. Antioxidant properties of EOCs eluted from PCL 15% HPβCD7% fibers after soaking in PBS at 37ºC and 100 rpm during 24h.**

| Fiber type | DPPH scavenging effect (%) | DPPH (µg/ml) |
|---|---|---|
| **PCL 15% HPβCD7%** | 5.72 ± 2.85 | 30.52 ±0.16 |
| **PCL 15% HPβCD7% carvacrol 5%** | 22.11 ± 2.64 **** | 25.04 ± 0.93 |
| **PCL 15% HPβCD7% carvacrol 10%** | 27.20 ± 0.95 **** | 23.33 ± 0.30 |
| **PCL 15% HPβCD7% citronellol 5%** | 9.37 ± 3.22 | 29.32 ± 1.63 |
| **PCL 15% HPβCD7% citronellol 10%** | 7.27 ± 2.47 | 30.00 ± 0.23 |
| **PCL 15% HPβCD7% cinnamic acid 10%** | 4.84 ± 5.11 | 30.81 ± 1.02 |
| **PCL 15% HPβCD7% cinnamic acid 20%** | 11.99 ± 2.77 | 28.42 ± 0.19 |
| **PCL 15% HPβCD7% carvacrol-citronellol 5%** | 27.62 ± 2.52 **** | 23.50 ± 0.49 |
| **PCL 15% HPβCD7% carvacrol-cinnamic acid 10%** | 55.30 ± 4.50 **** | 13.90 ± 1.50 |
| **PCL 15% HPβCD7% citronellol-cinnamic acid 10%** | 4.63 ± 3.57 | 30.89 ± 0.57 |
| **PCL 15% HPβCD7% carvacrol-citronellol-cinnamic acid 5%** | 29.99 ± 2.21 **** | 22.38 ± 0.20 |

### 3.3.8 Hemolysis test

The fibers with the highest antimicrobial activity were also evaluated in terms of hemocompatibility as a preliminary screening of biocompatibility. All fibers tested showed excellent blood compatibility with hemolysis percentages lower than 5% even for the fibers containing the highest concentrations in binary mixtures of EOCs (**Figure 3.42.**).

USC UNIVERSIDADE DE SANTIAGO DE COMPOSTELA

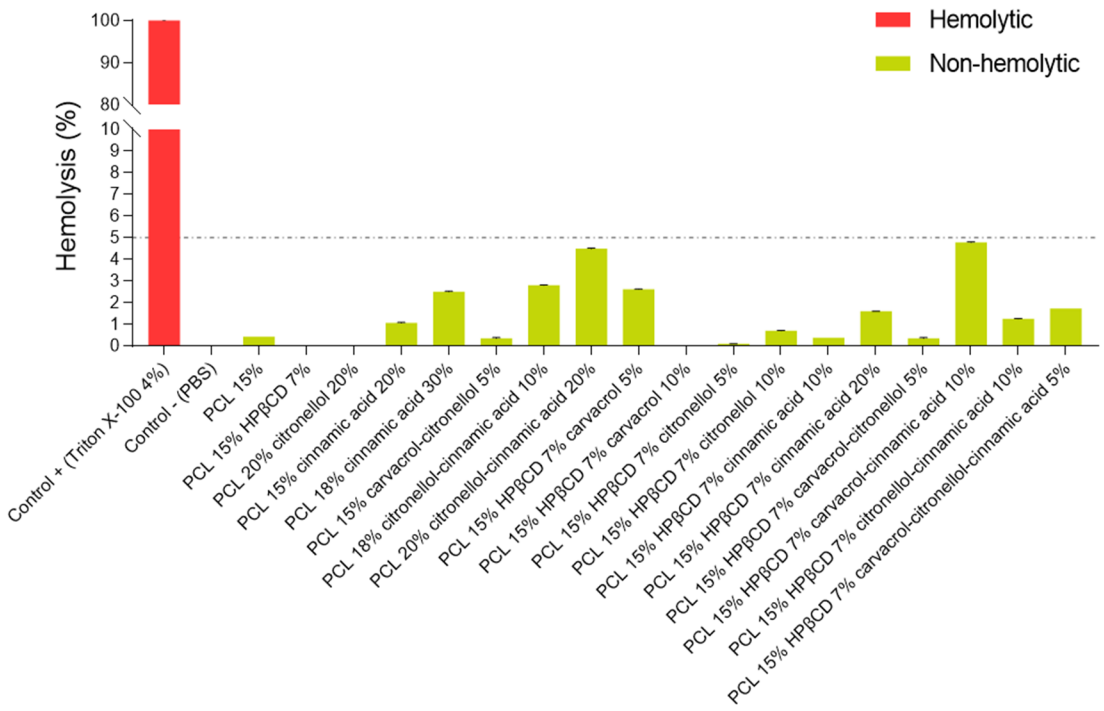



**Figure 3.42. Hemolysis recorded for the fibers loaded with different EOCs after 1 h incubation. Hemocompatibility threshold is shown as a dotted line.**

USC
UNIVERSIDADE DE SANTIAGO DE COMPOSTELA

### 3.3.9 *In ovo* tissue integration and angiogenesis evaluation

Finally, a CAM test was carried out to gain a further insight into biocompatibility, toxicity, angiogenesis response, and tissue integration of the developed mats. The CAM test has been proved to be a good alternative method to *in vivo* studies for formulations intended to be in contact with skin and mucosa, facilitating the reducing, replacement and refining of animal models [68,69]. The CAM test is more available and cost effective and allows complete accessibility to the circulatory system [49]. The CAM is a membrane sensitive to toxic agents and in few minutes can develop irritation signs such haemorrhage, vascular lysis or coagulation.

In our case, the fibers were in contact with the CAM for 5 days and no signs of hemolysis or toxicity were recorded. The integration and vascularization of the fibers are shown in **Figure 3.43 and 3.44**. All fibers had an integration score of 2 out of 3, showing good interaction with the surface that was in contact with the CAM. In general, vascularization was not affected, indicating that the amounts of EOC released from the fibers did not trigger angiogenic effects. Some authors reported that cinnamic acid and its derivatives have angiogenic capacities due to the regulation of VEGF and Flk-1/KDR expression [70]. Indeed, in the case of the fibers prepared without cyclodextrins, only those that incorporated cinnamic acid slightly increased the angiogenesis, but the change was not statistically different compared to the control (**Figure 3.43.C, D, F**).

USC
UNIVERSIDADE DE SANTIAGO DE COMPOSTELA

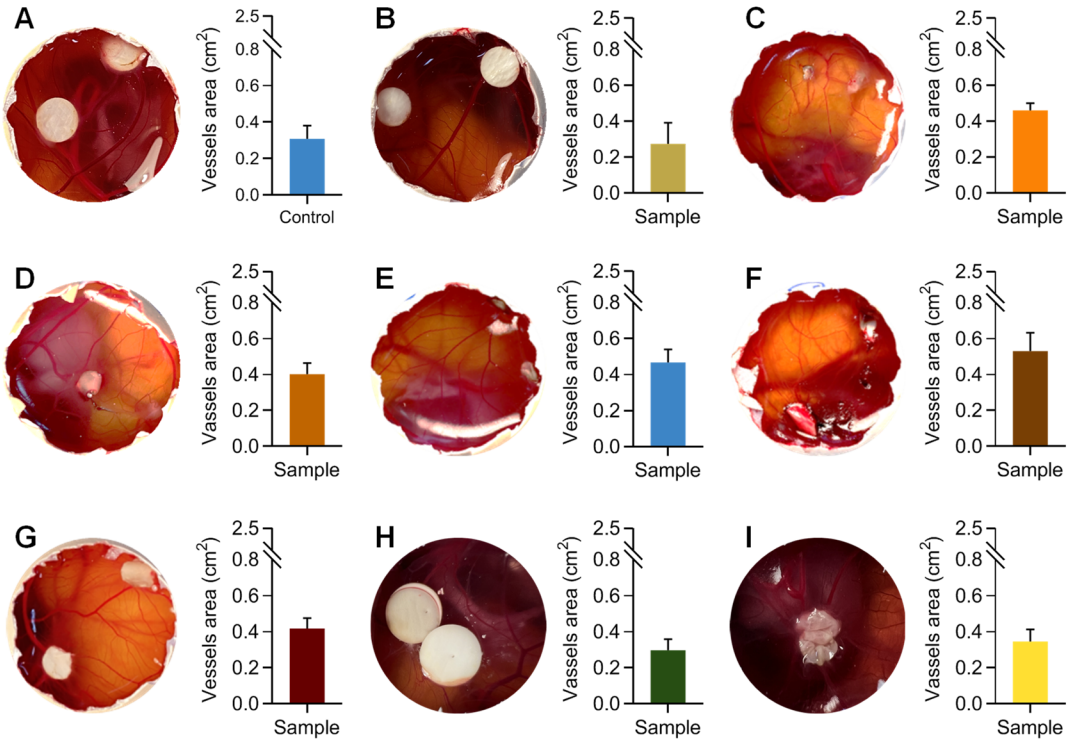



**Figure 3.43. CAM pictures and vascularization of A) PCL 15% (control), B) PCL 20% citronellol 20%, C) PCL 15% cinnamic acid 20%, D) PCL 18% cinnamic acid 30%, E) PCL 15% carvacrol-citronellol 5%, F) PCL 18% citronellol-cinnamic acid 10%, G) PCL 20% citronellol-cinnamic acid 20%, H) PCL 15% αCD 7% carvacrol 10%, and I) PCL 15% αCD 7% citronellol 5% mats. Data are presented as the mean ± standard deviation, n=4.**

When quantifying the area occupied by the blood vessels, fibers prepared with cyclodextrins performed similarly to PCL solely fibers, except for those prepared with the highest amount in carvacrol. PCL 15% HPβCD 7% carvacrol 10% exhibited angiogenic activity showing a significant increase compared to the controls ($p < 0.05$). Some authors have reported that carvacrol promotes angiogenesis at low concentrations by increasing VEGF levels and the formation of tubular arrays [71].

USC UNIVERSIDADE DE SANTIAGO DE COMPOSTELA

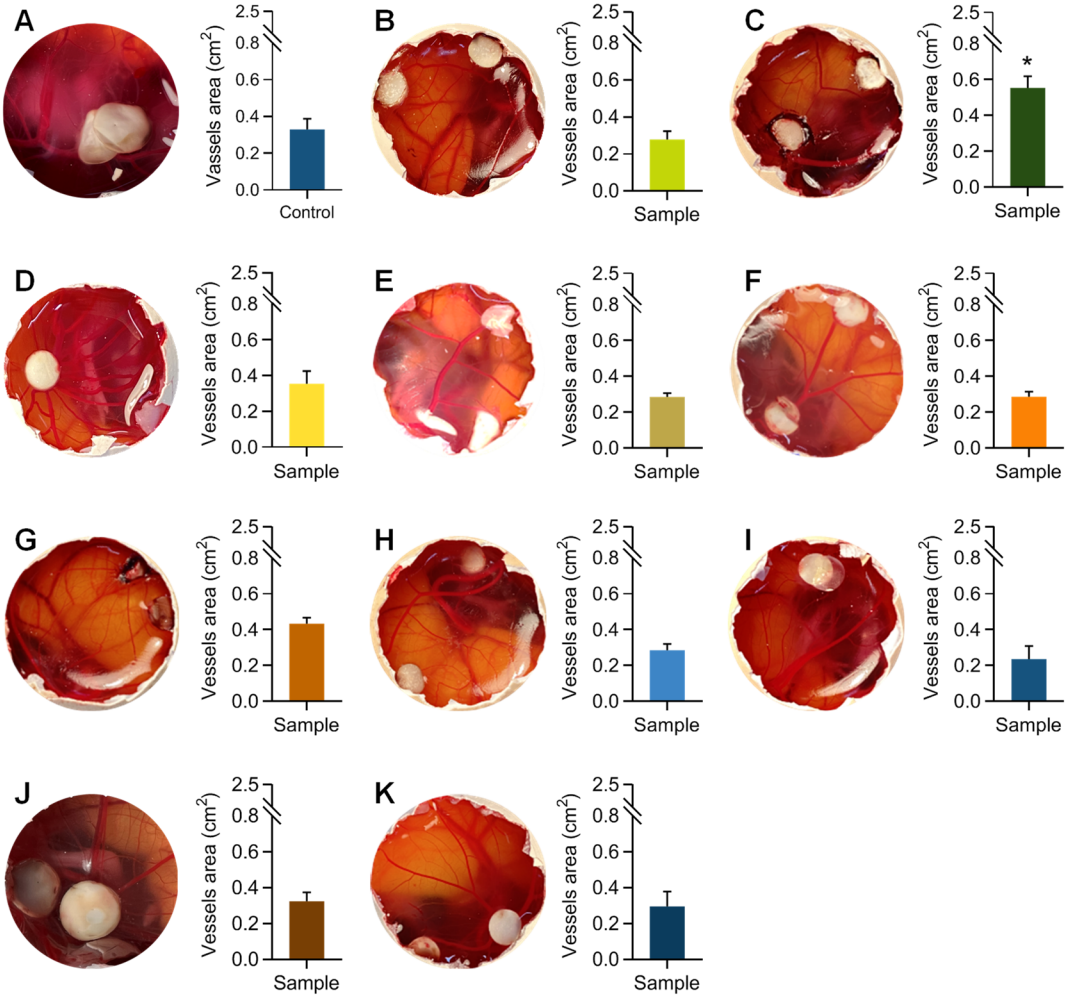



**Figure 3.44. CAM pictures and vascularization of A) PCL 15% HPβCD 7% (Control), B) PCL 15% HPβCD 7% carvacrol 5%, C) PCL 15% HPβCD 7% carvacrol 10%, D) PCL 15% HPβCD 7% citronellol 5%, E) PCL 15% HPβCD 7% citronellol 10%, F) PCL 15% HPβCD 7% cinnamic acid 10%, G) PCL 15% HPβCD 7% cinnamic acid 10%, H) PCL 15% HPβCD 7% carvacrol-citronellol 5%, I) PCL 15% HPβCD 7% carvacrol-carvacrol 10%, J) PCL 15% HPβCD 7% citronellol-cinnamic acid 10%, and K) PCL 15% HPβCD 7% carvacrol-citronellol-cinnamic acid 5% mats. Data are presented as the mean ± standard deviation, n=4, * p < 0.05.**

Overall, all the fibers tested showed good biocompatibility and no toxic effects despite the high concentration of EOCs with which they were loaded. In addition, these fibers had good integration scores, which may facilitate wound healing, also aided by angiogenesis in the case of those prepared with cinnamic acid and carvacrol.

## 3.4. CONCLUSIONS

USC UNIVERSIDADE DE SANTIAGO DE COMPOSTELA

Electrospun fibers loaded with single and combined EOCs were successfully prepared using PCL at 15-22% (w/v) as structural polymer and αCD 2-7% (w/v) or HPβCD 7%

(w/v) as encapsulating agent. Three types of EOCs of different physicochemical properties were investigated to demonstrate the versatility of the approach.

αCD promoted the formation of poly(pseudo)rotaxanes with PCL, reinforcing the mechanical properties of the fibers, but did not significantly contribute to facilitating the integration of the EOCs within the fibers. Differently, the greater capacity of HPβCD to form inclusion complexes with EOCs, and not form poly(pseudo)rotaxanes with PCL, facilitated the homogeneous incorporation of the EOCs. More specifically, HPβCD prevented from fusion of the fibers, attenuated the crystallization of cinnamic acid on the fibers surface, and provided an adequate balance of high loading and sufficiently rapid release of EOCs to obtain strong antimicrobial activity. Binary and ternary mixtures of EOCs shed light on the contribution of each EOC against *S. aureus* and *P. aeruginosa*. Carvacrol-loaded fibers were efficient against both bacteria, while fibers loaded with cinnamic acid solely were selective against the Gram-positive bacteria, which may be preferable when discriminating antimicrobial treatments are required.

Fibers of carvacrol solely and its binary mixtures also showed suitable mechanical properties and antioxidant effects to perform as wound dressings. In fact, the human blood compatibility tests and the *in ovo* CAM assay confirmed the excellent biocompatibility of the developed fibers.

Overall, the results obtained evidenced that by tuning the fibers composition it is possible to prepare environment-friendly, cost-effective, antibiotic-free antimicrobial wound dressings that might find an advantageous position in the arsenal against skin and soft tissue infections.

USC
UNIVERSIDADE DE SANTIAGO DE COMPOSTELA

## 3.5. REFERENCES

[1] D. Nathwani, M. Dryden, J. Garau, Early clinical assessment of response to treatment of skin and soft-tissue infections: how can it help clinicians? Perspectives from Europe, Int. J. Antimicrob. Agents. 48 (2016) 127-36, https://doi.org/10.1016/j.ijantimicag.2016.04.023.

[2] H.N. Leong, A. Kurup, M.Y. Tan, A.L.H. Kwa, K.H. Liau, M.H. Wilcox, Management of complicated skin and soft tissue infections with a special focus on the role of newer antibiotics, Infect. Drug Resist. 11 (2018) 1959–1974. https://doi.org/10.2147/IDR.S172366

[3] B. Silverberg, A structured approach to skin and soft tissue infections (SSTIS) in an ambulatory setting, Clin. Pract. 11 (2021) 65–74, https://doi.org/10.3390/clinpract11010011

[4] H.B. Fung, J.Y. Chang, S. Kuczynski, A practical guide to the treatment of complicated skin and soft tissue infections, Drugs 63 (2003) 1459–1480. https://doi.org/10.2165/00003495-200363140-00003

[5] A.K. Tiwari, R. Lal, Study to evaluate the role of severity stratification of skin and soft tissue infections (SSTIs) in formulating treatment strategies and predicting poor prognostic factors, Int. J. Surg. 12 (2014) 125–133. https://doi.org/10.1016/j.ijsu.2013.11.014

[6] M. Frieri, K. Kumar, A. Boutin, Antibiotic resistance, J. Infect. Public Health, 10 (2017) 369–378. https://doi.org/10.1016/j.jiph.2016.08.007

[7] Z. Yu, J. Tang, T. Khare, V. Kumar, The alarming antimicrobial resistance in ESKAPEE pathogens: Can essential oils come to the rescue?, Fitoterapia, 140 (2020) 104433. https://doi.org/10.1016/j.fitote.2019.104433

[8] U. Anand, N. Jacobo-Herrera, A. Altemimi, N. Lakhssassi, A comprehensive review on medicinal plants as antimicrobial therapeutics: Potential avenues of biocompatible drug discovery, Metabolites 9 (2019) 1–13. https://doi.org/10.3390/metabo9110258

USC UNIVERSIDADE DE SANTIAGO DE COMPOSTELA

[9] M. Raghavan, P. K. Linden, Newer treatment options for skin and soft tissue infections, Drugs 64 (2004) 1621-1642. https://doi.org/10.2165/00003495-200464150-00002

[10] N.A. Turner, B.K. Sharma-Kuinkel, S.A. Maskarinec, E.M. Eichenberger, P.P. Shah, M. Carugati, T.L. Holland, V.G. Fowler Jr, Methicillin-resistant *Staphylococcus aureus*: an overview of basic and clinical research, Nat. Rev. Microbiol. 17 (2019) 203-218. https://doi.org/10.1038/s41579-018-0147-4

[11] S. Santajit, N. Indrawattana, Mechanisms of antimicrobial resistance in ESKAPE pathogens, BioMed Res. Int. 2016 (2016) 2475067. https://doi.org/10.1155/2016/2475067

[12] S. Chouhan, K. Sharma, S. Guleria, Antimicrobial activity of some essential oils—Present status and future perspectives, Medicines, 4 (2017) 58. https://doi.org/10.3390/medicines4030058

[13] M.K. Swamy, M. S. Akhtar, U.R. Sinniah, Antimicrobial properties of plant essential oils against human pathogens and their mode of action: An updated review, Evid. Based Complement. Alternat. Med., 2016 (2016) 3012462. https://doi.org/10.1155/2016/3012462

[14] A. Bernardos, M. Bozik, S. Alvarez, M. Soskova, E. Perez-Esteve, P. Kloucek, M. Lhotka, A. Frankova, R. Martinez-Manez, The efficacy of essential oil components loaded into montmorillonite against *Aspergillus niger* and *Staphylococcus aureus*, Flavour Fragr. J. 34 (2019) 151–162. https://doi.org/10.1002/ffj.3488

[15] P.L. Santos, J.P.S.C.F. Matos, L. Picot, J.R.G.S. Almeida, J.S.S. Quintans, L.J. Quintans-Júnior, Citronellol, a monoterpene alcohol with promising pharmacological activities - A systematic review, Food Chem. Toxicol. 123 (2019) 459–469. https://doi.org/10.1016/j.fct.2018.11.030

[16] B. Melendez-Rodriguez, K.J. Figueroa-Lopez, A. Bernardos, R. Martínez-Máñez, L. Cabedo, S. Torres-Giner, J.M. Lagaron, Electrospun antimicrobial films of poly(3-hydroxybutyrate-co-3-hydroxyvalerate) containing eugenol essential oil encapsulated in mesoporous silica nanoparticles, Nanomaterials 9 (2019) 227. https://doi.org/10.3390/nano9020227

USC DE SANTIAGO DE COMPOSTELA

[17] A. Radisavljevic, D.B. Stojanovic, S. Perisic, V. Djokic, V. Radojevic, M. Rajilic-Stojanovic, P.S. Uskokovic, Cefazolin-loaded polycaprolactone fibers produced via different electrospinning methods: Characterization, drug release and antibacterial effect, Eur. J. Pharm. Sci., 124 (2018) 26–36. https://doi.org/10.1016/j.ejps.2018.08.023

[18] X. Hu, S. Liu, G. Zhou, Y. Huang, Z. Xie, X. Jing, Electrospinning of polymeric nanofibers for drug delivery applications, J. Control. Release, 185 (2014) 12–21. https://doi.org/10.1016/j.jconrel.2014.04.018

[19] N. Bhardwaj, S.C. Kundu, Electrospinning: A fascinating fiber fabrication technique, Biotechnol. Adv., 28 (2010) 325–347. https://doi.org/10.1016/j.biotechadv.2010.01.004

[20] F. Hemmati, A. Bahrami, A.F. Esfanjani, H. Hosseini, D.J. McClements, L. Williams, Electrospun antimicrobial materials: Advanced packaging materials for food applications, Trends Food Sci. Technol. 111 (2021) 520–533. https://doi.org/10.1016/j.tifs.2021.03.014

[21] D. Mondal, M. Griffith, S.S. Venkatraman, Polycaprolactone-based biomaterials for tissue engineering and drug delivery: Current scenario and challenges, Int. J. Polym. Mater., 65 (2016) 255-265. https://doi.org/10.1080/00914037.2015.1103241

[22] G. Narayanan, R. Aguda, M. Hartman, C. Chung, R. Boy, B.S. Gupta, A.E. Tonelli, Fabrication and characterization of poly(ε -caprolactone)/ α-cyclodextrin pseudorotaxane nanofibers, Biomacromolecules 17 (2016) 271–279. https://doi.org/10.1021/acs.biomac.5b01379

[23] F. Topuz, T. Uyar, Electrospinning of cyclodextrin functional nanofibers for drug delivery applications, Pharmaceutics 11 (2019) 6. https://doi.org/10.3390/pharmaceutics11010006

[24] F. Velázquez-Contreras, N. García-Caldera, J.D. Padilla de la Rosa, D. Martínez-Romero, E. Núñez-Delicado, J.A. Gabaldón, Effect of PLA active packaging containing monoterpene-cyclodextrin complexes on berries preservation, Polymers 13 (2021) 1399. https://doi.org/10.3390/polym13091399

[25] G. Narayanan, B.S. Gupta, A.E. Tonelli, Enhanced mechanical properties of poly (ε-caprolactone) nanofibers produced by the addition of non-stoichiometric inclusion

complexes of poly (ε-caprolactone) and α-cyclodextrin, Polymer, 76 (2015), 321-330. https://doi.org/10.1016/j.polymer.2015.08.045

[26] C. Alvarez-lorenzo, C.A. García-González, A. Concheiro, Cyclodextrins as versatile building blocks for regenerative medicine, J Control. Release, 268 (2017) 269–281. https://doi.org/10.1016/j.jconrel.2017.10.038

[27] A. Costoya, A. Concheiro, C.A. Alvarez-Lorenzo, Electrospun fibers of cyclodextrins and poly(cyclodextrins), Molecules, 22 (2017) 230. https://doi.org/10.3390/molecules22020230

[28] M. Dias Antunes, G. da Silva Dannenberg, A.M. Fiorentini, V.Z. Pinto, L.T. Lim, E. da Rosa Zavareze, A.R.G. Dias, Antimicrobial electrospun ultrafine fibers from zein containing eucalyptus essential oil/cyclodextrin inclusion complex, Int. J. Biol. Macromol. 104 (2017) 874–882. https://doi.org/10.1016/j.ijbiomac.2017.06.095

[29] Y. Liu, X. Liang, R. Zhang, W. Lan, W. Qin, Fabrication of electrospun polylactic acid/Cinnamaldehyde/β-cyclodextrin fibers as an antimicrobial wound dressing, Polymers, 9 (2017) 464. https://doi.org/10.3390/polym9100464

[30] Z.I. Yildiz, A. Celebioglu, M.E. Kilic, E. Durgun, T. Uyar, Fast-dissolving carvacrol/cyclodextrin inclusion complex electrospun fibers with enhanced thermal stability, water solubility, and antioxidant activity, J. Mater. Sci. 53 (2018) 15837–15849. https://doi.org/10.1007/s10853-018-2750-1

[31] Z.I. Yildiz, M.E. Kilic, E. Durgun, T. Uyar, Molecular encapsulation of cinnamaldehyde within cyclodextrin inclusion complex electrospun nanofibers: fast-dissolution, enhanced water solubility, high temperature stability, and antibacterial activity of cinnamaldehyde, J. Agricult. Food Chem., 67 (2019) 11066–11076. https://doi.org/10.1021/acs.jafc.9b02789

[32] L. Martins, C.E. dos Santos Cruxen, G. Pinheiro Bruni, A.M. Fiorentini, E. da Rosa Zavareze, L.T. Lim, A.R. Guerra Dias, Development of antimicrobial and antioxidant electrospun soluble potato starch nano fibers loaded with carvacrol, Int. J. Biol. Macromol. 139 (2019) 1182–1190. https://doi.org/10.1016/j.ijbiomac.2019.08.096

[33] A. Nostro, A.R. Blanco, M.A. Cannatelli, V. Enea, G. Flamini, I. Morelli, A.S. Roccaro, V. Alonzo, Susceptibility of methicillin-resistant staphylococci to oregano

essential oil, carvacrol and thymol. FEMS Microbiol. Let., 230 (2004), 191–195. https://doi.org/10.1016/S0378-1097(03)00890-5

[34] J.C. Lopez-Romero, H. González-Ríos, A. Borges, M. Simões, Antibacterial effects and mode of action of selected essential oils components against *Escherichia coli* and *Staphylococcus aureus*, Evid. Based Complement. Alternat. Med. 2015 (2015) 795435. https://doi.org/10.1155/2015/795435

[35] N. Ruwizhi, B.A. Aderibigbe, Cinnamic acid derivatives and their biological efficacy, Int. J. Mol. Sci., 21 (2020) 5712. https://doi.org/10.3390/ijms21165712

[36] J. Malheiro, I. Gomes, A. Borges, M.M.S.M. Bastos, J.Y. Maillard, F. Borges, M. Simões, Phytochemical profiling as a solution to palliate disinfectant limitations, Biofouling 32 (2016) 1007. https://doi.org/10.1080/08927014.2016.1220550

[37] J.F. Malheiro, J.Y. Maillard, F. Borges, M. Simões, Evaluation of cinnamaldehyde and cinnamic acid derivatives in microbial growth control, Int. Biodeterior. Biodegrad., 141 (2019) 71–78. https://doi.org/10.1016/j.ibiod.2018.06.003

[38] M. Ayaz, F. Ullah, A. Sadiq, F. Ullah, M. Ovais, J. Ahmed, H.P. Devkota, Synergistic interactions of phytochemicals with antimicrobial agents: Potential strategy to counteract drug resistance, Chem. Biol. Interact., 308 (2019) 294–303. https://doi.org/10.1016/j.cbi.2019.05.050

[39] I.M. Oliveira, A. Borges, F. Borges, M. Simões, Repurposing ibuprofen to control Staphylococcus aureus biofilms, Eur. J. Med. Chem. 166 (2019) 197–205. https://doi.org/10.1016/j.ejmech.2019.01.046

[40] M.M. Leitão, T.F. Vieira, S.F. Sousa, F. Borges, M. Simões, A. Borges, Dual action of benzaldehydes: Inhibiting quorum sensing and enhancing antibiotic efficacy for controlling *Pseudomonas aeruginosa* biofilms, Microb. Pathog. 2024 Jun;191:106663. doi: 10.1016/j.micpath.2024.106663.

[41] C. Wiegand, T. Heinze, U.C. Hipler, Comparative in vitro study on cytotoxicity, antimicrobial activity, and binding capacity for pathophysiological factors in chronic wounds of alginate and silver-containing alginate, Wound Repair Regen., 17 (2009) 511–521. https://doi.org/10.1111/j.1524-475X.2009.00503.x

USC UNIVERSIDADE DE SANTIAGO DE COMPOSTELA

[42] I.M. Oliveira, A. Borges, F. Borges, M. Simões, Repurposing ibuprofen to control Staphylococcus aureus biofilms, Eur. J. Med. Chem. 166 (2019) 197–205. https://doi.org/10.1016/j.ejmech.2019.01.046

[43] A. Borges, C. Ferreira, M.J. Saavedra, M. Simões, Antibacterial activity and mode of action of ferulic and gallic acids against pathogenic bacteria, Microb. Drug Resist. 19 (2013) 256-265. https://doi.org/10.1089/mdr.2012.0244.

[44] C.J. van Oss, M.K. Chaudhury, R.J. Good, Monopolar surfaces, Adv. Colloid Interfac. 28 (1987) 35–64. https://doi.org/10.1016/0001-8686(87)80008-8

[45] C.J. van Oss, R.J. Good, M.K. Chaudhury, Additive and nonadditive surface tension components and the interpretation of contact angles, Langmuir 4 (1988) 884–891. https://doi.org/10.1021/la00082a018

[46] C.J. van Oss, L. Ju, M.K. Chaudhury, R.J. Good, Estimation of the polar parameters of the surface tension of liquids by contact angle measurements on gels, J. Colloid Interface Sci. 128 (1989) 313–319. https://doi.org/10.1016/0021-9797(89)90345-7

[47] B. Janczuk, E. Chibowski, J.M. Bruque, M.L. Kerkeb, F.G. Caballero, On the consistency of surface free energy components as calculated from contact angles of different liquids: An application to the cholesterol surface, J. Colloid Interface Sci. 159 (1993) 421–428. https://doi.org/10.1006/jcis.1993.1342

[48] A. Contreras-García, E. Bucio, A. Concheiro, C. Alvarez-Lorenzo, Polypropylene grafted with NIPAAm and APMA for creating hemocompatible surfaces that load/elute nalidixic acid, React. Funct. Polym. 70 (2010) 836–842. https://doi.org/10.1016/j.reactfunctpolym.2010.07.019

[49] M.L. Ponce, H.K. Kleinmann, The chick chorioallantoic membrane as an in vivo angiogenesis model, Curr. Protoc. Cell Biol. 19 (2003) 1–6. doi: 10.1002/0471143030.cb1905s1

[50] B. R. Williamson, R. Krishnaswamy, A.E. Tonelli, Physical properties of poly(ε-caprolactone) coalesced from its α-cyclodextrin inclusion compound. Polymer 52 (2011) 4517–4527. https://doi.org/10.1016/j.polymer.2011.07.043

USC UNIVERSIDADE DE SANTIAGO DE COMPOSTELA

[51] C. Abril- Sánchez, A. Matencio, S. Navarro-Orcajada, F. García-Carmona, J.M. López-Nicolás, Evaluation of the properties of the essential oil citronellal nanoencapsulated by cyclodextrins, Chem. Phys. Lipids 219 (2019) 72–78. https://doi.org/10.1016/j.chemphyslip.2019.02.001

[52] M.I. Rodríguez-López, M.T. Mercader-Ros, J.A. Pellicer, V.M. Gómez-López, D. Martínez-Romero, E. Núñez-Delicado, J.A. Gabaldón, Evaluation of monoterpene-cyclodextrin complexes as bacterial growth effective hurdles, Food Control, 108 (2020) 106814. https://doi.org/10.1016/j.foodcont.2019.106814

[53] K.J. Figueroa-Lopez, D. Enescu, S. Torres-Giner, L. Cabedo, M.A. Cerqueira, L. Pastrana, P. Fuciños, J.M. Lagaron, Development of electrospun active films of poly(3-hydroxybutyrate-co-3-hydroxyvalerate) by the incorporation of cyclodextrin inclusion complexes containing oregano essential oil, Food Hydrocolloids, 108 (2020) 106013. https://doi.org/10.1016/j.foodhyd.2020.106013

[54] M.H. Cavanagh, R.E. Burrell, P.L. Nadworny, Evaluating antimicrobial efficacy of new commercially available silver dressings, Int. Wound J. 7 (2010), 394–405. https://doi.org/10.1111/j.1742-481X.2010.00705.x

[55] G. Mancuso, A. Midiri, E. Gerace, C. Biondo, Bacterial Antibiotic Resistance: The Most Critical Pathogens, Pathogens 10 (2021) 1310. https://doi.org/10.3390/pathogens10101310

[56] K.S. Letsididi, Z. Lou, R. Letsididi, K. Mohammed, B.L. Maguy, Antimicrobial and antibiofilm effects of trans-cinnamic acid nanoemulsion and its potential application on lettuce, LWT 94 (2018), 25–32. https://doi.org/10.1016/j.lwt.2018.04.018

[57] M.R. Tapia-Rodriguez, A. Hernandez-Mendoza, G.A. Gonzalez-Aguilar, M.A. Martinez-Tellez, C.M. Martins, J.F. Ayala-Zavala, Carvacrol as potential quorum sensing inhibitor of *Pseudomonas aeruginosa* and biofilm production on stainless steel surfaces, Food Control 75 (2017) 255-261, https://doi.org/10.1016/j.foodcont.2016.12.014.

[58] G. Brackman, M.J. Garcia-Fernandez, J. Lenoir, L. De Meyer, J.P. Remon, T. De Beer, A. Concheiro, C. Alvarez-Lorenzo, T. Coenye, Dressings loaded with cyclodextrin-hamamelitannin complexes increase *Staphylococcus aureus* susceptibility toward antibiotics both in single as well as in mixed biofilm communities, Macromol Biosci. 16 (2016) 859-69. https://doi.org/10.1002/mabi.201500437.

USC DE SANTIAGO DE COMPOSTELA

[59] M. Duplantier, E. Lohou, P. Sonnet, Quorum sensing inhibitors to quench *P. aeruginosa* pathogenicity, Pharmaceuticals 14 (2021) 1262. https://doi.org/10.3390/ph14121262.

[60] Z. Berkl, I. Fekete-Kertész, K. Buda, E. Vaszita, E. Fenyvesi, L. Szente, M. Molnár, effect of cyclodextrins on the biofilm formation capacity of *Pseudomonas aeruginosa* PAO1, Molecules 27 (2022) 3603. https://doi.org/10.3390/molecules27113603.

[61] T.K. Dash, V.B. Konkimalla, Poly-ϵ-caprolactone based formulations for drug delivery and tissue engineering: A review, J. Control. Release 158 (2012) 15-33. https://doi.org/10.1016/j.jconrel.2011.09.064.

[62] M.W. Tackenberg, C. Geisthövel, A. Marmann, H.P. Schuchmann, P. Kleinebudde, M. Thommes, Mechanistic study of carvacrol processing and stabilization as glassy solid solution and microcapsule, Int. J. Pharm., 478 (2015) 597-605. https://doi.org/10.1016/j.ijpharm.2014.12.012

[63] F. Menicucci, E. Palagano, M. Michelozzi, G. Cencetti, A. Raio, A. Bacchi, P.P. Mazzeo, O.A. Cuzman, A. Sidoti, S. Guarino, S. Basile, O. Riccobono, E. Peri, F. Vizza, A. Ienco, Effects of trapped-into-solids volatile organic compounds on paper biodeteriogens, Int. Biodeter. Biodegr. 174 (2022) 105469. https://doi.org/10.1016/j.ibiod.2022.105469.

[64] A.R. Albunia, P. Rizzo, G. Ianniello, C. Rufolo, G. Guerra, Syndiotactic polystyrene films with a cocrystalline phase including carvacrol guest molecules, J. Polym. Sci. Part B: Polym. Phys., 52 (2014) 657-665. https://doi.org/10.1002/polb.23464

[65] G. Narayanan, B.S. Gupta, A. Tonelli, Poly(ε-caprolactone) nanowebs functionalized with α- and γ-cyclodextrins, Biomacromolecules, 15 (2014) 4122–4133. https://doi.org/10.1021/bm501158w

[66] M. Lemos, A. Borges, J. Teodósio, P. Araújo, F. Mergulhão, L. Melo, M. Simões, The effects of ferulic and salicylic acids on *Bacillus cereus* and *Pseudomonas fluorescens* single- and dual-species biofilms, Int. Biodeterior. Biodegradation 86 (2014) 42–51. https://doi.org/10.1016/j.ibiod.2013.06.011

[67] S. López-Miranda, D. Berdejo, E. Pagán, D. García-Gonzalo, R. Pagán, Modified cyclodextrin type and dehydration methods exert a significant effect on the antimicrobial

activity of encapsulated carvacrol and thymol, J. Sci. Food Agric. 101 (2021) 3827-3835. https://doi.org/10.1002/jsfa.11017

[68] D. Ribatti, The chick embryo chorioallantoic membrane (CAM). A multifaceted experimental model, Mech. Dev. 141 (2016) 70-77. https://doi.org/10.1016/j.mod.2016.05.003.

[69] X. Farto-Vaamonde, L. Diaz-Gomez, A. Parga, A. Otero, A. Concheiro, C. Alvarez-Lorenzo, Perimeter and carvacrol-loading regulate angiogenesis and biofilm growth in 3D printed PLA scaffolds, J. Control Release. 352 (2022) 776-792. https://doi.org/10.1016/j.jconrel.2022.10.060

[70] D.Y. Choi, Y.H. Baek, J.E. Huh, J. M. Ko, H.S. Woo, J.D. Lee, D.S. Park, Stimulatory effect of *Cinnamomum cassia* and cinnamic acid on angiogenesis through up-regulation of VEGF and Flk-1/KDR expression, Int. Immunopharmacol. 9 (2009) 959–967.

[71] D. Matluobi, A. Araghi, B.F.A. Maragheh, A. Rezabakhsh, S. Soltani, M. Khaksar, V. Siavashi, A. Feyzi, H.S. Bagheri, R. Rahbarghazi, S. Montazersaheb, Carvacrol promotes angiogenic paracrine potential and endothelial differentiation of human mesenchymal stem cells at low concentrations, Microvasc. Res. 115 (2018) 20–27. https://doi.org/10.1016/j.mvr.2017.08.003

USC UNIVERSIDADE DE SANTIAGO DE COMPOSTELA

USC
UNIVERSIDADE
DE SANTIAGO
DE COMPOSTELA

# IV. DISULFIRAM-LOADED ELECTROSPUN FIBERS WITH ANTIMICROBIAL AND ANTITUMORAL PROPERTIES FOR GLIOBLASTOMA TREATMENT

USC
UNIVERSIDADE DE SANTIAGO DE COMPOSTELA

USC
UNIVERSIDADE
DE SANTIAGO
DE COMPOSTELA

# IV. DISULFIRAM-LOADED ELECTROSPUN FIBERS WITH ANTIMICROBIAL AND ANTITUMORAL PROPERTIES FOR GLIOBLASTOMA TREATMENT

Iago Gonzalez-Prada[1], Arthur Barcelos[2], Marine Dion[2], Beatriz Magariños[3], Clémentine Lapoujade[2], Audrey Rousseau[2,6], Angel Concheiro[1], Emmanuel Garcion[2,4,5,*] and Carmen Alvarez-Lorenzo[1*]

[1]Departamento de Farmacología, Farmacia y Tecnología Farmacéutica, I+D Farma (GI-1645), Facultad de Farmacia, Instituto de Materiales (iMATUS) and Health Research Institute of Santiago de Compostela (IDIS), Universidade de Santiago de Compostela, Spain.

[2]Inserm UMR 1307, CNRS UMR 6075, Université de Nantes, CRCI2NA, Université d'Angers, 49000 Angers, France.

[3]Departamento de Microbiología y Parasitología, Facultad de Biología, CIBUS, Universidade de Santiago de Compostela, Spain.

[4]PACEM (Plateforme d'Analyse Cellulaire et Moléculaire), Université d'Angers, SFR 4208, F-49000, Angers, France.

[5]PRIMEX (Plateforme de Radiobiologie et d'Imageries Expérimentales), Université d'Angers, SFR 4208, F-49000, Angers, France.

[6]Department of Pathology, University Hospital of Angers; F-49000 Angers, France.

This chapter has not been accepted or published yet.

USC UNIVERSIDADE DE SANTIAGO DE COMPOSTELA

**Abstract**

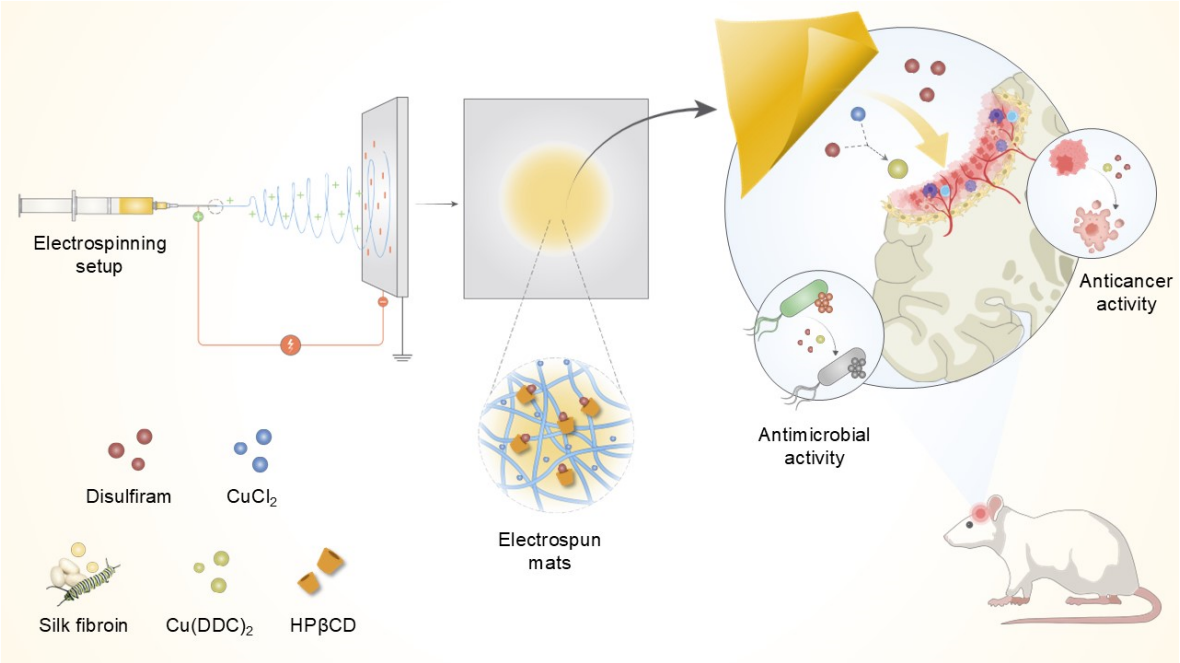
Glioblastoma (GBM) is a malignant tumor brain with one of the worst survival rates and high recurrence ratio owing to scarce and ineffective therapeutic arsenal. The repurposed drug disulfiram (DSF), approved for alcoholism treatment, shows promising anticancer and antimicrobial activity, but its poor biopharmaceutical properties hinder its applications. This work aimed to develop DSF-loaded silk fibroin (SF) fibers suitable for controlled release in the postsurgical resection cavity. Electrospinning was aided by the incorporation of hydroxypropyl-β-cyclodextrin (HPβCD) that formed inclusion complexes with DSF, increasing its release rate and antimicrobial activity (>3 logCFUs reduction) against *Staphylococcus aureus* and *Pseudomonas aeruginosa*. The incorporation of $CuCl_2$ to in situ form $Cu(DDC)_2$ complexes reinforced the antimicrobial and antitumoral effects of the fibers, which could be obtained in nanometric size (≤ 500 nm) while maintaining adequate mechanical properties. Selective toxicity of DSF and DSF-loaded fibers against glioblastoma cells, while sparing against astrocytes, was found highlighting the potential of the nanofibers loaded with DSF and its complex with Cu(II) as a targeted therapy for brain cancer. Increased potency of DSF at low concentrations when combined with SF fibers, HPβCD and copper was remarkable. These findings suggest that DSF delivery and bioavailability can be significantly optimized through electrospun nanofibers, which may also allow for more precise dosing. Combination with radiotherapy was also explored to assess the translational potential of DSF as part of a combination therapy regimen for glioblastoma. In vivo safety of selected formulations was confirmed in a complete normal brain rat model mimicking GBM surgery.

**Keywords**

Glioblastoma; disulfiram; silk fibroin; cyclodextrin; copper, electrospinning

USC
UNIVERSIDADE DE SANTIAGO DE COMPOSTELA

## Graphical abstract




USC UNIVERSIDADE DE SANTIAGO DE COMPOSTELA

## 4.1 INTRODUCTION

Glioblastoma multiforme (GBM) is a highly aggressive and lethal brain tumor characterized by a poor prognosis owing to its location, fast progression, and noteworthy invasive nature throughout the Central Nervous System [1]. Globally, approximately 49% of all primary brain tumors are GBMs and its incidence tends to increase with age, mainly affecting adults between 45 and 75 years of age. The current standard treatment for GBM consists of surgical resection to reduce the tumour mass effect followed by radiation and chemotherapy with temozolomide [2]. Different chemotherapeutic agents (*i.e.,* lomustine, carmustine, nimustine and, and regorafenib), immunotherapy (*i.e*., bevaciuzumab), and anti-mitotic therapies that generates Tumor Treating Fields (TTFields) (*i.e.* Optune™, previously known as the NovoTTF-100A System™) are explored as new treatment options. Despite the numerous investigations on GBM diagnosis and treatment, the overall 5-year survival remains at 9.8% due to multiple factors, including cellular heterogeneity, protection by the blood-brain barrier, dissemination capacity through neighboring tumor structures, and intrinsic resistance of the mesenchymal glioblastoma stem cells, also known as tumor-initiating cells [3]. Additionally, therapeutic alternatives usually come with high associated costs, present a poor treatment compliance, and have risks of neurologic deficits and severe side effects like suppression of bone marrow, hepatotoxicity, nephrotoxicity, necrosis, neurotoxicity, hematologic toxicity, and skin toxicity [4]. The intracranial local implant Gliadel® (carmustine wafer) approved by FDA for recurrent GBM has demonstrated an improvement in median of overall survival and progression-free survival of 2 months, supposing a quality-adjusted life years (QALY) of only 0.107 (5.6 weeks) [5] while it has remarkable limitations associated to the difficulty in handling, interferences with imaging (MRI), lack of wound healing, high probably of meningitis and oedema apparition, and short time therapy (6-8 weeks) leading a progressive clinical use reduction [6].

Considering the high attrition rates, substantial costs, and slow progress of the discovery and development of new therapeutic strategies, drug repurposing has emerged as an attractive alternative. Basically, drug repurposing (also referred as drug repositioning, reprofiling or re‑tasking) is an approach for identifying new uses for already approved or investigational drugs that are outside the scope of the original clinical indication [7]. Disulfiram is a good illustration of a drug repositioning opportunity that might offer an effective treatment for GBM therapy [8, 9].

USC DE SANTIAGO DE COMPOSTELA

Disulfiram (DSF) was approved by the Food and Drug Administration (FDA) in 1951 to treat chronic alcohol dependency (Antabuse®) by acting as an inhibitor on aldehyde dehydrogenase isoform-1A3 (ALDH1A3) [9]. Several preclinical and clinical studies have suggested that DSF could have potent anticancer properties against several types of cancer, including GBM. Although the mechanisms behind the cytotoxic effect of DSF on cancer cells remain not completely elucidated, the results obtained so far revealed an important versatile anticancer activity. As a divalent metal ion chelator, DFS can strongly chelate Cu(II) highly expressed in cancer cells to form a copper-DSF complex (Cu(II) bis(diethyldithiocarbamate); $Cu(DDC)_2$) that downregulates several copper-dependent signaling pathways responsible for DNA reparation and promotes reactive oxygen species (ROS) toxicity, resulting in a reduction of cancer cell viability by apoptosis induction [10-12]. This mechanism allows a targeted antitumoral activity, since cancer cells exhibit higher levels of intracellular Cu (2-3-fold) compared with healthy cells (e.g., the content in Cu of normal brain is 5.37 μg/g whilst malignant glioma tissue has 22.69 μg/g) [13]. Additionally, DSF may act as a proteasome inhibitor [14]. More specifically, DSF alone or in combination with Cu(II) targets nuclear protein localization protein 4 (NPL4), thus leading to their aggregation. Consequently, the p97-dependent protein turnover pathway is inactivated, followed by the induction of the unfolded protein response (UPR) causing an accumulation of misfolded proteins, endoplasmic reticulum stress and apoptosis [15-17]. $Cu(DCC)_2$ inhibits permanently the activity of P-gp efflux pump and its expression levels [18,19]. In parallel, DSF may be useful against drug-resistant cancer cells since it has demonstrated an inhibitory activity over the activation of the nuclear factor-κB (NF-κB) [20]. Also, DSF has cytotoxic activity over cancer stem cells that overexpresses several markers and transcription factors including aldehyde dehydrogenases (ALDHs), Sox2, Nanog and Oct3/4, which are targeted and inhibited by DSF [16]. DSF might also suppress cancer progression by inhibiting the proteolytic matrix metalloproteinases-2 [21], which regulates the migration and invasion features of cancer cells. Concomitant administration of DSF and temozolomide can cause synergistic effects, decreasing cell proliferation and self-renewal and successfully overcoming drug resistance [16]. Overall, DSF can be considered a multifunctional chemotherapeutic agent with a pronounced capacity to regulate cancer cell growth, differentiation, spontaneous metastasis, and drug resistance, all of which are vital to the development and progression of cancer.

USC DE COMPOSTELA

Apart from this important anticancer activity, DSF also presents anti-inflammatory and antibacterial properties. More specifically, DSF has revealed a strong activity against Gram-positive bacteria *Staphylococcus aureus (*MIC ranging from 0.37 to 64 μg/mL) and a slight activity against the Gram-negative bacteria *Pseudomonas aeruginosa (*MIC around 512 μg/mL) [22]. These properties may be particularly useful to prevent and control infections after surgical tumor resections in patients with GBM [23]. Collectively, the antitumor, antibacterial, and anti-inflammatory activities of DSF, make this drug one of the strongest ones to be repositioned to clinical GBM treatment. However, DSF is a biopharmaceutical classification system (BCS) class II drug (i.e., low solubility and high permeability) and its clinical applications in GBM treatment are limited by its lipophilicity (logP 4.16), poor water solubility (0.2 mg/mL), physiological instability, and short plasma half-life (*ca.* 7 h) [24,25]. Consequently, systemic administration demands high doses of free DSF (*ca.* 500-1000 mg once daily) or in combination with temozolomide (*ca.* 500 mg once daily) [17] to guarantee the desired therapeutic effect, but this causes marked hepatotoxicity, neurotoxicity, and low patient compliance, which urges the development of local delivery devices [26]. Moreover, the extremely low solubility of $Cu(DDC)_2$ (0.1-0.2 μg/mL, 50-fold more hydrophobic respect to DSF) and readily formation of aggregates makes practically impossible its systemic administration [18, 27].

The development of post-operative electrospun mats as locally implantable treatment for GBM is particularly appealing compared to conventional chemotherapy. The insertion of electrospun mats inside the tumor resection cavity would be negligibly invasive since surgery is part of the standard of care of patients with GBM. Electrospun fiber mats are highly versatile regarding drug (including DSF) entrapment efficiency and physical properties, provide high surface-to-volume ratio and porosity to promote drug release, and can be easily adapted to any space [28, 29]. Thereby, tumor-implanted electrospun mats avoid the blood-brain barrier crossing, increase cancer-targeted drug bioavailability, reduce systemic exposition, can mimic the native GBM extracellular matrix, and allow the concomitant administration of drugs with synergistic activities [29-31].

USC DE SANTIAGO DE COMPOSTELA

Considering all these aspects, this work was aimed to obtain an electrospun scaffold that can provide antitumoral and antimicrobial effects for recurrent GBM patients, using the repurposed drug DSF and its complex with copper, $Cu(DCC)_2$. Silk

fibroin (SF) was selected as main structural polymer of the fibers, HPβCD as encapsulating agent, and $CuCl_2$ as an adjuvant molecule. SF transition from α-helix to ß-sheet conformation communicates robust mechanical strength and toughness to a variety of scaffolds [32]. Notably, SF is a promising candidate for clinical use after GBM resection surgery, since it displays intrinsic bioactivities such as anti-inflammatory, hemostatic, neuroprotective, restorative neurological, and regenerative nerve process activities [33-35]. By forming inclusion complexes, HPβCD imparts stability and notably increases DSF apparent solubility [36]. HPβCD also displays neuroprotective and anticancer effects by forming complexes with fatty acids and cholesterol, mitigates the inflammatory effect response of immune cells, and reduces the production of interleukins (IL-10) and cytokines (TNF-α) [37]. Indeed, HPβCD has been approved as an orphan drug for the treatment of focal segment glomerulosis and the Niemann pick disease type C [38]. Combination of CDs and electrospinnable polymers may result in important synergies such as enhanced tensile strength, facilitated wetting of the mats, favored erosion or dissolution of the fibers, and most importantly a high encapsulation efficiency [39-41].

Some ongoing GBM clinical trials involve the administration of DSF and Cu(II) in separate and by different vias [19, 42] and result in the non-targeted exposition of the patient to high blood levels of both components (with toxic effects) for short periods of time (short have-life). As a relevant innovative approach, the developed electrospun fibers could function as local depots of both DSF and Cu(II) facilitating in situ formation of DSF-copper complex where it is needed. The DSF-loaded electrospun mats were produced by electrospinning and characterized using a wide range of analytical techniques including FTIR and SEM, contact angle measurements, and mechanical tests. After the structural characterization, hemocompatibility, and antimicrobial performance against relevant bacteria were investigated. Selective antitumoral activity against GBM was assessed using glioblastoma cell lines from murine (GL261) and human (U-87MG) origin, human glioblastoma astrocytoma cells (U-251MG) and also non-tumor fibroblasts (NIH/3T3) and non-tumor primary astrocytes. The use of Cu(II) in combination with DSF could be an attractive approach to increase the anticancer activity and reduce the amount of drug, leveraging the chelator activity of DSF for several organometallics, namely zinc, iron, and copper. $CuCl_2$ was chosen as a source of Cu(II) since both elements (Cu and Cl) are naturally present in human body [43]. Likewise, Cu is involved in different normal

USC UNIVERSIDADE DE SANTIAGO

homeostasis brain and neuronal process, including DNA regulation, cofactor of myriad enzymatic reactions, redox regulation, mitochondrial respiration, antioxidant defense, neural firing, cellular metabolism, and synaptic plasticity [44, 45]. Thus, the lack of this ion promotes the apparition of severe neurodegenerative disease (i.e., amyotrophic lateral sclerosis, Alzheimer, Huntington, and Parkinson disease). Moreover, brain has considerable tolerance at great amounts of copper (up to 125 μg/g dry weight) owing to the presence of astrocytes that recollect and store the copper to protect and supply the nervous system [46, 47]. Furthermore, Cu(II) could be an useful organometallic for scaffold due to the antimicrobial properties, decreasing the occurrence of infection and promoting vessel formation through the secretion of VEGF, angiogenin (hAmg), and fibroblast grow factor 1 (FGF1), IL-1, and IL-8 [48, 49]. The addition of Cu(II) in the electrospun fibers may allow increasing its intratumor concentration to easily generate high levels of $Cu(DDC)_2$, improving the effectiveness of the therapy and reducing inter-cancer and inter-patient differences, offering an alternative to intravenously injected DSF-loaded targeted nanoparticles [50].

## 4.2 MATERIALS AND METHODS

### 4.2.1 Materials

Fresh silk fibroin solution 7% (w/v) was supplied by IMIDA (Murcia, Spain). It was stored at -80ºC for 4 h and then freeze-dried for 48 h (LyoQuest, Telstar; Barcelona, Spain). 1,1,1,3,3,3-Hexafluoro-2-propanol (HFIP) was purchased from Acros (Waltham, MA, USA). Hydroxypropyl-β-cyclodextrin (HPβCD) was obtained from Roquette (Lestrem, France). Disulfiram (tetraethylthiuram disulfide), sodium diethyldithiocarbamate (DDC), Triton X-100, sodium dodecyl sulfate 95%, Dulbecco′s Modified Eagle′s Medium - high glucose (D6429), Dulbecco′s Phosphate Buffered Saline (D8537), Trypsin-EDTA solution (T3929), Antibiotic Antimycotic Solution (A5955), Fetal Bovine Serum (CVFSVF00-01), copper(II) chloride dihydrate (C3279), resazurin sodium salt (R7017), Giemsa stain (GS500), and dimethyl sulfoxide (DMSO, 41639) were purchased from Sigma-Aldrich (Steinheim, Germany). L-glutamine were provided by BioWhittaker (Verviers, Belgium). Dimethylformamide (DMF) and copper chloride (II) anhydride were provided by Thermo Fisher Scientific (Waltham, MA, USA). Phosphate-buffered saline (PBS) pH 7.4, 6.5, and 5.5 media were prepared as indicated in the European Pharmacopoeia 6$^{th}$ edition. For pH 7.4, 8 g/L NaCl, 2.38 g/L $Na_2HPO_4$

and 0.19 g/L $KH_2PO_4$ were mixed in ultrapure water. Acetonitrile and ethanol were provided by VWR Chemicals (Leuven, Belgium). Ultrapure water (resistivity>18.2 MΩ cm; Milli-Q®, Millipore Ibérica, Madrid, Spain) was obtained by reverse osmosis.

$Cu(DDC)_2$ was synthesized as previously reported [51] by mixing $CuCl_2$ (0.04 g in 500 mL water) and DDC (0.134 g in 500 mL water) under gentle agitation overnight. The obtained solid brown precipitate was filtered, washed with ultrapure water and recrystallized with pure ethanol (> 99%) to eliminate impurities and unreacted products. The final product was dried under vacuum and subsequently analyzed by FTIR (**Figure 4.1.**) to confirm $Cu(DDC)_2$ complex formation.

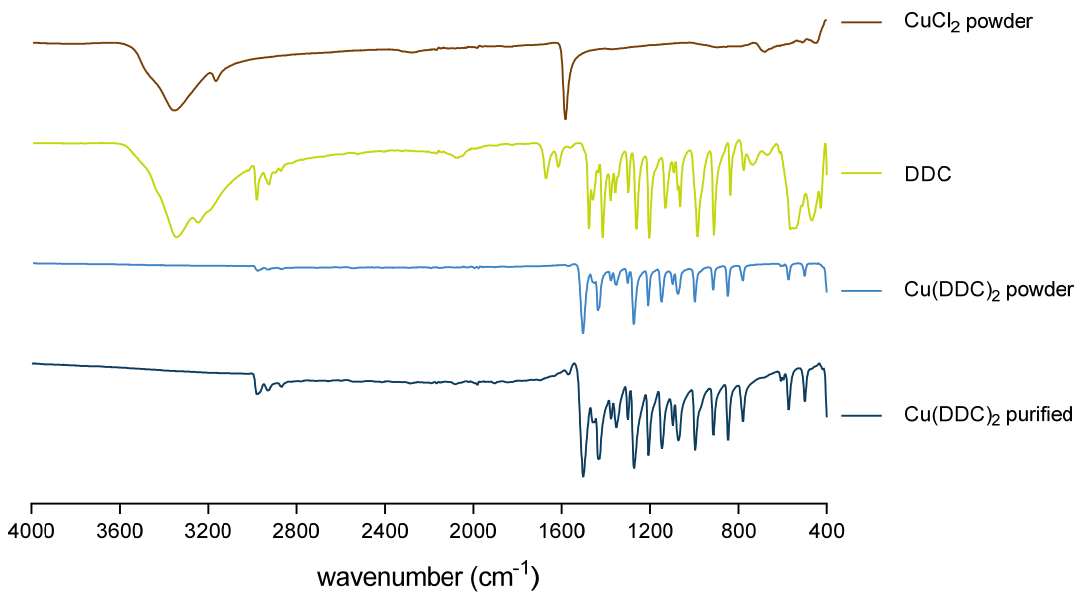



**Figure 4.1. FTIR spectra of $CuCl_2$ powder, DDC powder, synthetized $Cu(DDC)_2$, and synthetized $Cu(DDC)_2$ after purification in ethanol scanned in the region of 4000 $cm^{-1}$ to 400 $cm^{-1}$.**

### 4.2.2 Preparation of polymeric solution and electrospinning

Freeze-dried SF 12.5% (w/v) was dissolved in HFIP at 40 ºC under gentle agitation for 48 h and the solution was transferred to a syringe for the electrospinning. Disulfiram 0.5% and 5.0% (w/v) was added to some solutions and kept under stirring overnight before the electrospinning.

SF 12.5% (w/v) HPβCD 10% (w/v) fibers were prepared in two steps. Firstly, 1 g of freeze-dried SF was dissolved in 4 mL of HFIP at 40 ºC under gentle agitation for 12 h. In parallel, 0.8 g of HPβCD was dissolved in 4 mL of HFIP at room temperature under strong agitation overnight. Then, both solutions were mixed under gentle agitation

USC UNIVERSIDADE DE SANTIAGO DE COMPOSTELA

overnight. Finally, to prepare SF 12.5% (w/v) HPβCD 10% (w/v) disulfiram 0.5-5.0% (w/v) fibers disulfiram was added to the HPβCD solution to prepare the inclusion complex.

SF 6% (w/v) $CuCl_2$ 0.045% (w/v) fibers were prepared in two steps. Firstly, 0.5 g of freeze-dried SF was dissolved in 3.6 mL of HFIP at 40ºC under gentle agitation for 5 h. Meanwhile, 0.004 g of $CuCl_2$ was dissolved in 0.4 mL of DMF by strong agitation using a vortex for 1 minute, after that, the same volume of HFIP was added. Then, both solutions were mixed under strong agitation at 40 ºC drop by drop. To prepare the fibers with DSF at 0.5% and 5%, 0.05 g and 0.5 g were added to the previously homogeneous solution and mixed under gentle agitation overnight.

SF 5% (w/v) HPβCD 0.51-2.6% (w/v) $CuCl_2$ 0.045% (w/v) fibers were prepared in three steps. Firstly, 0.4 g of freeze-dried SF was dissolved in 2.6 mL of HFIP at 40ºC under gentle agitation for 5 h. Secondly, 0.004 g of $CuCl_2$ was dissolved in 0.4 mL of DMF by strong agitation using a vortex for 1 minute, after that, the same volume of HFIP was added. Then, both solutions were mixed under strong agitation at 40ºC drop by drop. Thirdly, HPβCD (0.51 g or 2.6 g) was dissolved in 1 mL of HFIP at room temperature for 2 h. DSF (0.05 g or 0.5 g) was added to the HPβCD solution at room temperature and kept under gentle agitation during 8 h. Finaly, this solution was incorporated to the aforementioned SF-$CuCl_2$ solution and kept under gentle agitation overnight.

A climate-controlled Yflow® Professional Electrospinning Machine (Yflow® S.D., Málaga, Spain) was used for fibers preparation. A series of experiments were carried out varying the electrospinning parameters to optimize the process. The applied voltages ranged between 10 and 15 kV, the collection distance was set at 15-25 cm, and the feeding rate was 1.0-2.0 mL/h. Composition and electrospinning condition for each fiber are summarized in **Table 4.1** and **Table 4.2.**, respectively.

**Table 4.1. Composition of the electrospun fibers expressed per gram of solid material.**

| Fiber type (w/v) | SF (mg) | HPβCD (mg) | DSF (mg) | Cu (mg) |
|---|---|---|---|---|
| SF (12.5%) | 1000 | | | |
| SF (12.5%) DSF (0.5%) | 962 | | 38 | |
| SF (12.5%) DSF (5%) | 714 | | 286 | |
| SF (12.5%) HPβCD (10%) | 556 | | 444 | |

USC UNIVERSIDADE DE SANTIAGO DE COMPOSTELA

| | | | | |
|---|---|---|---|---|
| SF (12.5%) HPβCD (2.6%) DSF (0.5%) | 801 | 167 | 32 | |
| SF (12.5%) HPβCD (10%) DSF (5%) | 455 | 364 | 182 | |
| SF (6%) $CuCl_2$ (0.045%) | 993 | | | 7 |
| SF (6%) DSF (0.1%) $CuCl_2$ (0.045%) | 976 | | 16 | 3.4 |
| SF (6%) DSF (0.5%) $CuCl_2$ (0.045%) | 917 | | 76 | 3.2 |
| SF (5%) HPβCD (0.51%) DSF (0.1%) $CuCl_2$ (0.045%) | 884 | 90 | 18 | 3.7 |
| SF (5%) HPβCD (2.6%) DSF (0.5%) $CuCl_2$ (0.045%) | 614 | 319 | 61 | 2.6 |

**Table 4.2. Electrospinning parameters for the manufacture of electrospun fibers. Nozzle-tip-collector distance was in all cases 25 cm.**

| Fiber type (w/v) | Solvent | Voltage (Kv) | Flow rate (mL/h) | Temperature (ºC) | Humidity (%) | Size (µm) |
|---|---|---|---|---|---|---|
| SF (12.5%) | HFIP | +8.75<br>-3.44 | 2 | 23.80 | 38.73 | 1.51 ± 0.42 |
| SF (12.5%)<br>HPβCD (10%) | HFIP | +8.58<br>-3.38 | 2 | 23.60 | 49.29 | 1.11 ± 0.22 |
| SF (12.5%)<br>DSF (0.5%) | HFIP | +8.92<br>-3.93 | 2 | 20.10 | 57.58 | 2.59 ± 0.67 |
| SF (12.5%)<br>DSF(5%) | HFIP | +9.10<br>-3.44 | 2 | 24.10 | 31.53 | 1.79 ± 0.37 |
| SF (12.5%)<br>HPβCD (2.6%)<br>DSF (0.5%) | HFIP | +7.61<br>-4.12 | 2 | 19.70 | 59.49 | 3.06 ± 0.76 |
| SF (12.5%)<br>HPβCD (10%)<br>DSF (5%) | HFIP | +8.58<br>-3.38 | 2 | 23.60 | 43.78 | 1.57 ± 0.3 |
| SF (12.5%)<br>$CuCl_2$ (0.045%) | HFIP :<br>DMF<br>(90:10) | +11.98<br>-2.84 | 1 | 21.70 | 52.92 | 0.41 ± 0.16 |
| SF (12.5%)<br>HPβCD (2.6%)<br>$CuCl_2$ (0.045%) | HFIP :<br>DMF<br>(90:10) | +7.12<br>-2.76 | 1 | 23.70 | 50.65 | 0.63 ± 0.21 |

USC UNIVERSIDADE DE SANTIAGO

| | | | | | | |
|---|---|---|---|---|---|---|
| SF (12.5%)<br>DSF (0.1%)<br>$CuCl_2$ (0.045%) | HFIP : DMF (90:10) | +9.89<br>-2.39 | 1 | 21.20 | 54.83 | 0.25 ± 0.08 |
| SF (12.5%)<br>DSF (0.5%)<br>$CuCl_2$ (0.045%) | HFIP : DMF (90:10) | +10.44<br>-2.39 | 1 | 22.30 | 58.17 | 0.44 ± 0.2 |
| SF (12.5%)<br>HPβCD (0.51%)<br>DSF (0.1%)<br>$CuCl_2$ (0.045%) | HFIP : DMF (90:10) | +12.37<br>-2.25 | 1 | 18.40 | 51.59 | 0.17 ± 0.06 |
| SF (12.5%)<br>HPβCD (2.6%)<br>DSF (0.5%)<br>$CuCl_2$ (0.045%) | HFIP : DMF (90:10) | +12.10<br>-2.25 | 1 | 22.50 | 50.20 | 0.19 ± 0.07 |

### 4.2.3 Fibers characterization

Electrospun mats were coated by sputtering gold under argon (Sputter Coater (Ou) - QUORUM Q150T-S) and observed using a ZEISS FESEM ULTRA Plus (Carl Zeiss, Oberkochen, Germany). The average diameter was determined using the ImageJ image analysis software.

Mechanical properties were analyzed, in triplicate, using a TA.XT plus Texture Analyzer (Stable Micro Systems, Surrey, UK) equipped with a 30 Kgf (~294 N) load cell under a crosshead speed of 10 mm/min. The fibers were cut as square pieces of 2.0 cm x 2.0 cm. The Young's modulus was determined as the slope of the linear (elastic) region of the stress-strain curve. Tensile strength and elongation at break (%) were also calculated.

The hydrophobicity of the fibers was determined from the contact angle of water, formamide and 1-bromonafthalene using an OCA 15 Plus equipment (Dataphysics Instruments, Germany), plugged with a videocamera for image acquisition and later data analysis. Pieces of the fibers (1 cm x 6 cm) were glued to a glass slide with double-sided tape, and 6 to 10 measurements were made at room temperature (23 ± 2 ºC) following a previously described protocol [41].

### 4.2.4 In vitro release study

USC UNIVERSIDADE DE SANTIAGO DE COMPOSTELA

SF mats containing disulfiram (1$cm^2$ square, average weight 0.035 g) were immersed in 2-10 mL of PBS (pH 7.4, 6.5, and 5.5) and incubated at 100 rpm and 37 °C

in a continuous shaker. At predetermined time points, 200 µL of solution was removed, filtered (Scharlau® Syringe Filter, 0.22 µm 13 mm HPPTFE), and replaced with 200 µL of fresh PBS. The release profile was determined using HPLC (AS-4140 autosampler, PU-4180 pump, LC-NetII/ADC interface box, CO-4060 column oven, MD-4010 photodiode array detector, JASCO, Tokyo, Japan) fitted with a C18 column (Waters Symmetry C18, 5 µm, 4.6 × 250 mm) and operated with ChromNAV software v.2. The mobile phase was acetonitrile:water 70:30 (v/v) over 9 min. The sample injection volume was 10 µL and the eluent was pumped at flow rate of 1 mL/min for 9 min. DSF was detected at 3.43 min at a wavelength of 217 nm (**Figure 4.2.**) and $Cu(DCC)_2$ was detected at 6.74 min at a wavelength of 432 nm (**Figure 4.4.**). The detection limit (LOD) and the quantification limit (LOQ) were determined to be 0.622 ppm and 1.882 ppm for DSF, and 0.088 ppm and 0.266 ppm for $Cu(DCC)_2$, respectively (**Figures 4.3 and 4.5**). The experiments were conducted in triplicate.

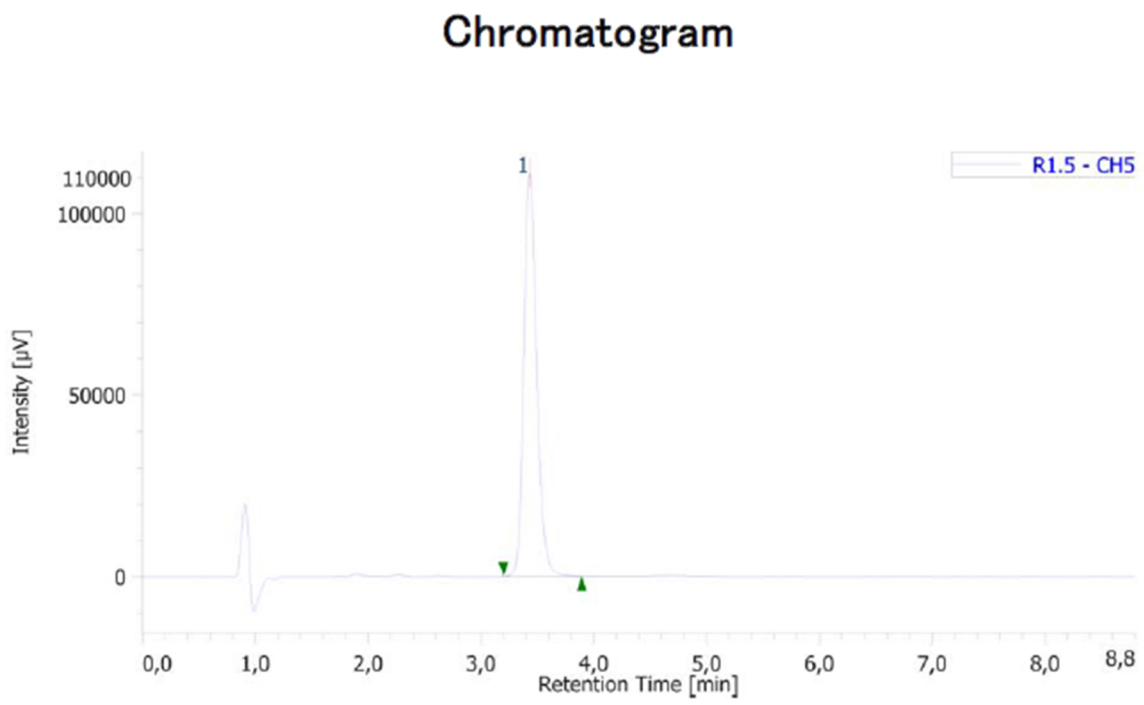



**Figure 4.2. HPLC chromatogram profile of 25 ppm of DSF dissolved in acetonitrile.**

USC UNIVERSIDADE DE SANTIAGO DE COMPOSTELA

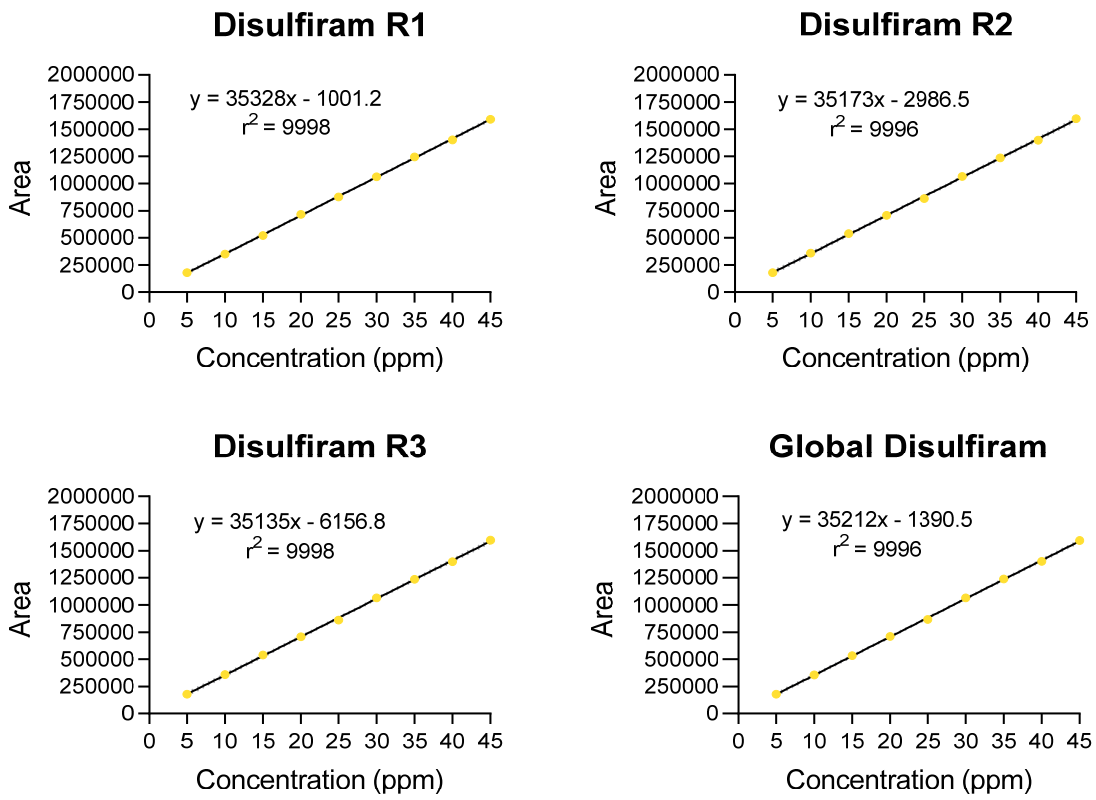



**Figure 4.3. Calibration curves of DSF determined by HPLC method.**

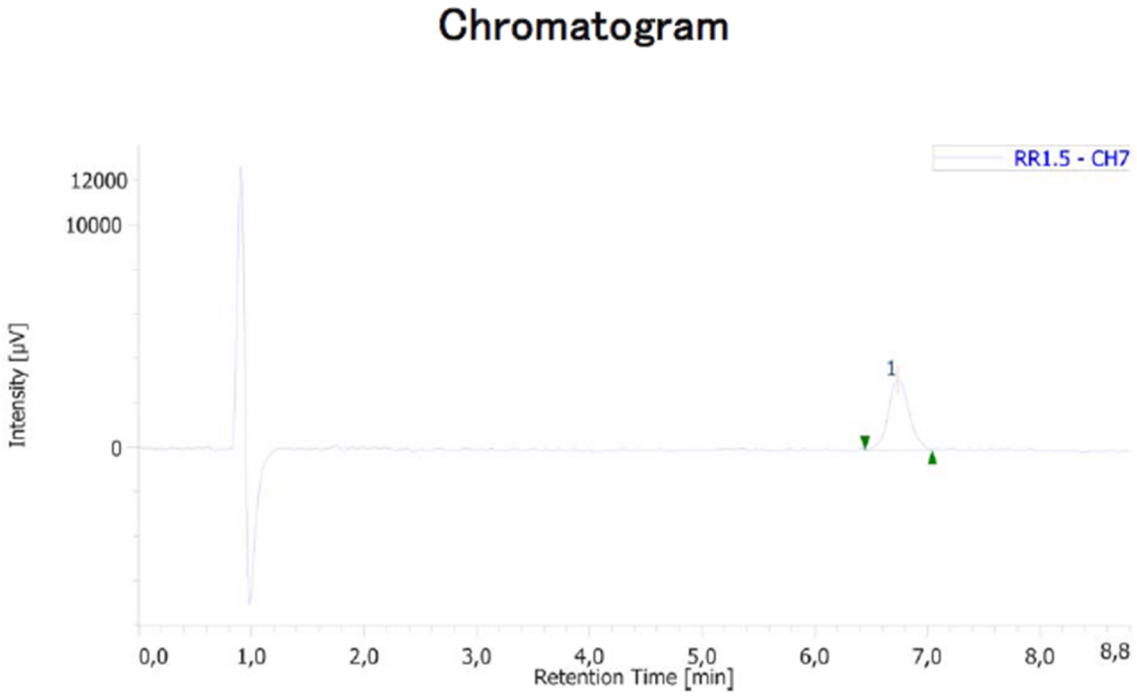



**Figure 4.4. HPLC chromatogram profile of 2.5 ppm of $Cu(DDC)_2$ dissolved in acetonitrile.**

USC UNIVERSIDADE DE SANTIAGO DE COMPOSTELA

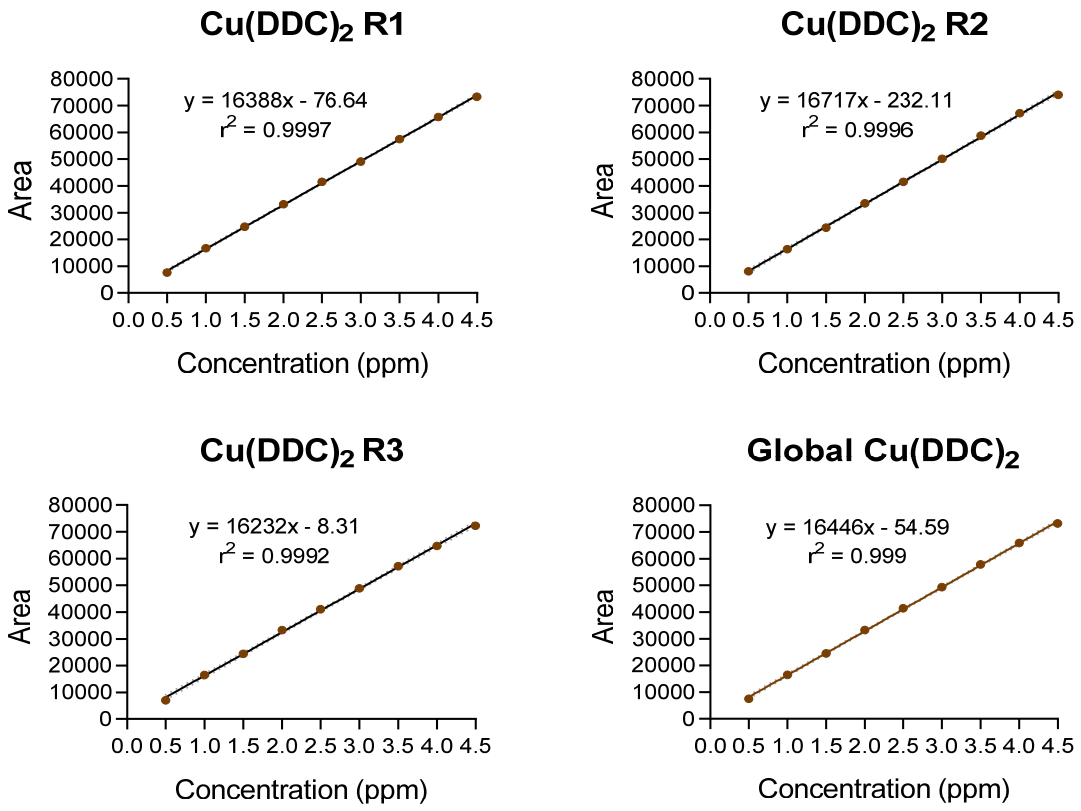



**Figure 4.5. Calibration curves of $Cu(DDC)_2$ determined by HPLC method.**

### 4.2.5 Blood compatibility

A 2.5 % (v/v) blood solution stock was prepared by diluting 5 mL of total blood provided by Galician Transfusion Center (ADOS) previously anticoagulated with EDTA in 200 mL of PBS (pH 7.4). SF mats (1 $cm^2$ square pieces) were immersed in 5 mL of 2.5 % (v/v) blood solution stock and incubated at 37 °C for 2 h under shaking. After that, the falcon tubes were centrifuged at 2,400 g for 10 min. Then, 150 µL of supernatant was taken and placed in a 96 well plate. The hemolytic activity was calculated as a function of the released hemoglobin which was measured by recording absorbance of the supernatant ($Abs_{sample}$) using a UV–visible microplate reader (Fluostar Optima, BMG Labtech, Germany) at 510 nm. Triton X-100 4% (v/v) solution was used as the positive control (PC) (100% lysis) and PBS (7.4) was added to blood stock solution and used as the negative control (NC). The hemolysis percentage was calculated using **Equation 4.1.**:

$$\% \text{ Hemolysis} = \frac{(Abs_{sample} - Abs_{NC})}{(Abs_{PC} - Abs_{NC})} \times 100 \qquad (4.1.)$$

USC UNIVERSIDADE DE SANTIAGO DE COMPOSTELA

### 4.2.6 Antimicrobial activity

#### 4.2.6.1. Bacterial strains and growth media

The antibacterial activity of the different SF electrospun mats were evaluated against *Staphylococcus aureus* (ATCC 25923) and *Pseudomonas aeruginosa* (CECT 110). All microbial strains were preserved at – 80ºC in cryovial and 30% glycerol and subcultured in trypticase soy agar (TSA) for *S. aureus* and Luria-Bertani´s lysogenic agar (LB) at 37ºC during 12 h before testing.

#### 4.2.6.2. Antimicrobial test

The method was based on the American Society for Testing and Materials (ASTM E-2149) standard. Briefly, the bacteria inoculum was prepared by aseptically transferring isolated colonies to 40 mL of trypticase soy agar (TSA) nutrient broth for *S. aureus* and 40 mL of Luria-Bertani´s lysogenic broth (LB) for *P. aeruginosa*, and then incubated for 12 h at 37 °C. After that, the inoculum was diluted at $OD_{620\ nm}$ of 0.04 ± 0.02 (corresponding to a concentration of ~$1\times10^8$ cells/mL; [41]). Electrospun mat pieces (1 $cm^2$; ≈ 0.35 mg) were sterilized under UV light for 15 min per side, placed in a sterile 24 well-plate with 2 mL microorganism suspension and incubated for 24 h at 37 ºC under slightly stirring (100 rpm). After that contact time, 100 µL of microorganism suspension of each sample was taken and added to 900 µL of PBS in an Eppendorf. Then, seven dilution factors 1:9 (v/v) were performed. For each dilution factor, 10 µL were spread on nutrient agar plates and incubated at 37 ºC for 24 h. Then, the viable colonies were counted, and results were expressed in log CFU/mL using **Equation 4.2** [52]:

$$\frac{CFU}{mL} = \frac{N}{SV \times Dilution} \qquad (4.2.)$$

where N is the number of CFU and SV is the volume of the sample in mL. The logarithmic reduction values were calculated according to **Equation 4.3** [52]:

$$\log reduction = \log CFU/mL_{control} - \log CFU/mL_{sample} \qquad (4.3.)$$

where the controls were SF 12.5% and SF 12.5% HPβCD 10% (without DSF) fibers, and the designation “sample” refers to fibers containing disulfiram.

USC UNIVERSIDADE DE SANTIAGO DE COMPOSTELA

Four replicate experiments were performed for each sample, testing two replicates in different weeks, and the growth reduction was evaluated according to the Japanese

Industrial Standard, as no antimicrobial activity (<0.5 log reduction), slight antimicrobial activity (0.5 to 1 log reduction), significant antimicrobial activity (1 to 3 log reduction) and strong antimicrobial activity (>3 log reduction) [53].

### 4.2.7 In Vitro test

#### 4.2.7.1 Cells and culture conditions

Non-tumor murine fibroblasts NIH/3T3 (CRL-1658™) and human glioblastoma cell line U-87MG (HTB-14 ™) were acquired from ATCC (Rockville, Maryland, USA). The murine glioblastoma cell line GL261 (RRID: CVCL_Y003) was kindly provided by Corinne Griguer and G. Yancey Gillespie of the University of Alabama at Birmingham, AL, USA. Human glioblastoma astrocytoma cell line U-251MG was a gift from C. Griguer and originally obtained from Dr. D.D. Bigner (Duke University, Durham, NC, USA). Cell lines were cultivated in Dulbecco's Modified Eagle's Medium - high glucose, supplemented with 10% fetal bovine serum and 1% antibiotic antimycotic solution. Cultures were maintained at 37°C in a 5% $CO_2$ environment. Purified newborn mice primary astrocytes were obtained by the mechanical dissociation method from cultures of cerebral cortex as originally described [54]. The cells were grown at 37 ºC/5% $CO_2$ in DMEM with glucose and L-glutamine containing 10% fetal bovine serum and 1% antibiotic antimycotic solution.

#### 4.2.7.2 Cytotoxicity assessment of DSF

The assessment of DSF cytotoxic potential, in association with 1 µM of $Cu^{2+}$, was conducted using the resazurin colorimetric assay based on the reduction of the oxidized blue dye by living cells into a pink, fluorescent resorufin product. For experimentation, $2.5x10^4$ (24 h) and $1.5x10^4$ cells (48 h) were seeded into 24-well plates and incubated at 37ºC in a 5% $CO_2$ atmosphere. DSF was initially dissolved in DMSO and subsequently diluted in complete medium. Concentrations ranging from 0.03 to 1 µM were tested. Control wells, consisting of negative (untreated), solvent (DMSO - 0.0297%), copper (1 µM), and positive (DMSO - 25%) controls, were included. Following a 24 or 48-h incubation period with DSF at 37ºC in a 5% $CO_2$ environment, the culture medium was aspirated to remove treatments before exposure to resazurin (44 µM). Microplates were then incubated at 37ºC in a 5% $CO_2$ environment for 2 h. Fluorescence intensity was measured using a multi-plate reader (CLARIOstar® Plus) with excitation at 544 nm (545-

USC UNIVERSIDADE DE SANTIAGO

20) and emission at 590 nm (600-40). Non-linear regression analysis was performed using GraphPad Prism to determine the sample concentration that inhibits 50% of cell viability ($IC_{50}$, half maximal inhibitory concentration).

4.2.7.3 Clonogenic Assay

The antiproliferative potential of DSF in combination with 1 μM of $Cu^{2+}$ was assessed using the clonogenic efficiency assay [55]. The exposure time and treatment concentrations were determined based on prior cytotoxicity assays. U-87MG, U-251MG, and GL261 cell suspensions were seeded into 6-well plates at a density of 300 cells per well. After allowing the cells to adhere during a 2-h incubation at 36.5°C in 5% $CO_2$, the cell lines were treated with varying concentrations of DSF (0.025 - 0.30 μM) in association with 1 μM of $Cu^{2+}$. Following 24 h of treatment, the culture medium was removed, and the cells were washed with PBS to eliminate any remaining treatment. The cells were then incubated to allow for at least six cell division cycles. After this incubation period, the colonies were washed with PBS, fixed with PFA 4%, and stained with Giemsa stain for 20 minutes. Finally, the colonies were counted, and the survival fraction was calculated according to the formula provided by Franken et al. [55].

4.2.7.4 Cytotoxicity assessment of DSF combined with beam radiation

The evaluation of cytotoxic potential of DSF-fibers in combination with irradiation was also performed using the resazurin colorimetric assay. For this experimentation, the test was conducted on the mouse primary astrocytes, and on cell lines NIH3T3 and GL261, seeded at a density of $1x10^4$ cells/mL in 24-well plates. After 24 h of incubation at 37ºC in a 5% $CO_2$ atmosphere the cells were exposed to different concentrations of DSF (dissolved in DMSO and diluted in complete medium) ranging from 0.03 μM to 0.12 μM. Control wells, consisting of negative (untreated), solvent (DMSO - 0.0297%), copper (1 μM), and positive (DMSO - 25%) controls, were included. Following a 24-hour incubation period with DSF at 37ºC in a 5% $CO_2$ environment, the culture medium was aspirated to remove treatments and replaced by fresh medium before an exposition to irradiation at 16GY (CP-160 cabinet X-ray system Faxitron, Edimex, Le Plessis Grammoire, Angers, France). After 48-h incubation, the cells were exposed to resazurin (44 μM), and microplates were incubated at 37ºC in a 5% $CO_2$ environment for 2 h. Fluorescence intensity was measured using a multi-plate reader (CLARIOstar® Plus) with excitation at 544 nm (545-20) and emission at 590 nm (600-40). Non-linear

USC DE COMPOSTELA

regression analysis was performed using GraphPad Prism to determine the sample concentration that inhibits 50% of cell viability ($IC_{50}$, half maximal inhibitory concentration).

4.2.7.5 Cytotoxicity assessment of DSF nanofibers

Cells were seeded at a density of $5x10^4$ cells/mL in 24-well plates and incubated for 24 h at 37ºC in a 5% $CO_2$ atmosphere. Subsequently, the cells were exposed to electrospun fiber pieces (4.91 mm², ≈ 0.20 mg) immerged in 1 mL of complete medium and further incubated at 37 °C for 24 h. Control wells encompassed negative controls (untreated), SF 12.5%, SF 6% $CuCl_2$ 0.045%, SF 6% HPβCD 2.6% $CuCl_2$ 0.045% solutions, and positive (DMSO - 25%) controls. Test wells contained SF 12.5% DSF 5% fibers, SF 12.5% DSF 0.5% fibers, SF 12.5% HPβCD 2.6% DSF 0.5% fibers, SF 6% DSF 0.5% $CuCl_2$ 0.045% fibers, SF 6% DSF 0.1% $CuCl_2$ 0.045% fibers, SF 5% HPβCD 2.6% DSF 0.5% $CuCl_2$ 0.045% fibers, and SF 5% HPβCD 0.51% DSF 0.1% $CuCl_2$ 0.045% fibers. Following a 24-h incubation at 37ºC, the culture medium was aspirated to remove treatments before exposure to resazurin (44 µM). Microplates were then incubated at 37ºC in a 5% $CO_2$ environment for 2 h. Fluorescence intensity was measured using a multi-plate reader (CLARIOstar® Plus) with excitation at 544 nm (545-20) and emission at 590 nm (600-40). Non-linear regression analysis was performed using GraphPad Prism to determine the effect of fibers on cell viability.

### 4.2.8 Evaluation of the toxicity of fibers In Vivo

4.2.8.1 Animals

15 Fisher female rats aged 9-11 weeks were obtained from Janvier Labs (Le Genest-Saint-Isle, France). The protocol was approved by the Ethical Committee for Animal Experimentation of Pays de la Loire region, France (authorization number APAFIS # 43915-2020032620074335). A minimum acclimatization period of one week was conducted before beginning the experiments. Rats were provided with *ad libitum* access to tap water and food. In this work, each rat represents an independent experimental unit.

4.2.8.2 Implantation of fibers

USC UNIVERSIDADE DE SANTIAGO

Two types of fibers were chosen to evaluate the toxicity in a complete normal brain: SF 12.5% HPβCD 2.6% DSF 0.5% fibers, and SF 5% HPβCD 2.6% DSF 0.5% $CuCl_2$

0.045% fibers. These fibers were first cut using a biopsy punch of 3 mm in diameter and sterilized under UV light for 15 min per side. Fisher rats were divided into three groups: a control group with 5 rats which undergo the surgery without receiving the fiber, a first treated group of 4 rats that received the fiber without cupper (one rat did not survive during the procedure) and a second treated group of 5 rats that received the fiber with cupper. Rats were anesthetized intraperitoneally with ketamine (0.8 mL/kg) and xylazine (0.62 mL/kg) and positioned in a Kopf stereotaxic instrument. A 10 mm incision was made along the midline to expose the surface of the skull. Subsequently, rats' skulls were pierced with a burr (Microtorque II) following these coordinates from the bregma (=0 mm): lateral: −2.9 mm, anteroposterior: +1 mm. A hole approximately 3 mm in diameter was created to allow a biopsy punch to access the cortex. The brain tissue was carefully cut and removed using vacuum suction, forming a cavity about 2 mm deep. One piece of fiber was gently placed into the cavity, the skull was then closed using bone wax and the wound was sutured. The rats were kept under observation for a week before euthanasia.

4.2.8.3 Histology and anatomocytopathology

After euthanasia, the brains were collected and subsequently fixed in 4% formaldehyde for around 10 days, followed by paraffin embedding. Afterward, 5 µm thick sections were obtained using an HM340E Microm Microtech microtome (France) and stained with hematoxylin and eosin (HE) for analysis. Several histopathological parameters were considered to assess the impact of fiber implantation on the brain such as multinucleated giant cells, acute inflammatory cells, necrosis, chronic inflammatory cells, neoangiogenesis, hemorrhage, hemosiderin deposition, and mineralization. Histopathological analyses were carried out at the Department of Cellular and Tissue Pathology of the University Hospital Center of Angers (CHU-Angers, France). The slides were scanned using an Aperio system

### 4.2.9 Statistical Analysis

Statistical analysis was performed using SPSS v.26.0 (IBM Co., Armonk, NY, USA). All results were expressed as mean ± standard deviation. Statistical analyses of the antimicrobial and antioxidant results (one-way ANOVA) were conducted, followed by the post hoc Tukey HSD multiple comparison test. Previously statistical analysis normality of all variables was evaluated using Kolmogorov-Smirnov test for groups ($n \geq 50$) and Shapiro–Wilk test for groups ($n \leq 50$). A confidence interval was used at least

USC DE COMPOSTELA

95%, to define statistical significance (* $p < 0.05$, ** $p < 0.005$, *** $p < 0.001$ and **** $p < 0.0001$).

## 4.3 Results and discussion

### 4.3.1 Fibers preparation and morphological and mechanical analysis

Preliminary studies were carried out to evaluate the effect of SF concentration (10% to 20% (w/v) range) on the spinnability and morphology of electrospun fibers (**Figure 4.6.)**. All SF solutions tested were electrospun under the same experimental conditions, but only SF 12.5% solution maintained an adequate Taylor cone for hours showing good properties for spinnability. SF fibers displayed continuous, smooth, homogeneous fibers without noticeable beads (**Figure 4.6.A**).

USC UNIVERSIDADE DE SANTIAGO DE COMPOSTELA

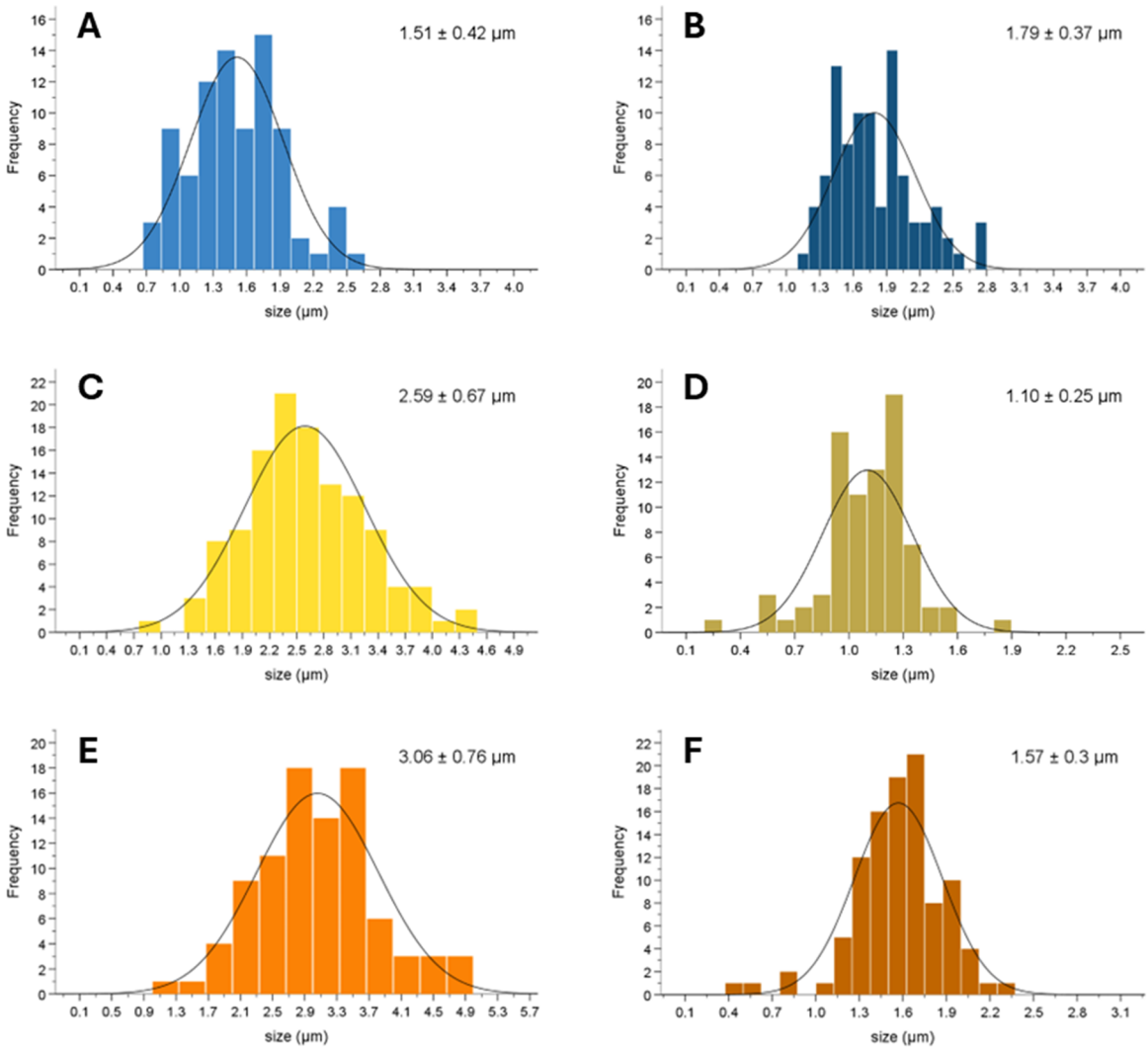



**Figure 4.6 Diameter distribution of fibers (n=200) measured in SEM micrographs of fibers made from solutions in HFIP of (A) SF 12.5% (w/v); (B) SF 12.5% (w/v) HPβCD 10% (w/v); (C) SF 12.5% (w/v) DSF 0.5% (w/v); (D) SF 12.5% (w/v) disulfiram 5% (w/v); (E) SF 12.5% (w/v) HPβCD 10% (w/v) DSF 0.5% (w/v); and (F) SF 12.5% (w/v) HPβCD 10% (w/v) disulfiram 5% (w/v).**

USC UNIVERSIDADE DE SANTIAGO DE COMPOSTELA

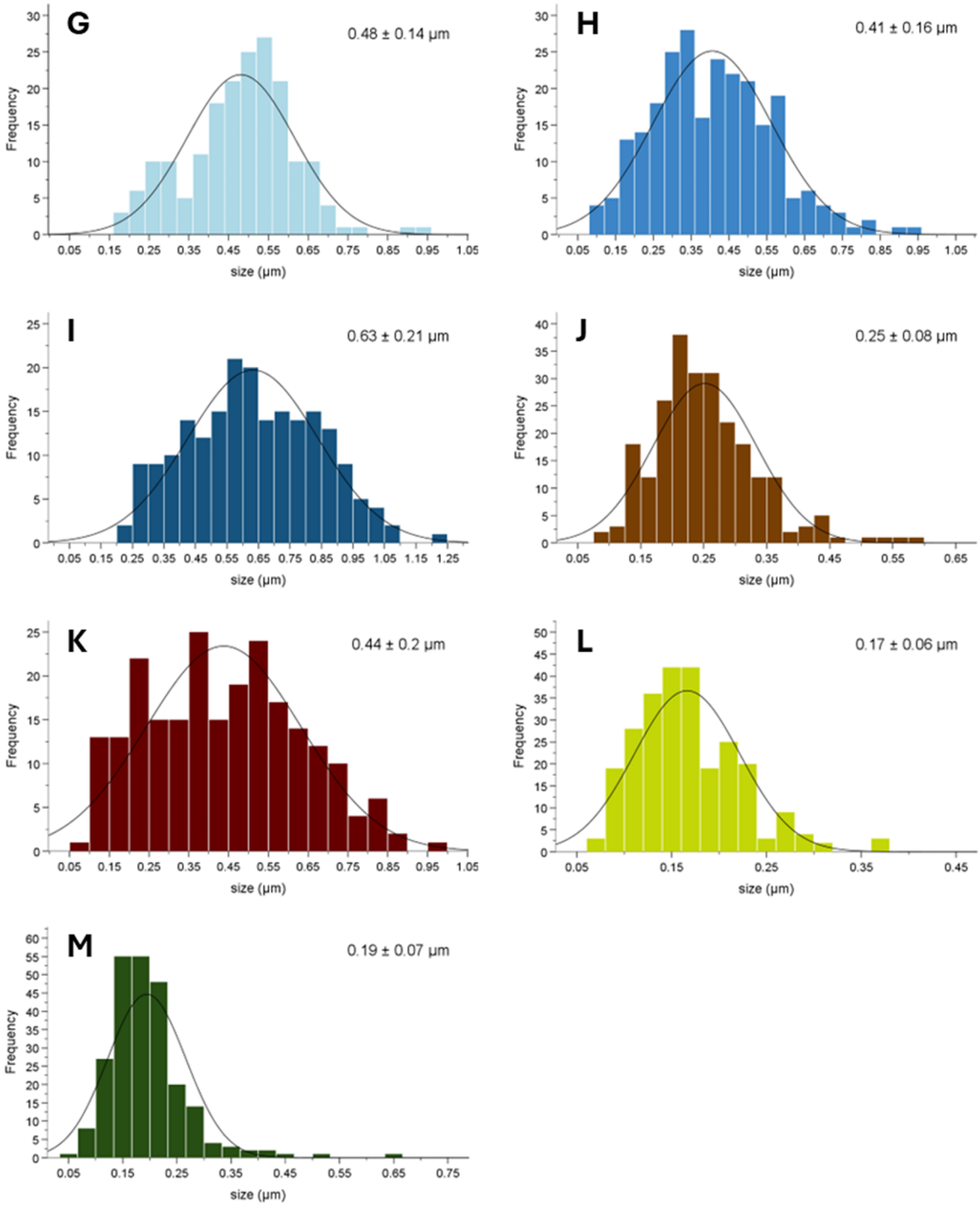



**Figure 4.6 (continuation). Diameter distribution of fibers (n=200) measured in SEM micrographs of fibers made from solutions in HFIP of (G) SF 4% (w/v) $CuCl_2$ 0.45% (w/v); (H) SF 6% (w/v) $CuCl_2$ 0.045% (w/v); (I) SF 6% (w/v) HPβCD 2.6% (w/v) $CuCl_2$ 0.045% (w/v); (J) SF 6% (w/v) $CuCl_2$ 0.045% (w/v) DSF 0.1% (w/v); (K) SF 6% (w/v) $CuCl_2$ 0.045% (w/v) DSF 0.5% (w/v); (L) SF 6% (w/v) HPβCD 2.6% (w/v) DSF 0.1% (w/v) $CuCl_2$ 0.045% (w/v); and (M) SF 6% (w/v) HPβCD 2.6% (w/v) DSF 0.5% (w/v) $CuCl_2$ 0.045% (w/v).**

USC UNIVERSIDADE DE SANTIAGO DE COMPOSTELA

Once SF concentration was fixed, the effect of HPβCD concentration was investigated. For the aim of this work, DSF concentration was chosen to be 0.5 or 5.0% (w/v). To encapsulate a large amount of drug (5.0% (w/v)), 20% (w/v) of HPβCD may be required if a 1:1 complex is considered [36, 56]. Unfortunately, the properties of SF solution were notably altered. The Taylor cone was unstable even many different parameters were attempted to be adjusted, and many drops were collected in the aluminum foil. Thus, HPβCD concentration had to be reduced to 10% (w/v) to obtain homogeneous electrospun fibers of SF 12.5% (w/v) HPβCD 10% (w/v) using the same parameters as for 12.5% (w/v) SF fibers (**Figure 4.7.B**).

Incorporation of disulfiram did not alter the electrospinnability, and electrospun fibers were obtained for SF 12.5% (w/v) DSF 0.5-5.0% (w/v) fibers, although the fiber diameter distribution was wider in the case of disulfiram 0.5% (**Figure 4.7.C**) compared to 5.0% (**Figure 4.7.D**). The drug was successfully encapsulated, and no disulfiram crystals were found lengthwise the fibers in the SEM images either.

As expected, the inclusion complex between HPβCD (10% w/v) and disulfiram (5% w/v) did not change the electrospun parameters (**Table 4.1.**). Overall, all fiber compositions provided continuous, smooth, homogeneous fibers without noticeable beads (**Figure 4.7.E-F.**). SF 12.5 % (w/v) fibers had a diameter of 1.51 ± 0.42 μm whereas SF 12.5% (w/v) HPβCD 10% (w/v) electrospun fiber diameter was 1.79 ± 0.37 μm (**Figure 4.7.N**). Therefore, no statistically significant differences were observed. The addition of disulfiram at 5% (w/v) to SF 12.5% (w/v) caused a minor decrease in the diameter of the fibers, 1.11 ± 0.22 μm. Differently, the addition of disulfiram to HPβCD solutions did not decrease the size of the fibers, reaching 1.57 ± 0.3 μm.

USC
UNIVERSIDADE DE SANTIAGO DE COMPOSTELA

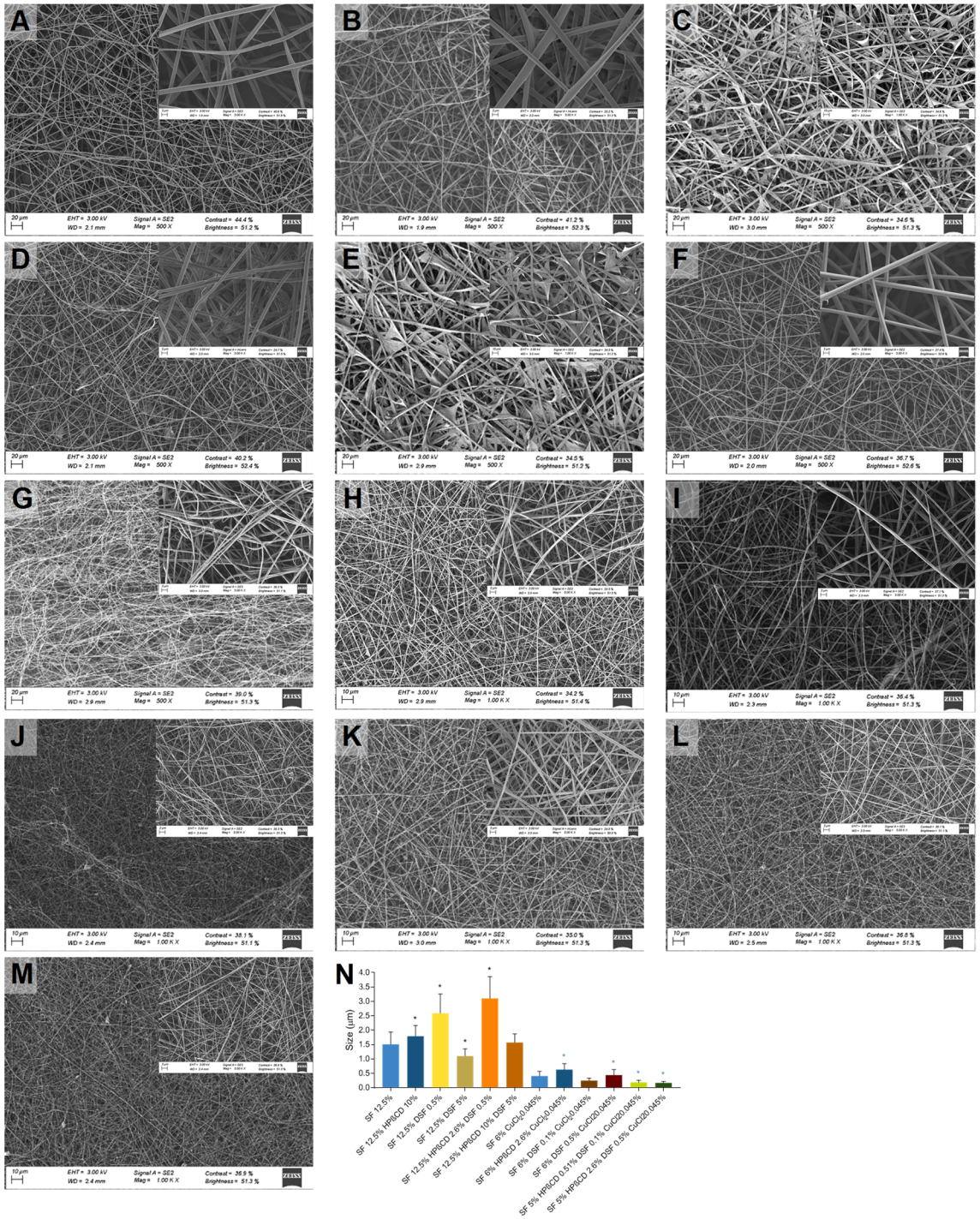



**Figure 4.7. SEM micrographs of fibers made from solutions in HFIP of (A) SF 12.5% (w/v); (B) SF 12.5% (w/v) HPβCD 10% (w/v); (C) SF 12.5% (w/v) DSF 0.5% (w/v); (D) SF 12.5% (w/v) DSF 5% (w/v); (E) SF 12.5% (w/v) HPβCD 2.6% (w/v) DSF 0.5% (w/v); (F) SF 12.5% (w/v) HPβCD 10% (w/v) DSF 5% (w/v); (G) SF 4% (w/v) $CuCl_2$ 0.45% (w/v); (H) SF 6% (w/v) $CuCl_2$ 0.045% (w/v); (I) SF 6% (w/v) HPβCD 2.6% (w/v) $CuCl_2$ 0.045% (w/v); (J) SF 6% (w/v) DSF 0.1% (w/v) $CuCl_2$ 0.045% (w/v); (K) SF 6% (w/v) DSF 0.5% (w/v) $CuCl_2$ 0.045% (w/v); (L) SF 6% (w/v) HPβCD 0.51% (w/v) DSF 0.1% (w/v) $CuCl_2$ 0.045% (w/v); and (M) SF 6% (w/v) HPβCD 2.6% (w/v) DSF 0.5% (w/v) $CuCl_2$ 0.045% (w/v); and (N) mean size and standard deviations (n=200) of fibers diameters.**

USC UNIVERSIDADE DE SANTIAGO DE COMPOSTELA

To reinforce the antitumor effect, $CuCl_2$ was added to the solutions to be electrospun. The incorporation of $CuCl_2$ at 0.045% (w/v) in the SF 6.0 % (w/v) solution was challenging due to its insolubility in solvents commonly used for dissolving and stabilizing silk fibroin in β-sheet conformation (i.e., formic acid and HFIP). DMF was selected as the most suitable solvent owing to its capacity to readily dissolve $CuCl_2$ at 0.45% (w/v) without inducing precipitation of SF at 4.0% (w/v) in HFIP at ratio of 10% (v/v). Indeed, homogeneous, continuous, smooth, and without beads fibers was obtained from this polymeric solution (**Figure 4.7.G**). The concentration of SF had to be decreased from 12.5 % (w/v) to 6.0 % (w/v) to avoid precipitation in the presence of $CuCl_2$ at 0.045% (w/v). This phenomenon was due to the interaction of Cu(II) ions with SF amino acid residues of histidine and tryptophan through coordination with both N and O atoms. Some authors reported that Cu(II) can chelate SF chains forming cross-linking networks. Moreover, metal ions change the conformation from helical conformation to β-sheet in several proteins including SF [57].

The reduction in SF concentration decreased the diameter of the fibers (reaching nano scale) and improved the morphology changing form ribbon structure to cylinder structure. Thus, SF 6% (w/v) $CuCl_2$ 0.045% (w/v) fibers were homogeneous, continuous, smooth and without undesired beads (**Figure 4.7.H**). The incorporation of HPβCD at 2.6% (w/v) and DSF at different concentrations 0.1- 0.5% (w/v) did not cause further changes (**Figure 4.7.I,J,K**). Nevertheless, SF 6% (w/v) HPβCD at 2.6% (w/v) $CuCl_2$ 0.045% (w/v) showed a slightly increase in the size fiber 0.63 ± 0.21 μm, if compared with SF 6% (w/v) $CuCl_2$ 0.045% (w/v) displaying a 0.41 ± 0.16 μm. As expected, SF 6% (w/v) DSF 0.1% (w/v) $CuCl_2$ 0.045% produced thinner fibers (0.25 ± 0.08 μm) than SF 6% (w/v) DSF 0.5% (w/v) $CuCl_2$ 0.045% (0.44 ± 0.20 μm). Smaller fibers were obtained with a further decrease in SF concentration to 5% (w/v) and incorporating HPβCD 0.51% (w/v) DSF 0.1% (w/v) $CuCl_2$ 0.045% (w/v) or HPβCD at 2.6% (w/v) DSF 0.5% (w/v) $CuCl_2$ 0.045% (w/v). Both fibers displayed diameters of 0.17 ± 0.10 μm and 0.19± 0.10 μm respectively, maintaining the same characteristics and morphology as the other SF mats (**Figure 4.7.L,M)**.

USC UNIVERSIDADE DE SANTIAGO DE COMPOSTELA

### 4.3.2 Mechanical, spectroscopical and hydrophobic properties of the fibers

SF 12.5% fibers showed high Young's modulus and tensile strength (**Table 4.3.)** due to its high content in SF in β-sheet conformation [58]. Addition of $CuCl_2$ notably reinforced the mechanical properties of the fibers despite the decrease in SF concentration. Differently, incorporation of HPβCD and DSF caused a weakening in the mechanical properties due to their intercalation between SF beta chains, suggesting an intermolecular disruption. Nevertheless, even the weaker mats had mechanical properties similarly to those of pure PCL electrospun mats [41] and ensured correct application in the resection cavity.

**Table 4.3 Mechanical properties of SF fibers and $CuCl_2$ - SF fibers prepared with different contents in HPβCD, and DSF.**

| Fiber type | Young's modulus (MPa) | Tensile strength (MPa) | Elongation at break (%) |
|---|---|---|---|
| **SF (12.5%)** | 7632 | 133.9 | 2.88 |
| **SF (12.5%) HPβCD (10%)** | 1079 | 26.20 | 1.55 |
| **SF (12.5%) DSF (0.5%)** | 2763 | 91.36 | 2.93 |
| **SF (12.5%) DSF (5%)** | 723 | 37.03 | 25.64 |
| **SF (12.5%) HPβCD (2.6%) DSF (0.5%)** | 301 | 18.72 | 6.53 |
| **SF (12.5%) HPβCD (10%) DSF (5%)** | 312 | 8.83 | 2.72 |
| **SF (6%) $CuCl_2$ (0.045%)** | 2807 | 101.14 | 5.87 |
| **SF (6%) HPβCD (2.6%) $CuCl_2$ (0.045%)** | 137 | 9.44 | 6.04 |
| **SF (6%) DSF (0.1%) $CuCl_2$ (0.045%)** | 3695 | 78.18 | 3.98 |
| **SF (6%) DSF (0.5%) $CuCl_2$ (0.045%)** | 83 | 25.66 | 9.91 |
| **SF (5%) HPβCD (0.51%) DSF (0.1%) $CuCl_2$ (0.045%)** | 4505 | 178.81 | 4.72 |
| **SF (5%) HPβCD (2.6%) DSF (0.5%) $CuCl_2$ (0.045%)** | 69 | 12.33 | 5.19 |

The presence of SF, HPβCD and disulfiram in the fibers was checked by comparing the FTIR spectra (**Figure 4.8.)**. The characteristic peaks of SF appeared at 1242 $cm^{-1}$ (C–N stretching vibration of amide III),1526 $cm^{-1}$ (N–H bending vibration and C–N stretching vibration of amide II), and 1631 $cm^{-1}$ (C–O stretching vibration of amide 1) assigned with numbers 3,5 and 6 in **Figure 4.8.**). These three bands indicated that SF was in ß-sheet conformation (silk II) [29]. Typical bands of HPβCD at 1027 $cm^{-1}$ (C−O bending) and 1152 $cm^{-1}$ (C−O bending/stretching) (assigned with numbers 1 and 2 in **Figure 4.8.**) were evident in all fibers containing HPβCD. The fibers that incorporated DSF showed a

characteristic peak at 1496 $cm^{-1}$, assigned to C–H symmetrical deformation vibrations [22]. No other relevant bands were detected.

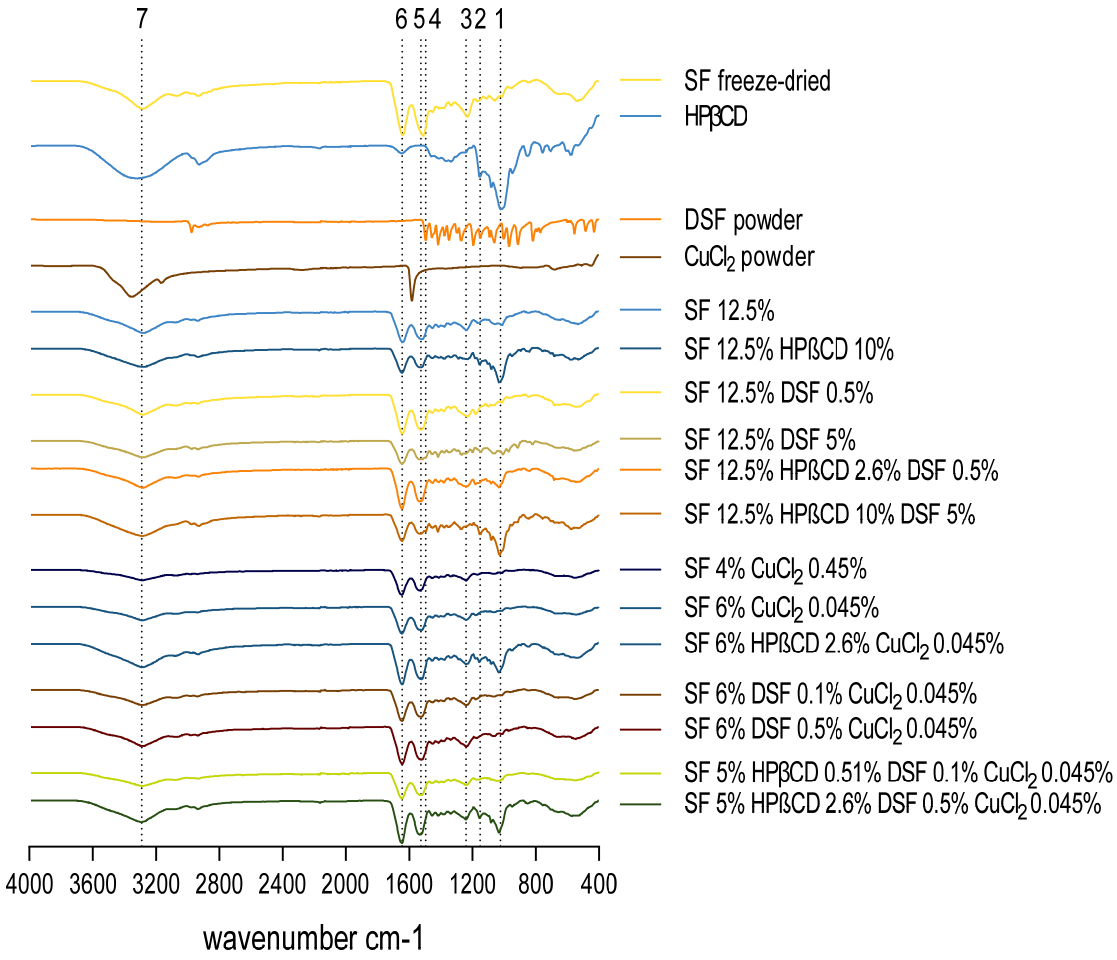



**Figure 4.8. FTIR spectra of freeze-dried SF, HPβCD powder, DSF powder, and of fibers prepared with SF 12.5% (w/v); SF 12.5% (w/v) HPβCD 10% (w/v); SF 12.5% (w/v) DSF 0.5% (w/v); SF 12.5% (w/v) DSF 5% (w/v); SF 12.5% (w/v) HPβCD 2.6% (w/v) DSF 0.5% (w/v); SF 12.5% (w/v) HPβCD 10% (w/v) DSF 5% (w/v); SF 4% (w/v) $CuCl_2$ 0.45% (w/v); SF 6% (w/v) $CuCl_2$ 0.045% (w/v); SF 6% (w/v) HPβCD 2.6% (w/v) $CuCl_2$ 0.045% (w/v); SF 6% (w/v) DSF 0.1% (w/v) $CuCl_2$ 0.045% (w/v); SF 6% (w/v) DSF 0.5% (w/v) $CuCl_2$ 0.045% (w/v); SF 6% (w/v) HPβCD 0.51% (w/v) DSF 0.1% (w/v) $CuCl_2$ 0.045% (w/v); and SF 6% (w/v) HPβCD 2.6% (w/v) DSF 0.5% (w/v) $CuCl_2$ 0.045% (w/v) in the region of 4000 $cm^{-1}$ to 400 $cm^{-1}$.**

Surface polarity of the fibers was calculated from the measurements of contact angle of water, formamide and 1-bromonafthalene. Apolar, polar and hydrophobic components of the surface tension are summarized in **Table 4.3.**. The two first

components were evaluated using the Lifshitz-van de Waals component $\gamma^{LW}$ and the Lewis acid-base component $\gamma^{AB}$. All fibers displayed a nonpolar component ( $\gamma^{LW}$) close to 40 mJ/m$^2$ in good agreement with the fact of that the main structural component is a biopolymer [59]. The polar surface tension component ( $\gamma^{AB}$) was calculated from the electron donor component ($\gamma^-$) and the electron acceptor component ($\gamma^+$) as reported previously [41]. The fibers with high contents in DSF showed high values of $\gamma^+$ due to the presence of electron-accepting ternary amide groups, whilst the fibers with high amounts of HPβCD displayed high values of $\gamma^-$ owing to the presence of electron-donor OH groups.

SF fibers with or without $CuCl_2$ showed $\Delta G^{TOT} < 0$ mJ/m$^2$, indicating that the prepared fibers had a hydrophobic surface owing to hydrophobic character of SF β-sheet, and the addition of the Cu(II) did not change the surface polarity. Differently, $\Delta G^{TOT} > 0$ mJ/m$^2$ values were recorded for fibers incorporating HPβCD. Such an increase in hydrophilicity may promote cell migration while hindering bacterial adhesion [60]. Thereby, these hydrophilic electrospun mats could stimulate and promote tissue whilst avoiding nosocomial infections.

**Table 4.3**. Contact angle of SF fibers and $CuCl_2$ – SF fibers with or without HPβCD loaded with DSF using water, bromonaphthalene and formamide at 23 ± 2ºC.

| Fiber type | Surface tension parameters (mJ/m$^2$) | | | | $\Delta G^{TOT}$ (mJ/m$^2$) | Picture | | |
|---|---|---|---|---|---|---|---|---|
| | $\gamma^{LW}$ | $\gamma^{AB}$ | $\gamma^+$ | $\gamma^-$ | | Water | Bromo-naphthalene | Formamide |
| SF (12.5%) | 41.07 | 0 | 0 | 1.06 | -87.22 |  |  |  |
| SF (12.5%) HPβCD (10%) | 41.11 | 10.28 | 0.56 | 47.49 | 25.63 |  |  |  |
| SF (12.5%) DSF (0.5%) | 41.20 | 0 | 0 | 0.01 | -106.19 |  |  |  |
| SF (12.5%) DSF (5%) | 40.83 | 0 | 6.96 | 0 | -54.64 |  |  |  |
| SF (12.5%) HPβCD (2.6%) DSF (0.5%) | 41.86 | 0 | 64.75 | 0 | 54.04 |  |  |  |

USC UNIVERSIDADE DE SANTIAGO DE COMPOSTELA

| | | | | | | | | |
|---|---|---|---|---|---|---|---|---|
| SF (12.5%)<br>HPβCD (10%)<br>DSF (5%) | 42.6 | 6.22 | 0.25 | 38.25 | 13.74 |  | | |
| SF (6%)<br>$CuCl_2$ (0.045%) | 40.77 | 0 | 0 | 1.47 | -83.39 |  | | |
| SF (12.5%)<br>HPβCD (2.6%)<br>$CuCl_2$ (0.045%) | 41.53 | 0 | 0 | 93.37 | 86.89 |  | | |
| SF (6%)<br>DSF (0.1%)<br>$CuCl_2$ (0.045%) | 41.04 | 0 | 0 | 0 | -108.03 |  | | |
| SF (6%)<br>DSF (0.5%)<br>$CuCl_2$ (0.045%) | 40.74 | 0 | 1.37 | 0 | -84.25 |  | | |
| SF (5%)<br>HPβCD (0.51%)<br>DSF (0.1%)<br>$CuCl_2$ (0.045%) | 40.32 | 0 | 0 | 0 | -107.5 |  | | |
| SF (5%)<br>HPβCD (2.6%)<br>DSF (0.5%)<br>$CuCl_2$ (0.045%) | 40.86 | 0 | 0 | 90 | 82.62 |  | | |

### 4.3.3 Disulfiram release profile

Release profiles of DSF from SF and SF-HPβCD fibers without $CuCl_2$ and with $CuCl_2$ are shown in **Figures 4.9.** and **4.10.**, respectively. The tests were carried out in PBS of three different pH (7.4, 6.5, and 5.5) trying to mimic all the possible scenarios that the fibers could be exposed to, depending on the GBM tumor resection location: "leading edge zone" that presents a normal pH 7.4, "cellular tumor zone" with a pH range values of 6.2 to 7, and "pseudo-palisading cell zone" of pH below 5.5 [61].

SF solely fibers showed slow release, with percentages of DSF released in the 1-5 % range. The low amount of DSF released could be due to the fact that fibroin in beta conformation (verified in section 3.2 FTIR) is hydrophobic and disulfiram is also a hydrophobic drug [25]. Changes in pH had minor impact on the amount of DSF released from SF solely fibers. A decrease in pH has been reported to trigger silk I to silk II transition [62], but this effect was not relevant in our case since the fibers were already prepared using silk II (beta-sheet, hydrophobic) conformation [63].

USC DE COMPOSTELA

Differently, SF-HPβCD fibers presented a relevant burst release in all PBS media. The release started as soon as the fibers entered in contact with water, reaching 25-51% released in the first two hours, due to the solubilizing capability of HPβCD. The effect of the pH was again unnoticeable. These fibers suffered partial dissolution in PBS, being more evident for SF 12.5% HPβCD 10% DSF 5% than for SF 12.5% HPβCD 2.6% DSF 0.5% due to the highest content in HPβCD.

In the case of the fibers containing Cu(II), DSF chelation of Cu(II) can occur spontaneously in aqueous medium and is favored by a decrease in the pH, which facilitates the rupture of the S-S bond and the formation of diethyldithiocarbamate (DDC) [64]. The concentration of both the DSF released from the fibers and the $Cu(DDC)_2$ spontaneously formed during the release was monitored (**Figure 4.10.**). For all formulations, $Cu(DDC)_2$ was detected since the first time point. Cu(II)-containing fibers had nanometric size (<500 nm), with a large surface-area in contact with the release medium. It should be noted that all fibers were prepared using the same concentration of $CuCl_2$ 0.045% (w/v), but the final contents in Cu(II) of the solid mats were slightly different depending on the other components ratio (as indicated in **Table 4.1.)** and ranged between 2.6 and 3.7 mg/g. Relevantly, the fibers combining Cu(II) with the lowest content in DSF (0.1% w/v) released the drug as a complex with Cu(II), namely as $Cu(DDC)_2$, which is the most active species against tumor cells and bacteria cells (**Figure 4.10.A** and **C**). These fibers were prepared with equimolar contents in Cu(II) and DSF, and the results confirmed the rapid decomposition of DSF in two molecules of DDC that chelate one Cu(II) ion, forming $Cu(DDC)_2$.

In the case of formulations prepared with 5 times more DSF (0.5% w/v), both DSF and $Cu(DDC)_2$ were detected in the medium (**Figure 4.10.B** and **D**). As observed for fibers without $CuCl_2$, incorporation of HPβCD significantly accelerated the release of intact DSF; the percentage released achieved 17% for SF 5% (w/v) HPβCD 2.6% (w/v) DSF 0.5% (w/v) $CuCl_2$ 0.045 (w/v) while it was approx. 5% released for SF 6% (w/v) DSF 0.5% (w/v) $CuCl_2$ 0.045 (w/v) after 24 h in the medium.

Overall, a wide range of DSF/$Cu(DDC)_2$ amounts released were obtained in the first hours of the study, also showing the capability of the fibers to retain encapsulated DSF under the tested in vitro conditions. These mats displayed high stability and reproducibility since they released similar amounts of DSF and its chelate disregarding

UBU UNIVERSIDAD

the changes in pH. Hence, these fibers may be potentially useful for supplying therapeutic amounts of DSF/$Cu(DDC)_2$ for GBM treatment disregarding the state of this disease.

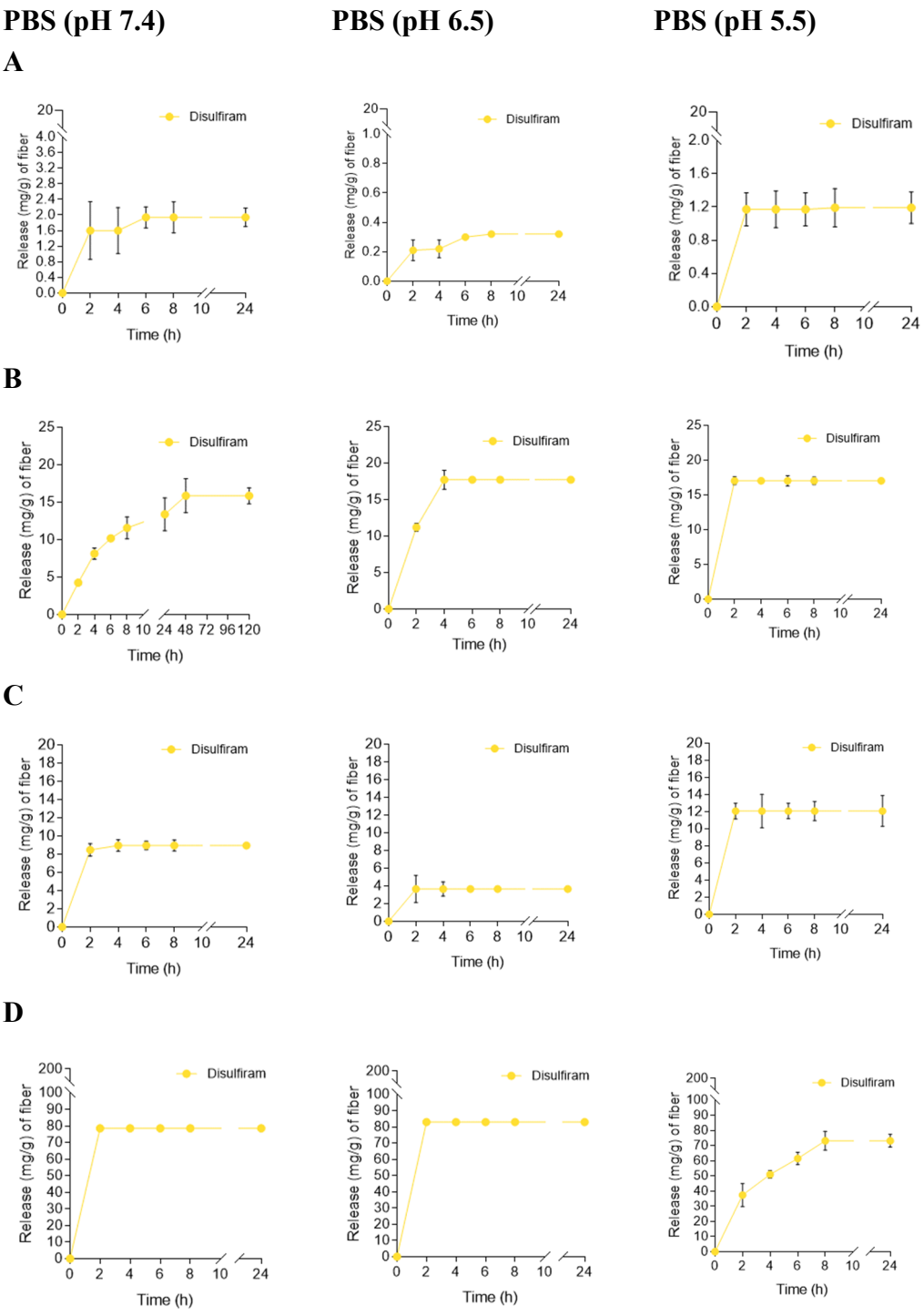



**Figure 4.9. Release profile of disulfiram from silk fibroin fibers prepared with and without HPβCD in PBS at different pHs under 100 rpm and at 37°C. (A) SF 12.5% (w/v) DSF 0.5% (w/v), (B) SF 12.5% (w/v) DSF 5% (w/v), (C) SF 12.5% (w/v) HPβCD 2.6% (w/v) DSF 0.5% (w/v), and (D) SF 12.5% (w/v) HPBCD 10% (w/v) DSF 5% (w/v).**

USC UNIVERSIDADE DE SANTIAGO DE COMPOSTELA

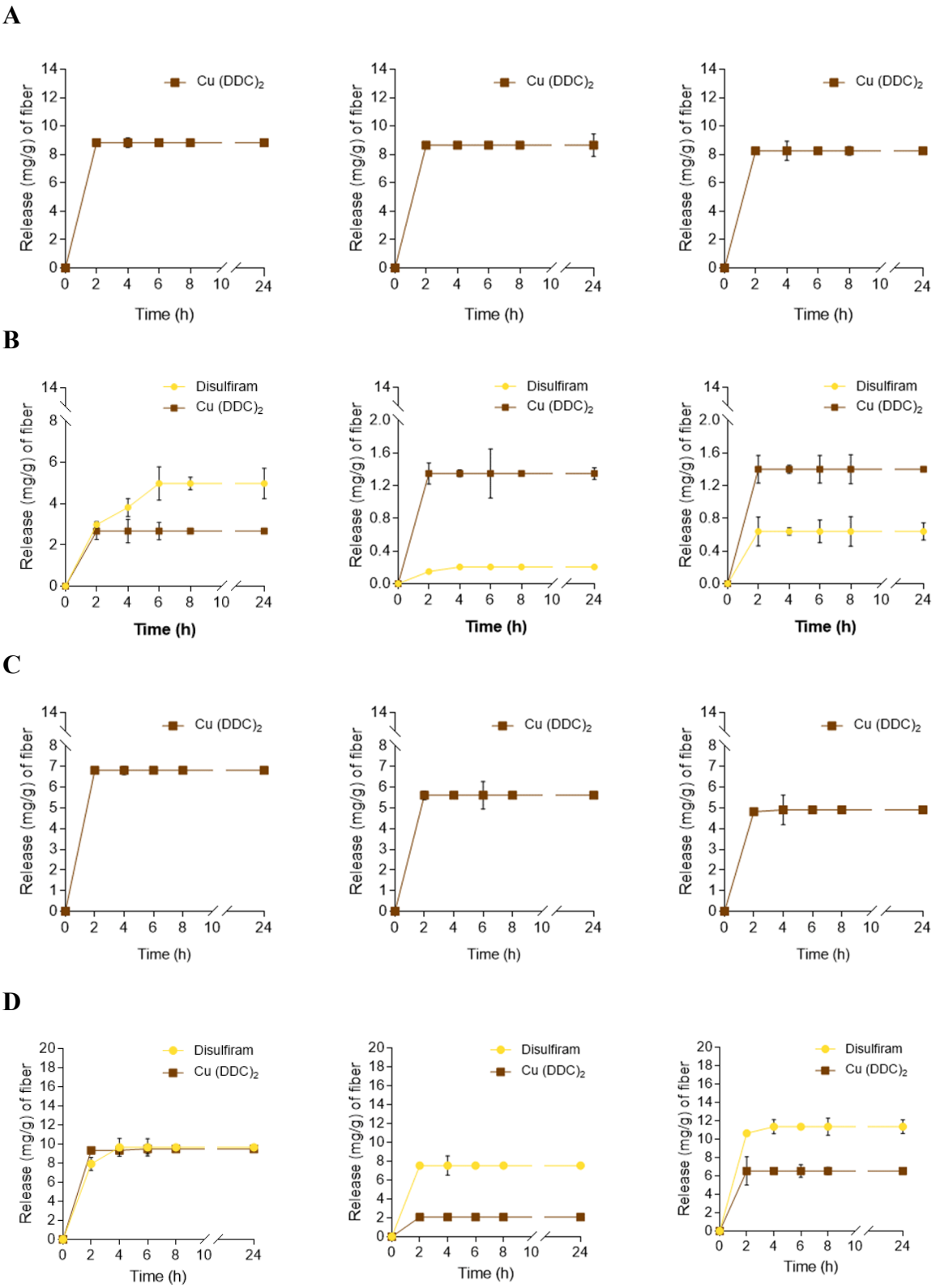



**Figure 4.10. Release profile of disulfiram and its chelate from silk fibroin fibers loaded with different concentrations of HPβCD, disulfiram and $CuCl_2$ (A) SF 6% (w/v) DSF 0.1% (w/v) $CuCl_2$ 0.045% (w/v), (B) SF 6% (w/v) DSF 0.5% (w/v) $CuCl_2$ 0.045% (w/v), (C) SF 5% (w/v) HPβCD 0.51% (w/v) DSF 0.1% (w/v) $CuCl_2$ 0.045% (w/v), and (D) SF 5% (w/v) HPBCD 2.6% (w/v) DSF 0.5% (w/v) $CuCl_2$ 0.045% (w/v) in PBS at different pHs under 100 rpm and at 37°C.**

USC UNIVERSIDADE DE SANTIAGO DE COMPOSTELA

### 4.3.4 Hemolysis

A first screening of biocompatibility was carried out testing the compatibility with human blood (**Figure 4.11.**). The fibers did not cause hemolysis. Even the SF 12.5% (w/v) HPβCD 10% (w/v) DSF 5% (w/v) fibers that released the highest concentrations of disulfiram had values well below the 5% hemolysis, set as the safe threshold.

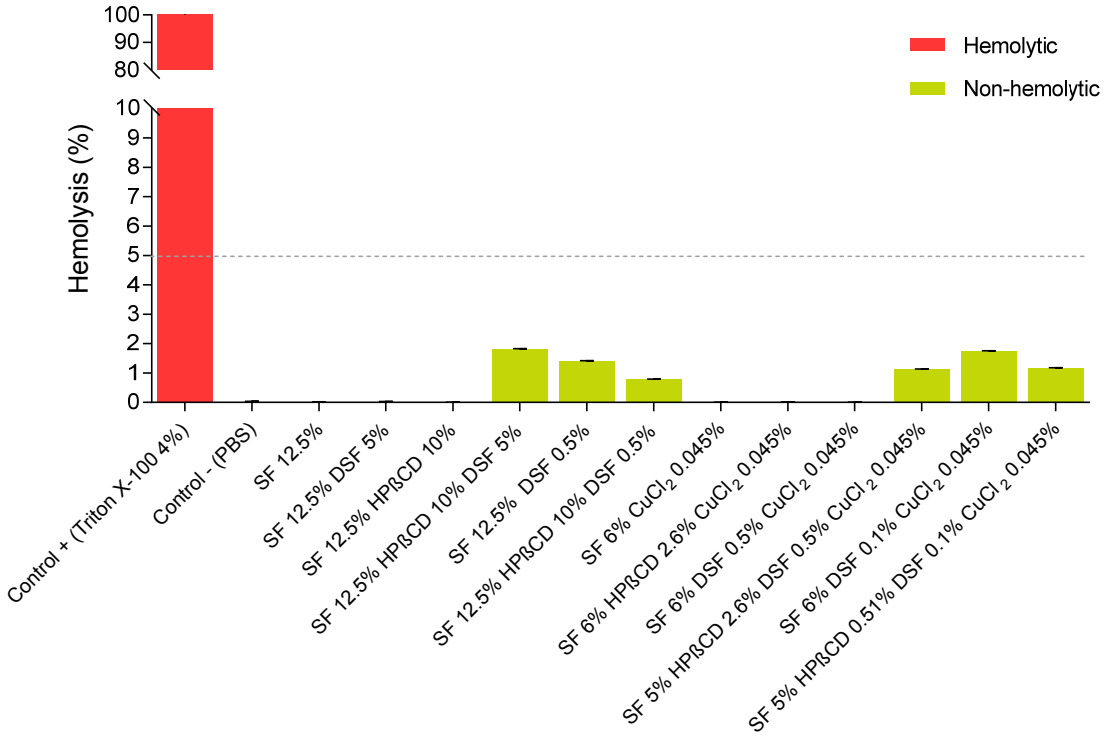



**Figure 4.11. Percentage of hemolysis produced by Triton X-100 4% (w/v) (positive control), PBS (negative control), and the prepared fibers after 2 h of incubation with diluted human blood at 37°C under gentle agitation.**

### 4.3.5 Antimicrobial activity

The antimicrobial activity of the fibers was tested against *S. aureus* and *P. aeruginosa* (**Figure 4.12** and **4.13**). SF 12.5% (w/v) HPβCD 10% (w/v) DSF 5% (w/v) fibers displayed the most intense antimicrobial activity against *S. aureus* reaching a reduction of up to 4.84 $Log_{10}$ (CFU/mL), which can be clearly attributed to the role of HPβCD as solubilizing agent and promoter of DSF release. SF 12.5% (w/v) DSF 5% (w/v) fibers (without HPβCD) showed a slight antimicrobial effect with a reduction of only 0.80 $Log_{10}$ (CFU/mL).

USC UNIVERSIDADE DE SANTIAGO

Interestingly, the fibers loaded with DSF 0.5% (w/v) displayed a similar antimicrobial activity if compared with SF 12.5% (w/v) DSF 5% (w/v) fibers (no statistically significant differences). The presence of $CuCl_2$ slightly increased the antimicrobial activity: SF 6% (w/v) DSF 0.5% (w/v) $CuCl_2$ 0.045% (w/v) caused a reduction of 0.59 $Log_{10}$ (CFU/mL) and SF 5% (w/v) HPβCD 2.6% (w/v) DSF 0.5% (w/v) $CuCl_2$ 0.045% (w/v) caused a reduction of 0.62 $Log_{10}$ (CFU/mL).

SF fibers loaded with lower amounts of DSF (0.1% w/v) did not show activity against *S. aureus* (< 0.5 log microbial growth reduction): SF 6% (w/v) DSF 0.1% (w/v) $CuCl_2$ 0.045% (w/v) with 0.39 $Log_{10}$ (CFU/mL), whilst SF 5% (w/v) HPβCD 0.51% (w/v) DSF 0.1% (w/v) $CuCl_2$ 0.045% (w/v) had 0.52 $Log_{10}$ (CFU/mL). Clearly both HPβCD (promoting DSF release) and Cu(II) (forming a chelate with DSF) enhanced the activity of the fibers against *S. aureus* [22, 65].

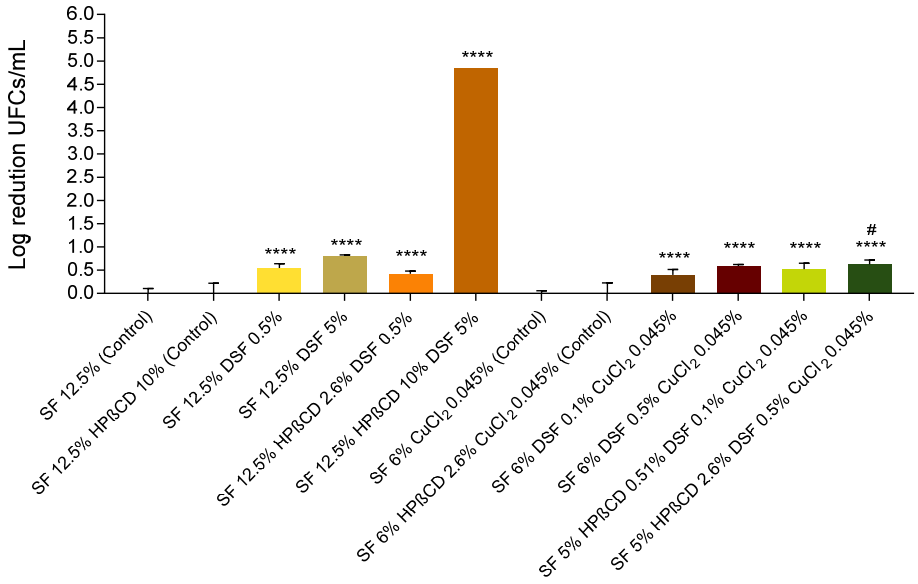



**Figure 4.12. Antimicrobial activity of SF fibers prepared with different concentrations of HPβCD, disulfiram, and $CuCl_2$ against *S. aureus*, in terms of reduction of culturable cells (log (CFU/mL) reduction) after 24 h of incubation at 37°C under gentle agitation. Mean ± standard deviation, n=4. Asterisk (*) was used to compare the antimicrobial activity of the fibers against the SF 12.5% (control fiber) and the number sign (#) was used to compare the antimicrobial activity of SF fibers without copper and with copper loaded with same content in DSF and HPβCD. * p < 0.05, ** p < 0.005, *** p < 0.001 and **** p < 0.0001.**

In the case of *P. aeruginosa,* SF 12.5% (w/v) HPβCD 10% (w/v) DSF 5% (w/v) fibers were again the most active ones, reaching a reduction of up to 5.96 $Log_{10}$ (CFU/mL), compared to SF 12.5% (w/v) DSF 5% (w/v), which were still active and

ranked the second ones, but caused a reduction of 0.75 $Log_{10}$ (CFU/mL) (**Figure 4.13.**). The other fibers did not cause antimicrobial effects, except for SF 5% (w/v) HPβCD 2.6% (w/v) DSF 0.5% (w/v) $CuCl_2$ 0.045% (w/v) with 0.47 $Log_{10}$ (CFU/mL). This last fiber showed the best antimicrobial activity of Cu(II)-containing fibers, displaying statistical differences ($^{\#}p < 0.05$) with similar fibers prepared in the absence of $CuCl_2$.

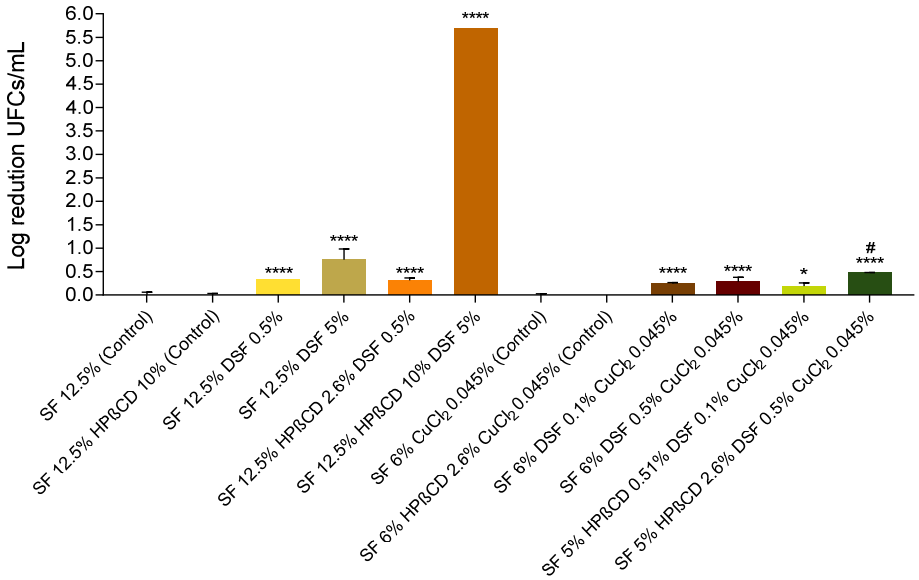



**Figure 4.13. Antimicrobial activity of SF fibers prepared with different concentrations of HPβCD, disulfiram, and $CuCl_2$ against *P. aeruginosa*, in terms of reduction of culturable cells (log (CFU/mL) reduction) after 24 h of incubation at 37°C under gentle agitation. Mean ± standard deviation, n=4. Asterisk (*) was used to compare the antimicrobial activity of the fibers against the SF 12.5% (control fiber) and number sign (#) was used to compare the antimicrobial activity of SF fibers without copper and with copper loaded with same content in DSF and HPβCD. * p < 0.05, ** p < 0.005, *** p < 0.001 and **** p < 0.0001.**

Results obtained in the antimicrobial tests agreed with the release tests since the best results were found for SF 12.5% (w/v) HPβCD 10% (w/v) DSF 5% (w/v) that released the highest amounts of disulfiram. Overall, DSF was revealed as a potential drug in infections or as a prophylactic agent with good antimicrobial properties

### 4.3.6 Anticancer activity on glioblastoma cells

As a first step, the effect of DSF on survival of glioblastoma cells was evaluated through a dose-response study on different murine and human glioblastoma cell lines (**Figure 4.14.**). The antitumoral activity of DSF in the presence of 1μM of copper in the medium strongly reduced the viability (resazurine assay) of glioblastoma cell lines at 24 and 48-hours treatment (**Figure 4.14.A**). The concentration needed to inhibit 50% of cell viability

($IC_{50}$) for GL261 was 0.12 µM after 24 and 48 h of treatment, meanwhile for the human glioblastoma cell lines (U-87MG and U-251MG) $IC_{50}$ was 0.20 µM and 0.30 µM at 24 h and decreased to 0.12 µM and 0.15 µM at 48 h respectively.

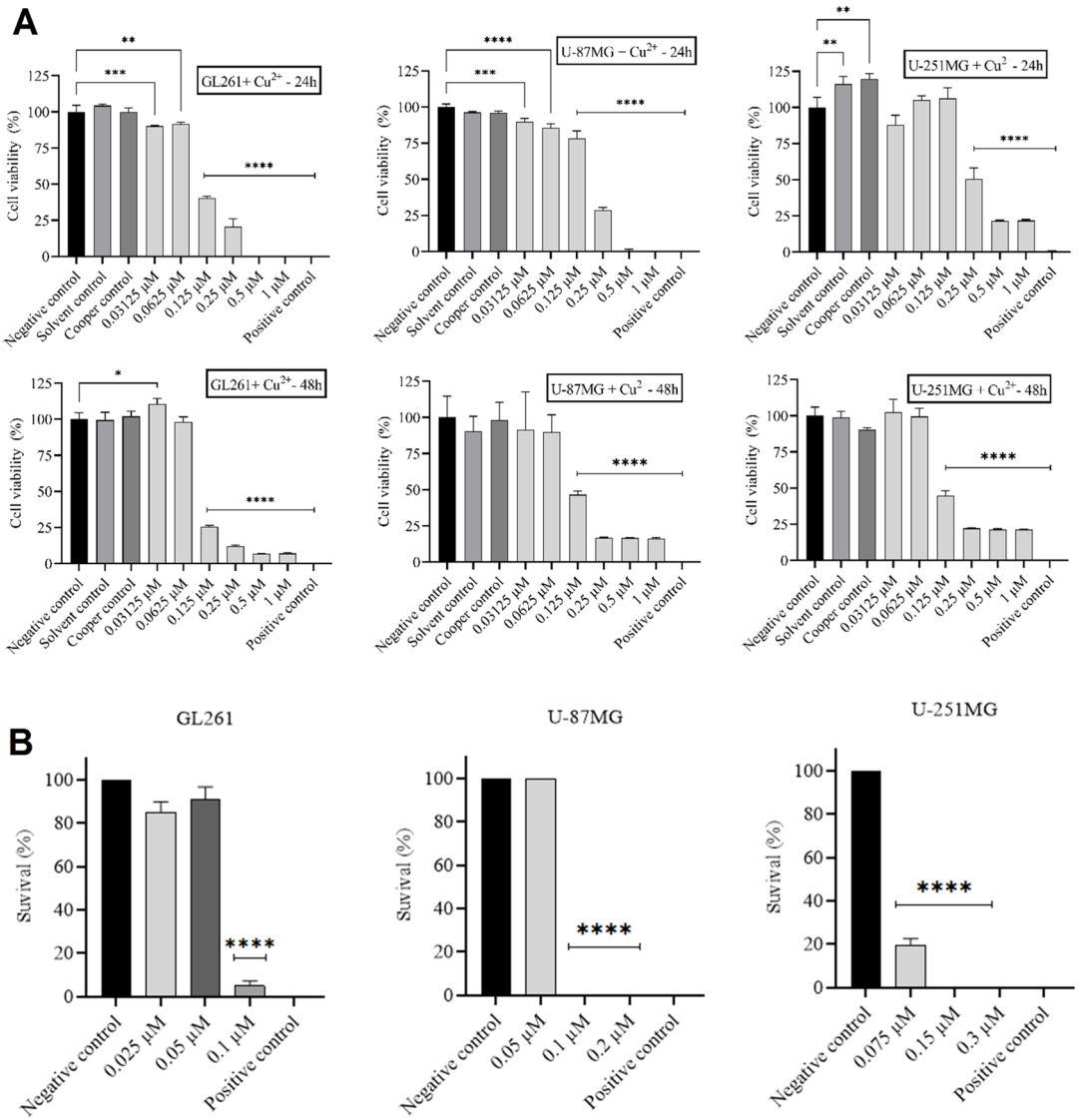



**Figure 4.14. Effect of disulfiram combined with cooper as an anticancer agent on glioblastoma cells. (A) Percentage of cell viability after exposition to different dose of disulfiram (0.03 – 1 µM) with 1 µM cooper in the medium, on GL261 (murine glioblastoma cell line), U-87MG and U-251MG (human glioblastoma cell line) after 24 or 48-h of treatment. (B) Percentage of colonies survival after 24 h of treatment of disulfiram (concentrations based on $IC_{50}$) in combination with 1 µM of copper, on GL261, U-87MG and U-251MG. Mean ± standard deviation, triplicate * p < 0.05, ** p < 0.005, *** p < 0.001 and **** p < 0.0001.**

Alongside these findings, the antiproliferative potential of DSF combined with copper was measured by studying the capacity of glioblastoma cells to form cell clones after treatment (done only after two hours of recovery after seeding of the cells) by using

the Giemsa stain technique [55]. As evidenced on **Figure 4.14.B**, this capacity was strongly decreased at concentrations greater than $IC_{50}$ for GL261 cells, while it was completely abolished in the human glioblastoma cell lines (U-87MG and U-251MG) at 0.10 μM and 0.15 μM, respectively. These results suggest a global effect of DSF beyond a particular subtype of cells within these heterogeneous cell lines. Results obtained were consistent with previous reports on the cytotoxic effect of DSF on glioblastoma cell lines U-87MG, U-251MG, and U-373MG [66], which evidenced that non-toxic copper is necessary to obtain this cytotoxic effect on cancer cells. In fact, DSF forms a complex with Cu(II) ions that inhibits the proteasome activity and NF- κB signaling, which causes the death of cancer cells [11, 67, 68]. These results show a potential use of DSF alone or in combination with other therapeutics for the development of a new therapy.

To gain further insight into the potential toxic effect of DSF beyond the anticancer properties in the central nervous system, and for future preclinical investigations, studies were also conducted on murine cells of the CNS that divide slowly in neutral conditions, astrocytes (to compare with GL261). As shown in **Figure 4.15.A**, the treatment had no effect on this type of cell. Differently, on murine fibroblast (NIH3T3 cell line) (**Figure 4.15.A**), which were still in cell cycle phase, DSF showed cytotoxic effects. This reveals a potential toxicity of DSF with copper on dividing cells. Regarding these results, potential toxic effects of the systemic administration of a high dose of DSF in the alcoholism treatment can be predicted. In our case, the locoregional and controlled administration of the treatment directly in the brain is an undeniable advantage.

To investigate more thoroughly potential synergies between the conventional treatment of glioblastoma which include beam radiation and the use of DSF, a study of association of treatment with a 16GY dose of radiation was conducted. Relevantly, DSF preserved its activity during irradiation, with a potentiation of the effects at 0.06 μM on GL261, while maintaining his harmlessness on astrocytes on which beam radiations had no effects (**Figure 4.15.B**). There is a slight toxicity of irradiation on murine fibroblasts (NIH3T3) but no synergic effect with DSF on this cell line (**Figure 4.15.B**). These results demonstrate that for a development of a combined therapeutic strategy (DSF + radiotherapy), it is possible to optimize the intensity and frequency of irradiation to have the best effect of the combination (synergy and lack of toxicity).

USC
UNIVERSIDADE DE SANTIAGO DE COMPOSTELA

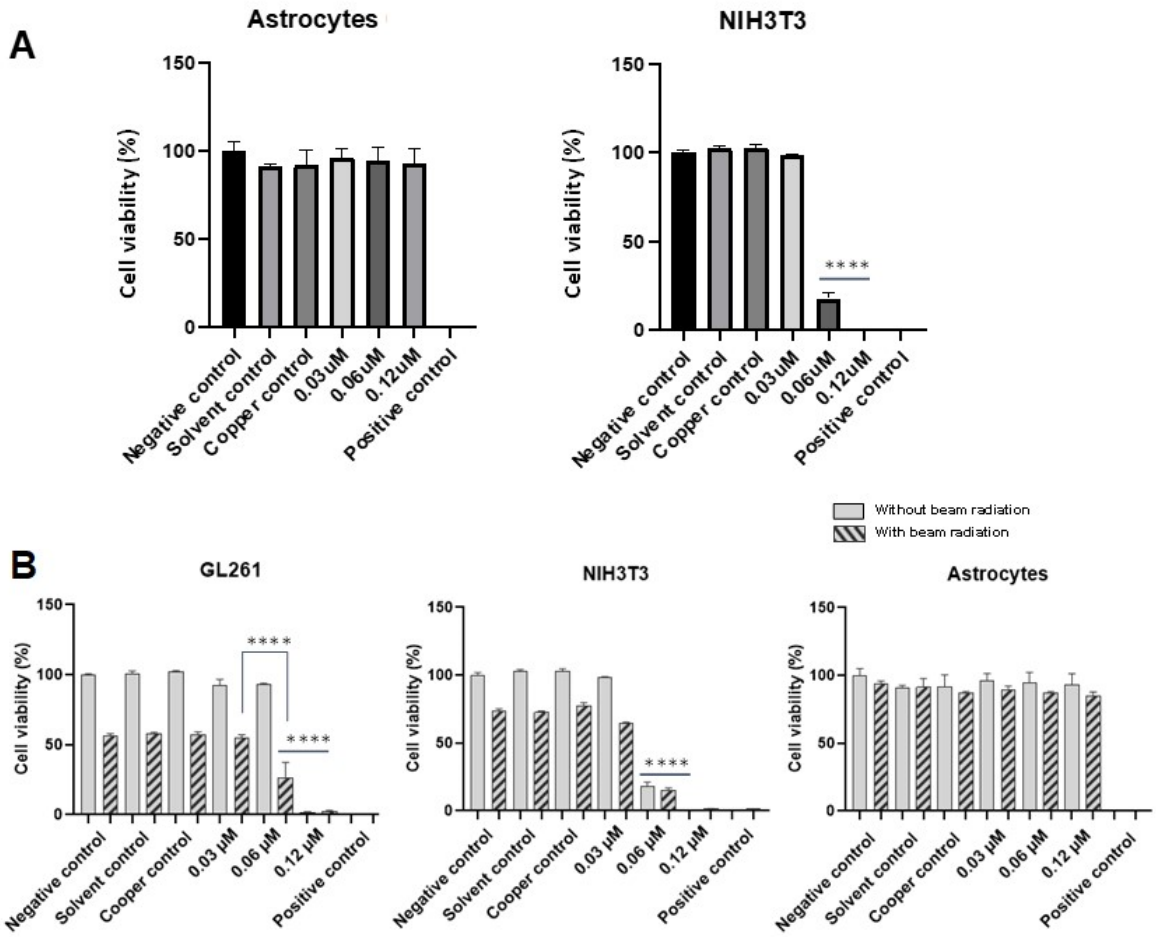



**Figure 4.15. Disulfiram toxicity on cycling cells (NIH3T3), central nervous system non cycling cells (astrocytes) and combination of treatment with beam radiation. (A) Percentage of cell viability after exposition to different dose of disulfiram (0.03 – 0.12 µM) with 1 µM cooper in the medium, on NIH3T3 and mouse primary astrocytes after 24h of treatment. (B) Percentage of cell viability after exposition to disulfiram (0.03 – 0.12µM) with cooper in combination with irradiation (16GY) on GL261, NIH3T3 and mouse primary astrocytes. Mean ± standard deviation, triplicate * p < 0.05, ** p < 0.005, *** p < 0.001 and **** p < 0.0001.**

Considering all these results, the possibility of administrating in safe and controlled manner DSF in the CNS was then investigated using the developed SF fibers (**Figure 4.16.**).

USC
UNIVERSIDADE DE SANTIAGO DE COMPOSTELA

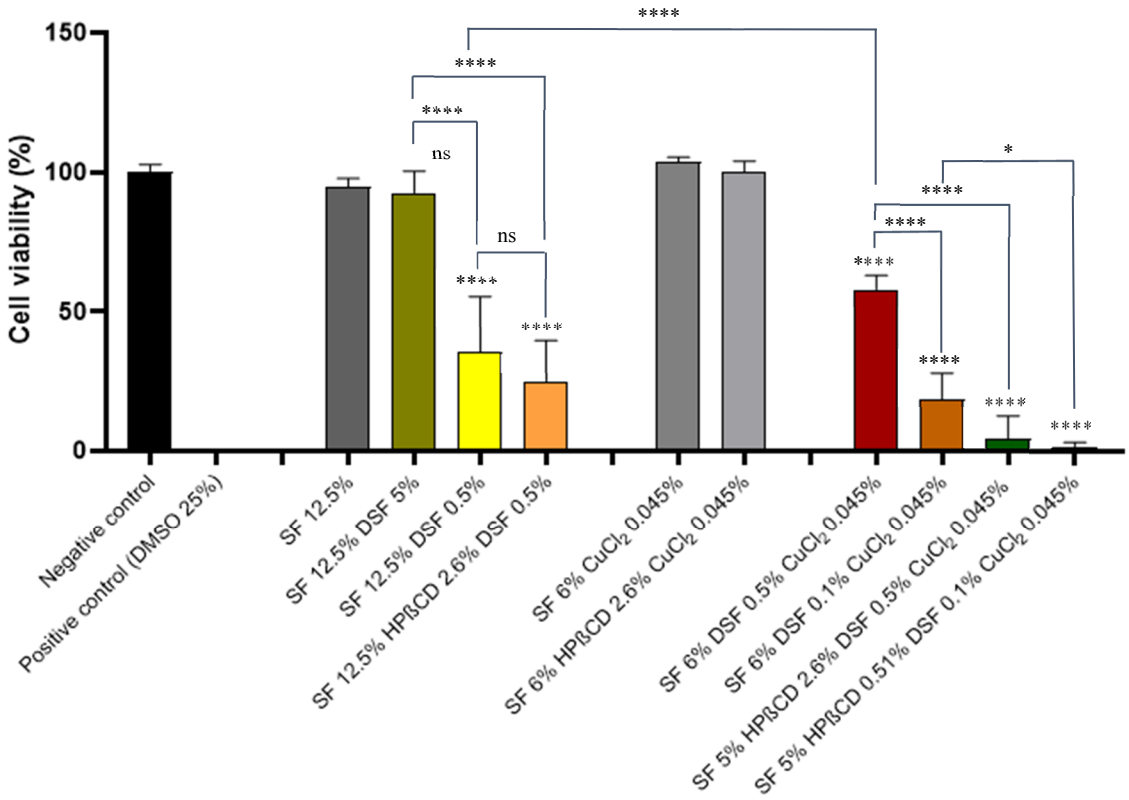



**Figure 4.16. Effect on cell viability of SF fibers prepared with different concentrations of HPßCD, disulfiram, and CuCl2 after 24 h of treatment on GL261. Mean ± standard deviation, n=3 * p < 0.05, ** p < 0.005, *** p < 0.001 and **** p < 0.0001.**

SF solely fibers (12.5%) did not cause any effect on cells. When DSF at 5% was added to the SF fibers, there was also a lack of effect on GL261 cells, which could be explained by the small amount of DSF released after 24 h of treatment (as recorded in the release tests). Lowering DSF proportion in the fiber remarkably promoted the cytotoxic effect, either in the absence or in the presence of HPβCD, as the fibers were more hydrophilic, and the release was facilitated. In the absence of DSF, the presence of $CuCl_2$ in the fibers did not trigger any cytotoxic effect on cancer cells. Differently, SF fibers prepared combining DSF, Cu(II) and HPβCD showed a strong antitumoral effect, with almost 100% of cell death after 24 h of treatment. Thus, SF 5% (w/v) HPßCD 2.6% (w/v) DSF 0.5% (w/v) $CuCl_2$ 0.045% (w/v) and SF 5% (w/v) HPβCD 0.51% (w/v) DSF 0.1% (w/v) and $CuCl_2$ 0.045% (w/v) fibers seems to be the best option to have a complete cytotoxic effect on glioblastoma cells.

USC UNIVERSIDADE DE SANTIAGO DE COMPOSTELA

### 4.3.7 *In vivo* medium-term biocompatibility of SF-fibers: locoregional histological analysis

A thorough *in vivo* anatomocytopathological study was conducted on naïve rats to investigate the locoregional cellular responses following the implantation of SF-fibers in healthy brain parenchyma. Two types of fibers, namely SF 12.5% (w/v) HPβCD 2.6% (w/v) DSF 0.5% (w/v) and SF 5% (w/v) HPβCD 2.6% (w/v) DSF 0.5% (w/v) $CuCl_2$ 0.045% (w/v), were directly implanted into a resection cavity in the cortex. The latter fibers were chosen considering together the antimicrobial and the antitumoral activities, while the former ones without Cu(II) were chosen as a reference to detect potential toxicity problems ascribed to the metal ions and the formation of the $Cu(DCC)_2$ chelate. Both types of fibers were verified to significantly reduce the proteasome activity in glioblastoma cells (**Figure 4.17.**), and thus may act as proteasome inhibitors able to alter the cell cycle and cause apoptosis of GBM cells [14]. The surgery mimicked GBM resection and implantation of a device that, if most tumor was removed, would be in contact with the healthy brain [32].

USC UNIVERSIDADE DE SANTIAGO DE COMPOSTELA

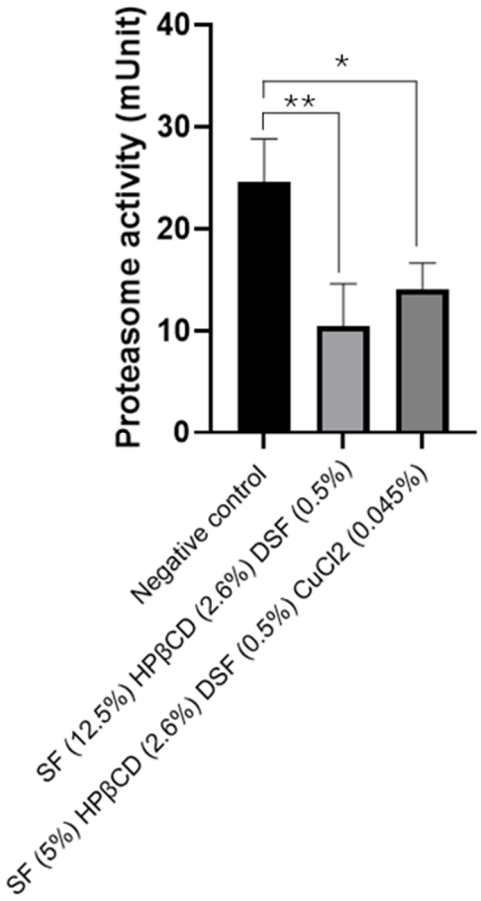



**Figure 4.17. Effect of disulfiram fibers on proteasome activity in GL261 cells: Proteasome activity levels were reduced following exposure to the fibers compared to the negative control. Mean ± standard deviation, n=3 * p < 0.05, ** p < 0.005, *** p < 0.001.**

One week after the implantation, brains were collected and stained with HE to investigate cellular and tissular responses that can occur following SF-fiber implantation in the cortex in comparison to the cavity control situation. As described in many brain surgical procedures, the results presented in **Figure 4.18.A and 4.18.B** indicated a mild but well identified inflammatory response in the control group. It was characterized by the presence of chronic inflammatory cells that include macrophages, lymphocytes and the occurrence of neoangiogenesis supporting tissue healing. Interestingly, no differences in terms of tissue response to surgery were noticed while comparing SF-fibers containing disulfiram at 0.5% and HPβCD to the cavity control. The recruitment of inflammatory cells was very similar with mild colonization of the tissue and no apparent signs of toxicity (**Figure 4.18.B**). In contrast, when using fibers containing disulfiram with HPβCD and $CuCl_2$, a higher global response was observed with more macrophages, lymphocytes recruited in several animal while being less homogeneous as in the other

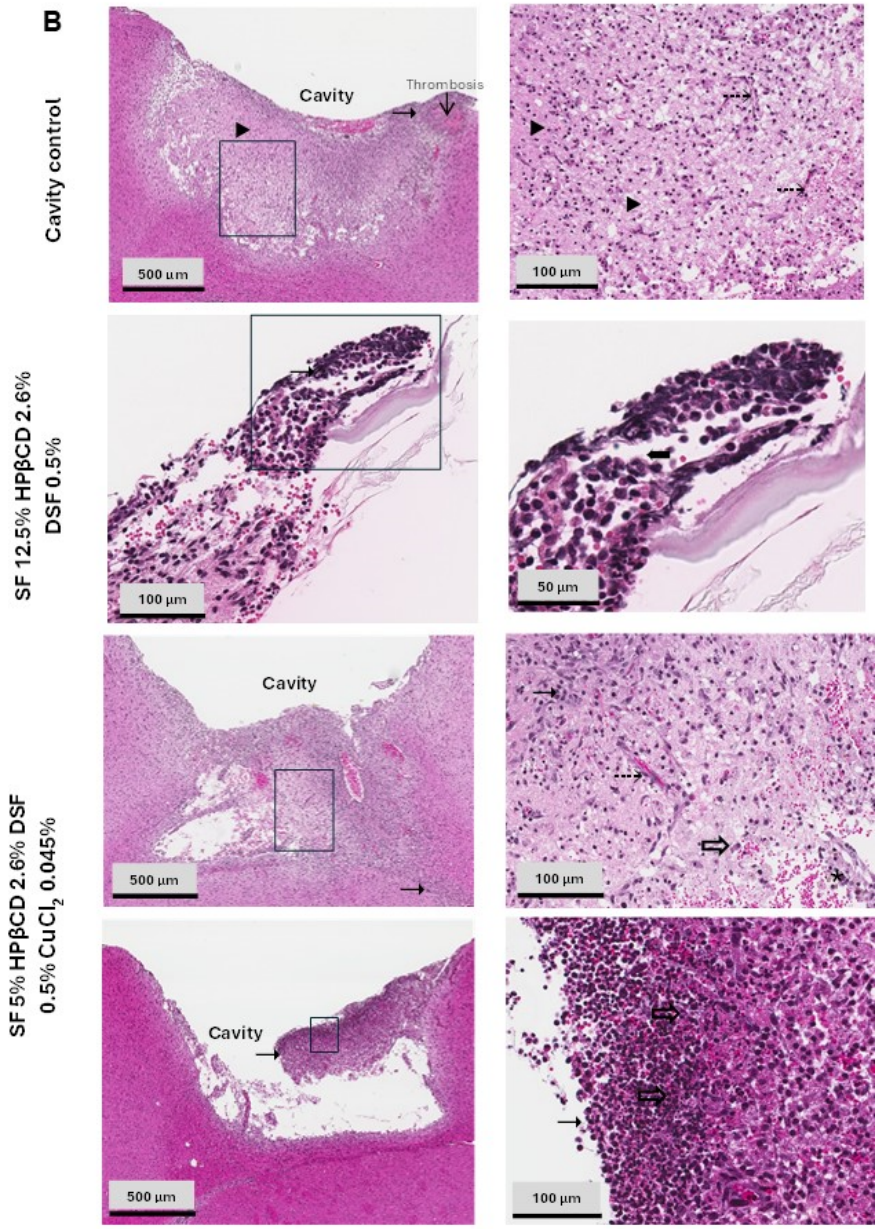
USC UNIVERSIDADE DE SANTIAGO

animal groups. Among the five rats included in this group, two exhibited an enhanced response, with a spread of inflammation and a notable presence of apoptotic bodies (**Figure 4.18.B**). All other tested parameters remained the same as for the control cavity (**Figure 4.18.A**).

**A**

| Cavity control n=5 | SF 12.5% HPβCD 2.6% DSF 0.5% n=4 | SF 5% HPβCD 2.6% DSF 0.5% $CuCl_2$ 0.045% n=5 | [ - -/+ + ++ +++ ] |
|---|---|---|---|
| - - - - - | - - - - | - - - - - | Multinucleated Giant cells |
| -/+ + - - - | - -/+ + - | - - + -/+ ++ | Acute inflammatory cells (PMN cells) |
| - - - - - | - - - - | - - - - ++ | Cellular debris and apoptotic bodies |
| + ++ ++ ++ ++ | ++ ++ ++ + | ++ + +++ ++ +++ | Chronic inflammatory cells |
| + ++ + ++ + | + + + + | ++ + +++ ++ + | Neoangiogenesis |
| - - - - - | - - - - | - - - - - | Haemorrhage |
| - -/+ - - - | - - - -/+ | + - -/+ + -/+ | Hemosiderin |
| - - - - - | -/+ - - - | -/+ - - - - | Mineralization |

**B**




USC UNIVERSIDADE DE SANTIAGO DE COMPOSTELA

**Figure 4.18. In vivo assessment of the impact of disulfiram fibers implantation in rat's brains. (A) Characterization of the *in vivo* cellular response to implanted fibers in the rat brain cortex. Scores are as follows: (−) = nil, (-/+) = rare, (+) = mild, (++) = moderate, and (+++) = marked. (B) Histological (H&E) staining (nuclei: blue/purple; cytoplasm: pink) images revealed the inflammatory response across the different study conditions one-week post-surgery. Symbols are as follows: Lymphocytes (→), Macrophages (▶), PMN cells (➡), neoangiogenesis (⇢), Hemosiderin (*), Apoptotic bodies (⇨). Interrupted-line bordered images are magnifications of the smaller squares indicated in their respective left images.**

This study on implantability and behavior of the brain parenchyma with respect to implanted SF-fibers does not prejudge the best possible candidate in terms of effectiveness but reflects a possible better acceptance of SF-fibers without Cu(II). It should also be noted that the very nature of fibers containing Cu(II) makes them mechanically more complex to handle. It remains to be seen whether *in vivo* experiments, beyond the *in vitro* experiments that have demonstrated the essential role of Cu(II) in the effectiveness of vectorized DSF, can demonstrate that *in situ* brain physiological levels of Cu(II) are sufficient for the effectiveness of DSF.

## 4.4. CONCLUSIONS

Electrospun fibers prepared using freeze-dried SF as main component revealed to be highly versatile to encapsulate considerable amounts of DSF and HPβCD. Incorporating small proportions of Cu(II) in the fibers allowed reducing the dose of DSF. However, the production of electrospun fibers of SF with Cu(II) was quite challenging due to the lack of solubility of the inorganic salt in HFIP and the strong interaction between both components, which caused the precipitation of SF. This problem was overcome tuning SF and Cu(II) concentration and using DMF as cosolvent and resulted in the obtaining of nanometric fibers of adequate mechanical properties.

Both HPβCD and $CuCl_2$ were shown to play very relevant roles in the control of DSF release and the in-situ formation of the DSF-copper chelate, which ultimately determined the performance of the fibers as antimicrobial and antitumor implantable devices. Relevantly, the release rate of DSF and in situ formation of $Cu(DDC)_2$ were not altered by pH changes in the range typical of healthy and tumoral brain tissues. The fibers allowed obtaining a good synchronization of the supply of the two therapeutic agents together from the same formulation, overcoming the need of administering DSF and Cu(II) in separate. The increased potency of DSF at lower concentrations when combined with SF fibers prepared with HPβCD and copper is particularly noteworthy. These

USC UNIVERSIDADE DE SANTIAGO DE COMPOSTELA

findings suggest that DSF delivery and bioavailability can be significantly optimized through these combinations, which may also allow for more precise dosing. The interaction with copper, given DSF known role in copper chelation and the generation of reactive oxygen species, might also provide a mechanistic explanation for this enhanced activity. As a limitation of the developed formulations, it should be mentioned that SF 5% HPßCD 2.6% DSF 0.5% $CuCl_2$ 0.045% fibers are weaker than the others, which makes their handling more difficult. On the other hand, they are the ones that best imitate the biological softness of the brain. Thus, the balance in mechanical properties requires further studies.

Of outmost importance from a regulatory perspective, the fibers were blood-compatible and did not trigger any toxic effect when loaded with DSF or $CuCl_2$ in separate. Moreover, selectivity against tumor cells compared to normal astrocytes is particularly relevant. This specificity is significant in the context of brain cancer treatment, where preserving healthy tissue is paramount. The observed toxicity on fibroblasts, in contrast, suggests that DSF may have a broader range of cellular targets, linked to differential metabolic pathways or variations in copper metabolism between cell types. Exploring this mechanism further could provide valuable insights. Additionally, the fibers are biodegradable and when its therapeutic purpose is complete (i.e., the release of DSF), all components could be reused by a variety of cells; for example, SF amino acids could be utilized for myriads of process (*e.g.* energy obtention), HPβCD can capture toxic substances forming inclusion complexes to be cleared from the body, and Cu(II) could be stored by astrocytes and reused to maintain a correct homeostasis or participate in neuronal synapses.

The obtained results collectively underscore the potential of DSF-loaded electrospun fibers containing Cu(II) for clinical translation as part of a combination therapy regimen for glioblastoma.

USC
UNIVERSIDADE DE SANTIAGO DE COMPOSTELA

### 4.5. References

[1] Louis D.N., Perry A., Wesseling P., Brat D.J., Cree I.A., Figarella-Branger D., Hawkins C., Ng H.K., Pfister S.M., Reifenberger G., Soffietti R., von Deimling A., Ellison D.W. The 2021 WHO Classification of Tumors of the Central Nervous System: a summary. Neuro Oncol. 23(8) (2021)1231-1251. https://doi.org/10.1093/neuonc/noab106.

[2] van Solinge T.S., Nieland L., Chiocca E.A. et al. Advances in local therapy for glioblastoma — taking the fight to the tumour. Nat Rev Neurol 18 (2022) 221–236. https://doi.org/10.1038/s41582-022-00621-0.

[3] Weller M., Wick W., Aldape K., Brada M., Berger M., Pfister S. M., Nishikawa R., Rosenthal M., Wen P. Y., Stupp R., Reifenberger, G. Glioma. Nature Rev Dis Primers 1 (2015) 15017. https://doi.org/10.1038/nrdp.2015.17

[4] Ragucci F., Sireci F., Cavallieri F., Rossi J., Biagini G., Tosi G., Lucchi C., Molina-Pena R., Ferreira N. H., Zarur M., Ferreiros A., Bourgeois W., Berger F., Abal M., Rousseau A., Boury F. Insights into Healthcare Professionals' Perceptions and Attitudes toward Nanotechnological Device Application : What Is the Current Situation in Glioblastoma Research ?. Biomedicines 11 (2023) 1854. https://doi.org/10.3390/biomedicines11071854

[5] Foo C. Y., Munir N., Kumaria A., Akhtar Q., Bullock C. J., Narayanan A., Fu R. Z. Medical Device Advances in the Treatment of Glioblastoma. Cancers 14 (2022) 5341. https://doi.org/10.3390/cancers14215341

[6] Iqbal T., Rewatkar P., Ahmed-Cox A., Saeed I., Mansfeld F. M., Kulshreshtha R., Kumeria T., Ziegler D. S., Kavallaris M., Mazzieri R., Popat A. Frontiers in the treatment of glioblastoma: Past, present and emerging. Adv Drug Del Rev 171 (2021) 108–138. https://doi.org/10.1016/j.addr.2021.01.012

[7] Pushpakom S., Iorio F., Eyers P. A., Escott K. J., Hopper S., Wells A., Doig A., Guilliams T., Latimer J., McNamee C., Norris A., Sanseau P., Cavalla D., Pirmohamed M. Drug repurposing: progress, challenges and recommendations. Nat Rev Drug Discov 18(1) (2019) 41–58. https://doi.org/10.1038/nrd.2018.168

USC UNIVERSIDADE DE SANTIAGO DE COMPOSTELA

[8] Cvek B. Nonprofit drugs as the salvation of the world's healthcare systems: the case of Antabuse (disulfiram). Drug Discov Today 17(9–10) (2012) 409–412. https://doi.org/10.1016/j.drudis.2011.12.010

[9] Benkő B. M., Lamprou D. A., Sebestyén A., Zelkó R., Sebe I. Clinical, pharmacological, and formulation evaluation of disulfiram in the treatment of glioblastoma - a systematic literature review. Expert Opin. Drug Deliv. 20(4) (2023) 541–557. https://doi.org/10.1080/17425247.2023.2190581

[10] Denoyer D., Masaldan S., Fontaine L., Cater M. A. Targeting copper in cancer therapy: 'Copper That Cancer'. Metallomics 7 (2015) 1459–1476. https://doi.org/10.1039/C5MT00149H

[11] Lun X., Wells J. C., Grinshtein N., King J. C., Hao X., Dang N., Wang X., Aman A., Uehling D., Datti A., Wrana J. L., Easaw J. C., Luchman A., Weiss S., Cairncross J. G., Kaplan D. R., Robbins S. M. Disulfiram when combined with copper enhances the therapeutic effects of temozolomide for the treatment of glioblastoma. Clin Cancer Res 22(15) (2016) 3860-3875. https://doi.org/10.1158/1078-0432.CCR-15-1798

[12] Zhang Y., Ding S., Li J., Peng X., Li J., Chang J. In vivo formation of $Cu(DDC)_2$ complex induced by nanomedicine for mesothelioma chemotherapy. Chinese Chem Lett, 31(12) (2020) 3168–3172. https://doi.org/10.1016/j.cclet.2020.04.051

[13] Yoshida D., Ikeda Y., Nakazawa S. Quantitative analysis of copper, zinc and copper/zinc ratio in selected human brain tumors. J. Neurooncol. 16 (2) (1993) 109-115. https://doi.org/10.1007/BF01324697.

[14] Gozdz A. Proteasome inhibitors against glioblastoma-overview of molecular mechanisms of cytotoxicity, progress in clinical trials, and perspective for use in personalized medicine. Curr Oncol. 30(11) (2023) 9676-9688. https://doi.org/10.3390/curroncol30110702.

[15] Brien P. S. O., Xi Y., Miller J. R., Brownell A. L., Zeng Q., Yoo G. H., Garshott D. M., Brien M. B. O., Galinato A. E., Cai P., Narula N., Callaghan M. U., Kaufman R. J., Fribley A. M. Disulfiram (Antabuse) activates ROS-dependent ER stress and apoptosis in oral cavity squamous cell carcinoma. J Clin Med. 8(5) (2019) 611. https://doi.org/10.3390/jcm8050611.

USC DE SANTIAGO DE COMPOSTELA

[16] Triscott J., Pambid M. R., Dunn S.E. Concise review: Bullseye: targeting cancer stem cells to improve the treatment of gliomas by repurposing disulfiram. Stem Cells 33(4) (2015) 1042-106. https://doi.org/10.1002/stem.1956.

[17] Lu C., Li X., Ren Y., Zhang X. Disulfiram: a novel repurposed drug for cancer therapy. Cancer Chemother Pharmacol. 87(2) (2021) 159–172. https://doi.org/10.1007/s00280-020-04216-8

[18] Mcmahon A., Chen W., Li F. Old wine in new bottles: Advanced drug delivery systems for disulfiram-based cancer therapy. J Control Release 319 (2020) 352–359. https://doi.org/10.1016/j.jconrel.2020.01.001

[19] Kannappan V., Ali M., Small B., Rajendran G., Elzhenni S., Taj H., Wang W., Dou Q. P. Recent advances in repurposing disulfiram and disulfiram derivatives as copper-dependent anticancer agents. Front Mol Biosci. 8 (2021) 741316. https://doi.org/10.3389/fmolb.2021.741316

[20] Xu B., Wang S., Li R., Chen K., He L., Deng M., Kannappan V., Zha J., Dong H., Wang W. Disulfiram/copper selectively eradicates AML leukemia stem cells in vitro and in vivo by simultaneous induction of ROS-JNK and inhibition of NF-κB and Nrf2. Cell Death Dis. 8(5) (2017) e2797. https://doi.org/10.1038/CDDIS.2017.176

[21] Li X., Xu F., He Y., Li Y., Hou J., Yang G., Zhou S. A hierarchical structured ultrafine fiber device for preventing postoperative recurrence and metastasis of breast cancer. Adv Funct Mater 30 (45) (2020) 2004851. https://doi.org/10.1002/adfm.202004851

[22] Meneguello J. E., Murase L. S., de Souza J. V. P., de Oliveira C. G., Ghiraldi-Lopes L. D., Teixeira J. J. V., Scodro R. B. de L., Ferracioli K. R. C., Siqueira V. L. D., Campanerut-Sá P. A. Z., Cardoso R. F. Systematic review of disulfiram as an antibacterial agent: what is the evidence?. Int J Antimicrob Agents 59(5) (2022) 106578. https://doi.org/10.1016/j.ijantimicag.2022.106578.

[23] Thakare R., Shukla M., Kaul G., Dasgupta A., Chopra S. Repurposing disulfiram for treatment of *Staphylococcus aureus* infections. Int J Antimicrob Agents 53(6) (2019) 709–715. https://doi.org/10.1016/j.ijantimicag.2019.03.024

[24] Xie C., Yan J., Cao S., Liu R., Sun B., Xie Y., Qu K., Zhang W., Weng Z., Wang Z. Bi-layered disulfiram-loaded fiber membranes with antibacterial properties for wound

dressing. Appl Biochem Biotechnol. 194(3) (2022) 1359–1372. https://doi.org/10.1007/s12010-021-03663-0

[25] Ramadhani N., Shabir M., McConville C. Preparation and characterisation of Kolliphor®P 188 and P 237 solid dispersion oral tablets containing the poorly water-soluble drug disulfiram. Int J Pharm. 475(1) (2014) 514–522. https://doi.org/10.1016/j.ijpharm.2014.09.013

[26] El Fawal G., Abu-Serie M. M., El-Gendi H., El-Fakharany E. M. Fabrication, characterization and in vitro evaluation of disulfiram-loaded cellulose acetate/poly(ethylene oxide) nanofiber scaffold for breast and colon cancer cell lines treatment. Int J Biol Macromol. 204 (2022) 555–564. https://doi.org/10.1016/j.ijbiomac.2022.01.145

[27] Wang P., Luo Q., Zhang L., Qu X., Che X., Cai S., Liu Y. A disulfiram / copper gluconate co-loaded bi-layered long-term drug delivery system for intraperitoneal treatment of peritoneal carcinomatosis. Colloids Surf. B 231 (2023) 113558. https://doi.org/10.1016/j.colsurfb.2023.113558

[28] Zhao J., Cui W. Functional electrospun fibers for local therapy of cancer. Adv Fiber Mater. 2 (2020) 229–245. https://doi.org/10.1007/s42765-020-00053-9

[29] El Fawal G., Abu-Serie M. M., Mo X., Wang H. Diethyldithiocarbamate/silk fibroin/polyethylene oxide nanofibrous for cancer therapy: Fabrication, characterization and in vitro evaluation. Int J Biol Macromol. 193 (2021) 293–299. https://doi.org/10.1016/j.ijbiomac.2021.10.039

[30] Han D., Serra R., Gorelick N., Fatima U., Eberhart C. G., Brem H., Tyler B., Steckl A. J. Multi-layered core-sheath fiber membranes for controlled drug release in the local treatment of brain tumor. Sci Rep. 9 (2019) 17936. https://doi.org/10.1038/s41598-019-54283-y

[31] Khodadadi M., Alijani S., Montazeri M., Esmaeilizadeh N., Younes S. S. Recent advances in electrospun nanofiber-mediated drug delivery strategies for localized cancer chemotherapy. J Biomed Mater Res A 108 (7) (2020) 1444–1458. https://doi.org/10.1002/jbm.a.36912

[32] Molina-Peña R., Ferreira N.H., Roy C., Roncali L., Najberg M., Avril S., Zarur M., Bourgeois W., Ferreirós A., Lucchi C., Cavallieri F., Hindré F., Tosi G., Biagini G.,

Valzania F., Berger F., Abal M., Rousseau A., Boury F., Alvarez-Lorenzo C., Garcion E. Implantable SDF-1α-loaded silk fibroin hyaluronic acid aerogel sponges as an instructive component of the glioblastoma ecosystem: Between chemoattraction and tumor shaping into resection cavities. Acta Biomater. 173 (2024) 261-282. https://doi.org/10.1016/j.actbio.2023.10.022.

[33] Sabarees G., Tamilarasi G. P., Velmurugan V., Alagarsamy V., Sibuh B. Z., Sikarwar M., Taneja P., Kumar A., Gupta, P. K. (2023). Emerging trends in silk fibroin-based nanofibers for impaired wound healing. J Drug Deliv Sci Technol. 79 (2023) 103994. https://doi.org/10.1016/j.jddst.2022.103994

[34] Kundu B., Rajkhowa R., Kundu S. C., Wang, X. Silk fibroin biomaterials for tissue regenerations. Adv Drug Deliv Rev. 65(4) (2013) 457–470. https://doi.org/10.1016/j.addr.2012.09.043

[35] Moisenovich M. M., Plotnikov E. Y., Moysenovich A. M., Silachev D. N., Danilina T. I., Savchenko E. S., Bobrova M. M., Safonova L. A., Tatarskiy V. V., Kotliarova M. S., Agapov I. I., Zorov D. B. Effect of silk fibroin on neuroregeneration after traumatic brain injury. Neurochemical Res. 44(10) (2019) 2261–2272. https://doi.org/10.1007/s11064-018-2691-8

[36] Qu Y., Sun X., Ma L., Li C., Xu Z., Ma W., Zhou Y., Zhao Z., Ma D. Therapeutic effect of disulfiram inclusion complex embedded in hydroxypropyl-β-cyclodextrin on intracranial glioma-bearing male rats via intranasal route. Eur J Pharm Sci. 156 (2021) 105590. https://doi.org/10.1016/j.ejps.2020.105590

[37] Matassoli F. L., Leão I. C., Bezerra B. B., Pollard R. B., Lütjohann D., Hildreth J. E. K., Arruda, L. B. de. Hydroxypropyl-beta-cyclodextrin reduces inflammatory signaling from monocytes: possible implications for suppression of HIV chronic immune activation. mSphere 3(6) (2018) 101128. https://doi.org/10.1128/msphere.00497-18

[38] Malanga M., Szemán J., Fenyvesi É., Puskás I., Csabai K., Gyémánt G., Fenyvesi F., Szente L. “Back to the Future”: A new look at hydroxypropyl beta-cyclodextrins. J Pharm Sci. 105(9) (2016) 2921–2931. https://doi.org/10.1016/j.xphs.2016.04.034

[39] Alvarez-lorenzo C., García-González C. A., Concheiro A. Cyclodextrins as versatile building blocks for regenerative medicine. J. Control. Release 268 (2017) 269–281. https://doi.org/10.1016/j.jconrel.2017.10.038

USC DE SANTIAGO DE COMPOSTELA

[40] Costoya A., Concheiro A., Alvarez-lorenzo C. Electrospun fibers of cyclodextrins and poly(cyclodextrins). Molecules 22(2) (2017) 230. https://doi.org/10.3390/molecules22020230

[41] Gonzalez-Prada I., Borges A., Santos-Torres B., Magariños B., Simões M., Concheiro A., Alvarez-Lorenzo C. Antimicrobial cyclodextrin-assisted electrospun fibers loaded with carvacrol, citronellol and cinnamic acid for wound healing. Int J Biol Macromol. 277 (2024) 134154. https://doi.org/10.1016/j.ijbiomac.2024.134154.

[42] Li H., Wang J., Wu C., Wang L., Chen Z. The combination of disulfiram and copper for cancer treatment. Drug Discov Today 25(6) (2020) 1099–1108. https://doi.org/10.1016/j.drudis.2020.04.003

[43] Jomova K., Makova M., Alomar S. Y., Alwasel S. H., Nepovimova E., Kuca K., Rhodes C. J., Valko M. Essential metals in health and disease. Chem Biol Interact. 367 (2022) 110173. https://doi.org/10.1016/j.cbi.2022.110173

[44] Rihel J. Copper on the brain. Nat Chem Biol. 14 (2008) 638–639. https://doi.org/10.1038/s41589-018-0089-1

[45] Chen L., Min J., Wang F. Copper homeostasis and cuproptosis in health and disease. Sig Transduct Target Ther. 7 (2022) 378. https://doi.org/10.1038/s41392-022-01229-y

[46] Lech T., Sadlik J. K. Copper concentration in body tissues and fluids in normal subjects of southern Poland. Biol Trace Elem Res. 118 (2007) 10–15. https://doi.org/10.1007/s12011-007-0014-z

[47] Scheiber I. F., Dringen R. Astrocyte functions in the copper homeostasis of the brain. Neurochemistry Int. 62 (2013) 556–565. https://doi.org/10.1016/j.neuint.2012.08.017

[48] Jin S., Ren L., Yang K. Bio-functional Cu containing biomaterials: A new way to enhance bio-adaption of biomaterials. J Mater Sci Technol. 32(9) (2016) 835–839. https://doi.org/10.1016/j.jmst.2016.06.022

[49] Oliveri V. Biomedical applications of copper ionophores. Coord Chem Rev. 422 (2020) 213474. https://doi.org/10.1016/j.ccr.2020.213474

USC UNIVERSIDADE DE SANTIAGO DE COMPOSTELA

[50] Moon O. J., Yoon C. J., Lee J. S., Kim H. H., Seol Y. H., Lee J. Tumor-specific release of copper-incorporated diethyldithiocarbamate from an optimized apoferritin scaffold enables both potent and safe anti-cancer therapy. Chem Eng J. 473 (2023) 145176. https://doi.org/10.1016/j.cej.2023.145176

[51] Lu M., Pais A., Vitorino R., Fortuna A., Vitorino C. Expediting disulfiram assays through a systematic analytical quality by design approach. Chemosensors 9 (2021) 172. https://doi.org/10.3390/chemosensors9070172

[52] Leão C., Borges A., Simões M. NSAIDs as a drug repurposing strategy for biofilm control. Antibiotics 9(9) (2020) 591. https://doi.org/10.3390/antibiotics9090591

[53] Wiegand C., Heinze T., Hipler U. C. Comparative in vitro study on cytotoxicity, antimicrobial activity, and binding capacity for pathophysiological factors in chronic wounds of alginate and silver-containing alginate. Wound Repair Regen. 17(4) (2009) 511–521. https://doi.org/10.1111/j.1524-475X.2009.00503.x

[54] McCarthy K.D., de Vellis J. Preparation of separate astroglial and oligodendroglial cell cultures from rat cerebral tissue. J Cell Biol 85 (3) (1980) 890–902. https://doi.org/10.1083/jcb.85.3.890

[55] Franken N.A., Rodermond H.M., Stap J., Haveman J., van Bree C. Clonogenic assay of cells in vitro. Nat Protoc. 1(5) (2006) 2315-9. https://doi.org/10.1038/nprot.2006.339

[56] Benkő B.M., Tóth G., Moldvai D., Kádár S., Szabó E., Szabó Z.I., Kraszni M., Szente L., Fiser B., Sebestyén A., Zelkó R., Sebe I. Cyclodextrin encapsulation enabling the anticancer repositioning of disulfiram: Preparation, analytical and in vitro biological characterization of the inclusion complexes. Int J Pharm. 657 (2024) 124187. https://doi.org/10.1016/j.ijpharm.2024.124187.

[57] Hua J., You H., Li X., You R., Ma L. Cu(II) ion loading in silk fibroin scaffolds with silk I structure. Int J Biol Macromol 158 (2020) 275–281. https://doi.org/10.1016/j.ijbiomac.2020.04.094

[58] Altman G. H., Diaz F., Jakuba C., Calabro T., Horan R. L., Chen J., Lu H., Richmond J., Kaplan D. L. Silk-based biomaterials. Biomaterials 24 (2003) 401–416. https://doi.org/10.1016/S0142-9612(02)00353-8.

[59] van Oss C. J., Chaudhury M. K., Good R. J. Monopolar surfaces. Adv Colloid Interf Sci. 28(C) (1987) 35–64. https://doi.org/10.1016/0001-8686(87)80008-8

[60] Cai S., Wu C., Yang W., Liang W., Yu H., Liu L. Recent advance in surface modification for regulating cell adhesion and behaviors. Nanotechnol Rev. 9 (1) 2020 971-989. https://doi.org/10.1515/ntrev-2020-0076

[61] Halcrow P. W., Khan N., Datta G., Ohm J. E., Chen X., Geiger J. D. Importance of measuring endolysosome, cytosolic, and extracellular pH in understanding the pathogenesis of and possible treatments for glioblastoma multiforme. Cancer Reports 2(6) (2019) 2–7. https://doi.org/10.1002/cnr2.1193

[62] Lammel A. S., Hu X., Park S., Kaplan D. L., Scheibel T. R. Controlling silk fibroin particle features for drug delivery. Biomaterials 31(16) (2010) 4583–4591. https://doi.org/10.1016/j.biomaterials.2010.02.024

[63] Qiao X., Miller R. Influence of pH on the surface and foaming properties of aqueous silk fibroin solutions. Soft Matter 16 (2020) 3695–3704. https://doi.org/10.1039/c9sm02372k

[64] Shen X., Sheng H., Zhang Y., Dong X., Kou L., Yao Q., Zhao X. Nanomedicine-based disulfiram and metal ion co-delivery strategies for cancer treatment. Int J Pharm X, 7 (2024) 100248. https://doi.org/10.1016/j.ijpx.2024.100248

[65] Haeili M., Moore C., Davis C. J. C., Cochran J. B., Shah S., Shrestha T. B., Zhang Y., Bossmann S. H., Benjamin W. H., Kutsch O., Wolschendorf, F. Copper complexation screen reveals compounds with potent antibiotic properties against methicillin-resistant *Staphylococcus aureus*. Antimicrob Agents Chemother 58 (2014) https://doi.org/10.1128/AAC.02316-13

[66] Liu P., Brown S., Goktug T., Channathodiyil P., Kannappan V., Hugnot J.P., Guichet P.O., Bian X., Armesilla A.L., Darling J.L., Wang W. Cytotoxic effect of disulfiram/copper on human glioblastoma cell lines and ALDH-positive cancer-stem-like cells. Br J Cancer. 107(9) (2012) 1488-97. doi: 10.1038/bjc.2012.442.

[67] Chen D., Cui Q.C., Yang H., Dou Q.P. Disulfiram, a clinically used anti-alcoholism drug and copper-binding agent, induces apoptotic cell death in breast cancer cultures and xenografts via inhibition of the proteasome activity. Cancer Res. 66(21) (2006) 10425-33. https://doi.org/10.1158/0008-5472.CAN-06-2126.

[68] Westhoff M.A., Zhou S., Nonnenmacher L., Karpel-Massler G., Jennewein C., Schneider M., Halatsch M.E., Carragher N.O., Baumann B., Krause A., Simmet T., Bachem M.G., Wirtz C.R., Debatin K.M. Inhibition of NF-κB signaling ablates the invasive phenotype of glioblastoma. Mol Cancer Res. 11(12) (2013) 1611-23. https://doi.org/10.1158/1541-7786.MCR-13-0435-T

USC
UNIVERSIDADE DE SANTIAGO DE COMPOSTELA

# V. GENERAL DISCUSSION

USC
UNIVERSIDADE
DE SANTIAGO
DE COMPOSTELA

USC
UNIVERSIDADE
DE SANTIAGO
DE COMPOSTELA

# V. GENERAL DISCUSSION

This PhD Thesis highlights the opportunities offered by the electrospinning technique in the biomedical field, exemplified in the approach to two different disease conditions such as chronic wound infection and GBM. The development of chronic wound infection begins with a physical or chemical disruption (e.g., cut, fall, or burn) of the normal tissue that must be repaired, tiggering a coordinated process (i.e., homeostasis, inflammation, proliferation and remodelling) to immediately restore normal function [1]. However, in some cases this cascade fails due to several factors, events, and comorbidities, including the severity of the damage, chronic diseases, habits, interactions with specific medications or the age of the patient, preventing proper wound healing and promoting bacterial colonization, the absence of immune response or the failure of fibroblast and platelet activity [2]. Bacterial colonization is one of the most dramatic and worring events in wound healing failure due to the current alarming situation of AMR, being a global health crisis with 1.7 million of deaths in 2019 and surpassing cancer by 2050 with an expectation of 10 million deaths [3,4] Several factors caused this alarming scenario, the main factor being the misuse and overuse of antibiotics. These bad practices during the last decades have led to a significant reduction of the current therapeutic arsenal available, with research and development of new approaches being essential to combat the terrible group called ESKAPE and its superbugs [5,6].

One of the most promising approaches is the use of EOCs to prevent biofilms and treat different varieties of infections. Plant-derived EOCs are composed by mixtures of terpenes, terpenoids, phenylpropanoids and other molecules that provide to EOCs of antimicrobial activity and the other multi-target effects including antioxidant, angiogenic, and anti-inflammatory [7]. However, EOCs are labile and volatile compounds with low water solubility, which makes their use difficult [8]. To address these limitations, fiber mats loaded with EOCs carvacrol, citronellol and cinnamic acid within a PCL matrix were prepared using a uniaxial electrospinning technique. To prepare PCL fibers, it was

USC DE COMPOSTELA

essential to set the optimal concentration of PCL in a mixture of two protic polar solvents such as THF and DMF. The use of these solvents allows obtaining continuous, homogeneous, smooth fibers without undesirable beads, and dissolving large amounts of the three EOCs for their subsequent encapsulation into the formed fibers. Despite the high amount loaded and the good morphology obtained with interlocking pores exhibited by this type of electrospun mats, hardly any antimicrobial activity was recorded except for fibers loaded with citronellol and cinnamic acid at concentrations equal to or higher than 20% (w/v). Thus, a new approach was applied to reduce the amount of essential oil components and increase the antimicrobial activity. Thus, two different types of cyclodextrins were added to the polymeric solution, obtaining uneven results. Electrospun mats with αCD hardly improved the antimicrobial results but reinforced the mechanical properties of the fibers due to the formation of poly(pseudo)rotaxanes with long PCL chains. In contrast, HPβCD formed inclusion complexes with EOCs, reinforcing the antimicrobial properties due to an increase in the apparent solubility of these hydrophobic natural compounds. In this regard, PCL/HPβCD fibers loaded with carvacrol showed strong antimicrobial activity (> 3 log CFU/mL) against *S. aureus* and *P. aeruginosa*; citronellol alone displayed significant antimicrobial activity (1-3 log CFU/mL) against *S. aureus*; and cinnamic acid showed strong antimicrobial activity against S. aureus at different concentrations. The inclusion complexes formed between the EOCs and HPβCD enhanced the morphology of fibers, changed the release profile, and increased the amount of EOCs released. Furthermore, electrospun mats of carvacrol and cinnamic acid displayed antioxidant and angiogenic activity. All fibers prepared in this first part of the Thesis proved to be hemocompatible and exhibited excellent integration and biocompatibility in the in ovo test.

Overall, the first chapter of this Thesis highlights the performance of electrospun mats loaded with different essential oil components as active wound dressings. Thereby, the use of PCL as the main structural polymer allowed encapsulating a large amount of cyclodextrins and a variety EOCs, and conferred good mechanical properties and controlled release. The use of cyclodextrins was essential to improve the antimicrobial activity of EOCs through an increase in solubility and release rate, significatively reducing the MIC and MBC of EOCs [9]. An appropriate pre-selection of EOCs is indispensable to obtain a significant antimicrobial response. For biomedical purposes, EOCs with purity above 95% are preferable compared to plant extracts since few

USC UNIVERSIDADE

substances in the extract have antimicrobial properties and the other components could interfere with the encapsulation of the desirable active compounds. Furthermore, the physicochemical properties of EOCs *(i.e.*, structure, molecular weight and their functional groups, density, solubility in a variety of solvents, Log P, boiling and melting point, viscosity, macroscopic properties such liquid or solid, colour, odour, pH or osmotic pressure) are involved in several aspect such as possible interactions with solvents and polymer matrix, encapsulation efficiency and formation of inclusion complexes with the different cyclodextrins, and antimicrobial properties (low MIC and MBC), which are aspects that should be analysed in detail before the electrospun mats preparation.

The electrospun fibers prepared in this PhD Thesis could be a good alternative to traditional wound dressings, as the antimicrobial activity (reaching 99.99% of bacterial reduction or 4 log CFU/mL) was comparable with that of common commercially available products to treat infected wounds, such as those incorporating silver ions, namely Algicell™, PolyMem® Silver Non-Adhesive Pads, and PolyMem® Silver Shapes [10]. However, the available wound dressings only offer antimicrobial activity, without additional help to the skin regeneration process that is essential to prevent recurrence. The prepared electrospun mats demonstrated a variety of advantages in the different steps of wound healing, such as antioxidant activity, which prevents an exacerbated anti-inflammatory response and hinders the cascade of ROS species or macrophages response, and angiogenic activity in wound area. These two properties are vital in the homeostasis, anti-inflammatory and proliferation phases, which begin in the first 24 hours after injury and involve several process and mechanisms, including cell migration (e.g., platelets, neutrophils, macrophages, fibroblast, or keratinocytes), and the delivery of a variety of peptides, nutrients, gases and growth factors. In general, commercial wound dressings prevents wound wettability and transpiration, trapping exudates and hindering gas exchange due to the lack of a large pore network. Therefore, the use of electrospun mats is a suitable alternative to avoid these worrying deficiencies.

Comparing the developed EOC-loaded electrospun mats with those prepared by other researchers is a difficult task because each publication shows different ways to evaluate antimicrobial, biocompatibility and regenerative properties. However, there is a certain tendency to perform some tests or use some substances. Plant extracts and mixtures of synthetic and natural polymeric excipients, uniaxial electrospinning, antimicrobial tests by disk diffusion, and fibroblasts for cytotoxicity assessment are

USC DE SANTIAGO DE COMPOSTELA

common options in many publications, as summarized in **Table 1.1**. The use of plant extracts obtained by researchers themselves in their respective laboratories could be disadvantageous due to difficulties in replicating the plant source and extraction process in other laboratories; batch variability due to limited and unknown origin of the source, low traceability and lack of resources for correct application of GMP; and presence of impurities or uninteresting molecules with low or different activity. In this Thesis, the three essential oil components used were acquired from recognized chemical companies with high quality standards of production that reduce the disadvantages addressed above. According to other researchers, the use of synthetic polymers such as PCL remains a good option due to the various properties and advantages it offers, namely, high encapsulation ratio, controlled release, reproducibility and low variability, excellent mechanical properties (i.e., strength and flexibility), easy adjustment to increase precision to treat only the damaged area, comfort, avoiding material discard, great biocompatibility and low immunogenic response, as well as easy removal due to strength and low degradation in contact with water, enzymatic activity, and pH, temperature, and pressure changes that the tissue undergoes throughout the wound healing process and bacterial colonization [11, 12].

Another important aspect that follows the same direction as other publications is the choice of uniaxial electrospinning compared to other approaches to prepare EOCs-loaded products. The fibers were prepared using a uniaxial approach to obtain mats with a monolithic structure and the three essential oil components share with PCL a high hydrophobicity, facilitating the encapsulation process. Thus, uniaxial electrospinning was the best choice to accomplish all the predetermined aims in a simpler way than other approaches namely, coaxial, triaxial or Janus electrospinning, which are the most used when incompatibility between polymers, solvents, active agents or other compounds is observed. However, the antimicrobial test performed in this Thesis diverges compared to the most widely reported technique which is the disk diffusion assay. This test only offers qualitative results, while the CFU count is a quantitative test that provides more information and facilitates the comparison with other formulations. Only three reports recorded in **Table 1.1**. expressed their results in CFU/mL. The first formulation used polyurethane loaded with Nigella sativa, inoculating the fibers with 3.8 - $4\times10^5$ of *S. aureus* and *E. coli.* After 24 hours, the fibers showed $3.7\times10^4$ CFU/mL of *S. aureus* and $1.7\times10^4$ CFU/mL of *E.coli* [13]. The second formulation used cellulose acetate and

USC UNIVERSIDADE DE SANTIAGO

chitosan loaded with eucalyptus oil, inoculated with 1 log CFU/mL of *S. aureus*. After 24 hours, the fiber control showed a 3 log CFU/mL and the EOC fiber reached 0 log CFU/mL [14]. The last formulation used PLA and chitosan loaded with black paper oil and limonene, inoculated with $1\times10^7$- $1\times10^8$ of *S. aureus* and *P. aeruginosa*. After 24 hours, the fibers incorporating chitosan and black pepper displayed a 1 log reduction for both species tested, and the formulation without chitosan showed 1.5 log reduction against *S. aureus* whilst no log reduction was observed against *P. aeruginosa*. Meanwhile, the formulation with chitosan and limonene showed less than 1 log reduction against *S. aureus* and no log reduction against *P. aeruginosa* and the formulations without chitosan displayed no log reduction for both bacterial species. In this case, the incorporation of chitosan enhanced the antimicrobial activity of the fibers compared to the single PLA matrix fibers (control), reaching 3 - 5 log reduction against *S. aureus* and non-differences were shown for *P. aeruginosa*. The results reported in those three publications demonstrate the complexity to achieve strong antimicrobial activity using plant extracts or EOCs while showing good biocompatibility. Overall, the first part of the Thesis showed the possibility of obtaining strong antimicrobial performance against *S. aureus* and *P. aeruginosa* with an appropriate selection of essential oil components, taking advantage of other key properties for wound healing such as antioxidant and antimicrobial ones. In particular, the incorporation of encapsulating agents such as cyclodextrins is a crucial aspect to overcome the poor physicochemical properties of EOCs. Furthermore, polymers and solvents play an important role to obtain adequate encapsulation and desirable controlled release of the active agents. The results obtained in the Thesis encourage the use of EOC-loaded electrospun mats to prevent and treat chronic wound infections.

The second part of this PhD Thesis focussed on GBM, a highly aggressive brain tumor, characterized by rapid progression, invasiveness, and poor prognosis. GBM represents approximately 49% of all primary brain tumors with an incidence rate of 4.6 per 100,000 inhabitants, affecting human adults aged 45 to 75 years [15,16]. Currently, the therapeutic arsenal is insufficient, with temozolomide (TMZ) in combination with radiotherapy after a surgical resection being the standard treatment [17,18] . Therapeutic advances of the last century have had little significant impact on survival rate, as is the case of Gliadel® (carmustatine wafer), a local intracranial implant that increases overall survival by approximately 2 months and has several limitations associated with hard

USC UNIVERSIDADE DE SANTIAGO

handling, a high probably of developing meningitis and edema, and interference with imaging [19,20]. In recent years, few products have been approved, including Avastin®, with the monoclonal antibody bevacizumab, and NovoTTF-100A System™, an antimitotic agent that generates Tumor Treating Fields (TTFields)[21]. Thereby, only two new approaches reached healthcare systems, highlighting the difficulty of discovering and developing new treatments against this cancer.

Consequently, in the second part of this PhD Thesis, the formulation of DSF, a repurposed drug, was explored. DSF is an inhibitor of alcohol dehydrogenase isoform-1A3 (ALDH1A3) for the treatment of alcohol dependence under the name Antabuse® [22]. Several publications have demonstrated potential new properties of DSF, highlighting the anticancer and antimicrobial activities due to the chelating property and the different bacterial targets that this drug shows [23] Drug repurposing is increasingly being explored due to the multiple advantages it offers. Repurposing consists of identifying new indications for clinically approved drugs, maximizing the therapeutical properties that could be offered at first moment. The main advantages of repurposed drugs include well-established safety profiles and a shortened (3-5 years) drug development process, which allows new therapeutical alternatives to be clinically available in a short period of time [24]. Furthermore, DSF showed selective tumor activity in vitro due to the copper-dependent antitumor effect, limiting tumor metastasis, restricting angiogenesis, and avoiding drug resistance and treatment failure. However, DSF displayed several disadvantages that limit its practical use such as low water solubility (0.2 mg/mL), high lipophilicity (logP 4.16), physiological instability, and short plasma half-life (ca. 7 h) [25]. Therefore, the aim was to develop a locally implantable electrospun mat that can be placed into the resection cavity. Freeze-dried SF was chosen as the main matrix of the fibers due to its electrospinnability forming continuous, homogeneous, smooth fibers without beads when HFIP is used as a solvent. High concentrations of DSF could be loaded inside the polymeric matrix, displaying a sustained release due to the hydrophobic properties of the β-sheet conformation of SF after freeze-drying. Moreover, this conformation endowed the fibers with strong mechanical properties, comparable to those achieved with the synthetic polymer PCL used in the first part of the Thesis. However, fibers prepared with SF in the absence of other excipients showed hardly any antimicrobial and anticancer activity, reaching a slightly antimicrobial activity (0.5 log CFU/mL reduction) and no antitumor activity (95% of GL261 cell viability), only with

USC UNIVERSIDADE

the exception of the electrospun mat loaded with low amounts of DSF that displayed a significant anticancer activity (40% of GL261 cell viability).

To enhance the antimicrobial and anticancer activities, two approaches were explored: incorporation of HPβCD and/or CuCl2. The selection of this type of cyclodextrin was due to its ability to form inclusion complexes and the remarkable acceleration of the release observed in the first part of the Thesis. It should be noted that the molecular structure and physicochemical properties (*e.g.,* lipophilicity and molecular weight) of DSF are similar to those of EOCs. As hypothesized, incorporation of HPβCD enhanced the antimicrobial and antitumor activities of electrospun mats, reaching strong antimicrobial activity 4.5 log CFU/mL reduction against *S. aureus* and 5.5 log CFU/mL reduction against *P. aeruginosa* and significant anticancer activity (less than 25% of GL261 cell viability). Furthermore, the incorporation of HPβCD was essential to increase the amounts of DSF released and the surface polarity of the fibers which improved the wettability by physiological medium. However, the high concentrations of DSF detected could have detrimental effects on biocompatibility. Reducing the amount of DSF loaded and released without a drastic reduction in antimicrobial and anticancer activity was essential to obtain an optimal implantable electrospun mat, avoiding potential side effects. Therefore, $CuCl_2$ was added to the polymer solution to take advantage of the chelating properties of DSF and form in situ the desirable $Cu(DDC)_2$. The incorporation of $CuCl_2$ became a difficult challenge due to the insolubility in HFIP, which forced the use of DMF as a cosolvent and the reduction of SF to minimize cross-linking. Interestingly, these changes positively affected the formation of the fibers, causing a reduction in the size down to nanometer scale without compromising mechanical properties. Additionally, this type of fibers showed the ability to form $Cu(DDC)_2$ in the aqueous medium and released high amounts of DSF at the same time. As a result, significant antimicrobial activity was obtained. Ultimately, all proposed objectives were met, supporting the use of DSF as a promising active compound to treat GBM in combination with other approaches such as the use of cyclodextrin or molecules with Cu(II) ions to enhance antimicrobial and anticancer activity. The antimicrobial properties displayed by DSF against *S. aureus* and *P. aeruginosa* could prevent nosocomial infections in the resection cavity (e.g., meningitis), avoiding the use of antibiotics and thus reducing the selective pressure and AMR.

USC UNIVERSIDADE DE SANTIAGO DE COMPOSTELA

If the electrospun mats developed in the second part of the PhD Thesis are compared with previous publications on the use of the electrospinning technique to prepare a local therapy to treat GBM in animal models, several conclusions can be drawn. Most of the electrospun mats mentioned in **(Table 1.2.)** were loaded with commonly used drugs in cancer therapy such as PTX, BCNU, TMZ, and DOX, as the active agent alone or in combination with RNA derivatives, proteins, factors or other active molecules. Moreover, the vast majority of publications used synthetic polymers (*e.g.,* PCL, PLGA, or PLA) as a main components to obtain sustained release. All electrospun mats were prepared using uniaxial electrospinning, which remains the gold standard technique for the preparation of various types of fibers (monolithic, blend or emulsion). Although all electrospun mats showed good results and improved the survival rate of animals, most publications omitted essential aspects such as tissue repair analysis, local antimicrobial activity, and cost-effectiveness. Meanwhile, our electrospun mats were developed using a natural polymer SF to take advantage of wound healing properties. The repurposed drug DSF, which exhibits selective anticancer and antimicrobial properties, is relatively inexpensive, and the obtained fibers are biodegradable; the degradation components can be reused by the healthy cells to restore the missing tissue.

Both parts of the PhD Thesis have their similarities and differences depending on the requirements of each application. At first glance, GBM and chronic wounds are completely different diseases in terms of origin, prevalence, therapeutical arsenal and survival rates. However, a deeper study of the two diseases reveals certain similarities such as being diseases with unmet clinical demands due to unstoppable agents (bacteria and cancer cells) that offer great resistance to the available active ingredients through mechanisms that trick the immune system and develop survival strategies including barriers such as the tumor extracellular matrix and biofilm construct, and ability to transform the environment (*i.e.*, resistance to pH and temperature changes, modification of pH and pressure, fast response to decreased nutrients, salts or gases, secretion of enzymes and other molecules for create new vessels or cause debridement to secure nutrients and dissemination).

The two types of active compounds used in this Thesis have analogous advantages and disadvantages. For instance, EOCs have traditionally been used in perfumes and as food additives to improve the odour and tasty properties, whereas disulfiram is approved for the treatment of alcoholism. Thereby, these compounds had different initial

USC DE SANTIAGO DE COMPOSTELA

indications, but new properties were found, such as antimicrobial, angiogenic and antioxidant properties for EOCs, and antimicrobial and antitumor activity for DSF. EOCs are obtained from plant extract, while disulfiram is a synthetic compound. As natural compounds, EOCs have the advantages of an unlimited and environmentally friendly source and multitasking activity (*e.g.,* anti-inflammatory, angiogenic, antioxidant, antibacterial and antifungal properties)[26]. However, natural sources have several limitations, such as difficult control of impurities, large batch variability, stationary production (depending on ripening and harvesting time), and low traceability. On the other hand, synthetic compounds such as disulfiram overcome the disadvantages presented by natural compounds, displaying high purity rates (> 99%), equal batches, sustained production throughout the year, and high traceability. However, synthetic compounds exhibit a variety of disadvantages, namely, newer products have a high production cost associated to qualified staff, appropriate installations, expensive software programs, equipment and techniques, or high initial investment. Notably, the active agents used in this Thesis have two points in common, both exhibited a variety of properties due to multi-target activities and both have poor physicochemical properties (*i.e.,* low water solubility, low stability, and high lipophilicity) [25,27]. Likewise, two different polymers were selected for preparing both electrospun mats considering the main requirements of the intended applications. Thus, a synthetic polymer PCL was selected as main structural compound of fibers for treating chronic wounds because the application area suffers high stress forces and demands sustained release for at least 24 hours (a critical lapse time for a wound management), low degradability under various conditions (*e.g*., pH changes or enzymatic degradation) to preserve the characteristics and shape of the electrospun mats, and biocompatibility in direct contact with exudates, blood and soft tissues [12]. Nevertheless, PCL is a polymer with a long decomposition time (approximately 1-3 years) and lack of stimulation of wound healing, which could limited its application to other therapies. On the other hand, the natural polymer silk fibroin was selected for treating GBM after surgical resection due to optimal degradability rate (approximately 6 months) avoiding a second removal surgery, and its intrinsic bioactivities *(e.g.,* anti-inflammatory, hemostatic, neuroprotective, restorative neurological and regenerative nerve process activities, and promotion of cell growth and migration, neo-vascularization, and re-epithelialization), robust mechanical strength and toughness and easy polarity switching due to the alpha or beta conformation. However, using silk fibroin was a difficult challenge due to the limitation in suitable solvents, being

USC DE COMPOSTELA

restricted to formic acid and HFIP for dissolving silk fibroin in β-sheet conformation; high susceptibility to environmental changes, causing morphological modifications of the fibers; and the need to apply a freeze-drying process to the supplied silk fibroin aqueous solution to avoid undesirable variability between batches. As noted above, all advantages and disadvantages described for synthetic and natural active agents could apply to the two selected polymers.

The incorporation of cyclodextrins to encapsulate the active compounds was essential to improve the solubility and increase the amounts loaded and released for both electrospun mats. In both types of fibers, HPβCD demonstrated several advantages, including high encapsulation efficiency for different agents with different origin, chemical structure, solubility, lipophilicity and molecular weight; great versatility and affinity for different organic solvents (*i.e.,* DMF and HFIP); improvement of wettability and change of hydrophobicity; modification of mechanical properties; remarkable increase of the amounts of active compounds released in aqueous medium; and change of release profiles obtaining a desirable initial burst. As a result of these changes, both electrospun formulations experienced remarkable antimicrobial activity with a significant reduction of amounts of active compounds, leading to a substantial enhancement of biocompatibility and toxicity profile.

In this Thesis, the technique used to prepare the electrospun mats was uniaxial electrospinning. Uniaxial electrospinning was the first and the simplest, versatile, and easy to handle and operate, requiring only a syringe pump, a high-voltage power supply, a single metallic blunt needle, and a collector for the optimal performance [28]. Furthermore, this technique allows preparing fibers using a monolithic or blended polymeric matrix dissolved in a single solvent or in a mixture of different ones. Uniaxial electrospinning is particularly suitable for laboratory use (i.e., less complex setup and low production) with high reproducibility, easy optimization of different conditions and useful to explore the spinnability of new matters and combinations [29]. According to the literature, this technique displays great versatility: a variety of different organic or inorganic compounds could be used, such as a synthetic polymer PCL and a natural polymer SF dissolved in a single solvent or in a mixture of solvents THF, THF/DMF, HFIP and HFIP/DMF to prepare blend matrix fibers. Uniaxial electrospinning also allows the incorporation of various and large amounts of cyclodextrins within the polymeric matrix without modifying the fiber structure. Furthermore, various and large amounts of

USC DE SANTIAGO DE COMPOSTELA

active compounds with different origin, properties and characteristic can be successfully encapsulated, obtaining different release profiles (*i.e.*, sustained, controlled, burst, and biphasic release). Particularly, the technique allowed loading large amounts of copper chloride, an inorganic salt that interacts with silk fibroin, tiggering conformational changes that affect to the morphology and the mechanical properties of the fiber, and that form chelates with disulfiram enhancing its anticancer and antimicrobial activities.

In both parts of the Thesis, continuous, homogeneous, smooth and bead-free fibers were obtained despite using a variety of materials with different physicochemical properties, prepared in a long-time span, and showing high reproducibility. Likewise, several mechanical and surface properties were recorded demonstrating the versatility and easy modification of these properties with simple changes in the amounts of the different components and electrospinning parameters. Another essential aspect was the ease of handling and adjustment, as different shapes and sized were required depending on the test. As shown throughout the Thesis, the square shape was used for the release, antioxidant, hemolysis, and antimicrobial tests; the rectangle shape was used for the mechanical and contact angle tests; and the circular shape was used for the in ovo and antitumor activity tests. Ultimately, this Thesis confirmed the multiple advantages of using the electrospinning technique, including high loading capacity, high encapsulation efficiency, high surface-to-volume ratio, simultaneous release of several active agents, adjustable porosity, malleability to conform scaffolds of different sizes and shapes, easy handling and reliability, reproducibility, and cost-effectiveness [30,31].

Although both electrospun mats were designed for different applications and diseases, it was possible to compare different outcomes obtained in the same tests prepared in both chapters. The EOC-loaded electrospun mats exhibited mild to significant antimicrobial activity due to the high MIC and MBC values shown by each essential oil component, while the electrospun mats incorporating inclusion complexes with HPβCD showed strong antimicrobial activity. Likewise, similar results were obtained in the case of DSF due to the high MIC and MBC shown by this repurposed drug. In both cases, it was essential to use more than 5% (w/v) of active compound and more than 7% (w/v) of HPβCD to reach strong antimicrobial activity and exceed 3 log CFU/mL decrease of *S. aureus* and *P. aeruginosa*. Despite the high amounts loaded and released, both electrospun mats exhibited good hemocompatibility and the possibility of using the active

USC DE SANTIAGO DE COMPOSTELA

compound at 5% (w/v) and an equal molar rate of HPβCD to reinforce the therapeutic activities of the tested active ingredients.

Overall, this Thesis demonstrates the feasibility of using a variety of EOCs to achieve strong antimicrobial response and take advantage of other invaluable properties such as antioxidant and angiogenic activity for the healing of chronic wounds. In this way, it will be possible to reduce the selective pressure produced by current antibiotics in healthcare systems worldwide and reduce the expected deaths due to dreaded AMR. On the other hand, this Thesis fulfilled one of the most important objectives proposed, namely, to develop a new approach that could reverse the dramatic situation faced by GBM patients due to the limited arsenal of available therapies. To this end, a molecule used for treating alcoholism dependence was selected, demonstrating the multiple possibilities and benefits of repositioning. Disulfiram showed significant anticancer and antimicrobial activities after the optimization of the electrospun formulations. Incorporation of cyclodextrins for tuning the release profiles and Cu(II) ions for improving the anticancer and antimicrobial activities of disulfiram were revealed to be highly beneficial. In short, the electrospinning technique, together with the optimization of compositions, is positioned as a century-old technique with a bright future to address the numerous health challenges existing in the biomedical field.

USC
UNIVERSIDADE DE SANTIAGO DE COMPOSTELA

# REFERENCES

USC
UNIVERSIDADE
DE SANTIAGO
DE COMPOSTELA

USC
UNIVERSIDADE
DE SANTIAGO
DE COMPOSTELA

## References

[1] L. M. Morton and T. J. Phillips, “Wound healing and treating wounds Differential diagnosis and evaluation of chronic wounds,” J. Am. Acad. Dermatol., vol. 74, no. 4, pp. 589–605, 2016, doi: 10.1016/j.jaad.2015.08.068.

[2] B. A. Mast and G. S. Schultz, “Interactions of cytokines, growth factors, and proteases in acute and chronic wounds,” Wound Repair Regen., vol. 4, no. 4, pp. 411–420, 1996, doi: 10.1046/j.1524-475X.1996.40404.x.

[3] C. J. Murray et al., “Global burden of bacterial antimicrobial resistance in 2019: a systematic analysis,” Lancet, vol. 399, no. 10325, pp. 629–655, 2022, doi: 10.1016/S0140-6736(21)02724-0.

[4] J. O’Neill, “Tackling Drug-Resistance Infections Globally: Final Report and Recommendations. The review on Antimicrobial Resistance Chaired by Jim O'Neill.[Online …,” no. May, pp. 1–84, 2016, [Online]. Available: https://amr-review.org/sites/default/files/160518_Final paper_with cover.pdf

[5] S. K. Ahmed et al., “Antimicrobial resistance: Impacts, challenges, and future prospects,” J. Med. Surgery, Public Heal., vol. 2, no. March, p. 100081, 2024, doi: 10.1016/j.glmedi.2024.100081.

[6] W. R. Miller and C. A. Arias, “ESKAPE pathogens: antimicrobial resistance, epidemiology, clinical impact and therapeutics,” Nat. Rev. Microbiol., vol. 22, no. 10, pp. 598–616, 2024, doi: 10.1038/s41579-024-01054-w.

[7] J. S. Raut and S. M. Karuppayil, “A status review on the medicinal properties of essential oils,” Ind. Crops Prod., vol. 62, pp. 250–264, 2014, doi: https://doi.org/10.1016/j.indcrop.2014.05.055.

[8] A. El Asbahani et al., “Essential oils: From extraction to encapsulation,” Int. J. Pharm., vol. 483, no. 1–2, pp. 220–243, 2015, doi: 10.1016/j.ijpharm.2014.12.069.

[9] K. J. Figueroa-Lopez et al., “Development of electrospun active films of poly(3-hydroxybutyrate-co-3-hydroxyvalerate) by the incorporation of cyclodextrin inclusion complexes containing oregano essential oil,” Food Hydrocoll., vol. 108, no. January, 2020, doi: 10.1016/j.foodhyd.2020.106013.

USC UNIVERSIDADE DE SANTIAGO DE COMPOSTELA

[10] M. H. Cavanagh, R. E. Burrell, and P. L. Nadworny, “Evaluating antimicrobial efficacy of new commercially available silver dressings,” Int. Wound J., vol. 7, no. 5, pp. 394–405, 2010, doi: 10.1111/j.1742-481X.2010.00705.x.

[11] R. S. Tiğli, N. M. Kazaroğlu, B. Maviş, and M. Gumusderelioglu, “Cellular behavior on epidermal growth factor (EGF)-immobilized PCL/gelatin nanofibrous scaffolds,” J. Biomater. Sci. Polym. Ed., vol. 22, no. 1–3, pp. 207–223, 2011, doi: 10.1163/092050609X12591500475424.

[12] K. Las Heras, M. Igartua, E. Santos-Vizcaino, and R. M. Hernandez, “Chronic wounds: Current status, available strategies and emerging therapeutic solutions,” J. Control. Release, vol. 328, no. September, pp. 532–550, 2020, doi: 10.1016/j.jconrel.2020.09.039.

[13] C. Aras, E. Tümay Özer, G. Göktalay, G. Saat, and E. Karaca, “Evaluation of Nigella sativa oil loaded electrospun polyurethane nanofibrous mat as wound dressing,” J. Biomater. Sci. Polym. Ed., vol. 32, no. 13, pp. 1718–1735, 2021, doi: 10.1080/09205063.2021.1937463.

[14] N. A. Elbhnsawi et al., “Nano-Chitosan/Eucalyptus Oil/Cellulose Acetate Nanofibers: Manufacturing, Antibacterial and Wound Healing Activities,” Membranes (Basel)., vol. 13, no. 6, 2023, doi: 10.3390/membranes13060604.

[15] O. Visser et al., “Survival of adults with primary malignant brain tumours in Europe ; Results of the EUROCARE-5 study,” pp. 2231–2241, 2015, doi: 10.1016/j.ejca.2015.07.032.

[16] D. Abdelnabi et al., “Local administration of irinotecan using an implantable drug delivery device stops high-grade glioma tumor recurrence in a glioblastoma tumor model,” Drug Deliv. Transl. Res., vol. 14, no. 11, pp. 3070–3088, 2024, doi: 10.1007/s13346-024-01524-x.

[17] M. Weller et al., “Glioma,” Nat. Rev. Dis. Prim., vol. 1, no. July, 2015, doi: 10.1038/nrdp.2015.17.

[18] K. J. Wolf, J. Chen, J. D. Coombes, M. K. Aghi, and S. Kumar, “Dissecting and rebuilding the glioblastoma microenvironment with engineered materials,” Nat. Rev. Mater., vol. 4, no. 10, pp. 651–668, 2019, doi: 10.1038/s41578-019-0135-y.

[19] C. Y. Foo et al., “Medical Device Advances in the Treatment of Glioblastoma,” Cancers (Basel)., vol. 14, no. 5341, pp. 1–33, 2022, doi: https://doi.org/10.3390/cancers14215341.

[20] T. Iqbal et al., “Frontiers in the treatment of glioblastoma : Past , present and emerging,” Adv. Drug Deliv. Rev., vol. 171, pp. 108–138, 2021, doi: 10.1016/j.addr.2021.01.012.

[21] D. Lenz, M. Ries, and P. Johann, “The drug development pipeline for glioblastoma—A cross sectional assessment of the FDA Orphan Drug Product designation database,” PLoS One, vol. 16, no. 7 July, pp. 1–14, 2021, doi: 10.1371/journal.pone.0252924.

[22] B.-M. Benkő, D. A. Lamprou, A. Sebestyén, R. Zelkó, and I. Sebe, “Clinical, pharmacological, and formulation evaluation of disulfiram in the treatment of glioblastoma - a systematic literature review,” Expert Opin. Drug Deliv., vol. 20, no. 4, pp. 541–557, Apr. 2023, doi: 10.1080/17425247.2023.2190581.

[23] B. J. Mason and C. J. Heyser, “A LCOHOL U SE D ISORDER : T HE R OLE OF M EDICATION IN R ECOVERY,” vol. 41, no. 1, pp. 1–17, 2021.

[24] F. Ragucci et al., “Insights into Healthcare Professionals ’ Perceptions and Attitudes toward Nanotechnological Device Application : What Is the Current Situation in Glioblastoma Research ?,” Biomedicines, vol. 11, p. 1854, 2023, doi: https://doi.org/10.3390/ biomedicines11071854 Academic.

[25] N. Ramadhani, M. Shabir, and C. McConville, “Preparation and characterisation of Kolliphor®P 188 and P 237 solid dispersion oral tablets containing the poorly water soluble drug disulfiram,” Int. J. Pharm., vol. 475, no. 1, pp. 514–522, 2014, doi: 10.1016/j.ijpharm.2014.09.013.

[26] F. Nazzaro, F. Fratianni, and L. De Martino, “Effect of Essential Oils on Pathogenic Bacteria,” pp. 1451–1474, 2013, doi: 10.3390/ph6121451.

[27] S. Chouhan, K. Sharma, and S. Guleria, “Antimicrobial Activity of Some Essential Oils—Present Status and Future Perspectives,” Medicines, vol. 4, no. 3, p. 58, 2017, doi: 10.3390/medicines4030058.

USC UNIVERSIDADE DE SANTIAGO DE COMPOSTELA

[28] N. Bhardwaj and S. C. Kundu, “Electrospinning: A fascinating fiber fabrication technique,” Biotechnol. Adv., vol. 28, no. 3, pp. 325–347, 2010, doi: 10.1016/j.biotechadv.2010.01.004.

[29] A. Keirouz, Z. Wang, V. S. Reddy, and Z. K. Nagy, “The History of Electrospinning : Past , Present , and Future Developments,” vol. 2201723, pp. 1–34, 2023, doi: 10.1002/admt.202201723.

[30] S. Chakraborty, I. C. Liao, A. Adler, and K. W. Leong, “Electrohydrodynamics: A facile technique to fabricate drug delivery systems,” Adv. Drug Deliv. Rev., vol. 61, no. 12, pp. 1043–1054, 2009, doi: 10.1016/j.addr.2009.07.013.

[31] N. Aminu et al., “Journal of Drug Delivery Science and Technology Applications of nanofibers drug delivery system in cancer therapy,” J. Drug Deliv. Sci. Technol., vol. 90, no. October, p. 105128, 2023, doi: 10.1016/j.jddst.2023.105128.

USC
UNIVERSIDADE DE SANTIAGO DE COMPOSTELA

# VI. CONCLUSIONS

USC
UNIVERSIDADE
DE SANTIAGO
DE COMPOSTELA

USC
UNIVERSIDADE
DE SANTIAGO
DE COMPOSTELA

# VI. CONCLUSIONS

According to the aims of this PhD Thesis, a variety of electrospun mats were developed for encapsulating different essential oil components as antimicrobial agents for treating infected chronic wounds and the repurposed drug disulfiram for treating glioblastoma after a resection surgery. The research was divided in two main sections and summarized in the following conclusions:

1. Carvacrol, citronellol and cinnamic acid as single, binary and ternary mixtures were successfully encapsulated within PCL matrix using electrospinning. The fibers displayed suitable morphology, optimal mechanical properties, and sustained release in relevant physiologic medium. However, mostly of the fibers prepared had limited antimicrobial properties against *S. aureus* and *P. aeruginosa*, mainly because of the low amount of essential oil released. The effects of the addition of cyclodextrins, αCD and HPβCD, were investigated and found to be quite opposite. αCD showed more affinity for the long chains of PCL and promoted the formation of poly(pseudo)rotaxanes, reinforcing the mechanical properties of the fibers, whilst HPβCD formed inclusion complexes with the essential oil components, facilitated the formation of the fibers, and notably enhaced the drug release rate with a marked burst in the first hours. Overall, these effects allowed reaching strong antimicrobial activity against *S. aureus* and significant activity against *P. aeruginosa*. Notably, carvacrol and cinnamic acid displayed major antioxidant and angiogenic activities, being the most promising essential oil components for wound healing management. Furthermore, all fibers prepared in the first part of the PhD Thesis demonstrated good hemocompatibility and biocompatibility and tissue integration in an in ovo model. In sum, the electrospun mats loaded with different essential oil components assisted by cyclodextrins could became a promising approach for the treatment of chronic infected wounds, avoiding the use of antibiotics and accelerating the wound healing process.

USC UNIVERSIDADE DE SANTIAGO DE COMPOSTELA

2. Disulfiram, a repurposing drug for cancer treatment, was formulated as electrospun nanofibers of silk fibroin. The freeze-dried silk fibroin demonstrated suitable properties to prepare electrospun fibers with a high content in disulfiram. The β-sheet conformation of silk fibroin after the freeze-drying communicated good mechanical properties to the fibers and prevented from their rapid disintegration in aqueous medium, which enabled sustained release of disulfiram during days. Nonetheless, these electrospun mats showed poor antitumoral and antimicrobial properties against *S. aureus* and *P. aeruginosa*. The incorporation of HPβCD to form an inclusion complex with disulfiram and the co-encapsulation of small proportions of Cu(II) for the *in situ* formation of the $Cu(DDC)_2$ complex notably enhanced the amount of disulfiram released and its antitumoral and antimicrobial properties. Tuning the content in silk fibroin, disulfiram, HPβCD and Cu(II) rendered nanofibers fibers that were blood-compatible and did not trigger any toxic effect normal astrocytes, while showing selectivity against tumor glioblastoma cells. This specificity is significant in the context of brain cancer treatment, where preserving healthy tissue is paramount. Additionally, the fibers are biodegradable and when its therapeutic purpose is complete (*i.e.*, the release of DSF), all components could be reused by a variety of cells; for example, silk fibroin amino acids could be utilized for myriads of process (*e.g.,* energy obtention), HPβCD can capture toxic substances forming inclusion complexes to be cleared from the body, and Cu(II) could be stored by astrocytes and reused to maintain a correct homeostasis or participate in neuronal synapses. The obtained results collectively underscore the potential of DSF-loaded electrospun fibers containing Cu(II) for clinical translation as part of a combination therapy regimen for glioblastoma.

USC UNIVERSIDADE DE SANTIAGO DE COMPOSTELA

# VII. GENERAL BIBLIOGRAPHY

USC
UNIVERSIDADE
DE SANTIAGO
DE COMPOSTELA

USC
UNIVERSIDADE
DE SANTIAGO
DE COMPOSTELA

# VII. General bibliography

[1] X. Hu, S. Liu, G. Zhou, Y. Huang, Z. Xie, and X. Jing, "Electrospinning of polymeric nanofibers for drug delivery applications," J. Control. Release, vol. 185, no. 1, pp. 12–21, 2014, doi: 10.1016/j.jconrel.2014.04.018.

[1] D. Nathwani, M. Dryden, J. Garau, Early clinical assessment of response to treatment of skin and soft-tissue infections: how can it help clinicians? Perspectives from Europe, Int. J. Antimicrob. Agents. 48 (2016) 127-36, https://doi.org/10.1016/j.ijantimicag.2016.04.023.

[1] Louis D.N., Perry A., Wesseling P., Brat D.J., Cree I.A., Figarella-Branger D., Hawkins C., Ng H.K., Pfister S.M., Reifenberger G., Soffietti R., von Deimling A., Ellison D.W. The 2021 WHO Classification of Tumors of the Central Nervous System: a summary. Neuro Oncol. 23(8) (2021)1231-1251. https://doi.org/10.1093/neuonc/noab106.

[1] L. M. Morton and T. J. Phillips, "Wound healing and treating wounds Differential diagnosis and evaluation of chronic wounds," J. Am. Acad. Dermatol., vol. 74, no. 4, pp. 589–605, 2016, doi: 10.1016/j.jaad.2015.08.068.

[2] N. Bhardwaj and S. C. Kundu, "Electrospinning: A fascinating fiber fabrication technique," Biotechnol. Adv., vol. 28, no. 3, pp. 325–347, 2010, doi: 10.1016/j.biotechadv.2010.01.004.

[2] H.N. Leong, A. Kurup, M.Y. Tan, A.L.H. Kwa, K.H. Liau, M.H. Wilcox, Management of complicated skin and soft tissue infections with a special focus on the role of newer antibiotics, Infect. Drug Resist. 11 (2018) 1959–1974. https://doi.org/10.2147/IDR.S172366

[2] van Solinge T.S., Nieland L., Chiocca E.A. et al. Advances in local therapy for glioblastoma — taking the fight to the tumour. Nat Rev Neurol 18 (2022) 221–236. https://doi.org/10.1038/s41582-022-00621-0.

[2] B. A. Mast and G. S. Schultz, "Interactions of cytokines, growth factors, and proteases in acute and chronic wounds," Wound Repair Regen., vol. 4, no. 4, pp. 411–420, 1996, doi: 10.1046/j.1524-475X.1996.40404.x.

USC UNIVERSIDADE DE SANTIAGO DE COMPOSTELA

[3] S. Chakraborty, I. C. Liao, A. Adler, and K. W. Leong, "Electrohydrodynamics: A facile technique to fabricate drug delivery systems," Adv. Drug Deliv. Rev., vol. 61, no. 12, pp. 1043–1054, 2009, doi: 10.1016/j.addr.2009.07.013.

[3] B. Silverberg, A structured approach to skin and soft tissue infections (SSTIS) in an ambulatory setting, Clin. Pract. 11 (2021) 65–74, https://doi.org/10.3390/clinpract11010011

[3] Weller M., Wick W., Aldape K., Brada M., Berger M., Pfister S. M., Nishikawa R., Rosenthal M., Wen P. Y., Stupp R., Reifenberger, G. Glioma. Nature Rev Dis Primers 1 (2015) 15017. https://doi.org/10.1038/nrdp.2015.17

[3] C. J. Murray et al., "Global burden of bacterial antimicrobial resistance in 2019: a systematic analysis," Lancet, vol. 399, no. 10325, pp. 629–655, 2022, doi: 10.1016/S0140-6736(21)02724-0.

[4] N. Aminu et al., "Journal of Drug Delivery Science and Technology Applications of nanofibers drug delivery system in cancer therapy," J. Drug Deliv. Sci. Technol., vol. 90, no. October, p. 105128, 2023, doi: 10.1016/j.jddst.2023.105128.

[4] H.B. Fung, J.Y. Chang, S. Kuczynski, A practical guide to the treatment of complicated skin and soft tissue infections, Drugs 63 (2003) 1459–1480. https://doi.org/10.2165/00003495-200363140-00003

[4] Ragucci F., Sireci F., Cavallieri F., Rossi J., Biagini G., Tosi G., Lucchi C., Molina-Pena R., Ferreira N. H., Zarur M., Ferreiros A., Bourgeois W., Berger F., Abal M., Rousseau A., Boury F. Insights into Healthcare Professionals' Perceptions and Attitudes toward Nanotechnological Device Application : What Is the Current Situation in Glioblastoma Research ?. Biomedicines 11 (2023) 1854. https://doi.org/10.3390/biomedicines11071854

[4] J. O'Neill, "Tackling Drug-Resistance Infections Globally: Final Report and Recommendations. The review on Antimicrobial Resistance Chaired by Jim O'Neill.[Online …," no. May, pp. 1–84, 2016, [Online]. Available: https://amr-review.org/sites/default/files/160518_Final paper_with cover.pdf

[5] S. Thenmozhi, N. Dharmaraj, K. Kadirvelu, and H. Y. Kim, "Electrospun nanofibers: New generation materials for advanced applications," Mater. Sci. Eng. B, vol. 217, pp. 36–48, 2017, doi: 10.1016/j.mseb.2017.01.001.

[5] A.K. Tiwari, R. Lal, Study to evaluate the role of severity stratification of skin and soft tissue infections (SSTIs) in formulating treatment strategies and predicting poor prognostic factors, Int. J. Surg. 12 (2014) 125–133. https://doi.org/10.1016/j.ijsu.2013.11.014

[5] Foo C. Y., Munir N., Kumaria A., Akhtar Q., Bullock C. J., Narayanan A., Fu R. Z. Medical Device Advances in the Treatment of Glioblastoma. Cancers 14 (2022) 5341. https://doi.org/10.3390/cancers14215341

[5] S. K. Ahmed et al., "Antimicrobial resistance: Impacts, challenges, and future prospects," J. Med. Surgery, Public Heal., vol. 2, no. March, p. 100081, 2024, doi: 10.1016/j.glmedi.2024.100081.

[6] J. Zeleny, "The electrical discharge from liquid points, and a hydrostatic method of measuring the electric intensity at their surfaces," Phys. Rev., vol. 3, no. 2, pp. 69–91, 1914, doi: 10.1103/PhysRev.3.69.

[6] M. Frieri, K. Kumar, A. Boutin, Antibiotic resistance, J. Infect. Public Health, 10 (2017) 369–378. https://doi.org/10.1016/j.jiph.2016.08.007

[6] Iqbal T., Rewatkar P., Ahmed-Cox A., Saeed I., Mansfeld F. M., Kulshreshtha R., Kumeria T., Ziegler D. S., Kavallaris M., Mazzieri R., Popat A. Frontiers in the treatment of glioblastoma: Past, present and emerging. Adv Drug Del Rev 171 (2021) 108–138. https://doi.org/10.1016/j.addr.2021.01.012

[6] W. R. Miller and C. A. Arias, "ESKAPE pathogens: antimicrobial resistance, epidemiology, clinical impact and therapeutics," Nat. Rev. Microbiol., vol. 22, no. 10, pp. 598–616, 2024, doi: 10.1038/s41579-024-01054-w.

[7] A. Formhals, "PROCESS AND APPARATUS FOR PREPARING ARTIFICIAL THREADS," United States paatent Off., vol. 1,095,504, 1934, doi: 10.1016/0042-6822(72)90565-x.

[7] Z. Yu, J. Tang, T. Khare, V. Kumar, The alarming antimicrobial resistance in ESKAPEE pathogens: Can essential oils come to the rescue?, Fitoterapia, 140 (2020) 104433. https://doi.org/10.1016/j.fitote.2019.104433

[7] Pushpakom S., Iorio F., Eyers P. A., Escott K. J., Hopper S., Wells A., Doig A., Guilliams T., Latimer J., McNamee C., Norris A., Sanseau P., Cavalla D., Pirmohamed

USC UNIVERSIDADE DE SANTIAGO

M. Drug repurposing: progress, challenges and recommendations. Nat Rev Drug Discov 18(1) (2019) 41–58. https://doi.org/10.1038/nrd.2018.168

[7] J. S. Raut and S. M. Karuppayil, "A status review on the medicinal properties of essential oils," Ind. Crops Prod., vol. 62, pp. 250–264, 2014, doi: https://doi.org/10.1016/j.indcrop.2014.05.055.

[8] G. Taylor and P. R. S. L. A, "Electrically driven jets," Proc. R. Soc. London. A. Math. Phys. Sci., vol. 313, no. 1515, pp. 453–475, 1969, doi: 10.1098/rspa.1969.0205.

[8] U. Anand, N. Jacobo-Herrera, A. Altemimi, N. Lakhssassi, A comprehensive review on medicinal plants as antimicrobial therapeutics: Potential avenues of biocompatible drug discovery, Metabolites 9 (2019) 1–13. https://doi.org/10.3390/metabo9110258

[8] Cvek B. Nonprofit drugs as the salvation of the world's healthcare systems: the case of Antabuse (disulfiram). Drug Discov Today 17(9–10) (2012) 409–412. https://doi.org/10.1016/j.drudis.2011.12.010

[8] A. El Asbahani et al., "Essential oils: From extraction to encapsulation," Int. J. Pharm., vol. 483, no. 1–2, pp. 220–243, 2015, doi: 10.1016/j.ijpharm.2014.12.069.

[9] Z. M. Huang, Y. Z. Zhang, M. Kotaki, and S. Ramakrishna, "A review on polymer nanofibers by electrospinning and their applications in nanocomposites," Compos. Sci. Technol., vol. 63, no. 15, pp. 2223–2253, 2003, doi: 10.1016/S0266-3538(03)00178-7.

[9] M. Raghavan, P. K. Linden, Newer treatment options for skin and soft tissue infections, Drugs 64 (2004) 1621-1642. https://doi.org/10.2165/00003495-200464150-00002

[9] Benkő B. M., Lamprou D. A., Sebestyén A., Zelkó R., Sebe I. Clinical, pharmacological, and formulation evaluation of disulfiram in the treatment of glioblastoma - a systematic literature review. Expert Opin. Drug Deliv. 20(4) (2023) 541–557. https://doi.org/10.1080/17425247.2023.2190581

[9] K. J. Figueroa-Lopez et al., "Development of electrospun active films of poly(3-hydroxybutyrate-co-3-hydroxyvalerate) by the incorporation of cyclodextrin inclusion

USC UNIVERSIDADE DE SANTIAGO DE COMPOSTELA

complexes containing oregano essential oil," Food Hydrocoll., vol. 108, no. January, 2020, doi: 10.1016/j.foodhyd.2020.106013.

[10] D. Han and A. J. Steckl, "Coaxial Electrospinning Formation of Complex Polymer Fibers and their Applications," Chempluschem, vol. 84, no. 10, pp. 1453–1497, 2019, doi: 10.1002/cplu.201900281.

[10] N.A. Turner, B.K. Sharma-Kuinkel, S.A. Maskarinec, E.M. Eichenberger, P.P. Shah, M. Carugati, T.L. Holland, V.G. Fowler Jr, Methicillin-resistant Staphylococcus aureus: an overview of basic and clinical research, Nat. Rev. Microbiol. 17 (2019) 203-218. https://doi.org/10.1038/s41579-018-0147-4

[10] Denoyer D., Masaldan S., Fontaine L., Cater M. A. Targeting copper in cancer therapy: 'Copper That Cancer'. Metallomics 7 (2015) 1459–1476. https://doi.org/10.1039/C5MT00149H

[10] M. H. Cavanagh, R. E. Burrell, and P. L. Nadworny, "Evaluating antimicrobial efficacy of new commercially available silver dressings," Int. Wound J., vol. 7, no. 5, pp. 394–405, 2010, doi: 10.1111/j.1742-481X.2010.00705.x.

[11] D. Ji et al., "Electrospinning of nanofibres," Nat. Rev. Methods Prim., vol. 4, no. 1, 2024, doi: 10.1038/s43586-023-00278-z.

[11] S. Santajit, N. Indrawattana, Mechanisms of antimicrobial resistance in ESKAPE pathogens, BioMed Res. Int. 2016 (2016) 2475067. https://doi.org/10.1155/2016/2475067

[11] Lun X., Wells J. C., Grinshtein N., King J. C., Hao X., Dang N., Wang X., Aman A., Uehling D., Datti A., Wrana J. L., Easaw J. C., Luchman A., Weiss S., Cairncross J. G., Kaplan D. R., Robbins S. M. Disulfiram when combined with copper enhances the therapeutic effects of temozolomide for the treatment of glioblastoma. Clin Cancer Res 22(15) (2016) 3860-3875. https://doi.org/10.1158/1078-0432.CCR-15-1798

[11] R. S. Tiğli, N. M. Kazaroğlu, B. Maviş, and M. Gumusderelioglu, "Cellular behavior on epidermal growth factor (EGF)-immobilized PCL/gelatin nanofibrous scaffolds," J. Biomater. Sci. Polym. Ed., vol. 22, no. 1–3, pp. 207–223, 2011, doi: 10.1163/092050609X12591500475424.

USC UNIVERSIDADE DE SANTIAGO DE COMPOSTELA

[12] P. R. Patel and R. V. N. Gundloori, "A review on electrospun nanofibers for multiple biomedical applications," Polym. Adv. Technol., vol. 34, no. 1, pp. 44–63, 2023, doi: 10.1002/pat.5896.

[12] S. Chouhan, K. Sharma, S. Guleria, Antimicrobial activity of some essential oils—Present status and future perspectives, Medicines, 4 (2017) 58. https://doi.org/10.3390/medicines4030058

[12] Zhang Y., Ding S., Li J., Peng X., Li J., Chang J. In vivo formation of Cu(DDC)2 complex induced by nanomedicine for mesothelioma chemotherapy. Chinese Chem Lett, 31(12) (2020) 3168–3172. https://doi.org/10.1016/j.cclet.2020.04.051

[12] K. Las Heras, M. Igartua, E. Santos-Vizcaino, and R. M. Hernandez, "Chronic wounds: Current status, available strategies and emerging therapeutic solutions," J. Control. Release, vol. 328, no. September, pp. 532–550, 2020, doi: 10.1016/j.jconrel.2020.09.039.

[13] A. Ghaderpour, Z. Hoseinkhani, R. Yarani, S. Mohammadiani, F. Amiri, and K. Mansouri, "Altering the characterization of nanofibers by changing the electrospinning parameters and their application in tissue engineering, drug delivery, and gene delivery systems," Polym. Adv. Technol., vol. 32, no. 5, pp. 1924–1950, 2021, doi: 10.1002/pat.5242.

[13] M.K. Swamy, M. S. Akhtar, U.R. Sinniah, Antimicrobial properties of plant essential oils against human pathogens and their mode of action: An updated review, Evid. Based Complement. Alternat. Med., 2016 (2016) 3012462. https://doi.org/10.1155/2016/3012462

[13] Yoshida D., Ikeda Y., Nakazawa S. Quantitative analysis of copper, zinc and copper/zinc ratio in selected human brain tumors. J. Neurooncol. 16 (2) (1993) 109-115. https://doi.org/10.1007/BF01324697.

[13] C. Aras, E. Tümay Özer, G. Göktalay, G. Saat, and E. Karaca, "Evaluation of Nigella sativa oil loaded electrospun polyurethane nanofibrous mat as wound dressing," J. Biomater. Sci. Polym. Ed., vol. 32, no. 13, pp. 1718–1735, 2021, doi: 10.1080/09205063.2021.1937463.

USC DE SANTIAGO DE COMPOSTELA

[14] A. Keirouz, Z. Wang, V. S. Reddy, and Z. K. Nagy, "The History of Electrospinning : Past , Present , and Future Developments," vol. 2201723, pp. 1–34, 2023, doi: 10.1002/admt.202201723.

[14] A. Bernardos, M. Bozik, S. Alvarez, M. Soskova, E. Perez-Esteve, P. Kloucek, M. Lhotka, A. Frankova, R. Martinez-Manez, The efficacy of essential oil components loaded into montmorillonite against Aspergillus niger and Staphylococcus aureus, Flavour Fragr. J. 34 (2019) 151–162. https://doi.org/10.1002/ffj.3488

[14] Gozdz A. Proteasome inhibitors against glioblastoma-overview of molecular mechanisms of cytotoxicity, progress in clinical trials, and perspective for use in personalized medicine. Curr Oncol. 30(11) (2023) 9676-9688. https://doi.org/10.3390/curroncol30110702.

[14] N. A. Elbhnsawi et al., "Nano-Chitosan/Eucalyptus Oil/Cellulose Acetate Nanofibers: Manufacturing, Antibacterial and Wound Healing Activities," Membranes (Basel)., vol. 13, no. 6, 2023, doi: 10.3390/membranes13060604.

[15] S. Mei et al., "Journal of Drug Delivery Science and Technology Electrospinning and its potential in fabricating pharmaceutical dosage form," vol. 76, no. May, 2022.

[15] P.L. Santos, J.P.S.C.F. Matos, L. Picot, J.R.G.S. Almeida, J.S.S. Quintans, L.J. Quintans-Júnior, Citronellol, a monoterpene alcohol with promising pharmacological activities - A systematic review, Food Chem. Toxicol. 123 (2019) 459–469. https://doi.org/10.1016/j.fct.2018.11.030

[15] Brien P. S. O., Xi Y., Miller J. R., Brownell A. L., Zeng Q., Yoo G. H., Garshott D. M., Brien M. B. O., Galinato A. E., Cai P., Narula N., Callaghan M. U., Kaufman R. J., Fribley A. M. Disulfiram (Antabuse) activates ROS-dependent ER stress and apoptosis in oral cavity squamous cell carcinoma. J Clin Med. 8(5) (2019) 611. https://doi.org/10.3390/jcm8050611.

[15] O. Visser et al., "Survival of adults with primary malignant brain tumours in Europe ; Results of the EUROCARE-5 study," pp. 2231–2241, 2015, doi: 10.1016/j.ejca.2015.07.032.

USC UNIVERSIDADE DE SANTIAGO DE COMPOSTELA

[16] G. H. Kim, Y. S. Cho, and W. D. Kim, "Stability analysis for multi-jets electrospinning process modified with a cylindrical electrode," Eur. Polym. J., vol. 42, no. 9, pp. 2031–2038, 2006, doi: 10.1016/j.eurpolymj.2006.01.026.

[16] B. Melendez-Rodriguez, K.J. Figueroa-Lopez, A. Bernardos, R. Martínez-Máñez, L. Cabedo, S. Torres-Giner, J.M. Lagaron, Electrospun antimicrobial films of poly(3-hydroxybutyrate-co-3-hydroxyvalerate) containing eugenol essential oil encapsulated in mesoporous silica nanoparticles, Nanomaterials 9 (2019) 227. https://doi.org/10.3390/nano9020227

[16] Triscott J., Pambid M. R., Dunn S.E. Concise review: Bullseye: targeting cancer stem cells to improve the treatment of gliomas by repurposing disulfiram. Stem Cells 33(4) (2015) 1042-106. https://doi.org/10.1002/stem.1956.

[16] D. Abdelnabi et al., "Local administration of irinotecan using an implantable drug delivery device stops high-grade glioma tumor recurrence in a glioblastoma tumor model," Drug Deliv. Transl. Res., vol. 14, no. 11, pp. 3070–3088, 2024, doi: 10.1007/s13346-024-01524-x.

[17] Y. Zheng, S. Xie, and Y. Zeng, "Electric field distribution and jet motion in electrospinning process: From needle to hole," J. Mater. Sci., vol. 48, no. 19, pp. 6647–6655, 2013, doi: 10.1007/s10853-013-7465-8.

[17] A. Radisavljevic, D.B. Stojanovic, S. Perisic, V. Djokic, V. Radojevic, M. Rajilic-Stojanovic, P.S. Uskokovic, Cefazolin-loaded polycaprolactone fibers produced via different electrospinning methods: Characterization, drug release and antibacterial effect, Eur. J. Pharm. Sci., 124 (2018) 26–36. https://doi.org/10.1016/j.ejps.2018.08.023

[17] Lu C., Li X., Ren Y., Zhang X. Disulfiram: a novel repurposed drug for cancer therapy. Cancer Chemother Pharmacol. 87(2) (2021) 159–172. https://doi.org/10.1007/s00280-020-04216-8

[17] M. Weller et al., "Glioma," Nat. Rev. Dis. Prim., vol. 1, no. July, 2015, doi: 10.1038/nrdp.2015.17.

[18] Y. Zheng, R. H. Gong, and Y. Zeng, "Multijet motion and deviation in electrospinning," RSC Adv., vol. 5, no. 60, pp. 48533–48540, 2015, doi: 10.1039/c5ra06049d.

USC

[18] X. Hu, S. Liu, G. Zhou, Y. Huang, Z. Xie, X. Jing, Electrospinning of polymeric nanofibers for drug delivery applications, J. Control. Release, 185 (2014) 12–21. https://doi.org/10.1016/j.jconrel.2014.04.018

[18] Mcmahon A., Chen W., Li F. Old wine in new bottles: Advanced drug delivery systems for disulfiram-based cancer therapy. J Control Release 319 (2020) 352–359. https://doi.org/10.1016/j.jconrel.2020.01.001

[18] K. J. Wolf, J. Chen, J. D. Coombes, M. K. Aghi, and S. Kumar, "Dissecting and rebuilding the glioblastoma microenvironment with engineered materials," Nat. Rev. Mater., vol. 4, no. 10, pp. 651–668, 2019, doi: 10.1038/s41578-019-0135-y.

[19] C. J. Angammana and S. H. Jayaram, "Fundamentals of electrospinning and processing technologies," Part. Sci. Technol., vol. 34, no. 1, pp. 72–82, 2016, doi: 10.1080/02726351.2015.1043678.

[19] N. Bhardwaj, S.C. Kundu, Electrospinning: A fascinating fiber fabrication technique, Biotechnol. Adv., 28 (2010) 325–347. https://doi.org/10.1016/j.biotechadv.2010.01.004

[19] Kannappan V., Ali M., Small B., Rajendran G., Elzhenni S., Taj H., Wang W., Dou Q. P. Recent advances in repurposing disulfiram and disulfiram derivatives as copper-dependent anticancer agents. Front Mol Biosci. 8 (2021) 741316. https://doi.org/10.3389/fmolb.2021.741316

[19] C. Y. Foo et al., "Medical Device Advances in the Treatment of Glioblastoma," Cancers (Basel)., vol. 14, no. 5341, pp. 1–33, 2022, doi: https://doi.org/10.3390/cancers14215341.

[20] N. M. Thoppey, J. R. Bochinski, L. I. Clarke, and R. E. Gorga, "Unconfined fluid electrospun into high quality nanofibers from a plate edge," Polymer (Guildf)., vol. 51, no. 21, pp. 4928–4936, 2010, doi: 10.1016/j.polymer.2010.07.046.

[20] F. Hemmati, A. Bahrami, A.F. Esfanjani, H. Hosseini, D.J. McClements, L. Williams, Electrospun antimicrobial materials: Advanced packaging materials for food applications, Trends Food Sci. Technol. 111 (2021) 520–533. https://doi.org/10.1016/j.tifs.2021.03.014

USC UNIVERSIDADE DE SANTIAGO DE COMPOSTELA

[20] Xu B., Wang S., Li R., Chen K., He L., Deng M., Kannappan V., Zha J., Dong H., Wang W. Disulfiram/copper selectively eradicates AML leukemia stem cells in vitro and in vivo by simultaneous induction of ROS-JNK and inhibition of NF-κB and Nrf2. Cell Death Dis. 8(5) (2017) e2797. https://doi.org/10.1038/CDDIS.2017.176

[20] T. Iqbal et al., "Frontiers in the treatment of glioblastoma : Past , present and emerging," Adv. Drug Deliv. Rev., vol. 171, pp. 108–138, 2021, doi: 10.1016/j.addr.2021.01.012.

[21] N. M. Thoppey, J. R. Bochinski, L. I. Clarke, and R. E. Gorga, "Edge electrospinning for high throughput production of quality nanofibers," Nanotechnology, vol. 22, no. 34, 2011, doi: 10.1088/0957-4484/22/34/345301.

[21] Li X., Xu F., He Y., Li Y., Hou J., Ya

[21] D. Mondal, M. Griffith, S.S. Venkatraman, Polycaprolactone-based biomaterials for tissue engineering and drug delivery: Current scenario and challenges, Int. J. Polym. Mater., 65 (2016) 255-265. https://doi.org/10.1080/00914037.2015.1103241

[21] D. Lenz, M. Ries, and P. Johann, "The drug development pipeline for glioblastoma—A cross sectional assessment of the FDA Orphan Drug Product designation database," PLoS One, vol. 16, no. 7 July, pp. 1–14, 2021, doi: 10.1371/journal.pone.0252924.

[22] J. Holopainen, T. Penttinen, E. Santala, and M. Ritala, "Needleless electrospinning with twisted wire spinneret," Nanotechnology, vol. 26, no. 2, p. 25301, 2015, doi: 10.1088/0957-4484/26/2/025301.

[22] G. Narayanan, R. Aguda, M. Hartman, C. Chung, R. Boy, B.S. Gupta, A.E. Tonelli, Fabrication and characterization of poly(ε -caprolactone)/ α-cyclodextrin pseudorotaxane nanofibers, Biomacromolecules 17 (2016) 271–279. https://doi.org/10.1021/acs.biomac.5b01379

[22] Meneguello J. E., Murase L. S., de Souza J. V. P., de Oliveira C. G., Ghiraldi-Lopes L. D., Teixeira J. J. V., Scodro R. B. de L., Ferracioli K. R. C., Siqueira V. L. D., Campanerut-Sá P. A. Z., Cardoso R. F. Systematic review of disulfiram as an antibacterial agent: what is the evidence?. Int J Antimicrob Agents 59(5) (2022) 106578. https://doi.org/10.1016/j.ijantimicag.2022.106578.

USC

[22] B.-M. Benkő, D. A. Lamprou, A. Sebestyén, R. Zelkó, and I. Sebe, "Clinical, pharmacological, and formulation evaluation of disulfiram in the treatment of glioblastoma - a systematic literature review," Expert Opin. Drug Deliv., vol. 20, no. 4, pp. 541–557, Apr. 2023, doi: 10.1080/17425247.2023.2190581.

[23] G. Jiang, S. Zhang, and X. Qin, "High throughput of quality nanofibers via one stepped pyramid-shaped spinneret," Mater. Lett., vol. 106, pp. 56–58, 2013, doi: 10.1016/j.matlet.2013.04.084.

[23] F. Topuz, T. Uyar, Electrospinning of cyclodextrin functional nanofibers for drug delivery applications, Pharmaceutics 11 (2019) 6. https://doi.org/10.3390/pharmaceutics11010006

[23] Thakare R., Shukla M., Kaul G., Dasgupta A., Chopra S. Repurposing disulfiram for treatment of *Staphylococcus aureus* infections. Int J Antimicrob Agents 53(6) (2019) 709–715. https://doi.org/10.1016/j.ijantimicag.2019.03.

[23] B. J. Mason and C. J. Heyser, "A LCOHOL U SE D ISORDER : T HE R OLE OF M EDICATION IN R ECOVERY," vol. 41, no. 1, pp. 1–17, 2021.

[24] X. Yan et al., "Slit-surface electrospinning: A novel process developed for high-throughput fabrication of core-sheath fibers," PLoS One, vol. 10, no. 5, pp. 1–11, 2015, doi: 10.1371/journal.pone.0125407.

[24] F. Velázquez-Contreras, N. García-Caldera, J.D. Padilla de la Rosa, D. Martínez-Romero, E. Núñez-Delicado, J.A. Gabaldón, Effect of PLA active packaging containing monoterpene-cyclodextrin complexes on berries preservation, Polymers 13 (2021) 1399. https://doi.org/10.3390/polym13091399

[24] Xie C., Yan J., Cao S., Liu R., Sun B., Xie Y., Qu K., Zhang W., Weng Z., Wang Z. Bi-layered disulfiram-loaded fiber membranes with antibacterial properties for wound dressing. Appl Biochem Biotechnol. 194(3) (2022) 1359–1372. https://doi.org/10.1007/s12010-021-03663-0

[24] F. Ragucci et al., "Insights into Healthcare Professionals ' Perceptions and Attitudes toward Nanotechnological Device Application : What Is the Current Situation in Glioblastoma Research ?," Biomedicines, vol. 11, p. 1854, 2023, doi: https://doi.org/10.3390/ biomedicines11071854 Academic.

USC

[25] G. Yan, H. Niu, H. Shao, X. Zhao, H. Zhou, and T. Lin, "Curved convex slot: an effective needleless electrospinning spinneret," J. Mater. Sci., vol. 52, no. 19, pp. 11749–11758, 2017, doi: 10.1007/s10853-017-1315-z.

[25] G. Narayanan, B.S. Gupta, A.E. Tonelli, Enhanced mechanical properties of poly (ε-caprolactone) nanofibers produced by the addition of non-stoichiometric inclusion complexes of poly (ε-caprolactone) and α-cyclodextrin, Polymer, 76 (2015), 321-330. https://doi.org/10.1016/j.polymer.2015.08.045

[25] Ramadhani N., Shabir M., McConville C. Preparation and characterisation of Kolliphor®P 188 and P 237 solid dispersion oral tablets containing the poorly water-soluble drug disulfiram. Int J Pharm. 475(1) (2014) 514–522. https://doi.org/10.1016/j.ijpharm.2014.09.013

[25] N. Ramadhani, M. Shabir, and C. McConville, "Preparation and characterisation of Kolliphor®P 188 and P 237 solid dispersion oral tablets containing the poorly water soluble drug disulfiram," Int. J. Pharm., vol. 475, no. 1, pp. 514–522, 2014, doi: 10.1016/j.ijpharm.2014.09.013.

[26] D. Lukas, A. Sarkar, and P. Pokorny, "Self-organization of jets in electrospinning from free liquid surface: A generalized approach," J. Appl. Phys., vol. 103, no. 8, 2008, doi: 10.1063/1.2907967.

[26] C. Alvarez-lorenzo, C.A. García-González, A. Concheiro, Cyclodextrins as versatile building blocks for regenerative medicine, J Control. Release, 268 (2017) 269–281. https://doi.org/10.1016/j.jconrel.2017.10.038

[26] El Fawal G., Abu-Serie M. M., El-Gendi H., El-Fakharany E. M. Fabrication, characterization and in vitro evaluation of disulfiram-loaded cellulose acetate/poly(ethylene oxide) nanofiber scaffold for breast and colon cancer cell lines treatment. Int J Biol Macromol. 204 (2022) 555–564. https://doi.org/10.1016/j.ijbiomac.2022.01.145

[26] F. Nazzaro, F. Fratianni, and L. De Martino, "Effect of Essential Oils on Pathogenic Bacteria," pp. 1451–1474, 2013, doi: 10.3390/ph6121451.

[27] K. Molnar and Z. K. Nagy, "Corona-electrospinning: Needleless method for high-throughput continuous nanofiber production," Eur. Polym. J., vol. 74, pp. 279–286, 2016, doi: 10.1016/j.eurpolymj.2015.11.028.

[27] A. Costoya, A. Concheiro, C.A. Alvarez-Lorenzo, Electrospun fibers of cyclodextrins and poly(cyclodextrins), Molecules, 22 (2017) 230. https://doi.org/10.3390/molecules22020230

[27] Wang P., Luo Q., Zhang L., Qu X., Che X., Cai S., Liu Y. A disulfiram / copper gluconate co-loaded bi-layered long-term drug delivery system for intraperitoneal treatment of peritoneal carcinomatosis. Colloids Surf. B 231 (2023) 113558. https://doi.org/10.1016/j.colsurfb.2023.113558

[27] S. Chouhan, K. Sharma, and S. Guleria, "Antimicrobial Activity of Some Essential Oils—Present Status and Future Perspectives," Medicines, vol. 4, no. 3, p. 58, 2017, doi: 10.3390/medicines4030058.

[28] I. Bhattacharyya, M. C. Molaro, R. D. Braatz, and G. C. Rutledge, "Free surface electrospinning of aqueous polymer solutions from a wire electrode," Chem. Eng. J., vol. 289, pp. 203–211, 2016, doi: 10.1016/j.cej.2015.12.067.

[28] M. Dias Antunes, G. da Silva Dannenberg, A.M. Fiorentini, V.Z. Pinto, L.T. Lim, E. da Rosa Zavareze, A.R.G. Dias, Antimicrobial electrospun ultrafine fibers from zein containing eucalyptus essential oil/cyclodextrin inclusion complex, Int. J. Biol. Macromol. 104 (2017) 874–882. https://doi.org/10.1016/j.ijbiomac.2017.06.095

[28] Zhao J., Cui W. Functional electrospun fibers for local therapy of cancer. Adv Fiber Mater. 2 (2020) 229–245. https://doi.org/10.1007/s42765-020-00053-9

[28] N. Bhardwaj and S. C. Kundu, "Electrospinning: A fascinating fiber fabrication technique," Biotechnol. Adv., vol. 28, no. 3, pp. 325–347, 2010, doi: 10.1016/j.biotechadv.2010.01.004.

[29] X. Wang, H. Niu, X. Wang, and T. Lin, "Needleless electrospinning of uniform nanofibers using spiral coil spinnerets," J. Nanomater., vol. 2012, 2012, doi: 10.1155/2012/785920.

[29] Y. Liu, X. Liang, R. Zhang, W. Lan, W. Qin, Fabrication of electrospun polylactic acid/Cinnamaldehyde/β-cyclodextrin fibers as an antimicrobial wound dressing, Polymers, 9 (2017) 464. https://doi.org/10.3390/polym9100464

[29] El Fawal G., Abu-Serie M. M., Mo X., Wang H. Diethyldithiocarbamate/silk fibroin/polyethylene oxide nanofibrous for cancer therapy: Fabrication, characterization

USC UNIVERSIDADE DE SANTIAGO

and in vitro evaluation. Int J Biol Macromol. 193 (2021) 293–299. https://doi.org/10.1016/j.ijbiomac.2021.10.039

[29] A. Keirouz, Z. Wang, V. S. Reddy, and Z. K. Nagy, "The History of Electrospinning : Past , Present , and Future Developments," vol. 2201723, pp. 1–34, 2023, doi: 10.1002/admt.202201723.

[30] S. L. Liu, Y. Y. Huang, H. D. Zhang, B. Sun, J. C. Zhang, and Y. Z. Long, "Needleless electrospinning for large scale production of ultrathin polymer fibres," Mater. Res. Innov., vol. 18, pp. S4833–S4837, 2014, doi: 10.1179/1432891714Z.000000000802.

[30] Z.I. Yildiz, A. Celebioglu, M.E. Kilic, E. Durgun, T. Uyar, Fast-dissolving carvacrol/cyclodextrin inclusion complex electrospun fibers with enhanced thermal stability, water solubility, and antioxidant activity, J. Mater. Sci. 53 (2018) 15837–15849. https://doi.org/10.1007/s10853-018-2750-1

[30] Han D., Serra R., Gorelick N., Fatima U., Eberhart C. G., Brem H., Tyler B., Steckl A. J. Multi-layered core-sheath fiber membranes for controlled drug release in the local treatment of brain tumor. Sci Rep. 9 (2019) 17936. https://doi.org/10.1038/s41598-019-54283-y

[30] S. Chakraborty, I. C. Liao, A. Adler, and K. W. Leong, "Electrohydrodynamics: A facile technique to fabricate drug delivery systems," Adv. Drug Deliv. Rev., vol. 61, no. 12, pp. 1043–1054, 2009, doi: 10.1016/j.addr.2009.07.013.

[31] C. Huang, H. Niu, J. Wu, Q. Ke, X. Mo, and T. Lin, "Needleless electrospinning of polystyrene fibers with an oriented surface line texture," J. Nanomater., vol. 2012, 2012, doi: 10.1155/2012/473872.

[31] Z.I. Yildiz, M.E. Kilic, E. Durgun, T. Uyar, Molecular encapsulation of cinnamaldehyde within cyclodextrin inclusion complex electrospun nanofibers: fast-dissolution, enhanced water solubility, high temperature stability, and antibacterial activity of cinnamaldehyde, J. Agricult. Food Chem., 67 (2019) 11066–11076. https://doi.org/10.1021/acs.jafc.9b02789

[31] Khodadadi M., Alijani S., Montazeri M., Esmaeilizadeh N., Younes S. S. Recent advances in electrospun nanofiber-mediated drug delivery strategies for localized cancer

chemotherapy. J Biomed Mater Res A 108 (7) (2020) 1444–1458. https://doi.org/10.1002/jbm.a.36912

[31] N. Aminu et al., "Journal of Drug Delivery Science and Technology Applications of nanofibers drug delivery system in cancer therapy," J. Drug Deliv. Sci. Technol., vol. 90, no. October, p. 105128, 2023, doi: 10.1016/j.jddst.2023.105128.

[32] T. Miloh, B. Spivak, and A. L. Yarin, "Needleless electrospinning: Electrically driven instability and multiple jetting from the free surface of a spherical liquid layer," J. Appl. Phys., vol. 106, no. 11, 2009, doi: 10.1063/1.3264884.

[32] L. Martins, C.E. dos Santos Cruxen, G. Pinheiro Bruni, A.M. Fiorentini, E. da Rosa Zavareze, L.T. Lim, A.R. Guerra Dias, Development of antimicrobial and antioxidant electrospun soluble potato starch nano fibers loaded with carvacrol, Int. J. Biol. Macromol. 139 (2019) 1182–1190. https://doi.org/10.1016/j.ijbiomac.2019.08.096

[32] Molina-Peña R., Ferreira N.H., Roy C., Roncali L., Najberg M., Avril S., Zarur M., Bourgeois W., Ferreirós A., Lucchi C., Cavallieri F., Hindré F., Tosi G., Biagini G., Valzania F., Berger F., Abal M., Rousseau A., Boury F., Alvarez-Lorenzo C., Garcion E. Implantable SDF-1α-loaded silk fibroin hyaluronic acid aerogel sponges as an instructive component of the glioblastoma ecosystem: Between chemoattraction and tumor shaping into resection cavities. Acta Biomater. 173 (2024) 261-282. https://doi.org/10.1016/j.actbio.2023.10.022.

[33] H. Niu, X. Wang, and T. Lin, "Needleless electrospinning: Influences of fibre generator geometry," J. Text. Inst., vol. 103, no. 7, pp. 787–794, 2012, doi: 10.1080/00405000.2011.608498.

[33] A. Nostro, A.R. Blanco, M.A. Cannatelli, V. Enea, G. Flamini, I. Morelli, A.S. Roccaro, V. Alonzo, Susceptibility of methicillin-resistant staphylococci to oregano essential oil, carvacrol and thymol. FEMS Microbiol. Let., 230 (2004), 191–195. https://doi.org/10.1016/S0378-1097(03)00890-5

[33] Sabarees G., Tamilarasi G. P., Velmurugan V., Alagarsamy V., Sibuh B. Z., Sikarwar M., Taneja P., Kumar A., Gupta, P. K. (2023). Emerging trends in silk fibroin-based nanofibers for impaired wound healing. J Drug Deliv Sci Technol. 79 (2023) 103994. https://doi.org/10.1016/j.jddst.2022.103994

USC DE SANTIAGO DE COMPOSTELA

[34] A. L. Yarin and E. Zussman, "Upward needleless electrospinning of multiple nanofibers," Polymer (Guildf)., vol. 45, no. 9, pp. 2977–2980, 2004, doi: 10.1016/j.polymer.2004.02.066.

[34] J.C. Lopez-Romero, H. González-Ríos, A. Borges, M. Simões, Antibacterial effects and mode of action of selected essential oils components against Escherichia coli and Staphylococcus aureus, Evid. Based Complement. Alternat. Med. 2015 (2015) 795435. https://doi.org/10.1155/2015/795435

[34] Kundu B., Rajkhowa R., Kundu S. C., Wang, X. Silk fibroin biomaterials for tissue regenerations. Adv Drug Deliv Rev. 65(4) (2013) 457–470. https://doi.org/10.1016/j.addr.2012.09.043

[35] Y. Li et al., "Developments of Advanced Electrospinning Techniques : A Critical Review," vol. 2100410, pp. 1–29, 2021, doi: 10.1002/admt.202100410.

[35] N. Ruwizhi, B.A. Aderibigbe, Cinnamic acid derivatives and their biological efficacy, Int. J. Mol. Sci., 21 (2020) 5712. https://doi.org/10.3390/ijms21165712

[35] Moisenovich M. M., Plotnikov E. Y., Moysenovich A. M., Silachev D. N., Danilina T. I., Savchenko E. S., Bobrova M. M., Safonova L. A., Tatarskiy V. V., Kotliarova M. S., Agapov I. I., Zorov D. B. Effect of silk fibroin on neuroregeneration after traumatic brain injury. Neurochemical Res. 44(10) (2019) 2261–2272. https://doi.org/10.1007/s11064-018-2691-8

[36] D. Li, Y. Wang, and Y. Xia, "Electrospinning of polymeric and ceramic nanofibers as uniaxially aligned arrays," Nano Lett., vol. 3, no. 8, pp. 1167–1171, 2003, doi: 10.1021/nl0344256.

[36] J. Malheiro, I. Gomes, A. Borges, M.M.S.M. Bastos, J.Y. Maillard, F. Borges, M. Simões, Phytochemical profiling as a solution to palliate disinfectant limitations, Biofouling 32 (2016) 1007. https://doi.org/10.1080/08927014.2016.1220550

[36] Qu Y., Sun X., Ma L., Li C., Xu Z., Ma W., Zhou Y., Zhao Z., Ma D. Therapeutic effect of disulfiram inclusion complex embedded in hydroxypropyl-β-cyclodextrin on intracranial glioma-bearing male rats via intranasal route. Eur J Pharm Sci. 156 (2021) 105590. https://doi.org/10.1016/j.ejps.2020.105590

USC UNIVERSIDADE DE SANTIAGO DE COMPOSTELA

[37] P. D. Dalton, D. Klee, and M. Möller, "Electrospinning with dual collection rings," Polymer (Guildf)., vol. 46, no. 3, pp. 611–614, 2005, doi: 10.1016/j.polymer.2004.11.075.

[37] J.F. Malheiro, J.Y. Maillard, F. Borges, M. Simões, Evaluation of cinnamaldehyde and cinnamic acid derivatives in microbial growth control, Int. Biodeterior. Biodegrad., 141 (2019) 71–78. https://doi.org/10.1016/j.ibiod.2018.06.003

[37] Matassoli F. L., Leão I. C., Bezerra B. B., Pollard R. B., Lütjohann D., Hildreth J. E. K., Arruda, L. B. de. Hydroxypropyl-beta-cyclodextrin reduces inflammatory signaling from monocytes: possible implications for suppression of HIV chronic immune activation. mSphere 3(6) (2018) 101128. https://doi.org/10.1128/msphere.00497-18

[38] J. Wu et al., "Electrospun nanoyarn scaffold and its application in tissue engineering," Mater. Lett., vol. 89, pp. 146–149, 2012, doi: 10.1016/j.matlet.2012.08.141.

[38] M. Ayaz, F. Ullah, A. Sadiq, F. Ullah, M. Ovais, J. Ahmed, H.P. Devkota, Synergistic interactions of phytochemicals with antimicrobial agents: Potential strategy to counteract drug resistance, Chem. Biol. Interact., 308 (2019) 294–303. https://doi.org/10.1016/j.cbi.2019.05.050

[38] Malanga M., Szemán J., Fenyvesi É., Puskás I., Csabai K., Gyémánt G., Fenyvesi F., Szente L. "Back to the Future": A new look at hydroxypropyl beta-cyclodextrins. J Pharm Sci. 105(9) (2016) 2921–2931. https://doi.org/10.1016/j.xphs.2016.04.034

[39] C. G. Taylor and E. L. Pendleton, "Characterization of an Epoxy-Anhydride Ablative System Using Computer Treatment of Analytical Results," J. Macromol. Sci. Part A - Chem., vol. 3, no. 3, pp. 453–470, 1969, doi: 10.1080/10601326908053822.

[39] I.M. Oliveira, A. Borges, F. Borges, M. Simões, Repurposing ibuprofen to control Staphylococcus aureus biofilms, Eur. J. Med. Chem. 166 (2019) 197–205. https://doi.org/10.1016/j.ejmech.2019.01.046

[39] Alvarez-lorenzo C., García-González C. A., Concheiro A. Cyclodextrins as versatile building blocks for regenerative medicine. J. Control. Release 268 (2017) 269–281. https://doi.org/10.1016/j.jconrel.2017.10.038

[40] G. Taylor and P. R. S. L. A, “Disintegration of water drops in an electric field,” Proc. R. Soc. London. Ser. A. Math. Phys. Sci., vol. 280, no. 1382, pp. 383–397, 1964, doi: 10.1098/rspa.1964.0151.

[40] M.M. Leitão, T.F. Vieira, S.F. Sousa, F. Borges, M. Simões, A. Borges, Dual action of benzaldehydes: Inhibiting quorum sensing and enhancing antibiotic efficacy for controlling Pseudomonas aeruginosa biofilms, Microb. Pathog. 2024 Jun;191:106663. doi: 10.1016/j.micpath.2024.106663.

[40] Costoya A., Concheiro A., Alvarez-lorenzo C. Electrospun fibers of cyclodextrins and poly(cyclodextrins). Molecules 22(2) (2017) 230. https://doi.org/10.3390/molecules22020230

[41] M. Jr and W. Ep, “Electrohydrodynamics of a current-carrying semi-insulating jet,” vol. 47, pp. 127–143, 1971.

[41] C. Wiegand, T. Heinze, U.C. Hipler, Comparative in vitro study on cytotoxicity, antimicrobial activity, and binding capacity for pathophysiological factors in chronic wounds of alginate and silver-containing alginate, Wound Repair Regen., 17 (2009) 511–521. https://doi.org/10.1111/j.1524-475X.2009.00503.x

[41] Gonzalez-Prada I., Borges A., Santos-Torres B., Magariños B., Simões M., Concheiro A., Alvarez-Lorenzo C. Antimicrobial cyclodextrin-assisted electrospun fibers loaded with carvacrol, citronellol and cinnamic acid for wound healing. Int J Biol Macromol. 277 (2024) 134154. https://doi.org/10.1016/j.ijbiomac.2024.134154.

[42] S. Kailasa, M. S. B. Reddy, M. R. Maurya, B. G. Rani, K. V. Rao, and K. K. Sadasivuni, “Electrospun Nanofibers: Materials, Synthesis Parameters, and Their Role in Sensing Applications,” Macromol. Mater. Eng., vol. 306, no. 11, pp. 1–36, 2021, doi: 10.1002/mame.202100410.

[42] I.M. Oliveira, A. Borges, F. Borges, M. Simões, Repurposing ibuprofen to control Staphylococcus aureus biofilms, Eur. J. Med. Chem. 166 (2019) 197–205. https://doi.org/10.1016/j.ejmech.2019.01.046

[42] Li H., Wang J., Wu C., Wang L., Chen Z. The combination of disulfiram and copper for cancer treatment. Drug Discov Today 25(6) (2020) 1099–1108. https://doi.org/10.1016/j.drudis.2020.04.003

[43] C. Zhang and X. Yuan, "EUROPEAN POLYMER Study on morphology of electrospun poly ( vinyl alcohol ) mats," vol. 41, pp. 423–432, 2005, doi: 10.1016/j.eurpolymj.2004.10.027.

[43] A. Borges, C. Ferreira, M.J. Saavedra, M. Simões, Antibacterial activity and mode of action of ferulic and gallic acids against pathogenic bacteria, Microb. Drug Resist. 19 (2013) 256-265. https://doi.org/10.1089/mdr.2012.0244.

[43] Jomova K., Makova M., Alomar S. Y., Alwasel S. H., Nepovimova E., Kuca K., Rhodes C. J., Valko M. Essential metals in health and disease. Chem Biol Interact. 367 (2022) 110173. https://doi.org/10.1016/j.cbi.2022.110173

[44] N. Joy, R. Anuraj, A. Viravalli, H. N. Dixit, and S. Samavedi, "Coupling between voltage and tip-to-collector distance in polymer electrospinning: Insights from analysis of regimes, transitions and cone/jet features," Chem. Eng. Sci., vol. 230, p. 116200, 2021, doi: 10.1016/j.ces.2020.116200.

[44] C.J. van Oss, M.K. Chaudhury, R.J. Good, Monopolar surfaces, Adv. Colloid Interfac. 28 (1987) 35–64. https://doi.org/10.1016/0001-8686(87)80008-8

[44] Rihel J. Copper on the brain. Nat Chem Biol. 14 (2008) 638–639. https://doi.org/10.1038/s41589-018-0089-1

[45] A. Asti and L. Gioglio, "Natural and synthetic biodegradable polymers: Different scaffolds for cell expansion and tissue formation," Int. J. Artif. Organs, vol. 37, no. 3, pp. 187–205, 2014, doi: 10.5301/ijao.5000307.

[45] C.J. van Oss, R.J. Good, M.K. Chaudhury, Additive and nonadditive surface tension components and the interpretation of contact angles, Langmuir 4 (1988) 884–891. https://doi.org/10.1021/la00082a018

[45] Chen L., Min J., Wang F. Copper homeostasis and cuproptosis in health and disease. Sig Transduct Target Ther. 7 (2022) 378. https://doi.org/10.1038/s41392-022-01229-y

[46] H. Seddiqi et al., Cellulose and its derivatives: towards biomedical applications, vol. 28, no. 4. Springer Netherlands, 2021. doi: 10.1007/s10570-020-03674-w.

[46] C.J. van Oss, L. Ju, M.K. Chaudhury, R.J. Good, Estimation of the polar parameters of the surface tension of liquids by contact angle measurements on gels, J.

USC UNIVERSIDADE DE SANTIAGO DE COMPOSTELA

Colloid Interface Sci. 128 (1989) 313–319. https://doi.org/10.1016/0021-9797(89)90345-7

[46] Lech T., Sadlik J. K. Copper concentration in body tissues and fluids in normal subjects of southern Poland. Biol Trace Elem Res. 118 (2007) 10–15. https://doi.org/10.1007/s12011-007-0014-z

[47] H. Rodríguez-Tobías, G. Morales, and D. Grande, "Comprehensive review on electrospinning techniques as versatile approaches toward antimicrobial biopolymeric composite fibers," Mater. Sci. Eng. C, vol. 101, no. March, pp. 306–322, 2019, doi: 10.1016/j.msec.2019.03.099.

[47] B. Janczuk, E. Chibowski, J.M. Bruque, M.L. Kerkeb, F.G. Caballero, On the consistency of surface free energy components as calculated from contact angles of different liquids: An application to the cholesterol surface, J. Colloid Interface Sci. 159 (1993) 421–428. https://doi.org/10.1006/jcis.1993.1342

[47] Scheiber I. F., Dringen R. Astrocyte functions in the copper homeostasis of the brain. Neurochemistry Int. 62 (2013) 556–565. https://doi.org/10.1016/j.neuint.2012.08.017

[48] V. Siracusa, "Microbial Degradation of Synthetic Biopolymers Waste," Polymers (Basel)., vol. 11, no. 6, 2019, doi: 10.3390/polym11061066.

[48] A. Contreras-García, E. Bucio, A. Concheiro, C. Alvarez-Lorenzo, Polypropylene grafted with NIPAAm and APMA for creating hemocompatible surfaces that load/elute nalidixic acid, React. Funct. Polym. 70 (2010) 836–842. https://doi.org/10.1016/j.reactfunctpolym.2010.07.019

[48] Jin S., Ren L., Yang K. Bio-functional Cu containing biomaterials: A new way to enhance bio-adaption of biomaterials. J Mater Sci Technol. 32(9) (2016) 835–839. https://doi.org/10.1016/j.jmst.2016.06.022

[49] A. K. Haghi and M. Akbari, "Trends in electrospinning of natural nanofibers," Phys. Status Solidi Appl. Mater. Sci., vol. 204, no. 6, pp. 1830–1834, 2007, doi: 10.1002/pssa.200675301.

USC UNIVERSIDADE DE SANTIAGO DE COMPOSTELA

[49] M.L. Ponce, H.K. Kleinmann, The chick chorioallantoic membrane as an in vivo angiogenesis model, Curr. Protoc. Cell Biol. 19 (2003) 1–6. doi: 10.1002/0471143030.cb1905s1

[49] Oliveri V. Biomedical applications of copper ionophores. Coord Chem Rev. 422 (2020) 213474. https://doi.org/10.1016/j.ccr.2020.213474

[50] S. Sukigara, M. Gandhi, J. Ayutsede, M. Micklus, and F. Ko, "Regeneration of Bombyx mori silk by electrospinning - Part 1: Processing parameters and geometric properties," Polymer (Guildf)., vol. 44, no. 19, pp. 5721–5727, 2003, doi: 10.1016/S0032-3861(03)00532-9.

[50] B. R. Williamson, R. Krishnaswamy, A.E. Tonelli, Physical properties of poly(ε-caprolactone) coalesced from its α-cyclodextrin inclusion compound. Polymer 52 (2011) 4517–4527. https://doi.org/10.1016/j.polymer.2011.07.043

[50] Moon O. J., Yoon C. J., Lee J. S., Kim H. H., Seol Y. H., Lee J. Tumor-specific release of copper-incorporated diethyldithiocarbamate from an optimized apoferritin scaffold enables both potent and safe anti-cancer therapy. Chem Eng J. 473 (2023) 145176. https://doi.org/10.1016/j.cej.2023.145176

[51] C. S. Ki, D. H. Baek, K. D. Gang, K. H. Lee, I. C. Um, and Y. H. Park, "Characterization of gelatin nanofiber prepared from gelatin-formic acid solution," Polymer (Guildf)., vol. 46, no. 14, pp. 5094–5102, 2005, doi: 10.1016/j.polymer.2005.04.040.

[51] C. Abril- Sánchez, A. Matencio, S. Navarro-Orcajada, F. García-Carmona, J.M. López-Nicolás, Evaluation of the properties of the essential oil citronellal nanoencapsulated by cyclodextrins, Chem. Phys. Lipids 219 (2019) 72–78. https://doi.org/10.1016/j.chemphyslip.2019.02.001

[51] Lu M., Pais A., Vitorino R., Fortuna A., Vitorino C. Expediting disulfiram assays through a systematic analytical quality by design approach. Chemosensors 9 (2021) 172. https://doi.org/10.3390/chemosensors9070172

[52] P. Gupta, C. Elkins, T. E. Long, and G. L. Wilkes, "Electrospinning of linear homopolymers of poly(methyl methacrylate): Exploring relationships between fiber formation, viscosity, molecular weight and concentration in a good solvent," Polymer (Guildf)., vol. 46, no. 13, pp. 4799–4810, 2005, doi: 10.1016/j.polymer.2005.04.021.

[52] M.I. Rodríguez-López, M.T. Mercader-Ros, J.A. Pellicer, V.M. Gómez-López, D. Martínez-Romero, E. Núñez-Delicado, J.A. Gabaldón, Evaluation of monoterpene-cyclodextrin complexes as bacterial growth effective hurdles, Food Control, 108 (2020) 106814. https://doi.org/10.1016/j.foodcont.2019.106814

[52] Leão C., Borges A., Simões M. NSAIDs as a drug repurposing strategy for biofilm control. Antibiotics 9(9) (2020) 591. https://doi.org/10.3390/antibiotics9090591

[53] S. S. Ojha, M. Afshari, R. Kotek, R. E. Gorga, and N. Carolina, "Morphology of Electrospun Nylon-6 Nanofibers as a Function of Molecular Weight and Processing Parameters," 2007, doi: 10.1002/app.

[53] K.J. Figueroa-Lopez, D. Enescu, S. Torres-Giner, L. Cabedo, M.A. Cerqueira, L. Pastrana, P. Fuciños, J.M. Lagaron, Development of electrospun active films of poly(3-hydroxybutyrate-co-3-hydroxyvalerate) by the incorporation of cyclodextrin inclusion complexes containing oregano essential oil, Food Hydrocolloids, 108 (2020) 106013. https://doi.org/10.1016/j.foodhyd.2020.106013

[53] Wiegand C., Heinze T., Hipler U. C. Comparative in vitro study on cytotoxicity, antimicrobial activity, and binding capacity for pathophysiological factors in chronic wounds of alginate and silver-containing alginate. Wound Repair Regen. 17(4) (2009) 511–521. https://doi.org/10.1111/j.1524-475X.2009.00503.x

[54] M. G. McKee, J. M. Layman, M. P. Cashion, and T. E. Long, "Phospholipid nonwoven electrospun membranes," Science (80-. )., vol. 311, no. 5759, pp. 353–355, 2006, doi: 10.1126/science.1119790.

[54] M.H. Cavanagh, R.E. Burrell, P.L. Nadworny, Evaluating antimicrobial efficacy of new commercially available silver dressings, Int. Wound J. 7 (2010), 394–405. https://doi.org/10.1111/j.1742-481X.2010.00705.x

[54] McCarthy K.D., de Vellis J. Preparation of separate astroglial and oligodendroglial cell cultures from rat cerebral tissue. J Cell Biol 85 (3) (1980) 890–902. https://doi.org/10.1083/jcb.85.3.890

[55] V. Pillay et al., "A Review of the Effect of Processing Variables on the Fabrication of Electrospun Nanofibers for Drug Delivery Applications," J. Nanomater., vol. 2013, p. 22, 2013, doi: http://dx.doi.org/10.1155/2013/789289.

[55] G. Mancuso, A. Midiri, E. Gerace, C. Biondo, Bacterial Antibiotic Resistance: The Most Critical Pathogens, Pathogens 10 (2021) 1310. https://doi.org/10.3390/pathogens10101310

[55] Franken N.A., Rodermond H.M., Stap J., Haveman J., van Bree C. Clonogenic assay of cells in vitro. Nat Protoc. 1(5) (2006) 2315-9. https://doi.org/10.1038/nprot.2006.339

[56] S. Tan, R. Inai, M. Kotaki, and S. Ramakrishna, "Systematic parameter study for ultra-fine fiber fabrication via electrospinning process," vol. 46, pp. 6128–6134, 2005, doi: 10.1016/j.polymer.2005.05.068.

[56] K.S. Letsididi, Z. Lou, R. Letsididi, K. Mohammed, B.L. Maguy, Antimicrobial and antibiofilm effects of trans-cinnamic acid nanoemulsion and its potential application on lettuce, LWT 94 (2018), 25–32. https://doi.org/10.1016/j.lwt.2018.04.018

[56] Benkő B.M., Tóth G., Moldvai D., Kádár S., Szabó E., Szabó Z.I., Kraszni M., Szente L., Fiser B., Sebestyén A., Zelkó R., Sebe I. Cyclodextrin encapsulation enabling the anticancer repositioning of disulfiram: Preparation, analytical and in vitro biological characterization of the inclusion complexes. Int J Pharm. 657 (2024) 124187. https://doi.org/10.1016/j.ijpharm.2024.124187.

[57] M. M. Hohman, M. Shin, G. Rutledge, and M. P. Brenner, "Electrospinning and electrically forced jets. II. Applications," Phys. Fluids, vol. 13, no. 8, pp. 2221–2236, 2001, doi: 10.1063/1.1384013.

[57] M.R. Tapia-Rodriguez, A. Hernandez-Mendoza, G.A. Gonzalez-Aguilar, M.A. Martinez-Tellez, C.M. Martins, J.F. Ayala-Zavala, Carvacrol as potential quorum sensing inhibitor of Pseudomonas aeruginosa and biofilm production on stainless steel surfaces, Food Control 75 (2017) 255-261, https://doi.org/10.1016/j.foodcont.2016.12.014.

[57] Hua J., You H., Li X., You R., Ma L. Cu(II) ion loading in silk fibroin scaffolds with silk I structure. Int J Biol Macromol 158 (2020) 275–281. https://doi.org/10.1016/j.ijbiomac.2020.04.094

[58] E. Polyetherimide, A. Abutaleb, D. Lolla, A. Aljuhani, and H. U. Shin, "Effects of Surfactants on the Morphology and," pp. 1–14, doi: 10.3390/fib5030033.

USC

[58] G. Brackman, M.J. Garcia-Fernandez, J. Lenoir, L. De Meyer, J.P. Remon, T. De Beer, A. Concheiro, C. Alvarez-Lorenzo, T. Coenye, Dressings loaded with cyclodextrin-hamamelitannin complexes increase Staphylococcus aureus susceptibility toward antibiotics both in single as well as in mixed biofilm communities, Macromol Biosci. 16 (2016) 859-69. https://doi.org/10.1002/mabi.201500437.

[58] Altman G. H., Diaz F., Jakuba C., Calabro T., Horan R. L., Chen J., Lu H., Richmond J., Kaplan D. L. Silk-based biomaterials. Biomaterials 24 (2003) 401–416. https://doi.org/10.1016/S0142-9612(02)00353-8.

[59] D. P. Bhattarai, L. E. Aguilar, C. H. Park, and C. S. Kim, "A Review on Properties of Natural and Synthetic Based Electrospun Fibrous Materials for Bone Tissue Engineering," 2018, doi: 10.3390/membranes8030062.

[59] M. Duplantier, E. Lohou, P. Sonnet, Quorum sensing inhibitors to quench P. aeruginosa pathogenicity, Pharmaceuticals 14 (2021) 1262. https://doi.org/10.3390/ph14121262.

[59] van Oss C. J., Chaudhury M. K., Good R. J. Monopolar surfaces. Adv Colloid Interf Sci. 28(C) (1987) 35–64. https://doi.org/10.1016/0001-8686(87)80008-8

[60] B. C. Xinhua Zonga, Kwangsok Kima, Dufei Fangb, Shaofeng Rana, Benjamin S. Hsiaoa,*, "Structure and process relationship of electrospun bioabsorbable nanofiber membranes," vol. 43, pp. 4403–4412, 202AD.

[60] Z. Berkl, I. Fekete-Kertész, K. Buda, E. Vaszita, E. Fenyvesi, L. Szente, M. Molnár, effect of cyclodextrins on the biofilm formation capacity of Pseudomonas aeruginosa PAO1, Molecules 27 (2022) 3603. https://doi.org/10.3390/molecules27113603.

[60] Cai S., Wu C., Yang W., Liang W., Yu H., Liu L. Recent advance in surface modification for regulating cell adhesion and behaviors. Nanotechnol Rev. 9 (1) 2020 971-989. https://doi.org/10.1515/ntrev-2020-0076

[61] I. Hayati, A. Bailey, and T. . Tadros, "Investigations into the mechanism of electrohydrodynamic spraying of liquids," J. Colloid Interface Sci., vol. 117, no. 1, pp. 222–230, 1987, doi: 10.1016/0021-9797(87)90186-x.

USC UNIVERSIDADE DE SANTIAGO DE COMPOSTELA

[61] T.K. Dash, V.B. Konkimalla, Poly-ϵ-caprolactone based formulations for drug delivery and tissue engineering: A review, J. Control. Release 158 (2012) 15-33. https://doi.org/10.1016/j.jconrel.2011.09.064.

[61] Halcrow P. W., Khan N., Datta G., Ohm J. E., Chen X., Geiger J. D. Importance of measuring endolysosome, cytosolic, and extracellular pH in understanding the pathogenesis of and possible treatments for glioblastoma multiforme. Cancer Reports 2(6) (2019) 2–7. https://doi.org/10.1002/cnr2.1193

[62] N. A. M. Barakat, M. A. Kanjwal, F. A. Sheikh, and H. Yong, "Spider-net within the N6 , PVA and PU electrospun nanofiber mats using salt addition : Novel strategy in the electrospinning process," Polymer (Guildf)., vol. 50, no. 18, pp. 4389–4396, 2009, doi: 10.1016/j.polymer.2009.07.005.

[62] M.W. Tackenberg, C. Geisthövel, A. Marmann, H.P. Schuchmann, P. Kleinebudde, M. Thommes, Mechanistic study of carvacrol processing and stabilization as glassy solid solution and microcapsule, Int. J. Pharm., 478 (2015) 597-605. https://doi.org/10.1016/j.ijpharm.2014.12.012

[62] Lammel A. S., Hu X., Park S., Kaplan D. L., Scheibel T. R. Controlling silk fibroin particle features for drug delivery. Biomaterials 31(16) (2010) 4583–4591. https://doi.org/10.1016/j.biomaterials.2010.02.024

[63] A. Ghaderpour and F. Amiri, "Altering the characterization of nanofibers by changing the electrospinning parameters and their application in tissue engineering , drug delivery , and gene delivery systems," no. January, 2021, doi: 10.1002/pat.5242.

[63] F. Menicucci, E. Palagano, M. Michelozzi, G. Cencetti, A. Raio, A. Bacchi, P.P. Mazzeo, O.A. Cuzman, A. Sidoti, S. Guarino, S. Basile, O. Riccobono, E. Peri, F. Vizza, A. Ienco, Effects of trapped-into-solids volatile organic compounds on paper biodeteriogens, Int. Biodeter. Biodegr. 174 (2022) 105469. https://doi.org/10.1016/j.ibiod.2022.105469.

[63] Qiao X., Miller R. Influence of pH on the surface and foaming properties of aqueous silk fibroin solutions. Soft Matter 16 (2020) 3695–3704. https://doi.org/10.1039/c9sm02372k

USC UNIVERSIDADE DE SANTIAGO DE COMPOSTELA

[64] Y. Su et al., "Temperature effect on electrospinning of nanobelts: The case of hafnium oxide," Nanotechnology, vol. 22, no. 28, 2011, doi: 10.1088/0957-4484/22/28/285609.

[64] A.R. Albunia, P. Rizzo, G. Ianniello, C. Rufolo, G. Guerra, Syndiotactic polystyrene films with a cocrystalline phase including carvacrol guest molecules, J. Polym. Sci. Part B: Polym. Phys., 52 (2014) 657-665. https://doi.org/10.1002/polb.23464

[64] Shen X., Sheng H., Zhang Y., Dong X., Kou L., Yao Q., Zhao X. Nanomedicine-based disulfiram and metal ion co-delivery strategies for cancer treatment. Int J Pharm X, 7 (2024) 100248. https://doi.org/10.1016/j.ijpx.2024.100248

[65] J. Pelipenko, J. Kristl, B. Jankovi, and P. Kocbek, "The impact of relative humidity during electrospinning on the morphology and mechanical properties of nanofibers," vol. 456, pp. 125–134, 2013, doi: 10.1016/j.ijpharm.2013.07.078.

[65] G. Narayanan, B.S. Gupta, A. Tonelli, Poly(ε-caprolactone) nanowebs functionalized with α- and γ-cyclodextrins, Biomacromolecules, 15 (2014) 4122–4133. https://doi.org/10.1021/bm501158w

[65] Haeili M., Moore C., Davis C. J. C., Cochran J. B., Shah S., Shrestha T. B., Zhang Y., Bossmann S. H., Benjamin W. H., Kutsch O., Wolschendorf, F. Copper complexation screen reveals compounds with potent antibiotic properties against methicillin-resistant Staphylococcus aureus. Antimicrob Agents Chemother 58 (2014) https://doi.org/10.1128/AAC.02316-13

[66] Y. Montoya, J. Cardenas, J. Bustamante, and R. Valencia, "Effect of sequential electrospinning and co-electrospinning on morphological and fluid mechanical wall properties of polycaprolactone and bovine gelatin scaffolds , for potential use in small diameter vascular grafts," Biomater. Res., vol. 25, no. 38, pp. 1–17, 2021, doi: https://doi.org/10.1186/s40824-021-00240-8.

[66] M. Lemos, A. Borges, J. Teodósio, P. Araújo, F. Mergulhão, L. Melo, M. Simões, The effects of ferulic and salicylic acids on Bacillus cereus and Pseudomonas fluorescens single- and dual-species biofilms, Int. Biodeterior. Biodegradation 86 (2014) 42–51. https://doi.org/10.1016/j.ibiod.2013.06.011

USC DE SANTIAGO DE COMPOSTELA

[66] Liu P., Brown S., Goktug T., Channathodiyil P., Kannappan V., Hugnot J.P., Guichet P.O., Bian X., Armesilla A.L., Darling J.L., Wang W. Cytotoxic effect of disulfiram/copper on human glioblastoma cell lines and ALDH-positive cancer-stem-like cells. Br J Cancer. 107(9) (2012) 1488-97. doi: 10.1038/bjc.2012.442.

[67] B. Z. Sun, E. Zussman, A. L. Yarin, J. H. Wendorff, and A. Greiner, "Compound Core ± Shell Polymer Nanofibers," no. 22, pp. 1929–1932, 2003, doi: 10.1002/adma.200305136.

[67] S. López-Miranda, D. Berdejo, E. Pagán, D. García-Gonzalo, R. Pagán, Modified cyclodextrin type and dehydration methods exert a significant effect on the antimicrobial activity of encapsulated carvacrol and thymol, J. Sci. Food Agric. 101 (2021) 3827-3835. https://doi.org/10.1002/jsfa.11017

[67] Chen D., Cui Q.C., Yang H., Dou Q.P. Disulfiram, a clinically used anti-alcoholism drug and copper-binding agent, induces apoptotic cell death in breast cancer cultures and xenografts via inhibition of the proteasome activity. Cancer Res. 66(21) (2006) 10425-33. https://doi.org/10.1158/0008-5472.CAN-06-2126.

[68] W. Huang, T. Hibino, S. Suye, and S. Fujita, "Electrospun collagen core/poly-l-lactic acid shell nanofibers for prolonged release of hydrophilic drug," pp. 5703–5711, 2021, doi: 10.1039/d0ra08353d.

[68] D. Ribatti, The chick embryo chorioallantoic membrane (CAM). A multifaceted experimental model, Mech. Dev. 141 (2016) 70-77. https://doi.org/10.1016/j.mod.2016.05.003.

[68] Westhoff M.A., Zhou S., Nonnenmacher L., Karpel-Massler G., Jennewein C., Schneider M., Halatsch M.E., Carragher N.O., Baumann B., Krause A., Simmet T., Bachem M.G., Wirtz C.R., Debatin K.M. Inhibition of NF-κB signaling ablates the invasive phenotype of glioblastoma. Mol Cancer Res. 11(12) (2013) 1611-23. https://doi.org/10.1158/1541-7786.MCR-13-0435-T

[69] Y. Xia, "Electrospinning of nanofibers with core-sheath , hollow , or porous structures Jesse T . McCann , Dan Li and Younan Xia *," J. Mater. Chem., vol. 15, no. 7, pp. 727–734, 2005, doi: https://doi.org/10.1039/B415094E.

[69] X. Farto-Vaamonde, L. Diaz-Gomez, A. Parga, A. Otero, A. Concheiro, C. Alvarez-Lorenzo, Perimeter and carvacrol-loading regulate angiogenesis and biofilm

growth in 3D printed PLA scaffolds, J. Control Release. 352 (2022) 776-792. https://doi.org/10.1016/j.jconrel.2022.10.060

[70] A. Khalf and S. V Madihally, "European Journal of Pharmaceutics and Biopharmaceutics Recent advances in multiaxial electrospinning for drug delivery," Eur. J. Pharm. Biopharm., vol. 112, pp. 1–17, 2017, doi: 10.1016/j.ejpb.2016.11.010.

[70] D.Y. Choi, Y.H. Baek, J.E. Huh, J. M. Ko, H.S. Woo, J.D. Lee, D.S. Park, Stimulatory effect of Cinnamomum cassia and cinnamic acid on angiogenesis through up-regulation of VEGF and Flk-1/KDR expression, Int. Immunopharmacol. 9 (2009) 959–967.

[71] V. Kalra, J. H. Lee, J. H. Park, M. Marquez, and Y. L. Joo, "Confined Assembly of Asymmetric Block-Copolymer Nanofibers via Multiaxial Jet Electrospinning," pp. 2323–2332, 2009, doi: 10.1002/smll.200900157.

[71] D. Matluobi, A. Araghi, B.F.A. Maragheh, A. Rezabakhsh, S. Soltani, M. Khaksar, V. Siavashi, A. Feyzi, H.S. Bagheri, R. Rahbarghazi, S. Montazersaheb, Carvacrol promotes angiogenic paracrine potential and endothelial differentiation of human mesenchymal stem cells at low concentrations, Microvasc. Res. 115 (2018) 20–27. https://doi.org/10.1016/j.mvr.2017.08.003

[72] D. Yu, X. Li, X. Wang, J. Yang, S. W. A. Bligh, and G. R. Williams, "Nano fi bers Fabricated Using Triaxial Electrospinning as Zero Order Drug Delivery Systems," 2015, doi: 10.1021/acsami.5b06007.

[73] X. Li, Y. He, J. Hou, G. Yang, and S. Zhou, "A Time-Programmed Release of Dual Drugs from an Implantable Trilayer Structured Fiber Device for Synergistic Treatment of Breast Cancer," vol. 1902262, pp. 1–14, 2020, doi: 10.1002/smll.201902262.

[74] W. K. Son, J. H. Youk, and W. H. Park, "Preparation of Ultrafine Oxidized Cellulose Mats via Electrospinning," vol. 5, no. 1, pp. 197–201, 2004, doi: https://doi.org/10.1021/bm034312g.

[75] M. Wang, D. Yu, S. Wan, and A. Bligh, "Progress in preparing electrospun Janus fibers and their applications," Appl. Mater. Today, vol. 31, no. October 2022, p. 101766, 2023, doi: 10.1016/j.apmt.2023.101766.

USC

[76] P. Gupta and G. L. Wilkes, “Some investigations on the fiber formation by utilizing a side-by-side bicomponent electrospinning approach,” vol. 44, pp. 6353–6359, 2003, doi: 10.1016/S0032-3861(03)00616-5.

[77] Y. Su, M. B. Taskin, M. Dong, X. Han, F. Besenbacher, and M. Chen, “A biocompatible artificial tendril with a spontaneous 3D Janus multi-helix-perversion configuration,” Mater. Chem. Front., vol. 4, no. 7, pp. 2149–2156, 2020, doi: 10.1039/d0qm00125b.

[78] G. Chen, Y. Xu, D. Yu, D. Zhang, N. P. Chatterton, and K. N. White, “Structure-tunable Janus fibers fabricated using spinnerets with varying port angles †,” Chem. Commun., vol. 51, pp. 4623–4626, 2015, doi: 10.1039/C5CC00378D.

[79] G. Jin, S. Lee, S. Kim, M. Kim, and J. Jang, “Bicomponent electrospinning to fabricate three-dimensional hydrogel-hybrid nanofibrous scaffolds with spatial fiber tortuosity,” pp. 793–804, 2014, doi: 10.1007/s10544-014-9883-z.

[80] Y. Li et al., “Developments of Advanced Electrospinning Techniques: A Critical Review,” Adv. Mater. Technol., vol. 6, no. 11, pp. 1–29, 2021, doi: 10.1002/admt.202100410.

[81] Y. Chen et al., “Preparation of Charged Mosaic Membrane of Sodium Polystyrene Sulfonate and Poly ( 4-vinyl pyridine ) by Conjugate Electrospinning,” vol. 40716, pp. 1–9, 2014, doi: 10.1002/app.40716.

[82] J. He, K. Qi, Y. Zhou, and S. Cui, “Multiple Conjugate Electrospinning Method for the Preparation of Continuous Polyacrylonitrile Nanofiber Yarn,” vol. 40137, pp. 2–7, 2014, doi: 10.1002/app.40137.

[83] R. S. Bhattarai, R. D. Bachu, S. H. S. Boddu, and S. Bhaduri, “Biomedical Applications of Electrospun Nanofibers : Drug and Nanoparticle Delivery,” 2018, doi: 10.3390/pharmaceutics11010005.

[84] R. Nayak, R. Padhye, and L. Arnold, Melt-electrospinning of nanofibers. Elsevier Ltd., 2017. doi: 10.1016/B978-0-08-100907-9.00002-7.

[85] W. Feng et al., “Coaxial electrospun membranes with thermal energy storage and shape memory functions for simultaneous thermal / moisture management in

USC UNIVERSIDADE DE SANTIAGO DE COMPOSTELA

personal cooling textiles," Eur. Polym. J., vol. 145, no. November 2020, p. 110245, 2021, doi: 10.1016/j.eurpolymj.2020.110245.

[86] H. Zhong, J. Huang, J. Wu, and J. Du, "Electrospinning nanofibers to 1D , 2D , and 3D scaffolds and their biomedical applications," Nano Res., vol. 15, no. 2, pp. 787–804, 2022, doi: https://doi.org/10.1007/s12274-021-3593-7.

[87] Y. Yokoyama, S. Hattori, C. Yoshikawa, Y. Yasuda, and H. Koyama, "Novel wet electrospinning system for fabrication of spongiform nano fi ber 3-dimensional fabric," Mater. Lett., vol. 63, no. 9–10, pp. 754–756, 2009, doi: 10.1016/j.matlet.2008.12.042.

[88] R. Nanomedicine et al., "3D electrospun silk fibroin nanofibers for fabrication of artificial skin," Nanomedicine Nanotechnology, Biol. Med., vol. 11, no. 3, pp. 681–691, 2015, doi: 10.1016/j.nano.2014.11.007.

[89] M. Vong, E. Speirs, C. Klomkliang, I. Akinwumi, W. Nuansing, and N. Radacsi, "RSC Advances," pp. 15501–15512, 2018, doi: 10.1039/c7ra13278f.

[90] P. Sofokleous, E. Stride, W. Bonfield, and M. Edirisinghe, "Design, construction and performance of a portable handheld electrohydrodynamic multi-needle spray gun for biomedical applications," Mater. Sci. Eng. C, vol. 33, no. 1, pp. 213–223, 2013, doi: 10.1016/j.msec.2012.08.033.

[91] S. C. Xu et al., "A battery-operated portable handheld electrospinning apparatus," Nanoscale, vol. 7, no. 29, pp. 12351–12355, 2015, doi: 10.1039/c5nr02922h.

[92] R. A. Revia, B. A. Wagner, and M. Zhang, "A portable electrospinner for nanofiber synthesis and its application for cosmetic treatment of alopecia," Nanomaterials, vol. 9, no. 9, 2019, doi: 10.3390/nano9091317.

[93] M. M. Abdul Hameed, S. A. P. Mohamed Khan, B. M. Thamer, N. Rajkumar, H. El-Hamshary, and M. El-Newehy, "Electrospun nanofibers for drug delivery applications: Methods and mechanism," Polym. Adv. Technol., vol. 34, no. 1, pp. 6–23, 2023, doi: 10.1002/pat.5884.

USC UNIVERSIDADE DE SANTIAGO DE COMPOSTELA

[94] Y. Liu, X. Chen, Y. Liu, Y. Gao, and P. Liu, "Electrospun Coaxial Fibers to Optimize the Release of Poorly Water-Soluble Drug," Polymers (Basel)., vol. 14, no. 469, pp. 1–13, 2022, doi: https://doi.org/ 10.3390/polym14030469.

[95] S. Kajdič, O. Planinšek, M. Gašperlin, and P. Kocbek, "Electrospun nanofibers for customized drug-delivery systems," J. Drug Deliv. Sci. Technol., vol. 51, no. March, pp. 672–681, 2019, doi: 10.1016/j.jddst.2019.03.038.

[96] P. P. P.Preetha, A.Srinivasa Rao, "Biphasic drug delivery in controlled release formulations – A review," Int. J. Pharm. Technol., vol. 6, no. 10, pp. 3046–3060, 2015.

[97] N. Nikmaram et al., "Emulsion-based systems for fabrication of electrospun nanofibers: Food, pharmaceutical and biomedical applications," RSC Adv., vol. 7, no. 46, pp. 28951–28964, 2017, doi: 10.1039/c7ra00179g.

[98] P. McClellan and W. J. Landis, "Recent Applications of Coaxial and Emulsion Electrospinning Methods in the Field of Tissue Engineering," Biores. Open Access, vol. 5, no. 1, pp. 212–227, 2016, doi: 10.1089/biores.2016.0022.

[99] X. Luo, C. Xie, H. Wang, C. Liu, S. Yan, and X. Li, "Antitumor activities of emulsion electrospun fibers with core loading of hydroxycamptothecin via intratumoral implantation," Int. J. Pharm., vol. 425, no. 1–2, pp. 19–28, 2012, doi: 10.1016/j.ijpharm.2012.01.012.

[100] S. P. Miguel et al., "Electrospun polymeric nanofibres as wound dressings: A review," Colloids Surfaces B Biointerfaces, vol. 169, pp. 60–71, 2018, doi: 10.1016/j.colsurfb.2018.05.011.

[101] A. Szentivanyi, T. Chakradeo, H. Zernetsch, and B. Glasmacher, "Electrospun cellular microenvironments : Understanding controlled release and scaffold structure," Adv. Drug Deliv. Rev., vol. 63, no. 4–5, pp. 209–220, 2011, doi: 10.1016/j.addr.2010.12.002.

[102] W. Song, Z. Ma, C. Wang, H. Li, and Y. He, "Pro-chondrogenic and immunomodulatory melatonin-loaded electrospun membranes for tendon-to-bone healing," J. Mater. Chem. B, vol. 7, no. 42, pp. 6564–6575, 2019, doi: 10.1039/c9tb01516g.

USC UNIVERSIDADE DE SANTIAGO DE COMPOSTELA

[103] G. Kuang, Z. Zhang, S. Liu, and D. Zhou, "Biomaterials Science Biphasic drug release from electrospun polyblend nano fi bers for optimized local cancer treatment †," 2017, doi: 10.1039/c7bm01018d.

[104] A. Laha, C. S. Sharma, and S. Majumdar, "Sustained drug release from multi-layered sequentially crosslinked electrospun gelatin nano fi ber mesh," Mater. Sci. Eng. C, vol. 76, pp. 782–786, 2017, doi: 10.1016/j.msec.2017.03.110.

[105] C. A. García-González, A. Concheiro, and C. Alvarez-Lorenzo, "Processing of Materials for Regenerative Medicine Using Supercritical Fluid Technology," Bioconjug. Chem., vol. 26, no. 7, pp. 1159–1171, 2015, doi: 10.1021/bc5005922.

[106] K. Li et al., "Three-dimensional magnetic fibrous scaffold with icariin expanded by supercritical CO2 for bone tissue engineering under static magnetic field," Compos. Part B Eng., vol. 226, no. July, p. 109304, 2021, doi: 10.1016/j.compositesb.2021.109304.

[107] J. Wang and M. Windbergs, "Functional electrospun fibers for the treatment of human skin wounds," Eur. J. Pharm. Biopharm., vol. 119, pp. 283–299, 2017, doi: 10.1016/j.ejpb.2017.07.001.

[108] R. S. Tiğli, N. M. Kazaroğlu, B. Maviş, and M. Gumusderelioglu, "Cellular behavior on epidermal growth factor (EGF)-immobilized PCL/gelatin nanofibrous scaffolds," J. Biomater. Sci. Polym. Ed., vol. 22, no. 1–3, pp. 207–223, 2011, doi: 10.1163/092050609X12591500475424.

[109] H. Daemi, M. Mashayekhi, and M. Pezeshki Modaress, "Facile fabrication of sulfated alginate electrospun nanofibers," Carbohydr. Polym., vol. 198, no. May, pp. 481–485, 2018, doi: 10.1016/j.carbpol.2018.06.105.

[110] J. S. Choi, K. W. Leong, and H. S. Yoo, "In vivo wound healing of diabetic ulcers using electrospun nanofibers immobilized with human epidermal growth factor (EGF)," Biomaterials, vol. 29, no. 5, pp. 587–596, 2008, doi: 10.1016/j.biomaterials.2007.10.012.

[111] X. Sun et al., "BFGF-grafted electrospun fibrous scaffolds via poly(dopamine) for skin wound healing," J. Mater. Chem. B, vol. 2, no. 23, pp. 3636–3645, 2014, doi: 10.1039/c3tb21814g.

USC

[112] Z. Yang, H. Peng, W. Wang, and T. Liu, "Crystallization behavior of poly(ε-caprolactone)/layered double hydroxide nanocomposites," J. Appl. Polym. Sci., vol. 116, no. 5, pp. 2658–2667, 2010, doi: 10.1002/app.

[113] S. Nam, S. Y. Lee, and H. Cho, "Journal of Colloid and Interface Science Phloretin-loaded fast dissolving nanofibers for the locoregional therapy of oral squamous cell carcinoma," J. Colloid Interface Sci., vol. 508, pp. 112–120, 2017, doi: 10.1016/j.jcis.2017.08.030.

[114] K. Anjireddy and S. Karpagam, "International Journal of Biological Macromolecules Chitosan nanofilm and electrospun nanofiber for quick drug release in the treatment of Alzheimer ' s disease : In vitro and in vivo evaluation," Int. J. Biol. Macromol., vol. 105, pp. 131–142, 2017, doi: 10.1016/j.ijbiomac.2017.07.021.

[115] W. Cui, X. Li, X. Zhu, G. Yu, S. Zhou, and J. Weng, "Investigation of Drug Release and Matrix Degradation of Electrospun Poly ( DL -lactide ) Fibers with Paracetanol Inoculation," Biomacromolecules, vol. 7, pp. 1623–1629, 2006, doi: 10.1021/bm060057z.

[116] J. Zeng et al., "Biodegradable electrospun fibers for drug delivery," vol. 92, pp. 227–231, 2003, doi: 10.1016/S0168-3659(03)00372-9.

[117] Y. You, B. Min, S. J. Lee, T. S. Lee, and W. H. Park, "In Vitro Degradation Behavior of Electrospun Polyglycolide , Polylactide , and Poly ( lactide- co -glycolide )," pp. 2–9, 2004, doi: 10.1002/app.21116.

[118] X. Zhu et al., "Anti-Neoplastic Cytotoxicity of SN-38-Loaded PCL / Gelatin Electrospun Composite Nanofiber Scaffolds against Human," J. Pharm. Sci., vol. 104, no. 12, pp. 4345–4354, 2015, doi: 10.1002/jps.24684.

[119] Q. Sang, G. R. Williams, H. Wu, K. Liu, H. Li, and L. Zhu, "Materials Science & Engineering C Electrospun gelatin / sodium bicarbonate and poly ( lactide- co - ε - caprolactone )/ sodium bicarbonate nano fi bers as drug delivery systems," Mater. Sci. Eng. C, vol. 81, no. July, pp. 359–365, 2017, doi: 10.1016/j.msec.2017.08.007.

[120] J. Hu, H. Li, G. R. Williams, H. Yang, L. Tao, and L. Zhu, "Electrospun Poly ( N-isopropylacrylamide )/ Ethyl Cellulose Nano fi bers as Thermoresponsive Drug Delivery Systems," vol. 105, pp. 1104–1112, 2016, doi: 10.1016/S0022-3549(15)00191-4.

[121] Y. Li et al., "Light responsive hybrid nanofibres for on-demand therapeutic drug and cell delivery," 2016, doi: 10.1002/term.

[122] J. Yun, J. S. Im, Y. Lee, and H. Kim, "Electro-responsive transdermal drug delivery behavior of PVA / PAA / MWCNT nanofibers," Eur. Polym. J., vol. 47, no. 10, pp. 1893–1902, 2011, doi: 10.1016/j.eurpolymj.2011.07.024.

[123] Y. Kim, M. Ebara, and T. Aoyagi, "FULL PAPER A Smart Hyperthermia Nanofi ber with Switchable Drug Release for Inducing Cancer Apoptosis," pp. 1–9, 2013, doi: 10.1002/adfm.201300746.

[124] X. Wang, D. Yu, X. Li, S. W. A. Bligh, and G. R. Williams, "Electrospun medicated shellac nano fi bers for colon-targeted drug delivery," Int. J. Pharm., vol. 490, no. 1–2, pp. 384–390, 2015, doi: 10.1016/j.ijpharm.2015.05.077.

[125] Y. Sakai et al., "Corticostriatal functional connectivity in non-medicated patients with," vol. 26, pp. 463–469, 2011, doi: 10.1016/j.eurpsy.2010.09.005.

[126] M. Ekor, "The growing use of herbal medicines : issues relating to adverse reactions and challenges in monitoring safety," vol. 4, no. January, pp. 1–10, 2014, doi: 10.3389/fphar.2013.00177.

[127] C. L. Ventola, "The Antibiotic Resistance Crisis Part 1 : Causes and Threats," Pharm. Ther., vol. 40, no. 4, pp. 277–283, 2015.

[128] D. Chinemerem Nwobodo et al., "Antibiotic resistance: The challenges and some emerging strategies for tackling a global menace," J. Clin. Lab. Anal., vol. 36, no. 9, pp. 1–10, 2022, doi: 10.1002/jcla.24655.

[129] C. H. Rammelkamp and T. Maxon, "Experimental Biology and Medicine," 1942, doi: 10.3181/00379727-51-13986.

[130] M. Gajdács, "The Continuing Threat of Methicillin-Resistant Staphylococcus aureus," Antibiotics, vol. 8, p. 52, 2019, doi: 10.3390/antibiotics8020052.

[131] J. O'Neill, "Tackling Drug-Resistance Infections Globally: Final Report and Recommendations. The review on Antimicrobial Resistance Chaired by Jim O'Neill.[Online …," no. May, pp. 1–84, 2016, [Online]. Available: https://amr-review.org/sites/default/files/160518_Final paper_with cover.pdf

USC DE COMPOSTELA

[132] The Lancet, "Antimicrobial resistance: time to repurpose the Global Fund," Lancet, vol. 399, no. 10322, p. 335, 2022, doi: 10.1016/S0140-6736(22)00091-5.

[133] M. Hosseini et al., "Prediction of tsunami of resistance to some antibiotics is not fetched which used during COVID- - 19 pandemic," no. January, pp. 1–10, 2023, doi: 10.1002/jcla.24959.

[134] EClinicalMedicine, "Antimicrobial resistance: a top ten global public health threat," eClinicalMedicine, vol. 41, p. 101221, 2021, doi: 10.1016/j.eclinm.2021.101221.

[135] C. J. Murray et al., "Global burden of bacterial antimicrobial resistance in 2019: a systematic analysis," Lancet, vol. 399, no. 10325, pp. 629–655, 2022, doi: 10.1016/S0140-6736(21)02724-0.

[136] A. Cassini et al., "Attributable deaths and disability-adjusted life-years caused by infections with antibiotic-resistant bacteria in the EU and the European Economic Area in 2015: a population-level modelling analysis," Lancet Infect. Dis., vol. 19, no. 1, pp. 56–66, 2019, doi: 10.1016/S1473-3099(18)30605-4.

[137] S. Basak, P. Singh, and M. Rajurkar, "Multidrug Resistant and Extensively Drug Resistant Bacteria: A Study," J. Pathog., vol. 2016, pp. 1–5, 2016, doi: 10.1155/2016/4065603.

[138] H. Endale, M. Mathewos, and D. Abdeta, "Potential Causes of Spread of Antimicrobial Resistance and Preventive Measures in One Health Perspective-A Review," Infect. Drug Resist., vol. 16, no. December, pp. 7515–7545, 2023, doi: 10.2147/IDR.S428837.

[139] S. K. Ahmed et al., "Antimicrobial resistance: Impacts, challenges, and future prospects," J. Med. Surgery, Public Heal., vol. 2, no. March, p. 100081, 2024, doi: 10.1016/j.glmedi.2024.100081.

[140] H. Mohanty, S. Pachpute, and R. P. Yadav, "Mechanism of drug resistance in bacteria: efflux pump modulation for designing of new antibiotic enhancers," Folia Microbiol. (Praha)., vol. 66, no. 5, pp. 727–739, 2021, doi: 10.1007/s12223-021-00910-z.

USC UNIVERSIDADE DE SANTIAGO DE COMPOSTELA

[141] A. Asghar et al., "An insights into emerging trends to control the threats of antimicrobial resistance (AMR): an address to public health risks," Arch. Microbiol., vol. 206, no. 2, 2024, doi: 10.1007/s00203-023-03800-9.

[142] J. L. Martinez, "Drug resistance General principles of antibiotic resistance in bacteria," Drug Discov. Today Technol., vol. 11, pp. 33–39, 2014, doi: 10.1016/j.ddtec.2014.02.001.

[143] E. Van Duijkeren, A. Schink, M. C. Roberts, Y. Wang, and S. Schwarz, "Mechanisms of Bacterial Resistance to Antimicrobial Agents," Microbiol. Spectr., vol. 6, no. 2, 2017, doi: 10.1128 /microbiolspec.ARBA-0019-2017.

[144] J. M. A. Blair, M. A. Webber, A. J. Baylay, D. O. Ogbolu, and L. J. V Piddock, "Molecular mechanisms of antibiotic resistance," Nat. Publ. Gr., vol. 13, no. 1, pp. 42–51, 2014, doi: 10.1038/nrmicro3380.

[145] G. Zhou, Q. Shi, X. Huang, and X. Xie, "The Three Bacterial Lines of Defense against Antimicrobial Agents," pp. 21711–21733, 2015, doi: 10.3390/ijms160921711.

[146] A. Tello, B. Austin, and T. C. Telfer, "Selective pressure of antibiotic pollution on bacteria of importance to public health," Environ. Health Perspect., vol. 120, no. 8, pp. 1100–1106, 2012, doi: 10.1289/ehp.1104650.

[147] H. N. Xian-Zhi Li, "Efflux-Mediated Drug Resistance in Bacteria: an Update," Drugs, vol. 69, no. 12, pp. 1555–1623, 2010, doi: 10.2165/11317030-000000000-00000.Efflux-Mediated.

[148] T. Li et al., "Bacterial resistance to antibacterial agents: Mechanisms, control strategies, and implications for global health," Sci. Total Environ., vol. 860, no. November 2022, p. 160461, 2023, doi: 10.1016/j.scitotenv.2022.160461.

[149] M. A. Kohanski, D. J. Dwyer, and J. J. Collins, "How antibiotics kill bacteria: From targets to networks," Nat. Rev. Microbiol., vol. 8, no. 6, pp. 423–435, 2010, doi: 10.1038/nrmicro2333.

[150] V. Kumar, S. L. Viviani, J. Ismail, S. Agarwal, A. Bonomo, and F. V. D. A. Id, "Structural analysis of the boronic acid β - lactamase inhibitor vaborbactam binding to Pseudomonas aeruginosa penicillin-binding protein 3," pp. 1–16, 2021, doi: 10.1371/journal.pone.0258359.

USC UNIVERSIDADE DE SANTIAGO

[151] L. S. Redgrave, S. B. Sutton, M. A. Webber, and L. J. V Piddock, "Fluoroquinolone resistance : mechanisms , impact on bacteria , and role in evolutionary success," Trends Microbiol., vol. 22, no. 8, pp. 438–445, 2014, doi: 10.1016/j.tim.2014.04.007.

[152] R. R. N. A. Methyltransferases, "A m i n o g l y c o s i d e Re s i s t a n c e The Emergence of Acquired 16S," Infect. Dis. Clin. NA, vol. 30, no. 2, pp. 523–537, 2016, doi: 10.1016/j.idc.2016.02.011.

[153] M. H. Muhammad, A. L. Idris, X. Fan, Y. Guo, Y. Yu, and X. Jin, "Beyond Risk : Bacterial Biofilms and Their Regulating Approaches," vol. 11, no. May, pp. 1–20, 2020, doi: 10.3389/fmicb.2020.00928.

[154] H. Flemming and J. Wingender, "Relevance of microbial extracellular polymeric substances ( EPSs ) – Part I : Structural and ecological aspects," Water Sci. Technol., vol. 43, no. 6, pp. 1–8, 2001, doi: https://doi.org/10.2166/wst.2001.0326.

[155] G. Laverty, S. P. Gorman, and B. F. Gilmore, "Biomolecular Mechanisms of Pseudomonas aeruginosa and Escherichia coli Biofilm Formation," pp. 596–632, 2014, doi: 10.3390/pathogens3030596.

[156] A. J. Weisberg and J. H. Chang, "Mobile Genetic Element Flexibility as an Underlying Principle to Bacterial Evolution," Annu. Rev. Microbiol., vol. 77, pp. 603–624, 2023, doi: 10.1146/annurev-micro-032521-022006.

[157] P. Gilbert, T. Maira-litran, and J. M, "The Physiology and Collective Recalcitrance of Microbial Biofilm Communities," Adv. Microb. Physiol., vol. 46, pp. 203–256, 2002, doi: https://doi.org/10.1016/S0065-2911(02)46005-5.

[158] W. R. Miller and C. A. Arias, "ESKAPE pathogens: antimicrobial resistance, epidemiology, clinical impact and therapeutics," Nat. Rev. Microbiol., vol. 22, no. 10, pp. 598–616, 2024, doi: 10.1038/s41579-024-01054-w.

[159] M. Vouga and G. Greub, "Emerging bacterial pathogens: The past and beyond," Clin. Microbiol. Infect., vol. 22, no. 1, pp. 12–21, 2016, doi: 10.1016/j.cmi.2015.10.010.

[160] G.-H. Tan, Q.-W. Low, H.-C. Lim, H.-K. Seah, and H.-K. Chan, "Inappropriate Antibiotic Utilization: Outpatient Prescription Review of a Regional Secondary

USC UNIVERSIDADE DE SANTIAGO

Hospital in Kedah, Malaysia," J. Pharm. Pract. Community Med., vol. 3, no. 4, pp. 215–219, 2017, doi: 10.5530/jppcm.2017.4.62.

[161] P. Dadgostar, "Antimicrobial resistance: implications and costs," Infect. Drug Resist., vol. 12, pp. 3903–3910, 2019, doi: 10.2147/IDR.S234610.

[162] I. Boszczowski, B. S. Kliemann, A. S. Levin, M. Luı, and J. J. Lewis, "Socioeconomic Determinants of Antibiotic Consumption in the State of S ã o Paulo , Brazil : The Effect of Restricting Over-The-Counter," no. Did, pp. 1–14, 2016, doi: 10.5061/dryad.mt685.

[163] T. Pulingam et al., "Antimicrobial resistance: Prevalence, economic burden, mechanisms of resistance and strategies to overcome," Eur. J. Pharm. Sci., vol. 170, p. 106103, 2022, doi: 10.1016/j.ejps.2021.106103.

[164] T. Mahtab et al., "Journal of Infection and Public Health Antibiotic resistance in microbes : History , mechanisms , therapeutic strategies and future prospects," vol. 14, pp. 1750–1766, 2021, doi: 10.1016/j.jiph.2021.10.020.

[165] R. Smith and J. Coast, "The true cost of antimicrobial resistance," BMJ, vol. 346, no. 7899, pp. 1–5, 2013, doi: 10.1136/bmj.f1493.

[166] E. Kobeissi, M. Menassa, K. Moussally, E. Repetto, I. Soboh, and M. Hajjar, "The socioeconomic burden of antibiotic resistance in conflict-affected settings and refugee hosting countries : a systematic scoping review," Confl. Health, vol. 15, no. 21, pp. 1–9, 2021, doi: https://doi.org/10.1186/s13031-021-00357-6.

[167] W. Wang et al., "Antibiotic resistance : a rundown of a global crisis," Infect. Drug Resist., vol. 11, pp. 1645–1658, 2018, doi: http://dx.doi.org/10.2147/IDR.S173867.

[168] X. Zhen, C. S. Lundborg, X. Sun, X. Hu, and H. Dong, "Economic burden of antibiotic resistance in ESKAPE organisms : a systematic review," Antimicrob. Resist. Infect. Control, vol. 7, no. 8, p. 137, 2019, doi: https://doi.org/10.1186/s13756-019-0590-7.

[169] F. Wan, M. D. T. Torres, J. Peng, and C. de la Fuente-Nunez, "Deep-learning-enabled antibiotic discovery through molecular de-extinction," Nat. Biomed. Eng., vol. 8, no. 7, pp. 854–871, 2024, doi: 10.1038/s41551-024-01201-x.

USC UNIVERSIDADE DE SANTIAGO DE COMPOSTELA

[170] F. Wong, C. de la Fuente-Nunez, and J. J. Collins, “Leveraging artificial intelligence in the fight against infectious diseases,” Science (80-. )., vol. 381, no. 6654, pp. 164–170, 2023, doi: 10.1126/science.adh1114.

[171] Y. Wang, K. J. Stebe, C. de la Fuente-Nunez, and R. Radhakrishnan, “Computational Design of Peptides for Biomaterials Applications,” ACS Appl. Bio Mater., vol. 7, no. 2, pp. 617–625, 2024, doi: 10.1021/acsabm.2c01023.

[172] M. D. T. Torres et al., “Mining human microbiomes reveals an untapped source of peptide antibiotics,” Cell, vol. 187, no. 19, pp. 5453-5467.e15, 2024, doi: 10.1016/j.cell.2024.07.027.

[173] C. de la Fuente-Nunez, “Toward Autonomous Antibiotic Discovery,” mSystems, vol. 4, no. 3, pp. 10–14, 2019, doi: 10.1128/msystems.00151-19.

[174] R. D. Forrest, “Early history of wound treatment,” J. R. Soc. Med., vol. 75, no. 3, pp. 198–205, 1982, doi: 10.1177/014107688207500310.

[175] J. B. Shah, “The history of wound care,” J. Am. Col. Certif. Wound Spec., vol. 3, no. 3, pp. 65–66, 2011, doi: 10.1016/j.jcws.2012.04.002.

[176] A. Scalise et al., “Microenvironment and microbiology of skin wounds: The role of bacterial biofilms and related factors,” Semin. Vasc. Surg., vol. 28, no. 3–4, pp. 151–159, 2015, doi: 10.1053/j.semvascsurg.2016.01.003.

[177] L. M. Morton and T. J. Phillips, “Wound healing and treating wounds Differential diagnosis and evaluation of chronic wounds,” J. Am. Acad. Dermatol., vol. 74, no. 4, pp. 589–605, 2016, doi: 10.1016/j.jaad.2015.08.068.

[178] B. K. Sun, Z. Siprashvili, and P. A. Khavari, “Advances in skin grafting and treatment of cutaneous wounds,” Science (80-. )., vol. 346, no. 6212, pp. 941–945, 2014, doi: 10.1126/science.1253836.

[179] M. Rodrigues, N. Kosaric, C. A. Bonham, and G. C. Gurtner, “Wound healing: A cellular perspective,” Physiol. Rev., vol. 99, no. 1, pp. 665–706, 2019, doi: 10.1152/physrev.00067.2017.

[180] J. R. S. Andrei Z. Budzynski, “Fibrinogen and fibrin: Biochemistry and pathophysiology,” Crit. Rev. Oncol. Hematol., vol. 6, no. 2, p. Pages 97-146, 1986, doi: https://doi.org/10.1016/S1040-8428(86)80019-1.

USC DE COMPOSTELA

[181] J. C. McDaniel, S. Roy, and T. A. Wilgus, "Neutrophil activity in chronic venous leg ulcers - A target for therapy?," Wound Repair Regen., vol. 21, no. 3, pp. 339–351, 2013, doi: 10.1111/wrr.12036.

[182] T. A. Wilgus, S. Roy, and J. C. McDaniel, "Neutrophils and Wound Repair: Positive Actions and Negative Reactions," Adv. Wound Care, vol. 2, no. 7, pp. 379–388, 2013, doi: 10.1089/wound.2012.0383.

[183] M. F. Shah, D. C. Mancuso, L. He, and S. Kozak, "Evaluation of the Medicaid Buy-In Program in Washington State: Outcomes for Workers With Disabilities Who Purchase Medicaid Coverage," J. Disabil. Policy Stud., vol. 22, no. 4, pp. 220–229, 2012, doi: 10.1177/1044207311427162.

[184] P. Krzyszczyk, R. Schloss, A. Palmer, and F. Berthiaume, "The role of macrophages in acute and chronic wound healing and interventions to promote pro-wound healing phenotypes," Front. Physiol., vol. 9, no. MAY, pp. 1–22, 2018, doi: 10.3389/fphys.2018.00419.

[185] I. Aukhil, "Biology of wound healing," Periodontol. 2000, vol. 22, no. 1, pp. 44–50, 2000, doi: 10.1034/j.1600-0757.2000.2220104.x.

[186] C. L. Grosskreutz et al., "Vascular endothelial growth factor-induced migration of vascular smooth muscle cells in vitro," Microvasc. Res., vol. 58, no. 2, pp. 128–136, 1999, doi: 10.1006/mvre.1999.2171.

[187] Brainbridge P, "Wound Healing and The Role of Fibroblast," J. Wound Care, vol. 22, no. 8, pp. 407–412, 2013, doi: https://doi.org/10.12968/jowc.2013.22.8.407.

[188] A. W. S. Yeung, A. C. Terentis, N. J. C. King, and S. R. Thomas, "Role of indoleamine 2,3-dioxygenase in health and disease," Clin. Sci., vol. 129, no. 7, pp. 601–672, 2015, doi: 10.1042/CS20140392.

[189] S. ichiro Motegi and O. Ishikawa, "Mesenchymal stem cells: The roles and functions in cutaneous wound healing and tumor growth," J. Dermatol. Sci., vol. 86, no. 2, pp. 83–89, 2017, doi: 10.1016/j.jdermsci.2016.11.005.

[190] A. Clinton and T. Carter, "Chronic wound biofilms: Pathogenesis and potential therapies," Lab Med., vol. 46, no. 4, pp. 277–284, 2015, doi: 10.1309/LMBNSWKUI4JPN7SO.

USC UNIVERSIDADE DE SANTIAGO

[191] G. A. James et al., "Biofilms in chronic wounds," Wound Repair Regen., vol. 16, no. 1, pp. 37–44, 2008, doi: 10.1111/j.1524-475X.2007.00321.x.

[192] B. A. Mast and G. S. Schultz, "Interactions of cytokines, growth factors, and proteases in acute and chronic wounds," Wound Repair Regen., vol. 4, no. 4, pp. 411–420, 1996, doi: 10.1046/j.1524-475X.1996.40404.x.

[193] N. J. Trengove, H. Bielefeldt-Ohmann, and M. C. Stacey, "Mitogenic activity and cytokine levels in non-healing and healing chronic leg ulcers," Wound Repair Regen., vol. 8, no. 1, pp. 13–25, 2000, doi: 10.1046/j.1524-475X.2000.00013.x.

[194] L. E. Tracy, R. A. Minasian, and E. J. Caterson, "Extracellular Matrix and Dermal Fibroblast Function in the Healing Wound," Adv. Wound Care, vol. 5, no. 3, pp. 119–136, 2016, doi: 10.1089/wound.2014.0561.

[195] S. Kadam, S. Nadkarni, J. Lele, S. Sakhalkar, P. Mokashi, and K. S. Kaushik, "Bioengineered Platforms for Chronic Wound Infection Studies: How Can We Make Them More Human-Relevant?," Front. Bioeng. Biotechnol., vol. 7, no. December, 2019, doi: 10.3389/fbioe.2019.00418.

[196] P. Taylor, S. L. Percival, and J. T. Walker, "Potable water and biofilms: A review of the public health implications," Biofouling, vol. 14, no. 2, pp. 99–115, 1999, doi: https://doi.org/10.1080/08927019909378402.

[197] T. K. Fisher, R. Wolcott, D. M. Wolk, M. Bharara, H. R. Kimbriel, and D. G. Armstrong, "Diabetic foot infections: A need for innovative assessments," Int. J. Low. Extrem. Wounds, vol. 9, no. 1, pp. 31–36, 2010, doi: 10.1177/1534734610363459.

[198] K. Rumbaugh, C. Watters, and T. Yuan, "Beneficial and deleterious bacterial–host interactions in chronic wound pathophysiology," Chronic Wound Care Manag. Res., p. 53, 2015, doi: 10.2147/cwcmr.s60317.

[199] M. Zhou, A. Yu, G. Wu, C. Xia, X. Hu, and B. Qi, "Role of different negative pressure values in the process of infected wounds treated by vacuum-assisted closure: An experimental study," Int. Wound J., vol. 10, no. 5, pp. 508–515, 2013, doi: 10.1111/j.1742-481X.2012.01008.x.

[200] A. Tankersley, M. B. Frank, M. Bebak, and R. Brennan, "Early effects of Staphylococcus aureus biofilm secreted products on inflammatory responses of human

USC UNIVERSIDADE DE SANTIAGO

epithelial keratinocytes," J. Inflamm. (United Kingdom), vol. 11, no. 1, pp. 1–11, 2014, doi: 10.1186/1476-9255-11-17.

[201] R. Prabhakara, J. M. Harro, J. G. Leid, M. Harris, and M. E. Shirtliff, "Murine immune response to a chronic Staphylococcus aureus biofilm infection," Infect. Immun., vol. 79, no. 4, pp. 1789–1796, 2011, doi: 10.1128/IAI.01386-10.

[202] E. R. Zielins et al., "Wound healing: An update," Regen. Med., vol. 9, no. 6, pp. 817–830, 2014, doi: 10.2217/rme.14.54.

[203] C. Albanesi, S. Madonna, P. Gisondi, and G. Girolomoni, "The interplay between keratinocytes and immune cells in the pathogenesis of psoriasis," Front. Immunol., vol. 9, no. JUL, pp. 1–7, 2018, doi: 10.3389/fimmu.2018.01549.

[204] C. W. Hall and T. F. Mah, "Molecular mechanisms of biofilm-based antibiotic resistance and tolerance in pathogenic bacteria," FEMS Microbiol. Rev., vol. 41, no. 3, pp. 276–301, 2017, doi: 10.1093/femsre/fux010.

[205] D. M. Castilla, Z.-J. Liu, and O. C. Velazquez, "Oxygen: Implications for Wound Healing," Adv. Wound Care, vol. 1, no. 6, pp. 225–230, 2012, doi: 10.1089/wound.2011.0319.

[206] C. Dunnill et al., "Reactive oxygen species (ROS) and wound healing: the functional role of ROS and emerging ROS-modulating technologies for augmentation of the healing process," Int. Wound J., vol. 14, no. 1, pp. 89–96, 2017, doi: 10.1111/iwj.12557.

[207] S. L. Percival, S. McCarty, J. A. Hunt, and E. J. Woods, "The effects of pH on wound healing, biofilms, and antimicrobial efficacy," Wound Repair Regen., vol. 22, no. 2, pp. 174–186, 2014, doi: 10.1111/wrr.12125.

[208] G. Daeschlein, "Antimicrobial and antiseptic strategies in wound management," Int. Wound J., vol. 10, no. S1, pp. 9–14, 2013, doi: 10.1111/iwj.12175.

[209] L. A. Barnes et al., "Mechanical Forces in Cutaneous Wound Healing: Emerging Therapies to Minimize Scar Formation," Adv. Wound Care, vol. 7, no. 2, pp. 47–56, 2018, doi: 10.1089/wound.2016.0709.

[210] P. Thomen, J. Robert, A. Monmeyran, A. F. Bitbol, C. Douarche, and N. Henry, "Bacterial biofilm under flow: First a physical struggle to stay, then a matter of

USC DE COMPOSTELA

breathing," PLoS One, vol. 12, no. 4, pp. 1–24, 2017, doi: 10.1371/journal.pone.0175197.

[211] R. Agha, R. Ogawa, G. Pietramaggiori, and D. P. Orgill, "A review of the role of mechanical forces in cutaneous wound healing," J. Surg. Res., vol. 171, no. 2, pp. 700–708, 2011, doi: 10.1016/j.jss.2011.07.007.

[212] P. G. Bowler, B. I. Duerden, and D. G. Armstrong, "Wound microbiology and associated approaches to wound management," Clin. Microbiol. Rev., vol. 14, no. 2, pp. 244–269, 2001, doi: 10.1128/CMR.14.2.244-269.2001.

[213] M. Fazli et al., "Nonrandom distribution of Pseudomonas aeruginosa and Staphylococcus aureus in chronic wounds," J. Clin. Microbiol., vol. 47, no. 12, pp. 4084–4089, 2009, doi: 10.1128/JCM.01395-09.

[214] K. Las Heras, M. Igartua, E. Santos-Vizcaino, and R. M. Hernandez, "Chronic wounds: Current status, available strategies and emerging therapeutic solutions," J. Control. Release, vol. 328, no. September, pp. 532–550, 2020, doi: 10.1016/j.jconrel.2020.09.039.

[215] S. Guo and L. A. DiPietro, "Critical review in oral biology & medicine: Factors affecting wound healing," J. Dent. Res., vol. 89, no. 3, pp. 219–229, 2010, doi: 10.1177/0022034509359125.

[216] C. D. Weller, V. Team, and G. Sussman, "First-Line Interactive Wound Dressing Update: A Comprehensive Review of the Evidence," Front. Pharmacol., vol. 11, no. February 2020, pp. 1–13, 2020, doi: 10.3389/fphar.2020.00155.

[217] T. Mustoe, "Understanding chronic wounds: A unifying hypothesis on their pathogenesis and implications for therapy," Am. J. Surg., vol. 187, no. 5 SUPPL. 1, pp. S65–S70, 2004, doi: 10.1016/S0002-9610(03)00306-4.

[218] V. Dubey, D. Mishra, A. Asthana, and N. K. Jain, "Transdermal delivery of a pineal hormone: Melatonin via elastic liposomes," Biomaterials, vol. 27, no. 18, pp. 3491–3496, 2006, doi: 10.1016/j.biomaterials.2006.01.060.

[219] Y. Xia, M. Sun, H. Huang, and W. L. Jin, "Drug repurposing for cancer therapy," Signal Transduct. Target. Ther., vol. 9, no. 1, 2024, doi: 10.1038/s41392-024-01808-1.

USC UNIVERSIDADE DE SANTIAGO

[220] K. Lee and S. Lee, "Electrospun Nanofibrous Membranes with Essential Oils for Wound Dressing Applications," Fibers Polym., vol. 21, no. 5, pp. 999–1012, 2020, doi: 10.1007/s12221-020-9300-6.

[221] L. Czaplewski et al., "Alternatives to antibiotics-a pipeline portfolio review," Lancet Infect. Dis., vol. 16, no. 2, pp. 239–251, 2016, doi: 10.1016/S1473-3099(15)00466-1.

[222] F. Nazzaro, F. Fratianni, L. De Martino, R. Coppola, and V. De Feo, "Effect of essential oils on pathogenic bacteria," Pharmaceuticals, vol. 6, no. 12, pp. 1451–1474, 2013, doi: 10.3390/ph6121451.

[223] J. S. Raut and S. M. Karuppayil, "A status review on the medicinal properties of essential oils," Ind. Crops Prod., vol. 62, pp. 250–264, 2014, doi: https://doi.org/10.1016/j.indcrop.2014.05.055.

[224] C. F. Bagamboula, M. Uyttendaele, and J. Debevere, "Inhibitory effect of thyme and basil essential oils, carvacrol, thymol, estragol, linalool and p-cymene towards Shigella sonnei and S. flexneri," Food Microbiol., vol. 21, no. 1, pp. 33–42, 2004, doi: 10.1016/S0740-0020(03)00046-7.

[225] A. Ben Arfa, S. Combes, L. Preziosi-Belloy, N. Gontard, and P. Chalier, "Antimicrobial activity of carvacrol related to its chemical structure," Lett. Appl. Microbiol., vol. 43, no. 2, pp. 149–154, 2006, doi: 10.1111/j.1472-765X.2006.01938.x.

[226] R. Di Pasqua, G. Betts, N. Hoskins, M. Edwards, D. Ercolini, and G. Mauriello, "Membrane toxicity of antimicrobial compounds from essential oils," J. Agric. Food Chem., vol. 55, no. 12, pp. 4863–4870, 2007, doi: 10.1021/jf0636465.

[227] C. V. Gabel and H. C. Berg, "The speed of the flagellar rotary motor of Escherichia coli varies linearly with protonmotive force," Proc. Natl. Acad. Sci. U. S. A., vol. 100, no. 15, pp. 8748–8751, 2003, doi: 10.1073/pnas.1533395100.

[228] A. Pauli and K. H. Kubeczka, "Antimicrobial properties of volatile phenylpropanes," Nat. Prod. Commun., vol. 5, no. 9, pp. 1387–1394, 2010, doi: 10.1177/1934578x1000500910.

USC UNIVERSIDADE DE SANTIAGO DE COMPOSTELA

[229] M. Hyldgaard, T. Mygind, and R. L. Meyer, "Essential oils in food preservation: Mode of action, synergies, and interactions with food matrix components," Front. Microbiol., vol. 3, no. JAN, pp. 1–24, 2012, doi: 10.3389/fmicb.2012.00012.

[230] I. M. Helander et al., "Characterization of the Action of Selected Essential Oil Components on Gram-Negative Bacteria," J. Agric. Food Chem., vol. 46, no. 9, pp. 3590–3595, 1998, doi: 10.1021/jf980154m.

[231] N. Y. Saad, C. D. Muller, and A. Lobstein, "Major bioactivities and mechanism of action of essential oils and their components," Flavour Fragr. J., vol. 28, no. 5, pp. 269–279, 2013, doi: 10.1002/ffj.3165.

[232] S. Burt, "Essential oils: Their antibacterial properties and potential applications in foods - A review," Int. J. Food Microbiol., vol. 94, no. 3, pp. 223–253, 2004, doi: 10.1016/j.ijfoodmicro.2004.03.022.

[233] B. K. Tiwari, V. P. Valdramidis, C. P. O'Donnell, K. Muthukumarappan, P. Bourke, and P. J. Cullen, "Application of natural antimicrobials for food preservation," J. Agric. Food Chem., vol. 57, no. 14, pp. 5987–6000, 2009, doi: 10.1021/jf900668n.

[234] H. Nikaido, "Prevention of Drug Access to Bacterial Targets: Permeability Barriers and Active Efflux," Science (80-. )., vol. 264, no. 5157, pp. 382–388, 1994, doi: 10.1126/science.8153625.

[235] D. Trombetta et al., "Mechanisms of antibacterial action of three monoterpenes," Antimicrob. Agents Chemother., vol. 49, no. 6, pp. 2474–2478, 2005, doi: 10.1128/AAC.49.6.2474-2478.2005.

[236] S. A. Burt and R. D. Reinders, "Antibacterial activity of selected plant essential oils against Escherichia coil O157:H7," Lett. Appl. Microbiol., vol. 36, no. 3, pp. 162–167, 2003, doi: 10.1046/j.1472-765X.2003.01285.x.

[237] P. Domadia, S. Swarup, A. Bhunia, J. Sivaraman, and D. Dasgupta, "Inhibition of bacterial cell division protein FtsZ by cinnamaldehyde," Biochem. Pharmacol., vol. 74, no. 6, pp. 831–840, 2007, doi: 10.1016/j.bcp.2007.06.029.

[238] R. Di Pasqua, G. Mauriello, G. Mamone, and D. Ercolini, "Expression of DnaK, HtpG, GroEL and Tf chaperones and the corresponding encoding genes during growth of Salmonella Thompson in presence of thymol alone or in combination with salt and

USC UNIVERSIDADE DE SANTIAGO

cold stress," Food Res. Int., vol. 52, no. 1, pp. 153–159, 2013, doi: 10.1016/j.foodres.2013.02.050.

[239] M. Oussalah, S. Caillet, L. Saucier, and M. Lacroix, "Antimicrobial effects of selected plant essential oils on the growth of a Pseudomonas putida strain isolated from meat," Meat Sci., vol. 73, no. 2, pp. 236–244, 2006, doi: 10.1016/j.meatsci.2005.11.019.

[240] Y. H. Li and X. Tian, "Quorum sensing and bacterial social interactions in biofilms," Sensors, vol. 12, no. 3, pp. 2519–2538, 2012, doi: 10.3390/s120302519.

[241] P. Williams, "Quorum sensing, communication and cross-kingdom signalling in the bacterial world," Microbiology, vol. 153, no. 12, pp. 3923–3938, 2007, doi: 10.1099/mic.0.2007/012856-0.

[242] B. L. Bassler, "How bacteria talk to each other: Regulation of gene expression by quorum sensing," Curr. Opin. Microbiol., vol. 2, no. 6, pp. 582–587, 1999, doi: 10.1016/S1369-5274(99)00025-9.

[243] M. E. Taga, J. L. Semmelhack, and B. L. Bassler, "The LuxS-dependent autoinducer Al-2 controls the expression of an ABC transporter that functions in Al-2 uptake in Salmonella typhimurium," Mol. Microbiol., vol. 42, no. 3, pp. 777–793, 2001, doi: 10.1046/j.1365-2958.2001.02669.x.

[244] B. K. Hammer and B. L. Bassler, "Quorum sensing controls biofilm formation in Vibrio cholerae," Mol. Microbiol., vol. 50, no. 1, pp. 101–104, 2003, doi: 10.1046/j.1365-2958.2003.03688.x.

[245] F. Nazzaro, F. Fratianni, and R. Coppola, "Quorum sensing and phytochemicals," Int. J. Mol. Sci., vol. 14, no. 6, pp. 12607–12619, 2013, doi: 10.3390/ijms140612607.

[246] J. M. McCord, "The evolution of free radicals and oxidative stress," Am. J. Med., vol. 108, no. 8, pp. 652–659, 2000, doi: 10.1016/S0002-9343(00)00412-5.

[247] A. Tomaino et al., "Influence of heating on antioxidant activity and the chemical composition of some spice essential oils," Food Chem., vol. 89, no. 4, pp. 549–554, 2005, doi: 10.1016/j.foodchem.2004.03.011.

USC UNIVERSIDADE DE SANTIAGO DE COMPOSTELA

[248] M. G. Miguel, "Antioxidant and anti-inflammatory activities of essential oils: A short review," Molecules, vol. 15, no. 12, pp. 9252–9287, 2010, doi: 10.3390/molecules15129252.

[249] A. El Asbahani et al., "Essential oils: From extraction to encapsulation," Int. J. Pharm., vol. 483, no. 1–2, pp. 220–243, 2015, doi: 10.1016/j.ijpharm.2014.12.069.

[250] Z. Drulis-Kawa and A. Dorotkiewicz-Jach, "Liposomes as delivery systems for antibiotics," Int. J. Pharm., vol. 387, no. 1–2, pp. 187–198, 2010, doi: 10.1016/j.ijpharm.2009.11.033.

[251] N. T. Ardekani, M. Khorram, K. Zomorodian, S. Yazdanpanah, H. Veisi, and H. Veisi, "Evaluation of electrospun poly (vinyl alcohol)-based nanofiber mats incorporated with Zataria multiflora essential oil as potential wound dressing," Int. J. Biol. Macromol., vol. 125, pp. 743–750, 2019, doi: 10.1016/j.ijbiomac.2018.12.085.

[252] I. Unalan et al., "Evaluation of Electrospun Poly(E-Caprolactone)/Gelatin Nanofiber Mats Containing Clove Essential Oil for Antibacterial Wound Dressing," Pharmaceutics, vol. 11, no. 11, p. 570, 2019, doi: https://doi.org/10.3390/pharmaceutics11110570.

[253] H. S. Sofi, T. Akram, A. H. Tamboli, A. Majeed, N. Shabir, and F. A. Sheikh, "Novel lavender oil and silver nanoparticles simultaneously loaded onto polyurethane nanofibers for wound-healing applications," Int. J. Pharm., vol. 569, no. April, 2019, doi: 10.1016/j.ijpharm.2019.118590.

[254] I. Unalan, B. Slavik, A. Buettner, W. H. Goldmann, G. Frank, and A. R. Boccaccini, "Physical and Antibacterial Properties of Peppermint Essential Oil Loaded Poly (ε-caprolactone) (PCL) Electrospun Fiber Mats for Wound Healing," Front. Bioeng. Biotechnol., vol. 7, no. November, pp. 1–11, 2019, doi: 10.3389/fbioe.2019.00346.

[255] M. Qin et al., "In Situ Electrospinning Wound Healing Films Composed of Zein and Clove Essential Oil," Macromol. Mater. Eng., vol. 305, no. 3, pp. 1–6, 2020, doi: 10.1002/mame.201900790.

[256] J. X. Liu et al., "In Situ Electrospun Zein/Thyme Essential Oil-Based Membranes as an Effective Antibacterial Wound Dressing," ACS Appl. Bio Mater., vol. 3, no. 1, pp. 302–307, 2020, doi: 10.1021/acsabm.9b00823.

[257] M. Salehi et al., "Porous electrospun poly(ε-caprolactone)/gelatin nanofibrous mat containing cinnamon for wound healing application: in vitro and in vivo study," Biomed. Eng. Lett., vol. 10, no. 1, pp. 149–161, 2020, doi: 10.1007/s13534-019-00138-4.

[258] H. Hosseinpor, A. Khaledi, and D. Esmaeili, "The properties of nanofiber scaffolds of polyurethane-Cinnamomum zeylanicum against pathogens of Pseudomonas aeruginosa and Staphylococcus aureus," Polym. Bull., vol. 78, no. 1, pp. 223–245, 2021, doi: 10.1007/s00289-019-03095-1.

[259] P. Sinsup et al., "Zingiber cassumunar roxb. Essential oil-loaded electrospun poly(lactic acid)/poly(ethylene oxide) fiber blend membrane for antibacterial wound dressing application," Membranes (Basel)., vol. 11, no. 9, 2021, doi: 10.3390/membranes11090648.

[260] G. Milanesi, B. Vigani, S. Rossi, G. Sandri, and E. Mele, "Chitosan-coated poly(Lactic acid) nanofibres loaded with essential oils for wound healing," Polymers (Basel)., vol. 13, no. 16, pp. 1–16, 2021, doi: 10.3390/polym13162582.

[261] C. Aras, E. Tümay Özer, G. Göktalay, G. Saat, and E. Karaca, "Evaluation of Nigella sativa oil loaded electrospun polyurethane nanofibrous mat as wound dressing," J. Biomater. Sci. Polym. Ed., vol. 32, no. 13, pp. 1718–1735, 2021, doi: 10.1080/09205063.2021.1937463.

[262] M. Reza, M. Khorram, S. Barzegar, F. Asadian, and K. Zomorodian, "Antimicrobial core – shell electrospun nanofibers containing Ajwain essential oil for accelerating infected wound healing," Int. J. Pharm., vol. 603, no. February, p. 120698, 2021, doi: 10.1016/j.ijpharm.2021.120698.

[263] D. Serbezeanu et al., "Electrospun polyvinyl alcohol loaded with phytotherapeutic agents for wound healing applications," Nanomaterials, vol. 11, no. 12, pp. 1–13, 2021, doi: 10.3390/nano11123336.

[264] M. Wang, D. G. Yu, G. R. Williams, and S. W. A. Bligh, "Co-Loading of Inorganic Nanoparticles and Natural Oil in the Electrospun Janus Nanofibers for a Synergetic Antibacterial Effect," Pharmaceutics, vol. 14, no. 6, 2022, doi: 10.3390/pharmaceutics14061208.

USC DE SANTIAGO DE COMPOSTELA

[265] A. S. Mohamed Ahmed Mohamady Hussein, Oguzhan Gunduz and M. M. Ibrahim Mohamed El-Sherbiny, "Dual Spinneret Electrospun Polyurethane/PVA-Gelatin Nanofibrous Scaffolds Containing Cinnamon Essential Oil and Nanoceria for Chronic Diabetic Wound Healing: Preparation, Physicochemical Characterization and In-Vitro Evaluation," Molecules, vol. 27, p. 2146, 2022, doi: https://doi.org/10.3390/molecules27072146.

[266] M. Najafiasl, S. Osfouri, R. Azin, and S. Zaeri, "Modeling of drug release and simultaneous enhancement of tensile strength and antioxidant activity of the electrospun nanofibres using naturally extracted oil from Pistacia atlantica," Polym. Test., vol. 107, p. 107492, 2022, doi: 10.1016/j.polymertesting.2022.107492.

[267] A. H. Rather et al., "Polyurethane and cellulose acetate micro-nanofibers containing rosemary essential oil, and decorated with silver nanoparticles for wound healing application," Int. J. Biol. Macromol., vol. 226, no. September 2022, pp. 690–705, 2023, doi: 10.1016/j.ijbiomac.2022.12.048.

[268] C. R. ustundag and M. B. Piskin, "Investigation of electrospun poly (ε-caprolactone) fiber mats loaded with Calophyllum inophyllum essential oil for wound dressing applications: Morphology, drug release and in vitro evaluation," Mater. Technol., vol. 38, no. 1, 2023, doi: 10.1080/10667857.2023.2223018.

[269] S. Khataei, M. H.Al-Musawi, K. Asadi, S. Ramezani, M. Abbasian, and M. Ghorbani, "Effect of molecular weight and content of polyvinylpyrrolidone on cell proliferation, loading capacity and properties of electrospun green tea essential oil-incorporated polyamide-6/polyvinylpyrrolidone nanofibers," J. Drug Deliv. Sci. Technol., vol. 82, no. September 2022, p. 104310, 2023, doi: 10.1016/j.jddst.2023.104310.

[270] V. Reisi-Vanani et al., "Engineering of a core-shell polyvinyl alcohol/gelatin fibrous scaffold for dual delivery of Thymus daenensis essential oil and Glycyrrhiza glabra L. extract as an antibacterial and functional wound dressing," J. Drug Deliv. Sci. Technol., vol. 81, no. February, p. 104282, 2023, doi: 10.1016/j.jddst.2023.104282.

[271] V. Sadaiyandi, R. Ramalingam, K. D. Arunachalam, and J. T. D, "Essential Oils Infused Poly-ε-Caprolactone/Gelatin Electrospun Nanofibrous Mats: Biocompatibility

USC UNIVERSIDADE DE SANTIAGO DE COMPOSTELA

and Antibacterial Study," Appl. Biochem. Biotechnol., vol. 196, no. 1, pp. 296–313, 2024, doi: 10.1007/s12010-023-04530-w.

[272] S. Rathinavel, M. Sugumar, E. Swaminathan, S. Kubendren, K. Samvasivan, and D. Sangeetha, "Development of electrospun Plectranthus amboinicus loaded PCL polymeric nanofibrous scaffold for skin wound healing application: in-vitro and in-silico analysis," J. Polym. Res., vol. 30, no. 3, 2023, doi: 10.1007/s10965-023-03474-3.

[273] P. Nezhad-Mokhtari et al., "Matricaria chamomilla essential oil-loaded hybrid electrospun nanofibers based on polycaprolactone/sulfonated chitosan/ZIF-8 nanoparticles for wound healing acceleration," Int. J. Biol. Macromol., vol. 247, no. July, p. 125718, 2023, doi: 10.1016/j.ijbiomac.2023.125718.

[274] M. Heydari et al., "A two-layer nanofiber-Tragacanth hydrogel composite containing Lavender extract and Mupirocin as a wound dressing," Polym. Bull., vol. 81, no. 1, pp. 373–389, 2024, doi: 10.1007/s00289-022-04655-8.

[275] N. A. Elbhnsawi et al., "Nano-Chitosan/Eucalyptus Oil/Cellulose Acetate Nanofibers: Manufacturing, Antibacterial and Wound Healing Activities," Membranes (Basel)., vol. 13, no. 6, 2023, doi: 10.3390/membranes13060604.

[276] P. Mishra, P. Gupta, R. Srivastava, A. K. Srivastava, K. M. Poluri, and R. Prasad, "Exploration of Antibiofilm and In Vivo Wound Healing Activity of p-Cymene-Loaded Gellan/PVA Nanofibers," ACS Appl. Bio Mater., vol. 6, no. 5, pp. 1816–1831, 2023, doi: 10.1021/acsabm.3c00047.

[277] A. Akturk, "Enrichment of Cellulose Acetate Nanofibrous Scaffolds with Retinyl Palmitate and Clove Essential Oil for Wound Healing Applications," ACS Omega, vol. 8, no. 6, pp. 5553–5560, 2023, doi: 10.1021/acsomega.2c06881.

[278] Z. Fakhri, N. Karimi, F. Saba, and M. Ghorbanpour, "Synthesis composit electrospun based gum-resin/polycaprolactone fibers for biomedical application," J. Drug Deliv. Sci. Technol., vol. 100, no. July, p. 106010, 2024, doi: 10.1016/j.jddst.2024.106010.

[279] D. Serra et al., "Electrospun Nanofibers Encapsulated with Natural Products: A Novel Strategy to Counteract Skin Aging," Int. J. Mol. Sci., vol. 25, no. 3, pp. 1–16, 2024, doi: 10.3390/ijms25031908.

USC

[280] D. Hanahan and R. A. Weinberg, “The Hallmarks of Cancer,” Cell, vol. 100, pp. 57–100, 2000, doi: 10.1016/S0092-8674(00)81683-9.

[281] D. Hanahan and R. A. Weinberg, “Hallmarks of cancer: The next generation,” Cell, vol. 144, no. 5, pp. 646–674, 2011, doi: 10.1016/j.cell.2011.02.013.

[282] D. Hanahan, “Hallmarks of Cancer: New Dimensions,” Cancer Discov., vol. 12, no. 1, pp. 31–46, 2022, doi: 10.1158/2159-8290.CD-21-1059.

[283] D. Hanahan and M. Monje, “Cancer hallmarks intersect with neuroscience in the tumor microenvironment,” Cancer Cell, vol. 41, no. 3, pp. 573–580, 2023, doi: 10.1016/j.ccell.2023.02.012.

[284] O. Visser et al., “Survival of adults with primary malignant brain tumours in Europe ; Results of the EUROCARE-5 study,” pp. 2231–2241, 2015, doi: 10.1016/j.ejca.2015.07.032.

[285] D. Abdelnabi et al., “Local administration of irinotecan using an implantable drug delivery device stops high-grade glioma tumor recurrence in a glioblastoma tumor model,” Drug Deliv. Transl. Res., vol. 14, no. 11, pp. 3070–3088, 2024, doi: 10.1007/s13346-024-01524-x.

[286] D. N. Louis et al., “The 2021 WHO classification of tumors of the central nervous system: A summary,” Neuro. Oncol., vol. 23, no. 8, pp. 1231–1251, 2021, doi: 10.1093/neuonc/noab106.

[287] K. J. Wolf, J. Chen, J. D. Coombes, M. K. Aghi, and S. Kumar, “Dissecting and rebuilding the glioblastoma microenvironment with engineered materials,” Nat. Rev. Mater., vol. 4, no. 10, pp. 651–668, 2019, doi: 10.1038/s41578-019-0135-y.

[288] P. Peruzzi et al., “Intratumoral drug-releasing microdevices allow in situ high-throughput pharmaco phenotyping in patients with gliomas,” Sci. Transl. Med., vol. 15, no. 712, 2023, doi: 10.1126/SCITRANSLMED.ADI0069.

[289] D. Lenz, M. Ries, and P. Johann, “The drug development pipeline for glioblastoma—A cross sectional assessment of the FDA Orphan Drug Product designation database,” PLoS One, vol. 16, no. 7 July, pp. 1–14, 2021, doi: 10.1371/journal.pone.0252924.

USC UNIVERSIDADE DE SANTIAGO DE COMPOSTELA

[290] T. S. van Solinge, L. Nieland, E. A. Chiocca, and M. L. D. Broekman, "Advances in local therapy for glioblastoma — taking the fight to the tumour," Nat. Rev. Neurol., vol. 18, no. 4, pp. 221–236, 2022, doi: 10.1038/s41582-022-00621-0.

[291] K. Lin, S. E. Gueble, R. K. Sundaram, E. D. Huseman, R. S. Bindra, and S. B. Herzon, "Mechanism-based design of agents that selectively target drug-resistant glioma," Science (80-. )., vol. 377, no. 6605, pp. 502–511, 2022, doi: 10.1126/science.abn7570.

[292] M. L. Broekman, S. L. N. Maas, E. R. Abels, T. R. Mempel, A. M. Krichevsky, and X. O. Breakefield, "Multidimensional communication in the microenvirons of glioblastoma," Nat. Rev. Neurol., vol. 14, no. 8, pp. 482–495, 2018, doi: 10.1038/s41582-018-0025-8.

[293] N. A. De Vries, J. H. Beijnen, W. Boogerd, and O. Van Tellingen, "Blood-brain barrier and chemotherapeutic treatment of brain tumors," Expert Rev. Neurother., vol. 6, no. 8, pp. 1199–1209, 2006, doi: 10.1586/14737175.6.8.1199.

[294] C. Nimsky et al., "Preoperative and intraoperative diffusion tensor imaging-based fiber tracking in glioma surgery," Neurosurgery, vol. 56, no. 1, pp. 130–137, 2005, doi: 10.1227/01.NEU.0000144842.18771.30.

[295] S. Pushpakom et al., "Drug repurposing: progress, challenges and recommendations," Nat. Rev. Drug Discov., vol. 18, no. 1, pp. 41–58, 2019, doi: 10.1038/nrd.2018.168.

[296] F. Ragucci et al., "Insights into Healthcare Professionals ' Perceptions and Attitudes toward Nanotechnological Device Application : What Is the Current Situation in Glioblastoma Research ?," Biomedicines, vol. 11, p. 1854, 2023, doi: https://doi.org/10.3390/ biomedicines11071854 Academic.

[297] J. Basso, A. Miranda, J. Sousa, A. Pais, and C. Vitorino, "Repurposing drugs for glioblastoma: From bench to bedside," Cancer Lett., vol. 428, pp. 173–183, 2018, doi: 10.1016/j.canlet.2018.04.039.

[298] S. Alomari et al., "Drug repurposing for glioblastoma and current advances in drug delivery—A comprehensive review of the literature," Biomolecules, vol. 11, no. 12, 2021, doi: 10.3390/biom11121870.

[299] B. Cvek, "Nonprofit drugs as the salvation of the world's healthcare systems: the case of Antabuse (disulfiram)," Drug Discov. Today, vol. 17, no. 9–10, pp. 409–412, 2012, doi: 10.1016/j.drudis.2011.12.010.

[300] Z. Skrott et al., "Alcohol-abuse drug disulfiram targets," Nat. Publ. Gr., 2017, doi: 10.1038/nature25016.

[301] Y. Lu et al., "Leveraging disulfiram to treat cancer: Mechanisms of action, delivery strategies, and treatment regimens," Biomaterials, vol. 281, no. September 2021, p. 121335, 2022, doi: 10.1016/j.biomaterials.2021.121335.

[302] M. Pan et al., "Seesaw conformations of Npl4 in the human p97 complex and the inhibitory mechanism of a disulfiram derivative," Nat. Commun., vol. 12, no. 1, 2021, doi: 10.1038/s41467-020-20359-x.

[303] Y. Terashima et al., "Targeting FROUNT with disulfiram suppresses macrophage accumulation and its tumor-promoting properties," Nat. Commun., vol. 11, no. 1, 2020, doi: 10.1038/s41467-020-14338-5.

[304] J. Sesen et al., "Metformin inhibits growth of human glioblastoma cells and enhances therapeutic response," PLoS One, vol. 10, no. 4, pp. 1–24, 2015, doi: 10.1371/journal.pone.0123721.

[305] M. Gritti et al., "Metformin repositioning as antitumoral agent: Selective antiproliferative effects in human glioblastoma stem cells, via inhibition of CLIC1-mediated ion current," Oncotarget, vol. 5, no. 22, pp. 11252–11268, 2014, doi: 10.18632/oncotarget.2617.

[306] E. Nance, S. H. Pun, R. Saigal, and D. L. Sellers, "Drug delivery to the central nervous system," Nat. Rev. Mater., vol. 7, no. 4, pp. 314–331, 2022, doi: 10.1038/s41578-021-00394-w.

[307] M. Weller et al., "Glioma," Nat. Rev. Dis. Prim., vol. 10, no. 1, 2024, doi: 10.1038/s41572-024-00516-y.

[308] R. Ramachandran et al., "Theranostic 3-Dimensional nano brain-implant for prolonged and localized treatment of recurrent glioma," Sci. Rep., vol. 7, no. October 2016, pp. 1–16, 2017, doi: 10.1038/srep43271.

USC UNIVERSIDADE DE SANTIAGO DE COMPOSTELA

[309] Y. Y. Tseng, J. Y. Liao, W. A. Chen, Y. C. Kao, and S. J. Liu, "Sustainable release of carmustine from biodegradable poly[(d,l)-lactide-co- glycolide] nanofibrous membranes in the cerebral cavity: In vitro and in vivo studies," Expert Opin. Drug Deliv., vol. 10, no. 7, pp. 879–888, 2013, doi: 10.1517/17425247.2013.758102.

[310] A. B. Fleming and W. M. Saltzman, "Pharmacokinetics of the carmustine implant," Clin. Pharmacokinet., vol. 41, no. 6, pp. 403–419, 2002, doi: 10.2165/00003088-200241060-00002.

[311] F. Ahmed, R. I. Pakunlu, A. Brannan, F. Bates, T. Minko, and D. E. Discher, "Biodegradable polymersomes loaded with both paclitaxel and doxorubicin permeate and shrink tumors, inducing apoptosis in proportion to accumulated drug," J. Control. Release, vol. 116, no. 2 SPEC. ISS., pp. 150–158, 2006, doi: 10.1016/j.jconrel.2006.07.012.

[312] S. H. Ranganath and C. H. Wang, "Biodegradable microfiber implants delivering paclitaxel for post-surgical chemotherapy against malignant glioma," Biomaterials, vol. 29, no. 20, pp. 2996–3003, 2008, doi: 10.1016/j.biomaterials.2008.04.002.

[313] P. Kumar Naraharisetti, B. Yung Sheng Ong, J. Wei Xie, T. Kam Yiu Lee, C. H. Wang, and N. V. Sahinidis, "In vivo performance of implantable biodegradable preparations delivering Paclitaxel and Etanidazole for the treatment of glioma," Biomaterials, vol. 28, no. 5, pp. 886–894, 2007, doi: 10.1016/j.biomaterials.2006.09.044.

[314] D. Hernán Pérez de la Ossa et al., "Local Delivery of Cannabinoid-Loaded Microparticles Inhibits Tumor Growth in a Murine Xenograft Model of Glioblastoma Multiforme," PLoS One, vol. 8, no. 1, pp. 2–9, 2013, doi: 10.1371/journal.pone.0054795.

[315] A. W. Scott et al., "Intracranial microcapsule drug delivery device for the treatment of an experimental gliosarcoma model," Biomaterials, vol. 32, no. 10, pp. 2532–2539, 2011, doi: 10.1016/j.biomaterials.2010.12.020.

[316] G. Y. Kim et al., "Resorbable polymer microchips releasing BCNU inhibit tumor growth in the rat 9L flank model," J. Control. Release, vol. 123, no. 2, pp. 172–178, 2007, doi: 10.1016/j.jconrel.2007.08.003.

USC DE SANTIAGO DE COMPOSTELA

[317] M. Y. Hua et al., "The effectiveness of a magnetic nanoparticle-based delivery system for BCNU in the treatment of gliomas," Biomaterials, vol. 32, no. 2, pp. 516–527, 2011, doi: 10.1016/j.biomaterials.2010.09.065.

[318] R. Ramachandran et al., "A polymer-protein core-shell nanomedicine for inhibiting cancer migration followed by photo-triggered killing," J. Biomed. Nanotechnol., vol. 10, no. 8, pp. 1401–1415, 2014, doi: 10.1166/jbn.2014.1847.

[319] V. R. Recinos et al., "Combination of intracranial temozolomide with intracranial carmustine improves survival when compared with either treatment alone in a rodent glioma model," Neurosurgery, vol. 66, no. 3, pp. 530–537, 2010, doi: 10.1227/01.NEU.0000365263.14725.39.

[320] S. Brem et al., "Local delivery of temozolomide by biodegradable polymers is superior to oral administration in a rodent glioma model," Cancer Chemother. Pharmacol., vol. 60, no. 5, pp. 643–650, 2007, doi: 10.1007/s00280-006-0407-2.

[321] S. Anai et al., "Antitumor effect of fibrin glue containing temozolomide against malignant glioma," Cancer Sci., vol. 105, no. 5, pp. 583–591, 2014, doi: 10.1111/cas.12397.

[322] S. H. Ranganath et al., "The use of submicron/nanoscale PLGA implants to deliver paclitaxel with enhanced pharmacokinetics and therapeutic efficacy in intracranial glioblastoma in mice," Biomaterials, vol. 31, no. 19, pp. 5199–5207, 2010, doi: 10.1016/j.biomaterials.2010.03.002.

[323] B. Y. S. Ong et al., "Paclitaxel delivery from PLGA foams for controlled release in post-surgical chemotherapy against glioblastoma multiforme," Biomaterials, vol. 30, no. 18, pp. 3189–3196, 2009, doi: 10.1016/j.biomaterials.2009.02.030.

[324] M. S. Lesniak, U. Upadhyay, R. Goodwin, B. Tyler, and H. Brem, "Local delivery of doxorubicin for the treatment of malignant brain tumors in rats," Anticancer Res., vol. 25, no. 6 B, pp. 3825–3831, 2005.

[325] Y. Manome et al., "Local delivery of doxorubicin for malignant glioma by a biodegradable PLGA polymer sheet," Anticancer Res., vol. 26, no. 5 A, pp. 3317–3326, 2006.

USC UNIVERSIDADE DE SANTIAGO DE COMPOSTELA

[326] P. Menei et al., “Local and sustained delivery of 5-fluorouracil from biodegradable microspheres for the radiosensitization of glioblastoma: A pilot study,” Cancer, vol. 86, no. 2, pp. 325–330, 1999, doi: 10.1002/(SICI)1097-0142(19990715)86:2<325::AID-CNCR17>3.0.CO;2-S.

[327] J. D. Weingart, R. C. Thompson, B. Tyler, O. M. Colvin, and H. Brem, “Local delivery of the topoisomerase I inhibitor camptothecin sodium prolongs survival in the rat intracranial 9L gliosarcoma model,” Int. J. Cancer, vol. 62, no. 5, pp. 605–609, 1995, doi: 10.1002/ijc.2910620519.

[328] J. Zhao and W. Cui, “Functional Electrospun Fibers for Local Therapy of Cancer,” Adv. Fiber Mater., vol. 2, pp. 229–245, 2020, doi: https://doi.org/10.1007/s42765-020-00053-9.

[329] X. Xu et al., “BCNU-loaded PEG – PLLA ultrafine fibers and their in vitro antitumor activity against Glioma C6 cells,” vol. 114, pp. 307–316, 2006, doi: 10.1016/j.jconrel.2006.05.031.

[330] Z. Jiang et al., Nanofiber Scaffolds as Drug Delivery Systems Promoting Wound Healing, vol. 15, no. 7. 2023. doi: 10.3390/pharmaceutics15071829.

[331] Y. Y. Tseng et al., “Advanced interstitial chemotherapy combined with targeted treatment of malignant glioma in rats by using drug-loaded nanofibrous membranes,” Oncotarget, vol. 7, no. 37, pp. 59902–59916, 2016, doi: 10.18632/oncotarget.10989.

[332] C. Lei, Y. Cui, L. Zheng, P. K. Chow, and C. Wang, “Biomaterials Development of a gene / drug dual delivery system for brain tumor therapy : Potent inhibition via RNA interference and synergistic effects,” Biomaterials, vol. 34, no. 30, pp. 7483–7494, 2013, doi: 10.1016/j.biomaterials.2013.06.010.

[333] J. R. Bagó et al., “Biomaterials Electrospun nanofibrous scaffolds increase the efficacy of stem cell-mediated therapy of surgically resected glioblastoma,” vol. 90, pp. 116–125, 2016, doi: 10.1016/j.biomaterials.2016.03.008.

[334] B. Liu et al., “Electrospun poly ( L-lactic acid )/ gelatine membranes loaded with doxorubicin for effective suppression of glioblastoma cell growth in vitro and in vivo,” no. July, pp. 1–12, 2021, doi: 10.1093/rb/rbab043.

USC UNIVERSIDADE DE SANTIAGO DE COMPOSTELA

[335] J. Gustavo et al., "Nek1-inhibitor and temozolomide-loaded microfibers as a co-therapy strategy for glioblastoma treatment," vol. 617, no. November 2021, 2022, doi: 10.1016/j.ijpharm.2022.121584.

[336] M. Haji et al., "Nanoparticle-containing electrospun nanofibrous scaffolds for sustained release of SDF-1 α," vol. 610, no. May, 2021, doi: 10.1016/j.ijpharm.2021.121205.

[337] S. Spadaro et al., "PEG-PLGA electrospun nanofibrous membranes loaded with Au@Fe2O3 nanoparticles for drug delivery applications," Front. Phys., vol. 13, no. 1, pp. 1–9, 2018, doi: 10.1007/s11467-017-0703-9.

[338] A. Contreras-García, E. Bucio, A. Concheiro, and C. Alvarez-Lorenzo, "Polypropylene grafted with NIPAAm and APMA for creating hemocompatible surfaces that load/elute nalidixic acid," React. Funct. Polym., vol. 70, no. 10, pp. 836–842, 2010, doi: 10.1016/j.reactfunctpolym.2010.07.019.

[339] K. J. Figueroa-Lopez et al., "Development of electrospun active films of poly(3-hydroxybutyrate-co-3-hydroxyvalerate) by the incorporation of cyclodextrin inclusion complexes containing oregano essential oil," Food Hydrocoll., vol. 108, no. January, 2020, doi: 10.1016/j.foodhyd.2020.106013.

[340] J. E. Meneguello et al., "Systematic review of disulfiram as an antibacterial agent: what is the evidence?," Int. J. Antimicrob. Agents, vol. 59, no. 5, p. 106578, 2022, doi: 10.1016/j.ijantimicag.2022.106578.

[341] M. Lemos et al., "The effects of ferulic and salicylic acids on Bacillus cereus and Pseudomonas fluorescens single- and dual-species biofilms," Int. Biodeterior. Biodegrad., vol. 86, pp. 42–51, 2014, doi: 10.1016/j.ibiod.2013.06.011.

[342] M. H. Cavanagh, R. E. Burrell, and P. L. Nadworny, "Evaluating antimicrobial efficacy of new commercially available silver dressings," Int. Wound J., vol. 7, no. 5, pp. 394–405, 2010, doi: 10.1111/j.1742-481X.2010.00705.x.

[343] M. Weller et al., "Glioma," Nat. Rev. Dis. Prim., vol. 1, no. July, 2015, doi: 10.1038/nrdp.2015.17.

[344] C. Y. Foo et al., "Medical Device Advances in the Treatment of Glioblastoma," pp. 1–33, 2022.

USC UNIVERSIDADE DE SANTIAGO DE COMPOSTELA

[345] T. Iqbal et al., “Frontiers in the treatment of glioblastoma : Past , present and emerging,” Adv. Drug Deliv. Rev., vol. 171, pp. 108–138, 2021, doi: 10.1016/j.addr.2021.01.012.

[346] B. J. Mason and C. J. Heyser, “ALCOHOL USE DISORDER : THE ROLE OF MEDICATION IN RECOVERY,” vol. 41, no. 1, pp. 1–17, 2021.

[347] N. Ramadhani, M. Shabir, and C. McConville, “Preparation and characterisation of Kolliphor®P 188 and P 237 solid dispersion oral tablets containing the poorly water soluble drug disulfiram,” Int. J. Pharm., vol. 475, no. 1, pp. 514–522, 2014, doi: 10.1016/j.ijpharm.2014.09.013.

[348] F. Nazzaro, F. Fratianni, and L. De Martino, “Effect of Essential Oils on Pathogenic Bacteria,” pp. 1451–1474, 2013, doi: 10.3390/ph6121451.

[349] S. Chouhan, K. Sharma, and S. Guleria, “Antimicrobial Activity of Some Essential Oils—Present Status and Future Perspectives,” Medicines, vol. 4, no. 3, p. 58, 2017, doi: 10.3390/medicines4030058.

USC UNIVERSIDADE DE SANTIAGO DE COMPOSTELA

# VII. ANNEXES

USC
UNIVERSIDADE
DE SANTIAGO
DE COMPOSTELA

USC
UNIVERSIDADE
DE SANTIAGO
DE COMPOSTELA

# ANNEX A

## A.1. CONFLICT OF INTEREST

The doctoral student declares that there is no conflict of interest regarding the doctoral thesis.

## A.2. LIST OF PUBLICATIONS

CHAPTER I

TITLE: Antimicrobial cyclodextrin-assisted electrospun fibers loaded with carvacrol, citronellol and cinnamic acid for wound healing

AUTHORS: Iago Gonzalez-Prada, Anabela Borges, Beatriz Santos-Torres, Beatriz Magariños, Manuel Simões, Angel Concheiro, Carmen Alvarez-Lorenzo

JOURNAL: International Journal of Biological Macromolecules

YEAR: 2024

PUBLISHER: ELSEVIER

LINK: https://doi.org/10.1016/j.ijbiomac.2024.134154

JOURNAL IMPACT FACTOR (year 2024, latest update JCR Clarivate): 7.7 (Q1-chemical and biological aspects of all natural macromolecules.)

AUTHOR CONTRIBUTION: I. Gonzalez-Prada: Conceptualization; Data curation; Formal analysis; Investigation; Methodology; Software; Writing - original draft; and Writing - review & editing

INFORMATION REGARDING COPYRIGHT AND USE: Please note that, as the author of this Elsevier article, you retain the right to include it in a thesis or dissertation, provided it is not published commercially. Permission is not required, but please ensure that you reference the journal as the original source. https://www.elsevier.com/about/policies-and-standards/copyright/permissions

USC UNIVERSIDADE DE SANTIAGO DE COMPOSTELA

Can I include/use my article in my thesis/dissertation?

Yes. Authors can include their articles in full or in part in a thesis or dissertation for non-commercial purposes.

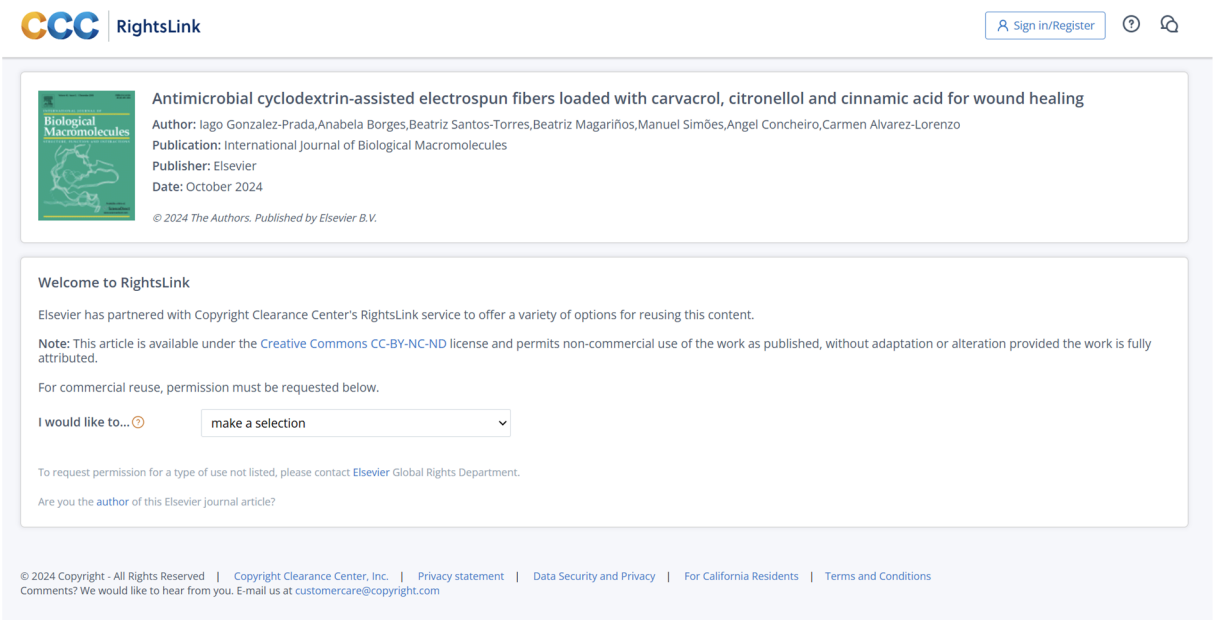
***For any further clarifications, you can submit your query via our online form***

Can I use material from my Elsevier journal article within my thesis/dissertation?

As an Elsevier journal author, you have the right to Include the article in a thesis or dissertation (provided that this is not to be published commercially) whether in full or in part, subject to proper acknowledgment; see the Copyright page for more information. No written permission from Elsevier is necessary.

This right extends to the posting of your thesis to your university's repository provided that if you include the published journal article, it is embedded in your thesis and not separately downloadable.

***For any further clarifications, you can submit your query via our online form***




## A.3. Figures Authorship

The author declares that all unreferenced figures of this Thesis are from published articles and the student has permission from the publisher to include them in the thesis. Figures included in the unpublished works are of his authorship.

USC UNIVERSIDADE DE SANTIAGO DE COMPOSTELA

# ANNEX B

## B.1. PERMISSION FOR THE IN VIVO STUDY

MINISTÈRE
DE L'ENSEIGNEMENT
SUPÉRIEUR
ET DE LA RECHERCHE
*Liberté*
*Égalité*
*Fraternité*

**Service de la performance, du financement et de la contractualisation avec les organismes de recherche**

**Département des pratiques de recherche réglementées**

**Cellule Animaux utilisés à des Fins Scientifiques - AFiS**

Affaire suivie par : V. Delassault et V. Gomez
Tél : 01 55 55 97 27 / 77 58
Mél : autorisation-projet@recherche.gouv.fr

1, rue Descartes
75231 Paris SP 05

**Direction générale**
**de la recherche et de l'innovation**

Paris, le 13 septembre 2023

**Autorisation de projet utilisant des animaux à des fins scientifiques**

En application des dispositions du code rural et de la pêche maritime, notamment ses articles R.214-87 à R.214-126, le projet :

1. référencé sous le numéro APAFIS #43915-2020032620074335 v11
2. ayant pour titre : Etude des effets thérapeutiques lors du traitement par radiothérapie interne via l'utilisation de nanoparticules chargées au Rhénium-188 et d'un bio-implant dans le cas du glioblastome chez le rat (1/2)
3. déposé par l'établissement utilisateur : Service Commun Animalerie Hospitalo-Universitaire (SCAHU) - Université Angers, numéro d'agrément F49007002, dont le responsable est Monsieur Pierre ASFAR
4. et dont la responsabilité de la mise en œuvre générale et de la conformité à l'autorisation est assurée par : Monsieur Emmanuel GARCION, Monsieur Loris RONCALI, Madame Charlotte ROY,

est autorisé.

L'autorisation de projet est accordée, sous réserve de la validité de l'agrément de l'établissement, pour une durée de 5 ans à compter de la présente notification.

Le projet précité a été évalué sur le plan éthique par le comité d'éthique en expérimentation animale n°006 et a reçu un avis favorable.

Ce projet n'est pas soumis à l'obligation d'une appréciation rétrospective à l'issue de sa réalisation.

Pour la ministre et par délégation
le chef du département des pratiques
de recherche réglementées

Laurent PINON

Monsieur Pierre ASFAR
Service Commun Animalerie Hospitalo-Universitaire (SCAHU) - Université Angers

USC
UNIVERSIDADE
DE SANTIAGO
DE COMPOSTELA

## B.2. ARRIVE CHECKLIST

CHECKLIST FOR THESIS THAT INCLUDE EXPERIMENTAL ANIMALS.

EXPERIMENTAL ANIMALS ARRIVE

| Yes/No/NA | | Page |
|---|---|---|
| | **Title** | |
| Yes | Provide as accurate and concise a description of the content of the article as possible. | 221 |
| | **Abstract** | |
| Yes | Provide an accurate summary of the background, research objectives, including details of the species or strain of animal used, key methods, principal findings and conclusions of the study | 222 |
| | **Background** | |
| Yes | Provide an accurate summary of the background, research objectives, including details of the species or strain of animal used, key methods, principal findings and conclusions of the study. | 222-275 |
| Yes | Explain how and why the animal species and model being used can address the scientific objectives and, where appropriate, the study's relevance to human biology. | 239-240, 262-265 |
| | **Objectives** | |
| Yes | Clearly describe the primary and any secondary objectives of the study, or specific hypotheses being tested. | 239-240 |
| | **Methods** | |
| | **Ethical statement** | |
| Yes | Indicate the nature of the ethical review permissions, relevant licenses, and national or institutional guidelines for the care and use of animals, that cover the research. | 239-240, 305 |
| | **Study design** | |
| Yes | Number of experimental and control groups | 239 |
| Yes | Steps taken to minimize the effects of subjective bias when allocating animals to treatment (e.g. randomization procedure) and when assessing results (e.g. if done, describe who was blinded and when). | 239-240 |
| Yes | The experimental unit (e.g. a single animal, group or cage of animals). A time-line diagram or flow chart can be useful to illustrate how complex study designs were carried out. | 239-240 |
| | **Experimental procedures** | |
| Yes | How (e.g. drug formulation and dose, site and route of administration, anesthesia and analgesia used [including monitoring], surgical procedure, method of euthanasia). Provide details of any specialist equipment used, including supplier(s). | 239-240 |
| Yes | When (e.g. time of day). | 239-240 |

USC UNIVERSIDADE DE SANTIAGO DE COMPOSTELA

| | | |
|---|---|---|
| Yes | Where (e.g. home cage, laboratory, water maze). | 239-240 |
| Yes | Why (e.g. rationale for choice of specific anesthetic, route of administration, drug dose used). | 239-240 |
| | **Experimental animals** | |
| Yes | Provide details of the animals used, including species, strain, sex, developmental stage (e.g. mean or median age plus age range) and weight (e.g. mean or median weight plus weight range). | 239-240 |
| Yes | Provide further relevant information such as the source of animals, international strain nomenclature, genetic modification status (e.g.knock-out or transgenic), genotype, health/immune status, drug or test naïve, previous procedures, etc. | 239-240 |
| | **Housing and husbandry** | |
| Yes | Housing (type of facility e.g. specific pathogen free [SPF]; type of cage or housing; bedding material; number of cage companions; tank shape and material etc. for fish). | 239-240 |
| Yes | Husbandry conditions (e.g. breeding program, light/dark cycle, temperature, quality of water etc for fish, type of food, access to food and water, environmental enrichment). | 239-240 |
| Yes | Welfare-related assessments and interventions that were carried out prior to, during, or after the experiment. | 239-240 |
| | **Sample size** | |
| Yes | Specify the total number of animals used in each experiment, and the number of animals in each experimental group. | 239-240 |
| Yes | Explain how the number of animals was arrived at. Provide details of any sample size calculation used. | 239-240 |
| Yes | Indicate the number of independent replications of each experiment, if relevant. | 239-240 |
| Yes | Allocating animals to experimental groups | 239-240 |
| Yes | Indicate the number of independent replications of each experiment, if relevant. | 239-240 |
| Yes | Describe the order in which the animals in the different experimental groups were treated and assessed. | 239-240 |
| | **Experimental outcomes** | |
| Yes | Clearly define the primary and secondary experimental outcomes assessed (e.g. cell death, molecular markers, behavioral changes). | 239-240 |
| | **Statistical methods** | |
| Yes | Provide details of the statistical methods used for each analysis. | 240-241 |
| Yes | Specify the unit of analysis for each dataset (e.g. single animal, group of animals, single neuron). | 240-241 |
| Yes | Describe any methods used to assess whether the data met the assumptions of the statistical approach. | 240-241 |
| | **Results and discussion** | |
| | **Basal data** | |

USC UNIVERSIDADE DE SANTIAGO DE COMPOSTELA

| | | |
|---|---|---|
| Yes | For each experimental group, report relevant characteristics and health status of animals (e.g. weight, microbiological status, and drug or test naïve) prior to treatment or testing (this information can often be tabulated). | 262-266 |
| | **Numbers analyzed** | |
| Yes | Report the number of animals in each group included in each analysis. Report absolute numbers (e.g. 10/20, not 50%). | 262-266 |
| Yes | If any animals or data were not included in the analysis, explain why. | 262-266 |
| | **Outcomes and estimation** | |
| Yes | Report the results for each analysis carried out, with a measure of precision (e.g. standard error or confidence interval). | 262-266 |
| | **Adverse events** | |
| NA | Give details of all important adverse events in each experimental group. | |
| NA | Describe any modifications to the experimental protocols made to reduce adverse events. | |
| | **Interpretation/scientific implications** | |
| Yes | Interpret the results, taking into account the study objectives and hypotheses, current theory and other relevant studies in the literature. | 262-266 |
| NA | Comment on the study limitations including any potential sources of bias, any limitations of the animal model, and the imprecision associated with the results. | |
| NA | Describe any implications of your experimental methods or findings for the replacement, refinement or reduction (the 3Rs) of the use of animals in research. | |
| | **Generalizability/translation** | |
| Yes | Comment on whether, and how, the findings of this study are likely to translate to other species or systems, including any relevance to human biology. | 265-266 |
| | **Funding** | |
| Yes | List all funding sources (including grant number) and the role of the funder(s) in the study. | 305 |

Based on The ARRIVE guidelines: Animal Research: Reporting of In Vivo Experiments.

USC UNIVERSIDADE DE SANTIAGO DE COMPOSTELA







This PhD Thesis focuses on developing alternative approaches for treating two major societal challenges: antimicrobial resistance and cancer, with a particular emphasis on glioblastoma. To address these issues, a range of electrospun mats were prepared. Various essential oils —namely carvacrol, citronellol, and cinnamic acid— displaying antimicrobial, anti-inflammatory, and angiogenic properties were evaluated for treating infected chronic wounds. Additionally, the repurposed drug disulfiram was encapsulated to leverage its anticancer and antimicrobial properties in the presence of selective amounts of Cu(II), forming the $Cu(DDC)_2$ complex that enhanced the activity and reduced the toxicity. Cyclodextrins such as αCD and HPβCD were used to encapsulate these active compounds, improving their poor physicochemical properties and tuning the release profiles. This work highlights the advantages and versatility of the electrospinning technique in producing fiber-based scaffolds for biomedical applications.